

ORIGINAL FROM  
IN-46-CR

25669  
P 623

The University of Alabama in Huntsville

Annual Report for Grant NAG8-834  
Due Date: June 24, 1991

**"Theoretical and Experimental Studies Relevant to  
Interpretation of Auroral Emissions"**

Submitted to

George C. Marshall Space Flight Center  
Space Science Laboratory  
National Aeronautics and Space Administration  
Marshall Space Flight Center, AL 35812

by

Charles E. Keffer  
Charles E. Keffer  
Principal Investigator  
The University of Alabama in Huntsville  
Physics Department  
Huntsville, AL 35899

(NASA-CR-188491) THEORETICAL AND  
EXPERIMENTAL STUDIES RELEVANT TO  
INTERPRETATION OF AURORAL EMISSIONS Annual  
Report (Alabama Univ.) 623 p CSCL 04A

N91-26637

Unclas  
53/46 0025669



The University of Alabama in Huntsville

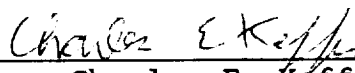
Annual Report for Grant NAG8-834  
Due Date: June 24, 1991

**"Theoretical and Experimental Studies Relevant to  
Interpretation of Auroral Emissions"**

Submitted to

George C. Marshall Space Flight Center  
Space Science Laboratory  
National Aeronautics and Space Administration  
Marshall Space Flight Center, AL 35812

by

  
\_\_\_\_\_  
Charles E. Keffer  
Principal Investigator  
The University of Alabama in Huntsville  
Physics Department  
Huntsville, AL 35899





## Table of Contents

1.	Introduction . . . . .	1
2.	Space Vehicle Contamination Study . . . . .	2
	2.1 Laboratory Measurements . . . . .	2
	2.2 Induced Environment Workshop . . . . .	5
3.	Auroral Modeling . . . . .	7
	3.1 Auroral Modeling . . . . .	7
	3.2 UVI Workshops . . . . .	12
4.	REFERENCES . . . . .	14
5.	APPENDIX A . . . . .	15
6.	APPENDIX B . . . . .	26
7.	APPENDIX C . . . . .	31
8.	APPENDIX D . . . . .	236



## **Theoretical and Experimental Studies Relevant to Interpretation of Auroral Emissions**

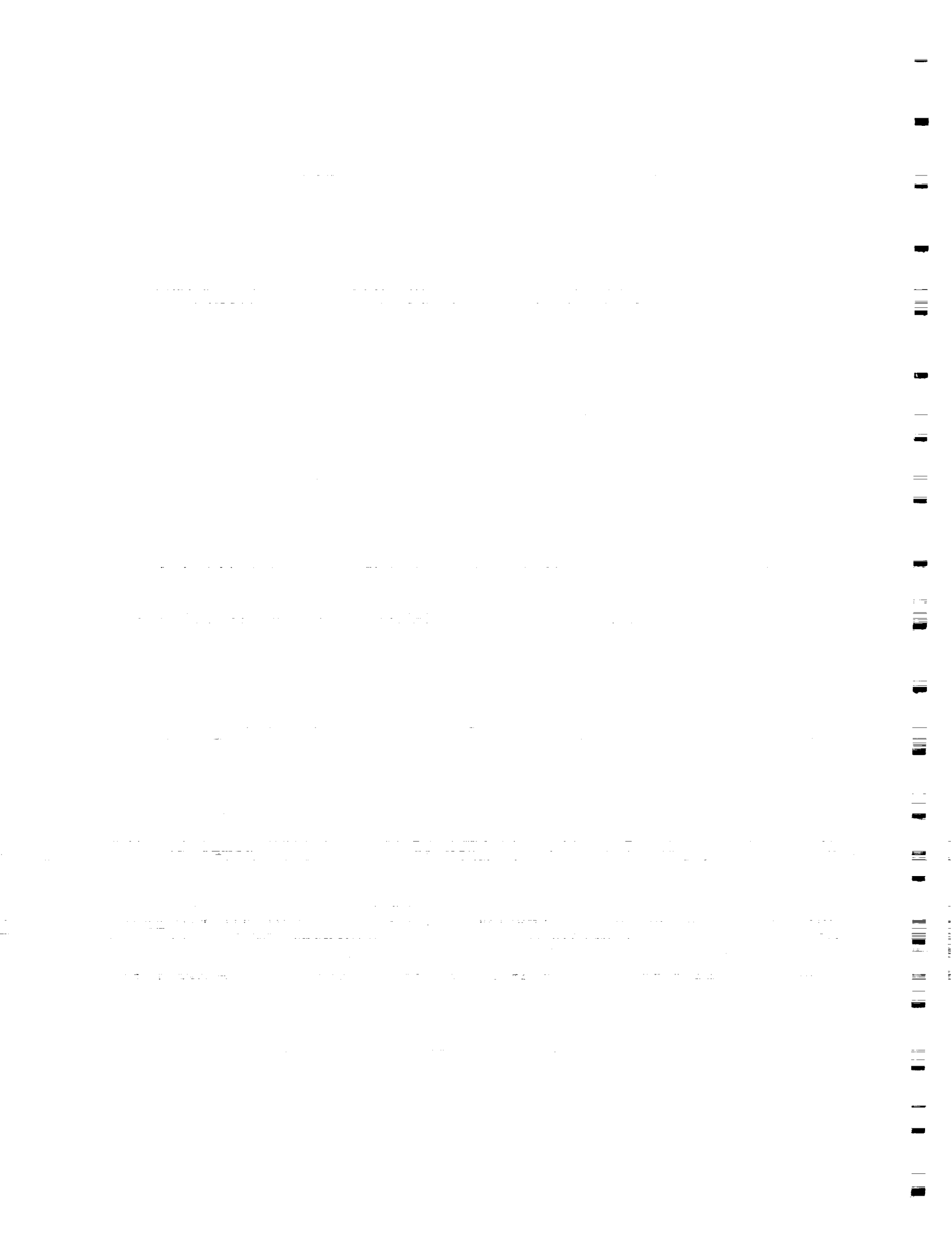
### **1. Introduction**

Increasingly, space based observations of upper atmospheric emissions are supplanting their ground-based counterparts as the methods of choice for the study of the Earth's upper atmosphere and its interaction with the solar environment. Auroral imaging from an orbiting platform, in particular, offers the opportunity to provide details on the total auroral energy influx and characteristic energy of the incident auroral particles, as well as the capability to map and relate these parameters from the ionosphere/thermosphere to the various regions of the Earth's magnetosphere.

This report details the accomplishments of the first year of what is intended to be a three year collaborative effort with MSFC focused on the interpretation of auroral emissions and studies of potential spacecraft-induced contamination effects. Accordingly, the research has been divided into two tasks. The first task is designed to add to our understanding of space vehicle induced external contamination. An experimental facility for simulation of the external environment for a spacecraft in low Earth orbit has been developed. The facility has been used to make laboratory measurements of important phenomena required for improving our understanding of the space vehicle induced external environment and its effect on measurement of auroral emissions from space-based platforms. A workshop was sponsored to provide a forum for presentation of the latest research by nationally recognized experts on space vehicle contamination and to discuss the impact of this research on future missions involving space-based platforms.

The second task is to add an ab initio auroral calculation to the extant ionospheric/thermospheric global modeling capabilities at our disposal. Once the addition of the code was complete, the combined model was to be used to compare the relative intensities and behavior of various emission sources (dayglow, aurora, etc.). Such studies are essential to an understanding of the types of VUV auroral images which are expected to be available within two years with the successful deployment of the Ultraviolet Imager (UVI) on the ISTP POLAR spacecraft. In anticipation of this, the second task includes support for meetings of the science working group for the UVI to discuss operational and data analysis needs.

Taken together, the proposed tasks outline a course of study designed to make significant contributions to the field of space-based auroral imaging. The accomplishments of each task for the past year are discussed in detail below and in the appendices.



## 2. Space Vehicle Contamination Study

### 2.1 Laboratory Measurements

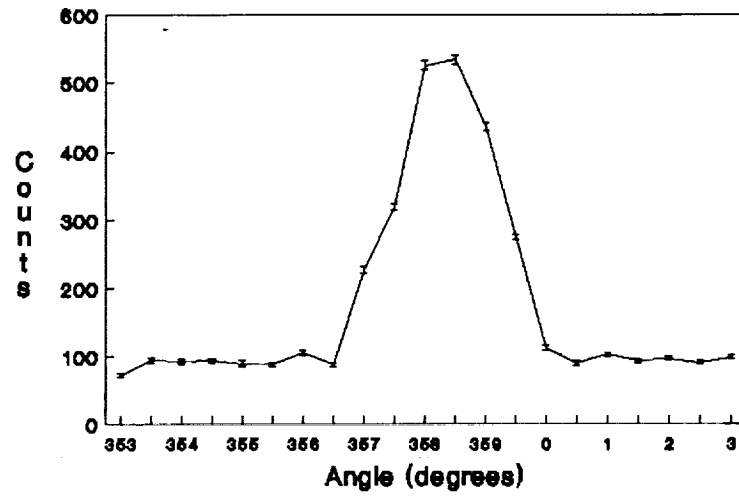
The laboratory work under this grant has all been performed in our Cross Section Facility. The Facility is described in the paper entitled "Laboratory Facility for Simulation of Vehicle-Environment Interactions" which was presented by Dr. Keffer at the Vehicle-Environment Interactions Conference held at the Applied Physics Laboratory, Laurel, Maryland on March 11-13, 1991. The paper is attached as Appendix A of this report.

Work performed during the last year has emphasized gas-gas interactions in crossed molecular beam experiments. Appendix B contains the Semiannual Report which covers the first six months of this period. Briefly summarizing that report, characterization of the two pulsed molecular beams has been completed using thermal energy oxygen and nitrogen beams. Figures 1 and 2 show typical spatial and temporal profiles of the beam pulses. Thermal energy differential scattering cross sections were also measured using the oxygen and nitrogen beams. The result is shown in Figure 3. This cross section has been compared with classical scattering theory and shown to be in satisfactory agreement. These characterization measurements have demonstrated that the Cross Section Facility can be used to make differential scattering measurements without serious systematic errors.

Atomic oxygen plays a pivotal role both in contributing to the induced external environment around orbiting space vehicles and in the chemistry of the earth's atmosphere. Consequently, development and characterization of an energetic, high flux source of atomic oxygen is one of the crucial tasks in this laboratory effort. Work in this area has progressed well during the last six months and substantial progress has been made toward completion of the task. A reliable and reproducible energetic oxygen source is currently being routinely operated. A large number of measurements have been made of the velocity and composition of the source. Figure 4 illustrates the type of beam velocity measurements which have been made. Two peaks are evident in the intensity vs time plot of the mass spectrometer signal. The first peak is due to photons from the plasma discharge formed when the molecular oxygen pulse is dissociated by a pulse from a CO<sub>2</sub> laser. These photons arrive at the detector essentially coincident with the formation of the fast O atoms. The second peak in the figure is due to the fast O atoms. The velocity of the atoms is calculated from the known distance from the pulsed valve to the mass spectrometer divided by the time between the two peaks since this time represents the time of flight for the fast O atoms. The velocity for the measurement shown is 6.8 km/sec. Mass spectrometer measurements of the fast oxygen beam have demonstrated that it is composed predominantly of oxygen atoms with some oxygen molecules and a small percentage of atomic oxygen ions and some impurities such as hydrogen atoms and nitrogen



## O2 Spatial Profile



## N2 Spatial Profile

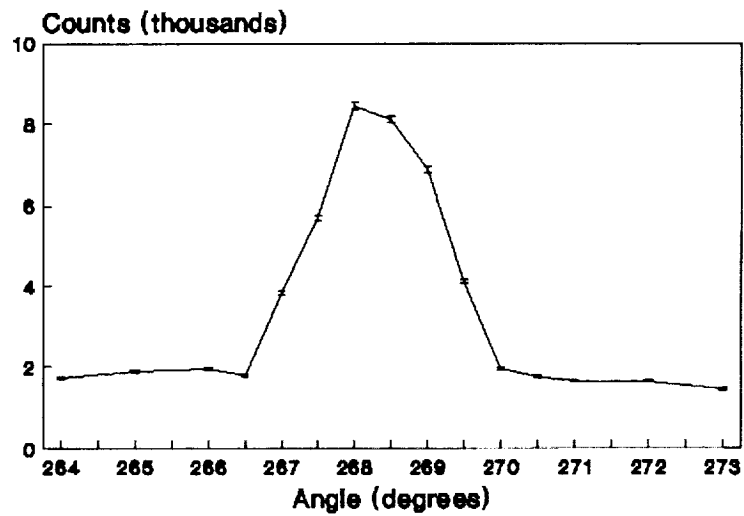
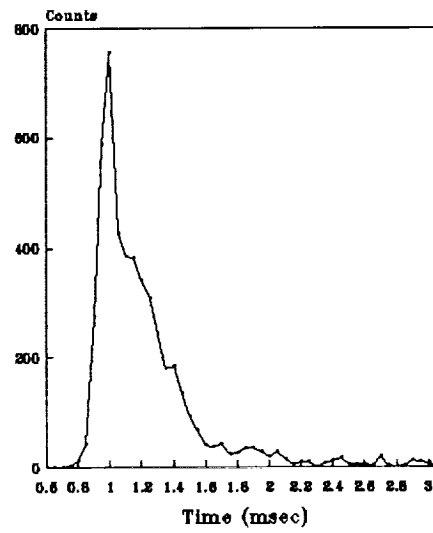


Figure 1





## O<sub>2</sub> Temporal Profile



## N<sub>2</sub> Temporal Profile

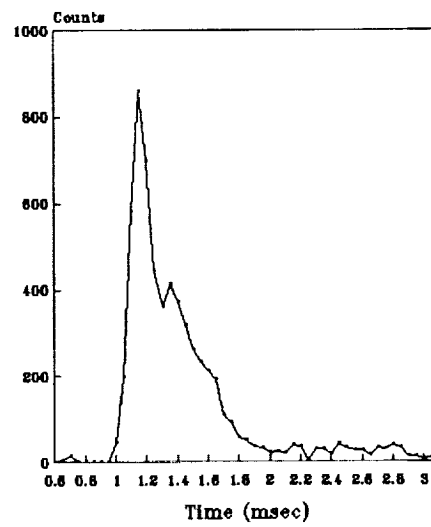


Figure 2



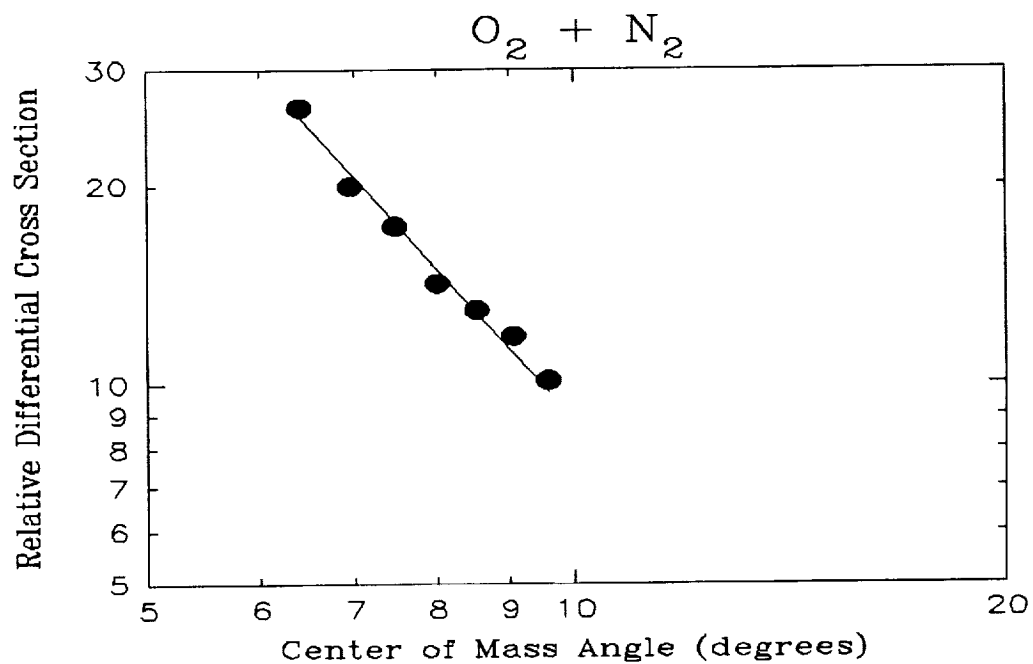


Figure 3

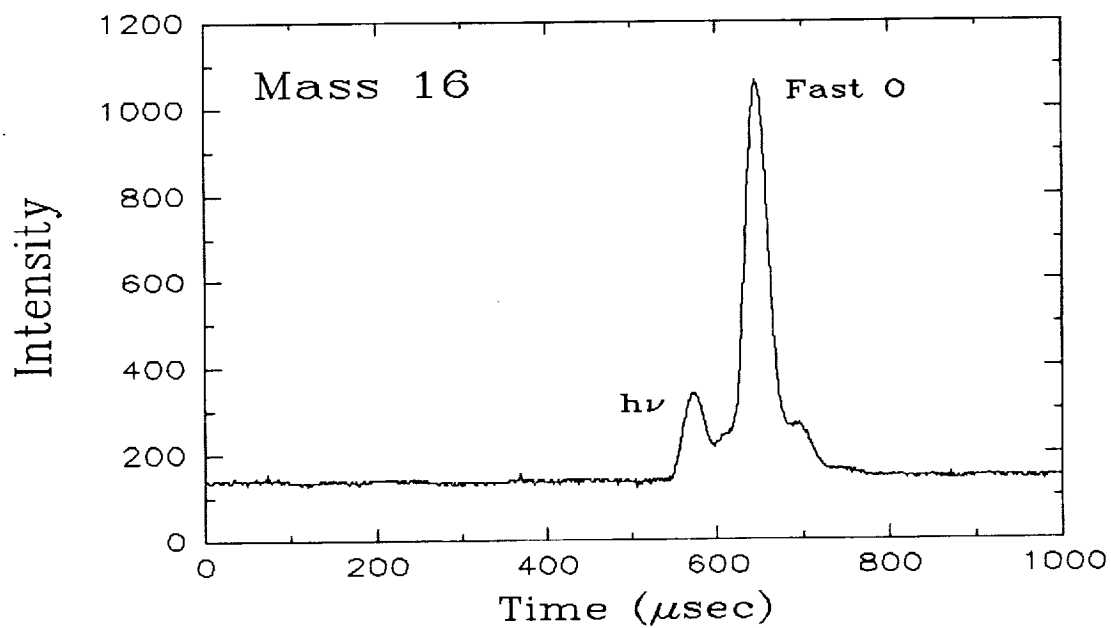


Figure 4



molecules. Characteristics of the energetic oxygen atom source are summarized in Table 1.

Velocity Range	3 to 11 km/sec
Oxygen Atoms	> 80 %
Oxygen Molecules	< 20 %
Total Ions	< 1 %
Impurities (H, N <sub>2</sub> , etc.)	< 1 %

Table 1: Energetic oxygen atom source operating characteristics.

In addition to these thorough facility characterization measurements completed during the last year, work is in progress toward achieving additional goals of the proposed multi-year effort. Preliminary evaluations have been performed using the energetic oxygen atom source for differential scattering cross section measurements and for surface scattering measurements. Work is continuing in both of these areas.

## 2.2 Induced Environment Workshop

A workshop has been sponsored by this grant to provide a forum for presentation and discussion of the latest research in the area of space vehicle induced external environments. A group of nationally recognized experts on space vehicle contamination met January 30-31, 1991 in Huntsville, Alabama. Twenty invited participants each presented a paper in their particular area of expertise. The papers and the discussion which followed was designed to address three questions:

- (1) What is our current state of knowledge of the likely induced external environment for a large space-based platform in low Earth orbit?
- (2) What progress has been made during the last two years in the vehicle contamination knowledge data base and in the predictive capability of induced vehicle contamination for future missions?
- (3) What issues remain unresolved and are the most important to investigate in future studies?

A proceedings of this workshop entitled "*Workshop on the Induced Environment of Space Station Freedom*" is attached to this report as Appendix C. Included in the workshop proceedings is an agenda of the meeting and a list of the attendees. A paper



entitled "Cross Section Work at UAH/MSFC" presented by the Principal Investigator, Dr. Charles E. Keffer, is included in the workshop proceedings.

### 3. Auroral Modeling

Modeling activities of the past year have included a series of parameter sensitivity studies of modeled auroral and dayglow emissions, the integration of auroral and global ionospheric/thermospheric modeling capabilities, and support of a science workshop for discussion of future science needs. Initial sensitivity studies of modeled auroral emissions discussed in the December 1990 progress report (see Appendix B) have been subsequently extended to include modeled dayglow emissions as provided by the Field Line Interhemispheric Plasma (FLIP) model. This concurrent aurora/dayglow sensitivity study represents the type of integrated auroral/global thermospheric studies toward which the modeling program is directed. It is also a measure of our success in meeting one of our stated research goals--the simultaneous modeling of global airglow emissions with auroral emissions.

In addition, a science working group meeting for the Ultraviolet Imager (UVI) was held in August 1990 in Park City, Utah. Attendees met for two days of informal discussion of operational and data analysis issues. Preliminary contacts have been made in support of a second workshop.

#### 3.1 Auroral Modeling

A necessary and important first step in the process of interpreting auroral images is a series of parameter sensitivity studies to determine the dependence of modeled and measured emissions on such variables as atmospheric composition, auroral energy distribution, and level of solar activity. In a previous study [Germany et al., 1990], carried out under contract NAS8-37586, the sensitivity of modeled VUV auroral emissions to likely uncertainties and anticipated changes in the neutral atmosphere was investigated. In particular, it was shown that selected ratios of OI 1356 and LBH emissions could be used to extract the characteristic energy of a modeled aurora. The utility of these intensity ratios, however, is characterized by their sensitivity to changes in the modeled neutral atmosphere, with the LBH ratio being much more stable than the OI ratio. Figure 5 shows both the OI 1356-to-LBH 1838 ratio and the LBH 1838-to-LBH 1464 ratios for ranges of levels of solar activities and for both winter and summer conditions. As can be seen, the LBH ratio shows much less variation than the OI 1356 ratio for the same model conditions. The difference in stability of the two ratios and the utility of the LBH ratio as a determinate of incident characteristic energy was discussed for the first time by Germany





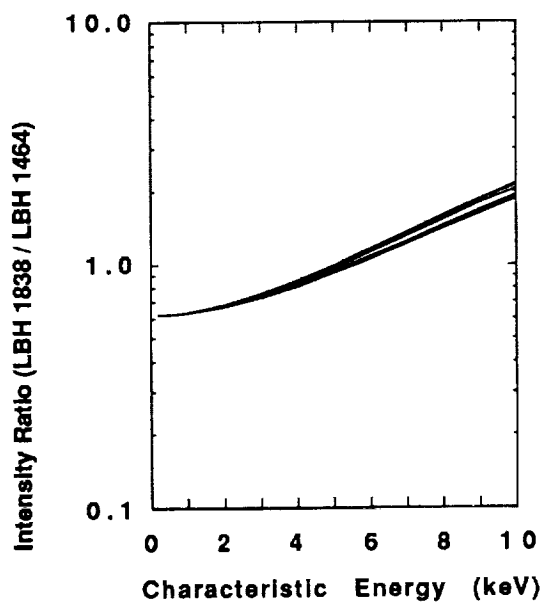
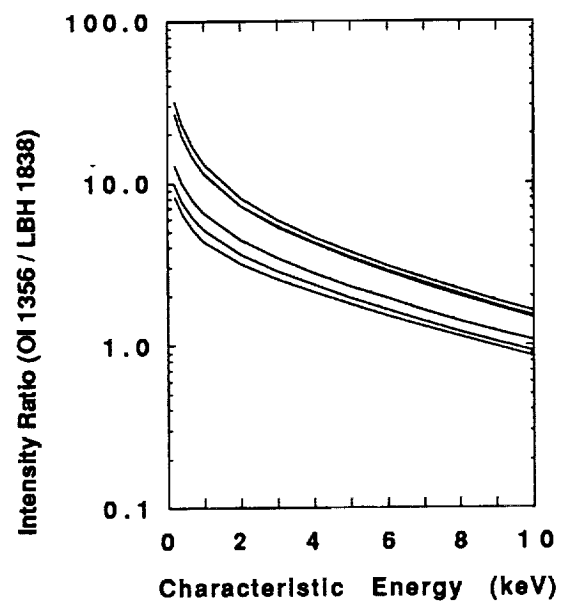


Figure 5



et al., [1990].

This initial investigation has been followed by a study designed to determine the sensitivity of modeled auroral emissions to the choice of electron energy distribution. Four distributions were employed: Maxwellian, Gaussian, and two arbitrary distributions designed to have either a very broad or a very narrow energy range. The behavior of modeled VUV auroral emissions (OI 1356, LBH 1464, LBH 1838) was investigated as a function of the energy distribution of the incident electron flux. For a given average energy, changes from broader to more narrow distributions lead to increased column intensities, provided the wavelength of the modeled emission lies within the O<sub>2</sub> Schumann-Runge absorption band. This is shown in Figure 6 where the ratio of the column integrated auroral emission modeled with a narrow Gaussian distribution to that from a broad Maxwellian is given. This is interpreted as increased O<sub>2</sub> absorption loss from the distribution with the more energetic electrons, in this case, the Maxwellian. Electrons with more energy penetrate to lower altitudes where they encounter greater O<sub>2</sub> densities. Subsequent emissions are then reduced by the local absorption process.

Even without the O<sub>2</sub> loss mechanism, the high altitude dominance of atomic oxygen leads to a dependence on energy distribution due to increased competition with lower altitude species. Despite the (often) large differences in the shape of the incident auroral energy distributions investigated, the magnitude of the differences in subsequent emission intensities is generally less than 25%, provided the average energy and total energy flux are held constant. This implies that the choice of electron distribution used in our models should not be a limitation in the interpretation of auroral images.

Another major goal of the modeling program is the incorporation of the two stream auroral model within the larger and more comprehensive FLIP model. The initial work on this goal was accomplished in the first six months of support and was reported in the December report. With the addition of simultaneous modeling of auroral and dayglow emissions, sensitivity studies of total (aurora + dayglow) emissions are now possible. Since observation of VUV emissions allows imaging of the aurora against a sunlit dayglow background, a study of a typical aurora with concurrent dayglow emissions for local noon on the sunlit Earth is underway.

The dayglow emissions are modeled with the FLIP code, used in conjunction with the two stream auroral model. The relative sensitivity of the dayglow and auroral emissions to changes in the level of solar activity are studied. With increasing levels of solar activity, the total modeled emission (aurora + dayglow) increases significantly. In fact, the total emission is much more dependent on solar activity than are the individual auroral emissions alone. Figure 7 shows column integrated emissions for OI



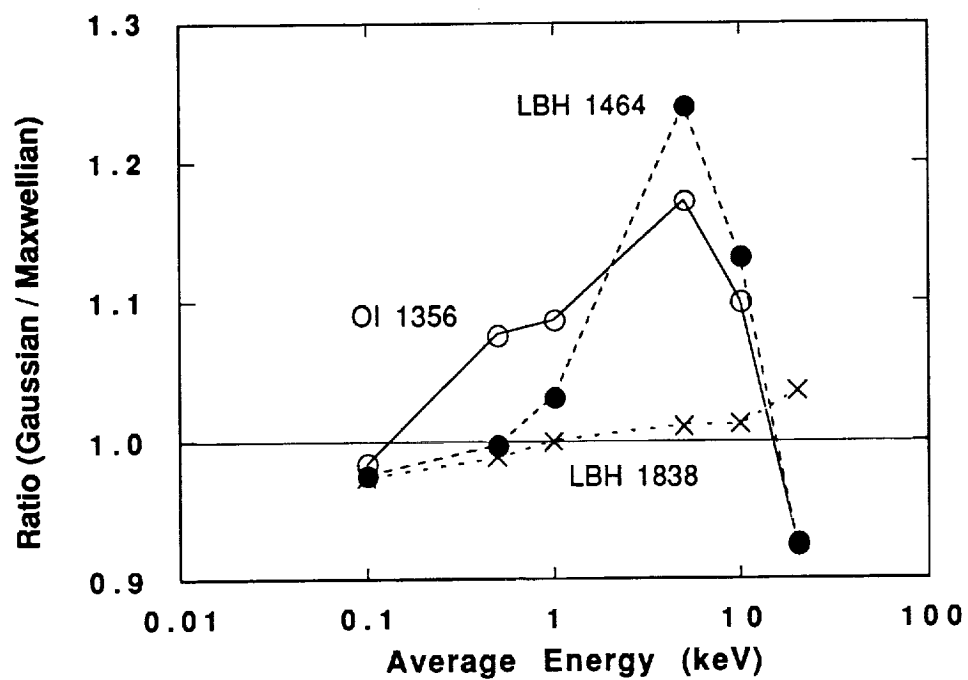


Figure 6



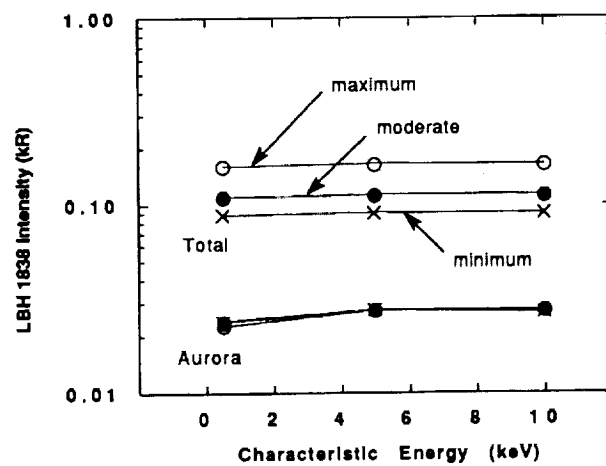
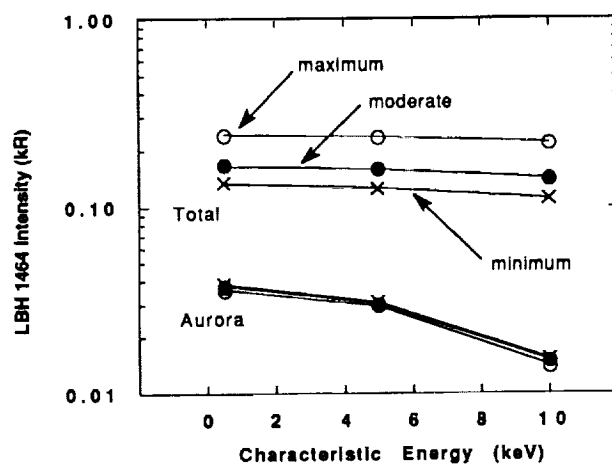
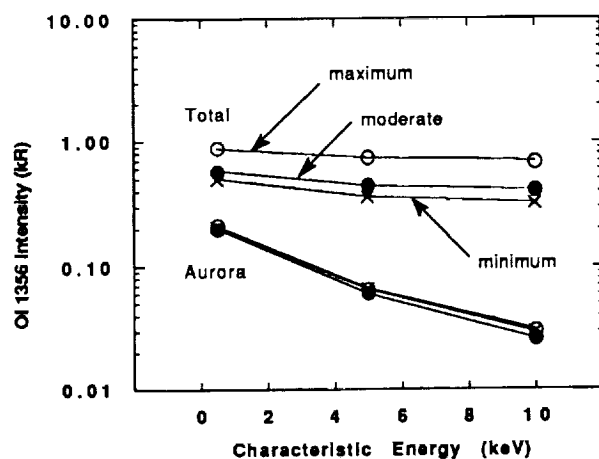


Figure 7





1356, LBH 1464, and LBH 1838 as a function of incident characteristic energy and as a function of solar cyclic variations. The variation of the total (dayglow + aurora) emission with solar activity is noted. The matching variations of the individual auroral emissions are virtually indistinguishable. The auroral emissions thus represent a smaller fraction of the total emission for solar maximum conditions than for solar minimum conditions. In addition, the dayglow will, of course, be independent of the auroral characteristic energies. Therefore the shorter wavelength auroral emissions will represent a decreasing contribution to the total with increasing characteristic energy. For example, the OI 1356 emission contributes about 42% of the total column brightness for low energy (1 keV) electrons. For 10 keV electrons, however, this contribution drops to less than 10% of the total column brightness.

The study of the combined auroral emissions is being extended to include investigation of the relative emission intensities as a function of the incident energy flux and of solar zenith angle. The results of both this study and the energy distribution study discussed above will be submitted for publication in the immediate future.

### 3.2 UVI Workshops

The original modeling task included support for a UVI science working group meeting in the second and third years of support. It readily became apparent, however, that there were several issues that needed immediate discussion by the group. Therefore, the first Ultraviolet Imager (UVI) workshop was held on 15 & 16 August 1990 in Park City, Utah. The attendees included prominent scientists in the fields of ionospheric and magnetospheric physics and chemistry and are listed in Table 2 along with the meeting's agenda. A major focus of the workshop was the mission science planning and the specific science requirements of each participant for the UVI instrument. The workshop was deliberately informal, with each participant giving presentations about science planning and analysis topics of particular interest to them. Copies of all presentations were collected and distributed to each attendee for reference. A copy of these presentations is attached to this report as Appendix D.

The planning and coordination of the meeting was the responsibility of Dr. Germany. His responsibilities included arrangement of meeting facilities, communication with the science team members, and preparation of post workshop mailings in addition to his participation in the workshop discussions presentations.

The first meeting was considered a success by all and, pending second year support, initial contacts have been made in support of a second UVI workshop. Initial responses are favorable and indicate that attendance at a second workshop held in August of

1. The first part of the document is a letter from the President of the United States to the Congress, dated January 3, 1862. It is a very important document, as it contains the President's annual message to Congress, which is a key document in the history of the United States.

2. The second part of the document is a letter from the Secretary of the Treasury to the President, dated January 3, 1862. It is a very important document, as it contains the Secretary's report to the President on the state of the Treasury, which is a key document in the history of the United States.

3. The third part of the document is a letter from the Secretary of the Navy to the President, dated January 3, 1862. It is a very important document, as it contains the Secretary's report to the President on the state of the Navy, which is a key document in the history of the United States.

4. The fourth part of the document is a letter from the Secretary of the War to the President, dated January 3, 1862. It is a very important document, as it contains the Secretary's report to the President on the state of the War, which is a key document in the history of the United States.

5. The fifth part of the document is a letter from the Secretary of the Interior to the President, dated January 3, 1862. It is a very important document, as it contains the Secretary's report to the President on the state of the Interior, which is a key document in the history of the United States.

6. The sixth part of the document is a letter from the Secretary of the Agriculture to the President, dated January 3, 1862. It is a very important document, as it contains the Secretary's report to the President on the state of the Agriculture, which is a key document in the history of the United States.

7. The seventh part of the document is a letter from the Secretary of the Education to the President, dated January 3, 1862. It is a very important document, as it contains the Secretary's report to the President on the state of the Education, which is a key document in the history of the United States.

8. The eighth part of the document is a letter from the Secretary of the Commerce to the President, dated January 3, 1862. It is a very important document, as it contains the Secretary's report to the President on the state of the Commerce, which is a key document in the history of the United States.

9. The ninth part of the document is a letter from the Secretary of the Marine to the President, dated January 3, 1862. It is a very important document, as it contains the Secretary's report to the President on the state of the Marine, which is a key document in the history of the United States.

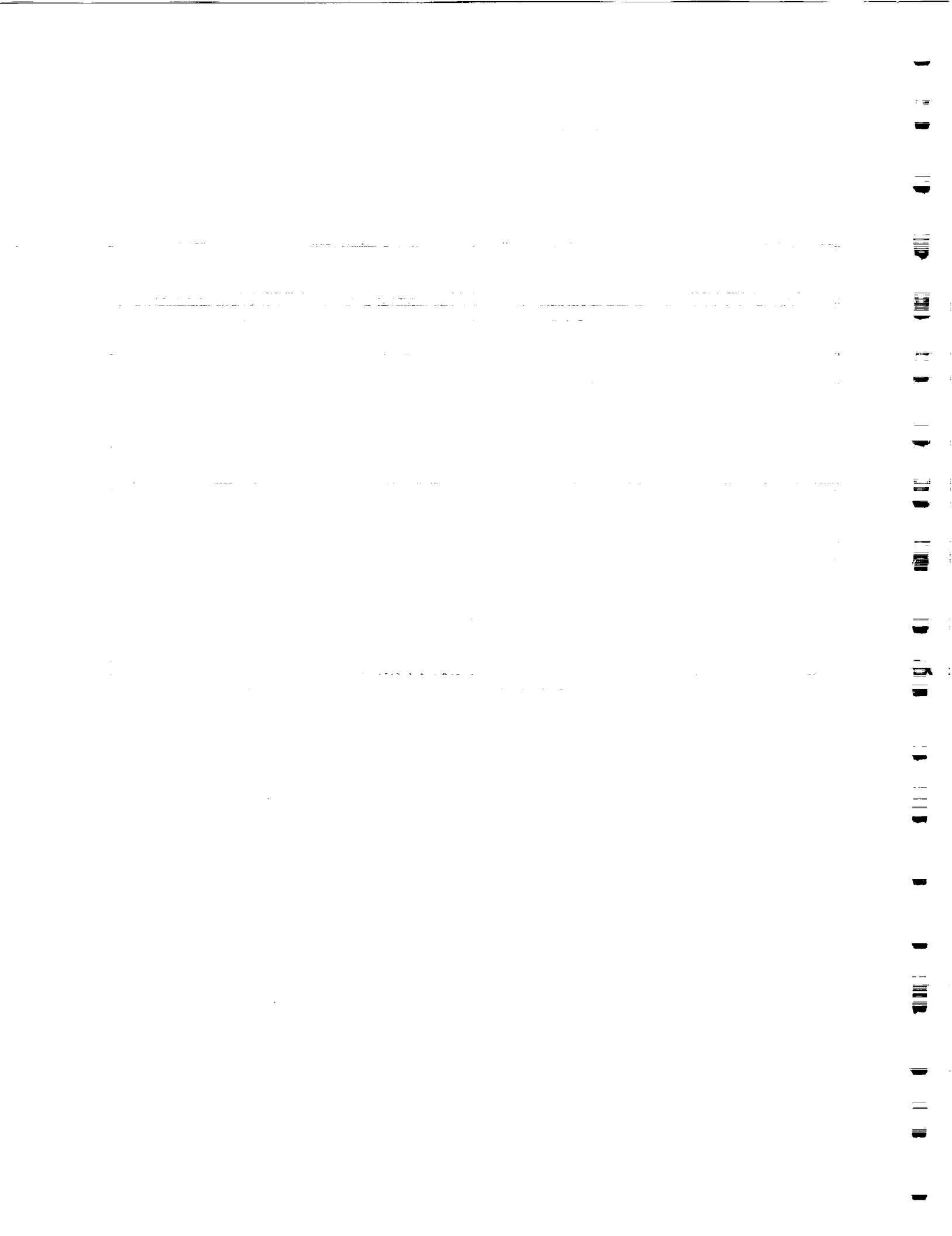
10. The tenth part of the document is a letter from the Secretary of the Air to the President, dated January 3, 1862. It is a very important document, as it contains the Secretary's report to the President on the state of the Air, which is a key document in the history of the United States.

11. The eleventh part of the document is a letter from the Secretary of the Space to the President, dated January 3, 1862. It is a very important document, as it contains the Secretary's report to the President on the state of the Space, which is a key document in the history of the United States.

this year would exceed that at the first meeting.

<b>Agenda</b>	
August 15, 1990	August 16, 1990
Introduction	Discussion of Analysis Tools
Instrument Observing Sequences	Discussion of Signal Extraction
Review of Science Objectives	Revised Data Analysis Plan
	Summary
<b>Attendees</b>	
Dr. Joe Ajello	Jet Propulsion Laboratory
Dr. Ken Clark	University of Washington
Dr. Bob Clauer	University of Michigan
Dr. Glynn Germany	University of Alabama in Huntsville
Dr. George Parks	University of Washington
Dr. Jim Spann	NASA/MSFC
Dr. Doug Torr	University of Alabama in Huntsville
Dr. Marsha Torr	NASA/MSFC

Table 2. Attendees and agenda of the UVI workshop



#### 4. REFERENCES

Germany, G. A., M. R. Torr, P. G. Richards, and D. G. Torr, The dependence of modeled OI 1356 and N2 Lyman Birge Hopfield auroral emissions on the neutral atmosphere, J. Geophys. Res., 95, 7725, 1990.



5. **APPENDIX A**

"Laboratory Facility for Simulation of  
Vehicle-Environment Interactions"

Presented by Dr. Charles E. Keffer

at

Vehicle-Environment Interactions Conference  
Applied Physics Laboratory  
Laurel, Maryland  
March 11-13, 1991





## **Laboratory Facility for Simulation of Vehicle-Environment Interactions**

Charles E. Keffer  
University of Alabama in Huntsville  
Physics Department  
Huntsville, AL 35899

Marsha R. Torr  
NASA Marshall Space Flight Center  
Space Science Laboratory  
Huntsville, AL 35812

### **ABSTRACT**

A facility for simulation and study of interactions between a spacecraft in low Earth orbit (LEO) and its ambient environment is described. The facility is composed of a crossed beam apparatus with a rotatable mass spectrometer detector. It can be used for a wide variety of vehicle interaction studies including both gas phase and gas-surface interactions. Measurements of differential scattering cross sections, surface scattering phenomena, and spacecraft glow are representative examples. A key element in the facility is a laser-induced discharge energetic oxygen atom source for simulation of the ambient vehicle environment. Measurements of important characteristics of the oxygen atom source, including velocity and beam composition, are presented. Performance of differential scattering cross section measurements is evaluated using low angle scattering from thermal energy collisions between beams of oxygen and nitrogen molecules.

### **INTRODUCTION**

Spacecraft in low Earth orbit (200-700 km) are exposed to an intense flux of atomic and molecular species from the atmosphere. At these altitudes the major constituent of the atmosphere is atomic oxygen which is created by solar UV photodissociation of molecular oxygen. Typical orbital velocities of 8 km/sec produce an atomic oxygen kinetic energy relative to the spacecraft of nominally 5 eV. The density of atomic oxygen varies with the amount of solar activity, but an average value for 250 km is about  $10^9$  atoms/cm<sup>3</sup>. The flux of atomic oxygen impinging on spacecraft surfaces under these conditions is thus approximately  $10^{15}$  atoms/cm<sup>2</sup>/sec. This environment is known to cause a variety of phenomena including severe surface erosion of polymers and some metals as well as induced optical emissions in the ultraviolet, visible, and infrared portions of the electromagnetic spectrum [Bareiss et al., 1987].

Since the discovery of these effects several years ago,



a significant effort has been made to study them. A combination of spacecraft glow data (see, e.g., Torr et al., 1977; Banks et al., 1983; Mende et al., 1988) and several recent laboratory investigations (Arnold and Coleman, 1988; Caledonia et al., 1990; Holtzclaw et al., 1990; Orient et al., 1990) has led to the development of a preliminary data base for the spacecraft glow phenomena. However, very little is yet known about such fundamental atomic and molecular parameters as scattering, excitation, or ionization cross sections for 5 eV oxygen colliding with other species. Mechanisms for the spacecraft glow phenomena and the surface chemistry processes (Kofsky and Barrett 1986) are just beginning to be understood with much still remaining to be learned.

An improved understanding of these atomic oxygen effects on orbiting spacecraft is important to the success of Space Station Freedom and to future Space Shuttle missions with payloads which are sensitive to the induced environment around the vehicle. Atomic oxygen also plays a fundamental role in the chemistry of the upper atmosphere and in high temperature combustion reactions.

#### **FACILITY DESCRIPTION**

Figure 1 shows a schematic diagram of the facility. The basic design consists of two orthogonal fixed beam sources and an in-plane quadrupole mass spectrometer detector which is rotatable around the collision region of the two gas beams [Lee et al., 1969]. The beam sources are pulsed to minimize pumping requirements and to optimize the energetic oxygen atom source in one of the beams. The configuration shown illustrates the setup for making differential scattering cross section measurements. For surface scattering measurements only one beam valve is used and the surface material is placed at the center of rotation of the mass spectrometer detector.

#### **Vacuum System**

The cylindrical vacuum chamber is fabricated from 304L stainless steel with an inside diameter of 47" and height of 25.5" (see Figure 2). The walls are made thick to limit distortion and misalignment due to atmospheric pressure. The lid, which is removable to allow access to the interior of the chamber, is 1.5" thick, the bottom is 1" thick and the cylinder wall is 0.5" thick. The main chamber is pumped by a 3000 l/sec cryopump which removes essentially all of the gas from each pulse prior to the arrival of the next pulse at the usual 0.5 Hz repetition rate of the valves.

The pulsed valves are in differentially pumped chambers each evacuated by a 1000 l/sec turbomolecular pump. A 1 mm diameter beam skimmer separates each pulsed valve chamber from

1. The first part of the document is a letter from the President of the United States to the Congress, dated January 3, 1862. It is a very important document, as it contains the President's annual message to Congress, which is a key document in the history of the United States.

2. The second part of the document is a report from the Secretary of the Interior, dated January 3, 1862. It is a very important document, as it contains the Secretary's annual report to the President, which is a key document in the history of the United States.

3. The third part of the document is a report from the Secretary of the Treasury, dated January 3, 1862. It is a very important document, as it contains the Secretary's annual report to the President, which is a key document in the history of the United States.

4. The fourth part of the document is a report from the Secretary of the War, dated January 3, 1862. It is a very important document, as it contains the Secretary's annual report to the President, which is a key document in the history of the United States.

5. The fifth part of the document is a report from the Secretary of the Navy, dated January 3, 1862. It is a very important document, as it contains the Secretary's annual report to the President, which is a key document in the history of the United States.

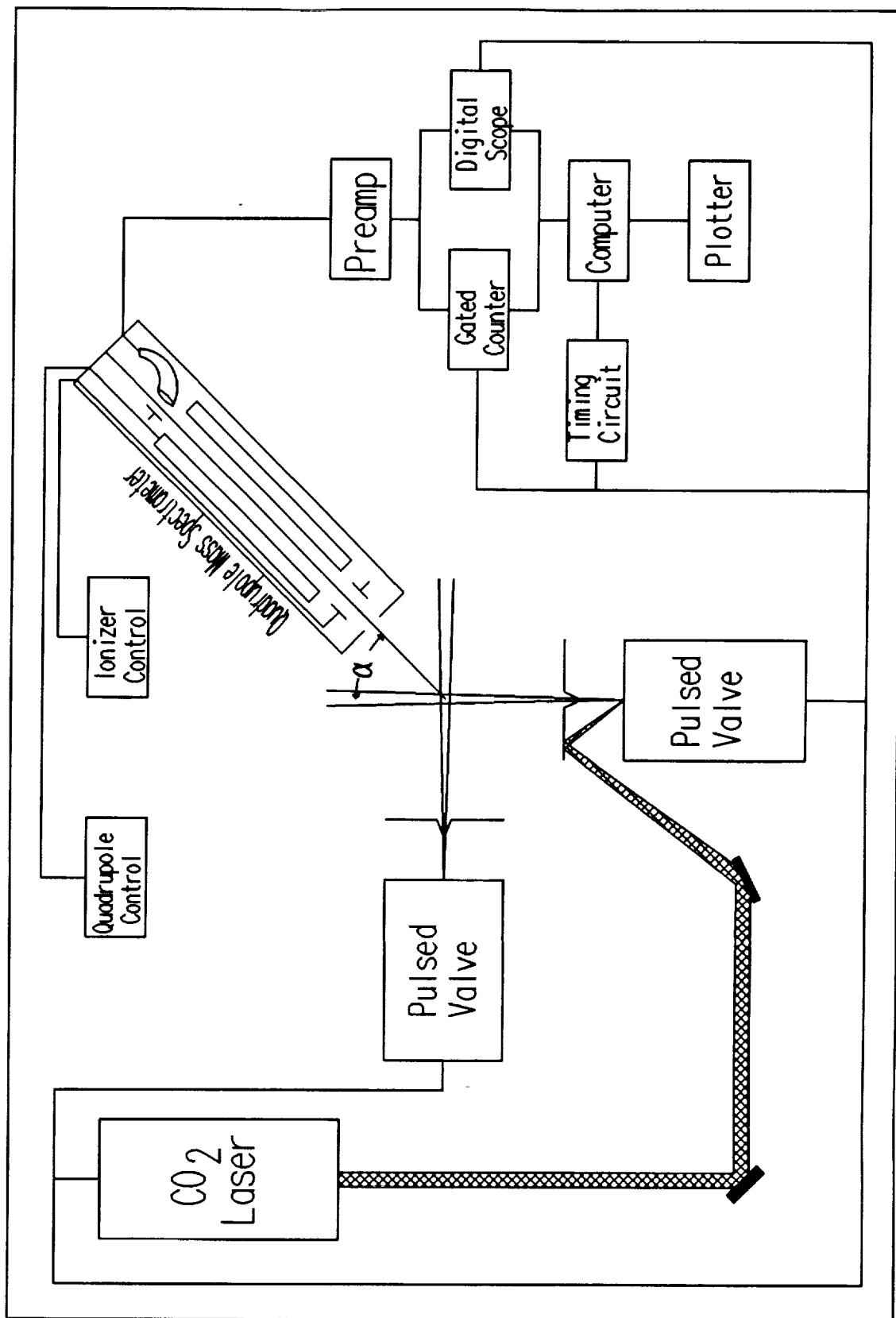
6. The sixth part of the document is a report from the Secretary of the State, dated January 3, 1862. It is a very important document, as it contains the Secretary's annual report to the President, which is a key document in the history of the United States.

7. The seventh part of the document is a report from the Secretary of the War, dated January 3, 1862. It is a very important document, as it contains the Secretary's annual report to the President, which is a key document in the history of the United States.

8. The eighth part of the document is a report from the Secretary of the Navy, dated January 3, 1862. It is a very important document, as it contains the Secretary's annual report to the President, which is a key document in the history of the United States.

9. The ninth part of the document is a report from the Secretary of the State, dated January 3, 1862. It is a very important document, as it contains the Secretary's annual report to the President, which is a key document in the history of the United States.

10. The tenth part of the document is a report from the Secretary of the War, dated January 3, 1862. It is a very important document, as it contains the Secretary's annual report to the President, which is a key document in the history of the United States.



**Figure 1.** Schematic diagram of cross section facility.

[illegible][illegible]

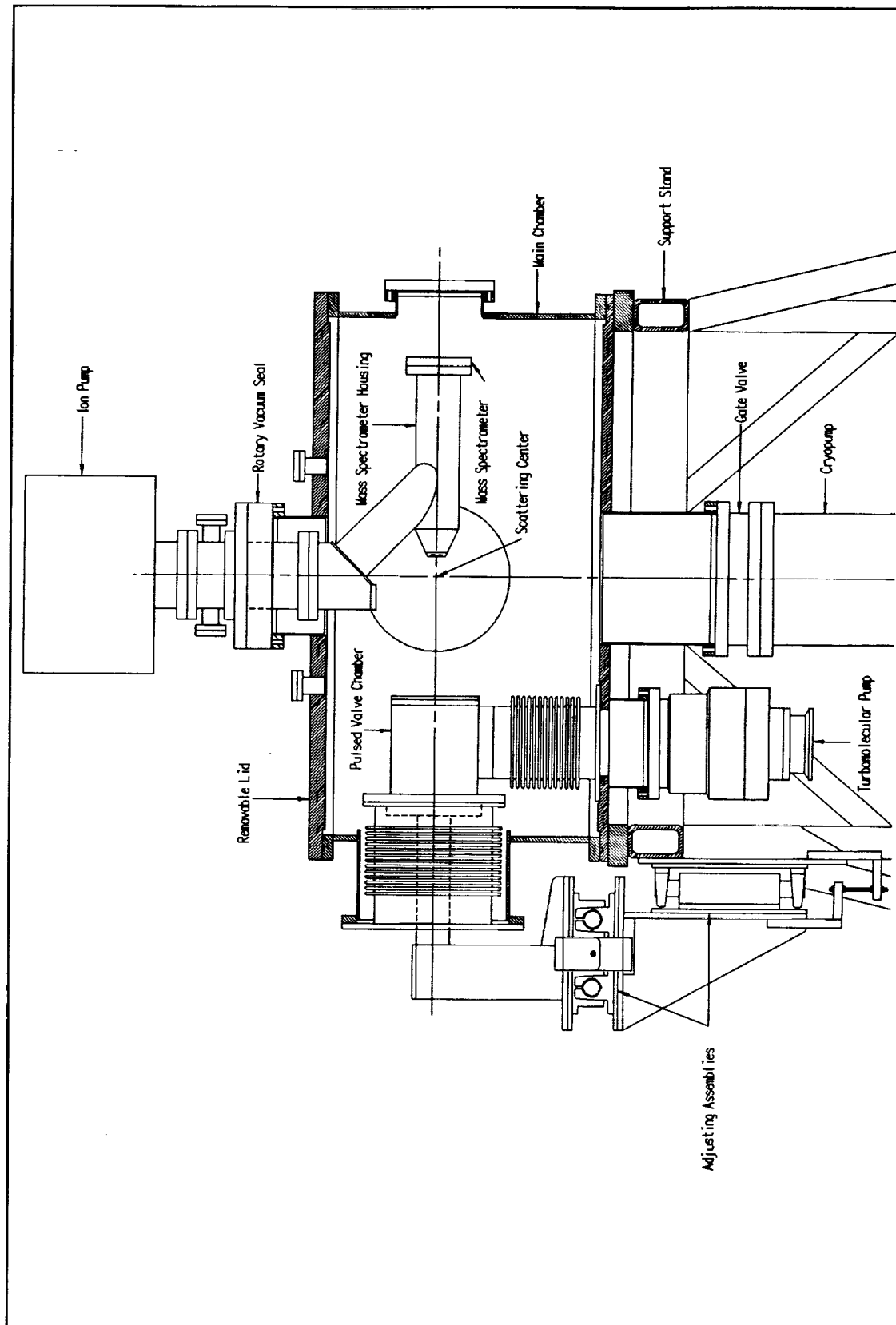


Figure 2. Sectional view of vacuum chamber.





the main chamber and collimates the gas beam. Flexible bellows in the pulsed valve chambers, together with horizontal and vertical adjusting assemblies, allow the gas beams to be aligned so as to collide at the center of rotation of the mass spectrometer detector. Precision bearings and shafts in the adjusting assemblies allow an alignment accuracy of  $\pm .005''$ . Pressure in the pulsed valve chambers is kept below  $10^{-4}$  Torr during operation to limit loss in beam intensity due to scattering.

The mass spectrometer is mounted inside of a housing which is differentially pumped by a 230 l/sec ion pump. Interchangeable apertures on the front of the housing and the entrance to the mass spectrometer ionizer limit the acceptance angle of the mass spectrometer to the region of overlap of the two gas beams. The mass spectrometer housing is suspended from a rotary vacuum seal which is differentially pumped by a small mechanical pump and a small ion pump. This arrangement allows the mass spectrometer to be rotated about the scattering center through approximately 200 degrees without significantly effecting the pressure in the main chamber or in the mass spectrometer housing. Base pressure in the mass spectrometer housing is  $10^{-9}$  Torr. No measurable effect on the pressure in the mass spectrometer occurs from operation of the pulsed valves.

#### **Atomic Oxygen Source**

Atomic oxygen is formed in one of the beam sources by pulsed laser-induced breakdown of pure molecular oxygen in the manner developed and described by Caledonia et al., 1987. A sectional view of the atomic oxygen source is shown in Figure 3. A pulsed valve in the center of the figure introduces a short pulse of molecular oxygen into a conical expansion nozzle. An approximately 8 J  $\text{CO}_2$  laser beam passes through a 1 meter focal length  $\text{BaF}_2$  lens shown at the lower left of the figure. The  $\text{CO}_2$  laser beam then passes through an AR coated ZnSe window which separates the vacuum in the pulsed valve chamber from atmospheric pressure. The beam is focussed to about  $1 \text{ cm}^2$  on a gold coated nickel copper mirror. A smaller spot size results in an energy density on the mirror which can cause significant damage to the mirror coating. The 50 cm radius of curvature of the gold coated mirror focusses the  $\text{CO}_2$  laser beam to about  $1 \text{ mm}^2$  near the orifice of the valve. A direct hit on the valve orifice is avoided since this damages the o-ring tip which seals the valve closed between pulses. The energy density in the focussed laser beam is sufficient to dissociate the molecular oxygen creating a high temperature plasma near the throat of the nozzle. The hot plasma accelerates down the expansion nozzle as a blast wave dissociating and accelerating most of the remaining molecular oxygen. Fast oxygen atoms exiting the nozzle are collimated by a 1 mm diameter skimmer as they enter the main vacuum chamber. Residual gas deflected by the skimmer is removed

1. The first part of the document is a letter from the President of the United States to the Congress, dated January 3, 1862. It is a very important document, as it contains the President's annual message to Congress, which is a key part of the executive branch's communication with the legislative branch.

2. The second part of the document is a report from the Secretary of the Interior, dated January 10, 1862. It contains information about the state of the Department of the Interior, including the status of the various bureaus and the progress of the work.

3. The third part of the document is a report from the Secretary of the Treasury, dated January 10, 1862. It contains information about the state of the Department of the Treasury, including the status of the various bureaus and the progress of the work.

4. The fourth part of the document is a report from the Secretary of the War, dated January 10, 1862. It contains information about the state of the Department of the War, including the status of the various bureaus and the progress of the work.

5. The fifth part of the document is a report from the Secretary of the Navy, dated January 10, 1862. It contains information about the state of the Department of the Navy, including the status of the various bureaus and the progress of the work.

6. The sixth part of the document is a report from the Secretary of the Army, dated January 10, 1862. It contains information about the state of the Department of the Army, including the status of the various bureaus and the progress of the work.

7. The seventh part of the document is a report from the Secretary of the Post Office, dated January 10, 1862. It contains information about the state of the Department of the Post Office, including the status of the various bureaus and the progress of the work.

8. The eighth part of the document is a report from the Secretary of the Land Office, dated January 10, 1862. It contains information about the state of the Department of the Land Office, including the status of the various bureaus and the progress of the work.

9. The ninth part of the document is a report from the Secretary of the Indian Affairs, dated January 10, 1862. It contains information about the state of the Department of the Indian Affairs, including the status of the various bureaus and the progress of the work.

10. The tenth part of the document is a report from the Secretary of the Marine Corps, dated January 10, 1862. It contains information about the state of the Department of the Marine Corps, including the status of the various bureaus and the progress of the work.

11. The eleventh part of the document is a report from the Secretary of the Cavalry, dated January 10, 1862. It contains information about the state of the Department of the Cavalry, including the status of the various bureaus and the progress of the work.

12. The twelfth part of the document is a report from the Secretary of the Artillery, dated January 10, 1862. It contains information about the state of the Department of the Artillery, including the status of the various bureaus and the progress of the work.

13. The thirteenth part of the document is a report from the Secretary of the Engineers, dated January 10, 1862. It contains information about the state of the Department of the Engineers, including the status of the various bureaus and the progress of the work.

14. The fourteenth part of the document is a report from the Secretary of the Ordnance, dated January 10, 1862. It contains information about the state of the Department of the Ordnance, including the status of the various bureaus and the progress of the work.

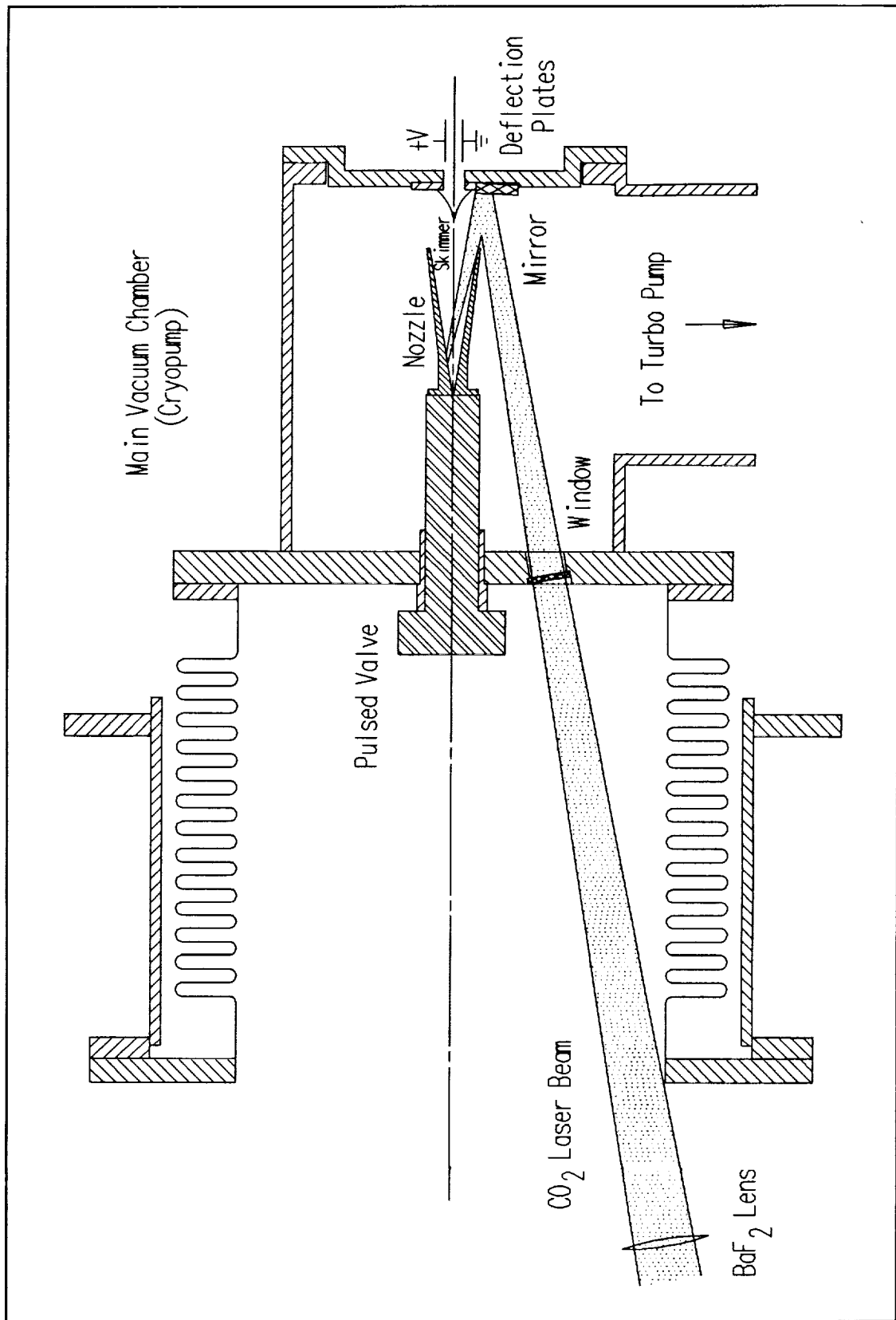


Figure 3. O atom source sectional view.



from the pulsed valve chamber by the turbomolecular pump. A small fraction of the fast gas pulse is composed of ions. These are readily removed from the pulse by deflection plates in the main vacuum chamber. These deflection plates are spaced 1 cm apart and biased with a few hundred volts potential difference.

## FACILITY PERFORMANCE

### Differential Scattering

Classical scattering theory predicts that an intermolecular potential of the form

$$V(r) \propto -1/r^6 \quad (1),$$

where  $r$  is the intermolecular distance, should have a low-angle differential scattering cross section equal to

$$I(\theta) \propto \theta^{-7/3} \quad (2),$$

where  $\theta$  is the center-of-mass scattering angle (Bernstein, 1964). This functional form of the potential is typical of the long range attractive van der Waals forces between atoms and molecules. Experimental results presented as log-log plots of differential scattering cross section vs center-of-mass angle have confirmed this predicted behavior in the range of center-of-mass angles from roughly 1 to 10 degrees for a large number of collision partners (Bernstein, 1964). We have used this simple relationship to validate the capability of our facility for making differential scattering cross section measurements without serious systematic errors. Collisions between beams of thermal energy oxygen and nitrogen molecules have been used as a test system. Several sets of data were taken for center-of-mass angles less than 10 degrees. A least squares fit to the log of the scattered intensity vs the log of the center-of-mass angle resulted in an experimental value for the exponent of  $-2.37 \pm .14$ . This is within one standard deviation of the theoretical value and so indicates satisfactory agreement.

### Atomic Oxygen Source

Measurements have been made on the atomic oxygen source to determine the velocity of the atom beam. Figure 4 indicates the type of measurements which have been made. The figure shows two peaks. The first one is due to photons from the oxygen plasma discharge which strike the Channeltron detector of the mass spectrometer while the second peak is due to fast oxygen atoms. The photon peak serves as a time marker since the arrival of the photons at the detector is essentially coincident in time with the formation of the fast atoms. So, the time between the two peaks represents the time

1. The first part of the document is a list of the names of the persons who have been appointed to the various offices of the city.

2. The second part of the document is a list of the names of the persons who have been appointed to the various offices of the city.

3. The third part of the document is a list of the names of the persons who have been appointed to the various offices of the city.

4. The fourth part of the document is a list of the names of the persons who have been appointed to the various offices of the city.

5. The fifth part of the document is a list of the names of the persons who have been appointed to the various offices of the city.

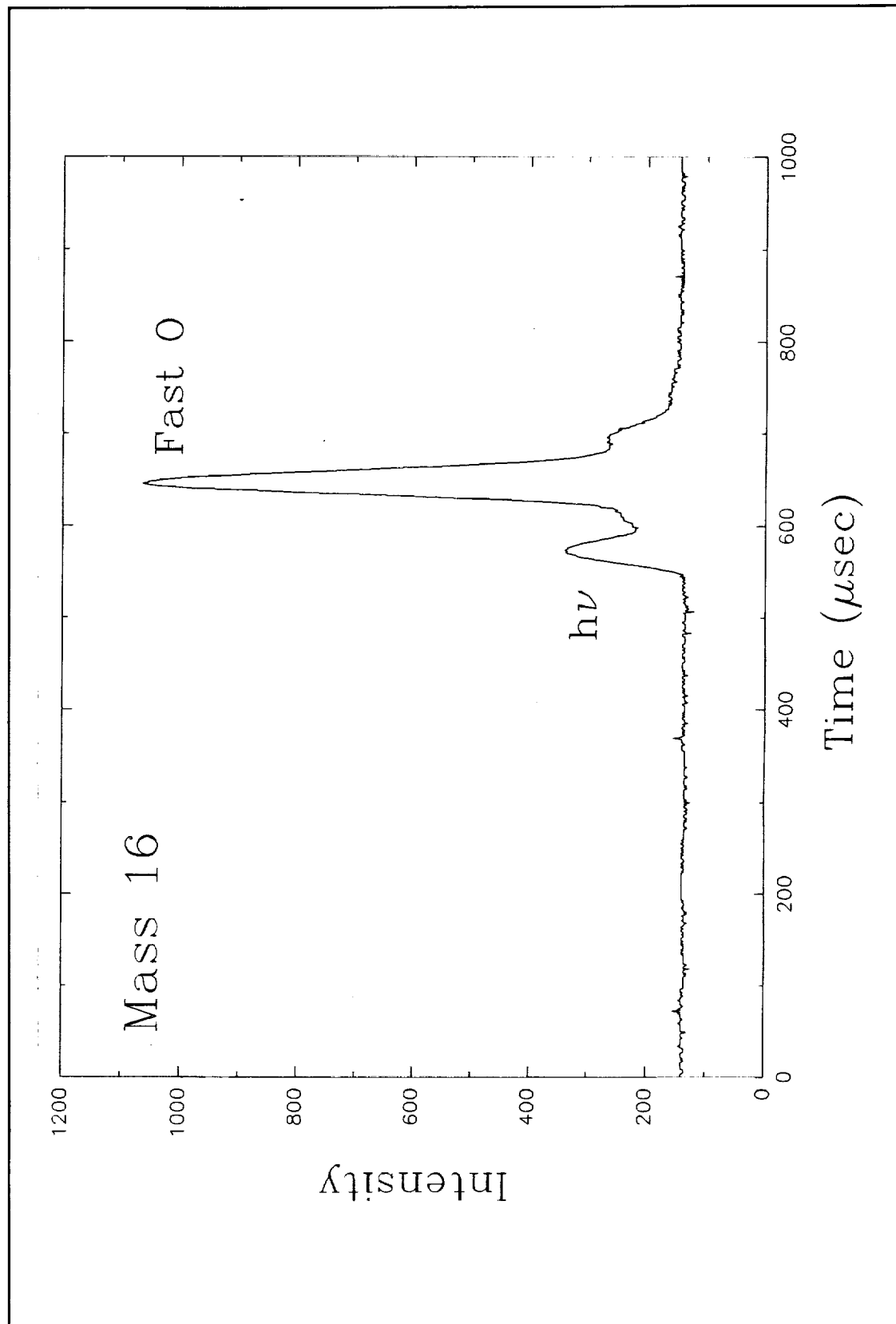
6. The sixth part of the document is a list of the names of the persons who have been appointed to the various offices of the city.

7. The seventh part of the document is a list of the names of the persons who have been appointed to the various offices of the city.

8. The eighth part of the document is a list of the names of the persons who have been appointed to the various offices of the city.

9. The ninth part of the document is a list of the names of the persons who have been appointed to the various offices of the city.

10. The tenth part of the document is a list of the names of the persons who have been appointed to the various offices of the city.



**Figure 4.** Oxygen atom velocity measurement.





of flight for the oxygen atoms. The velocity is thus calculated from the time of flight and known distance from the valve to mass spectrometer. The average velocity is 6.8 km/sec for the oxygen atom pulse shown in Figure 4. The velocity of the oxygen atoms can be varied by changing the laser intensity or the amount of gas per pulse. A velocity range of 3 to 11 km/sec has been measured for this source.

The fast atom beam composition has also been measured to determine the ratio of oxygen atoms to oxygen molecules and to identify the presence of any impurities in the beam. Mass spectrometer measurements of the beam have been made with a range of 80 % to 95 % atoms in the beam. There are no metal surfaces in the direct line-of-sight for the oxygen atoms as they enter the mass spectrometer ionizer. However, some recombination of atoms may occur in the mass spectrometer during the duration of the fast pulse resulting in a loss of atoms in the beam. The mass spectrometer measurements are thus a lower limit on the percentage of atoms in the beam. So, the fast atom beam is conservatively estimated to be > 80 % atomic oxygen and < 20% molecular oxygen. Some oxygen ions are also present at less than 1 % of the beam. These ions are readily removed from the beam by the deflection plates described above. Impurities at other masses also represent less than 1 % of the beam.

#### **ACKNOWLEDGEMENTS**

This work was supported by NASA Marshall Space Flight Center under Grant No. NAG8-834 to The University of Alabama in Huntsville.



## REFERENCES

- Arnold, G. S., and D. J. Coleman, Surface Mediated Radical Recombination Luminescence:  $O + NO + Ni$ , J. Chem. Phys., **88**, 7147-7156, 1988.
- Banks, P. M., P. R. Williamson, W. J. Raitt, Space Shuttle Glow Observations, Geophys. Res. Lett., **10**, 118-121, 1983.
- Bareiss, L. E., R. M. Payton, and H. A. Papazian, Shuttle/Spacelab Contamination Environment and Effects Handbook, NASA Contractor Report 4053, George C. Marshall Space Flight Center, Huntsville, AL, 1987.
- Bernstein, R. B., Molecular Beam Scattering at Thermal Energies, Science, **144**, 141-150, 1964.
- Caledonia, G. E., R. H. Krech, and B. D. Green, A High Flux Source of Energetic Oxygen Atoms for Material Degradation Studies, AIAA J., **25**, 59-63, 1987.
- Caledonia, G. E., K. W. Holtzclaw, B. D. Green, R. H. Krech, A. Leone, and G. R. Swenson, Laboratory Investigation of Shuttle Glow Mechanisms, Geophys. Res. Lett., **17**, 1881-1884, 1990.
- Holtzclaw, K. W., M. E. Fraser, and A. Gelb, Infrared Emission from the Reaction of High-Velocity Atomic Oxygen with Graphite and Polyethylene, J. Geophys. Res., **95**, 4147-4153, 1990.
- Kofsky, I. L., and J. L. Barrett, Spacecraft Glows from Surface-Catalyzed Reactions, Planet. Space Sci., **34**, 665-681, 1986.
- Lee, Y. T., J. D. McDonald, P. R. LeBreton, and D. R. Herschbach, Molecular Beam Reactive Scattering Apparatus with Electron Bombardment Detector, Rev. Sci. Instrum., **40**, 1402-1408, 1969.
- Mende, S. B., G. R. Swenson, and E. J. Llewellyn, Adv. Space Res., **8**, 229, 1988.
- Orient, O. J., A. Chutjian, and E. Murad, Recombination Reactions of 5-eV  $O(^3P)$  Atoms on a  $MgF_2$  Surface, Phys. Rev. A, **41**, 4106-4108, 1990.
- Torr, M. R., P. B. Hays, B. C. Kennedy, and J. C. G. Walker, Intercalibration of Airglow Observatories with the Atmosphere Explorer Satellite, Planet. Space Sci., **25**, 173-184, 1977.

1. The first part of the document is a letter from the President of the United States to the Congress, dated January 3, 1862. It is a very important document, as it contains the President's annual message to Congress. The letter is written in a formal, dignified style, and it is one of the most important documents in the history of the United States.

2. The second part of the document is a report from the Secretary of the Interior, dated January 3, 1862. It is a very important document, as it contains the Secretary's annual report to the President. The report is written in a formal, dignified style, and it is one of the most important documents in the history of the United States.

3. The third part of the document is a report from the Secretary of the Treasury, dated January 3, 1862. It is a very important document, as it contains the Secretary's annual report to the President. The report is written in a formal, dignified style, and it is one of the most important documents in the history of the United States.

4. The fourth part of the document is a report from the Secretary of the War, dated January 3, 1862. It is a very important document, as it contains the Secretary's annual report to the President. The report is written in a formal, dignified style, and it is one of the most important documents in the history of the United States.

5. The fifth part of the document is a report from the Secretary of the Navy, dated January 3, 1862. It is a very important document, as it contains the Secretary's annual report to the President. The report is written in a formal, dignified style, and it is one of the most important documents in the history of the United States.

6. The sixth part of the document is a report from the Secretary of the Army, dated January 3, 1862. It is a very important document, as it contains the Secretary's annual report to the President. The report is written in a formal, dignified style, and it is one of the most important documents in the history of the United States.

7. The seventh part of the document is a report from the Secretary of the Marine Corps, dated January 3, 1862. It is a very important document, as it contains the Secretary's annual report to the President. The report is written in a formal, dignified style, and it is one of the most important documents in the history of the United States.

8. The eighth part of the document is a report from the Secretary of the Coast and Geodetic Survey, dated January 3, 1862. It is a very important document, as it contains the Secretary's annual report to the President. The report is written in a formal, dignified style, and it is one of the most important documents in the history of the United States.

9. The ninth part of the document is a report from the Secretary of the Smithsonian Institution, dated January 3, 1862. It is a very important document, as it contains the Secretary's annual report to the President. The report is written in a formal, dignified style, and it is one of the most important documents in the history of the United States.

10. The tenth part of the document is a report from the Secretary of the Department of the Interior, dated January 3, 1862. It is a very important document, as it contains the Secretary's annual report to the President. The report is written in a formal, dignified style, and it is one of the most important documents in the history of the United States.

6. **APPENDIX B**

Semiannual Status Report for Grant NAG8-834  
December 24, 1990



The University of Alabama in Huntsville

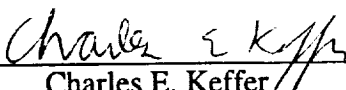
Semiannual Status Report for Grant NAG8-834  
Due Date: December 24, 1990

"Theoretical and Experimental Studies Relevant to  
Interpretation of Auroral Emissions"

Submitted to

George C. Marshall Space Flight Center  
Space Science Laboratory  
National Aeronautics and Space Administration  
Marshall Space Flight Center, AL 35812

by

  
Charles E. Keffer  
Principal Investigator  
The University of Alabama in Huntsville  
Physics Department  
Huntsville, AL 35899





# **Theoretical and Experimental Studies Relevant to Interpretation of Auroral Emissions**

## **1. Introduction**

Work under this contract is divided into two tasks. Task one is a laboratory study designed to improve our understanding of the space vehicle induced external environment and its effect on measurement of auroral emissions from space-based platforms. Task two is a modeling program to develop the capability of using auroral images at various wavelengths to infer the total energy influx and characteristic energy of the incident auroral particles. Together they provide a significant contribution to the field of space-based auroral imaging.

## **2. Space Vehicle Contamination Study**

### **2.1 Workshop Support**

Planning has been initiated for a Space Vehicle Induced External Environment Workshop. A group of experts is being convened to review our current knowledge of induced vehicle environments, to assess progress that has been made in our understanding of this environment, and to discuss priorities for conducting future studies. Preworkshop support which has been provided during the first semiannual reporting period includes invitation of participants, arrangement of meeting facilities, and preparation of a meeting agenda. The workshop will be held on January 30-31, 1991 during the next six month reporting period.

### **2.2 Laboratory Measurements**

The first six months of laboratory effort have focussed on a thorough characterization of the facility. This is essential to insure that measurement of gas-gas interactions such as differential scattering cross sections can be made without any serious systematic errors. Specifically, we have completed characterization of thermal energy beams of O<sub>2</sub> and N<sub>2</sub>. The spatial profile of these beams has been measured to insure proper alignment and to determine their geometric extent. Also, the temporal profiles of the thermal energy O<sub>2</sub> and N<sub>2</sub> beams have been measured to confirm that the pulses from each valve arrive at the scattering region at the same point in time. Thermal energy differential scattering cross section measurements for O<sub>2</sub> on N<sub>2</sub> collisions have also been completed. Results of these measurements have been compared with classical scattering theory and are in good agreement. This serves as an indication that there are no serious systematic errors in differential scattering cross section measurements made with our facility. Work has begun on characterization of a laser induced energetic oxygen atom source. Preliminary measurements indicate that a beam of oxygen atoms traveling at > 6 km/sec has been formed. The ion content of the fast oxygen atom beam has been estimated to be less than 1%. Use of parallel plate deflectors reduces the ion content of the beam to a negligible level. Characterization of the energetic oxygen atom source is continuing and will be completed during the next reporting period.

THE UNIVERSITY OF CHICAGO PRESS  
54 EAST LAKE STREET, CHICAGO, ILL. 60601-3043  
TEL: (773) 837-3000 FAX: (773) 837-1500  
WWW.CHICAGO.PRESS.EDU

CHICAGO, ILL. 60601-3043

THE UNIVERSITY OF CHICAGO PRESS  
54 EAST LAKE STREET, CHICAGO, ILL. 60601-3043  
TEL: (773) 837-3000 FAX: (773) 837-1500  
WWW.CHICAGO.PRESS.EDU

THE UNIVERSITY OF CHICAGO PRESS  
54 EAST LAKE STREET, CHICAGO, ILL. 60601-3043  
TEL: (773) 837-3000 FAX: (773) 837-1500  
WWW.CHICAGO.PRESS.EDU

THE UNIVERSITY OF CHICAGO PRESS  
54 EAST LAKE STREET, CHICAGO, ILL. 60601-3043  
TEL: (773) 837-3000 FAX: (773) 837-1500  
WWW.CHICAGO.PRESS.EDU

THE UNIVERSITY OF CHICAGO PRESS  
54 EAST LAKE STREET, CHICAGO, ILL. 60601-3043  
TEL: (773) 837-3000 FAX: (773) 837-1500  
WWW.CHICAGO.PRESS.EDU

### **3. Auroral Modeling**

Modeling activities through the end of 1990 included an energy sensitivity study, initial use of an integrated global-auroral model, and the support of a science workshop for discussion of future science needs.

#### **3.1 Sensitivity Studies**

One of the first applications of the two-stream auroral code (AURCODE) was a study, carried out under contract NAS8-37586, of the sensitivity of modeled parameters to the choice of neutral atmosphere. This initial study has been followed by a study designed to determine the sensitivity of modeled auroral emissions to the choice of electron energy distribution. Four distributions were employed: Maxwellian, Gaussian, and two arbitrary distributions designed to have very broad or very narrow energy ranges.

The results of the study indicate the average energy of the incident electron flux may have more bearing than the energy distribution. As long as the average energy of the selected distribution is held constant, the modeled emissions vary by less than 25%. Visible  $N_2$  and  $N_2^+$  emissions are virtually independent of energy distribution. In addition, observed variations in  $N_2$  LBH emissions are entirely due to  $O_2$  absorption effects. Indeed, much of the observed dependence is due to  $O_2$  absorption effects. If this effect is removed, only the modeled emissions from atomic oxygen exhibit dependence on choice of energy distribution.

The small size of the variability most likely precludes the use of auroral images alone to determine electron energy distributions. On the other hand, the study does indicate that the observed emissions are not overly sensitive to the choice of incident electron energy distribution.

#### **3.2 Global Modeling**

Integration of the two-stream auroral code into the global FLIP model has begun. A version of AURCODE was transferred from its native VMS operating environment to the MSFC Cray computer to allow its use with the FLIP model. After code transfer and modification was complete, the auroral electron flux was then used to add the modeled auroral emissions to the FLIP airglow emission.

With the successful addition of auroral fluxes to the FLIP model, sensitivity studies have begun. Specifically, the intensity of the auroral emissions relative to the modeled dayglow emissions is to be investigated as a function of solar cyclic behavior and possibly as a function of neutral atmospheric composition.

#### **3.3 UVI Workshops**

The first Ultraviolet Imager (UVI) workshop was held on 15 & 16 August 1990. The workshop allowed each of the attendees to participate in the mission science planning and to address their specific science requirements for the UVI instrument. A major focus of the workshop was a review of the UVI operational and science objectives.

The attendees included nationally prominent scientists in the fields of ionospheric and magnetospheric physics and chemistry. The workshop participants and agenda are given in Table 1.



August 15, 1990

Introduction  
Instrument Observing Sequences  
Review of Science Objectives

August 16, 1990

Discussion of Analysis Tools  
Discussion of Signal Extraction  
Revised Data Analysis Plan  
Summary

Dr. Joe Ajello  
Dr. Ken Clark  
Dr. Bob Clauer  
Dr. Glynn Germany  
Dr. George Parks  
Dr. Jim Spann  
Dr. Doug Torr  
Dr. Marsha Torr

Jet Propulsion Laboratory  
University of Washington  
University of Michigan  
University of Alabama in Huntsville  
University of Washington  
NASA/MSFC  
University of Alabama in Huntsville  
NASA/MSFC

Table 1. Attendees and agenda of the UVI workshop.

Dr. Germany was responsible for coordination of the meeting, which was held in Park City, Utah. His responsibilities included arrangement of meeting facilities, communication with the science team members, and preparation of post workshop mailings. In addition, Dr. Germany participated in the workshop discussions and gave a presentation on the extraction of characteristic energy from auroral images via auroral modeling.

THE UNIVERSITY OF CHICAGO  
LIBRARY

THE UNIVERSITY OF CHICAGO  
LIBRARY

THE UNIVERSITY OF CHICAGO  
LIBRARY

THE UNIVERSITY OF CHICAGO  
LIBRARY

THE UNIVERSITY OF CHICAGO  
LIBRARY

THE UNIVERSITY OF CHICAGO  
LIBRARY

THE UNIVERSITY OF CHICAGO  
LIBRARY

THE UNIVERSITY OF CHICAGO  
LIBRARY

THE UNIVERSITY OF CHICAGO  
LIBRARY

7. **APPENDIX C**

Workshop on the Induced Environment of Space Station Freedom  
Huntsville, Alabama  
January 30-31, 1991

THESE DOCUMENTS SONT LA PROPRIETE DE LA BIBLIOTHEQUE DE LA MAIRIE DE MONTREAL  
CEUX QUI LES PRETENT SONT TENUS DE LES RENDRE A LA BIBLIOTHEQUE A LA DEMANDE



# Workshop on the Induced Environment of Space Station Freedom

Proceedings of a workshop held at  
George C. Marshall Space Flight Center  
Huntsville, Alabama  
January 30-31, 1991



# **Summary Report on the Workshop on the Induced Environment of Space Station Freedom**

**Huntsville, Alabama, January 30-31, 1991**

**prepared by Dr Marsha R. Torr/MSFC**

**Introduction.** A workshop was held in Huntsville on January 30-31, 1991 for the purpose of reviewing the state of knowledge of the likely induced external environment around Space Station Freedom. This workshop was chaired by Dr Marsha R. Torr and was a continuation of an activity coordinated by the Marshall Space Flight Center since 1987 and sponsored by the Office of Space Science and Applications and more recently by the Space Station Utilization Office at Reston. Two previous workshops have been held (one in October 1987 and one in May 1988) with the express purpose of assessing our understanding of the causative mechanisms underlying the various phenomena in the induced environment (glows, ionization, surface effects, gas envelope, etc). Both of the previous meetings led to the publication of NASA Conference Proceedings which document the contributions. As a result of the earlier reviews, a limited number of studies were funded in an attempt to obtain information on certain of the more fundamental processes involved. The activity has also been used to assist NASA Headquarters in assessing the impact of various Station design issues on potential attached payloads. Information gathered applies just as readily to critical Station systems such as the solar arrays.

The purpose of this meeting was to address three questions:

- 1) Where are we in our knowledge of the likely induced environment?
- 2) What progress have we made in the past two years in understanding this environment?
- 3) What areas of study are the most important for the next two years?

Copies of the material presented at the meeting are available.



**Proceedings of Meeting.** The agenda for the meeting is included here as Attachment I. The list of attendees is included as Attachment II. The meeting attendance was intentionally limited to the participants and NASA invitees. Some additional observers attended on a space available basis. The objective was to keep the meeting rather small so as to facilitate a good working environment. As with the previous two workshops, however, it was clear that as word of the meeting got out, the interest in attending was high and we had to turn a relatively large number of people away. This may indicate the desirability of scheduling a wider attendance "tutorial" meeting at some point to serve the purpose of briefing various personnel working on the Station design on the issues that this panel of experts is addressing.

As part of the first question above, reviews were presented of various related activities that have been conducted over the past year, including a rather sizable DOD effort on vehicle glows, and a summary of the early findings from the LDEF program. In addition, presentations were made of the various studies that have been funded by this and other MSFC programs.

Despite the very limited funding that has gone into the effort, the progress that has been made since the 1988 workshop was found to be considerable. This is largely due to the fact that the external Station environment represents a region of most unusual physical processes, including both gas phase and surface phase interactions, so that scientists in fields of appropriate expertise are challenged by the task of understanding the phenomena. A number of facilities have been put in place for the purpose of studying such environments in the laboratory and early results are beginning to emerge. The progress in developing models of the environment has made excellent progress. Almost three years ago we had very little to work with apart from unexplained Shuttle phenomena, and "back-of-the-envelope" projections for Space Station Freedom. Now we are at a point where we have the tools to begin to do believable evaluations.



**Recommendations.** In order to predict the external Station environment, it is necessary that we are able to understand the nature of the processes taking place within it. At present, the state of knowledge is very poor. Over the past three years, with very nominal resources (~\$150K per year), it has been possible to make progress in the field and to set in place important tools which are now available for use in further studies.

At some point we anticipate that the Space Station Freedom will be used for purposes of attaching external payloads. If NASA is to remain a "smart buyer" in this area it is most important that we continue the efforts (albeit at a low level of effort) to understand the environment in which these systems will operate, and what the limitations on them will be. Maintenance of a multidisciplinary pool of expertise, such as is represented by the panels put together for these workshops and study efforts, is a valuable, if not essential, activity.

At present there are several activities that we would recommend for immediate attention. For example, in order to conduct almost any assessment of the external environment, one must first model the gas concentrations surrounding the vehicle. Once this is known, one can proceed to model the induced optical emission and the induced ionization. With these established one can compute the backscatter fluxes, arcing, plasma discharges, optical thresholds, etc. One can optimize the placement of vents, and establish the impact of leaks. However, a fundamental input to models of the neutral gas environment is the gas phase collision cross sections. Those relevant to this problem are essentially unknown. It is important to measure these cross sections in the laboratory and then input them to the models. During a shuttle docking the Station surfaces can become flooded with contaminants. We do not know what the residence times of these contaminants are on the surfaces, and in the induced environment. These lifetimes can be measured in the laboratory and it is recommended that studies be made for key likely species such as water. If attached payloads are initially to be mounted on the JEM, it is important that we try to establish the environment for this location first. Relevant new evidence of synergistic effects is emerging from the LDEF studies. These need to be examined in the light of the Space Station Freedom external environment work. A summary of the specific recommendations made by individual panel members is included here as Attachment III.

1. The first part of the document is a list of the names of the persons who have been appointed to the various offices of the city of New York.

2. The second part of the document is a list of the names of the persons who have been appointed to the various offices of the city of New York.

3.

4.

5. The third part of the document is a list of the names of the persons who have been appointed to the various offices of the city of New York.

6. The fourth part of the document is a list of the names of the persons who have been appointed to the various offices of the city of New York.

7. The fifth part of the document is a list of the names of the persons who have been appointed to the various offices of the city of New York.

8.



**ATTACHMENT I:**

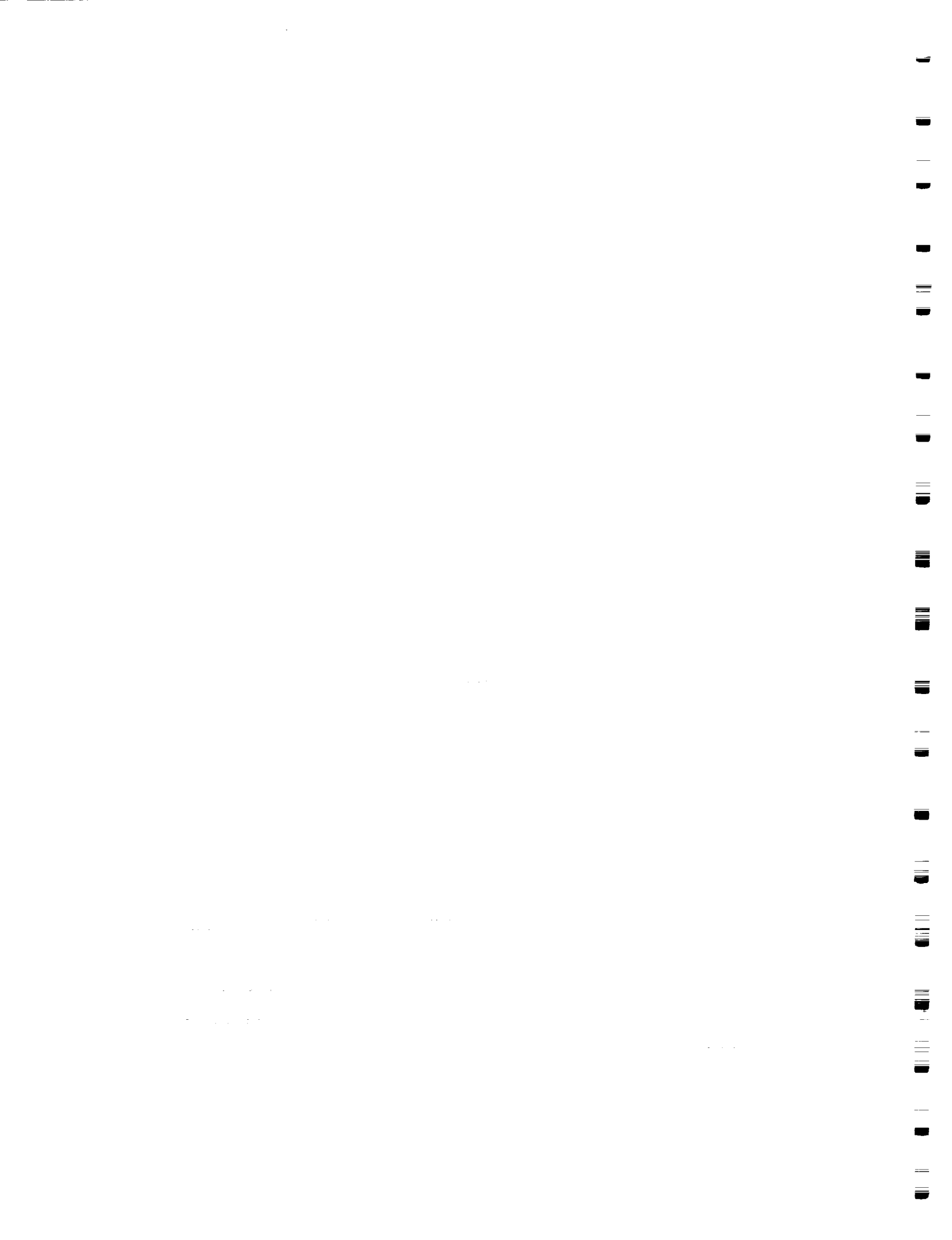
**WORKSHOP on the INDUCED ENVIRONMENT of  
SPACE STATION FREEDOM**

**Radisson Hotel, Huntsville, Alabama**

**January 30-31, 1991**

**Wednesday, January 30, 1991**

8:30AM	Introduction and Objectives of Workshop	M. Torr
8:45AM	Environmental Definition and Assessment Program	D. Brewer
9:15AM	Current Requirements and Plans to Verify These	L. Leger
9:45AM	Status of Planned Investigations Attached to Space Station Freedom	M. Sistilli
10:15AM	BREAK	
10:30AM	Environmental Issues from the Utilization Viewpoint	K. Schaefer
11:00AM	Vehicle Interaction Program at JHU/APL	C. Meng
11:30AM	LUNCH	
1:00PM	Gloves, Accommodation and Surface Residence Times	G. Caledonia
1:30PM	Summary of Space Station Grounding Issues	R. Carruth
2:00PM	LDEF: Lessons Learned	convenor: A. Whitaker R. Linton R. Rantanen
3:15PM	BREAK	



**January 30, 1991, continued:**

3:30PM	Overview of Spacecraft Glow	T. Slanger
4:00PM	Summary of JPL Workshop on Modeling Tools	J. Murphy
4:30PM	Discussion	
5:00PM	End of Formal Presentations for the Day	
6:00PM	SPECIAL EVENT AT ALABAMA SPACE AND ROCKET CENTER see attached sheet	

**Thursday, January 31, 1991**

8:30AM	ISEM Space Station Model Update	T. Gordon
9:00AM	Cross Section Work at Rice	K. Smith
9:30AM	Cross Section Work at UAH/MSFC	C. Keffer
10:00AM	BREAK	
10:15AM	Induced Emissions	D. Torr
10:45AM	Atomic Oxygen Studies at PPPL	J. Cuthbertson
11:15AM	Spacecraft Glow Studies and Mechanisms	S. Mende
11:45AM	LUNCH	
1:00PM	Visit to Space Station Mockup	
2:30PM	Surface Temperature Dependent Glow Mechanisms in Space	N. Tolk
3:00PM	What Have We Learned?	
3:30PM	BREAK	
3:45PM	Where do we go from here?	
4:30PM	End of Meeting	



**ATTACHMENT II:**

**LIST OF ATTENDEES**

Marsha Torr, Chairperson	NASA\MSFC
Charles Keffer	UAH
Anderson, Jeff	NASA/MSFC
Blanchette, Fred	McDonnell Douglas Space Systems Co.
Brewer, Dana	NASA/HQ
Caledonia, George	Physical Sciences Inc.
Carruth, Ralph	NASA/MSFC
Chappell, Rick	NASA/MSFC
Collier, Jack	NASA/HQ
Crane, Mike	Boeing
Cuthbertson, John	Princeton Plasma Physics Lab
Erlandson, Bob	Applied Physics Lab
Espy, Pat	NASA/MSFC
Feddes, Allan	Boeing
Fichtl, George	NASA/MSFC
Gordon, Tim	Applied Science Technologies
Hefling-Miller, Hilda	Grumman SSPSD
Hwang, Kai-Shen	Grumman SSEIC
Jongward, Gary	S-Cubed
Katz, Ira	S-Cubed
Leifer, Joel	Booz-Allen & Hamilton
Linton, Roger	NASA/MSFC
McCombs, Roger	BA&E
Mende, Steve	Lockheed Palo Alto Research Lab
Melendez, Daniel	NRC
Meng, Ching	Applied Physics Lab
Murphy, Gerry	JPL
Nahra, Henry	NASA/Lewis
Nebolsine, Peter	Physical Sciences Inc.
O'Keefe, Ed	Boeing
Plaster, Teresa	Grumman Space Station Integration
Rantanen, Ray	ROR Enterprises
Schaefer, Kevin	NASA/Reston



Sistilli, Mark  
Slanger, Tom  
Smith, Ken  
Snyder, Dave  
Suggs, Rob  
Taylor, Bill  
Tolk, Norman  
Torr, Doug  
Whitaker, Ann  
Wyman, Pete  
Young, Dave

NASA/HQ  
SRI International  
Rice University  
NASA/Lewis  
Grumman Space Station Integration  
NASA/HQ  
Vanderbilt University  
UAH  
NASA/MSFC  
NASA/HQ  
Grumman





### ATTACHMENT III:

Recommendations Made by Individual Panel Members (in alphabetical order).

Brewer(HQ/MSS):

- \*Cross comparison of model results used by station engineers and science community using station vent, leakage and outgassing data for

- each stage in assembly sequence to identify potential problems early on

- identification of sensitive surfaces (which will change orientation as a function of stage)

- \*Identification/quantification of neutral/plasma effects on Station hardware.

Carruth(MSFC/EH12)

- \*Needed:

- definition of data required and models for environment

- meeting of atomic oxygen facility groups

- determine the causative processes involved in new LDEF phenomena (i.e. fluorescence and synergistic effects)

- studies of basic interactions which affect surfaces rather subtly over time

- investigations of plasma phenomena (interactions) on SSF systems and of mitigating techniques

Cuthbertson(PPPL):

For further progress we need:

- \*laboratory investigation of synergistic phenomena (UV, temperature cycling)









# Environment Management and Control for the Space Station Freedom Program

Dana A. Brewer  
Space Station Freedom  
Program Office  
January 30, 1991

1000

1000

1000

1000

1000

1000

1000

1000

1000

1000

1000

1000

1000

1000

1000

1000

1000

1000

1000

1000

1000

1000

1000

1000

1000

1000

1000

1000

1000

1000

1000

1000

1000

1000

1000

1000

1000

1000

1000

1000

1000

1000



# Environment Management and Control for the Space Station Freedom Program



- **Objective: Build the Space Station Freedom that provides:**
  - Equipment that operates with no unintentional operational constraints due to the natural and induced environments
  - A safe, habitable environment for the crew
  - A useful station for experiments
- **Why does the Space Station Freedom need this?**
  - The space environment is harsh
  - If no compensation, the lifetime and functionality of station may be severely degraded

# How is Environment Management and Control Achieved?



- **By defining the components of environments assessment:**

- Define the environments
- Define the environment effects
- Define requirements to control or accommodate the environment and its effects
  - Includes requirements for whole Space Station Freedom (SSF) and its hardware components
- Define methods to control or accommodate the environment and its effects
  - Includes verification methods for whole SSF and its hardware components
- Define the management process to control or accommodate the environment and its effects
  - Management process includes requirements development, verification, and interactions with the payload community



# Environment Management and Control: Overall Activities



- **Documentation for environment management:**
  - Environment management plan:
    - Roadmap for all environments activities in the SSFP
  - Environment Definition And Assessment (EDAP) requirements document
    - Specifies requirements for interfacing SSFP data bases and models with environments data bases and models
  - Environments models and data bases are standardized (configuration controlled)

# Environment Management and Control: Overall Activities (Cont'd)



- **Documentation for Environment Management (Cont'd):**
  - EDAP Implementation Plan
    - Describes the plan for developing interaction models, tools, and data bases which can be used to perform analyses of combined environmental effects
    - Describes how the EDAP will be used for both payload accommodation and engineering analyses
  - EDAP Software Product Assurance Plan
    - Describes standards for documenting and benchmarking environments models and data bases
  - EDAP Configuration Management Plan
    - Describes how environments models, tools, and data bases will be tracked, changed, and augmented

# Environment Management and Control: Overall Activities (Cont'd)



- **Documentation for Environment Management (Cont'd):**
  - Environment Assessment Plan
    - Describes the methodology used to develop environments definitions, requirements, and effects requirements
  - Environment Control Process
  - Environment Assessment Reports, Vols. I and II
    - Vol. I: Data Bases And Models (and their interfaces)
      - Describes the Interrelationship between the environments models, tools, and data bases and the SSFP data bases
    - Vol. II: Reports of Level II Assessments
  - Environment Discipline Implementation Plans
    - Describes the procedures for identifying the requirements, performing the review, performing waiver analyses, and maintaining environment definitions
  - TMIS Requirements Definition Document
    - Describes the requirements placed on TMIS to support environment activities
      - Includes communications support, data exchange, configuration control during data transmittal

# Natural Environment



- **Definition:** The environment in the absence of the SSF
- **Sub-disciplines (all external):**
  - Magnetic and gravitational fields – Neutral atmosphere
  - Atmospheric density – Solar activity
  - Thermospheric winds – Plasma
  - Ionizing radiation – Electromagnetic radiation
  - Meteoroids and orbital debris – Physical constants
- **Defined in SSP 30425, Space Station Program Natural Environment Definition for Design**
- **Requirement to accommodate the natural environment and its effects are given in SSP 30000, Sec. 3 and the ACDs**



# Status of Natural Environment Documents



- SSP 30425, Space Station Program Natural Environment Definition for Design, is being revised in two stages
  - Stage 1: Every environment except the meteoroid and orbital debris environments
    - BB000884A
  - Stage 2: The meteoroid and orbital debris environment
    - BB000883A
- SSP 30000, Sec. 3 Design Requirements for Every Natural Environment Except the Meteoroid and Orbital Debris Environments are being transferred from the baselined version of SSP 30425
  - Included in BB000884A

# External Neutral Environment

FREEDOM



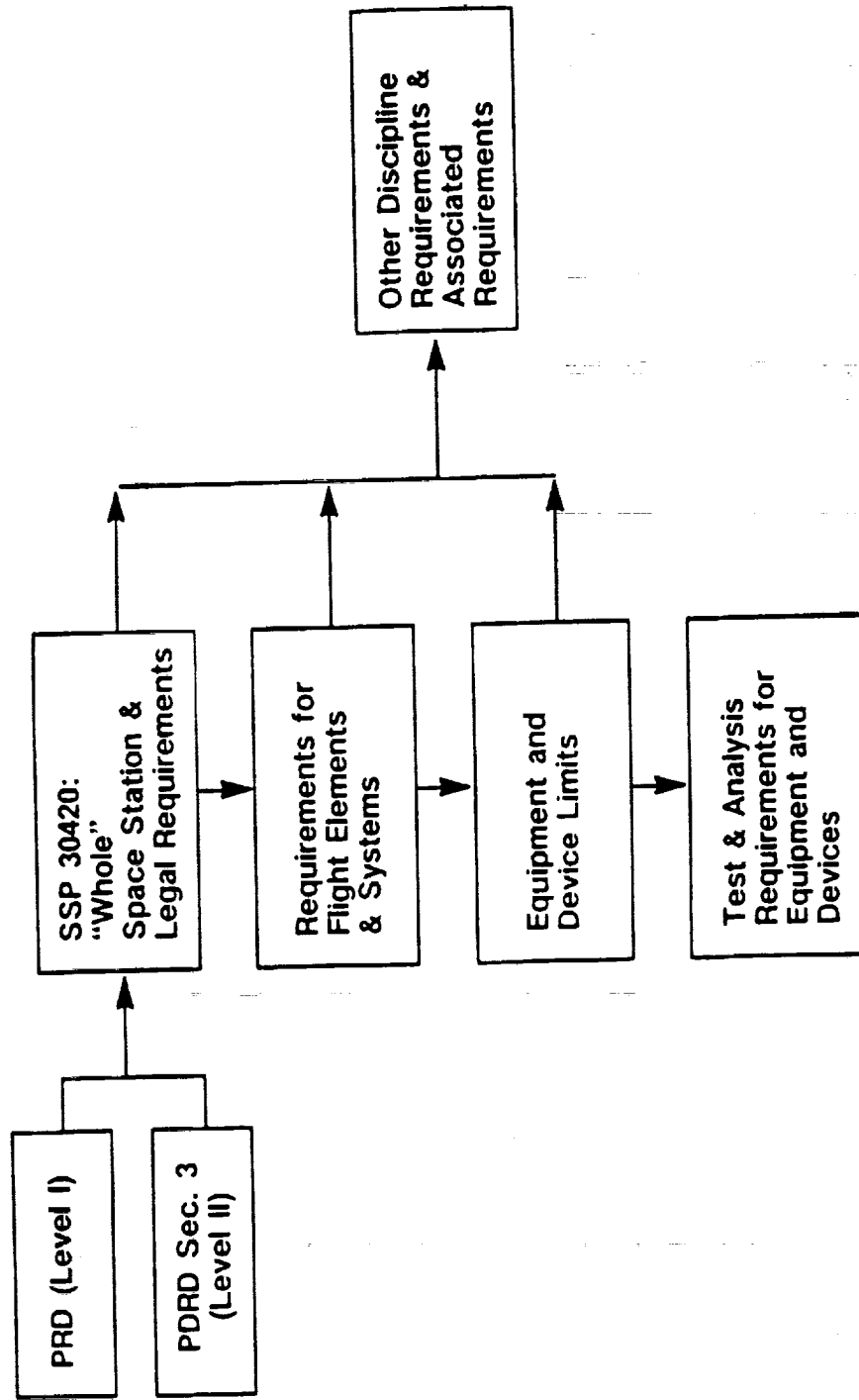
- The environment is comprised of electrically neutral chemicals; sources are from the natural environment and station operations, such as:
  - Venting – Leakage
  - Outgassing and offgassing – Thruster Firing
  - Attitude control firing – Airlock operations
  - EVA – Shuttle docking/berthing
- Definition and control of this environment impacts:
  - Attached payload operations
  - Lifetimes of surface materials
    - Deposition on thermal radiators and solar arrays
    - Atomic oxygen degradation
- This environment is defined and controlled by:
  - Design and use of vents – Materials outgassing requirements
  - Design and use of thrusters – EVA EMU venting
  - Operational constraints on times and rates of venting
  - Methods for shuttle docking/berthing

## External Neutral Environment: Requirements



- **SSP 30426, Space Station External Contamination Control Requirements**
  - Requirements for contamination levels for “Whole SSF”
  - Document is being updated based upon CBR and revised user requirements
    - BB000874
  - Cleanest areas are defined as “Prime Measurement Points”
  - Requires preparation and review of a “Contamination” control plan, a DR
    - Prepared by element integrators – work packages and International Partners
- **SSP TBD, External Contamination Implementation Plan, is being prepared**
  - Performs budget allocation for venting for each work package and International Partner
  - Develops content of the External Contamination Control Plan
  - Develops methodology for Level II review of plans and maintenance of external particulate and gas environment definition and assessments

# Structure of Particle and Wave Requirements





# **Ionizing Radiation**



- **An induced environment:** The natural ionizing radiation environment perturbed by shielding from station hardware
- **The environment is defined and its effects are controlled:**
  - To ensure that external legal requirements are satisfied
  - To ensure that Electrical, Electronic, and Electromechanical (EEE) equipment is designed to accommodate the space ionizing radiation environment
- **Legal requirements:**
  - Report sources and types of ionizing radiation sources to the Office of the President to ensure that:
    - The SSF will not endanger U.S. Citizens on the ground (environmental impact)
    - Treaties are not violated when ionizing radiation sources are used on the SSF
  - Satisfy U.S. Department of Labor requirements that the crew are treated as radiation health workers under OSHA
    - Satisfied by NASA Radiation Constraints Panel (established by NMI at JSC)

# **Ionizing Radiation: Requirements Status**



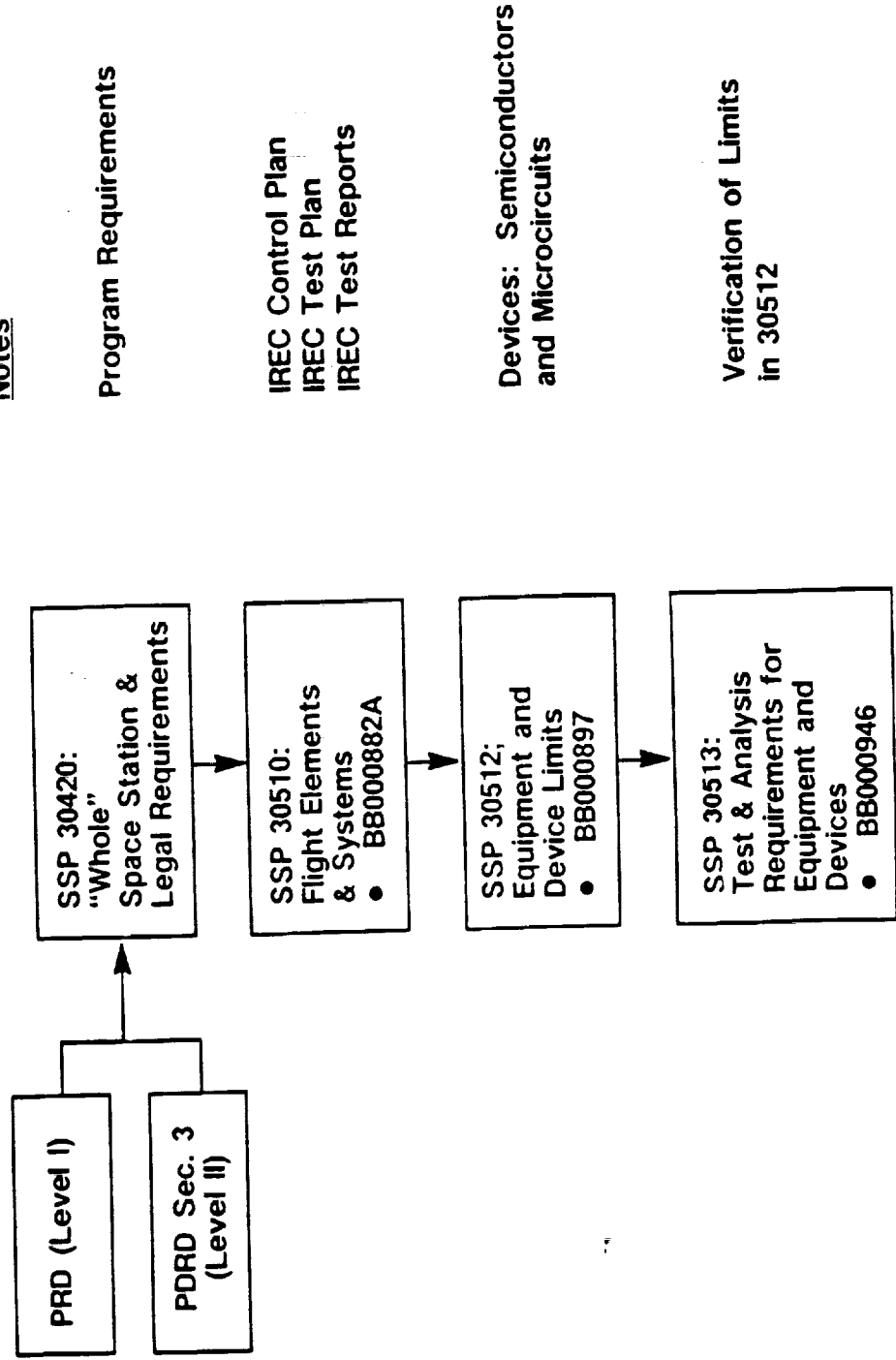
- **Baselined documents:**

- SSP 30420, Space Station Electromagnetic, Ionizing Radiation, and Plasma Definition and Design Requirements
  - Part of Level I and Level II baselines
- Calls out Ionizing Radiation Legal Requirements and Radiation Constraints Panel
- Requires Ionizing Radiation Control Plans, Test Plans, and Test Reports from element integrators (work packages and International Partners)
- Needs to be updated to clarify legal and “Whole SSF” requirements

- **Other baselined requirements:**

- Crew dose limits in SSP 30000, Sec. 3, Table 3–12

# Traceability for Ionizing Radiation Requirements Documents

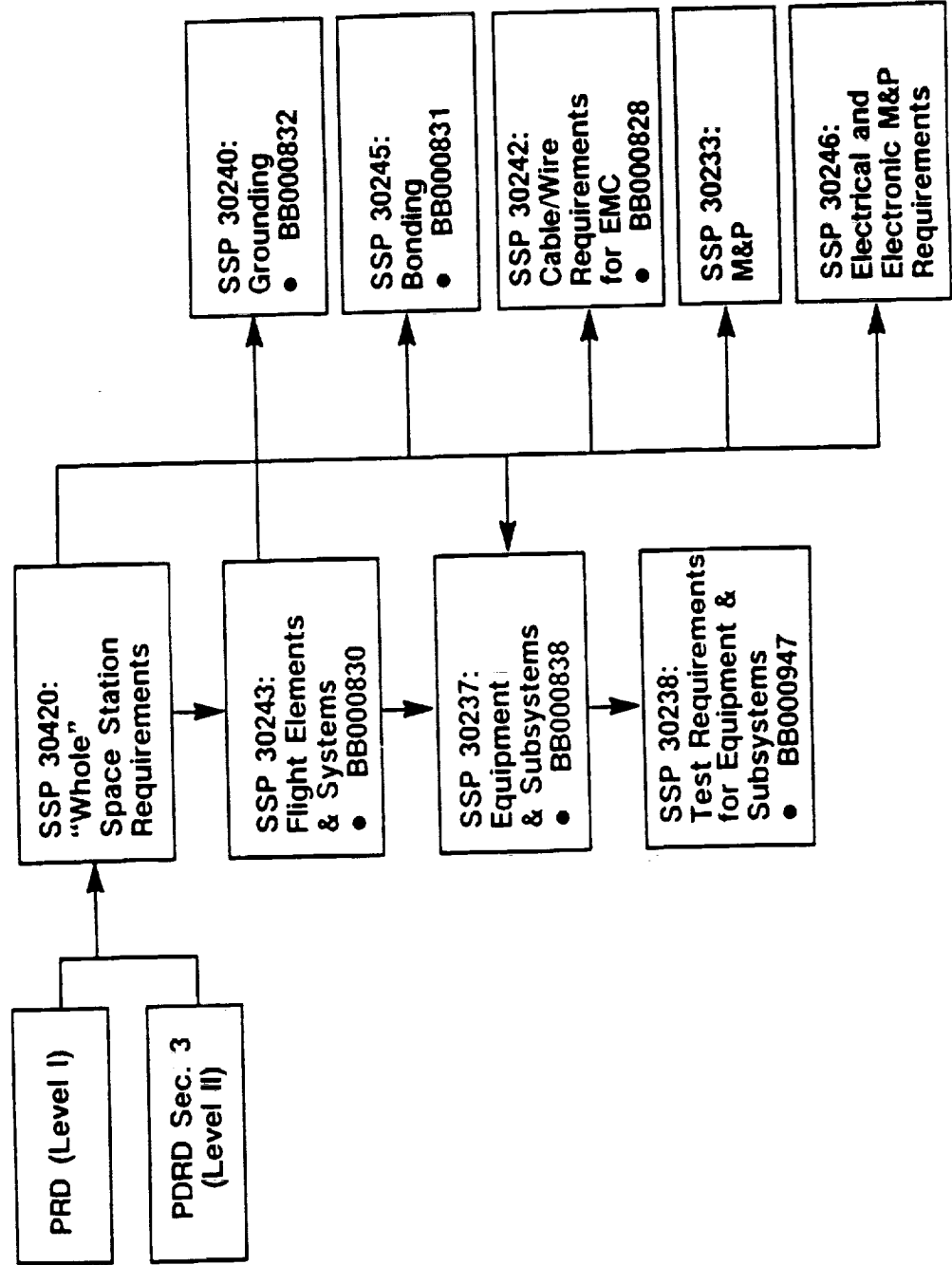


# Electromagnetic Radiation



- **An induced environment**
  - Natural environment: space electromagnetic radiation; external radiators
  - Environment due to presence of the SSF: effects transmitted down wires and through space
- **The environment is defined and its effects are controlled to ensure that:**
  - Equipment and systems that produce and use power do not interfere with each other
    - Example: Electromagnetic Interference (EMI) can inhibit C&T equipment from operating in the presence of power producing and transforming equipment
- **Requirements are patterned after military EMC requirements but have been tailored for the SSFP**

# Traceability for EMC Requirements Documents

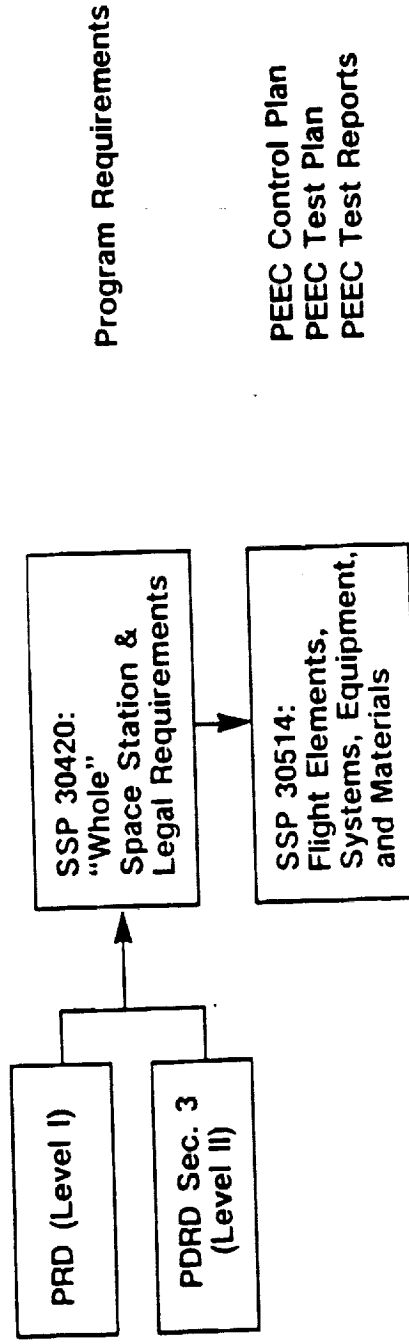


- **An induced environment with a natural component and a component due to the presence of the SSF**
  - Natural component: Space Plasma
  - Component due to presence of the SSF: Ram/Wake effects; potential effects due to grounding
- **The environment is defined and its effects are controlled to ensure that equipment and systems do not degrade due to arcing, corona, sputtering, and EMI induced by plasma**

# Traceability for Plasma Requirements Documents



## Notes



## Observations



- **Electrical Grounding of 160 volt photovoltaic arrays may result in plasma environmental effects**
  - Corona, arcing, EMI, sputtering, kapton pyrolyzation
  - An electrical grounding tiger team has been formed to quantify the effects through tests and analysis
    - Engineers and plasma physicists are participating
- **The user organizations (OSSA, OAET, OCP) are now members of the Space Station**
  - Direct participants in the SSFP
- **Several technology issues remain to be solved**
  - Users are invited to participate in solving these issues



**STATUS OF PLANNED OSSA ATTACHED PAYLOAD  
INVESTIGATIONS ON SPACE STATION FREEDOM**

**MARK SISTILLI  
OSSA PROGRAM MANAGER  
FOR ATTACHED PAYLOADS  
JANUARY 30, 1991**

## STATUS:

- SSFP ISSUED A STOP-WORK ORDER TO GSFC (WP-3) ON APAE PROJECT EFFECTIVE 11/5/90.
- SSFP INDEFINITELY DEFERRED (ELIMINATED) ALL OTHER ATTACHED PAYLOAD ACCOMMODATIONS FROM THE SSF (EXCLUDING THE JEM EF).
  - POSSIBLE ADD-BACK OF SOME ACCOMMODATIONS AFTER CONCLUSION OF SSFP 90-DAY RESTRUCTURE STUDY - TBD
- OSSA ATTACHED PAYLOAD FY 91 FUNDING (EXCLUDING EOS) REDUCED TO MINIMUM LEVEL NECESSARY TO KEEP CONTRACTS IN EFFECT THROUGH THIS FISCAL YEAR.
- PROGRESS OF MSFC PHASE A PAYLOAD POINTING SYSTEM STUDY WAS REVIEWED ON 11/27/90. STUDY NOW ON HOLD PENDING THE RESULTS OF THE RESTRUCTURING ACTIVITY.
- MAJOR ATTACHED PAYLOAD-RELATED LEVEL I AND II CRs (INCLUDING SRR-A ACCOMMODATIONS) HAVE BEEN DEFERRED.

## FLIGHT PROJECTS DESCRIPTION:

FLIGHT PROJECT (14 TOTAL)		SCIENCE MISSION GOAL
ASTROMAG FACILITY	• MEASUREMENT OF COSMIC RAY ARTICLES (WIZARD)	SEARCH FOR COSMIC ANTIMATTER SOURCES ( $Z < 4$ )
	• LARGE ISOTOPE SPECTROMETER FOR ASTROMAG (LISA)	SEARCH FOR COSMIC ANTIMATTER SOURCES ( $Z > 4$ )
	• SPECTRA, COMPOSITION, AND INTERACTION OF COSMIC RAY NUCLEI (SCIN)	VERY HIGH ENERGY COSMIC RAY PARTICLE STUDIES ( $E > 10^{14}$ eV)
COSMIC DUST COLLECTION FACILITY	• COSMIC DUST EXPERIMENT (CODE)	CAPTURE OF DUST PARTICLES, STUDY OF COMPOSITION, CORRELATION OF DUST PARTICLES TRAJECTORIES WITH INTER PLANETARY SOURCE BODIES
	• COSMIC DUST ORBIT CAPTURE EXPERIMENT (CDOCE)	CORRELATION OF CHARGED DUST PARTICLE TRAJECTORIES WITH INTER PLANETARY SOURCE BODIES
	• EXOBIOLOGY INTACT CAPTURE EXPERIMENT (EXO-ICE)	CAPTURE OF DUST PARTICLES, AND STUDY OF COMPOSITION
• SOLAR VIEWING PROJECT:	• HEAVY NUCLEI COLLECTOR (HNC)	SEARCH FOR COSMIC SUPER HEAVY ELEMENT SOURCES ( $Z > 92$ )
	• LARGE AREA MODULAR ARRAY OF REFLECTORS (LAMAR)	STUDY OF DISCRETE CELESTIAL X-RAY SOURCES (STELLAR, GALACTIC, COSMIC QUASARS)
	• X-RAY BACKGROUND SURVEY SPECTROMETER (XRBS)	STUDY OF DIFFUSE CELESTIAL X-RAY SOURCES (PROTO-STELLAR)
EOS ON MANNED STATION	• ULTRA HIGH RESOLUTION EXTREME ULTRAVIOLET SPECTROHELIOGRAPH (UHEXS)	EUV (40Å - 1600Å) STUDY OF SOLAR ATMOSPHERIC FINE STRUCTURE AND INTERACTION WITH SOLAR FLARES, SOLAR WIND
	• CLOUDS AND THE EARTH'S RADIANT ENERGY SYSTEM (CERES)	UV-VISIBLE-IR STUDY OF EARTH/SOLAR RADIATION BALANCE AND INTERACTION WITH GLOBAL EARTH CLIMATE
	• STRATOSPHERIC AEROSOL AND GAS EXPERIMENTS (SAGE III)	EARTH LIMB STUDY (VISIBLE-IR) OF GLOBAL DISTRIBUTION OF ATMOSPHERIC OZONE, WATER, NO <sub>2</sub> , AEROSOLS, AND INTERACTION WITH GLOBAL EARTH CLIMATE
• EARTH VIEWING PROJECTS:	• LIGHTNING IMAGING SENSOR (LIS)	MEASUREMENT (IR-774Å) OF GLOBAL DISTRIBUTION OF LIGHTNING AND INTERACTION WITH ATMOSPHERIC CHARGE TRANSPORT MECHANISMS
	• LASER COMMUNICATIONS TRANCEIVER (LCTI)	SPACE-BASED LASER (IR) OPTICAL COMMUNICATIONS TECHNOLOGIES STUDY

## CONCEPT STUDIES DESCRIPTION:


<u>CONCEPT STUDY (13 TOTAL)</u>	<u>SCIENCE MISSION GOAL</u>
<u>• ⑤ CELESTIAL VIEWING CONCEPTS STUDIES:</u> <ul style="list-style-type: none"> <li>• ORBITING STELLAR INTERFEROMETER (OSI)</li> <li>• PRECISION OPTICAL INTERFEROMETER (POINTS)</li> <li>• ENERGETIC X-RAY OBSERVER (EXOSS)</li> <li>• HIGH RESOLUTION IMAGING SPECTROMETER AT TERAHERTZ FREQUENCIES (HRISTF)</li> <li>• ACTIVE COLLECTOR OF COSMIC DUST (ACCD)</li> </ul>	BOTH ASTROMETRIC (10 MICRO-ARCSECONDS) AND IMAGING (m=20) OBSERVATIONS USING INTERFEROMETRIC TECHNIQUES  ASTROMETRIC MAPPING, DETECTION OF EXTRA-SOLAR PLANETARY SYSTEMS (INDIRECT), SOLAR SYSTEM TEST OF GENERAL RELATIVITY, DIRECT DETERMINATION OF CEPHEID DISTANCE SCALE  CODED APERTURE X-RAY IMAGING (3 KeV-511 KeV), AND SPECTROSCOPY OF CELESTIAL X-RAY SOURCES  DETERMINE THE ORIGIN AND PROPAGATION OF ULTRAVIOLET RADIATION IN THE GALAXY BY STUDY OF ATOMIC CARBON, OXYGEN EXCITATION AT SUBMILLIMETER WAVELENGTHS  UNCONTAMINATED, INTACT CAPTURE OF DUST PARTICLES FOR EXOBIOLOGICAL ANALYSIS
<u>• ① SOLAR VIEWING CONCEPT STUDY:</u> <ul style="list-style-type: none"> <li>• PINHOLE/OCCULTER FACILITY (POF)</li> </ul>	SOLAR IMAGING (X-RAY, GAMMA-RAY, NEUTRONS) WITH 0.2 ARCSEC SPATIAL RESOLUTION, IN ORDER TO STUDY SOLAR PARTICLE ACCELERATION AND CORONAL PHYSICS
<u>• ⑥ EARTH VIEWING CONCEPT STUDIES:</u> <ul style="list-style-type: none"> <li>• LASER/ATMOSPHERIC WIND SOUNDER (LAWS)</li> <li>• TROPICAL REGIONS IMAGING SPECTROMETER (IRIS) (T/N)</li> <li>• ADVANCED SCATTEROMETER FOR STUDIES IN METEOROLOGY AND OCEANOGRAPHY (SCANSAT)</li> <li>• GLOBAL POSITIONING SYSTEM GEOSCIENCE INSTRUMENT (GGI)</li> <li>• TROPICAL RAIN MAPPING RADAR (IRAMAR)</li> <li>• HIGH RESOLUTION MICROWAVE SPECTROMETER SOUNDER (HIMSS)</li> </ul>	DETERMINE WIND VELOCITY AT 100 KM HORIZONTAL RESOLUTION, 1 KM VERTICAL RESOLUTION WITH ACCURACY OF 1 TO 5 M/SEC  THIS T-MEASURE VEGETATION, CHLOROPHYLL CONCENTRATIONS THIS N-MEASURE SURFACE TEMPERATURE (LAND AND OCEAN)  MEASURE SURFACE VELOCITY OVER OCEAN AS INPUT INTO AIR-SEA INTERACTION STUDIES  TO PROVIDE REAL TIME POSITIONING (~1M) AND ATTITUDE (20-40 ARCSEC)  MEASURE TROPICAL REGION'S RAIN RATE AS INPUT INTO GLOBAL ENERGY BALANCE STUDIES  MEASURE PRECIPITATION RATES, SEA ICE COVERAGE, SNOW COVER DEPTH AND WATER EQUIVALENT
<u>• ① MAGNETOSPHERIC CONCEPT STUDY</u> <ul style="list-style-type: none"> <li>• PLASMA INTERACTIONS EXPERIMENT</li> </ul>	STUDY OF DYNAMIC INTERACTIONS BETWEEN HIGH DENSITY PLASMA AND NEUTRAL GAS CLOUDS ARTIFICIALLY INJECTED INTO THE IONOSPHERE

# **Factors Influencing Vent design**


**Space Station Freedom Induced  
Environment Workshop**


**January 30-31**

**Kevin Schaefer/MSU-1  
(703) 487-7088**

		Primary Contaminant Sources	
Kevin Schaefer (703) 487-7088		Factors Influencing Vent Design	
Date: 1-30-91		Page: 2	


- Primary gas, liquid and particulate source categories:
  - Surfaces
  - Leaks
  - Vents
- Allocation part of total environment to each category
- Sub-divide allocations by system/element


	<b>Requirements Status</b>	<b>Factors Influencing Vent Design</b>	
Kevin Schaefer (703) 487-7088		Date: 1-30-91	Page: 3
<ul style="list-style-type: none"><li>• SSP 30426 defines total neutral environment<ul style="list-style-type: none"><li>•• Not linked to PDRD, but CR in work</li></ul></li><li>• CR does not contain allocations<ul style="list-style-type: none"><li>•• No leak rates by system</li><li>•• No outgasing rates by surface</li><li>•• No vent rates by system</li></ul></li><li>• Leak detection and vent design requirements are vague</li></ul>			


	Vent Types			Factors Influencing Vent Design		
				Kevin Schaefer (703) 487-7088	Date: 1-30-91	Page: 4

- **Waste:** dispose of SSF and payload by-products
- **Drain or vacuum:** empty a system or enclosed space
- **Purge:** replace one gas or liquid with another
- **Pressure Relief:** prevent excessive pressure buildup
- **Bleed:** remove gases from a liquid system
- **Outgas:** allow the escape of gases from enclosed spaces




	Design Parameters	Factors Influencing Vent Design	
		Kevin Schaefer (703) 487-7088	Date: 1-30-91 Page: 5
<ul style="list-style-type: none"><li>• <b>Direction:</b> Main axis of undisturbed plume</li><li>• <b>Location:</b> Centroid of exit plane</li><li>• <b>Nozzle design:</b> Mass flow rate, expansion ratio, thrust, Plume "shape"</li><li>• <b>Vented material composition:</b> Liquid/gas ratio; Breakdown by species</li><li>• <b>Operation:</b> Frequency and duration of operation</li></ul>			

	Orbit Lifetime	Factors Influencing Vent Design	
		Kevin Schaefer (703) 487-7088	Date: 1-30-91 Page: 6
<ul style="list-style-type: none"><li>• Maximize SSF orbit lifetime:<ul style="list-style-type: none"><li>•• Nozzle design, direction, operation, and SSF mass</li></ul></li><li>• Direction of thrust through SSF CG:<ul style="list-style-type: none"><li>•• Ram: accelerates orbit decay</li><li>•• Wake: slows orbit decay</li><li>•• Zenith or nadir: increases eccentricity; slows decay</li><li>•• <math>\pm Y</math> LVLH: no effect</li></ul></li><li>• Maximizing orbit lifetime:<ul style="list-style-type: none"><li>•• Maximize thrust</li><li>•• No thrust component in Ram direction</li></ul></li></ul>			

	Attitude Control		Factors Influencing Vent Design	
			Kevin Schaefer (703) 487-7088	Date: 1-30-91
				Page: 7


- Resultant torque about CG cannot exceed CMG limits:
  - Vent location, direction, and nozzle design
- Optimizing attitude control:
  - Minimize thrust
  - Direct thrust through CG
  - Simultaneous operation of symmetric vent pairs

	Micro-Gravity		Factors Influencing Vent Design	
			Kevin Schaefer (703) 487-7088	Date: 1-30-91 Page: 8


- Minimize accelerations and vibrations to  $\mu$ -g payloads:
  - Nozzle design, direction, operation, and SSF mass
- $\mu$ -g requirements apply only during 30 day quiescent period
- Minimizing  $\mu$ -g disturbances
  - Limit vent operation in quiescent periods
  - Minimize thrust
  - Direct thrust through CG
  - Locate vents far from  $\mu$ -g payloads

	Molecular and Particulate Deposition			Factors Influencing Vent Design	
				Kevin Schaefer (703) 487-7088	Date: 1-30-91

- Minimize deposition on sensitive surfaces:
  - Thermal radiators, windows, solar arrays, star trackers, cameras, and external payload sensors, etc.
  - Location and direction determine plume impingement
  - Nozzle design and vented material composition determine sticking coefficient
- Minimizing deposition:
  - Design nozzle to minimize plume "spread"
  - Direct plumes away from critical surfaces

	Light Scattering		Factors Influencing Vent Design	
			Kevin Schaefer (703) 487-7088	Date: 1-30-91 Page: 10

- Minimize Background Spectral Irradiance (BSI):
  - Gas/particulate column density/composition as a function of direction
  - Location and direction of light sources
  - Location and viewing direction of sensor
- BSI and vent design:
  - Nozzle design, location, and direction determine Molecular Column Density (MCD)
  - Material composition determines wavelengths of light scattered

	More Light Scattering	Factors Influencing Vent Design	
Kevin Schaefer (703) 487-7088		Date: 1-30-91	Page: 11
<ul style="list-style-type: none"><li>• BSI requirement applies only in 14 day quiescent periods</li><li>• SSF structures block viewing along main truss</li><li>• Air glow layer above horizon already has high BSI</li><li>• MCD high towards Earth</li><li>• Minimizing light scattering:<ul style="list-style-type: none"><li>•• Limit vent operation in quiescent periods</li><li>•• Coordinate vent operation with payload viewing</li><li>•• Direct plumes towards blocked viewing directions, air glow layer, or Earth</li></ul></li></ul>			



# Structural Blockage

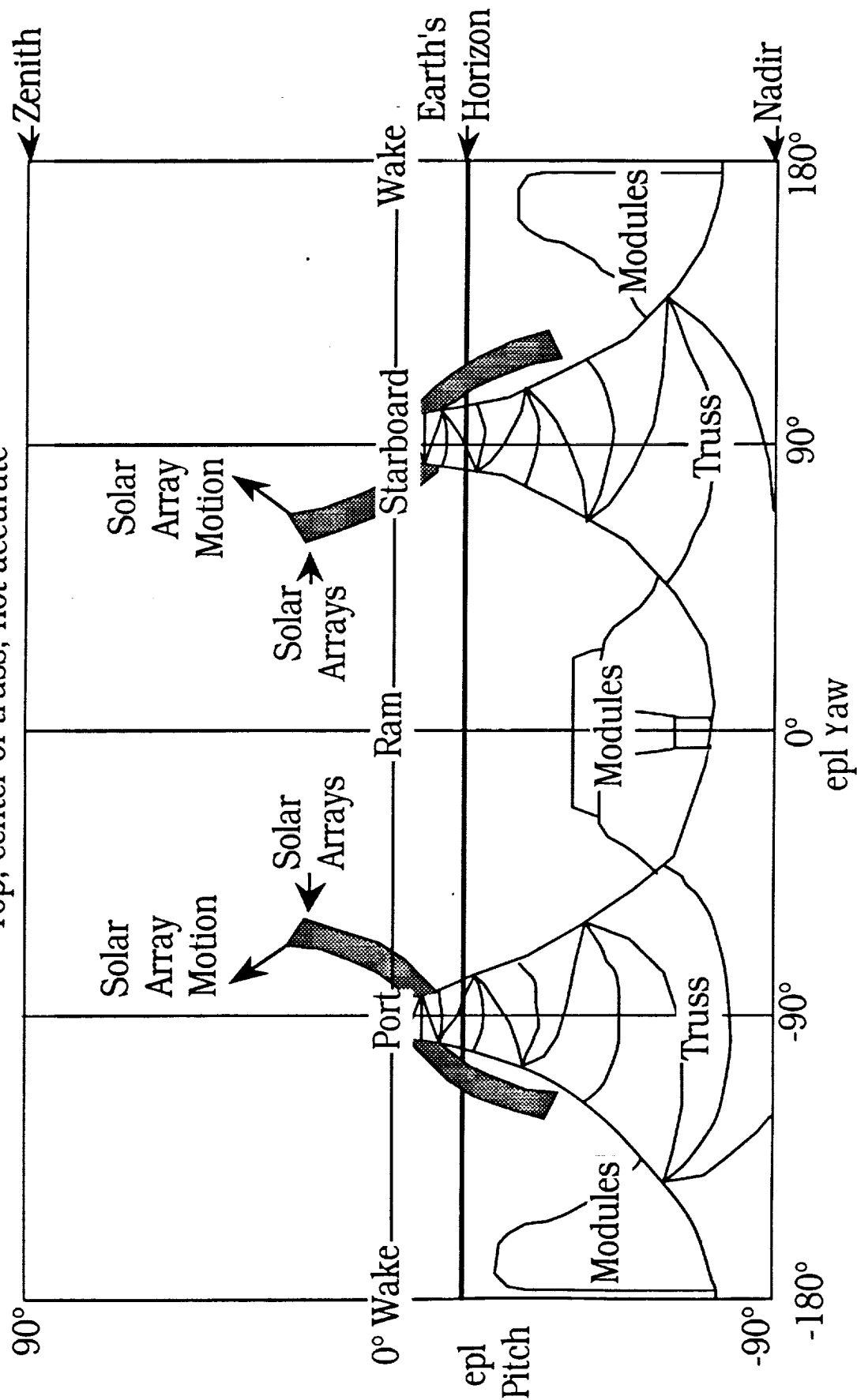
Factors Influencing  
Vent Design

Kevin Schaefer  
(703) 487-7088

Date: 1-30-91

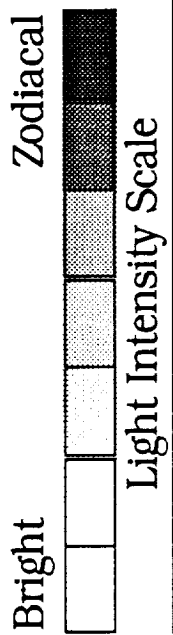
Page: 12

Top, center of truss; not accurate

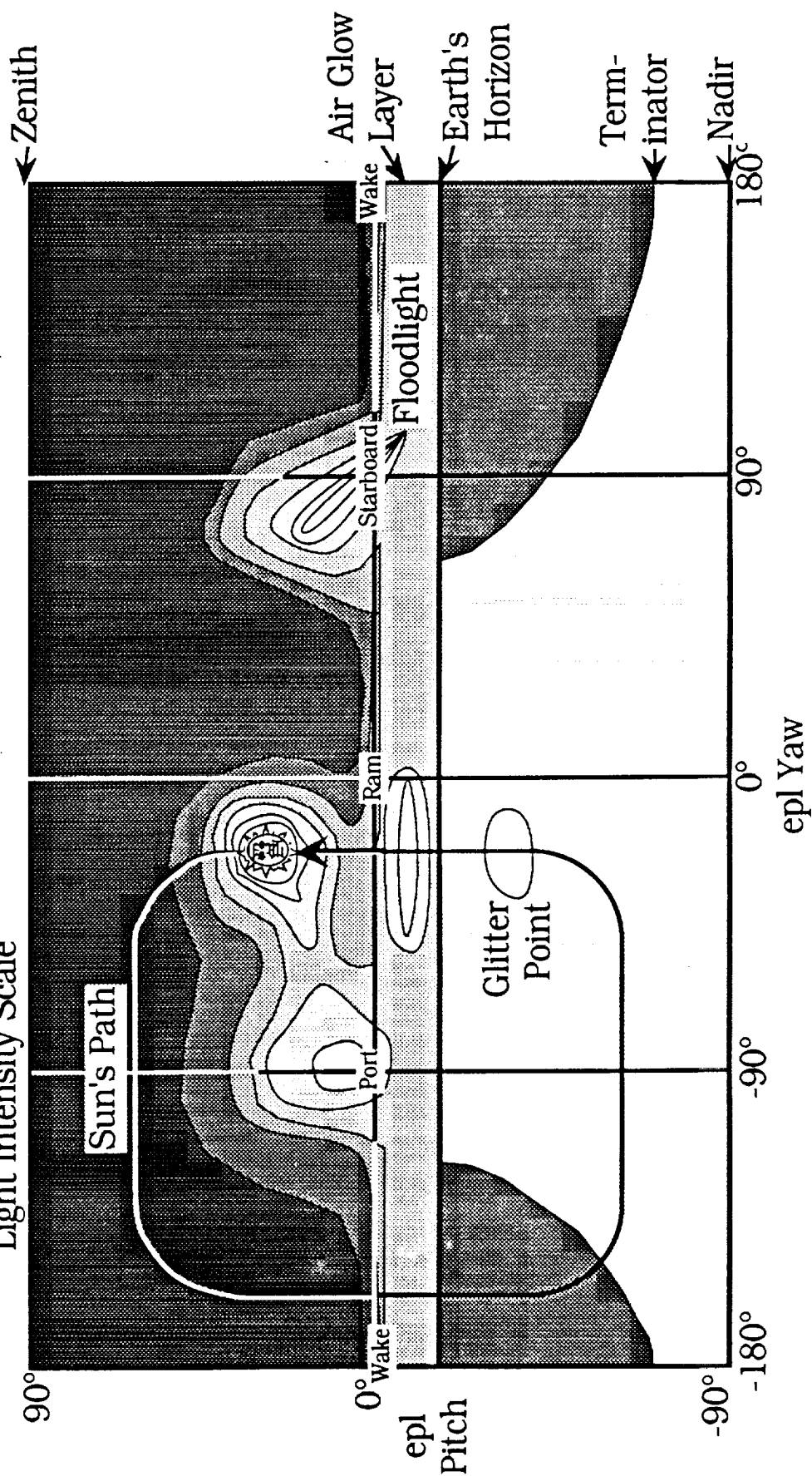




	<b>Background Spectral Irradiance</b>		<b>Factors Influencing Vent Design</b>	
	Kevin Schaefer (703) 487-7088		Date: 1-30-91	
		Page: 13		



Not Accurate





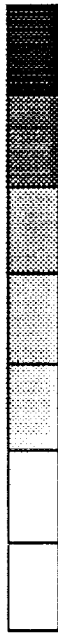
# Molecular Column Density

Factors Influencing  
Vent Design

Kevin Schaefer  
(703) 487-7088

Date: 1-30-91  
Page: 14

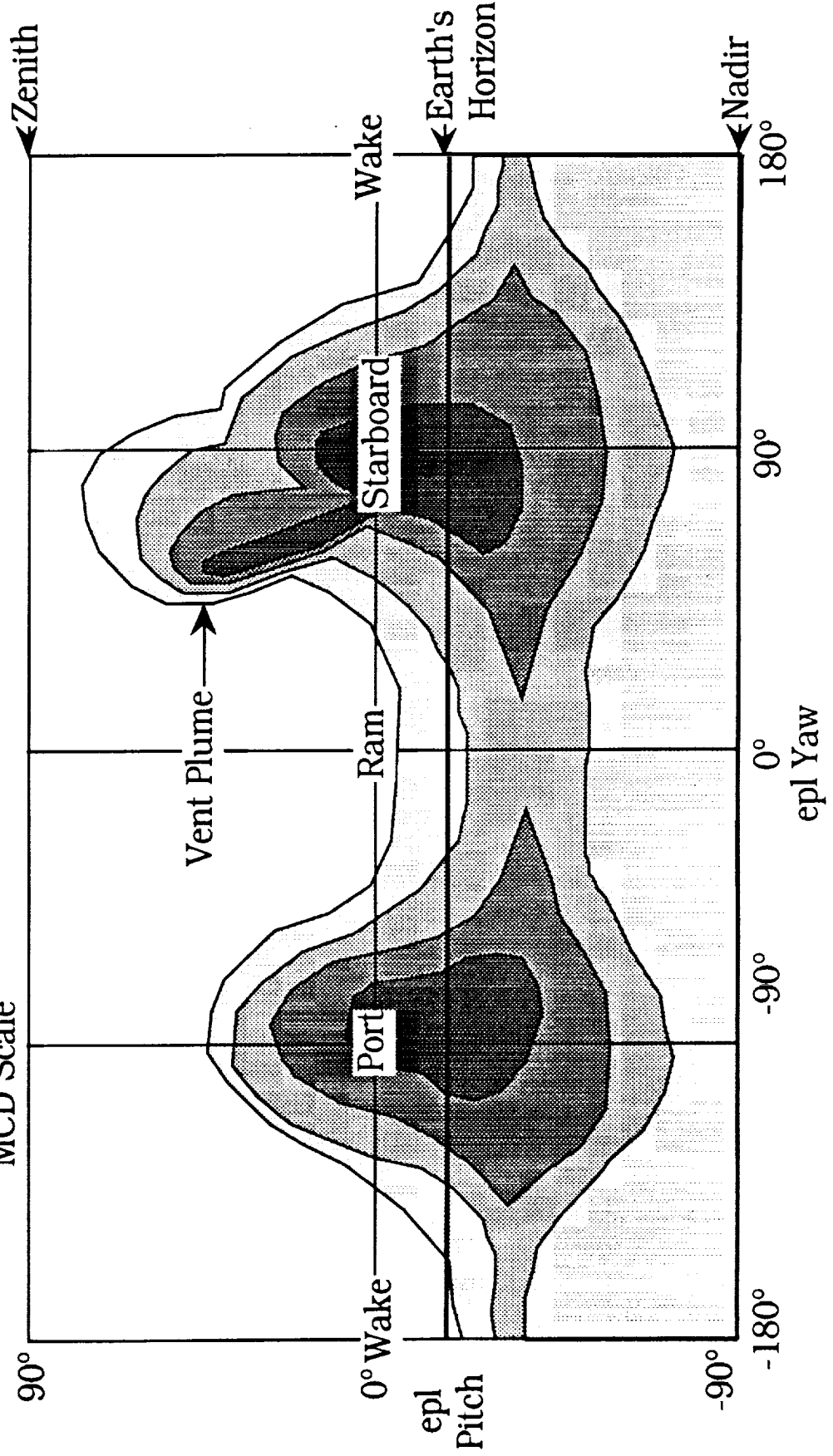
Low





MCD Scale


High

Top, center of truss; not accurate



	Other Considerations		Factors Influencing Vent Design	
			Kevin Schaefer (703) 487-7088	Date: 1-30-91
			Page: 15	
<ul style="list-style-type: none"><li>• Plume ionization:<ul style="list-style-type: none"><li>•• Arcing, EMI, light scattering and molecular deposition</li></ul></li><li>• System servicing:<ul style="list-style-type: none"><li>•• ORU accessibility, fluid replenishment</li></ul></li><li>• Crew safety</li></ul>				

	<h2>General Conclusions</h2>	<h3>Factors Influencing Vent Design</h3>	
Kevin Schaefer (703) 487-7088		Date: 1-30-91	Page: 16
<ul style="list-style-type: none"><li>• Balance requirements, design parameters, and cost<ul style="list-style-type: none"><li>•• Operational constraints</li><li>•• Plume direction</li><li>•• Nozzle design</li><li>•• Location</li><li>•• Vented materials composition</li></ul></li><li>• Consider the additive effects of all vents</li><li>• Include ram/wake interactions</li><li>• Include reactions between species</li></ul>			

	<b>Specific Conclusions</b>	<b>Factors Influencing Vent Design</b>	
Kevin Schaefer (703) 487-7088		Date: 1-30-91	Page: 17
<ul style="list-style-type: none"><li>• <b>Direction:</b><ul style="list-style-type: none"><li>•• Thrust through CG</li><li>•• Away from sensitive surfaces and ram</li><li>•• Towards horizon or Earth</li></ul></li><li>• <b>Location:</b><ul style="list-style-type: none"><li>•• Away from <math>\mu</math>-g payloads</li></ul></li><li>• <b>Nozzle design:</b><ul style="list-style-type: none"><li>•• Minimize plume "spread" and thrust</li></ul></li><li>• <b>Operations:</b><ul style="list-style-type: none"><li>•• Limit vent operation in quiescent periods</li><li>•• Coordinate vent operations</li></ul></li></ul>			



## What Next?

### Factors Influencing

#### Vent Design

Kevin Schaefer  
(703) 487-7088

Date: 1-30-91

Page: 18

- Compile complete vent list:
  - Vent location and direction
  - Plume characteristics, thrust profile (forcing function)
  - Vented material composition and mass flow rate
  - Operation frequency/duration
- Identify sensitive surfaces (Prime Measurement Points)
  - Size, shape, orientation, location, maximum deposition
  - Payload viewing locations
- Define consistent computer models
- Report at  $\mu$ -g Workshop, February 28-March 1



**JHU/APL**

**Vehicle Interaction  
and  
Spacecraft Contamination Activities**

**Ching I. Meng & Robert E. Erlandson**

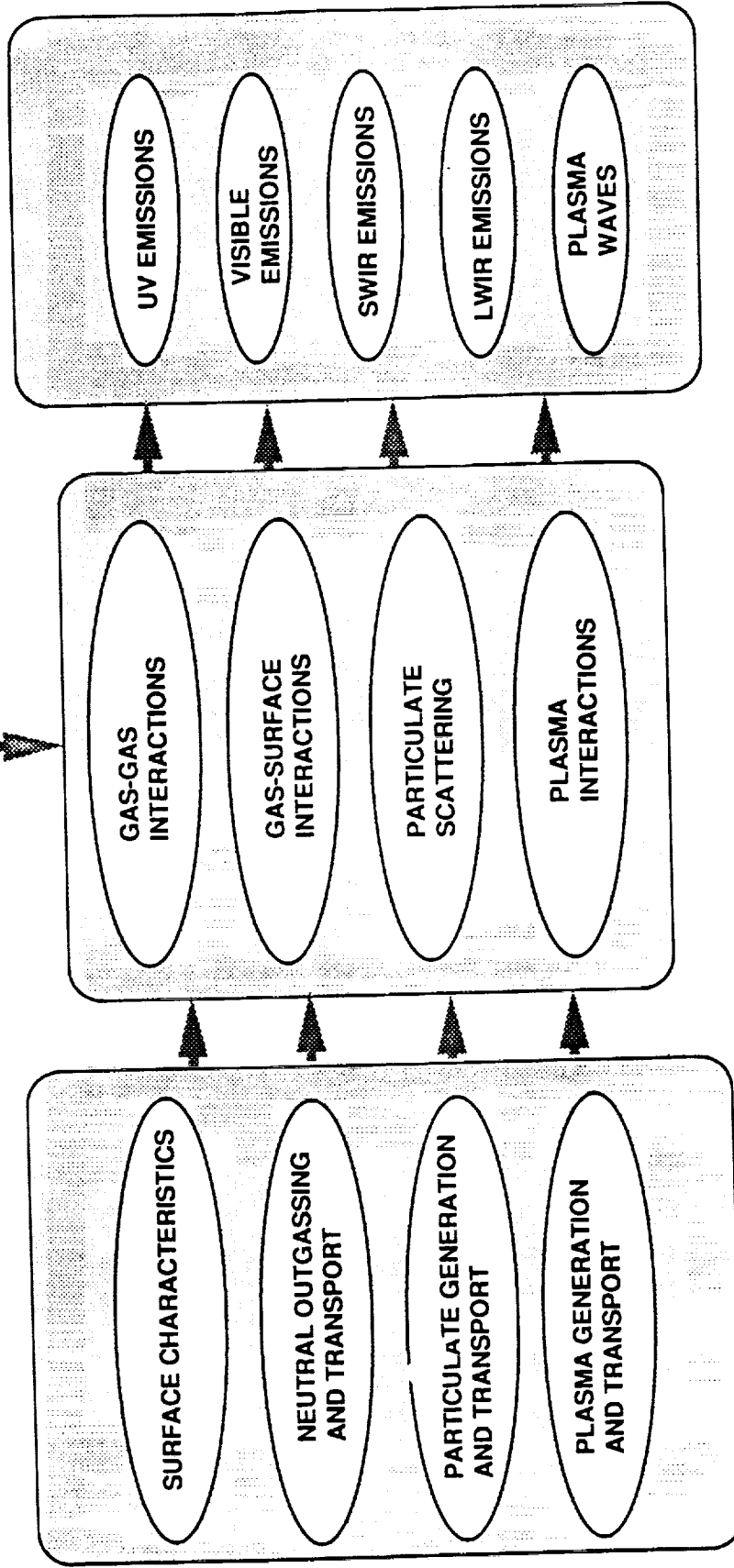
**Workshop on the Induced Environment of Space Station Freedom**

**January 30-31, 1991**



# PROGRAM PARADIGM

*Natural environment*







## **Vehicle Interactions Topics**

---

### **Research Areas:**

**Data Analysis**

**Laboratory Experiments**

**Modeling and Simulations**

**Theoretical Studies**



## Data Analysis Activities

<u>Investigator:</u>	<u>Objectives:</u>
J. Yee (U. Mich)	Spectral variation with altitude, surface temperature dependence, variation with time after launch, and ram angle dependence
J. Yee (U. Mich)	Investigation of high resolution glow spectra
G. Swenson (LMSC)	Investigation of role of OH and collisional excitation of H <sub>2</sub> O by O(3P)
D. Torr (SEA)	Analysis of EUV and VUV data. Investigation of LBH bands of N <sub>2</sub>
D. Torr (SEA)	Investigation of LBH bands of N <sub>2</sub> through comparison of ISO and S3-4 data



## Modeling and Simulations

<u>Investigator:</u>	<u>Objective:</u>
Y. Chiu (LMSC)	Particulate contamination modeling
D. Strickland (CPI)	Ambient environment model of neutral atmosphere, ionospheric density, and magnetic field strength.
D. Strickland (CPI)	Particulate Mie scattering model
D. Torr (SEA)	Interaction-chemistry model (ISEM)
M. Pervaiz (SSI)	Neutral contamination and interaction modeling (DSMC)
J. Raitt (USU)	Neutral contamination and interaction modeling



## Theoretical & Mechanism Studies

<u>Investigator:</u>	<u>Organization:</u>	<u>Objectives:</u>
P. Swaminathan	CPI	Theoretical calculations of cross sections for O + H <sub>2</sub> O vibrational excitations
G. Swenson	LMSC	OH, N <sub>2</sub> , and NO emission studies
D. Hastings	MIT	Water cloud electrodynamics
D. Torr	SEA	N <sub>2</sub> LBH emission studies
T. Slanger	SRI Intl.	OH, N <sub>2</sub> , NO, and O <sub>2</sub> emission studies
C. Goertz	U. Iowa	Neutral - Plasma interactions



## Laboratory Experiments

<u>Lab Experiment:</u>	<u>Organization:</u>	<u>Objectives:</u>
Neutral Beam Experiments	M. Fraser (PSI)	UV-IR glow due to O or N <sub>2</sub> beam bombardment of materials
Charged Particle Beam Exp.	R. Benson (APL), N. Tolk (Vanderbilt U.)	UV-Visible glow due to e- and ion beams on water ice and materials
Outgassing Exp.	J. Garrett (LMSC)	Material Outgassing measurements
Laboratory Glow Experiments	T. Slanger (SRI Intl.)	Determination of OH vib. levels ( $v=11-15$ ) and production effc. for N <sub>2</sub> (a' $\Pi_g$ ) generation from recomb. of N on surfaces
Particulate Charging	Y. Chiu (LMSC)	Particulate charging in plasma
Particulate Generation	D. Green (PSI)	Particulate generation under O beam bombardment



## **Recent Results: APL Sponsored Research**

---

**Results from APL funded research have been published in a number of scientific journals and have been presented at Fall AGU**



## Workshops & Conferences

---

Vehicle Environment Interaction Workshop #1      February 1989

Vehicle Interaction Program Science Workshop      June 1990

Vehicle Environment Interactions Conference      March 1991

March 11-13, 1991 at JHU/APL

March 11-12 open to government agencies and  
their contractors



## Low Altitude Satellite

### Satellite Summary:

Launch: 1993  
Circular-Polar Orbit: 900 km  
Mission Lifetime: 4 Years

### Satellite Sensors:

Optical Sensors  
Contamination Instruments

### Contamination Instruments:

Neutral Mass Spectrometer  
Bennett Ion Mass Spectrometer  
Quartz Crystal Microbalance (QCM)  
Pressure Sensor  
Xenon Lamp (Particulate Experiment)  
Krypton Lamp (Water Vapor Monitor)  
Mirror Cleaning Experiment (CO<sub>2</sub> Laser)





## Contamination Experiment

### Neutral Mass Spectrometer: University of Michigan

Mass Range: 2-150 amu  
Scan Rate: 0.17 s/amu

Sensitivity:  $10E+8$  #/cm<sup>2</sup>s  
Maximum Flux:  $10E+17$  #/cm<sup>2</sup>s

### Bennett Ion Mass Spectrometer: Ideas, Inc.

Mass Range: 1-56 amu  
Scan Rate: 2s/spectrum

Ion Sensitivity: 20 ions/cm<sup>3</sup>  
Scan Rate: 2 seconds/spectrum

### Pressure Sensor: Sentran

Range:  $1x10E-5$  to  $1x10E-10$  Torr      Rate: 5 Samples/s

### Quartz Crystal Microbalance:

Sensitivity:  $2x10E-9$  to  $2x10-4$  g/cm<sup>2</sup>

### Krypton Lamp/ OH Radiometer: Visidyne, Inc.

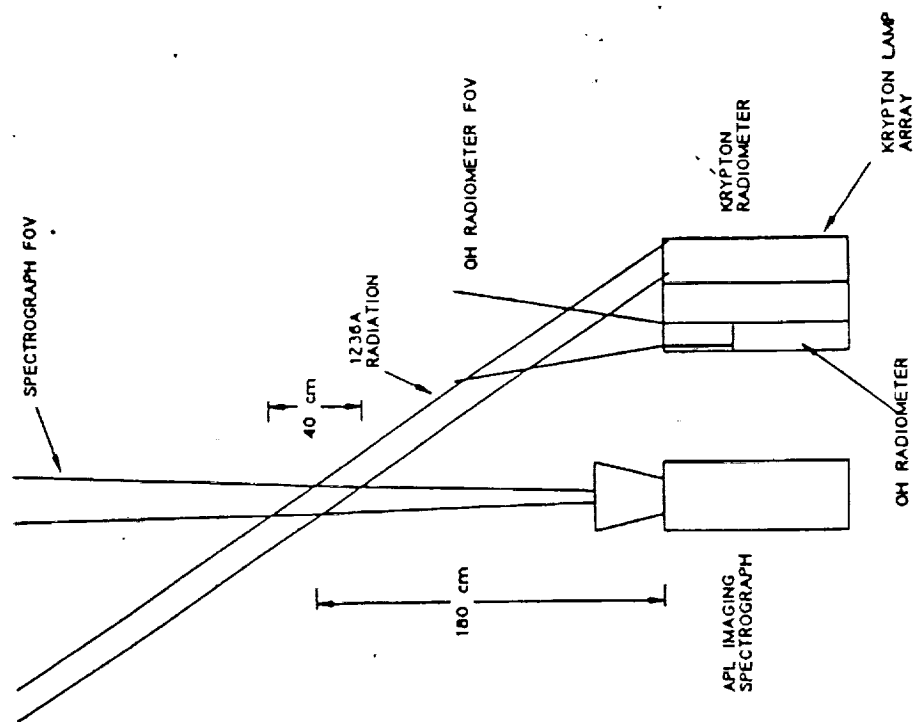
H<sub>2</sub>O Concentration Sensitivity:  $3x10E+6$  cm<sup>-3</sup>  
Dynamic Range:  $2x10E+4$

### Xenon Lamp/ Particulate Detection: Visidyne, Inc.

Minimum Particulate Size: 0.5  $\mu$ m

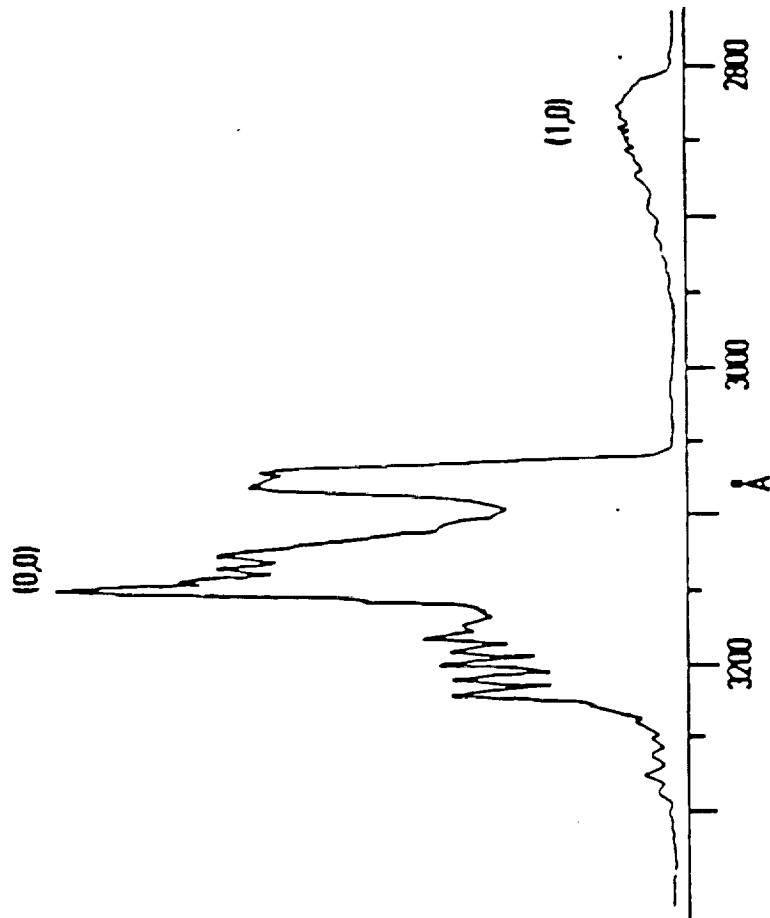


# Krypton Lamp Water Vapor Measurement Geometry





## Krypton Lamp OH (A-X) Emission Spectrum



Emission Results from the photodissociation  
of H<sub>2</sub>O with 1236 Å radiation



# Xenon Lamp Particulate Measurement Geometry

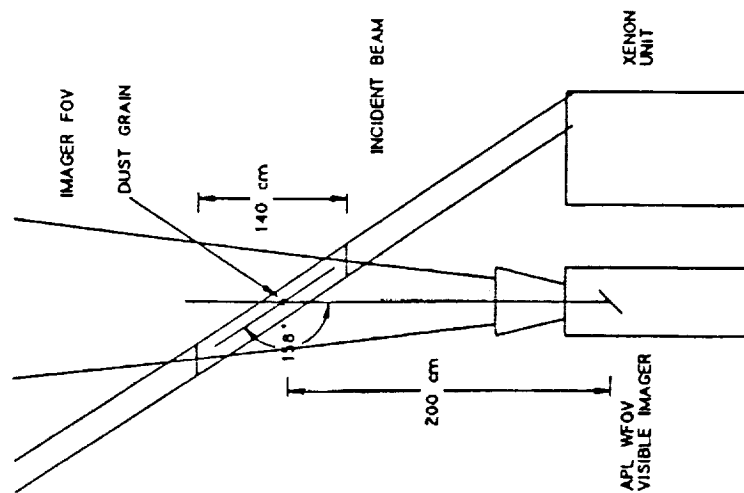


TABLE III  
MASS LOSS AND THICKNESS LOSS FOR  
AO171 COMPOSITE SAMPLES

<u>Composite Materials</u> <u>(No. of Specimens)</u>	<u>Mass Loss</u> <u>per Area</u> <u>(Mg/Cm<sup>2</sup>)</u>	<u>Average Thickness</u> <u>Loss (Mils)</u>	<u>Atomic Oxygen</u> <u>Reactivity</u> <u>10<sup>-24</sup> Cm/Atom</u>
HMF 322/P1700/±45°	18.46	4.7 to 11.5*	(1.9 - 4.6)
HMS 934/0°	11.79	2.5**	1.0
HMS 934/90°	11.31	2.7	1.1
P75S/934/90°	11.27	2.7	1.1
P75S/934/0°	10.29	2.8	1.1
"S" Glass-epoxy	2.40	0.36***	.14
Thermal Control Aluminized Taped "S" Glass-epoxy	0.59	Indeterminate	--

\* Matrix erosion much greater than fiber

\*\* Average of rates from 2 ends of sample; contamination likely on forward end

\*\*\* Fibers uneroded and become protective after initial matrix mass loss

ORGANIZATION:  CHART NO.:	EH11   	MARSHALL SPACE FLIGHT CENTER SPACE STATION INDUCED ENVIRONMENTS WORKSHOP	NAME: DR. ANN F. WHITAKER  DATE: JANUARY 30, 1991
<p style="text-align: center;">           SUMMARY OF GENERAL SPACE ENVIRONMENTAL EFFECTS            ON MATERIALS NOTED ON EXP. AO171         </p> <ul style="list-style-type: none"> <li>             O REEMPHASIZES THE NEED TO THERMAL/VACUUM BAKE MATERIALS TO CONTROL CONTAMINATION           </li> <li>             O ATOMIC OXYGEN EROSION GENERALLY AS EXPECTED           </li> <li>             O ATOMIC OXYGEN EFFECTS DOMINATE FOR MATERIALS THAT ARE BOTH AO AND UV SUSCEPTIBLE           </li> <li>             O HIGH SERIES RESISTANCE NOTED IN SOLAR CELLS           </li> <li>             O HIGH DENSITY OF MICROMETEOROID/SPACE DEBRIS IMPACTS HAVE IMPLICATIONS FOR MIRRORS, PROTECTIVE COATINGS, PAINTS, AND COMPOSITES           </li> <li>             O NEW SYNERGISTIC EFFECTS NOTED             <ul style="list-style-type: none"> <li>- AO + CONTAMINATION</li> <li>- FLUORESCENCE IN MANY MATERIALS</li> </ul> </li> </ul>			

ORGANIZATION:		MARSHALL SPACE FLIGHT CENTER		NAME:	ROGER LINTON
CHART NO.:		LDEF EXPERIMENT A0034		DATE:	JANUARY 1991
EH12					

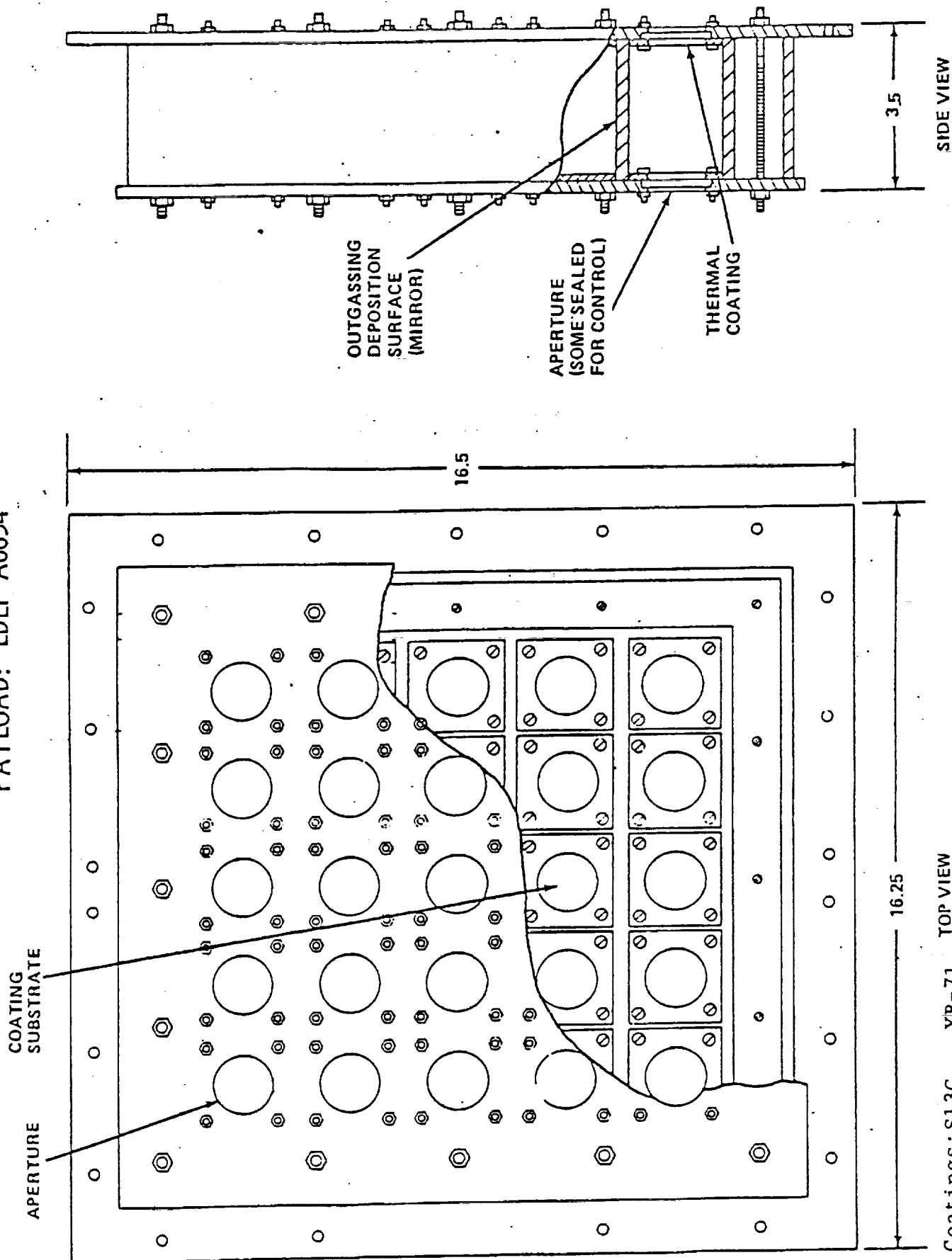
"ATOMIC OXYGEN STIMULATED OUTGASSING"

INVESTIGATORS: R. LINTON/EH12  
R. SCOTT/SOUTHERN UNIVERSITY

OBJECTIVE: EVALUATE ROLE OF ATOMIC OXYGEN IN  
THE DEGRADATION AND OUTGASSING OF  
THERMAL CONTROL COATINGS

APPROACH: PASSIVE CONTROLLED EXPOSURE OF SELECTED  
THERMAL CONTROL COATINGS ON THE LEADING  
(RAM) AND TRAILING (WAKE) EDGES  
OF THE LDEF, WITH CONTAMINANT COLLECTOR  
MIRRORS.

ATOMIC OXYGEN STIMULATED-OUTGASSING  
PAYLOAD: LDEF-A0034



Coatings: S13G YB-71 TOP VIEW  
S13GLO Z306  
.Z93 AZ76



ORGANIZATION:		MARSHALL SPACE FLIGHT CENTER		NAME:	
EH12				ROGER LINTON	
CHART NO.:		LDEF EXPERIMENT A0034		DATE:	
				JANUARY 1991	

"ATOMIC OXYGEN STIMULATED OUTGASSING"

1. S-13G (IITRI)
2. S-13G-LO (IITRI)
3. ZINC ORTHOTITANATE  $Zn_2TiO_4$
4. CHEMGLAZE-A276
5. CHEMGLAZE-Z-306
6. Z-93

ORGANIZATION:	EH12	MARSHALL SPACE FLIGHT CENTER	NAME:	ROGER LINTON
CHART NO.:		A0034	DATE:	SEPTEMBER 1991

# OPTICAL PROPERTIES OF TOP COVER (ANODIZED ALUMINUM)

## LEADING EDGE

## TRAILING EDGE

### EXPOSED FRONT

### EXPOSED FRONT

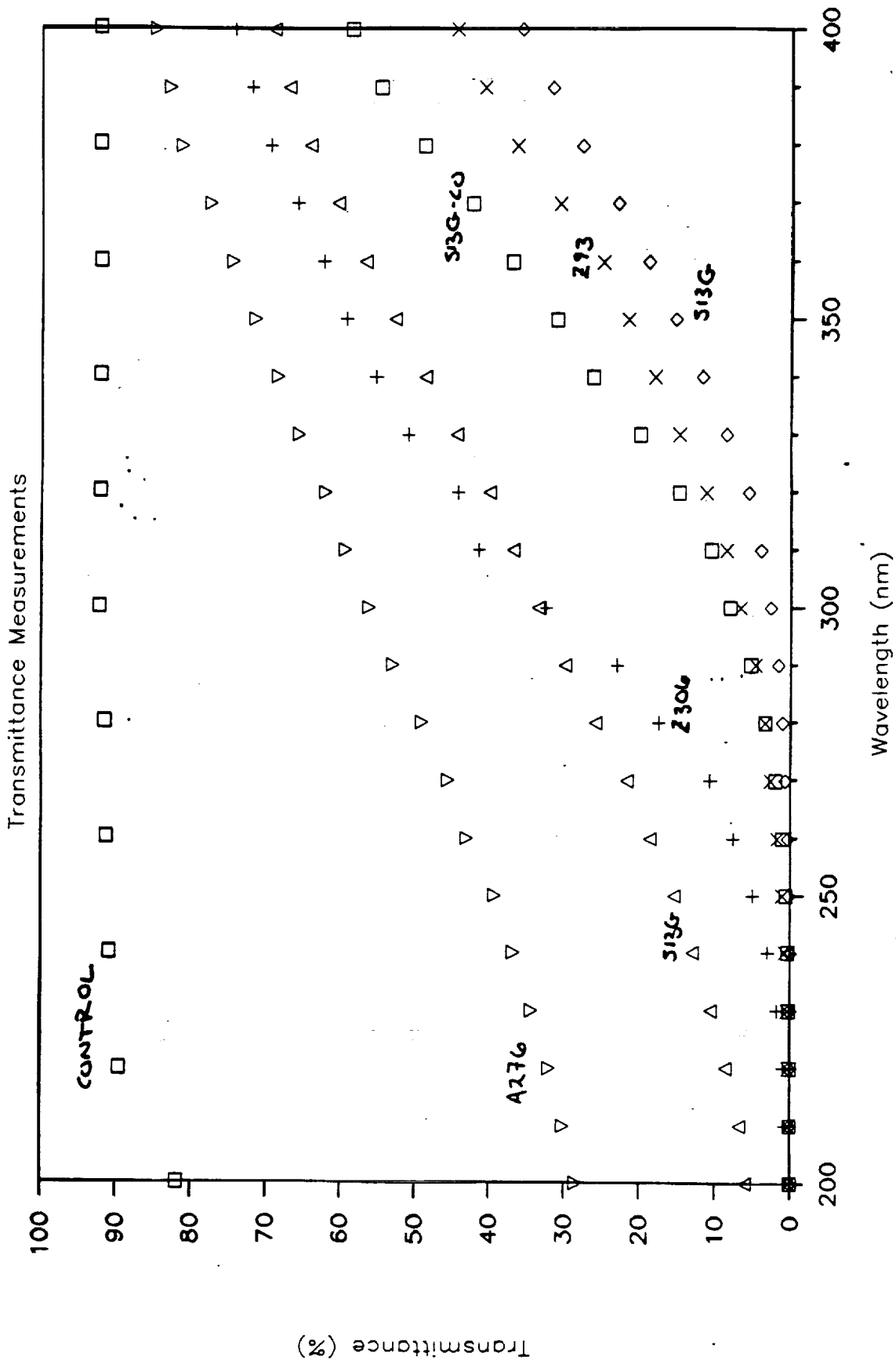
$\alpha_s$	$\epsilon_{FR}$	$\alpha_s$	$\epsilon_{FR}$
0.35-0.42	0.11-0.16	0.46-0.49	0.09-0.165
MEAN 0.38	0.13	MEAN 0.47	0.13

### UNEXPOSED BACK

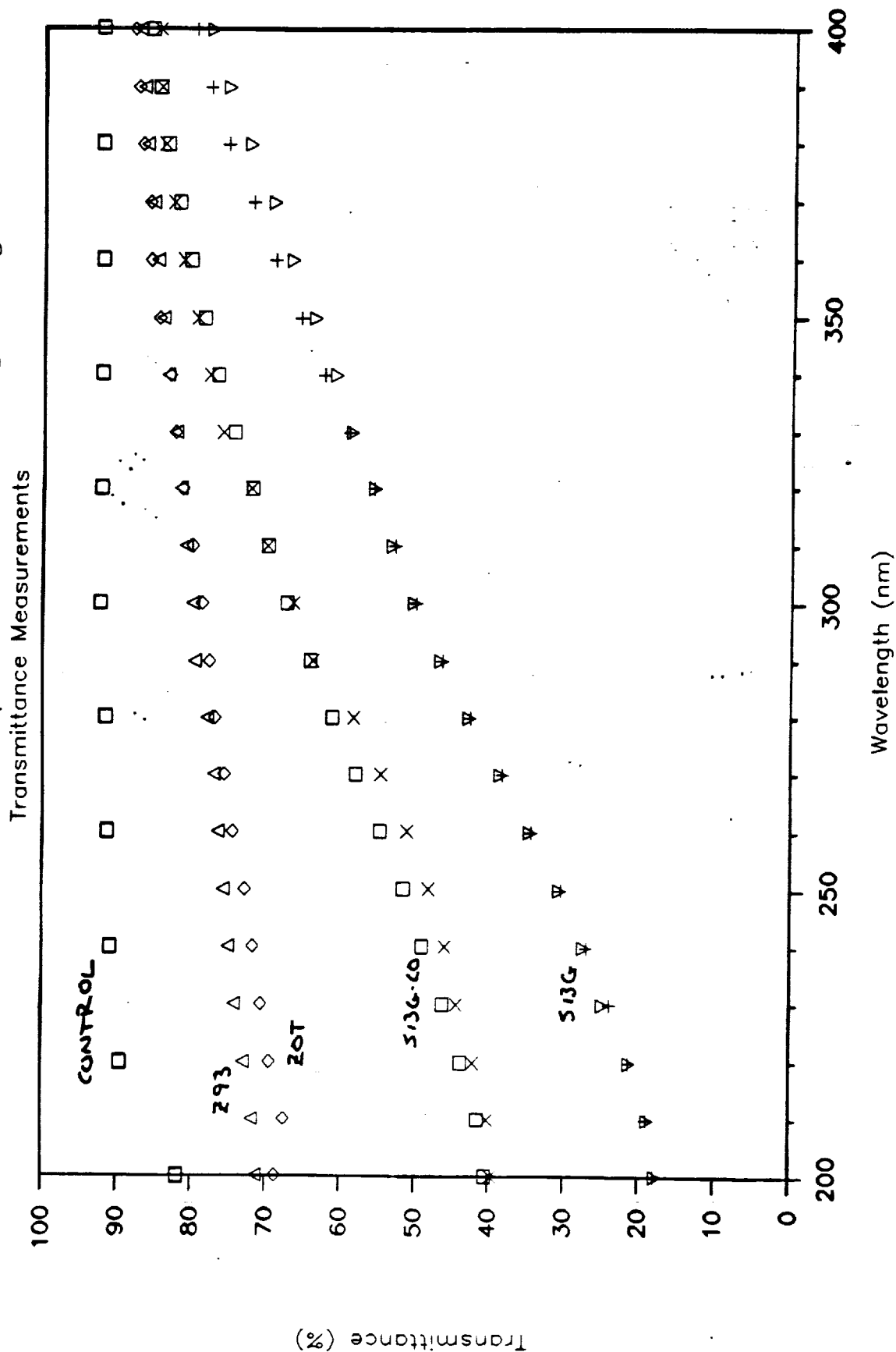
### UNEXPOSED BACK

0.40-0.46	0.13-0.16	0.40-0.50	0.08-0.176
MEAN 0.42	0.15	MEAN 0.45	0.14

# A0034 UV WINDOWS - Leading Edge



# A0034 UV WINDOWS - Trailing Edge



ORGANIZATION:	EH12	MARSHALL SPACE FLIGHT CENTER AO034	NAME: R. C. LINTON
CHART NO.:		"ATOMIC OXYGEN STIMULATED OUTGASSING"	DATE: SEPTEMBER 1990

SUMMARY OF RESULTS

SOLAR ABSORPTANCE MEASUREMENTS ( $\alpha_s$ )

LDEF LEADING EDGE

EXPOSURE:	<u>OPEN</u>	<u>COVERED</u>	<u>UV ONLY (WINDOW)</u>
<u>COATING</u>	<u>AVERAGE</u>	<u>AVERAGE</u>	<u>AVERAGE</u>
S13G	0.17*	0.17	0.18
S13G-LO	0.19	0.18	0.19
Z-93	0.17		0.17
ZnTiO <sub>4</sub>	0.17		
A276	0.22		0.35
Z306	0.96		0.95
<u>TRAILING EDGE</u>			
S13G	0.26	0.18	0.20
S13G-LO	0.28	0.17	0.21
Z-93	0.17	0.16	0.16
ZnTiO <sub>4</sub>	0.19	0.16	0.19

\*ONE @ 0.26

ORGANIZATION: <b>EH12</b>	MARSHALL SPACE FLIGHT CENTER <b>A0034</b>		NAME: <b>R. C. LINTON</b>
CHART NO.:	<b>"ATOMIC OXYGEN STIMULATED OUTGASSING"</b>		DATE: <b>SEPTEMBER 1980</b>

# SUMMARY OF RESULTS INFRARED EMITTANCE MEASUREMENTS ( $\epsilon_{IR}$ )

## LDEF LEADING EDGE

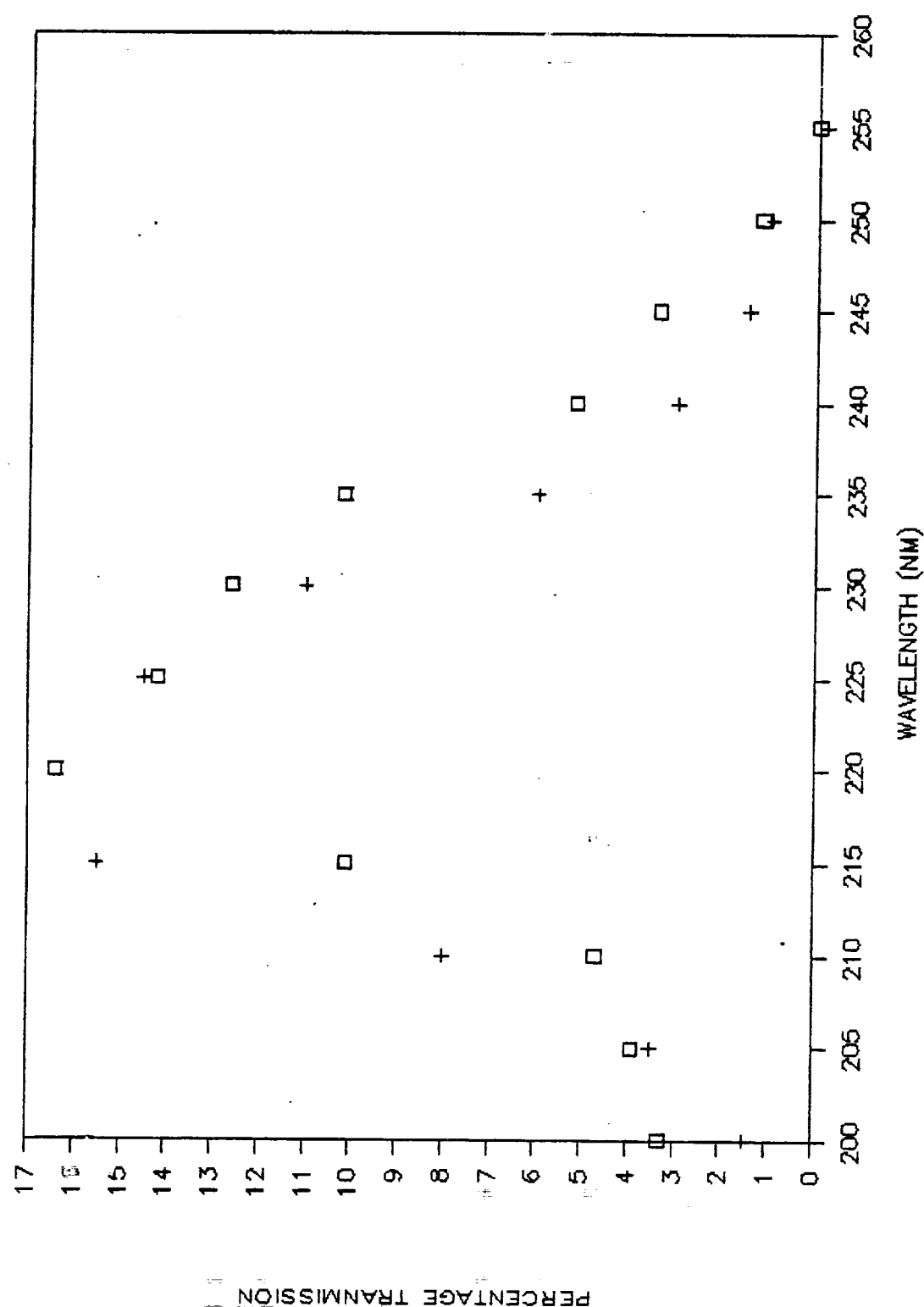
EXPOSURE:	<u>OPEN</u>	<u>COVERED</u>	<u>UV ONLY (WINDOW)</u>
	<u>AVERAGE</u>	<u>AVERAGE</u>	<u>AVERAGE</u>
S13G	0.88	0.90	0.90
S13G-LO	0.87	0.89	0.89
Z-93	0.92		0.93
ZnTiO <sub>4</sub>	0.89		
A276	0.92	0.87	0.87
Z306	0.80	0.83	0.83

## TRAILING EDGE

S13G	0.89	0.90
S13G-LO	0.91	0.89
Z-93	0.90	0.91
ZnTiO <sub>4</sub>	0.89	0.89

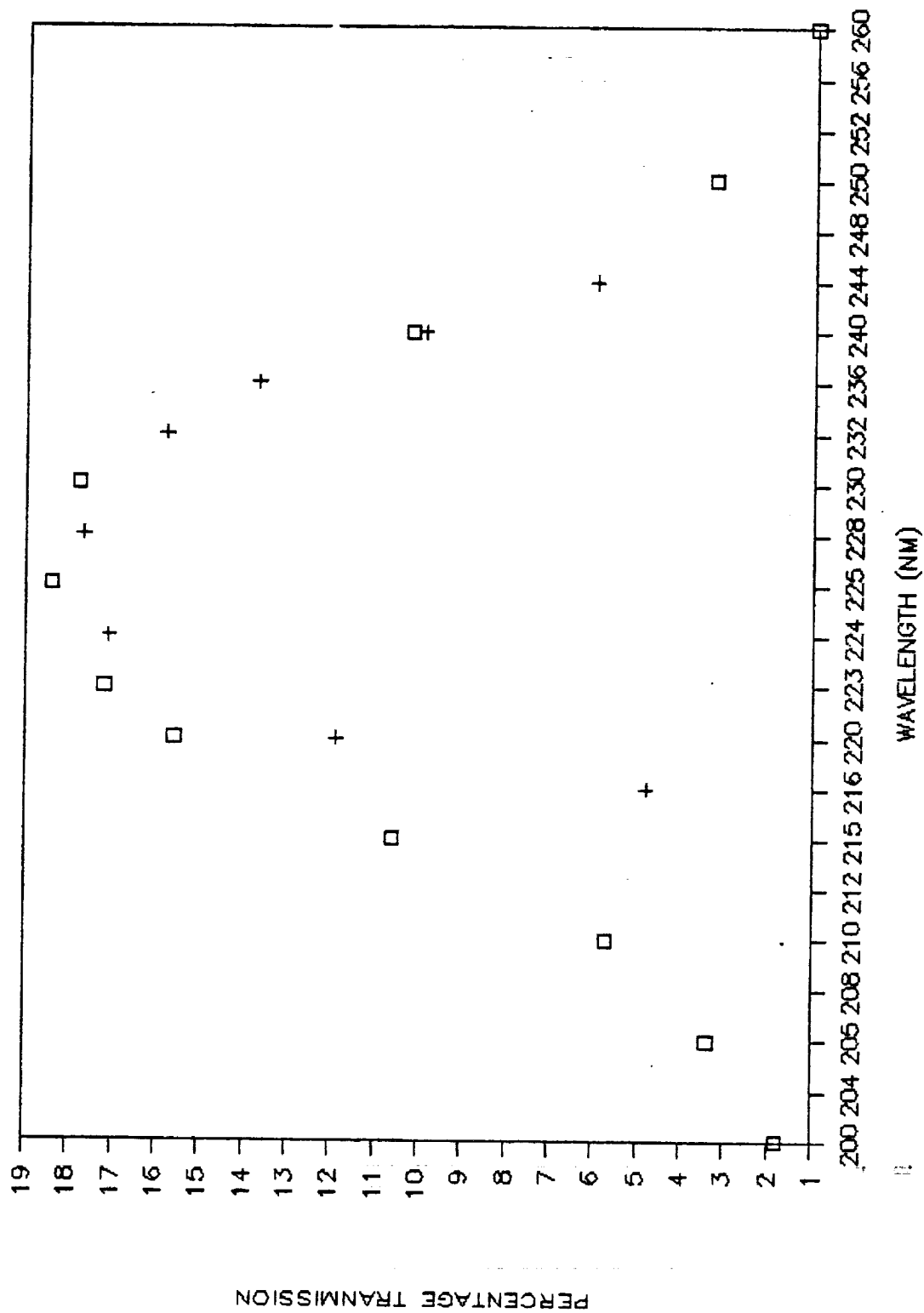
ORGANIZATION:		MARSHALL SPACE FLIGHT CENTER		NAME:		ROGER LINTON																			
CHART NO.:		LDEF EXPERIMENT A0034		DATE:		SEPT. 1990																			
<p style="text-align: center;">CONTAMINANT COLLECTOR MIRRORS EFFECTS OF THE NATURAL ENVIRONMENT</p> <table border="1"> <thead> <tr> <th>MIRROR TYPE</th> <th>LEADING EDGE</th> <th>TRAILING EDGE</th> </tr> </thead> <tbody> <tr> <td>SiO/PYREX</td> <td colspan="2" style="text-align: center;">CONTAMINANT COLORATION</td> </tr> <tr> <td>OSMIUM/QUARTZ</td> <td>TOTAL REMOVAL (60nm.) (ESTIM. REFLECTED FLUENCE= 2E20 ATOMS/CM2)</td> <td>PARTIAL REMOVAL (ESTIM. REFL. F= 1E19 ATOMS/CM2)</td> </tr> <tr> <td>SILVER/QUARTZ</td> <td>OXIDIZED/REMOVED (ESTIM. REFL. FLUENCE&gt; 1E19 ATOMS/CM2)</td> <td>OXIDIZED (ESTIM. REFL. F= 9E18 ATOMS/CM2)</td> </tr> <tr> <td>GOLD/QUARTZ</td> <td>SLIGHT VISUAL DIFF.</td> <td>NO OBVIOUS EFFECT</td> </tr> <tr> <td>MgF2/Al</td> <td>NO VISIBLE EFFECT (UV TRANSMISSION EFF.)</td> <td>NO VISIBLE EFFECT (UV %T EFFECT)</td> </tr> </tbody> </table>								MIRROR TYPE	LEADING EDGE	TRAILING EDGE	SiO/PYREX	CONTAMINANT COLORATION		OSMIUM/QUARTZ	TOTAL REMOVAL (60nm.) (ESTIM. REFLECTED FLUENCE= 2E20 ATOMS/CM2)	PARTIAL REMOVAL (ESTIM. REFL. F= 1E19 ATOMS/CM2)	SILVER/QUARTZ	OXIDIZED/REMOVED (ESTIM. REFL. FLUENCE> 1E19 ATOMS/CM2)	OXIDIZED (ESTIM. REFL. F= 9E18 ATOMS/CM2)	GOLD/QUARTZ	SLIGHT VISUAL DIFF.	NO OBVIOUS EFFECT	MgF2/Al	NO VISIBLE EFFECT (UV TRANSMISSION EFF.)	NO VISIBLE EFFECT (UV %T EFFECT)
MIRROR TYPE	LEADING EDGE	TRAILING EDGE																							
SiO/PYREX	CONTAMINANT COLORATION																								
OSMIUM/QUARTZ	TOTAL REMOVAL (60nm.) (ESTIM. REFLECTED FLUENCE= 2E20 ATOMS/CM2)	PARTIAL REMOVAL (ESTIM. REFL. F= 1E19 ATOMS/CM2)																							
SILVER/QUARTZ	OXIDIZED/REMOVED (ESTIM. REFL. FLUENCE> 1E19 ATOMS/CM2)	OXIDIZED (ESTIM. REFL. F= 9E18 ATOMS/CM2)																							
GOLD/QUARTZ	SLIGHT VISUAL DIFF.	NO OBVIOUS EFFECT																							
MgF2/Al	NO VISIBLE EFFECT (UV TRANSMISSION EFF.)	NO VISIBLE EFFECT (UV %T EFFECT)																							

# 220 N-T.E. - VS - ORIGINAL %T

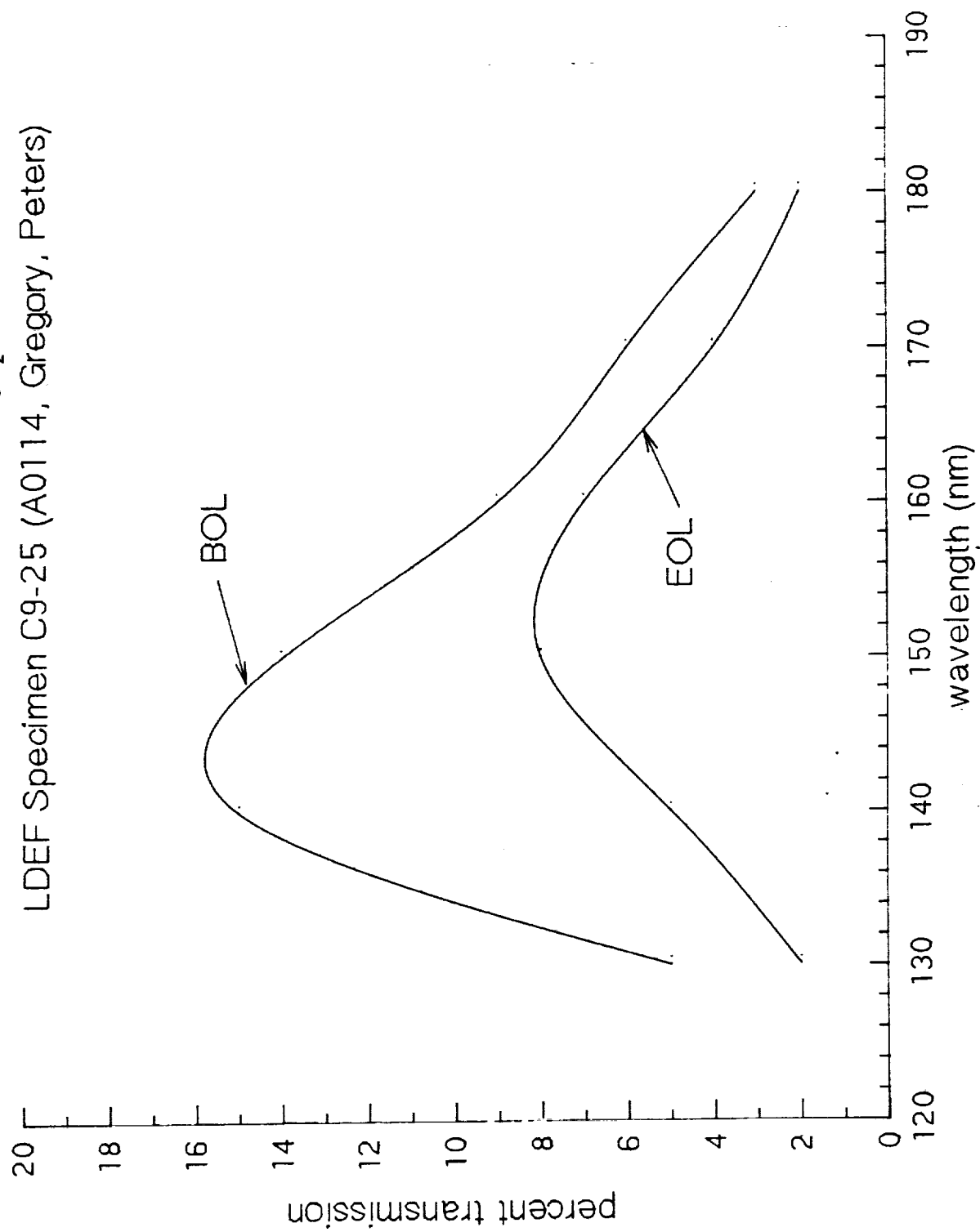


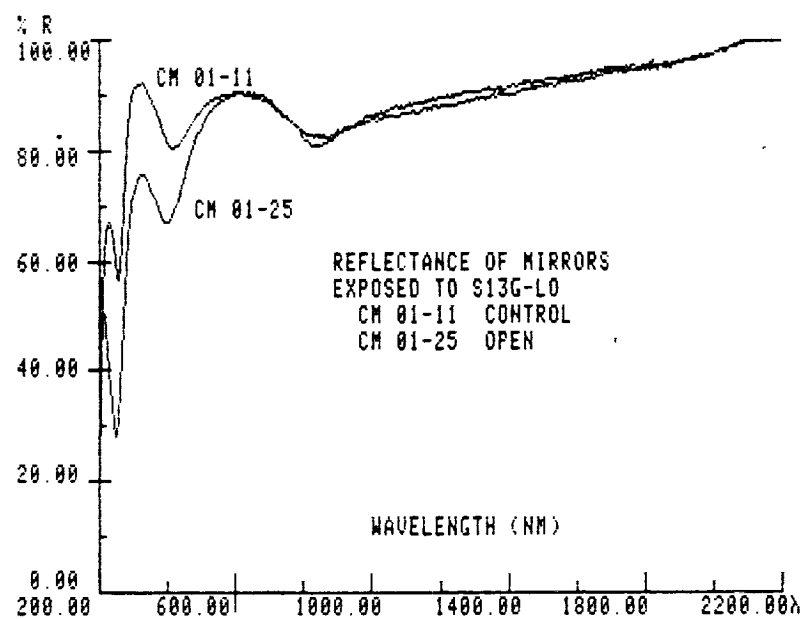


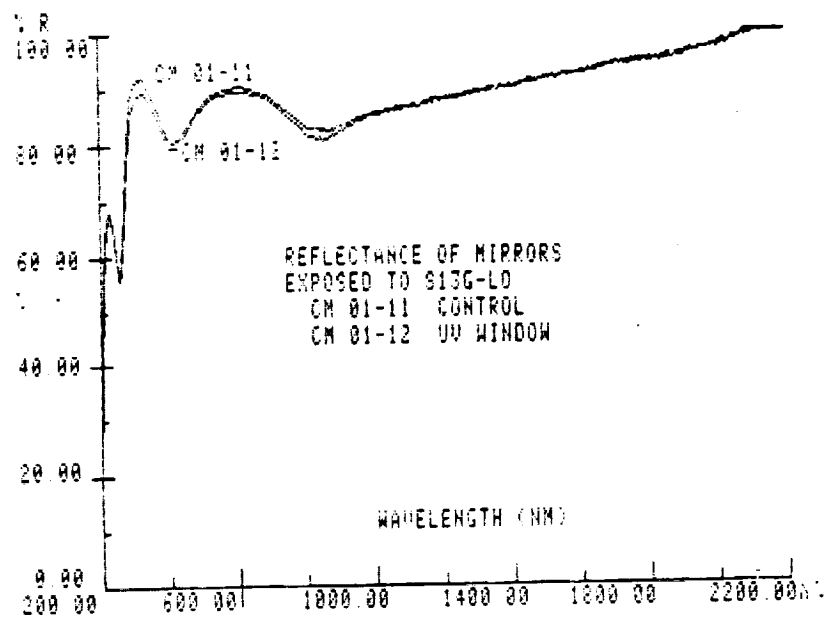
# 220 N-L.E. - V8 - Original %T

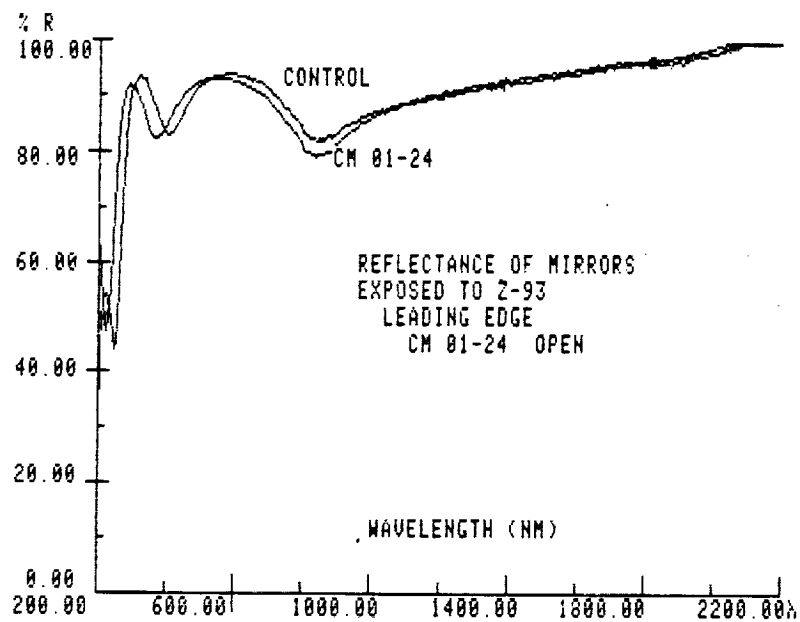


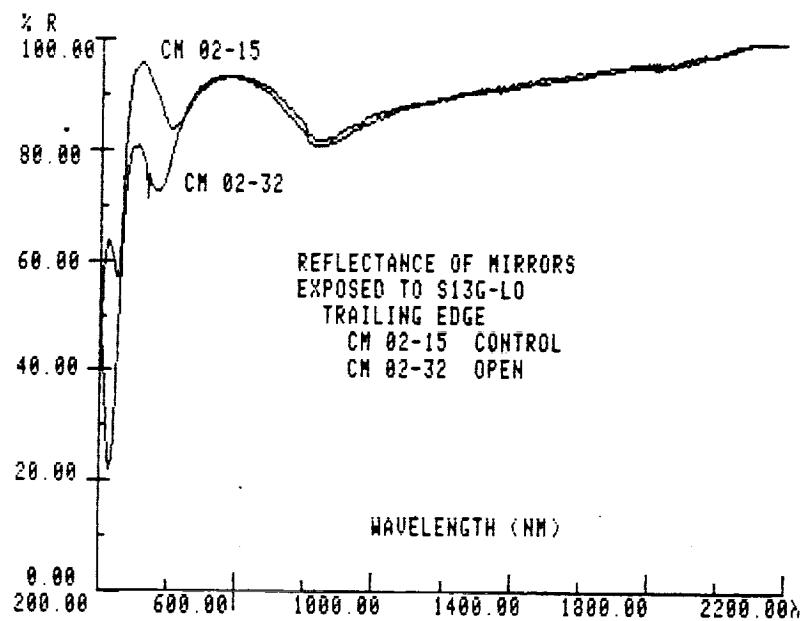
Vacuum UV Transmittance of  $\text{MgF}_2$  Filter  
LDEF Specimen C9-25 (A0114, Gregory, Peters)











# LDEF CONTAMINATION MODELING

PRESENTED BY:

R. RANTANEN AND T. GORDON

PRESENTED TO:

SPACE STATION ENVIRONMENT WORKSHOP

30 JANUARY 1991

HUNTSVILLE, ALABAMA

## OBJECTIVES

- o MODEL GAS CLOUD SURROUNDING LDEF
- o CHARACTERIZE DIFFERENT PERIODS ON ORBIT
- o DETERMINE SURFACE FLUXES OF AMBIENT, OUTGASSING AND ATOMIC OXYGEN EROSION PRODUCTS
- o EVALUATE PLUME SHAPE THROUGH OPENINGS IN EXTERNAL SURFACE OF LDEF OBSERVED ON INTERNAL SURFACES.
- o DETERMINE APPLICABILITY TO SPACE STATION AND UV IMAGER

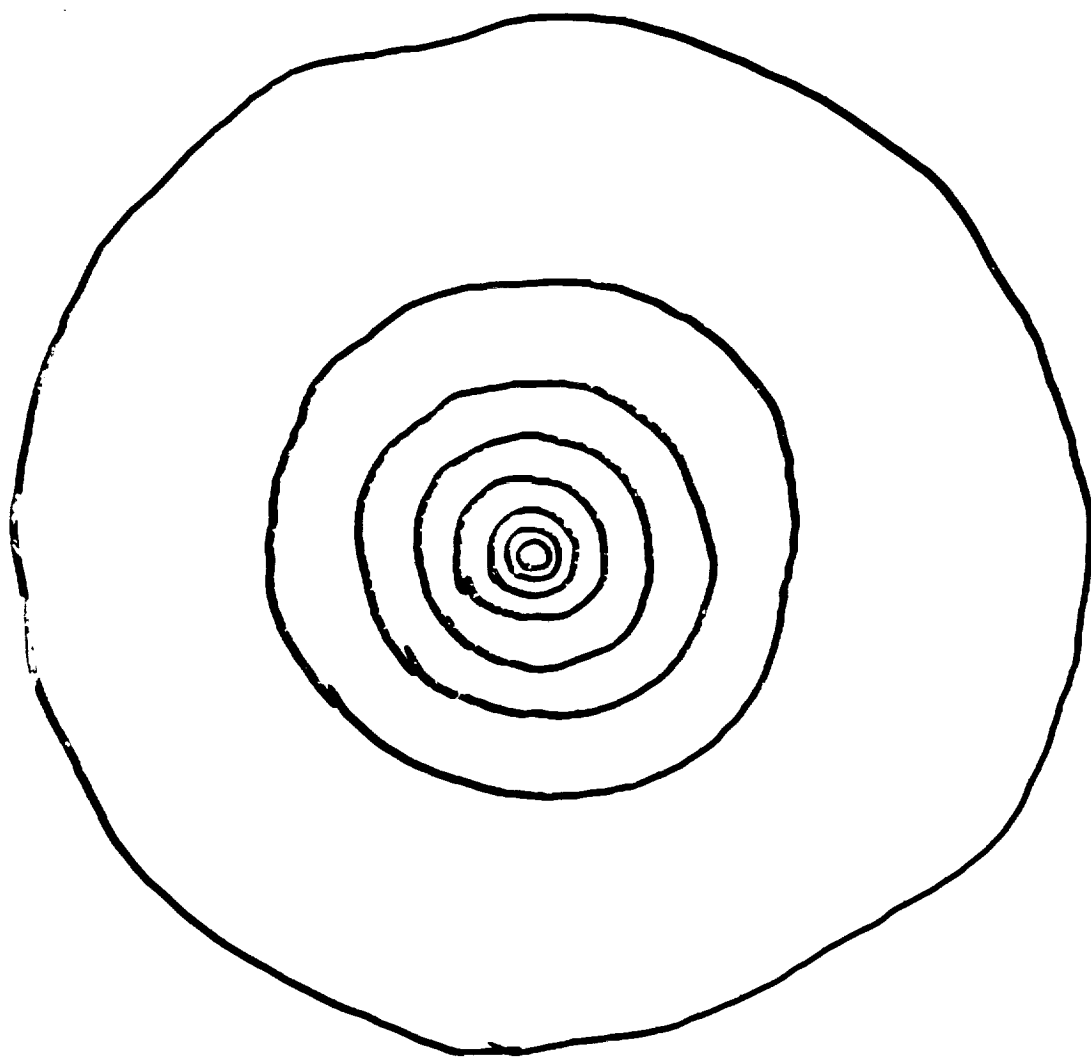


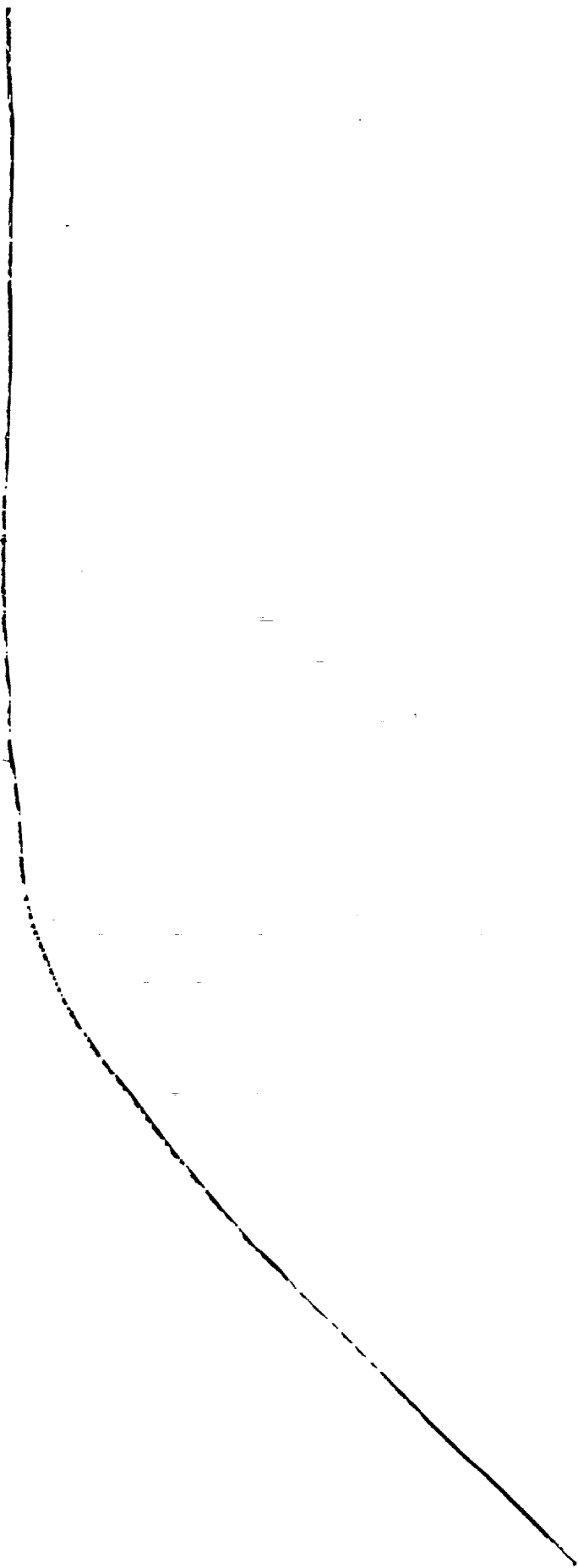
PERIODS MODELED DURING MISSION-MSIS 86

SPECIES /CM <sup>3</sup>	463KM 4/84	417KM 4/87	333KM 1/90
O	2.59(7)	3.48(7)	9.03(8)
O <sub>2</sub>	7.52(3)	1.43(4)	6.06(6)
N	6.65(5)	7.44(5)	3.28(7)
N <sub>2</sub>	4.23(5)	7.26(5)	2.03(8)
He	3.47(6)	3.85(6)	5.07(5)
H	1.63(5)	2.30(5)	2.66(4)
TOTAL	3.06(7)	4.04(7)	1.15(9)
O FLUX /cm <sup>2</sup>	2.0(13)	2.7(13)	7.0(14)

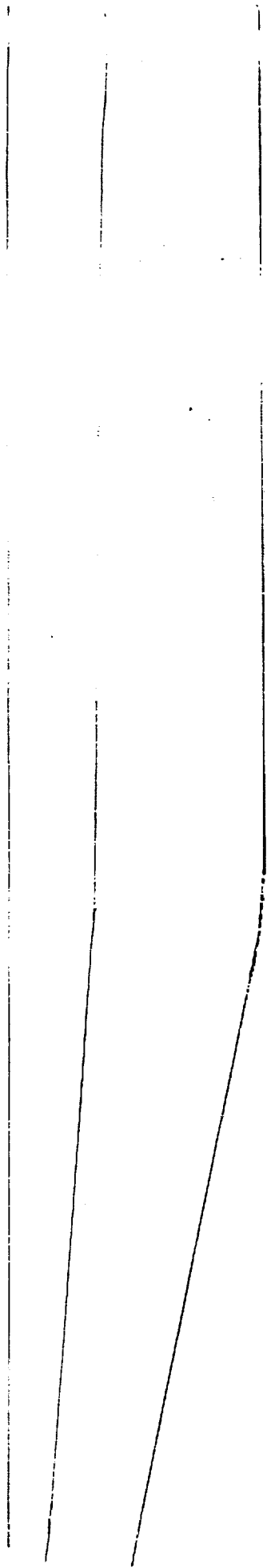
OUTGASSING AND EROSION RATES

RATE g.cm <sup>-2</sup> .sec <sup>-1</sup>	463KM	417KM	333KM
	4/84	4/87	1/90
-----			
EXTERNAL	2.0(-9)	2.6(-11)	1.4(-12)
INTERNAL	2.0(-10)	5.6(-12)	4.8(-13)
EROSION	6.3(-11)	8.5(-11)	2.2(-9)











## Summary

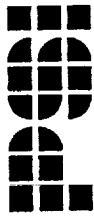
---

There is an existing program at APL whose objective is to understand vehicle interaction processes.

The research encompasses a wide variety of research topics which include understanding the source of spacecraft contamination, interactions with the spacecraft with the ambient environment, and the effects which result from these interactions.

Contamination activities at APL include a low altitude satellite which is instrumented to obtain observations of neutral gas contamination, contaminant ions, particulate contamination, and molecular contamination on satellite surfaces.

Contamination activities are designed to allow long term observations of the contamination environment of a satellite in low earth orbit



VG91-016

# **GLOWS, ACCOMMODATION, AND SURFACE RESIDENCE TIMES**

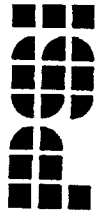
**G.E. Caledonia, K. Holtzclaw, D. Sonnenfroh, and R. Krech**

**Presented at**

**Workshop on the Induced Environment at  
Space Station Freedom**

**January 30, 1991**

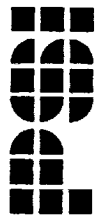




## PSI-FAST (8 km/s) O-ATOM ACTIVITIES

T-4009

- Material Erosion Studies
- Gas-Gas Interactions (visible, IR emissions)
- ★ Surface Glows (shuttle glow with A. Leone and G. Swenson, Lockheed)
- ★ Contamination Scouring
- ★ Accommodation Coefficients



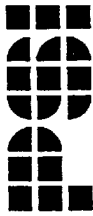
## O-ATOM BEAM

T-4010

- Utilizes pulsed laser induced breakdown of O<sub>2</sub> followed by hypersonic expansion

### Range of O-Beam Operating Characteristics

Beam Area	-	10 to 10 <sup>3</sup> cm <sup>2</sup> , ~flat radial profile
Beam Flux/Pulse	-	up to 10 <sup>15</sup> cm <sup>-2</sup> at an area 10 <sup>3</sup> cm <sup>2</sup>
Pulse Duration	-	30 to 100 μs
Velocity	-	5 to 12 km/s (selectable), ±15% spread
Atomic Content	-	>80% at 8 km/s
Ion Content	-	<1% at 8 km/s (controllable)

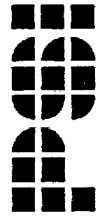


## THE SHUTTLE GLOW

T-4029

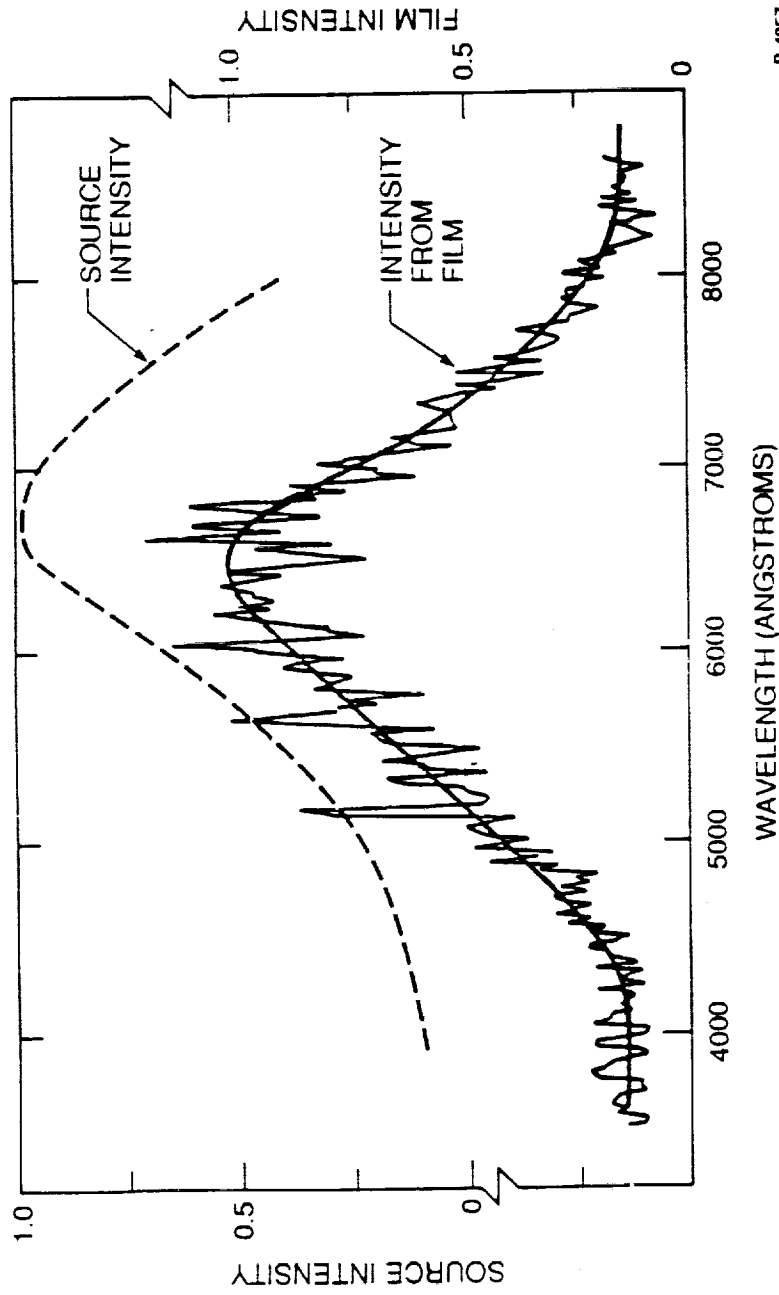
- Orange glow observed over ram surfaces in LEO
  - $\cos\theta$  law
- Scales with density
- Scales inversely with surface temperature
- Proposed mechanism – surface mediated  $\text{NO}_2$  recombination

★ See Garrett et al., J. Spacecraft 25, 321 (1988)  
Swenson et al., Nature 323, 519 (1986)



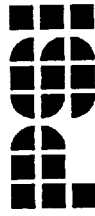
# SHUTTLE GLOW SPECTRUM STS-41D (Mende and Swenson A1AA-85-0909)

T-4030



B-4857

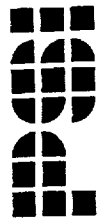
(Bottom) Six line average tracing of spacecraft glow observed with Hasselblad camera on STS-41D. The tracing has been corrected for the calibrated D-Log-E response of the film. The noise character in the data is primarily due to ion scintillations in the image intensifier which have accumulated in the image over the 30s exposure. (Top) Corrected spectrum of spacecraft glow where the instrument response has been applied to the curve drawn through the data shown in the bottom of the figure.



## LABORATORY STUDY

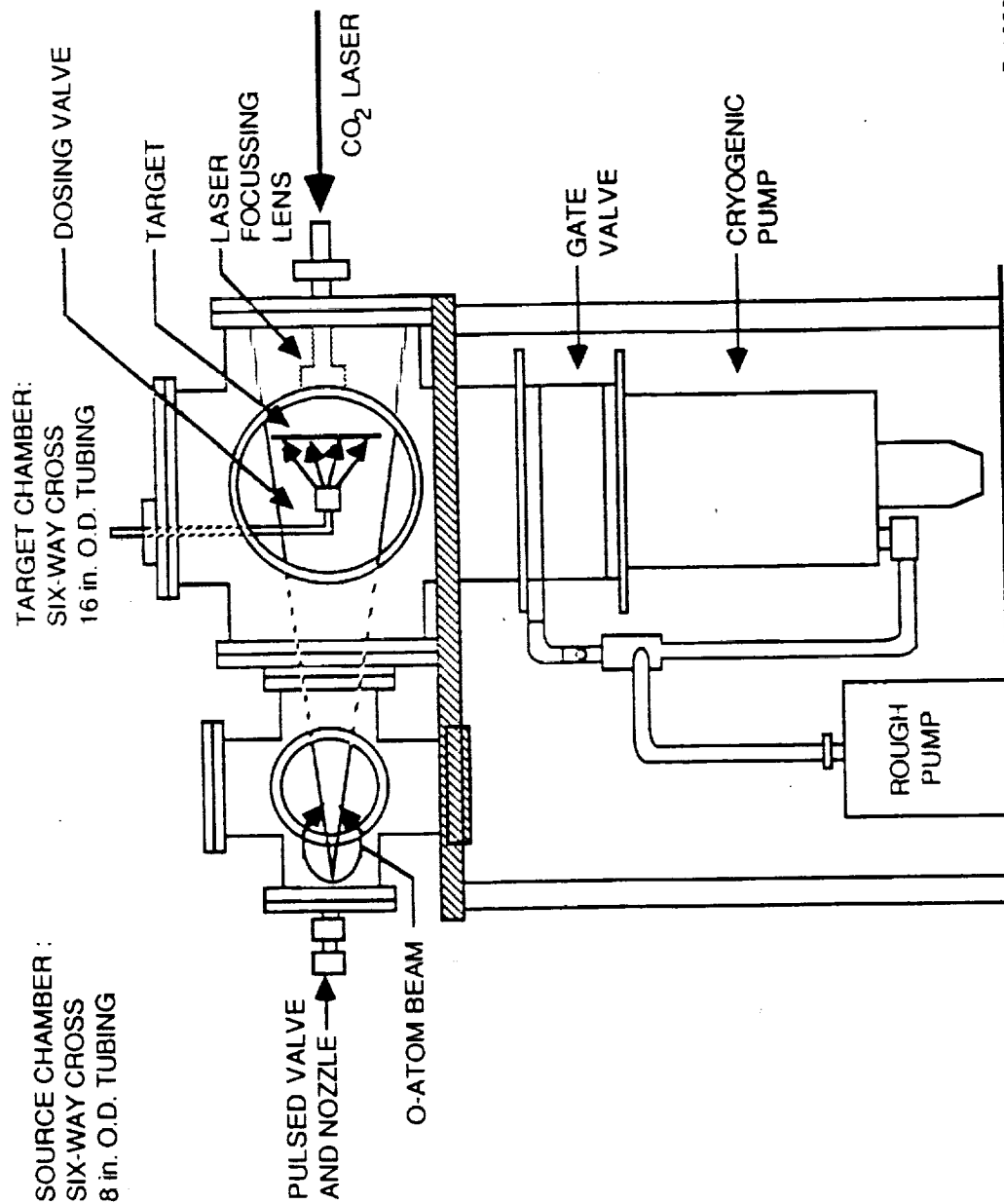
T-4031

- Test postulate for surface mediated  $\text{NO}_2$  glow
- Use PSI fast O-atom source
- Irradiate NO-doped targets (mono-layer doping)
  - Ni, Al, Z306
  - 77 K, 300 K
- Observe intensity, spectral shape of luminescence
- Diagnostics
  - Scanning monochromator
  - Imaging spectrometer

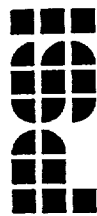


# EXPERIMENTAL APPARATUS

T-4032

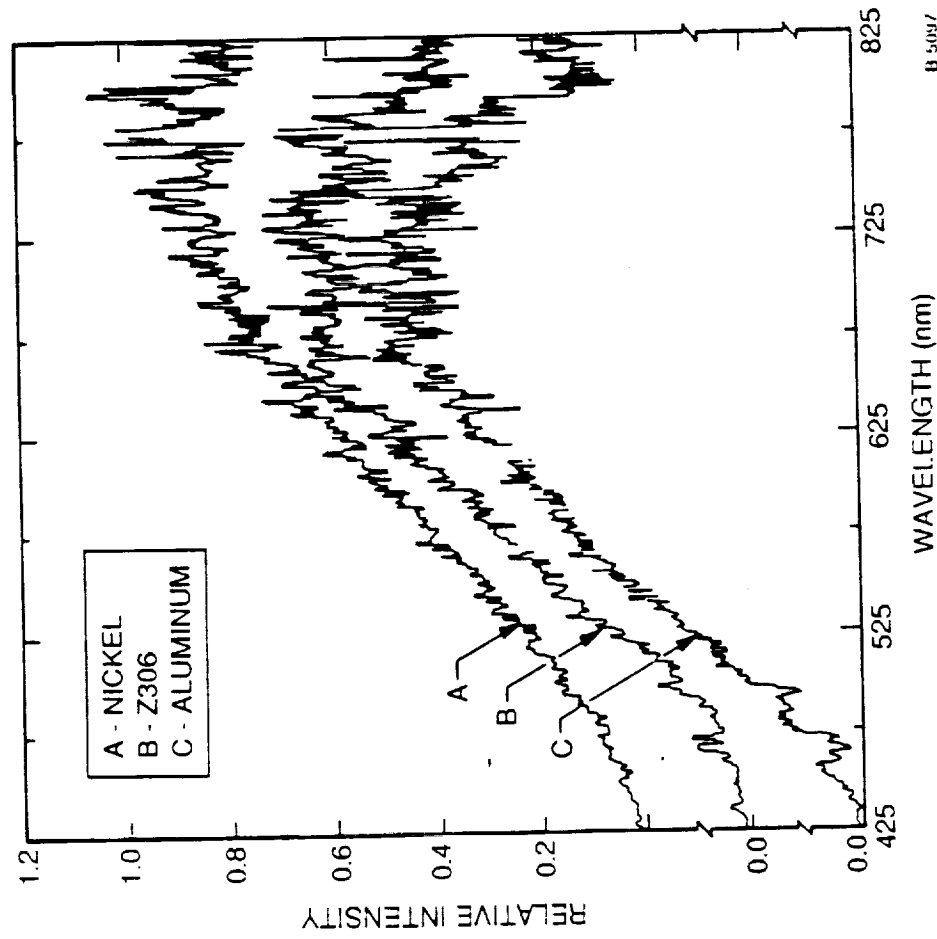


B-1828a

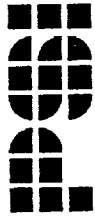


# RELATIVE GLOWS OBSERVED ABOVE THREE MATERIALS

T-4033

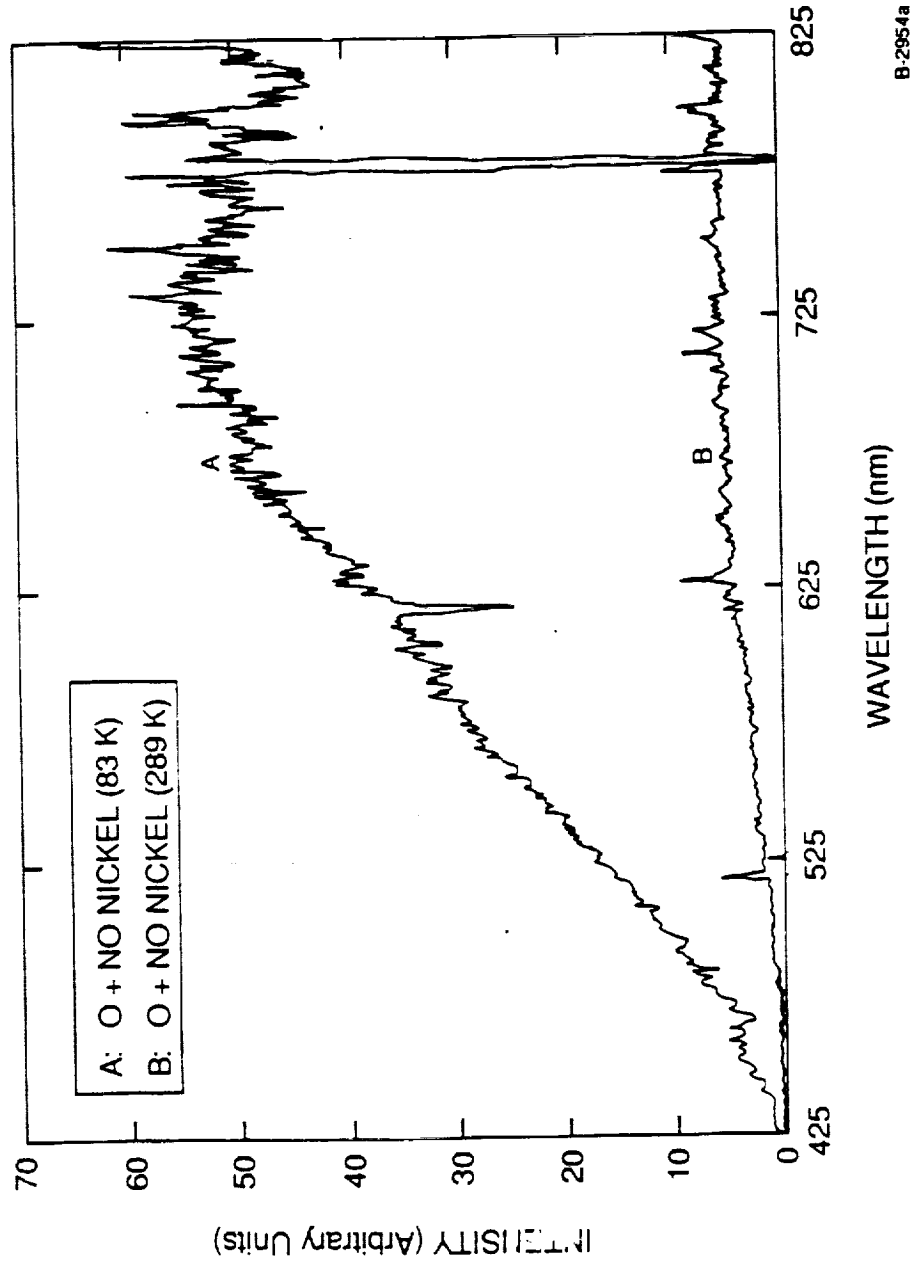


Relative glow intensities observed with monochromator above cooled Ni, Z306, and Al targets doped with NO.  $T \sim 83$  K.



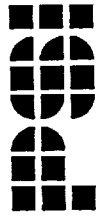
# OBSERVED TEMPERATURE VARIATION OF GLOW

T-4034



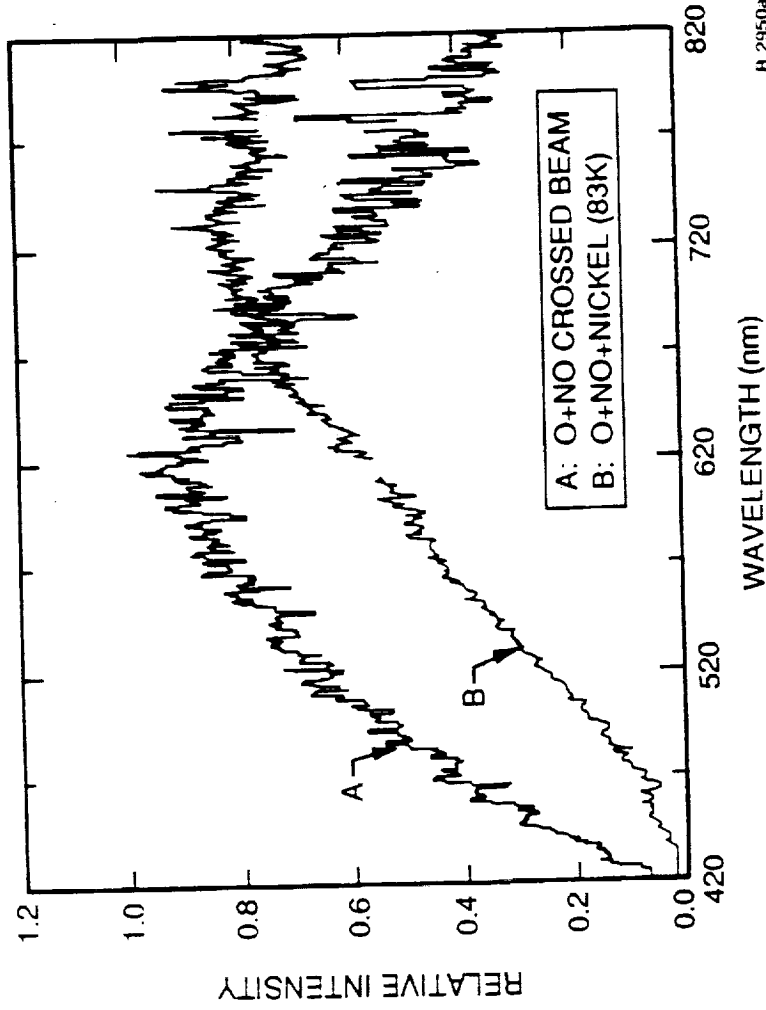
Spectra resulting from the impact of 8 km/s oxygen on warm nickel dosed with NO, and cold nickel dosed with NO. S/N of ~3 in room temperature data but spectral shape appears to be the same as in 83 K data.



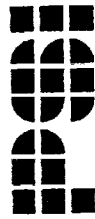


# RELATIVE GLOWS – 8 km/s O-ATOMS INTERACTING WITH GASEOUS NO AND NO-DOPED SURFACE

T-4035

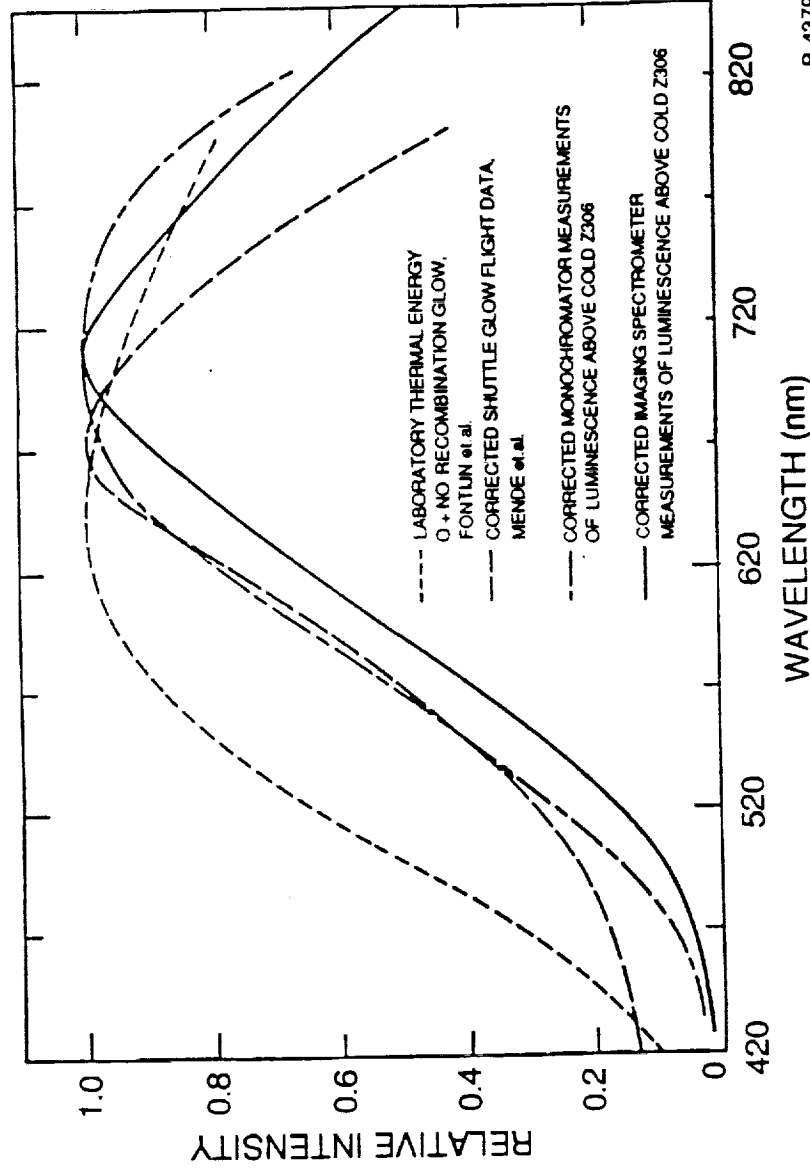


Contrast between relative glow observed with monochromator above an NO doped cooled nickel target and that observed in the interaction of the fast O-beam with a pulse of NO gas. Open regions in spectra correspond to signal interferences resulting from oxygen atom beam transitions at 615.7 and 777.4 nm. T ~83 K.



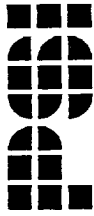
# SMOOTHED GLOW DATA CONTRASTED WITH SHUTTLE OBSERVATION AND GAS PHASE $\text{NO}_2$ CHEMILUMINESCENCE

T-4036



B-4379

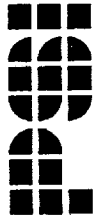
Spectral response corrected luminescence measured in the present study (as a result of 8 km/s O-atom interaction with NO doped Z306 chemglaze surfaces) using a scanning monochromator (pp S/N ~7 or 8 to 1) and imaging spectrometer (pp S/N ~10 to 1, for 15 min integration) are compared with shuttle flight data and thermal  $\text{NO}_2$  gas recombination continuum information



## BASIC OBSERVATIONS

T-4037

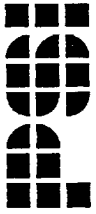
- All intensities within factor of two at 77 K
- Slight spectral variations from material to material
- Intensity drops an order of magnitude as temperature goes from 77 to 300 K
- Clear distinction between spectra resulting from 8 km/s O-atoms impacting either gas phase or surface-deposited NO



## SUMMARY

T-4038

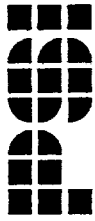
- Laboratory observations spectrally similar to shuttle observations
  - Slower decay to red
- Strong confirming evidence for NO<sub>2</sub> chemiluminescence postulate
- Differences with lab measurements taken under other conditions
  - See additional measurements
    - Arnold and Coleman, J. Chem. Phys. 88, 7147 (1988),  $v=1.4$  km/s, Ni, 300 K
    - Orient et al., Phys. Rev. A 41, 4106 (1990),  $v=8$  km/s, MgF<sub>2</sub>, 300 K



# SURFACE CONTAMINATION CLEANUP IN LOW EARTH ORBIT

T-4039

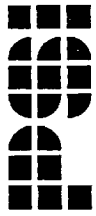
- Issue - What is the efficiency of 8 km/s O-atoms for removing contaminants from surfaces
  - Contaminants build up on leeward surfaces or during station activities, i.e., dumps, thruster firings
  - Ram removal rate, chemical interactions required for contamination model
- Approach - Irradiate contaminated surfaces with PSI's fast O-atom source
  - Monitor visible, IR radiation from "sputtered" contaminants



## PRESENT STUDIES

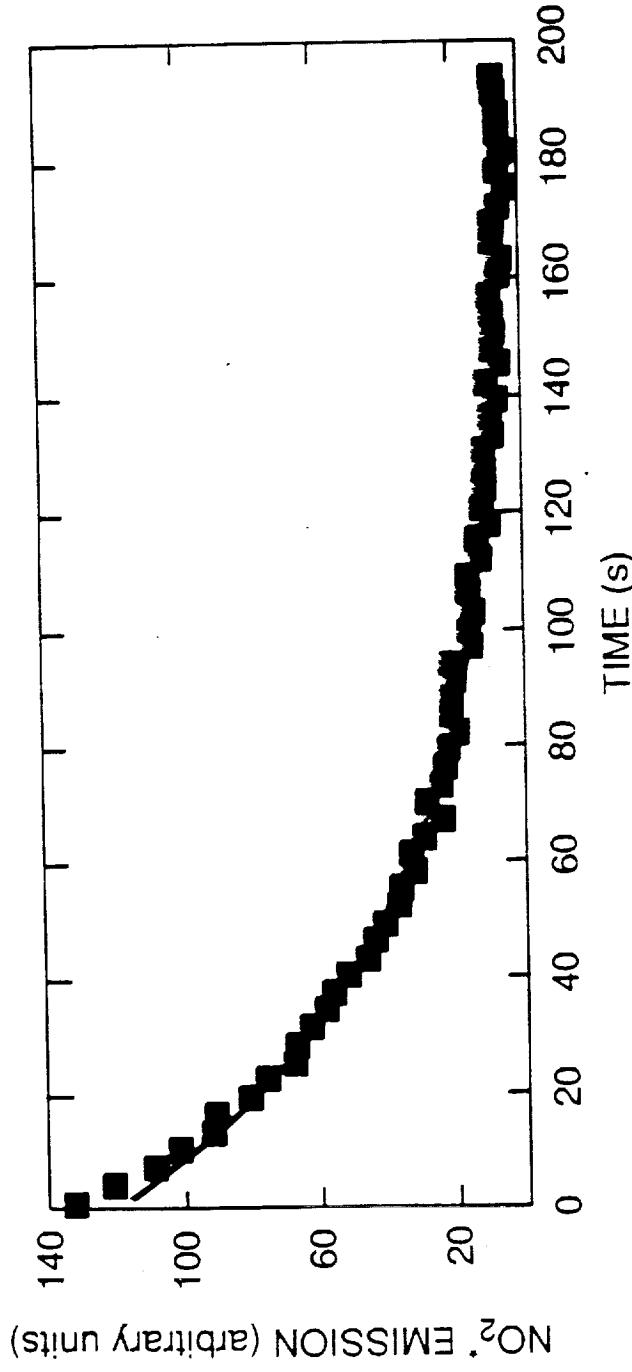
T-4040

- Three materials: Al, Z306 (Chemglaze) and Nickel
- Two contaminants
  - NO on surfaces cooled to 77 K
    - Mono-layer pre-dosing with pulsed valve
  - "Natural" contaminants on room temperature surfaces
- Normal incidence at 8 km/s



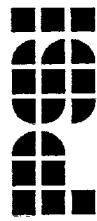
## TYPICAL SCOURING EXPERIMENT NO ON AI

T-4041



B-6268

- Typical experimental results illustrating emission of NO<sub>2</sub>\* at 675 nm decaying as a function of time (number of O-atom pulses) as the NO is scoured from an Al surface. Each point represents an average of 3 O-atom pulses. (1 Hz frequency) Solid line is a fit to a single exponential functional form.



## DATA ANALYSIS

T-4042

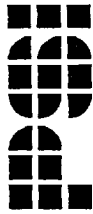


$$I(t) = I(0) \exp(- (k_{\text{pd}} + RN_{\text{O}}f)t)$$

$f$  = pulse repetition frequency

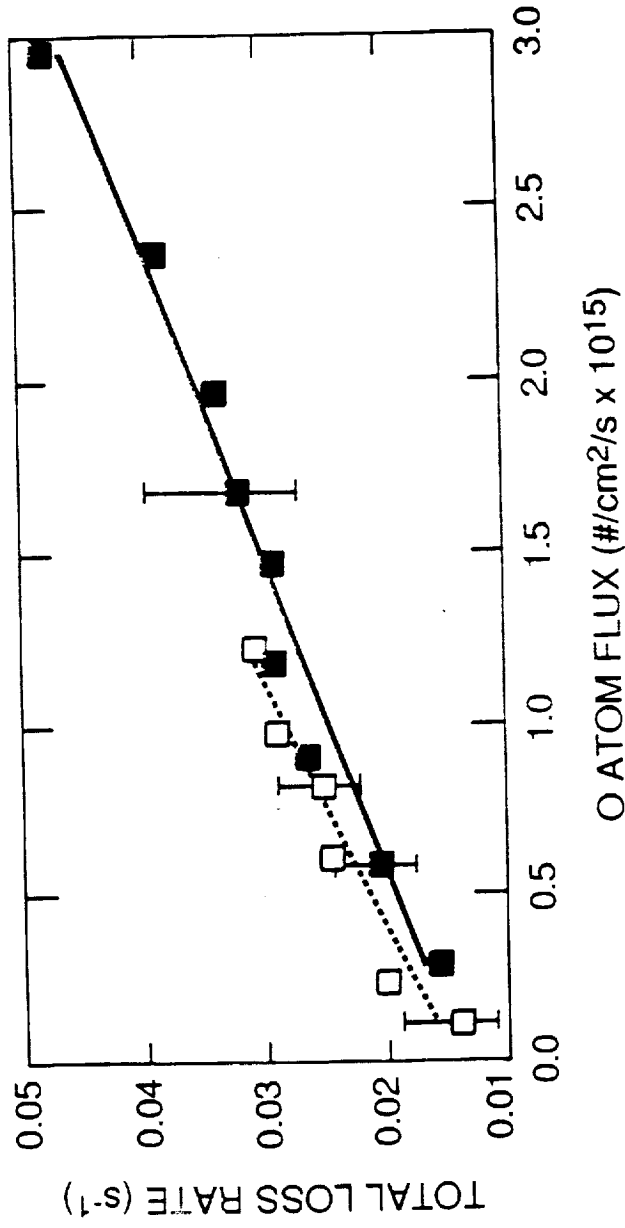
$N_{\text{O}}$  = O-atoms/pulse





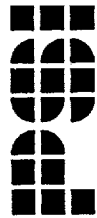
## TOTAL LOSS RATE VS O-ATOM FLUX NO ON AI

T-4043



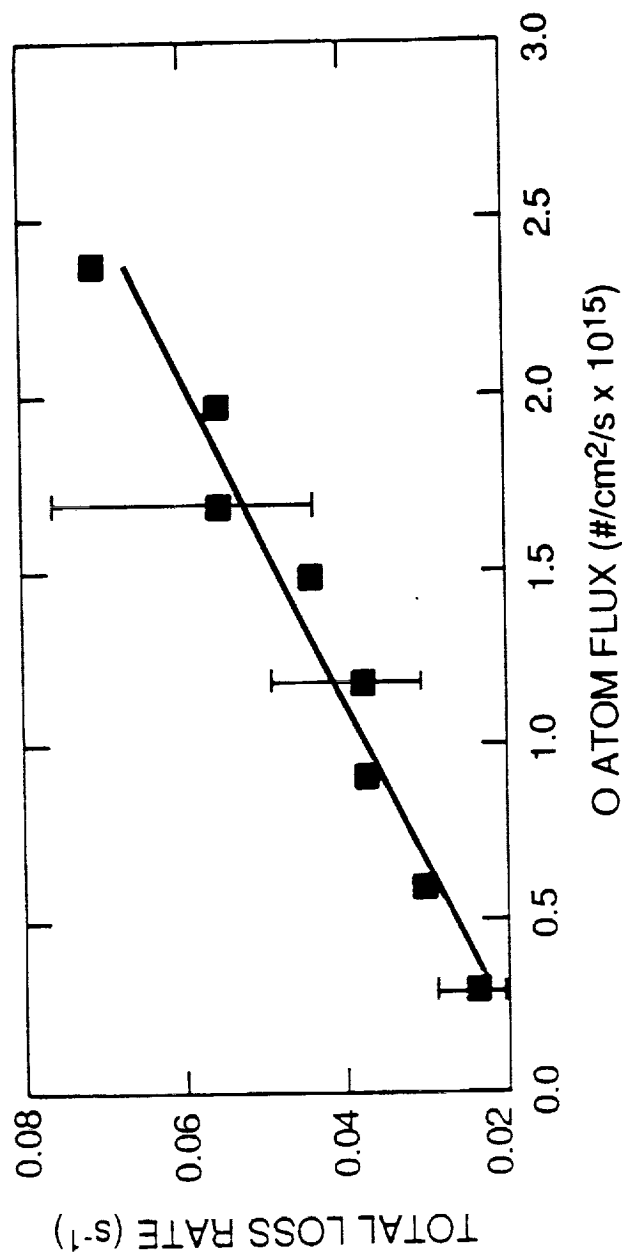
B-6269

- Total loss rate (as monitored by decay of NO<sub>2</sub><sup>\*</sup> emission) as a function of O-atom flux for NO on an Al surface. Open squares show data for an experiment in which the number of O-atoms/pulse was 1/2 that for the experiment indicated by the solid square.



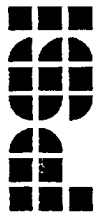
# TOTAL LOSS RATE VS O-ATOM FLUX NO ON Z306

T-4044



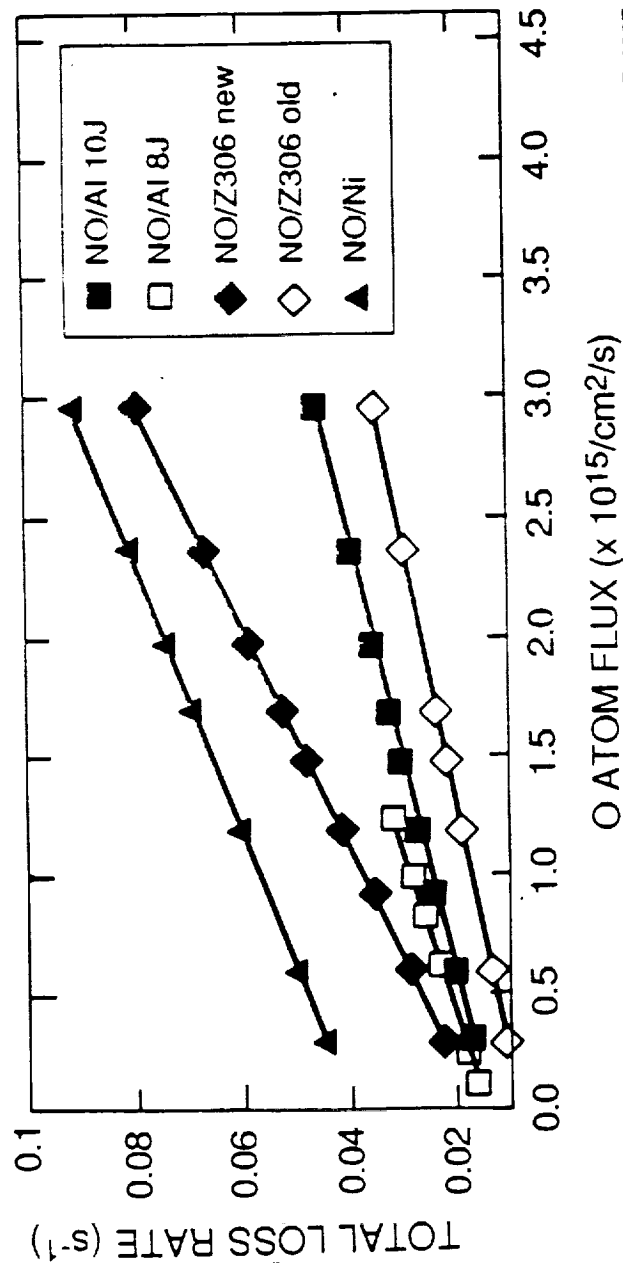
B-6270

- Total loss rate as a function of O-atom flux for NO on Z306



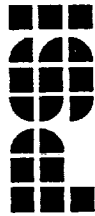
## SUMMARY PLOT

T-4045



B-6267

- Summary plot of fits to model for all experiments



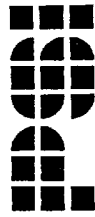
## DATA SUMMARY

T-4046

Experiment	k physi-desorption ( $s^{-1} \times 10^2$ )	k collisional desorption <sup>1</sup> ( $s^{-1} \times 10^2$ )	e-Folding O-atom Fluence, $cm^{-2}$
NO/Al (high flux)	$1.4 \pm 0.3$	$1.3 \pm 0.2$	$1.55 \times 10^{16}$
NO/Al (low flux)	$1.4 \pm 0.4$	$0.7 \pm 0.2$	$1.5 \times 10^{16}$
NO/Z306 (new)	$1.6 \pm 0.7$	$2.5 \pm 0.4$	$7.9 \times 10^{15}$
NO/Z306 (old)	$0.7 \pm 0.4$	$1.2 \pm 0.2$	$1.6 \times 10^{16}$
NO/Ni	$4.0 \pm 1.2$	$2.0 \pm 0.6$	$1.0 \times 10^{16}$

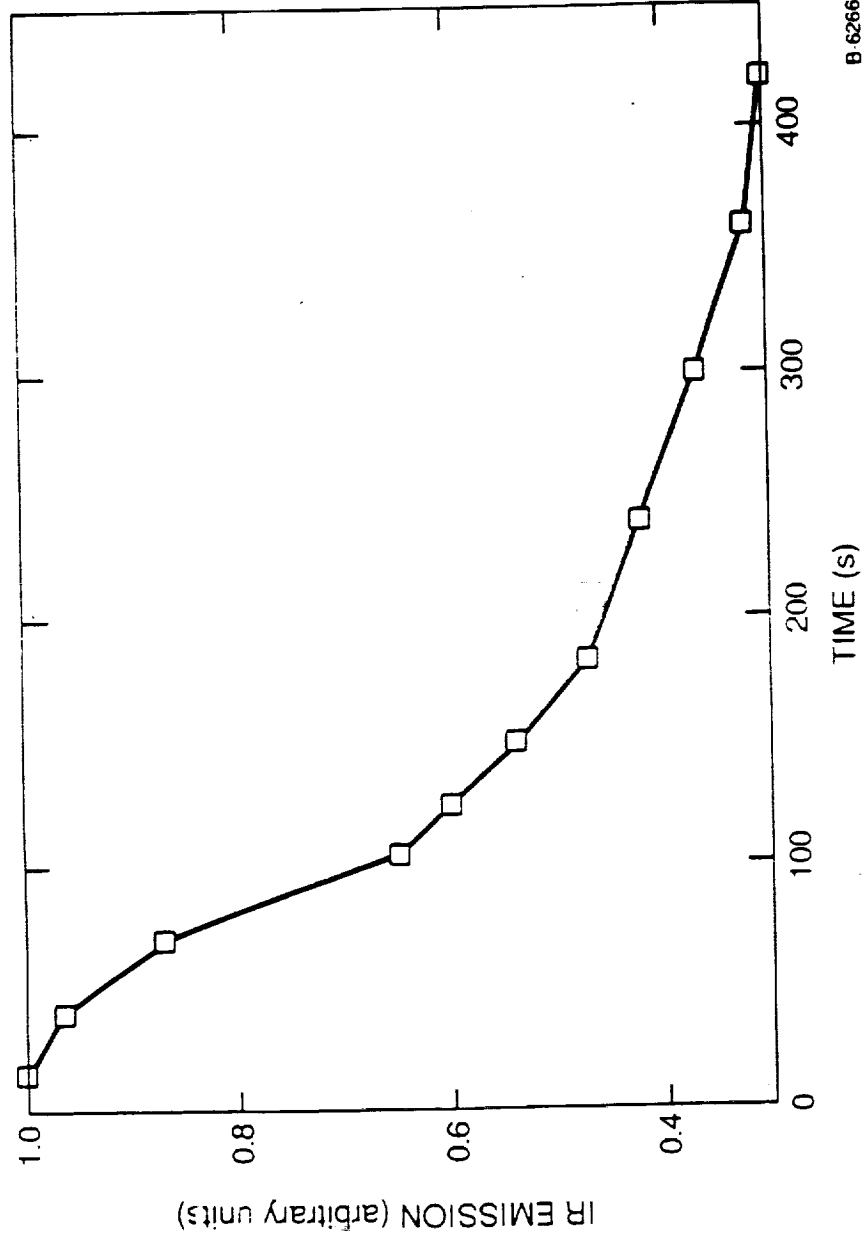
<sup>1</sup>At 1 Hz

Error bars represent 2 standard deviations on curve fit

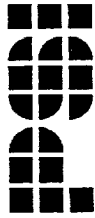


## Al TARGET BURN DOWN

T-4047

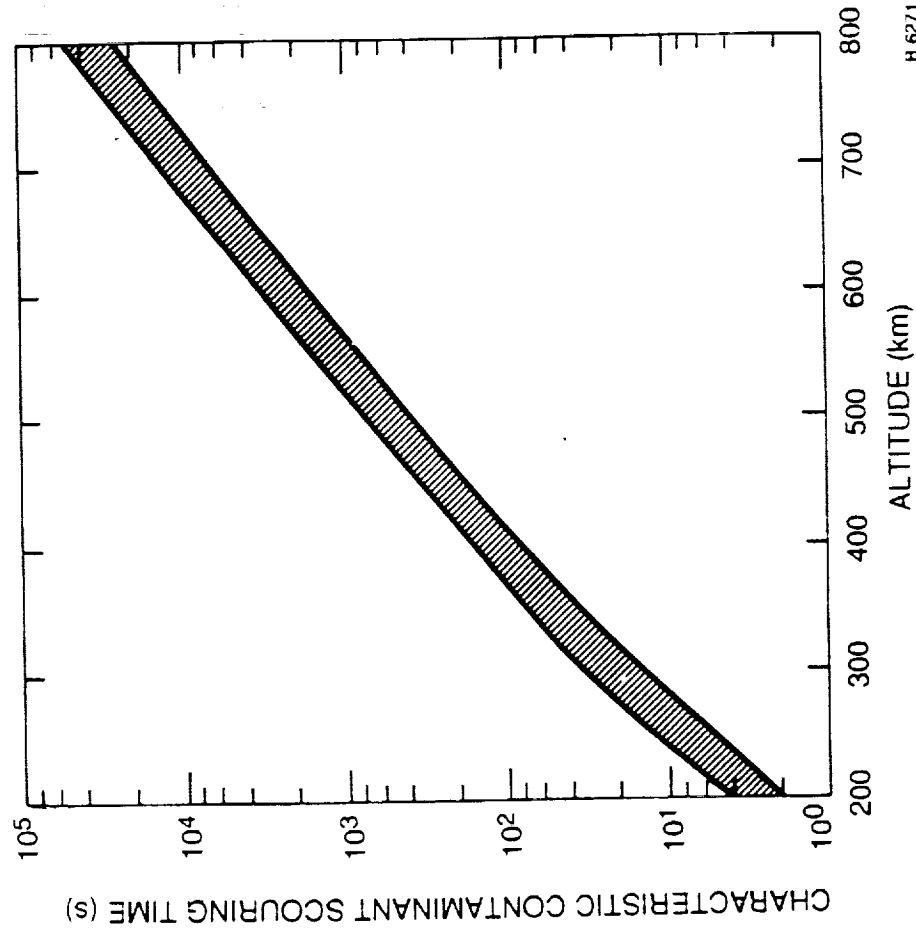


- Decay of IR Emission in the 4.0 to 5.1  $\mu\text{m}$  bandpass versus time as a "clean" Al target is subjected to O-atom pulses

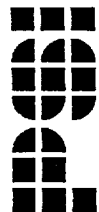


# CHARACTERISTIC O-ATOM SCOURING TMIE VS ALTITUDE

T-4048



An extrapolation of the laboratory data to LEO conditions assuming contaminant desorption can be neglected (O-atom profile corresponding to nominal solar activity conditions)

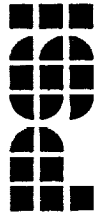


## SUMMARY

T-4011

PRECEDING PAGE BLANK NOT FILMED

- Observations on fast O-atom scouring of NO from Al, N<sub>i</sub> and Z306
  - Exponential decay
  - e-folding O-atom flux  $\sim 1.5 \times 10^{16} \text{ cm}^{-2}$
  - "Aging" effects observed on Z306
- Similar behavior observed in scouring of "original" contaminant layer
- Implications for LEO assessed, possible O-atom calibration technique

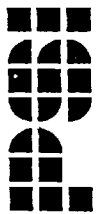


# ENERGY ACCOMMODATION

T-4012

- What fraction of O-atom kinetic (5 eV) and chemical (2.5 eV) energy is accommodated on surfaces?
- What is momentum accommodation?
  - Velocity and scattering angle distribution
- ★ First look at RCG, gold, aluminum

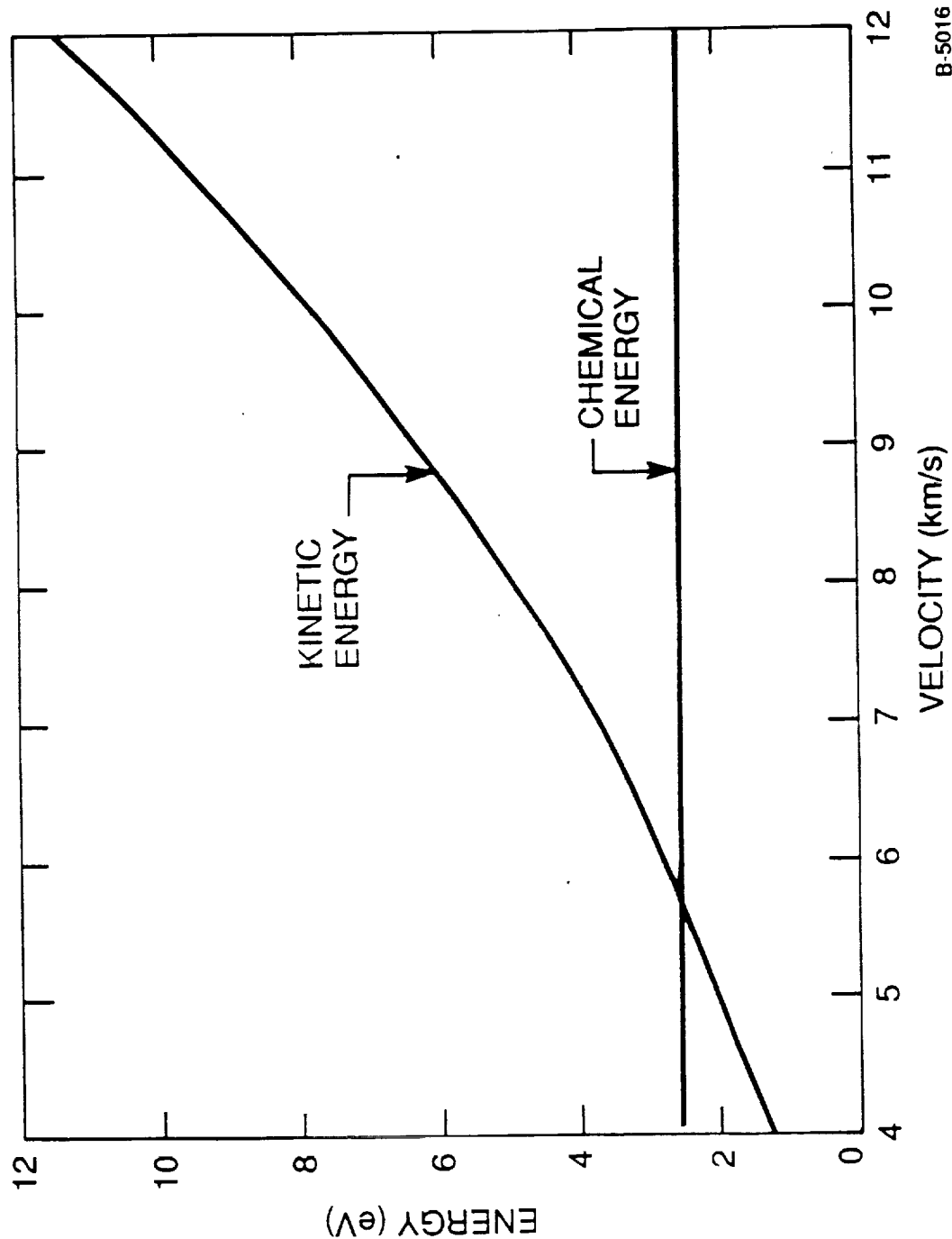




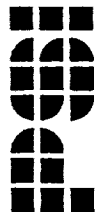
# OXYGEN ATOM ENERGY VERSUS VELOCITY

T-987

PRECEDING PAGE BLANK NOT FILMED



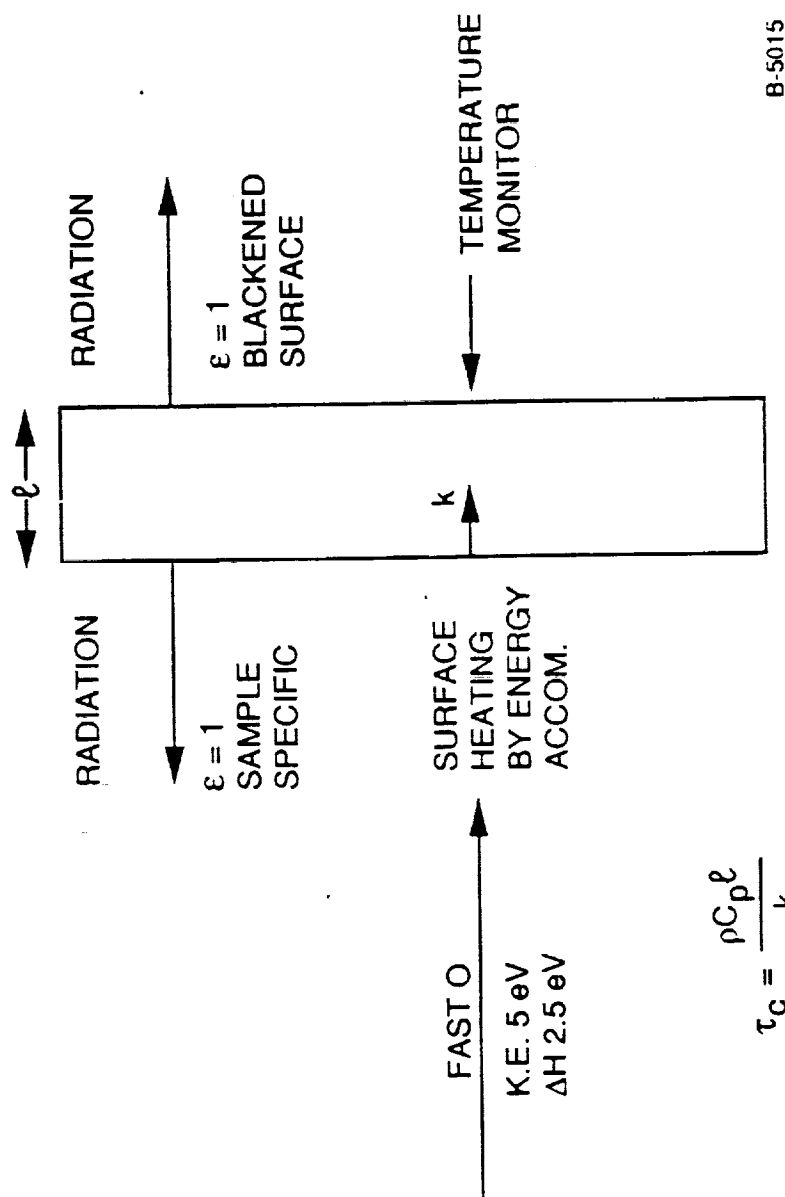
B-5016



# PHENOMENOLOGY

T-4013

## Thermally Isolated Target



$$\tau_c = \frac{\rho C_p l}{k}$$

B-5015



## SIMPLE HEATING MODEL

- Assumptions
  - 1) Heat conduction instantaneous
  - 2) Beam Approximated as CW
- Then
 
$$\rho C_p I \, dT/dt = aI - 2\epsilon \sigma (T^4 - T_o^4)$$

$a$  = energy accommodation coefficient  
 $I$  = available beam power (K.E. & Chem.)

- In steady state

$$\Delta T_{ss} = \frac{aI}{8\epsilon \sigma T_o^3}$$

— Independent of material property



## SIMPLE HEATING MODEL (CONT.)

T-983

- General solution

$$\Delta T = \frac{aI}{8\varepsilon \sigma T_o^3} \left( 1 - \exp\left(-8\varepsilon \sigma T_o^3 t / \rho C_p \ell\right) \right)$$

$$\text{whence } \tau = \frac{\rho C_p \ell}{3\varepsilon \sigma T_o^3}$$

- A similar decay time can be measured upon beam termination
- A cross check then is

$$\Delta T_{ss} = \frac{aI\tau}{\rho C_p \ell}$$

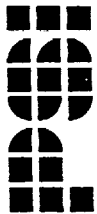


## APPARATUS AND EQUIPMENT

T-1039

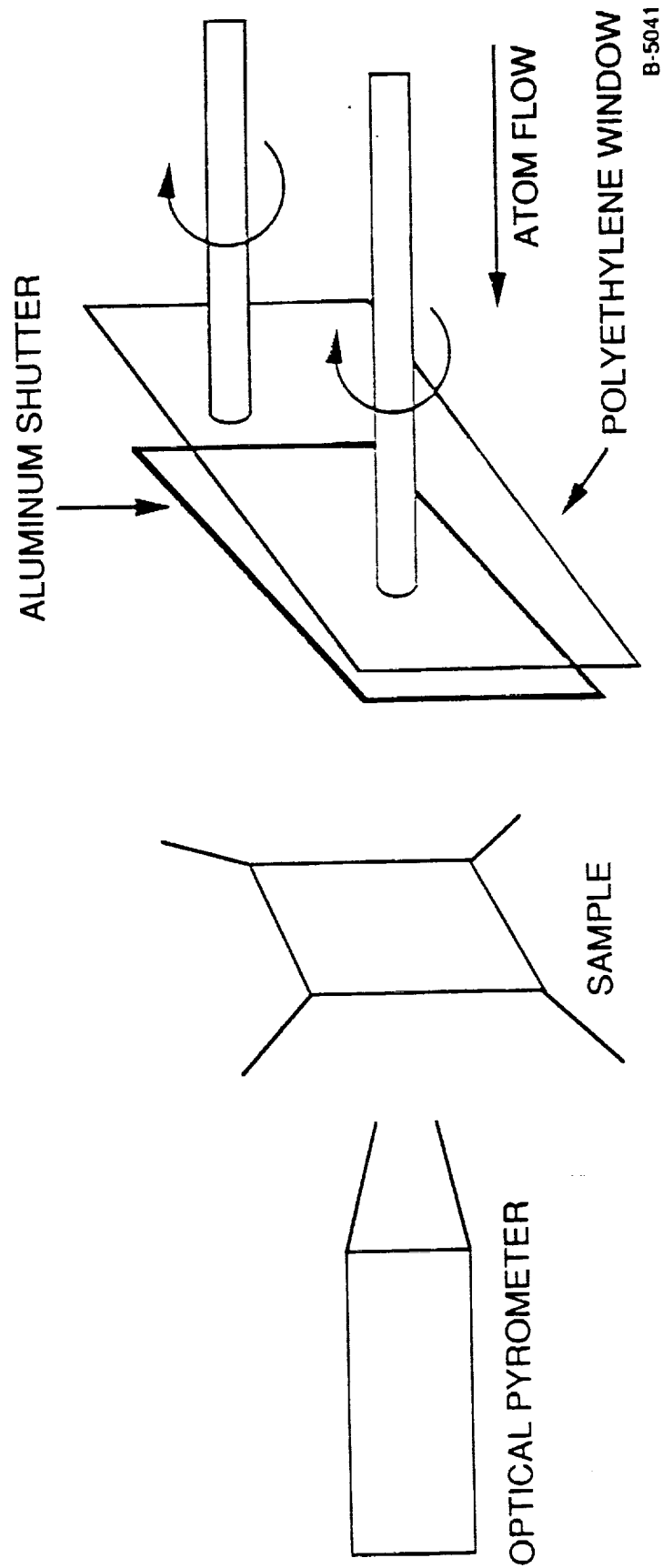
PRECEDING PAGE BLANK NOT FILMED

- Fast-2 chamber
- Omega optical pyrometers (2)
  - 0.1F sensitivity (0.1 mV)
  - 0 to 300°C (0 to 50°C)
  - 20 ms response time
  - Mounted inside chamber
  - Black painted rear surface FOV
- Aluminum shutter for radiative B.G.
- Polyethylene shutter for hv load
  - $T_{ave} = 0.85$  (0.2 to 16+  $\mu\text{m}$ )
- Samples suspended on 0.25  $\mu\text{m}$  SS wire on nylon screws for thermal isolation



# EXPERIMENTAL SCHEMATIC

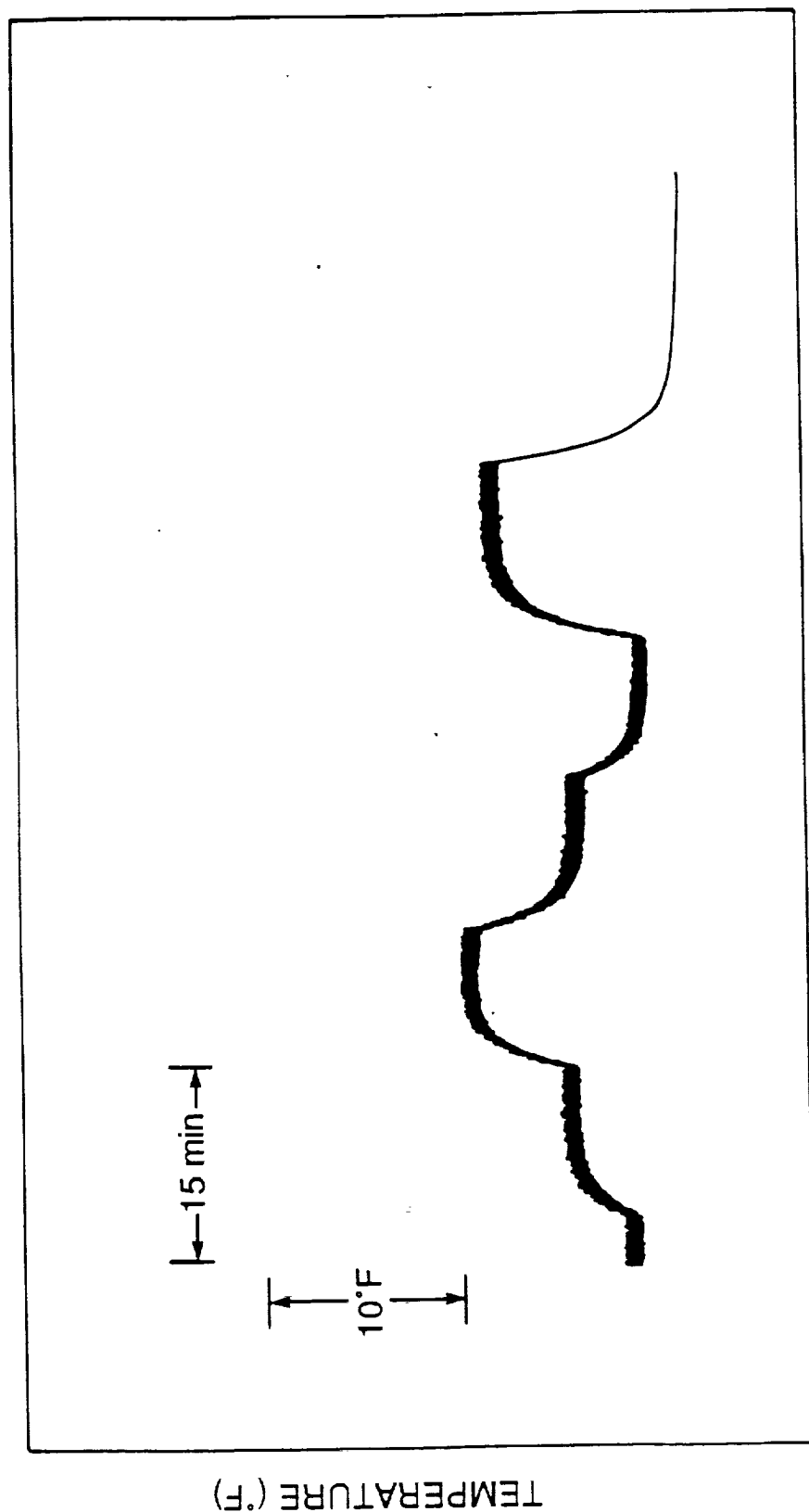
T-1040



B-5041

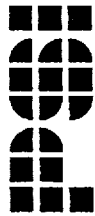
# TEMPERATURE VERSUS TIME GOLD

T-1043



TIME (min)

B-5044



# ACCOMMODATION EXPERIMENTS

T-1044

## Radiative Load Corrections

$$\alpha T_p I_{\text{scattered laser}} = 4(1 + \epsilon) \sigma T_o^3 \Delta T$$

$$\alpha = \frac{4(1 + \epsilon) \sigma T_o^3 \Delta T}{T_p I_{\text{scattered laser}}}$$

Material	$T_o$ (K)	$\Delta T$	$\alpha$	$I$ (W/cm <sup>2</sup> )
RCG	293.43	7.10	0.850	0.01
Nickel	291.59	0.89	0.060	0.01
Gold	292.54	1.72	0.124	0.01

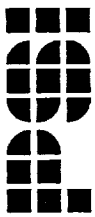
$$T_p = 0.85$$

$$\sigma = 5.67 \times 10^{-12} \text{ W/cm}^2 - \text{K}^4$$

$$\alpha = \text{absorptivity at } 10.6 \mu\text{m}$$

$$\epsilon = \text{average IR emissivity}$$



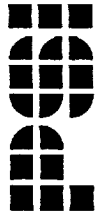


## DATA SUMMARY

PRECEDING PAGE BLANK NOT FILMED

T-4088

Material	Total Energy Coefficient	Translation Energy Only
Average Values of Three Measurements		
RCG	$0.36 \pm 0.08$ (23%)	$0.54 \pm 0.12$ (23%)
Nickel	$0.35 \pm 0.06$ (17%)	$0.53 \pm 0.09$ (17%)
Gold	$0.43 \pm 0.12$ (27%)	$0.64 \pm 0.1$ (27%)
Average All	$0.38 \pm 0.10$ (25%)	$0.57 \pm 0.14$ (25%)
Maximum Value of Three Measurements		
RCG	0.46	0.69
Nickel	0.43	0.65
Gold	0.59	0.88
Average Maximum All	$0.49 \pm 0.07$ (14%)	$0.74 \pm 0.10$ (14%0)



# ACCOMMODATION EXPERIMENTS

T-1046

## Radiative Balance Check

$$\tau = \frac{\rho C_p \Delta X}{4(1 + \varepsilon) \sigma T_o^3}$$

Material	$\rho C_p \Delta X$	$\tau_{\text{calc}}$	$\tau_{\text{obs}}$	%
RCG	0.33	311.0	300	96
Nickel	0.05	83.9	90	107
Gold	0.05	78.3	90	115

$\tau$  = 1/e equilibrium time

$\rho$  = density

$C_p$  = specific heat

$\Delta X$  = thickness



## SUMMARY

T-4014

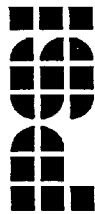
- Energy accommodation measured straightforwardly
  - Laser scattering problem can be minimized
- N/N<sub>2</sub> mixtures can be studied
- Momentum accommodation diagnostics defined
  - Coupled to energy accommodation
  - Large parameter space  $\theta$ ,  $\phi$ ,  $E$ ,  $T$ , material
- Possible space experiment



## GAS PHASE STUDIES

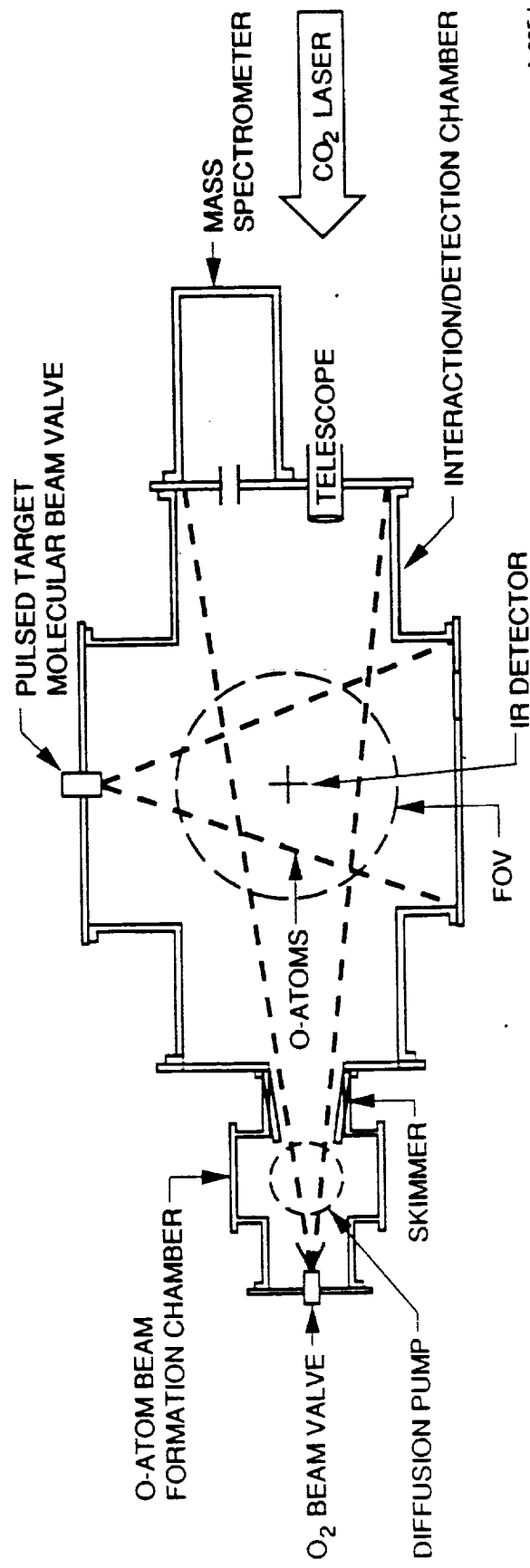
T-4015

- Ambient O-atom collisions with plume exhaust, vented or outgassed species can lead to significant IR signatures
- Present studies – cross section evaluation
  - O + CO, CO<sub>2</sub>, H<sub>2</sub>O, N<sub>2</sub>, UDMH
  - $\lambda = 1$  to 5.5  $\mu\text{m}$
  - O atom velocity 8 km/s
- High velocities open up new reaction channels
  - $\text{O} + \text{N}_2 \rightarrow \text{NO}^* + \text{N}$
  - $\text{O} + \text{H}_2\text{O} \rightarrow \text{OH}^* + \text{OH}$
  - $\text{O} + \text{CO}_2 \rightarrow \text{CO}^* + \text{O}_2$



# EXPERIMENTAL CONFIGURATION

T-3869



A-885d

- Interaction Region
  - O, target gas densities  $\sim 4 \times 10^{13} \text{ cm}^3$
  - $\sim 75 \mu\text{s}$  interaction time

# SUMMARY OF SPACE STATION GROUNDING ISSUES

M. R. CARRUTH, JR.

MARSHALL SPACE FLIGHT CENTER

WORKSHOP on the INDUCED ENVIRONMENT of  
SPACE STATION FREEDOM

January 30-31, 1991

## INTRODUCTION

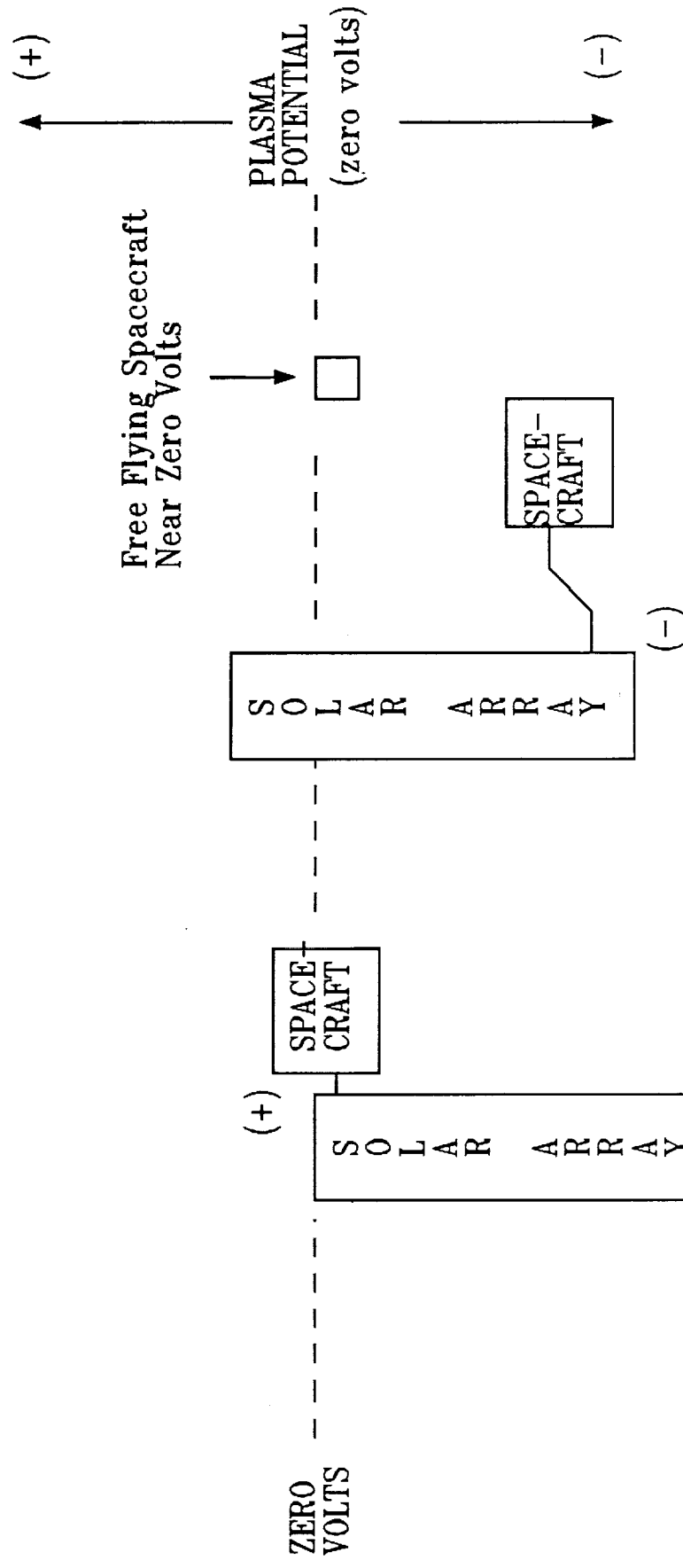
- o Plasma Interactions With Spacecraft Systems Have Been Under Study For a Number of Years
- o Previous Space Flight Experience Has Been With Low Voltage Power Systems and Smaller Physical Size
- o There Have Been Several Plasma Working Groups Who Have Been Addressing Space Station Interactions
- o The Earlier Power System Design (20 kHz) Made Plasma Concerns Minimal; DC Negative Ground is Worst Option From Environmental Considerations

## AMBIENT PLASMA/SPACECRAFT INTERACTION

- 0 Spacecraft Sitting in the Conductive Ambient Plasma Must Collect Zero Net Charge
- 0 A System With a Voltage Difference, Such as a Solar Array, Will 'Float'
  - 0 The Positive Part Will Collect Electrons
  - 0 The Negative Part Will Collect Ions
- 0 Electrons Are Very Mobile And Easily Collected; Ions Are Massive And Difficult to Collect
  - 0 A Small Percentage of the Solar Array Area Will Be Positive Relative to Plasma Potential and the Rest of it Will Be Negative



# SPACECRAFT WITH HIGH VOLTAGE SOLAR ARRAY IN IONOSPHERIC PLASMA



- o Spacecraft Negative and Must Consider Plasma Effects
- o Sputtering and Arcing
- o Docking and Safety
- o Structure Currents and EMI

# SOLAR ARRAY AND POWER DISTRIBUTION NEGATIVELY GROUNDED TO STRUCTURE

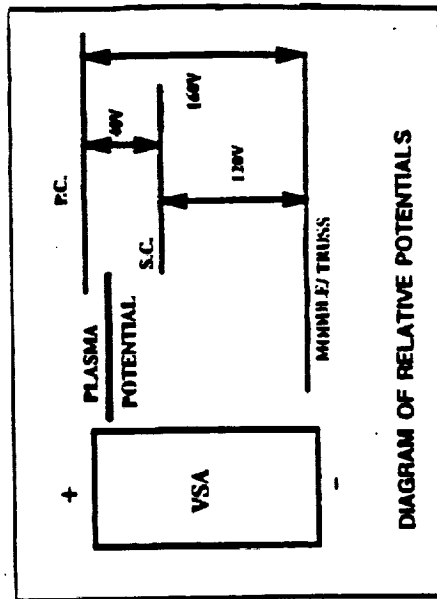
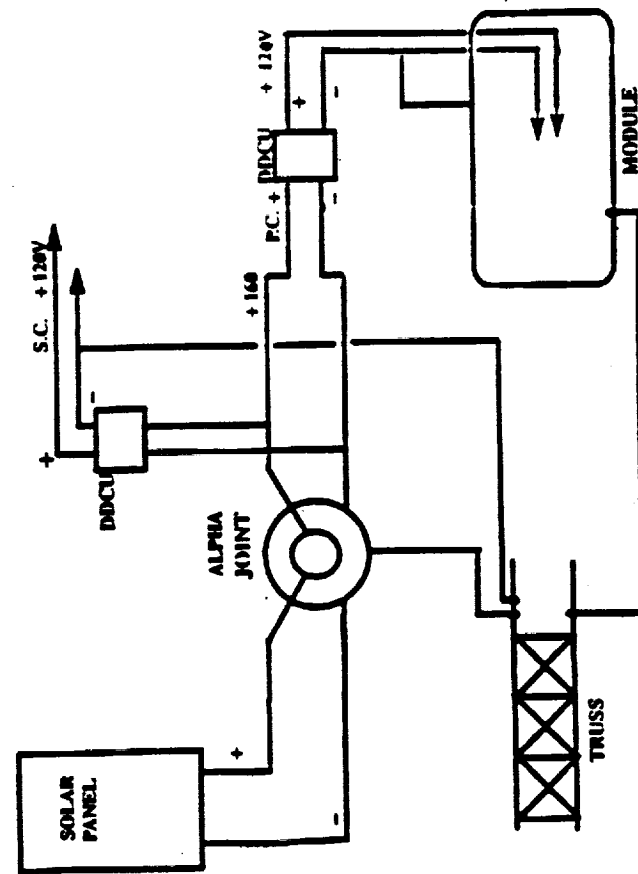


DIAGRAM OF RELATIVE POTENTIALS

VSA - SOLAR ARRAY VOLTAGE - 160V  
 PC - PRIMARY CABLE (160V) HOT SIDE  
 SC - SECONDARY CABLE (120V) HOT SIDE  
 DDCU - DC TO DC CONVERTER UNIT

The first configuration identified has the array grounded with the primary power distribution on its negative side and the secondary power distribution also grounded on the negative side. This is the concept currently being used in the power distribution design.

## HISTORY OF NEGATIVE GROUND INVESTIGATION

0 WORKSHOP AT LeRC	MAY 1990
0 ORIGINAL NEG GROUND CR	JUNE 1990
0 REQUEST FROM HEADQUARTERS TO REVIEW WORKSHOP REPORT	JUNE 1990
0 REQUEST FROM MSFC SSF ENGINEERING TO LABS TO REVIEW WORKSHOP REPORT	AUGUST 1990
0 REQUEST FROM MSFC SSFPO TO REVIEW CR WITH REPORT	AUGUST 1990
0 APPROVAL OF CR BY SSCB	OCTOBER 1990
0 ESTABLISHMENT OF TIGER TEAM	OCTOBER 1990
0 INITIAL TIGER TEAM MEETING AND DRAFT OF PLAN	NOVEMBER 1990

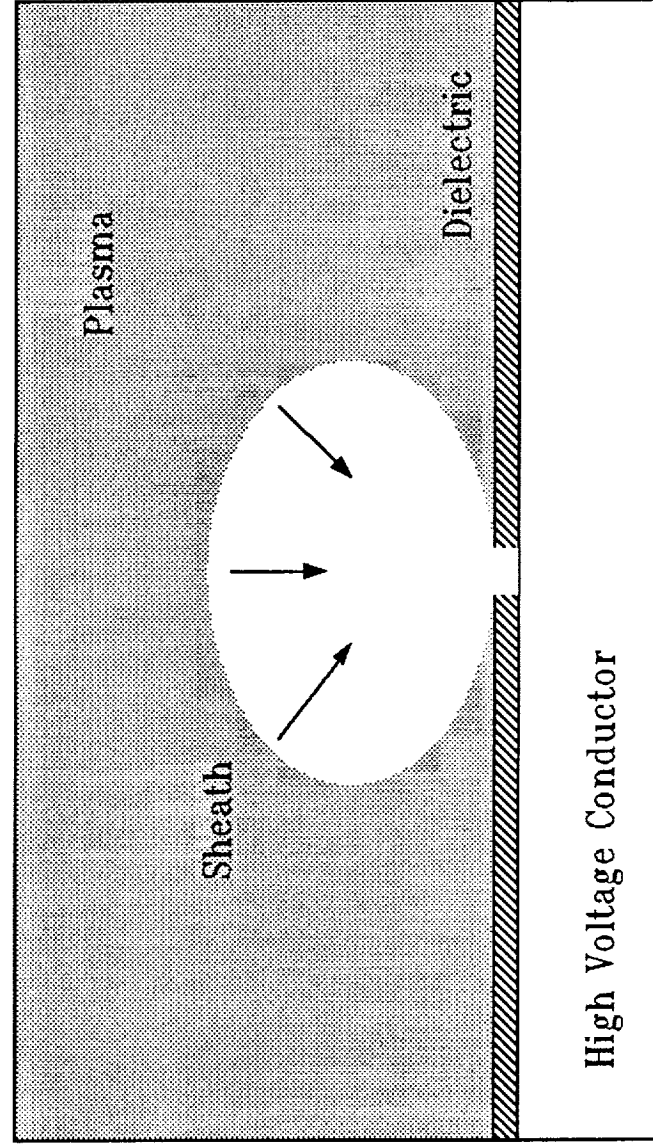
## PURPOSE AND GOALS OF TIGER TEAM

- 0 COST, SCHEDULE, SAFETY AND RELIABILITY AFFECTED BY INTERACTION BETWEEN SPACE STATION AND PLASMA ENVIRONMENT
- 0 TIGER TEAM MUST:
  - 0 SORT THROUGH EFFECTS TO DETERMINE WHICH ARE MOST SIGNIFICANT AND WHICH HAVE POSSIBLE 'FIXES'
  - 0 GATHER INFORMATION NECESSARY FOR ENGINEERING ASSESSMENT OF ISSUES RESULTING FROM INTERACTION
  - 0 DEVELOP AND IMPLEMENT SHORT TERM TEST AND ANALYSIS PLAN THAT LEADS TO PREPARATION OF DECISION PACKAGE
- 0 THREE-PHASE APPROACH ADOPTED:
  - 0 ESTABLISH BASIS FOR PREDICTING PERFORMANCE/LIFETIME OF BASELINE
  - 0 EVALUATE ALTERNATIVE DESIGN APPROACHES IF NECESSARY
  - 0 VALIDATE FLIGHT READINESS OF CHOSEN DESIGN

## NEGATIVE GROUND ISSUES ENVIRONMENTAL ISSUES

- 0 SPUTTERING OF EXPOSED CONDUCTOR
  - 0 Degradation of Surfaces
  - 0 Contamination Source From Deposition of Sputtered Material
- 0 DIELECTRIC BREAKDOWN AND ARCING EFFECTS
  - 0 Damage to Surface Due to Arc
  - 0 EMI Generated by Arcs and Transient Currents
- 0 KAPTON PYROLIZATION
  - 0 Electron Current Concentration at Pinholes on Solar Array May Cause 'Burning' of Kapton
- 0 DOCKING AND SAFETY
  - 0 Evaluation Indicates That This Is Not a Major Concern
- 0 PERTURBATION OF SCIENCE
  - 0 Transient Currents and Voltages: Arcs, Thruster Firings, v x B
  - 0 Induced Ionization Around Space Station

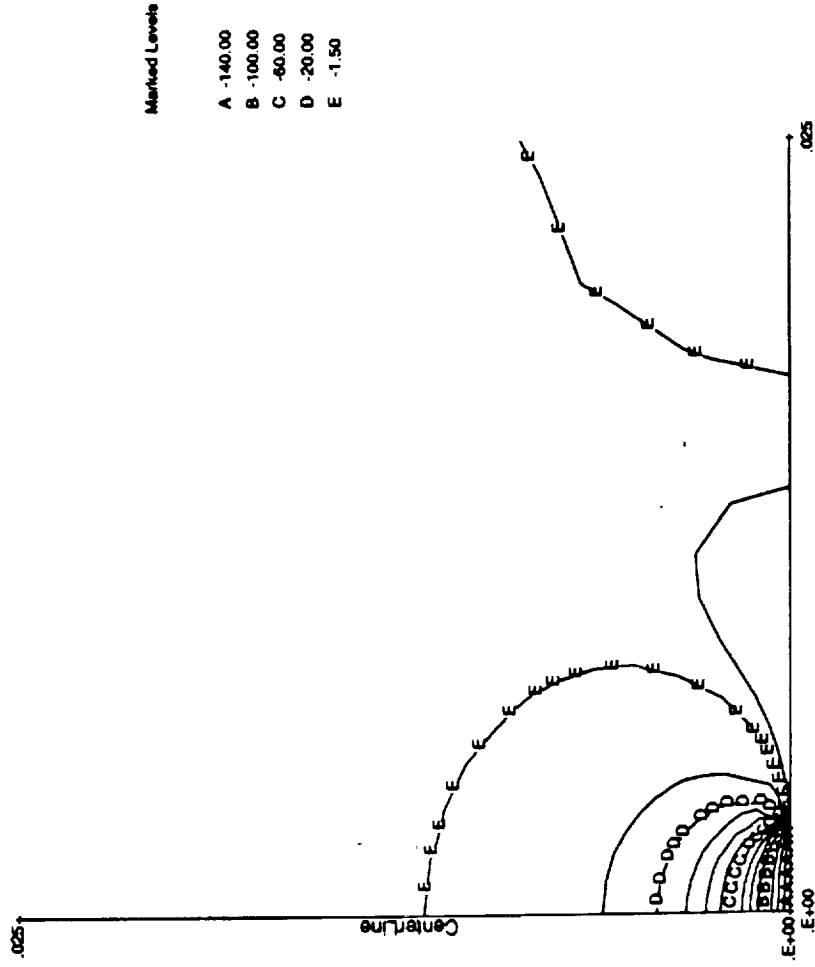
## SPUTTERING AT DEBRIS STRIKES



- o Sheath Growth Around Debris Strike or Other Penetration Can Cause Enhanced Sputtering of Conductor

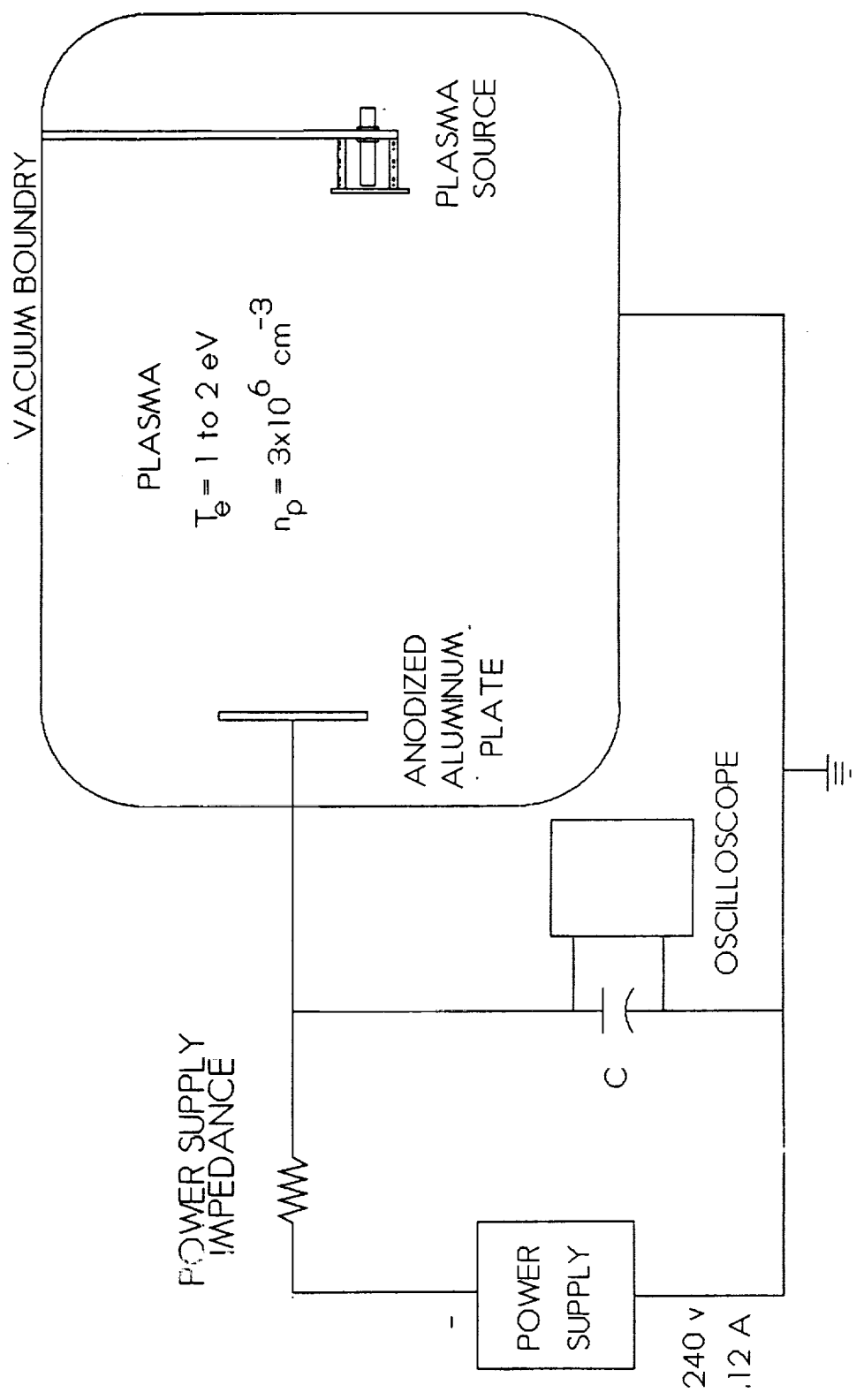


# Laboratory Plasma Sheath Potentials



$\phi_{\text{sheath}} = -1.4 \text{ volts}$   
 $\phi_{\text{surface}} = +2 \text{ to } -5.5 \text{ volts}$

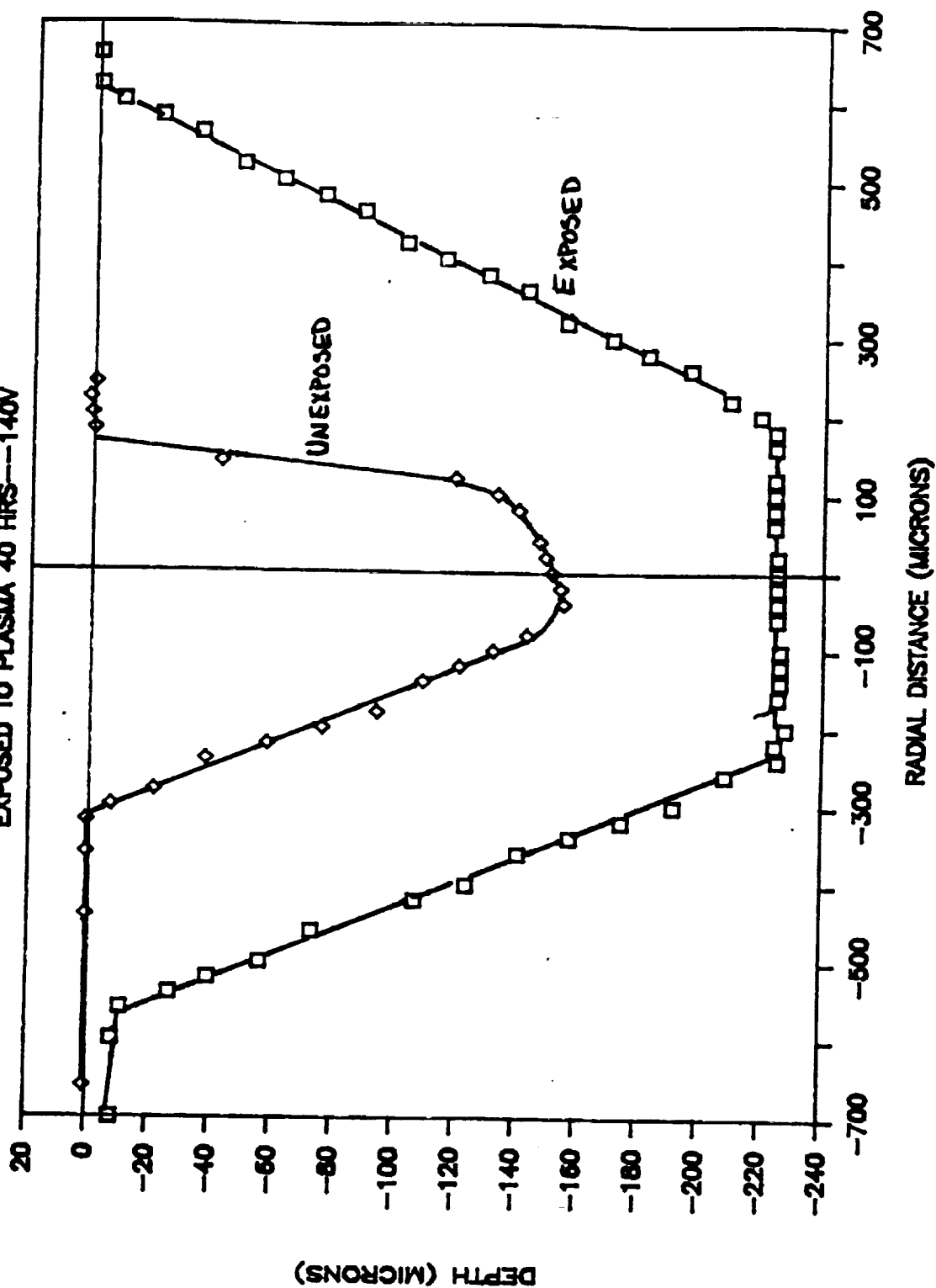
# SSF SOLAR ARRAY NEGATIVE GROUNDING TEST APPARATUS





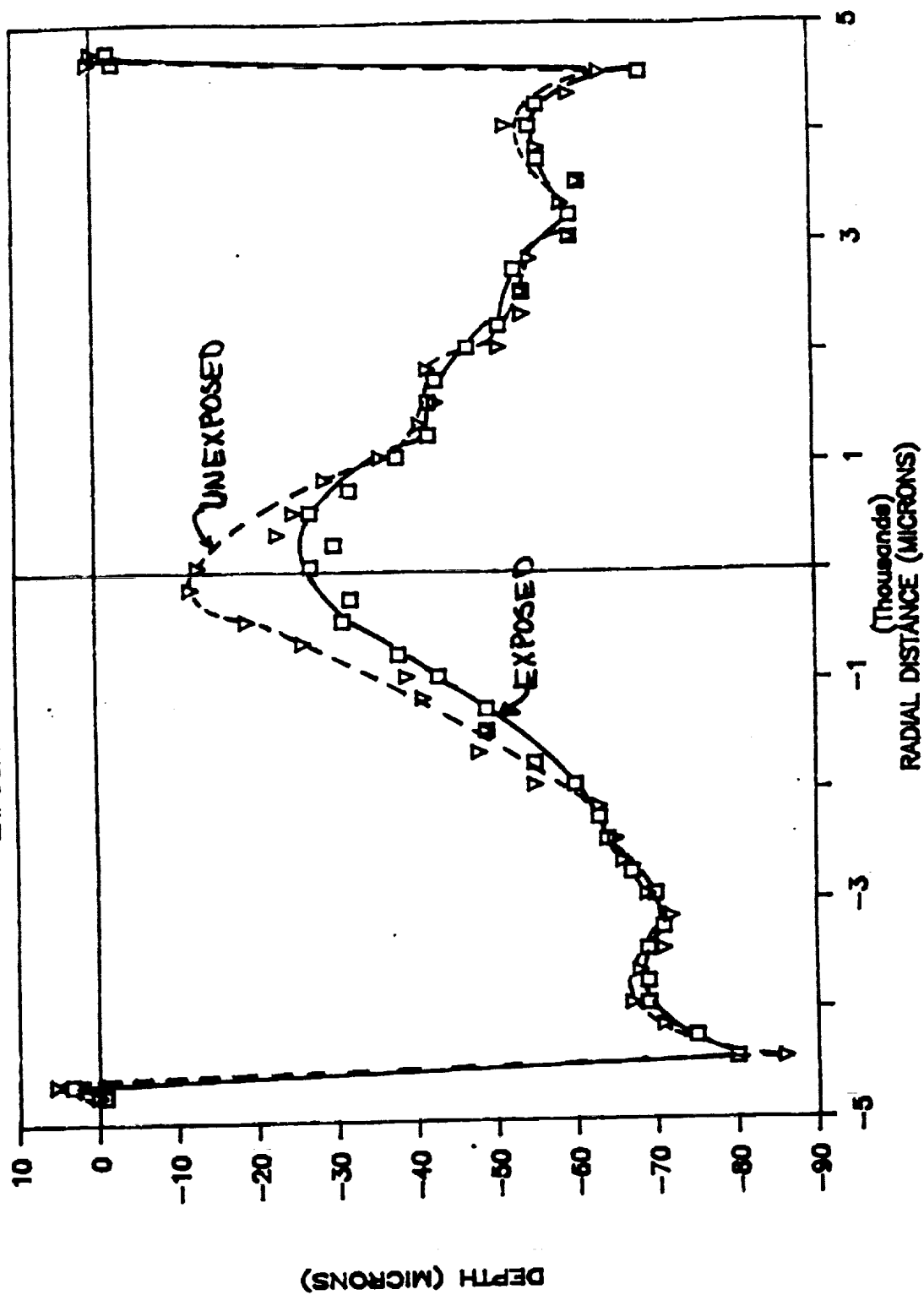
# DEPTH PROFILE OF PIN HOLE

EXPOSED TO PLASMA 40 HRS ---140V



# DEPTH PROFILE OF PIN HOLE

EXPOSED TO PLASMA 40 HRS ---140V



Exp. Cu-535 15:36 11/09/90

2.5x

RMS: 16.8nm

## SURFACE

WVLEN: 657.3nm

RA: 13.2nm

R Crv: -117.3m

P-V: 176nm

R Cyl: 11.06m  
5.2°

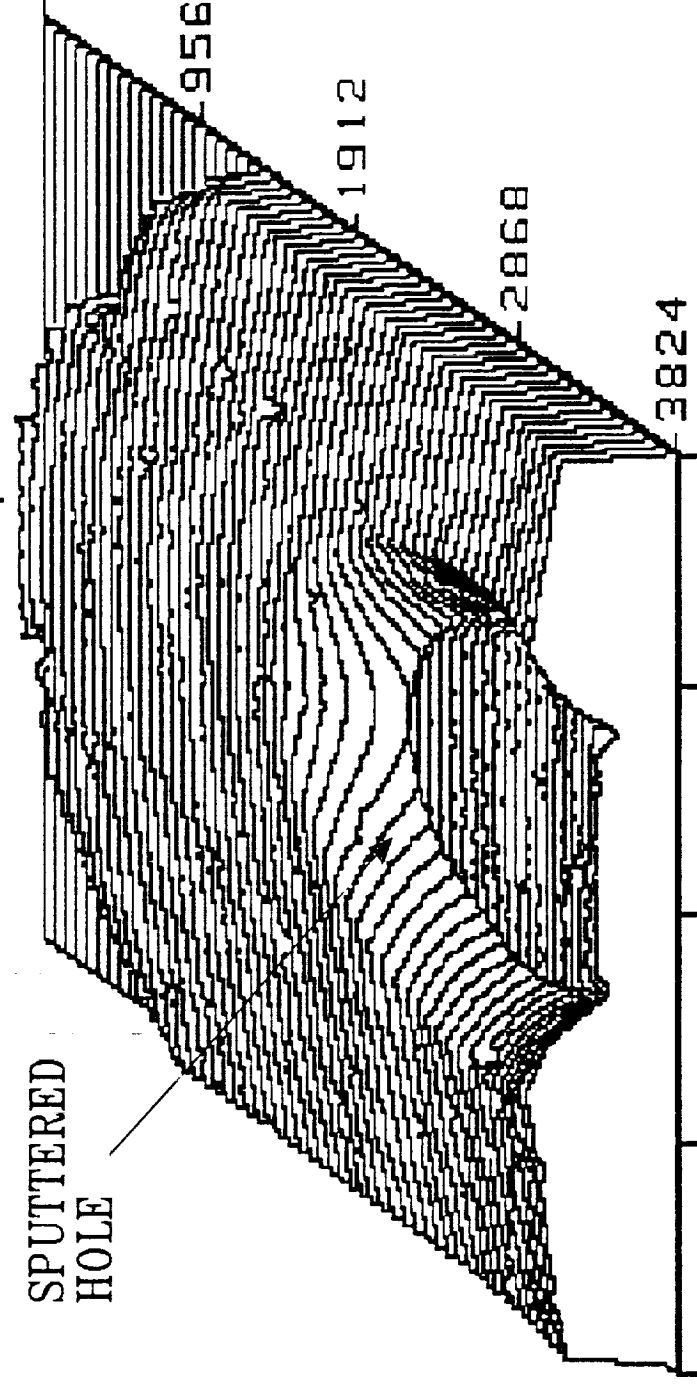
EXPOSED Cu

Orientation



(Front)

SPUTTERED  
HOLE



0 992 1984 2976 3968 3824

Distance (Microns)

U: 48nm

L: -73nm

J. K. Norwood / NASA-MSFC

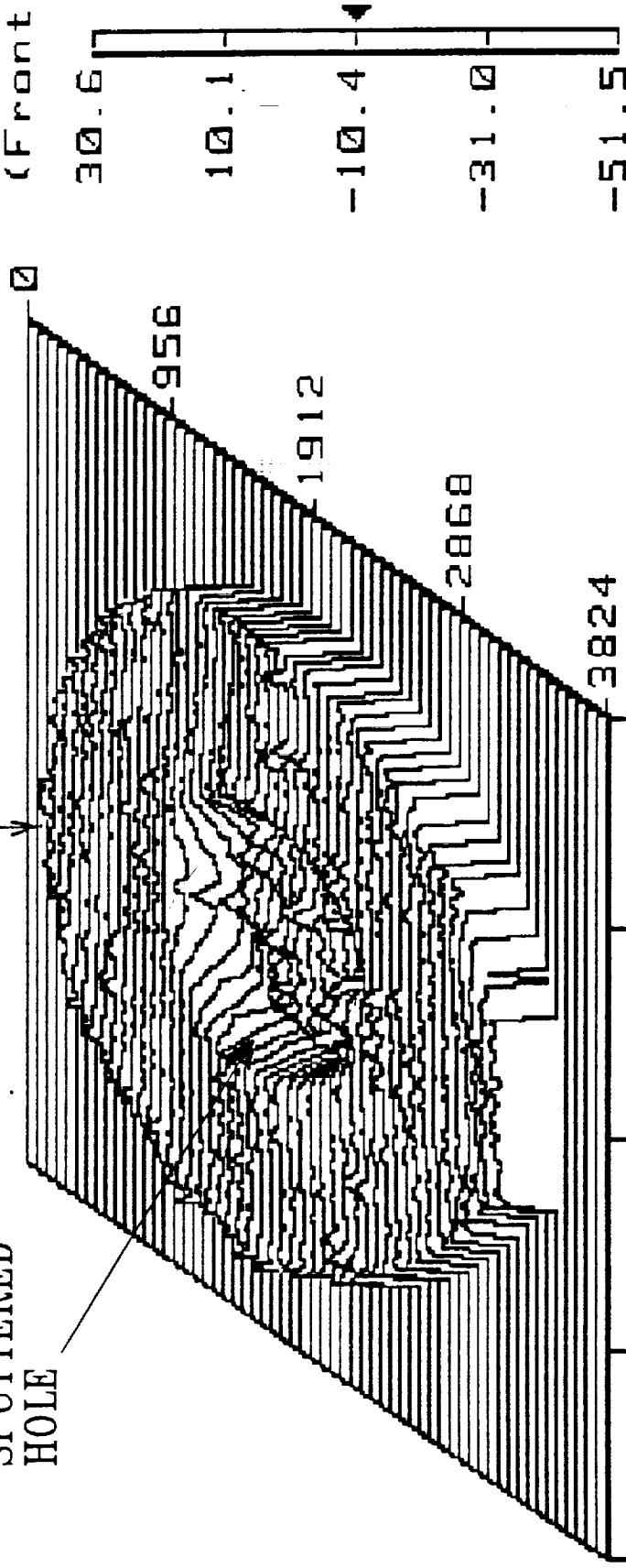
# WYKO

Exp. Cu-285 18:43 11/15/90 2.5x  
 RMS: 13.7nm WVLN: 657.3nm  
 RA: 9.18nm Tilt Removed  
 P-V: 82.1nm

EXPOSED Cu

SPUTTERED  
HOLE

(Front)



0 992 1984 2976 3968

Distance (Microns)

Cu-285 (Exposed) Horizontal Section

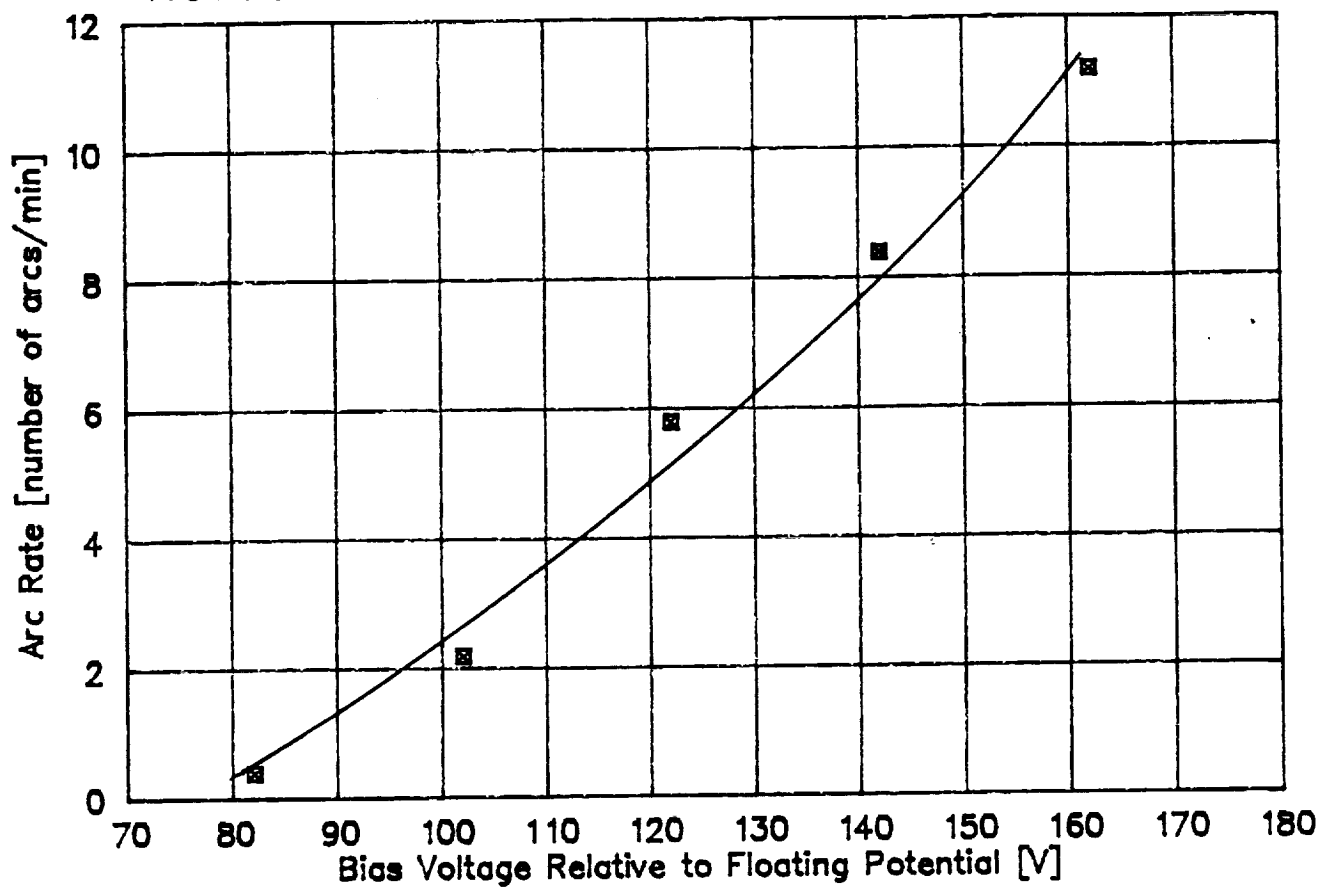
-- J. K. Norwood / NASA-MSFC

U: 30.6nm  
 L: -51.5nm

WYKO

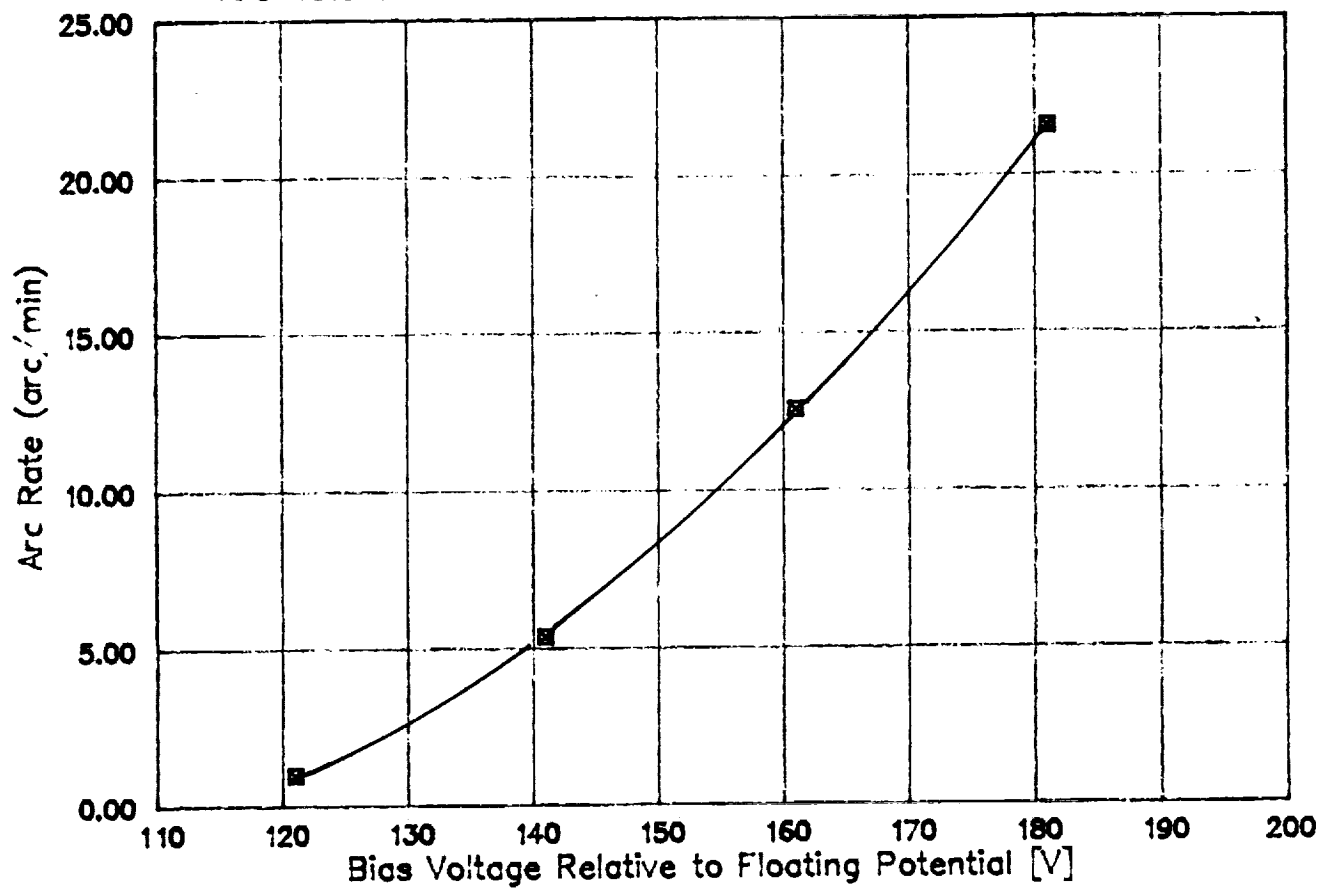
# SSF Solar Array Negative Grounding Effects

Arc Rate on JSC Chromic Acid Anodized Plate--0.16 mil Anodization



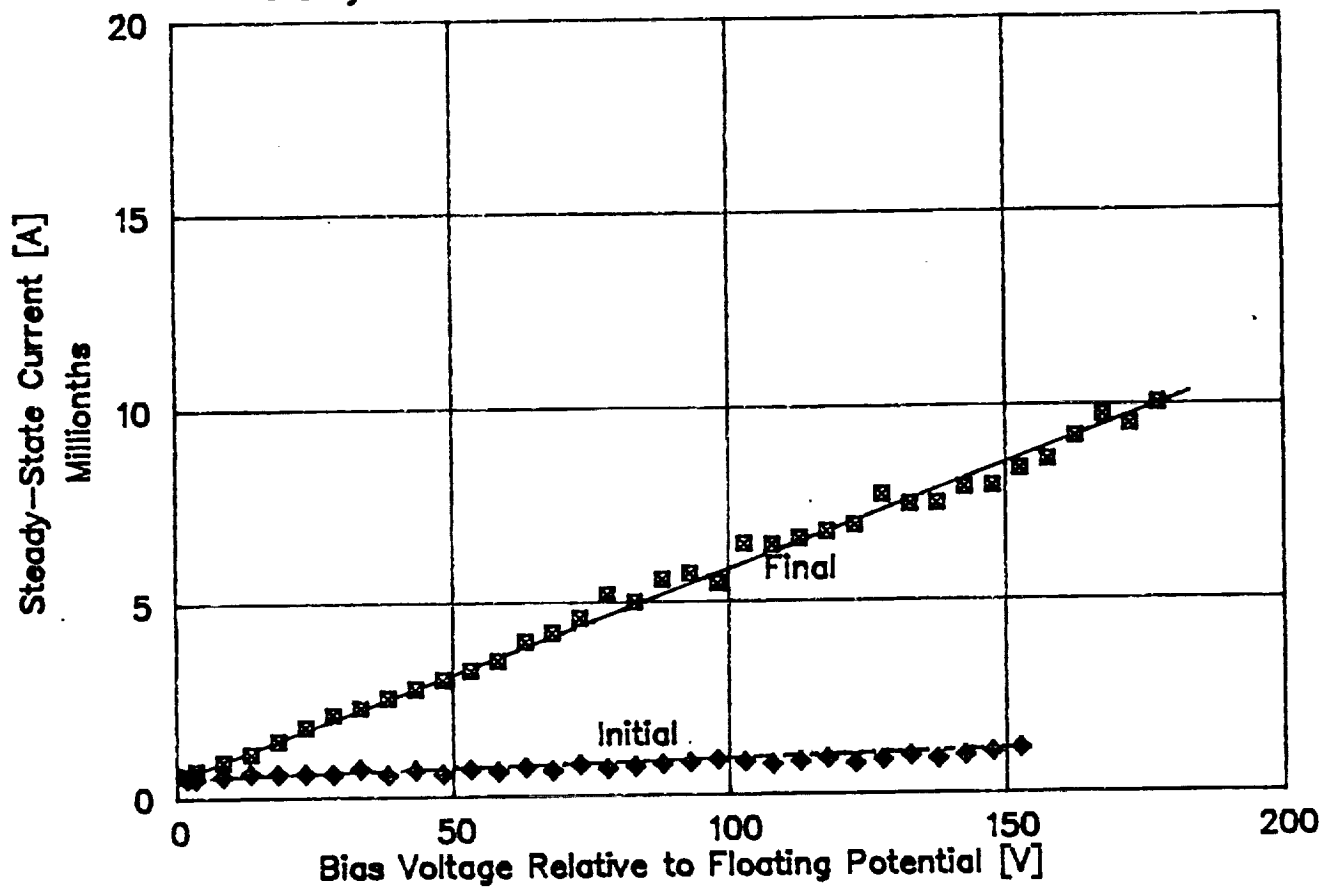
## SSF Solar Array Negative Grounding Effects

Arc Rate on Sulfuric Acid Anodized Plate—0.5 mil Anodization

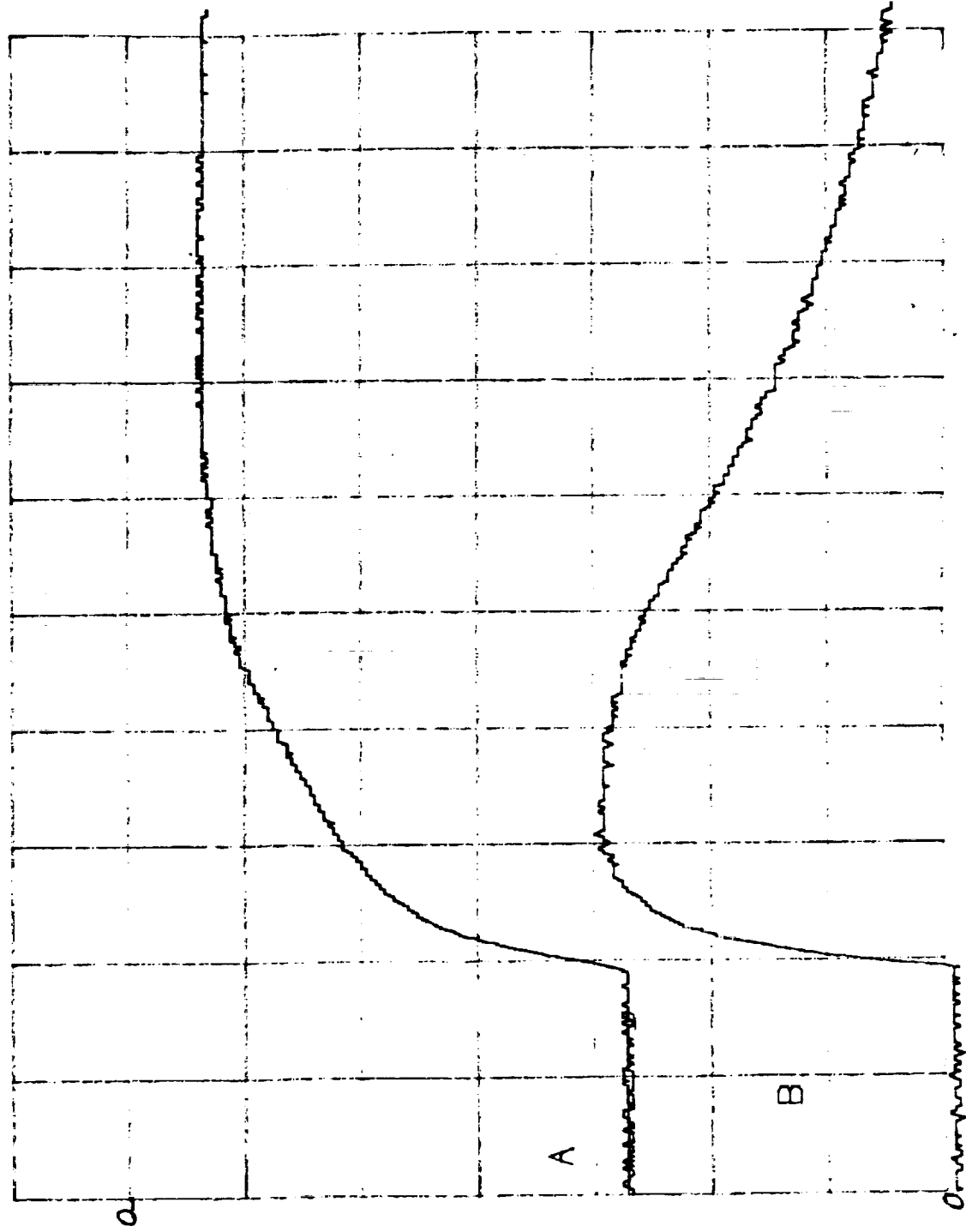


# SSF SOLAR ARRAY NEGATIVE GROUNDING EFFECTS

## Steady-State Current Collection of Sulfuric Anodized Plate



# ARC CURRENT AND CAPACITOR VOLTAGE



-160 VOLTS BIAS

C= 220 MICRO-FARAD

X=0.1 mSEC/DIV

Y(A)=40 V/DIV

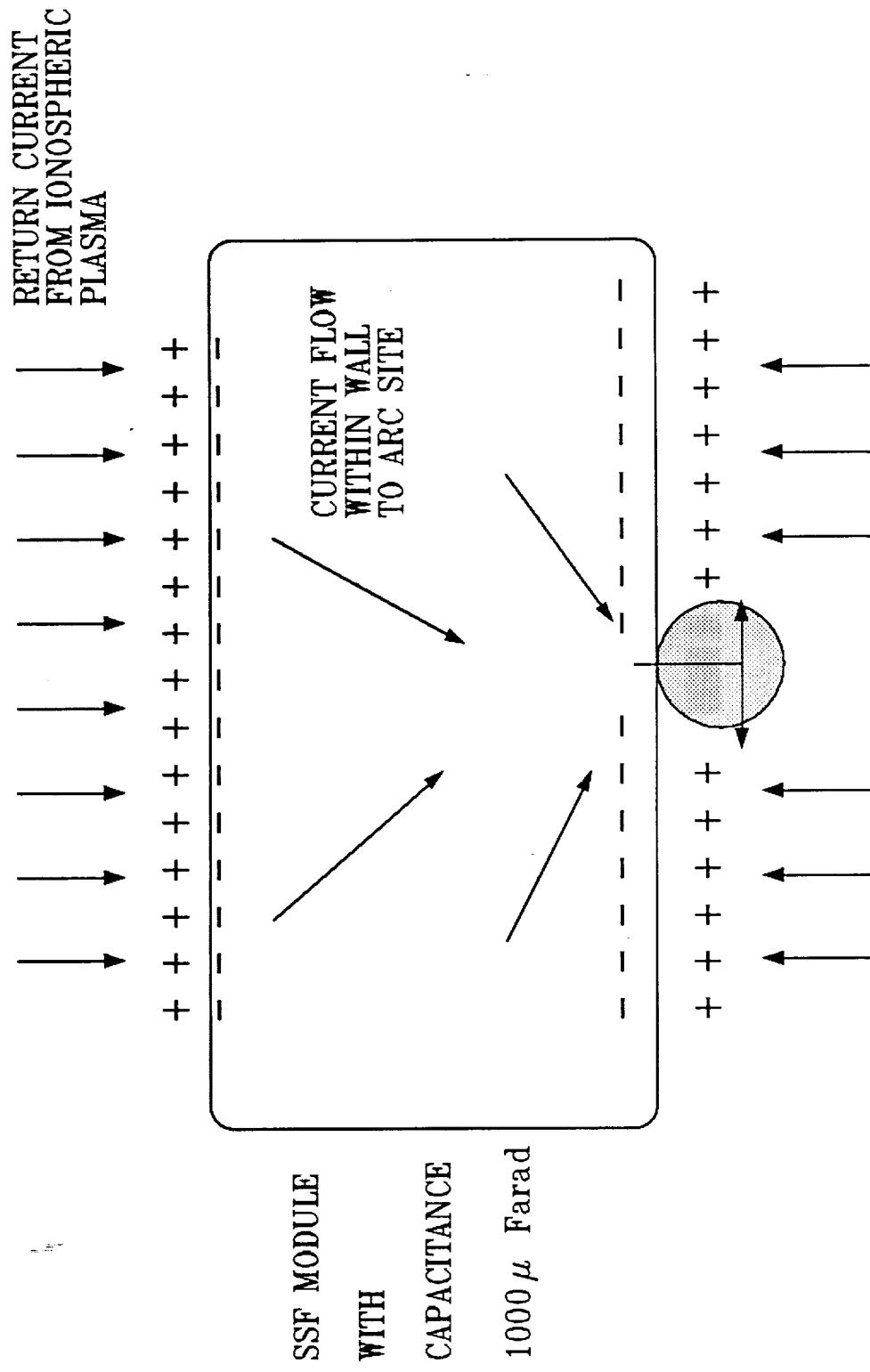
Y(B)=500 AMP/DIV

CURVE A= CAP VOLTS

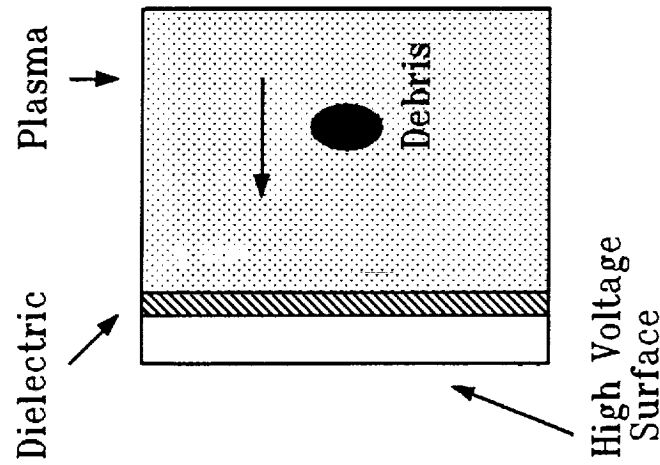
CURVE B= ARC CURRENT



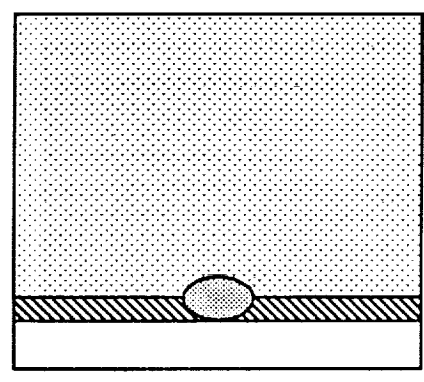
# CURRENT PATHS DURING AN ARC



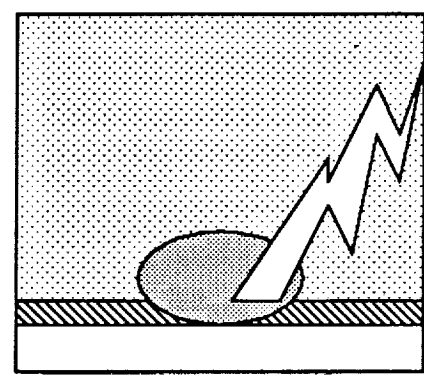
# DEBRIS STRIKE INITIATED ARC



(A) Debris Particle Incoming Through Plasma and Strikes Dielectric With High Voltage Surface Underneath



(B) Particle Strikes Surface Vaporizing and Ionizing; Penetrates to Underlying High Voltage Surface



(C) Dense Impact Plasma Couples High Voltage Surface to Outer Layer and Plasma Discharge

## DESIGN ALTERNATIVES AND MITIGATING TECHNIQUES

- 0 FLOATING OF THE SOLAR ARRAY AND PRIMARY POWER
- 0 POSITIVE GROUNDING OF THE SOLAR ARRAY
- 0 ESTABLISH STRUCTURE GROUND TO SOLAR ARRAY AT SOME POINT OTHER THAN THE POSITIVE OR NEGATIVE END
- 0 LARGE AREA ION COLLECTORS
- 0 USE OF PLASMA CONTACTOR TO CONTROL POTENTIAL OF THE STRUCTURE TO THE AMBIENT PLASMA

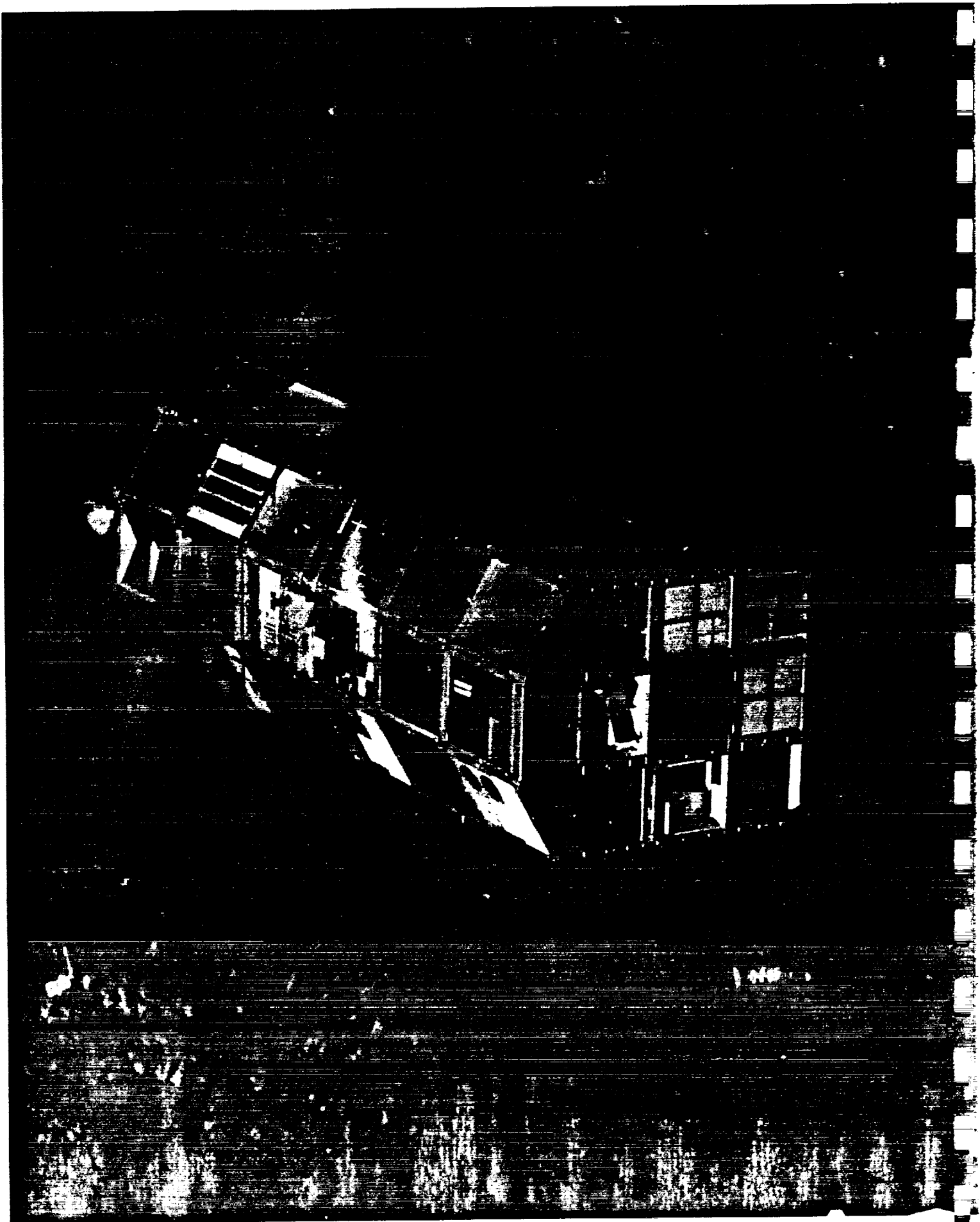
## SUMMARY

- 0 PRELIMINARY RESULTS SHOW THAT EFFECTS OF LEO PLASMA ON ANY LARGE PLATFORMS USING HIGH VOLTAGE MUST BE SERIOUSLY CONSIDERED IN DESIGN
- 0 TEST AND ANALYSIS PLAN FOR PHASE I COMPLETE WITH SOME TESTS AND ANALYSIS ALREADY IN PROGRESS
- 0 GOAL IS TO UNDERSTAND EFFECTS SUCH THAT
  - o REASONABLE MITIGATION TECHNIQUES IDENTIFIED
  - o RELIABLE ASSESSMENT OF ENVIRONMENTAL IMPACTS CAN BE MADE

ORGANIZATION:		MARSHALL SPACE FLIGHT CENTER		NAME:	DR. ANN F. WHITAKER
EH11		SPACE STATION INDUCED ENVIRONMENTS WORKSHOP		DATE:	JANUARY 30, 1991
CHART NO.:					
<p style="text-align: center;">LDEF INDUCED ENVIRONMENTS</p> <p>GENERAL ENVIRONMENTS, EXP. A0171 RESULTS      -      ANN WHITAKER</p> <p>LDEF CONTAMINATION MODELLING                              -      RAY RANTANEN</p> <p>EXPERIMENT A0034 RESULTS                                      -      ROGER LINTON</p>					

ORIGINAL PAGE IS  
OF POOR QUALITY

ORIGINAL PAGE  
BLACK AND WHITE PHOTOGRAPH



ORGANIZATION:  CHART NO.:	EH11  MARSHALL SPACE FLIGHT CENTER SPACE STATION INDUCED ENVIRONMENTS WORKSHOP	NAME: DR. ANN F. WHITAKER
		DATE: JANUARY 30, 1991

LDEF NATURAL ENVIRONMENTS

- 0 HIGH VACUUM -  $10^{-6}$  -  $10^{-7}$  TORR (VARIES RAM TO WAKE, LOCALLY)
- 0 UV RADIATION - 10.041 ESH • 1 SUN (EXP. A0171)
- 0 PROTON FLUENCE -  $10^9$  p<sup>+</sup>/CM<sup>2</sup> (.05 - 200 MeV)
- 0 ELECTRON FLUENCE -  $(10^{12} - 10^8$  e<sup>-</sup>/CM<sup>2</sup>)(.05 - 3.0 MeV)
- 0 ATOMIC OXYGEN -  $8.0 \times 10^{21}$  ATOMS/CM<sup>2</sup>
- 0 MICROMETEOROID/SPACE DEBRIS IMPACTS ~ 5000-6000. >1/2mm. 2-7 PER 25 IN<sup>2</sup>  
(A0171 EXP.), <1mm.
- 0 THERMAL CYCLES - ~ 32,000 CYCLES (THERMAL EXTREMES MATERIALS PECULIAR)

ORGANIZATION:		MARSHALL SPACE FLIGHT CENTER		NAME:	DR. ANN F. WHITAKER
CH11		SPACE STATION INDUCED ENVIRONMENTS WORKSHOP		DATE:	JANUARY 30, 1991
CHART NO.:					

**LDEF CONTAMINATION SOURCES**

**MAJOR SOURCES:**

ON-ORBIT

- UNBAKED Z306 POLYURETHANE BLACK PAINT ON LDEF INTERIOR SURFACES
- REFLECTORS ON END RINGS THAT FACE ALTERNATE ROWS
- UNBAKED ELECTRICAL CONNECTOR INSERTS

RETRIEVAL, TRANSPORT, AND GROUND HANDLING

- PARTICULATE METALLIZATIONS FROM ATOMIC OXYGEN ERODED THIN FILM SUBSTRATES

**OTHER SOURCES:**

- PARTICULATES FROM PREFLIGHT/ORBITAL OPERATIONS
- INSUFFICIENTLY T/V BAKED MATERIALS
- UNBAKED MATERIALS
- MICROMETEOROID/SPACE DEBRIS



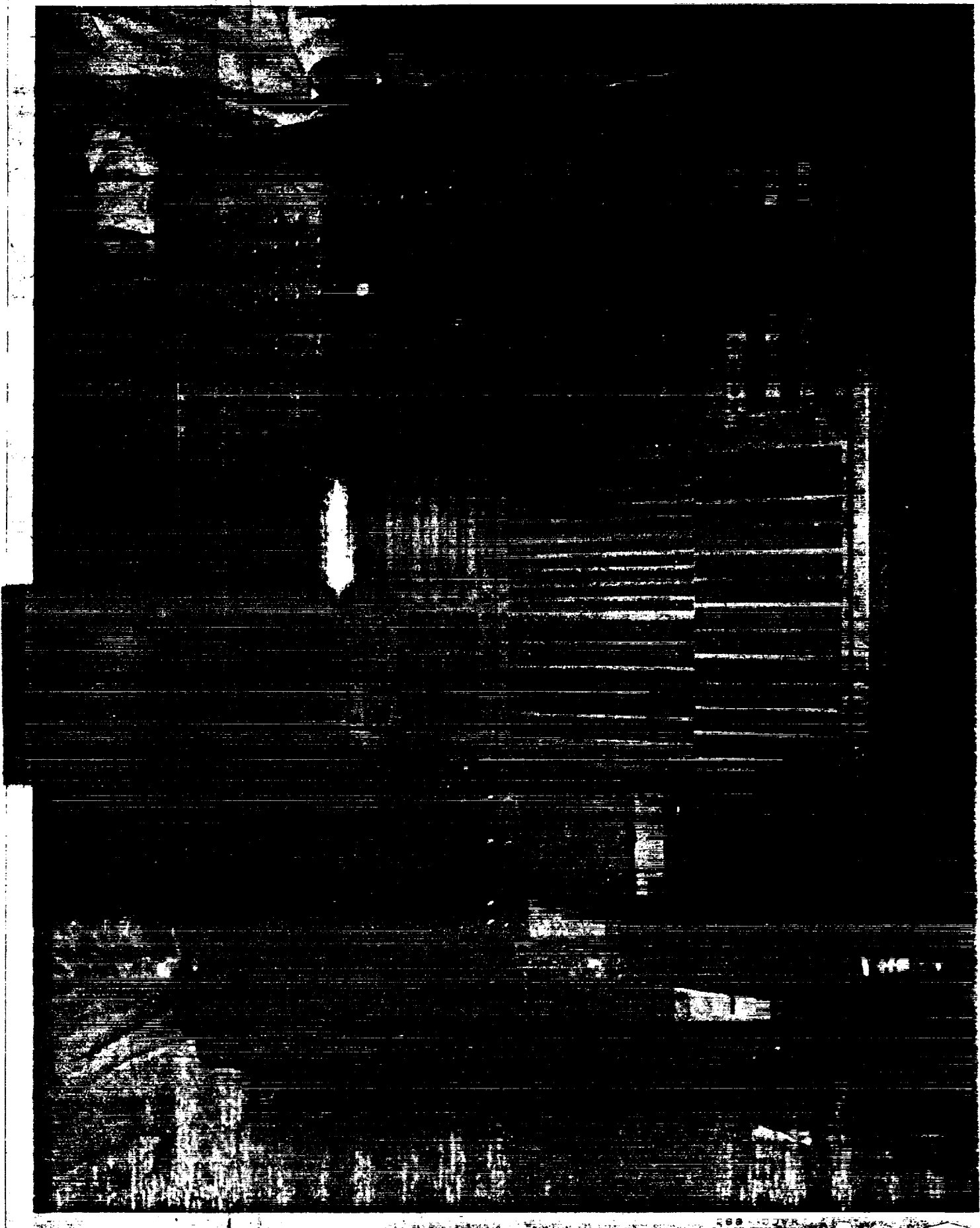
ORIGINAL PAGE IS  
OF POOR QUALITY

ORIGINAL PAGE  
BLACK AND WHITE PHOTOGRAPH



ORIGINAL PAGE IS  
OF POOR QUALITY

ORIGINAL PAGE  
BLACK AND WHITE PHOTOGRAPH



ORIGINAL PAGE IS  
OF POOR QUALITY

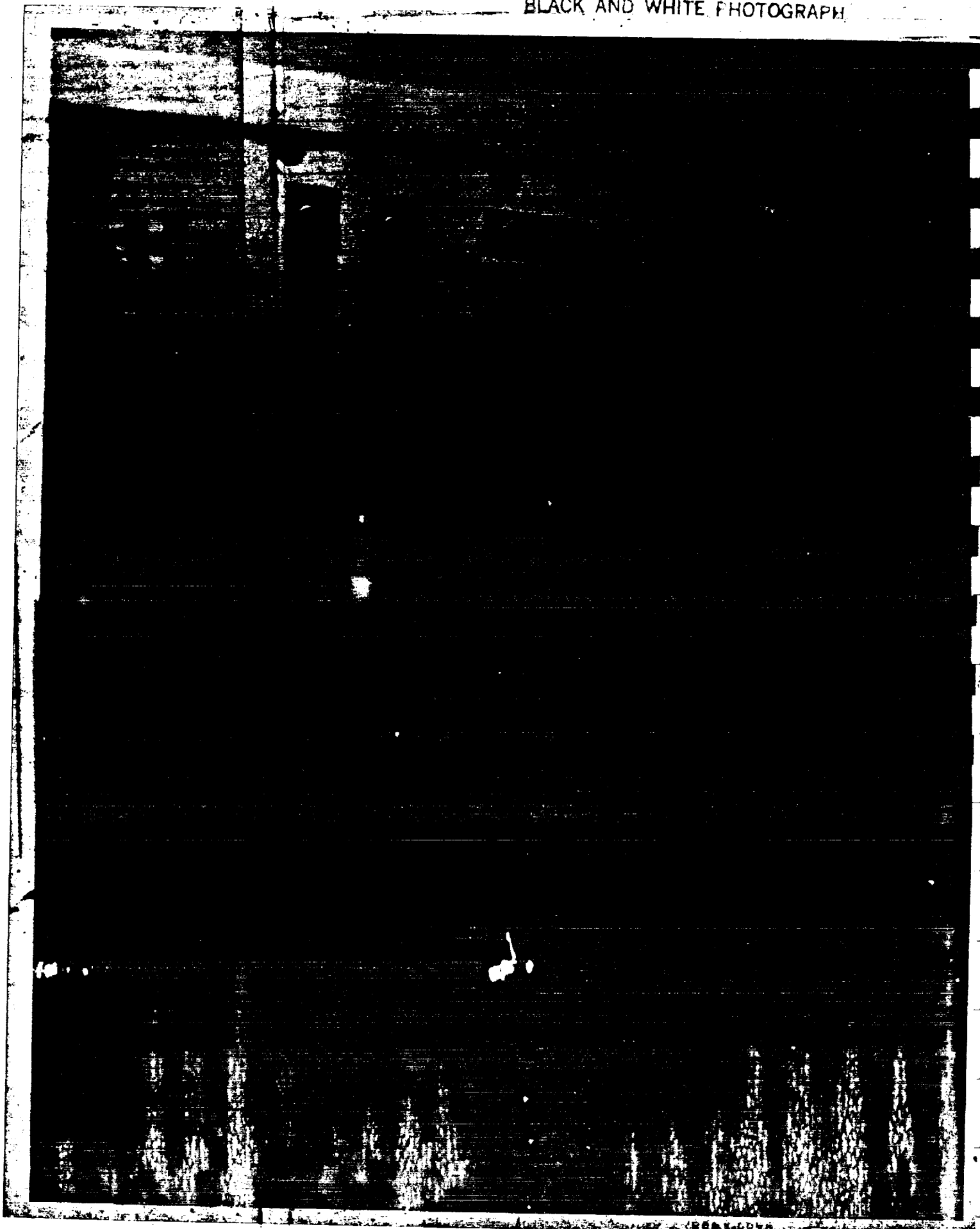
ORIGINAL PAGE  
BLACK AND WHITE PHOTOGRAPH

ORIGINAL PAGE IS  
OF POOR QUALITY

ORIGINAL PAGE  
BLACK AND WHITE PHOTOGRAPH

ORIGINAL PAGE IS  
OF POOR QUALITY

ORIGINAL PAGE  
BLACK AND WHITE PHOTOGRAPH





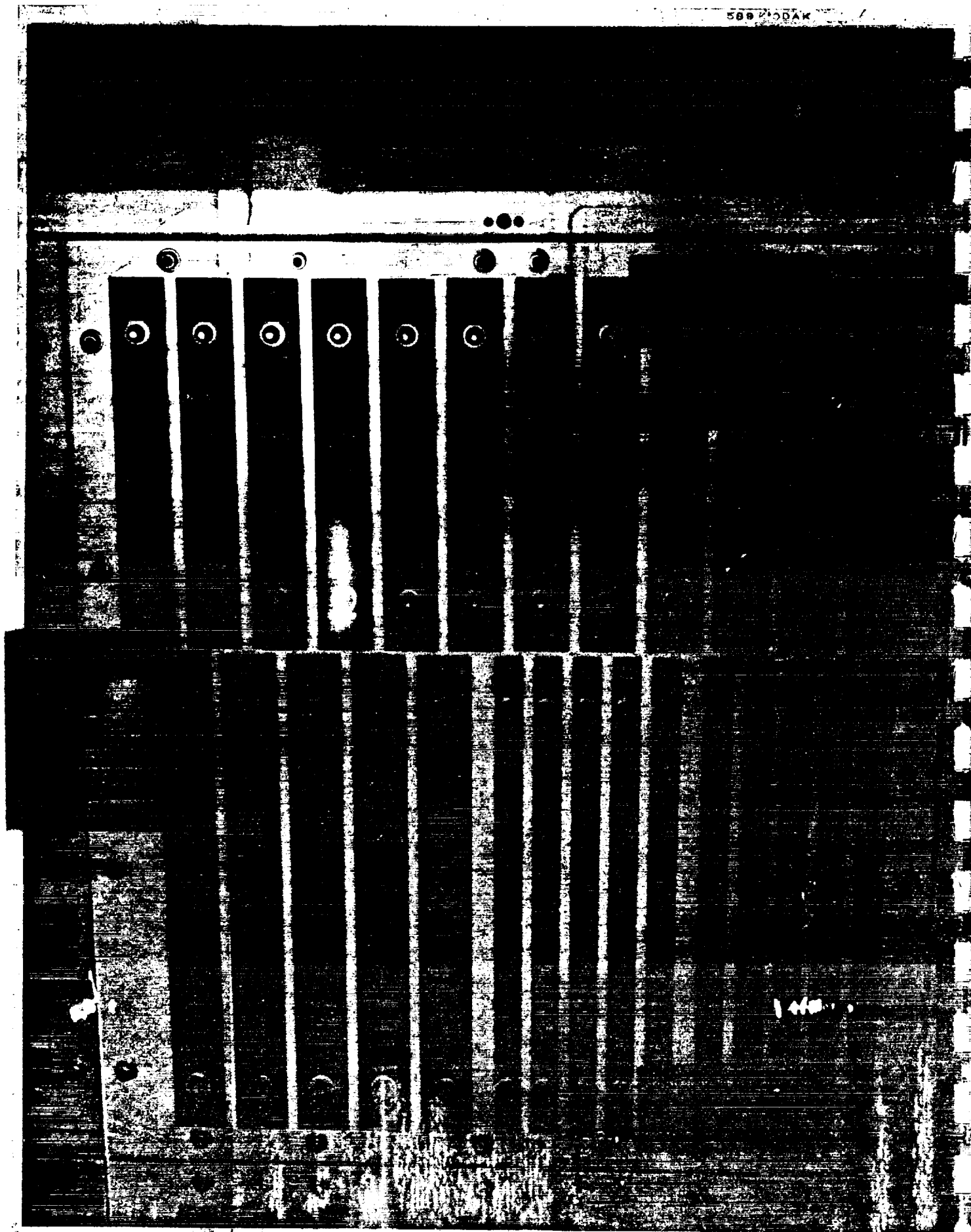
ORIGINAL PAGE IS  
OF POOR QUALITY

ORIGINAL PAGE  
BLACK AND WHITE PHOTOGRAPH

ORIGINAL PAGE IS  
OF POOR QUALITY

ORIGINAL PAGE  
BLACK AND WHITE PHOTOGRAPH

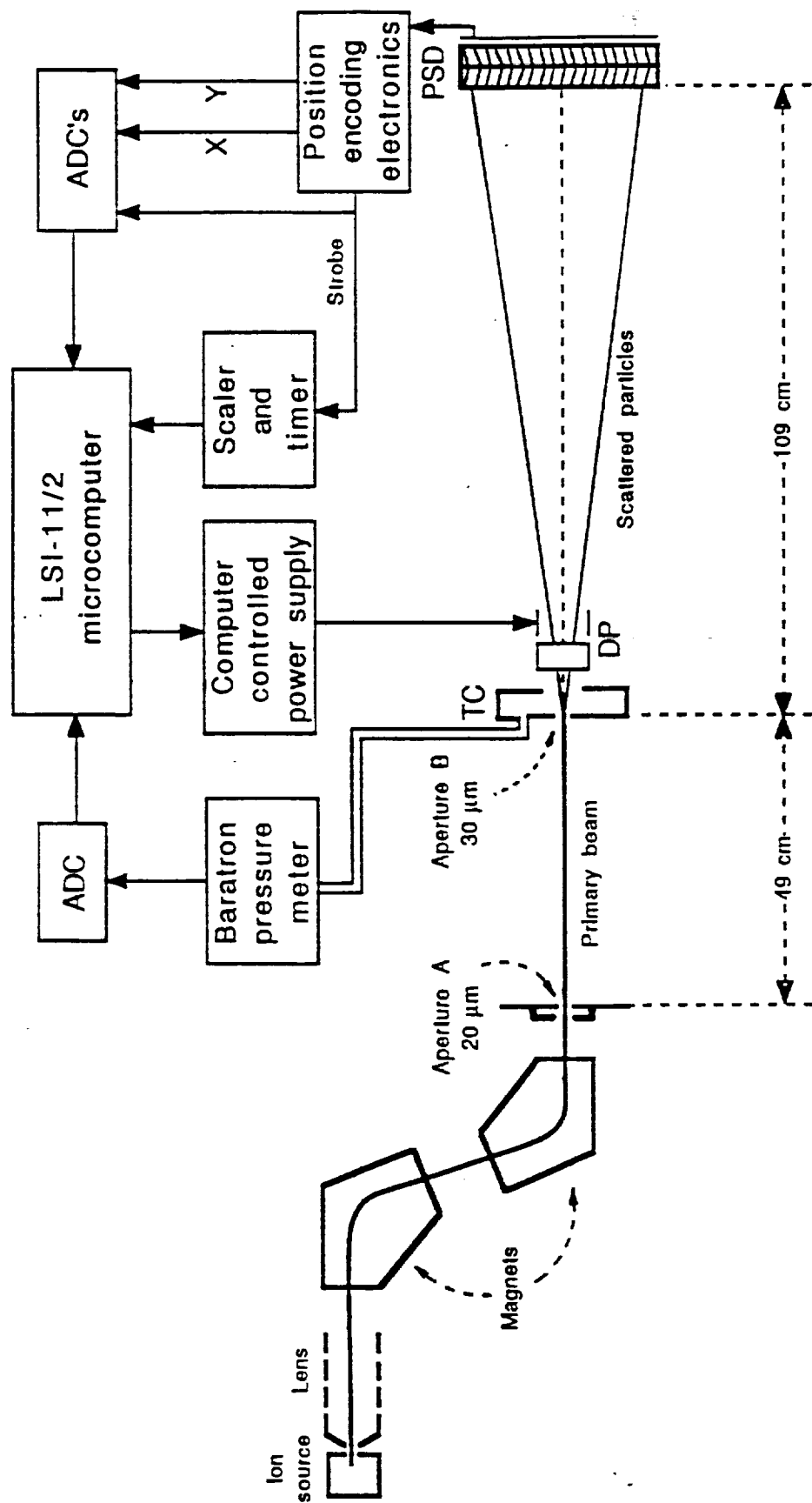
589 200AK



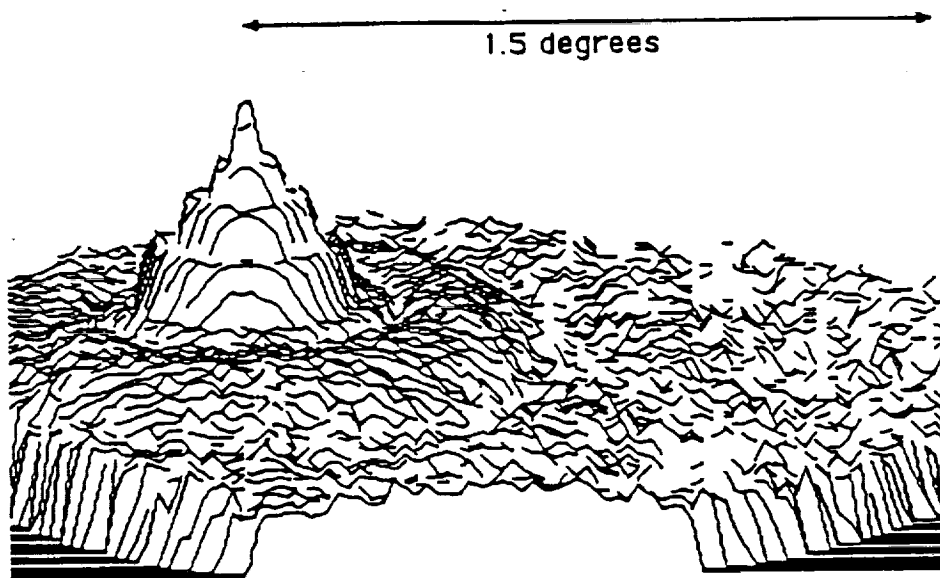
ORIGINAL PAGE IS  
OF POOR QUALITY

ORIGINAL PAGE  
BLACK AND WHITE PHOTOGRAPH

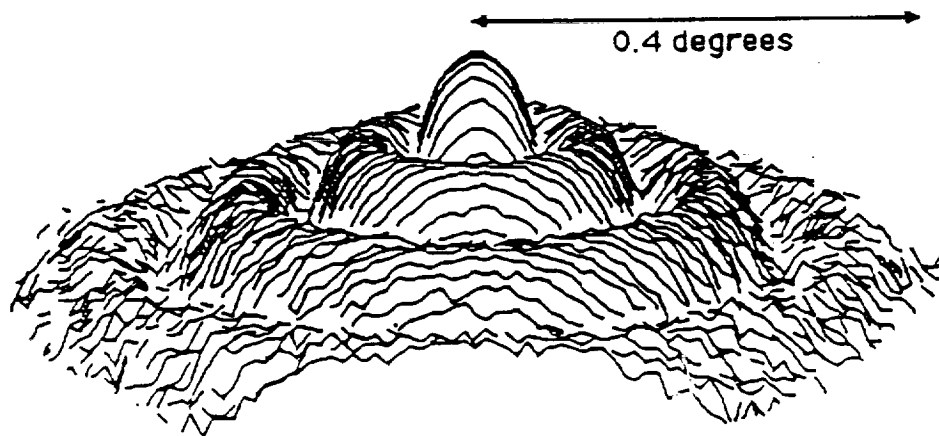




Schematic diagram of the apparatus

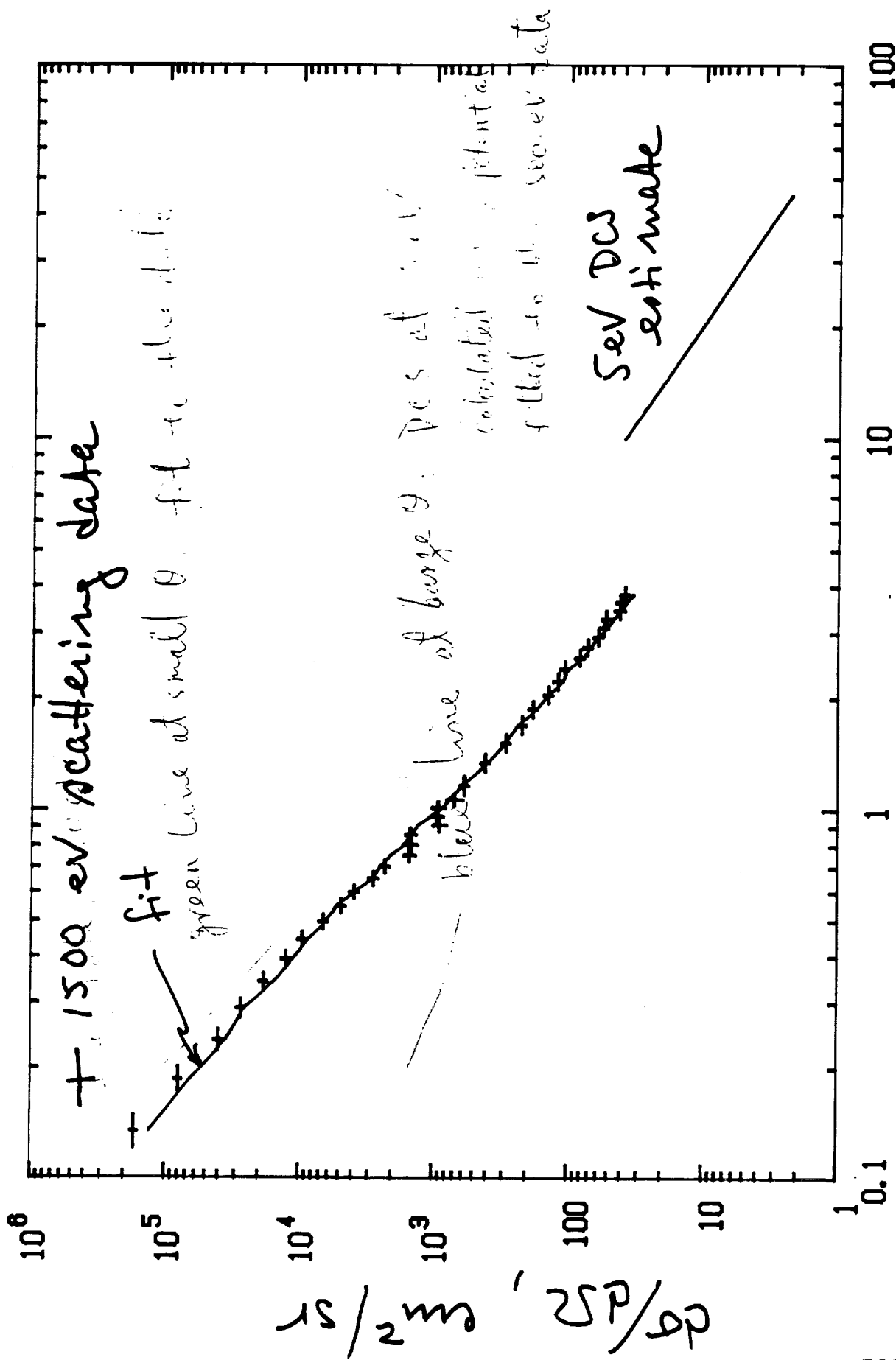


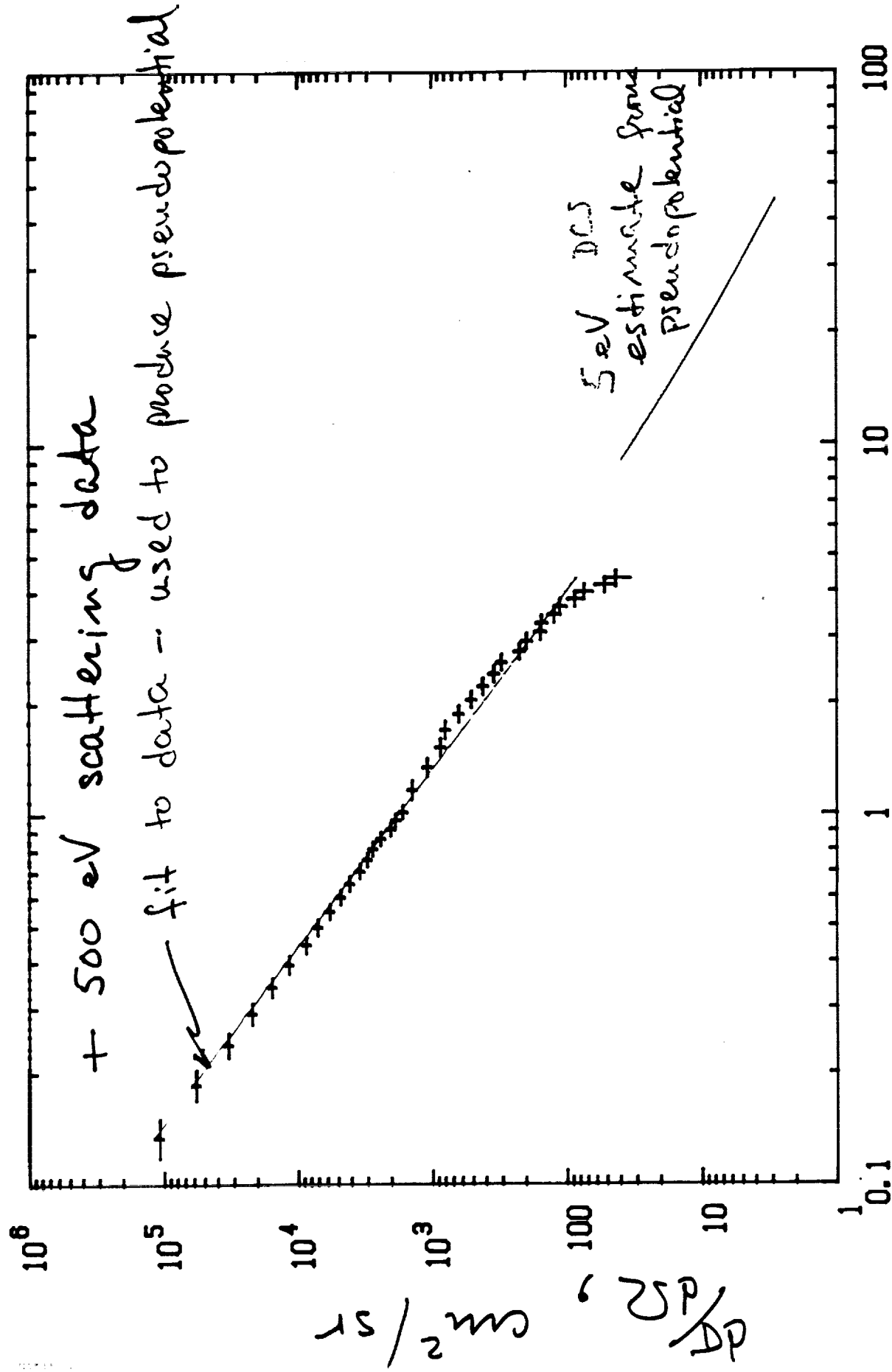
Map of particle impacts on the PSD for  $\text{He}^+(1.5 \text{ keV})$  - He charge-transfer scattering. PSD bin dimension was set to be  $436 \mu\text{m}$ .



Map of particle impacts on the PSD for  $\text{He}^+(1.5 \text{ keV})$  - He charge-transfer scattering. PSD bin dimension was set to be  $109 \mu\text{m}$ .

$O + N_2 DCS$







# Cross Section Work at UAH/MSFC

Charles E. Keffer  
UAH

Presented at Space Station Freedom  
Induced External Environment Review  
January 31, 1991

# INTRODUCTION

- Space Station Induced Environment
- Objectives for Cross Section Facility
- Cross Section Facility Description
- Recent Data
- Future Directions

# Space Station Induced Environment

## Contamination Issues

- Neutral Gas Abundance/Distribution
- Gas/Surface Interactions
- Optical Emission/Absorption
- Plasma Electromagnetic Effects
- Particulates



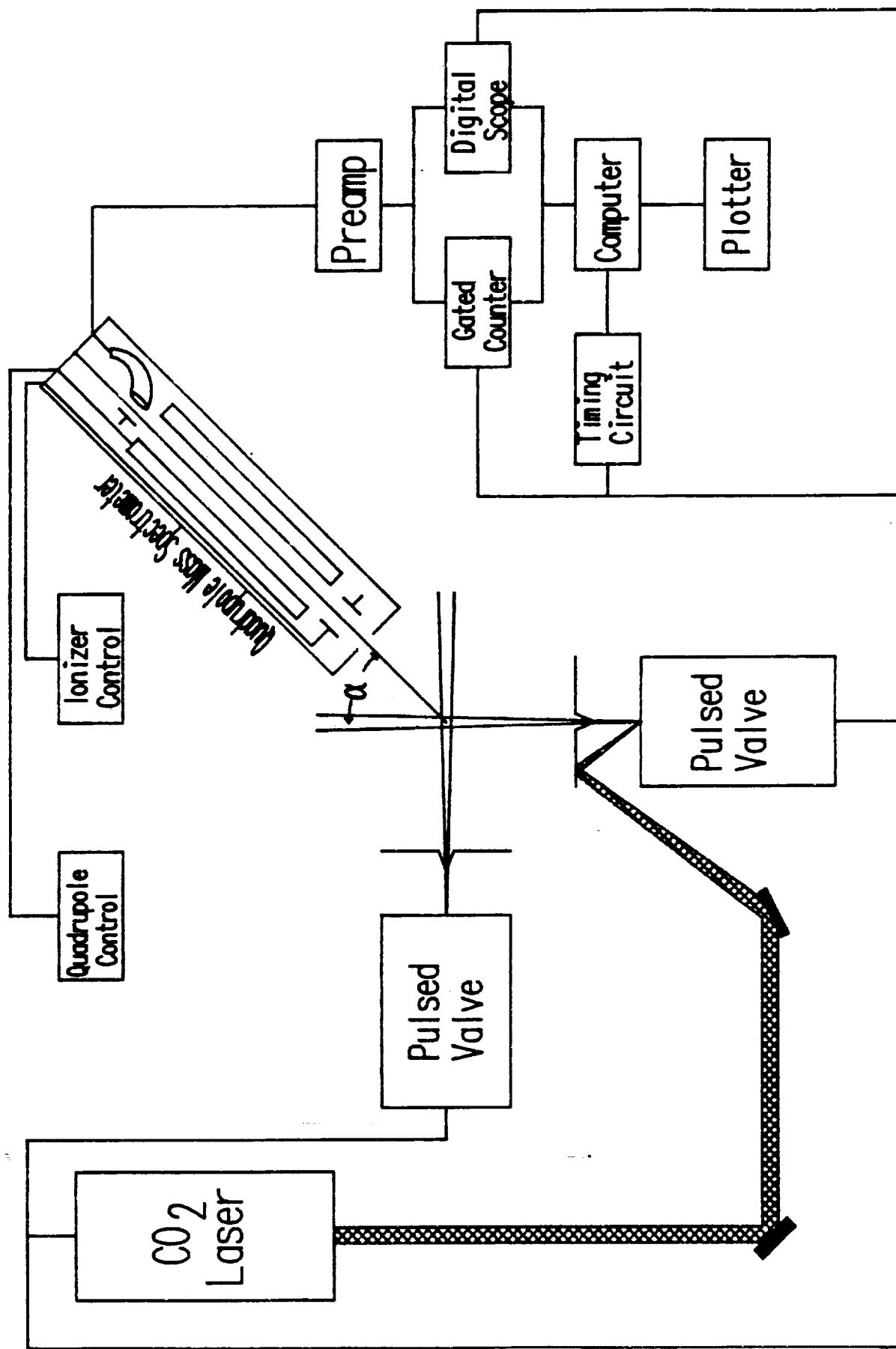
# Objectives for Cross Section Facility

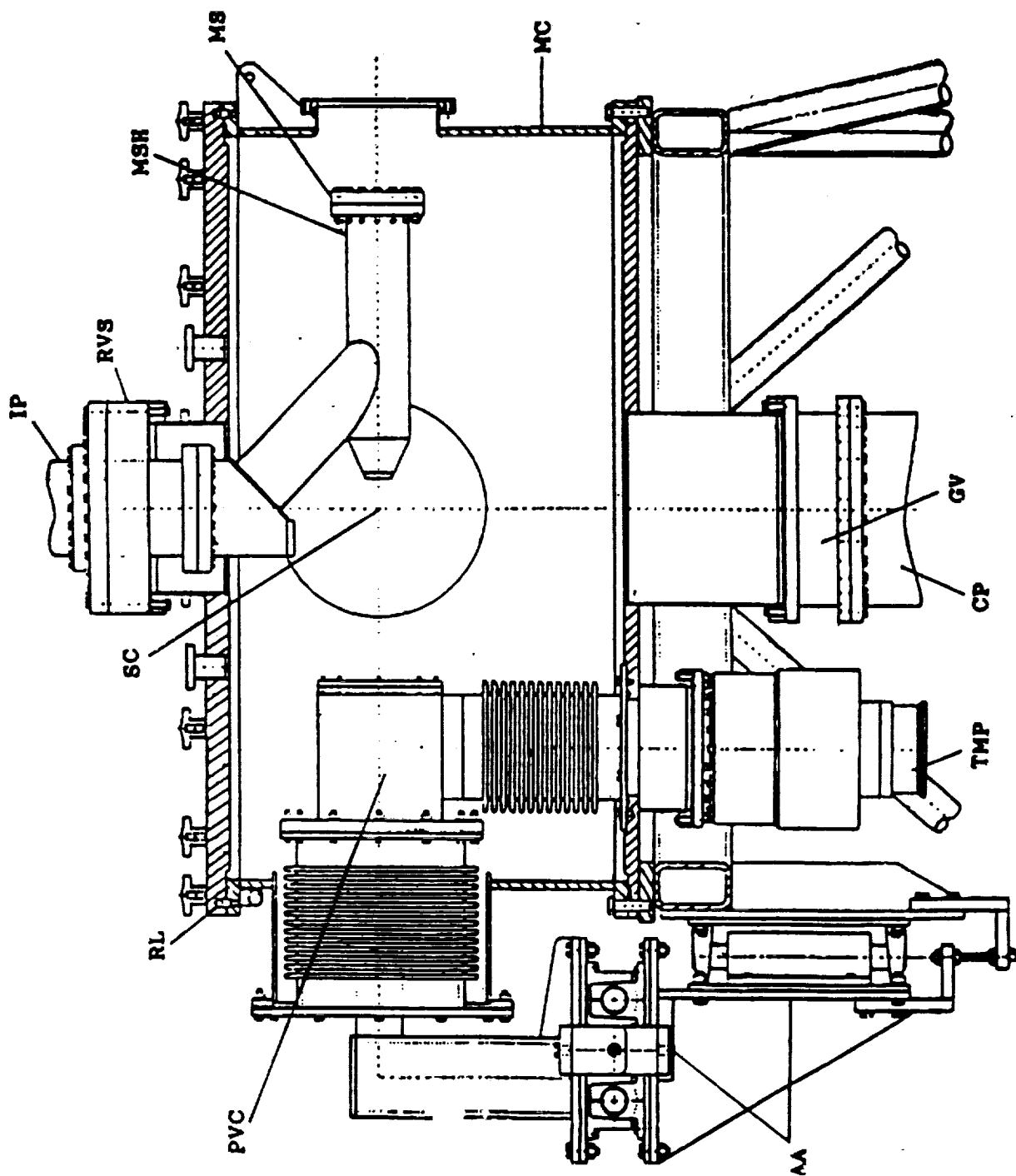
- Measure Atomic and Molecular Parameters
  - Differential Scattering Cross Sections
  - Charge Exchange Cross Sections
  - Reaction Cross Sections
- Study Gas/Surface Interactions
  - Sticking Coefficients
  - Reaction Products
  - Surface Temperature Effects
- Study Induced Emissions ("shuttle glow")

# Experimental Approach

- Crossed Beam Apparatus
- Rotatable Mass Spectrometer
- Differential Pumping and Pulsed Beams
- High Angular Resolution
- Laser-Induced Discharge Energetic  
O Atom Source
- Flexible System for Multiple Objectives

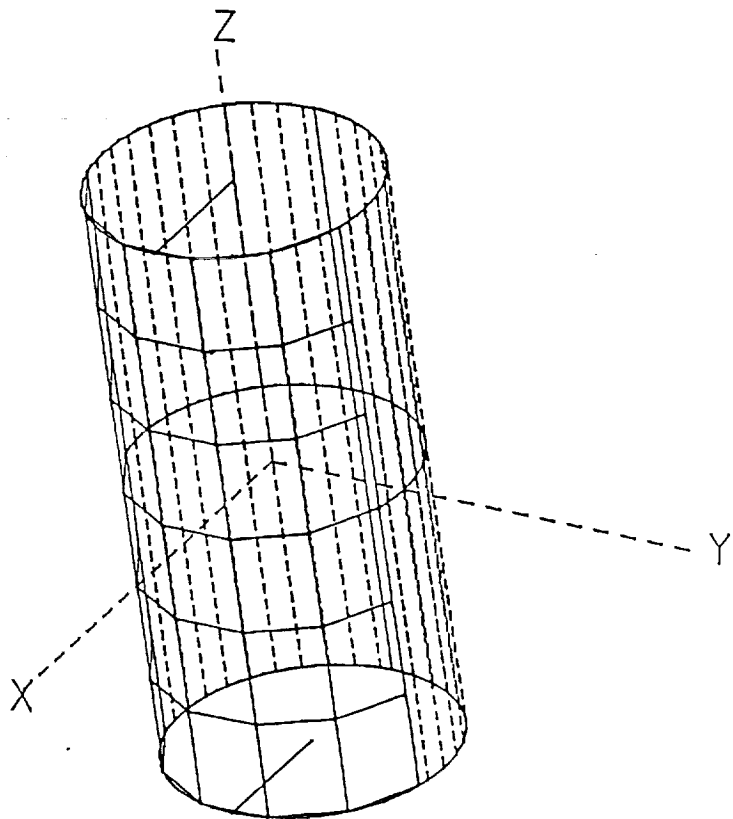
# Cross Section Facility





1. Side view of vacuum chamber. IP - ion pump, RVS - rotary vacuum seal, MSH - mass spectrometer housing, MS - mass spectrometer, MC - main chamber, GV - gate valve, CP - cryopump, TMP - turbomolecular pump, AA - adjusting assemblies, PVC - pulsed valve chamber, RL - removable lid, SC - scattering center.

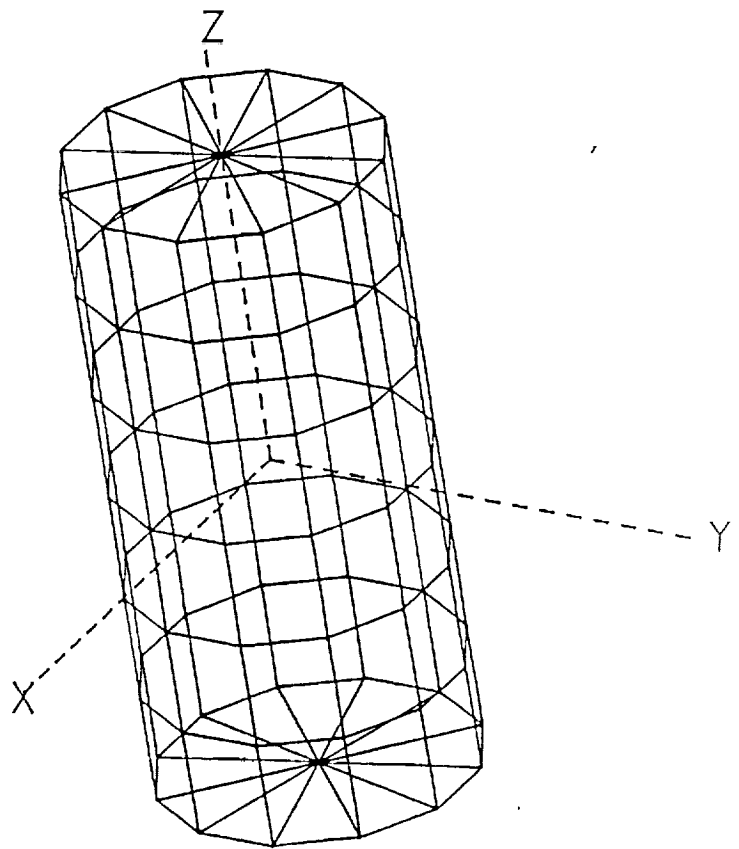
# LONG DURATION EXPOSURE FACILITY



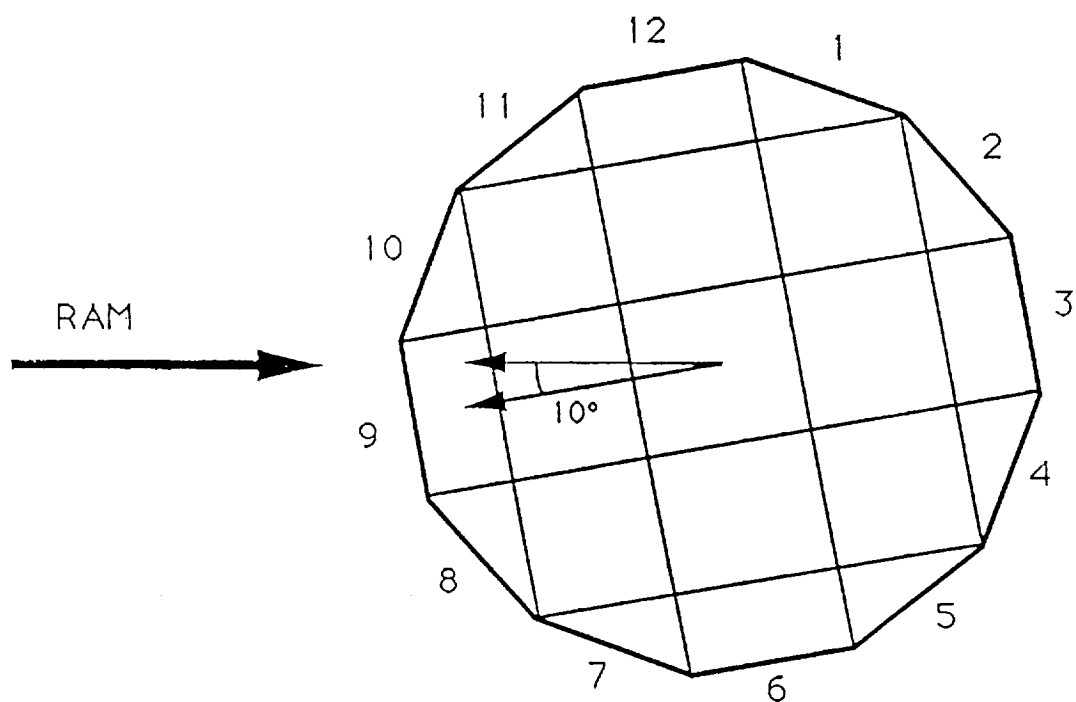
VIEW = 3-D  
SCALE = 0.1413  
NV = 1



# LONG DURATION EXPOSURE FACILITY



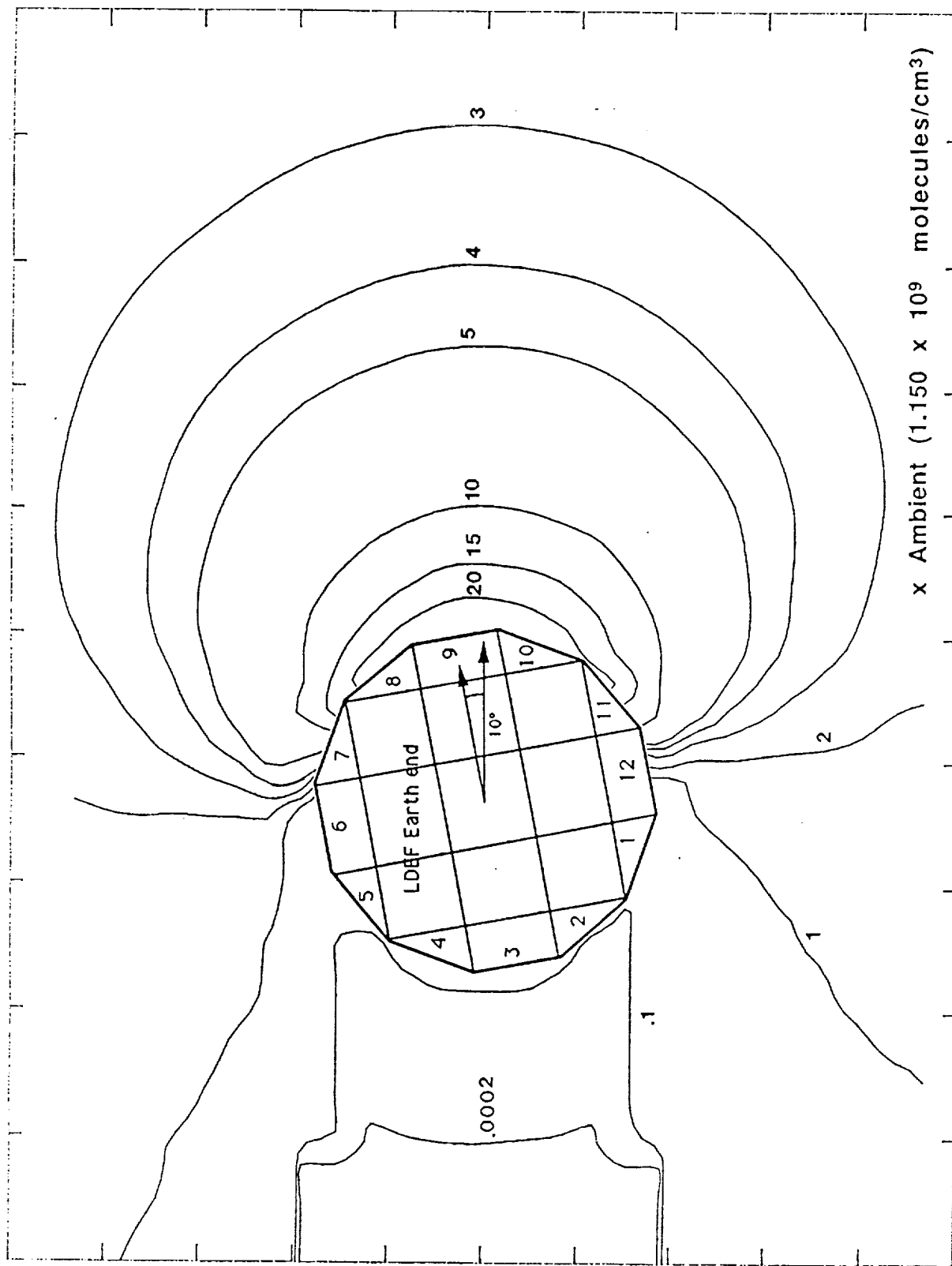
VIEW = 3-D  
SCALE = 0.1541  
NV = 1



# LDEF FACET IDENTIFICATION (FROM EARTH END)

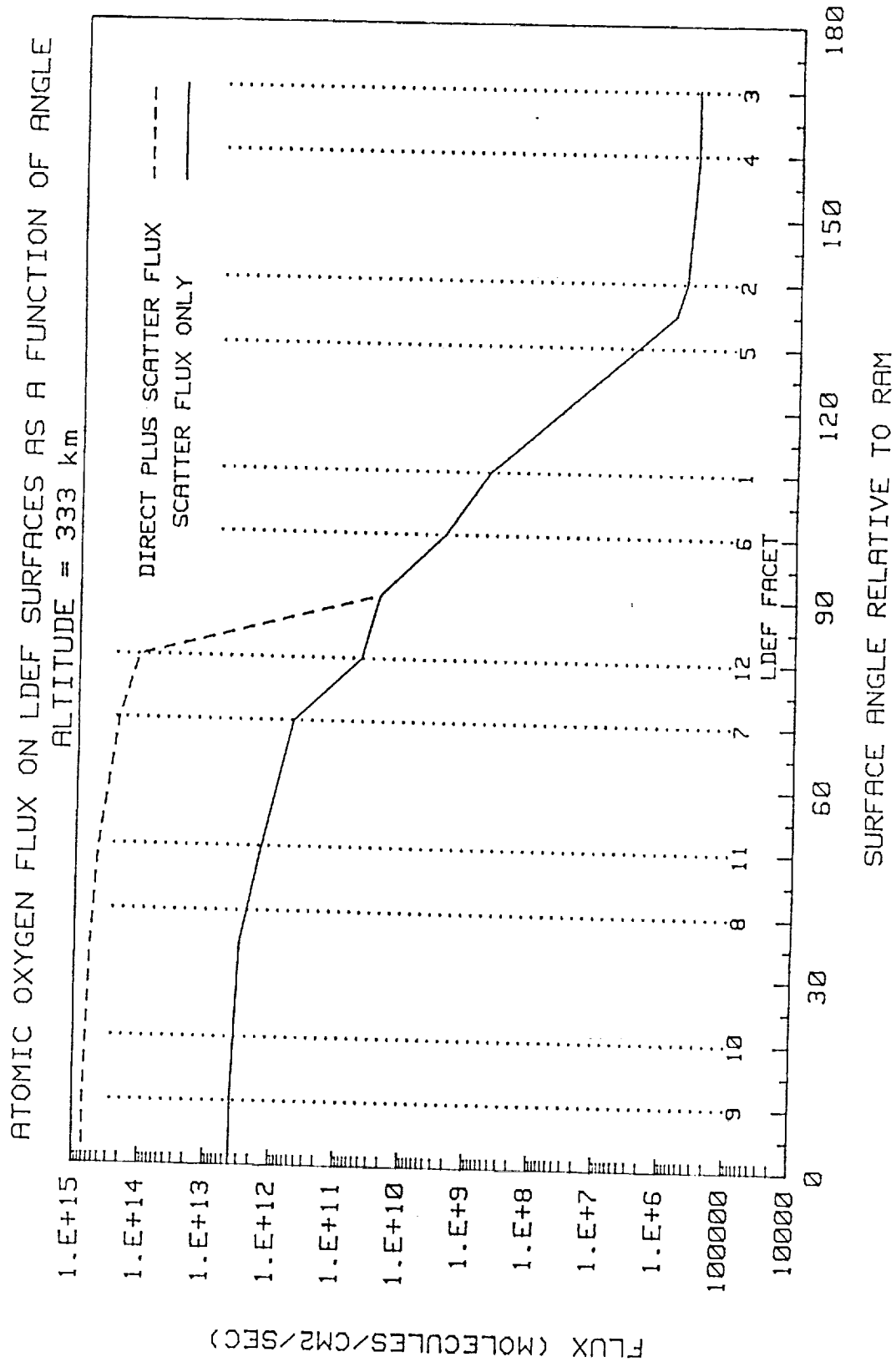
NOTE: 10° ROTATION REFERENCE "LDEF FLOW ANGLE MEASUREMENT SUMMARY", JASON A. VAUGHN, MSFC, 1990.

# TOTAL DENSITY X-Y PLANE AT 333 KM



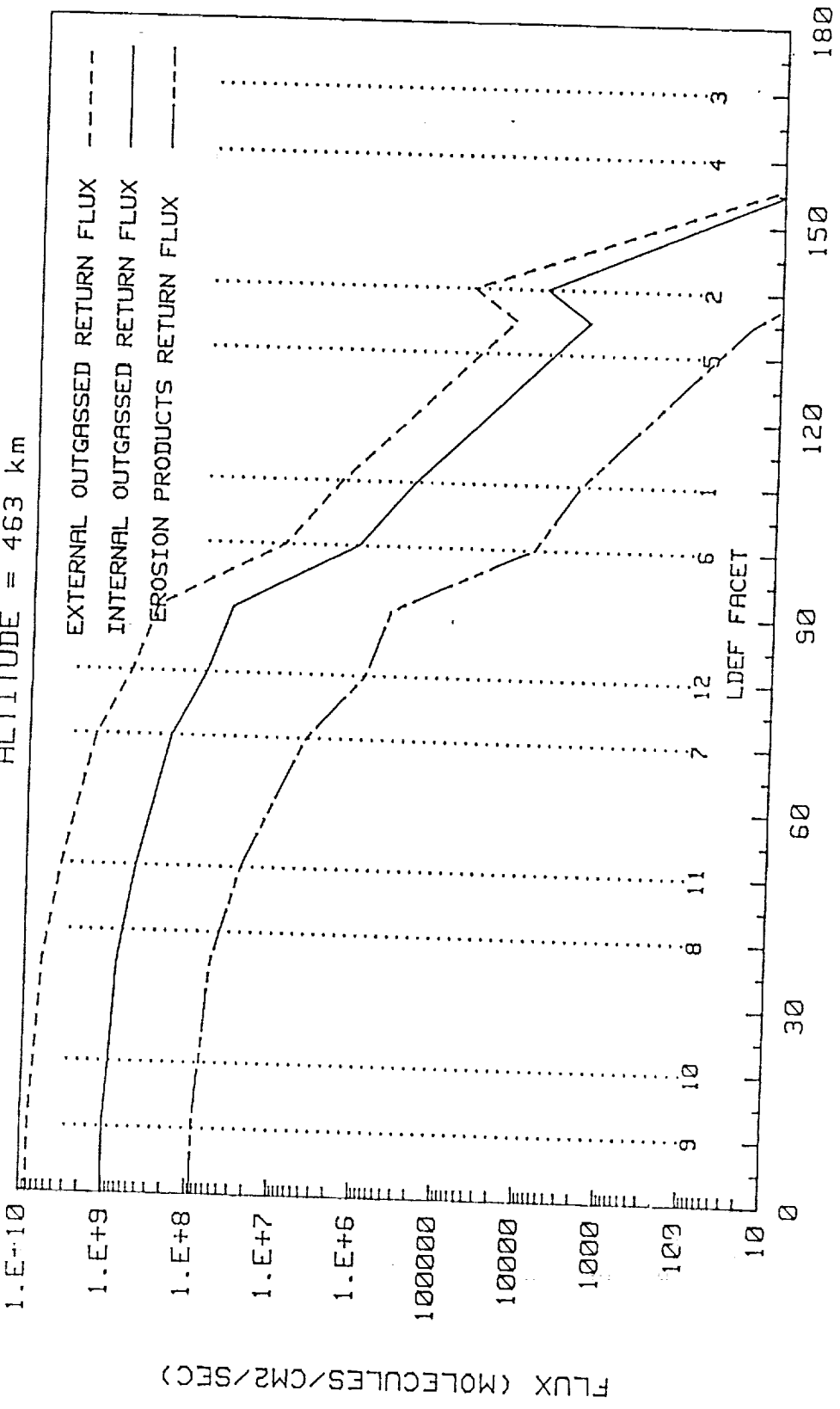
CONTOUR FROM 0.20000E-03 TO 20.000 CONTOUR INTERVAL OF IRREGULAR  
 X INTERVAL= 155.00 Y INTERVAL= 115.00





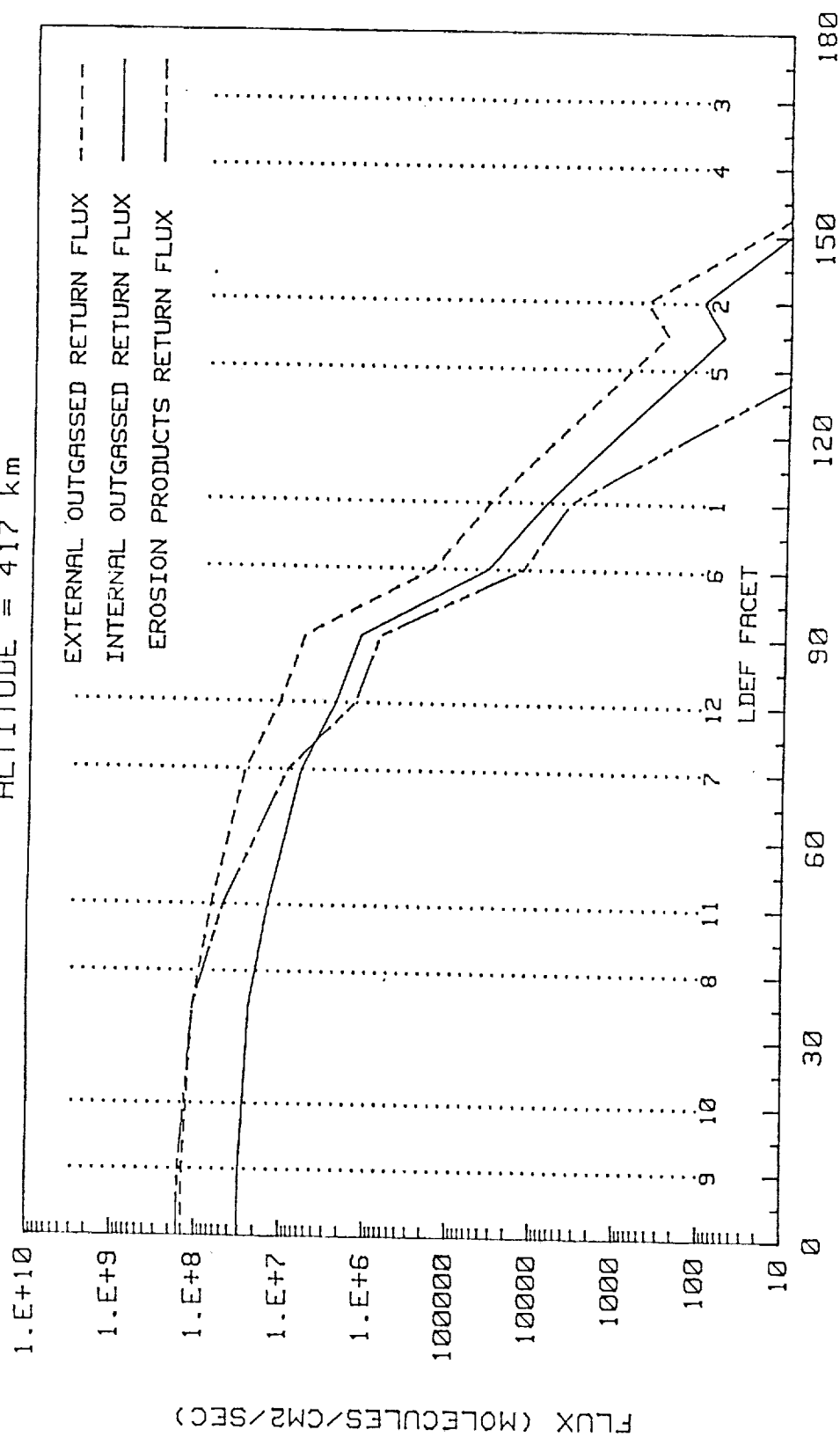
# OUTGAS AND EROSION PRODUCT FLUX ON LDEF SURFACES AS A FUNCTION OF ANGLE

ALTITUDE = 463 km



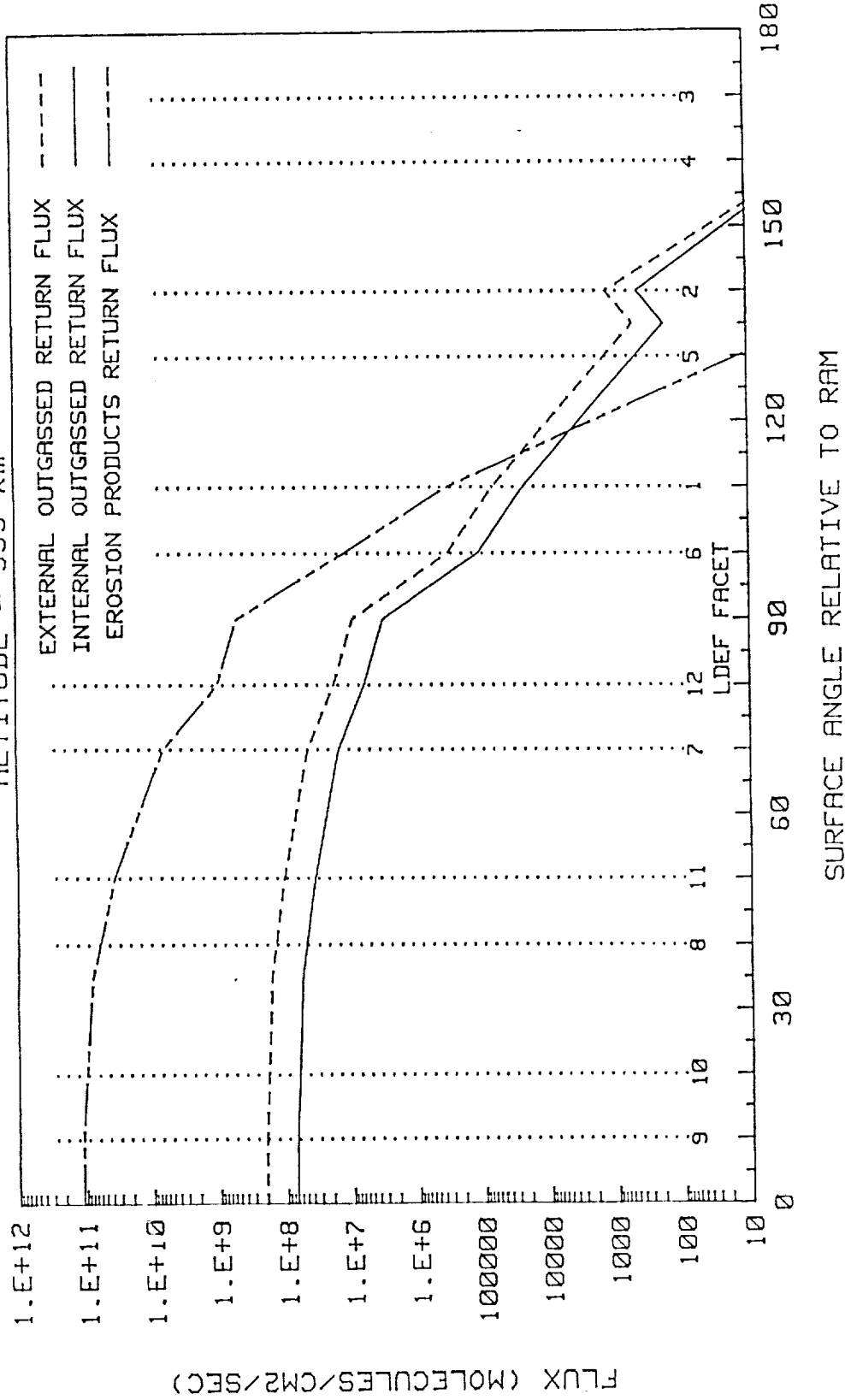
# OUTGAS AND EROSION PRODUCT FLUX ON LDEF SURFACES AS A FUNCTION OF ANGLE

ALTITUDE = 417 km



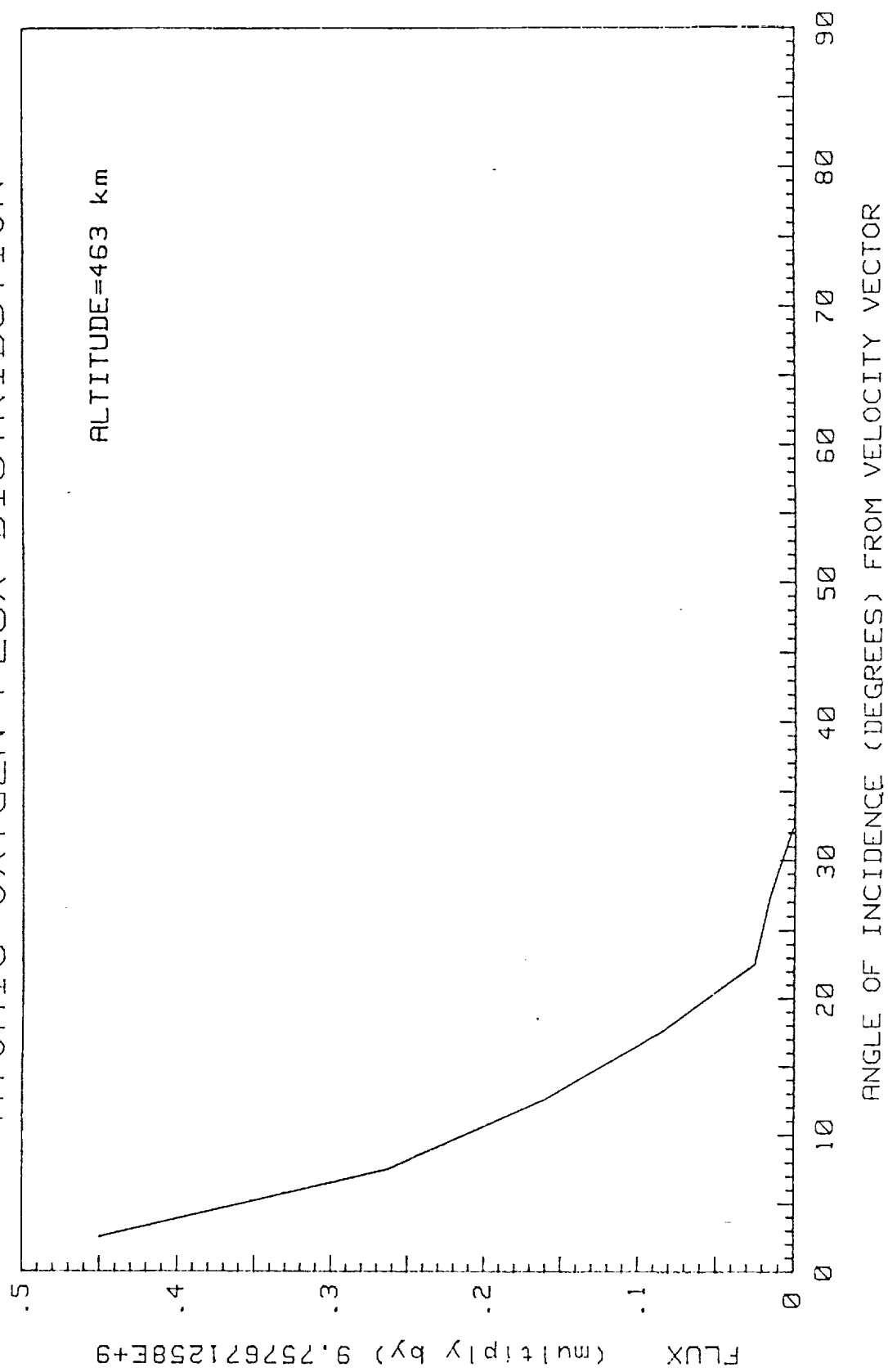
# OUTGAS AND EROSION PRODUCT FLUX ON LDEF SURFACES AS A FUNCTION OF ANGLE

ALTITUDE = 333 km



# ATOMIC OXYGEN FLUX DISTRIBUTION

ALTITUDE=463 km



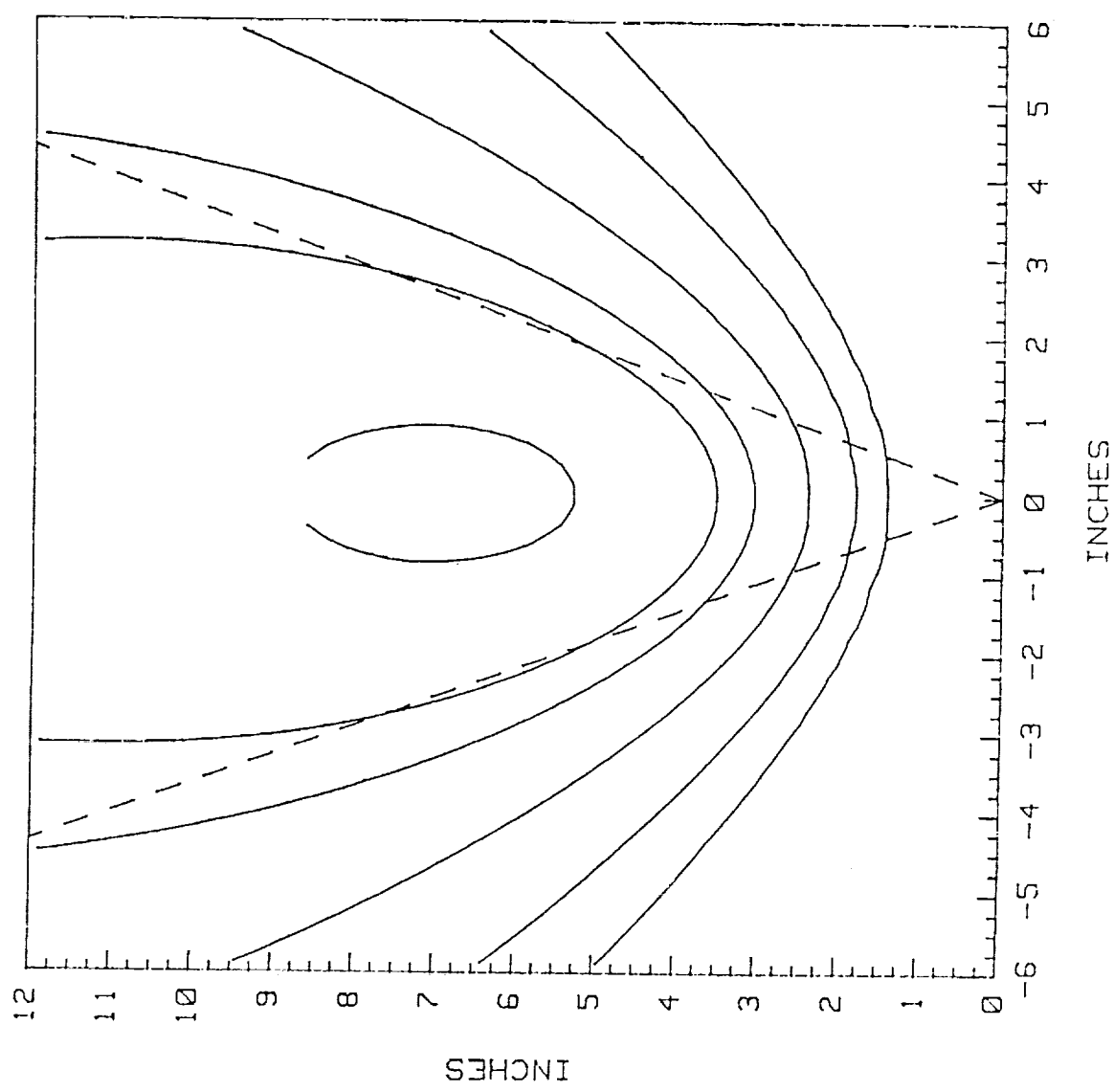
# INCIDENT SCATTER ISO-FLUX CONTOURS ON SURFACE

MOLECULAR SPECIES=  
ATOMIC OXYGEN

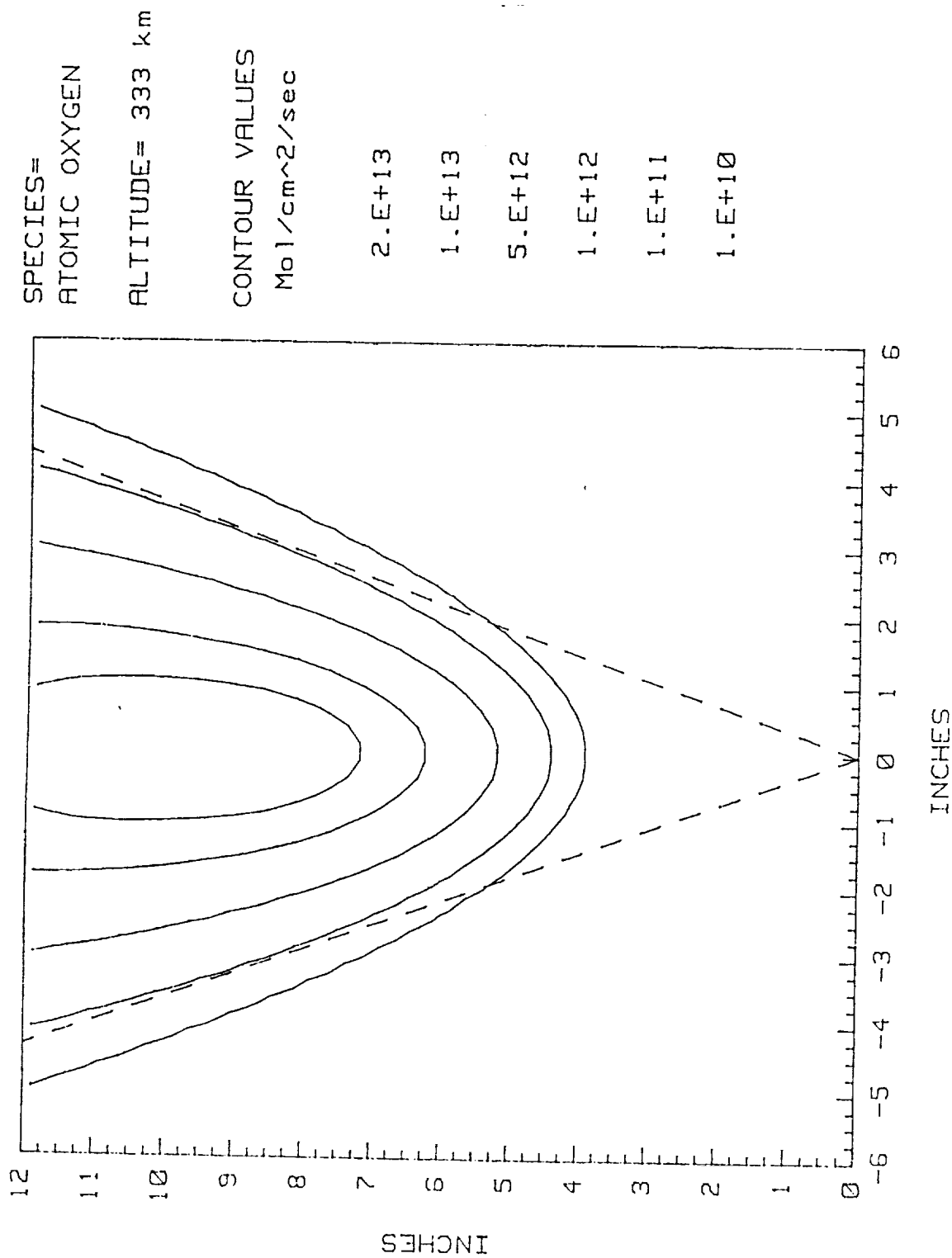
ALTITUDE= 333 km

CONTOUR VALUES  
 $\text{Mol}/\text{cm}^2/\text{sec}$

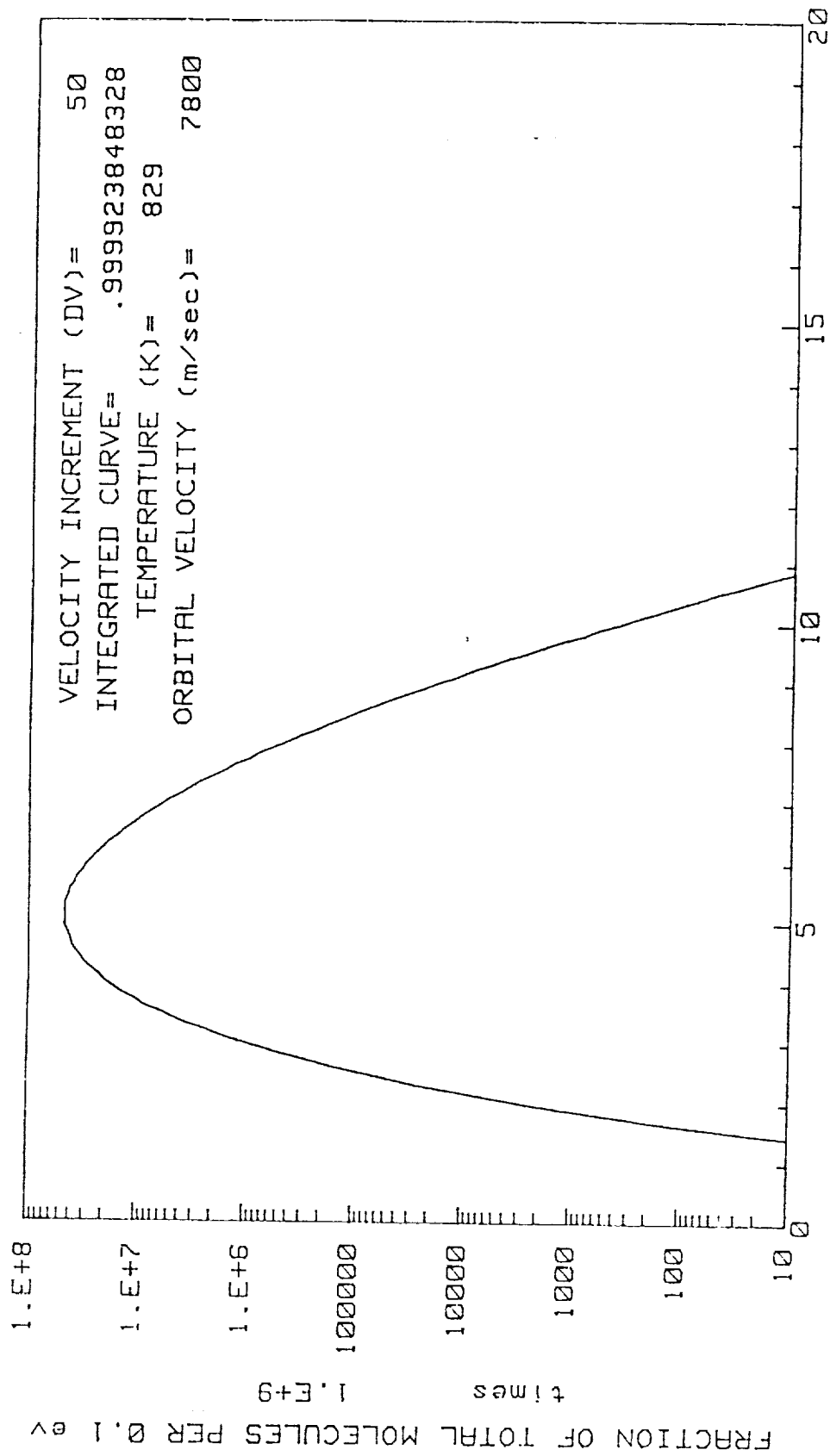
- 3.E+10
- 1.E+10
- 5.E+9
- 1.E+9
- 1.E+8
- 1.E+7



# INCIDENT ISO-FLUX CONTOURS ON SURFACE

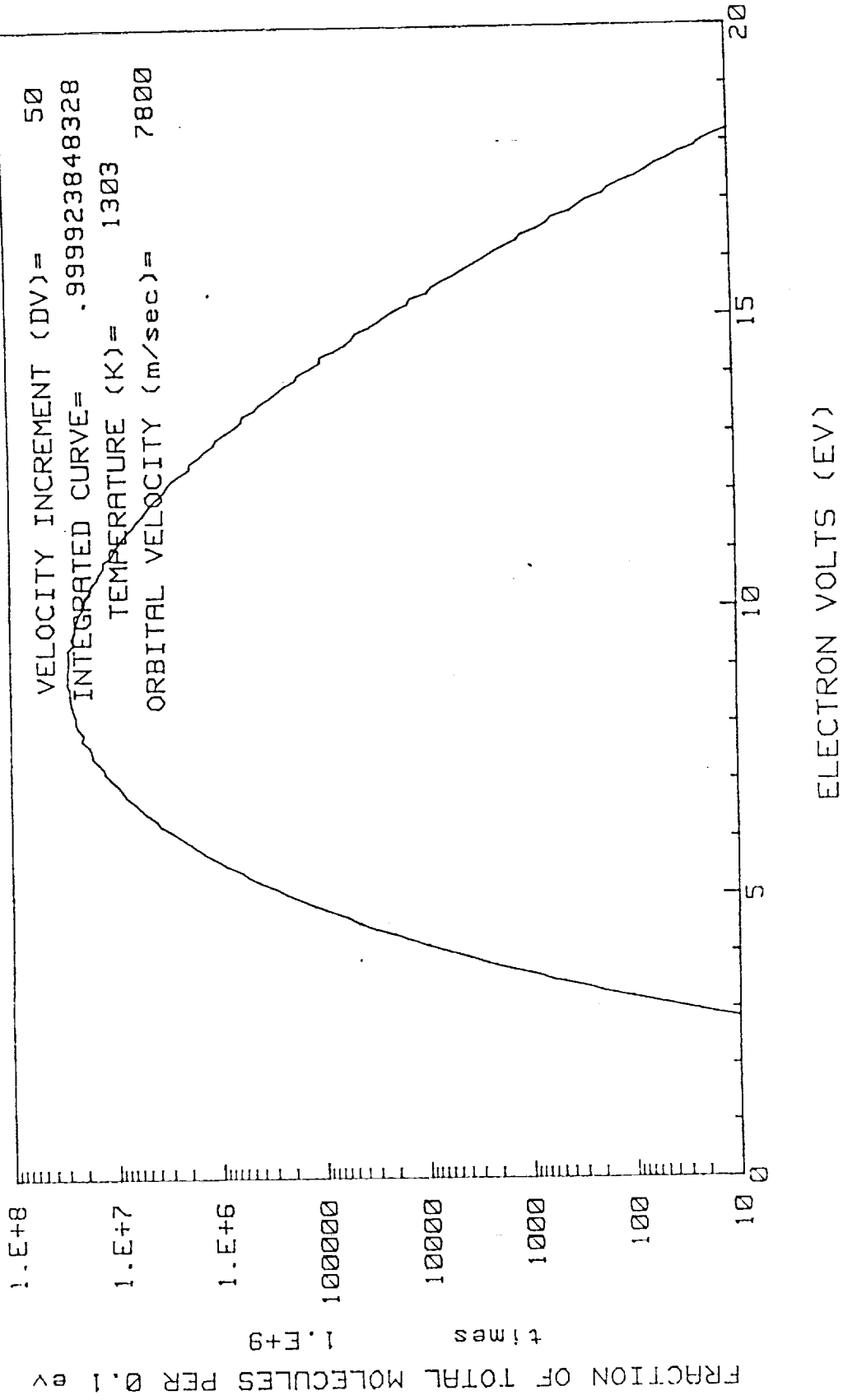


# EV DISTRIBUTION OF INCIDENT AMBIENT ATOMIC OXYGEN





# EV DISTRIBUTION OF INCIDENT AMBIENT NITROGEN



## CONCLUSIONS

- o THERMAL COMPONENT OF AMBIENT IMPORTANT FOR FLUXES THROUGH OPENINGS IN SURFACE
- o DIFFERENT COSINE SCATTERING MAINLY EFFECTS ANGLE OF INCIDENCE ON SURFACES
- o CONTAMINANT DEPOSIT PATTERNS ON INSIDE SURFACES APPEARS TO BE CAUSED BY ATOMIC OXYGEN FLUX FIXING OF CONTAMINANTS
- o ATOMIC OXYGEN EROSION RATES AT END OF MISSION ARE COMPARABLE TO INITIAL OUTGASSING RATES OF LDEF SURFACES
- o RETURN FLUX OF EROSION SPECIES NEAR END OF MISSION AN ORDER OF MAGNITUDE GREATER THAN RETURN FLUX OF OUTGASSED PRODUCTS EARLY IN THE MISSION
- o COSINE 20 TH POWER SCATTERING FOR HIGH SPEED COLLISIONS IMPORTANT FOR SURFACE ANGLE IMPINGEMENT
- o DETAILED MODELING OF AN EXPERIMENT TRAY RECOMMENDED FOR DEPOSIT IDENTIFICATION AND MODEL ALGORITHM VERIFICATION
- o RESULTS HAVE APPLICATION TO SPACE STATION AND UV IMAGER --FURTHER ANALYSIS WILL ADD TO THIS KNOWLEDGE.

# OVERVIEW OF SPACECRAFT GLOW ISSUES

T. G. SLANGER  
MOLECULAR PHYSICS LABORATORY  
SRI INTERNATIONAL  
MENLO PARK, CA

SPACE STATION FREEDOM INDUCED EXTERNAL ENVIRONMENT REVIEW  
MARSHA'S SPACE FLIGHT CENTER  
HUNTSVILLE, ALABAMA  
JAN. 30-31, 1991



## SPACECRAFT GLOW DEFINITION

Optical emission (UV-IR) resulting directly or indirectly from the interaction of atmospheric particles with or on the surface of space vehicles

With refers to chemical reactions involving the spacecraft material itself, or adsorbed contaminant species

On refers to surface-catalyzed processes, in which the surface of the craft is not degraded

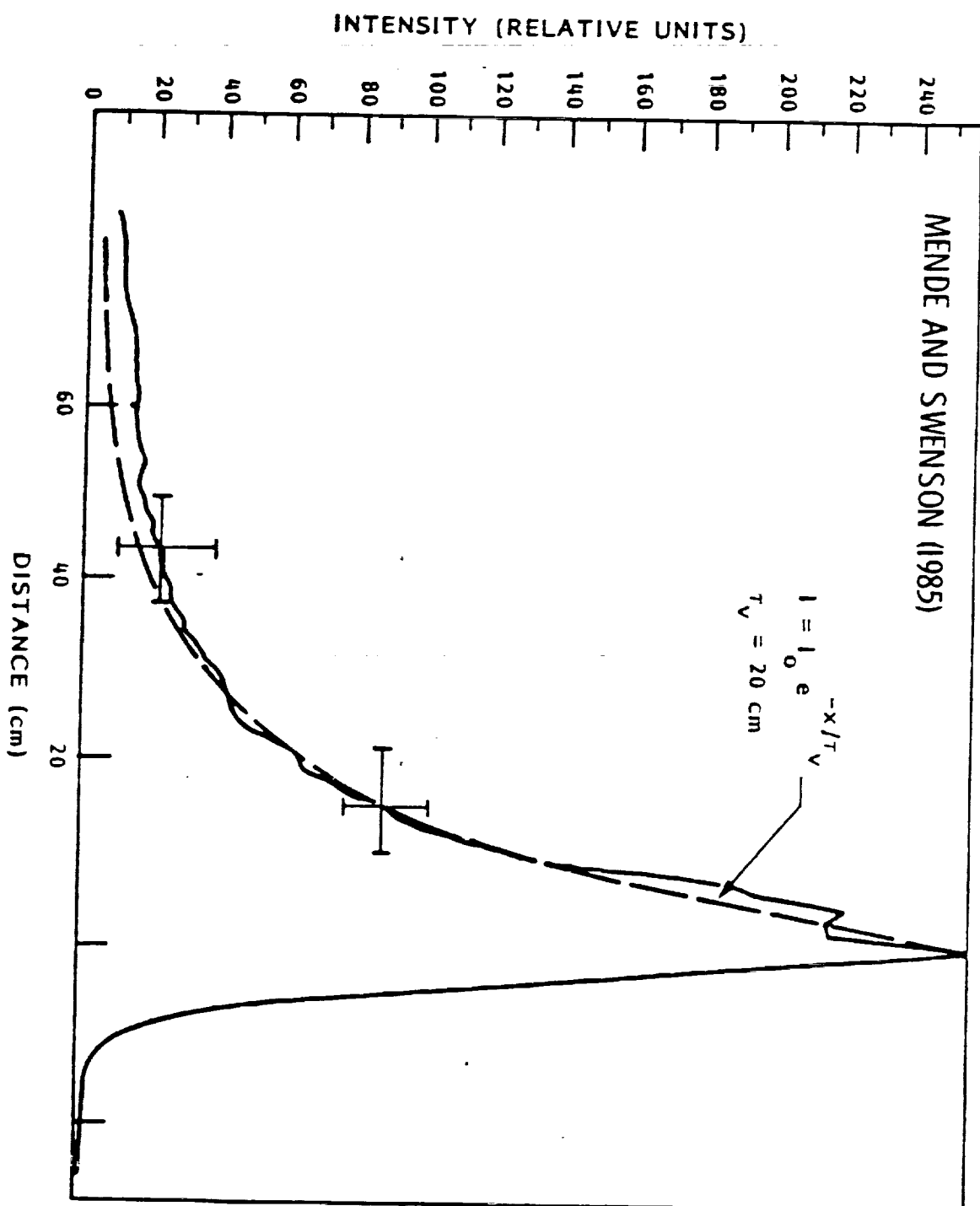
A secondary definition includes radiation caused by gas phase interaction between the incoming atmosphere and desorbed material, typically water

# CURRENT DATA BASE FOR SPACECRAFT GLOW

- 1) Space Shuttle  
Lockheed team (Mende, Swenson, et al.)  
Visible spectral region  
NO<sub>2</sub> identification
- 2) Atmospheric Explorer (AE)  
U. of Michigan/Harvard/Utah State (Yee, Abreu,  
Hays, Torr, Dalgarno, et al.)  
Non-dispersive filter measurements (280-730 nm)  
Altitude-dependent study
- 3) Dynamics Explorer (DE)  
U. of Michigan  
Fabry-Perot system at 732 nm  
Possible OH Meinel band identification
- 4) S3-4 DOD satellite  
NRL/AFGL (Meier, Conway, Huffman et al.)  
Nadir viewing  
UV/Vacuum uv (120-300 nm)  
N<sub>2</sub> LBH system identification
- 5) Ground-based shuttle overflight  
NASA Ames (Witteborn et al.)  
IR (1.4-1.8  $\mu$ m)  
Consistent with very hot OH Meinel bands  
Halo rather than surface glow

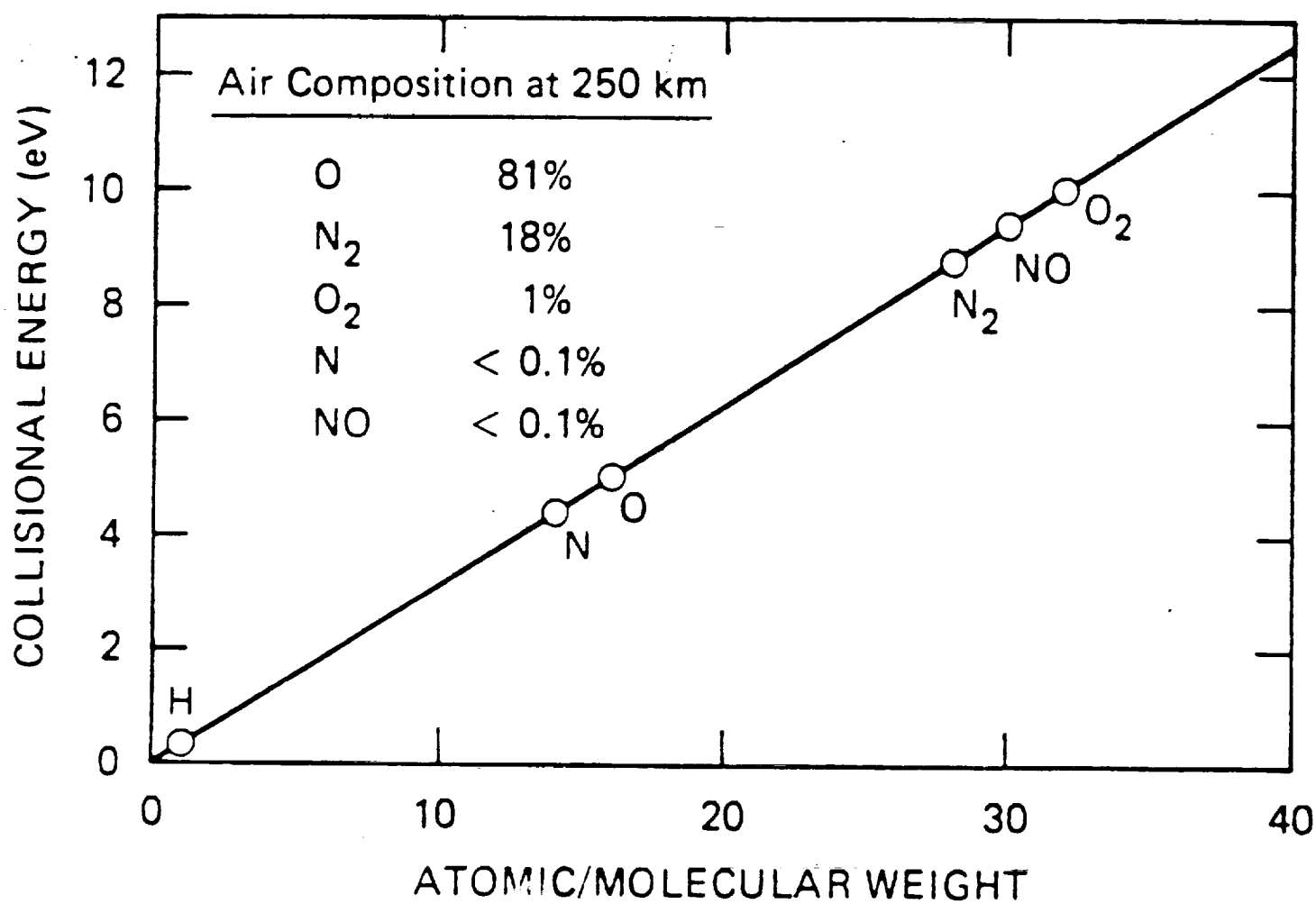
Other data exist, from Spacelab (Torr and Torr)  
and recent ground-based measurements (Murad et al.)

MENDE AND SWENSON (1985)

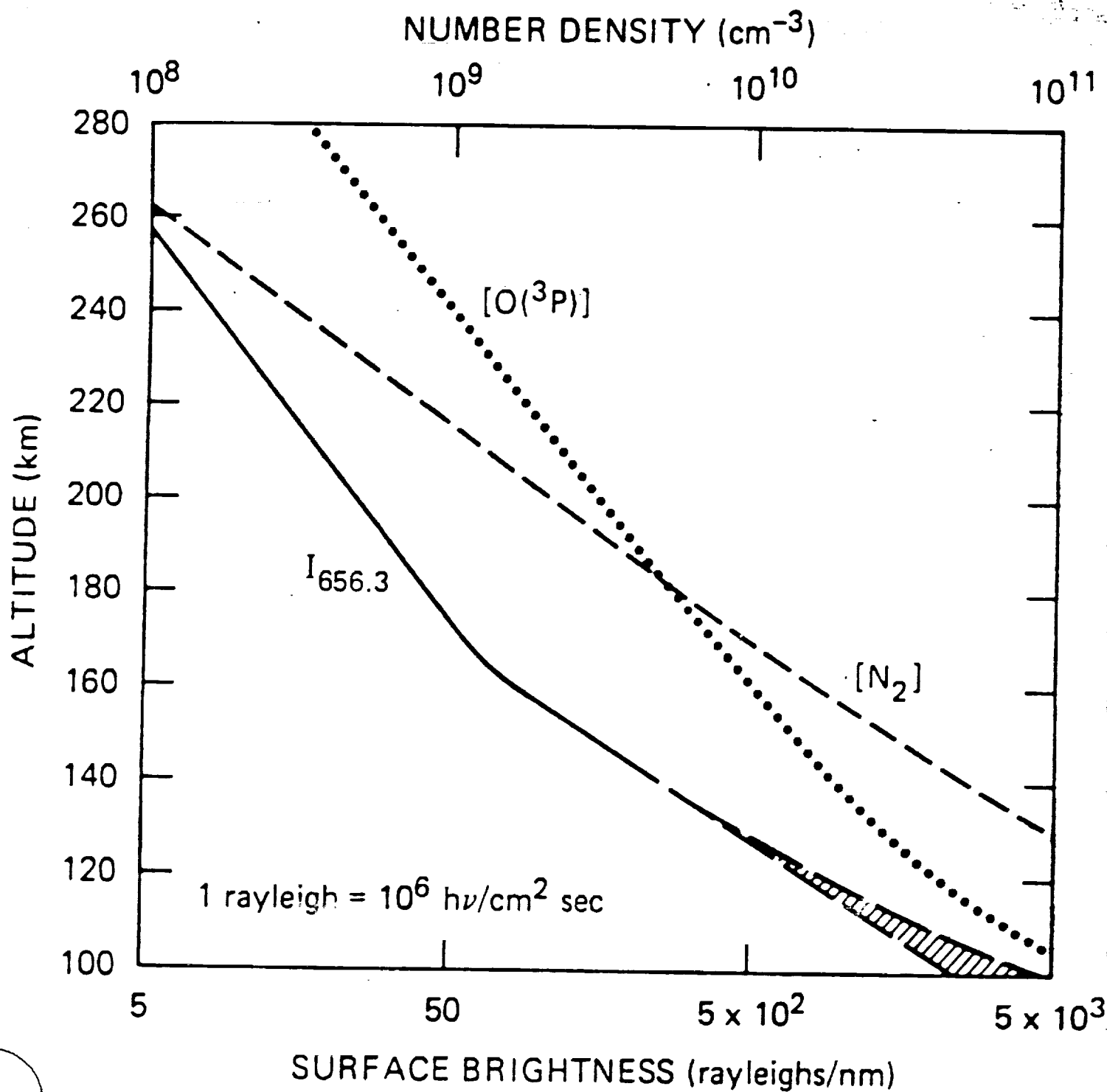


GLOW INTENSITY VS DISTANCE FROM TAIL SURFACE

# TRANSLATIONAL ENERGY VERSUS ATOMIC/MOLECULAR WEIGHT (Velocity = 7.8 km/s)

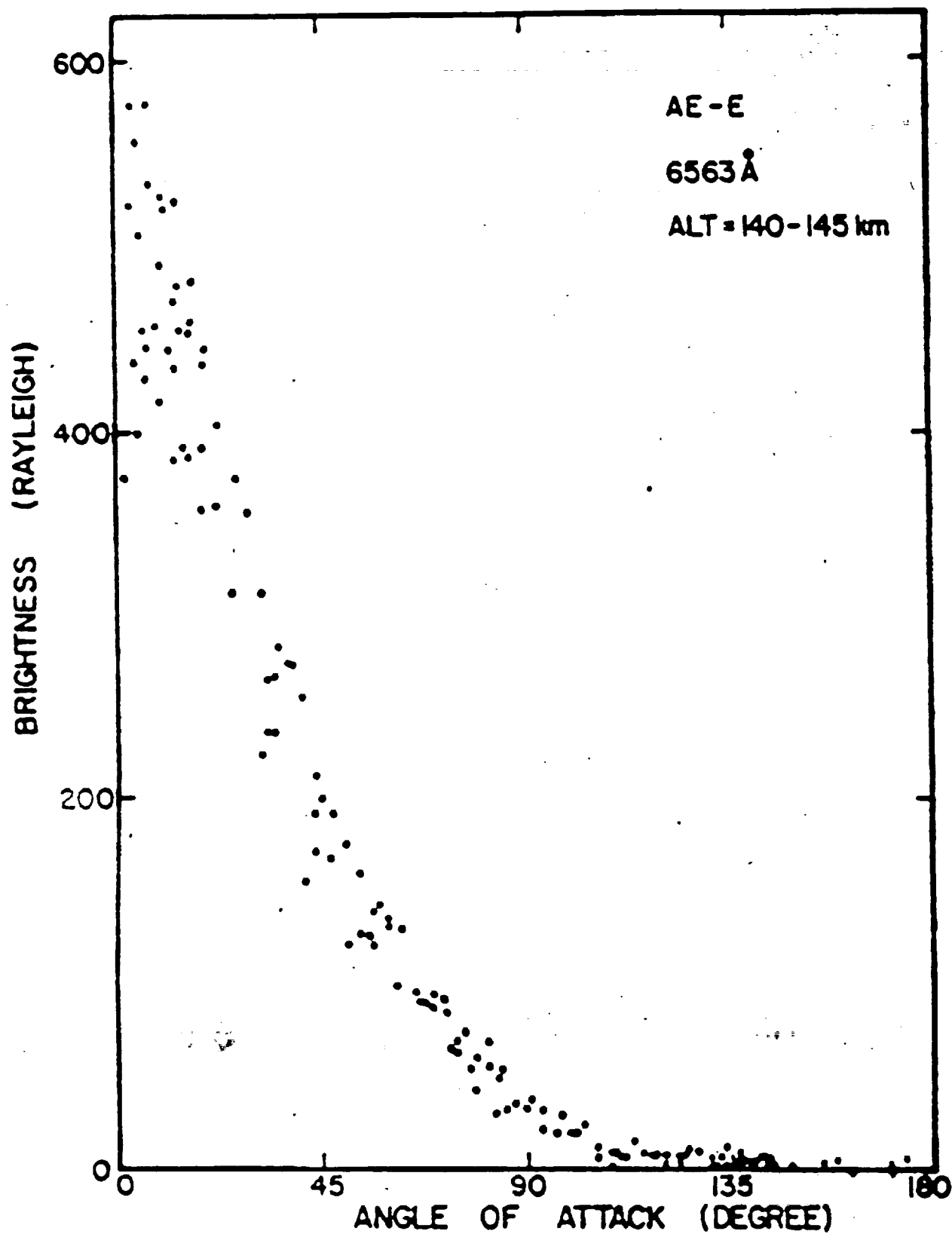


I(656.3 nm), [M] VERSUS ALTITUDE  
AE SATELLITE, YEE AND ABREU (1982)

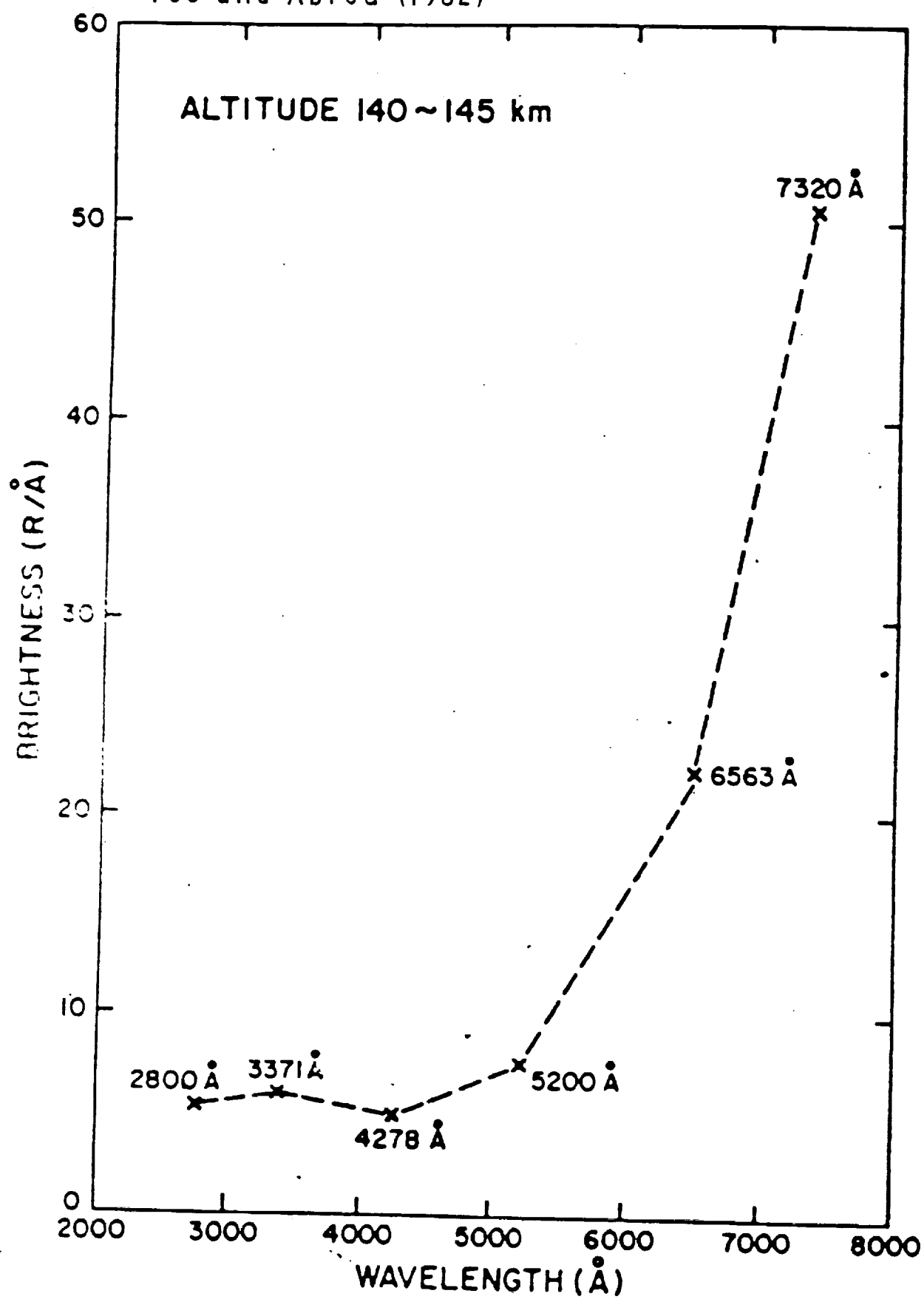




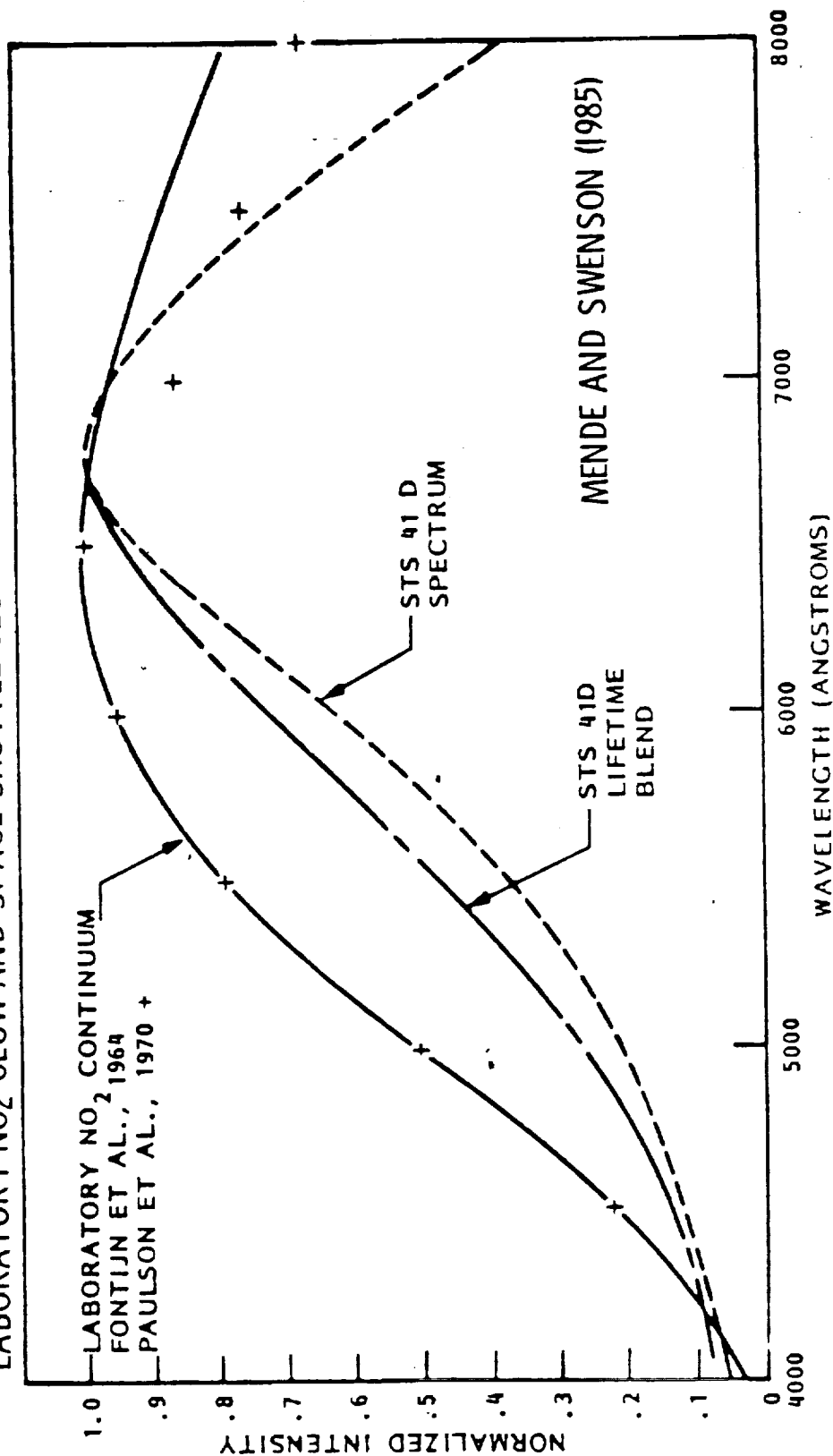
Yee and Abreu (1982)

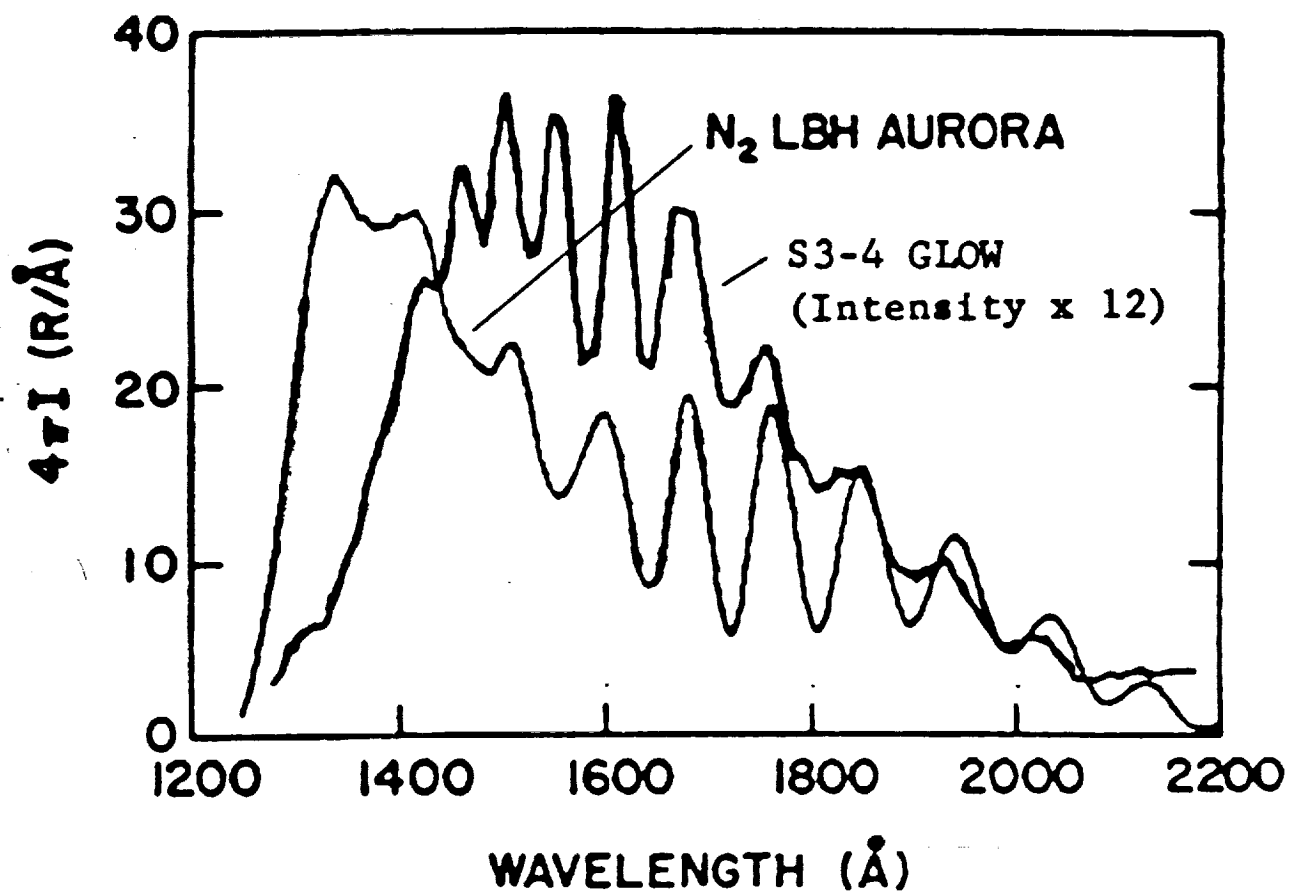


Yee and Abreu (1982)



# LABORATORY NO<sub>2</sub> GLOW AND SPACE SHUTTLE GLOW





## $\text{N}_2$ LBH AND $\text{NO}_2^*$ GLOWS

- 1) Common thread is nitrogen, implicating the participation of  $\text{N}_2$  chemistry
- 2) Meyerott and Swenson have discussed  $\text{N}_2/\text{O}$  interaction in the enhanced density region in front of the shuttle
- 3)  $\text{N}_2 + \text{O}(^3\text{P}) \rightarrow \text{N}(^4\text{S}) + \text{NO} - 3.3 \text{ eV}$
- 4) Both N and NO are products
- 5) Likeliest  $\text{NO}_2^*$  source is:  
 $\text{O} + \text{NO} \rightarrow \text{NO}_2^*(\text{surf}) \rightarrow \text{NO}_2^*(\text{gas}) \rightarrow \text{NO}_2 + h\nu \text{ (400-800 nm)}$
- 6) Likeliest  $\text{N}_2^*$  source is:  
 $\text{N}(^4\text{S}) + \text{N}(^4\text{S}) \rightarrow \text{N}_2^*(\text{surf}) \rightarrow \text{N}_2^*(\text{gas}) \rightarrow \text{N}_2 + h\nu \text{ (140-200 nm)}$

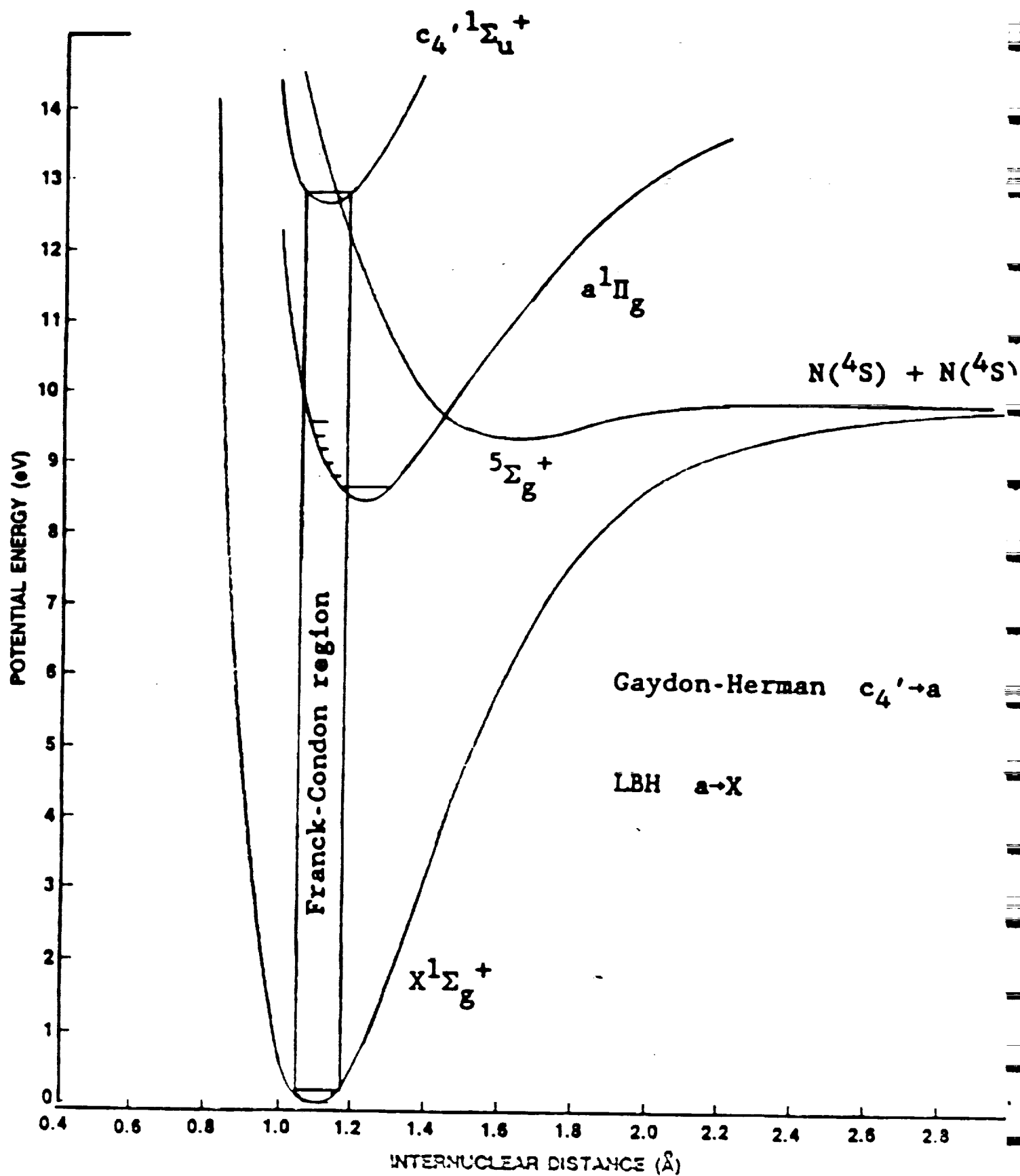
## THE ROLE OF TRANSLATIONAL ENERGY

- 1) Is there one?
- 2) If N and NO are scavenged from the atmosphere, it is not evident that the 5-10 eV translational energy is necessary for excited state production
- 3) If N and NO need to be produced in situ, then the endothermic  $N_2 + O$  reaction is where the translational energy is needed
- 4) Laboratory reactions with O-atom sources in which the system is doped with NO may therefore indicate no role for translational energy

## SURFACE vs GAS PHASE CHEMISTRY

- 1) Where do  $N_2$  and O interact?
- 2) Probability of  $N_2/O$  collision is far higher on the surface than in the plow cloud, at  $10^{11} \text{ cm}^{-3}$  particle density
- 3) Surface O-atom coverage is likely to be substantially higher than  $N_2$  coverage
- 4) Therefore, most probable interaction is fast  $N_2$  (9 eV) colliding with surface-bound  $O(^3P)$ , to generate  $N + NO$

# N<sub>2</sub> POTENTIALS

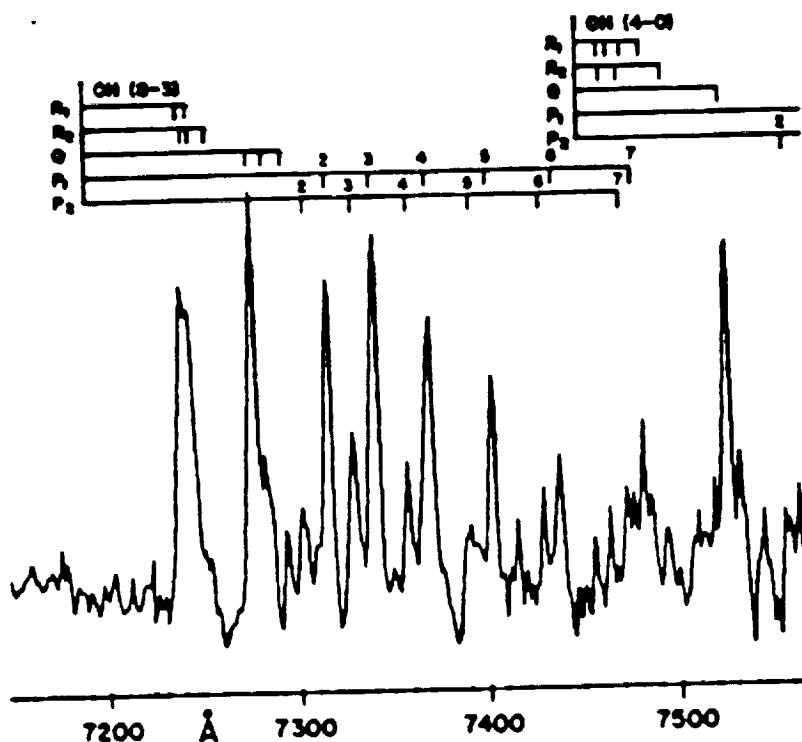




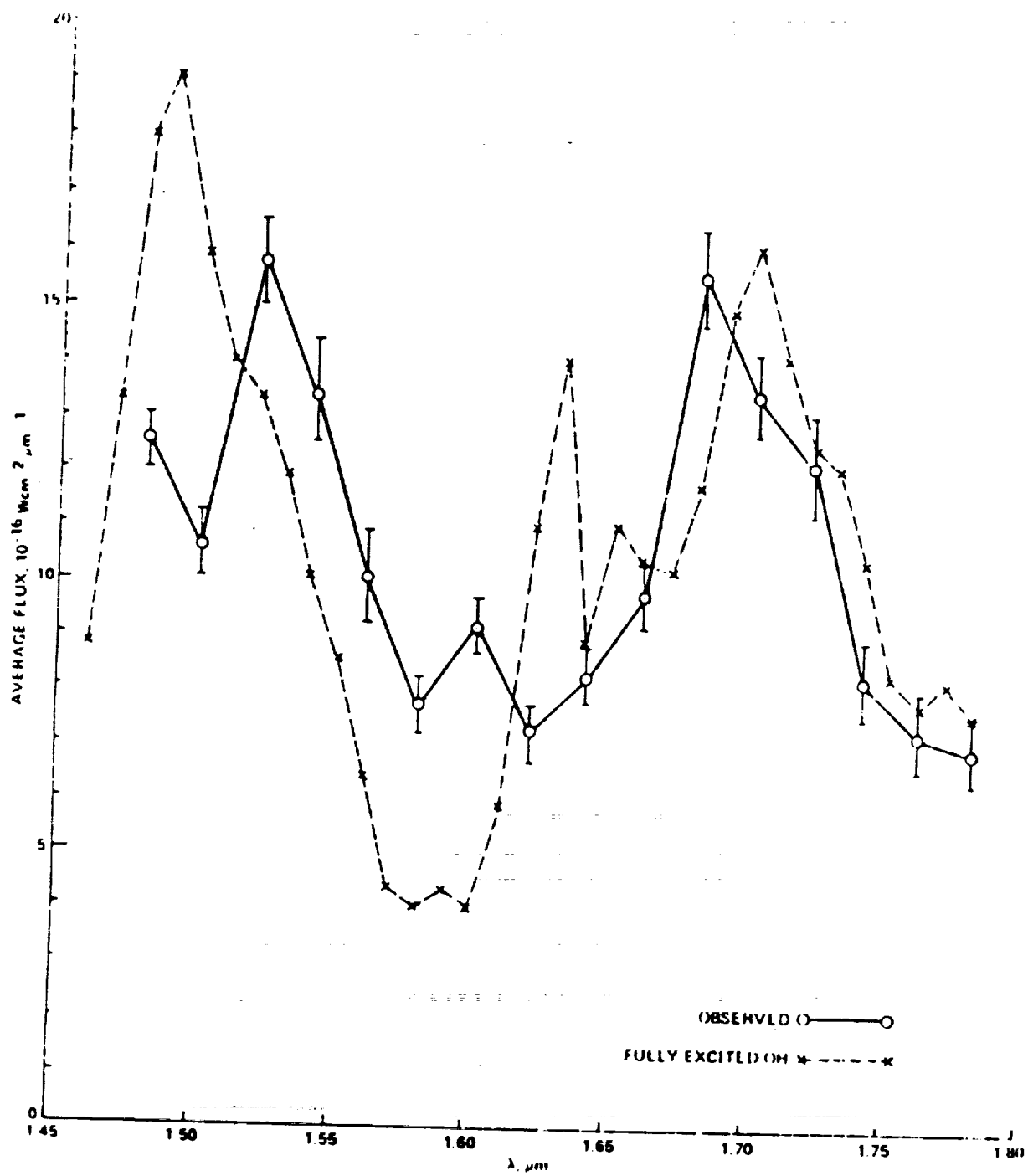
# THE OH MEINEL SYSTEM

## (VIBRATION/ROTATION BANDS)

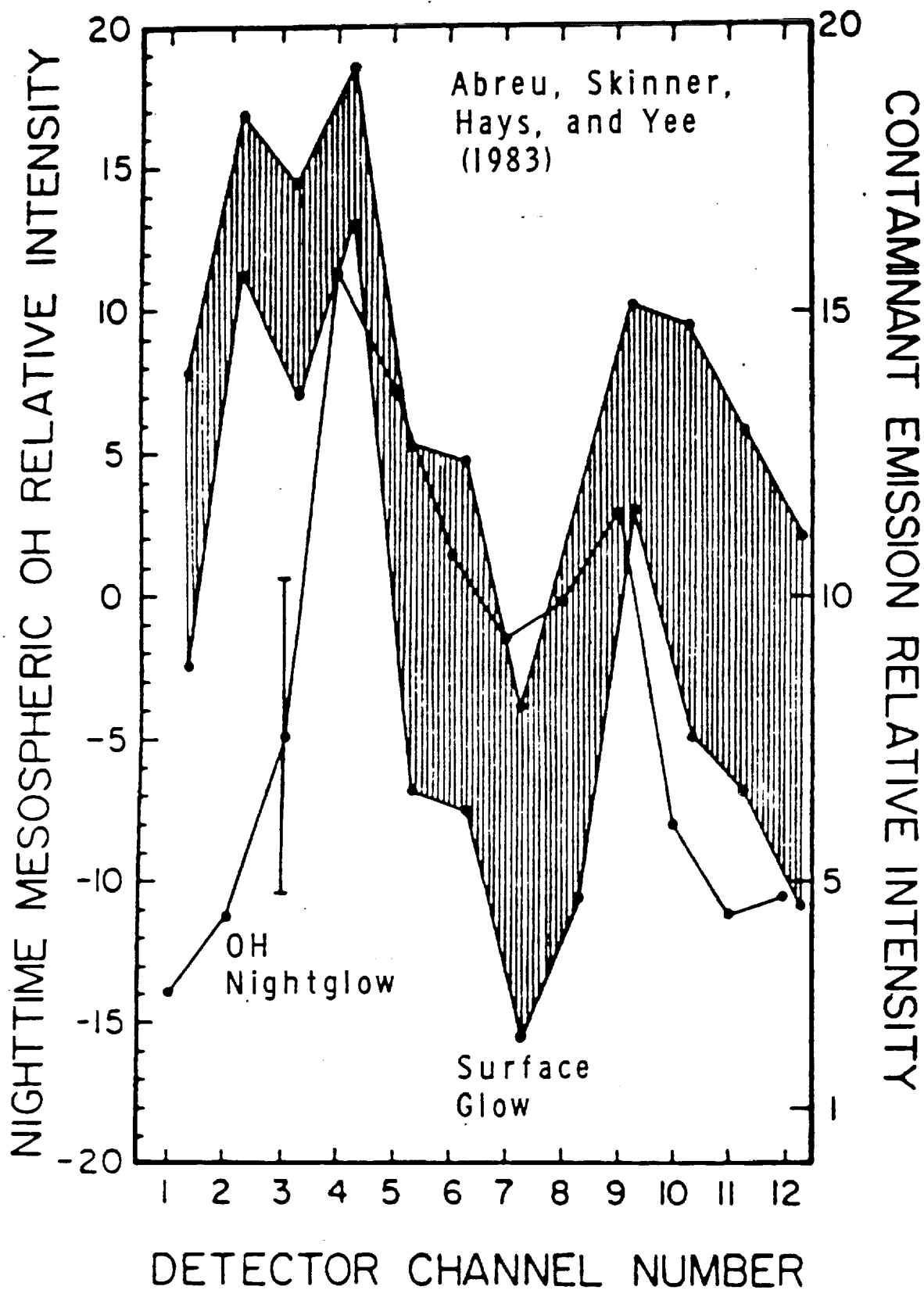
- 1) Atmospheric generation by  $\text{H} + \text{O}_3 \rightarrow \text{OH}(\text{vib}) + \text{O}_2$
- 2) Commonly seen in afterglow systems



Broadfoot and Kendall (1968)



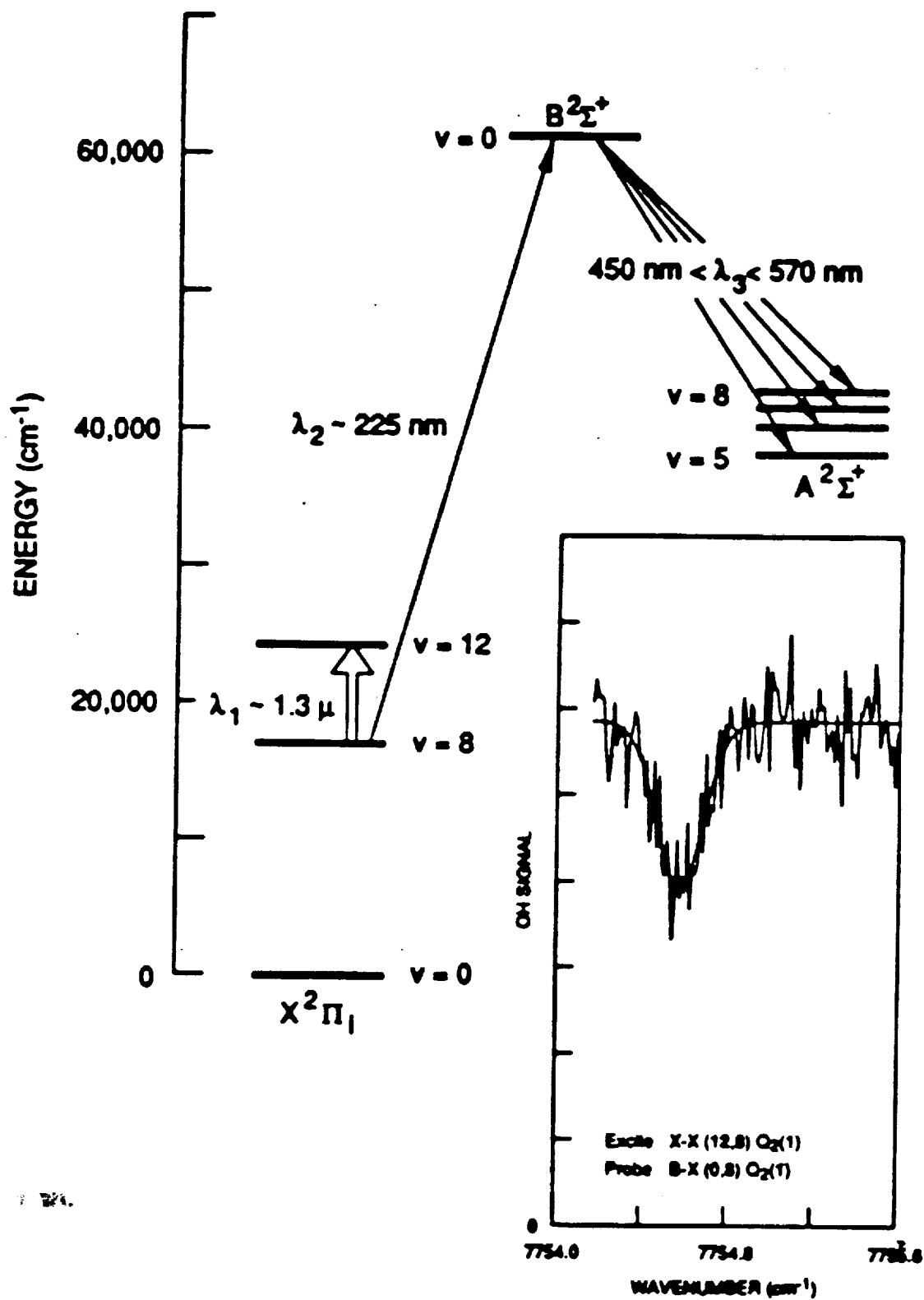
Witteborn, Caroff, Rank, and Ashley, unpublished results

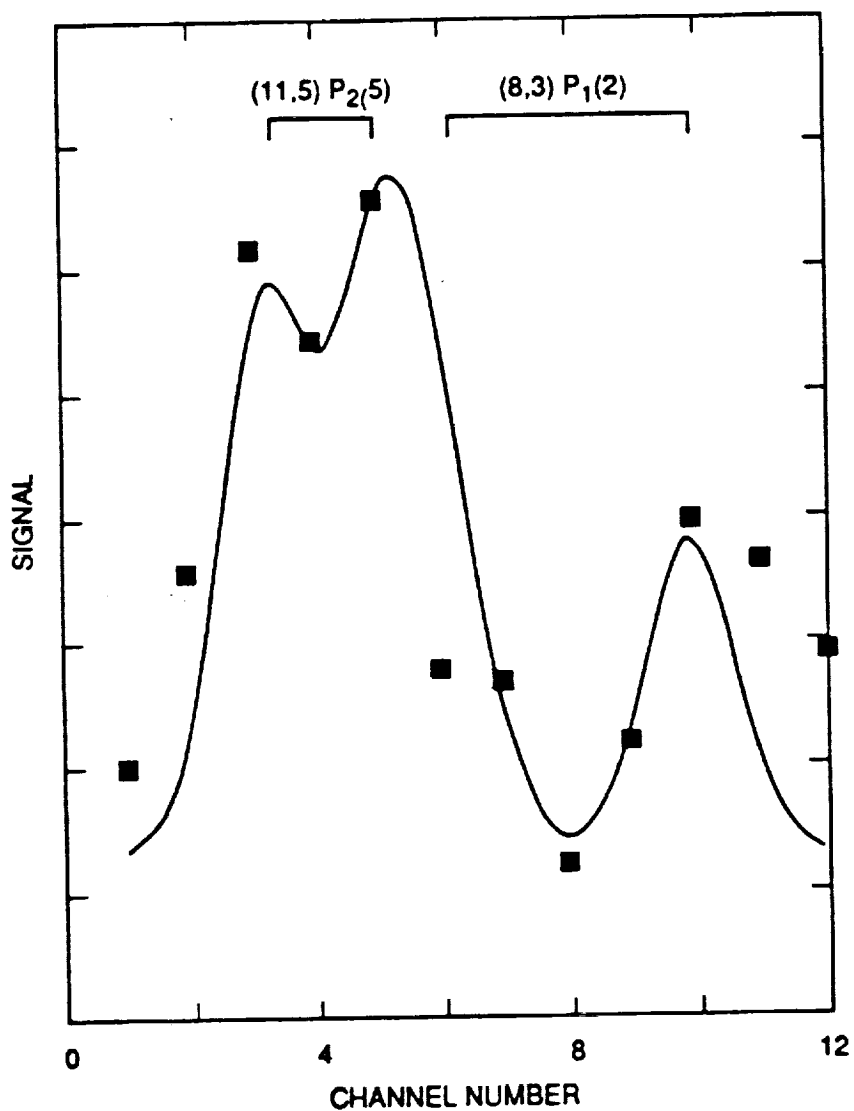


A comparison of the OH nightglow and the contaminant glow spectrum.

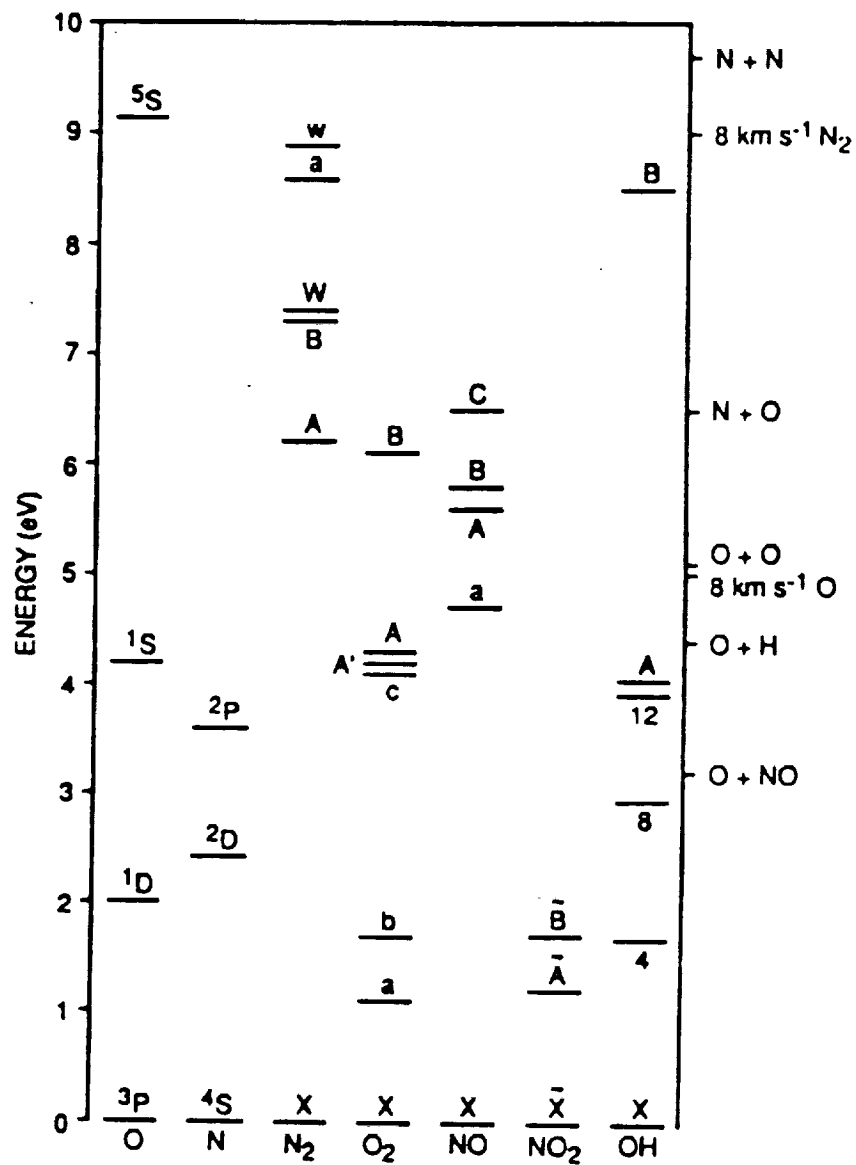
## EXPECTATIONS

- 1) Many low-lying molecular states are metastable, particularly for homonuclear molecules ( $N_2$ ,  $O_2$ )
- 2) Such states will not be seen to radiate from the emitting vehicle, but should be discernible from a distant platform. A particle with a 100 ms radiative lifetime travels ~50 meters at thermal velocity before radiating
- 3) The most prolifically produced molecule should be  $O_2$ , with large quantities of  $O_2(a^1\Delta_g)$  [ $\tau_r = 1$  hr],  $O_2(b^1\Sigma_g^+)$  [ $\tau_r = 12$  sec], and vibrationally excited  $O_2$  being generated
- 4) Non-radiating molecule production is likely to greatly exceed that of excited molecules (has been shown for  $NO_2$ )





COMPARISON OF DE FABRY-PEROT SPECTRUM (squares)  
AND SPECTRAL SIMULATION USING 11-5 AND  
8-3 OH LINES, T=550 K



## EXCITED STATE PRODUCTION

**RESULTS OF JPL WORKSHOP:  
LEVEL II ENVIRONMENT MODELING**

**G. MURPHY  
JAN. 30 1991**



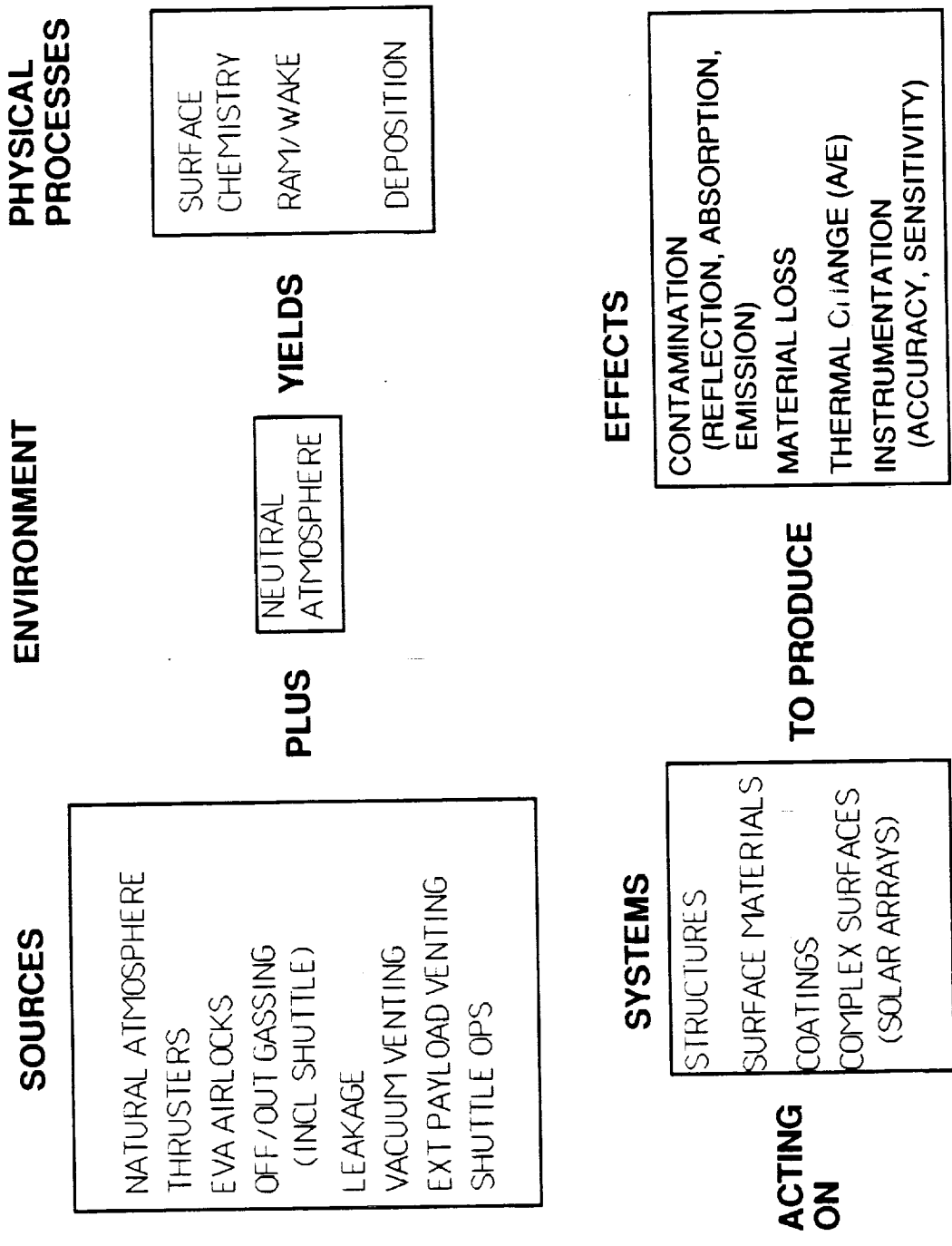
## **OUTLINE**

- **BACKGROUND**
- **PURPOSE AND SCOPE OF WORKSHOP**
- **EDAP--A PROGRAM FOR ENVIRONMENT DEFINITION AND ASSESSMENT**
- **WORKSHOP RECOMMENDATIONS**
- **SUMMARY**

## BACKGROUND

- SSF MUST MEET LIFETIME REQUIREMENTS IN LEO WITH REALISTIC MAINTENANCE AND COST ---- DESIGN MUST BE COMPATIBLE WITH ENVIRONMENT
- ALL WORK PACKAGE CENTERS, PRIMES, AND SUBS MUST WORK TO CONSISTENT SET OF REQUIREMENTS, BASED ON COMMON ENVIRONMENT THREATS
- ANALYSIS MUST BE BASED ON VALIDATED, CONFIGURATION CONTROLLED MODELS WITH KNOWN ASSUMPTIONS AND UNIFORM DATABASE
- PROGRAM MUST RETAIN KNOWLEDGE BASE AND BUILD ON IT THROUGH LIFE OF SSF

ENVIRONMENT/SYSTEM INTERACTION



SOURCES PLUS ENVIRONMENT RESULTS IN PHYSICAL PROCESSES WHICH ACT ON SYSTEMS TO PRODUCE EFFECTS

## WORKSHOP

- PURPOSE: EXAMINE POSSIBLE PROGRAM STRUCTURES AND CONCEPTS FOR ASSURING SYSTEM/ENVIRONMENT COMPATIBILITY BY INTEGRATING ANALYSIS SOFTWARE AND PHYSICAL/CONFIGURATION DATABASES.
- SCOPE:
  - DEVELOP LEVEL II PROGRAM THAT COORDINATES ENVIRONMENT/EFFECTS ANALYSIS AND DATA;
  - EXAMINE IMPLEMENTATION REQUIREMENTS SUCH THAT PROGRAM FULFILLS NEEDS OF CONTROL BOARDS, WORKING GROUPS, SYSTEM ENGINEERING, AND UTILIZATION.
  - ASSESS ISSUES ASSOCIATED WITH MODEL VALIDATION, VERIFICATION, INTEGRATION, AVAILABILITY, AND CONFIGURATION CONTROL

# **EDAP--ENVIRONMENT DEFINITION AND ASSESSMENT PROGRAM** **(EDAP)**

- **GOALS:**

- ASSURE CONSISTENT ANALYSES ACROSS THE PROGRAM DURING DESIGN, VERIFICATION, AND UTILIZATION PHASES.
- PROVIDE FOR COMPREHENSIVE ASSESSMENTS THAT CROSS WORK-PACKAGE AND DISCIPLINE BOUNDARIES.
- DEVELOP, ORGANIZE, CONTROL, AND DISTRIBUTE A CONSISTENT, COORDINATED SET OF ENVIRONMENT DEFINITION, INTERACTION, AND EFFECTS MODELS / TOOLS / DATABASES.

- **STRUCTURE:**

- LEVEL II ENVIRONMENT DEFINITION PANEL
- WORKING GROUPS AND CONTROL BOARDS
- ENVIRONMENT WORKBENCH (EWB)

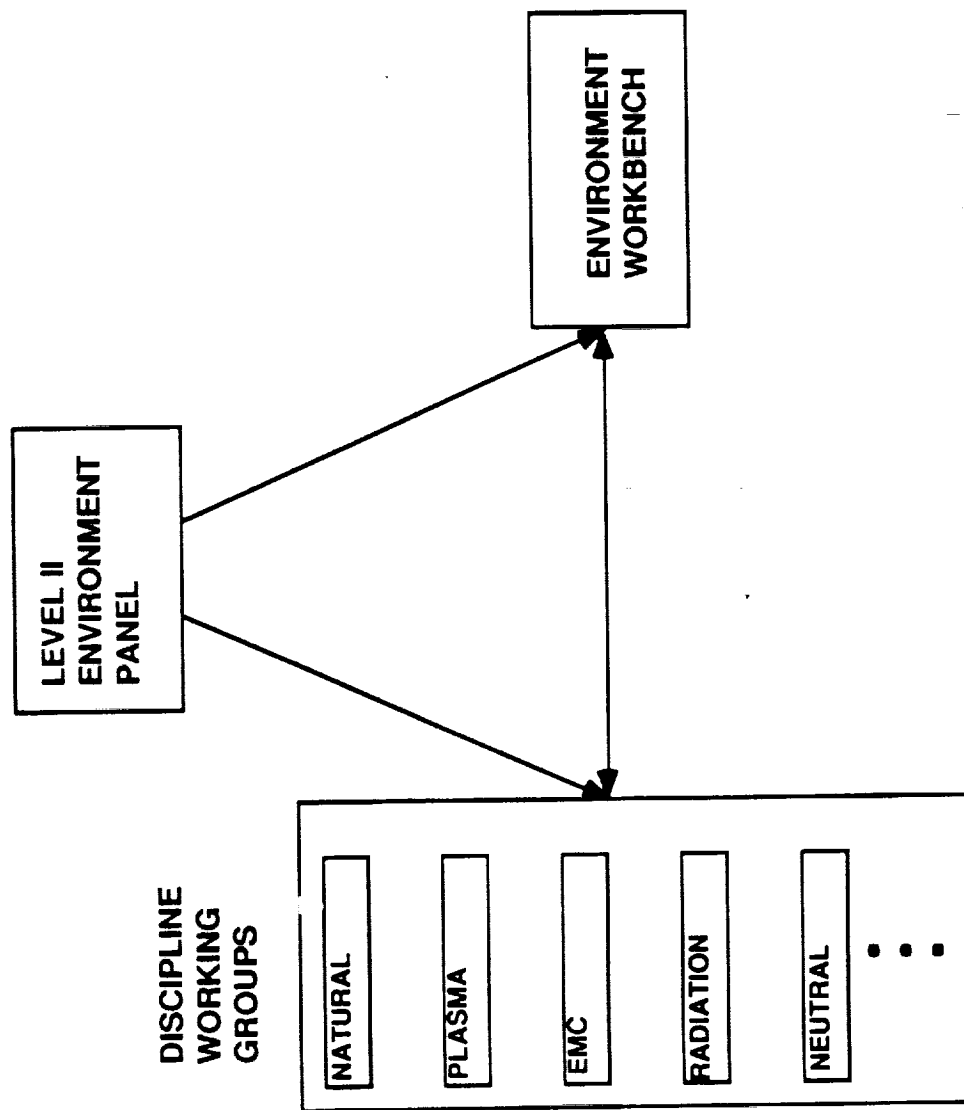
## **EDAP REQUIREMENTS**

- **BEGIN IMPLEMENTATION USING CURRENT RESOURCES**
- **ACCOMMODATE INTEGRATION OF EXISTING CODES**
- **FULLY FUNCTIONAL, INCREMENTAL DELIVERABLES THAT MATCH PROGRAM NEEDS AND RESOURCES--BEGIN DELIVERABLES IMMEDIATELY**
- **ACCOMMODATE NEEDS OF LEVEL II SE&I AND U&O, WORKING GROUPS, CONTROL BOARDS DURING LIFE OF SSF PROGRAM**
- **INCORPORATE LONGTERM COMPREHENSIVE PRODUCT ASSURANCE PROGRAM**

## **EDAP REQUIREMENTS (CONT)**

- **DEVELOP MODELS IN PARALLEL WITH EWB SYSTEM SOFTWARE**
- **INVOLVE ALL RELEVANT WORKING GROUPS AND DISCIPLINE EXPERTS**
- **SATISFY SHORT TERM REQUIREMENTS FOR DESIGN AND VERIFICATION--LONG TERM REQUIREMENTS FOR MAINTENANCE, CONFIGURATION CONTROL, EVOLUTION ETC.**
- **ASSURE MINIMAL LONG TERM EVOLUTION AND MAINTENANCE COST**

# ENVIRONMENT DEFINITION AND ASSESSMENT PROGRAM





## **EDAP PROGRAM STRUCTURE--ROLES AND RESPONSIBILITIES**

- LEVEL II ENVIRONMENT PANEL**
  - MODEL SELECTION GROUND RULES**
  - MODEL / DATABASE APPROVAL**
  - COORDINATE DEVELOPMENT OF CROSS-DISCIPLINE MODELS**
  - PROGRAM LEVEL SOFTWARE PRODUCT ASSURANCE RESPONSIBILITY**
  - WORKING GROUP AND EWB FUNDING**

## **EDAP ROLES AND RESPONSIBILITIES (CONT)**

- . DISCIPLINE WORKING GROUPS**

- DISCIPLINE MODEL RECOMMENDATIONS TO LEVEL II ENVIRONMENT PANEL**

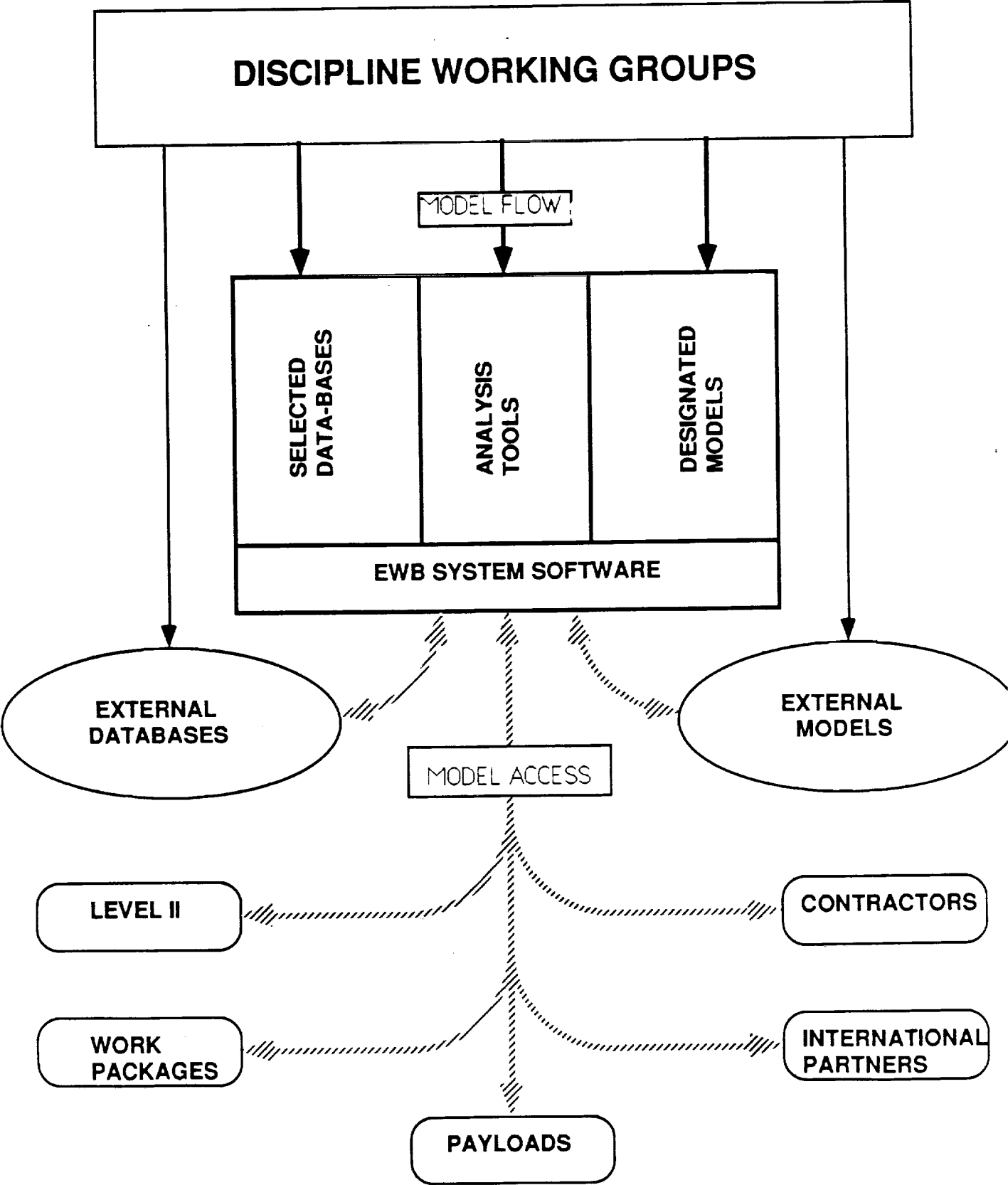
- PEER REVIEW OF ANALYSIS TECHNIQUES AND MODEL ASSUMPTIONS**

- MODEL VALIDATION**

- DISCIPLINE MODEL DEVELOPMENT**

- DATABASE REVIEW**

**EWB MODEL FLOW DIAGRAM**



## **EDAP ROLES AND RESPONSIBILITIES (CONT)**

- ENVIRONMENT WORKBENCH**

- DEVELOP SOFTWARE BUSS AND USER INTERFACE TO DATA / MODELS NEEDED BY EDAP**
- INCORPORATE EXISTING MODELS APPROVED BY WORKING GROUPS**
- INCLUDE MODELS APPROVED BY EDAP FOR ANALYSIS IN LIEU OF TEST**
- PROVIDE ANALYSIS TOOLS FOR QUICK ASSESSMENT**
- MODEL SYNERGISTIC EFFECTS OF NATURAL / INDUCED ENVIRONMENTS**
- INTEGRATE APPROPRIATE DATA BASES**
- INTEGRATE, CONTROL, DISTRIBUTE, AND MAINTAIN ANALYSIS TOOLS / DATA BASES**
- IMPLEMENT SPA FOR EWB SYSTEM AND MODELS**

## **WORKSHOP RECOMMENDATIONS**

- **WORKSHOP ADDRESSED:**

- IMPLEMENTATION PLAN FOR EDAP AND EWB

- EDAP AND EWB FUNCTIONAL REQUIREMENTS

- WORK BREAKDOWN STRUCTURE, SCHEDULE AND MILESTONES

- STANDARDS FOR ARCHITECTURE, INTERFACES, SOFTWARE

- SOFTWARE PRODUCT ASSURANCE

- SOURCES, PROCESSES AND EFFECTS ANALYSES

- **DETAILS OF SOURCES, PROCESSES AND EFFECTS ANALYSES FOR NEUTRAL ENVIRONMENT SUMMARIZED BELOW--OTHER RECOMMENDATIONS INCLUDED IN ATTACHMENT**

• ANALYZED RELATIONSHIP BETWEEN SOURCES AND ENVIRONMENT; PROCESSES AND EFFECTS

• BEGAN LISTING CANDIDATE CODES AND EVALUATED FOR:

-COMPLETION STATUS

-REQUIRED DEVELOPMENT TIME

-LEVEL OF VERIFICATION

-GROUND / SPACE TESTS REQUIRED TO COMPLETE VERIFICATION

SOURCES, PROCESSES, EFFECTS	CANDIDATE CODES	CODE STATUS	VERIFICATION	DEVELOPMENT TIME	GROUND OR SPACE TEST RQMT.
THRUSTER PLUME	VISMOC/TRAN78	COMP	?	0	UPCOMING
	DSMC, RAMP	COMP		0	SHUTTLE
	COMTAM	COMP		0	TESTS
EVA/AIRLOCKS	BLOVAC	90 %	VACUUM CHAMBER TEST	3MOS	MORE TESTS SHOULD BE DONE
VACUUM VENTING	AEDC TESTS	COMP	?	3MOS	SOME TESTS
	BLOVAC	90 %	YES	3MOS	PERFORMED
OFF/OUTGASSING	ISEM	COMP.			MATERIALS TESTS REQUIRED
	SOCRATES	COMP	?		
	MOLFLUX	COMP			
	SPACE II	COMP			
	LSMC TESTS	COMP			
HAB/LAB LEAKAGE	ISEM	COMP	?	?	?
	MOLFLUX	COMP			
WATER DUMPS	PIM 900	COMP	?	?	SHUTTLE
	LOCKEED STUDY	?			TEST
	SKYLAB DATA	COMP			DATA

SOURCES, PROCESSES, EFFECTS	CANDIDATE CODES	CODE STATUS	VERIFICATION	DEVELOPMENT TIME	GROUND OR SPACE TEST RQMT.
AO EROSION	EPSAT	COMP	NO	0	USES FLIGHT DATA
RAM	ISEM	COMP	?		DATA REQUIRED
	DSMC	COMP	?		DATA REQUIRED
WAKE	ISEM	COMP	?		DATA REQUIRED
	DSMC	COMP	?		DATA REQUIRED
DEPOSITION	EPSAT	COMP	?		
	IMP/SPECON	COMP	?	0	MATERIALS AND SYNERGISTIC TESTS
	ISEM	?	?	3 MOS	
	MOLFLUX	COMP	?	0	
MOLECULAR COLUMN DENSITY	CONTAM	COMP	?	0	
	ISEM/MOLFLUX	COMP	?	0	
	EPSAT	COMP	?	0	
	SOCRATES	COMP	?	0	
GLOW	PLMNCD	90 %	?	3 MOS	
	ISEM (UV, VIS)	IN WORK		6 MOS	SHUTTLE DATA
SURFACE CHEM	ISEM	COMP			YES



## SUMMARY

- LEVEL II REQUIRES CONSISTENT, VALIDATED, INTEGRATED SET OF MODELS OF THE NATURAL AND INDUCED ENVIRONMENT AND UNIFORM DATABASE INPUT FOR EVALUATING THE INDIVIDUAL AND SYNERGISTIC EFFECTS OF THIS ENVIRONMENT ON SSF HARDWARE AND OPERATIONS
- ENVIRONMENT DESIGN AND ASSESSMENT PROGRAM PROVIDES METHODOLOGY FOR IMPLEMENTATION OF THIS REQUIREMENT AT LEVEL II--EDAP IS THE INTEGRATED SOLUTION
- ENVIRONMENT WORKBENCH IS, WORKABLE, COST EFFECTIVE SOLUTION TO PROVIDING INTEGRATION, COORDINATION, CONFIGURATION CONTROL, AND MAINTENANCE FOR MODELS NEEDED BY THE EDAP
- EWB WILL MAINTAIN CORPORATE KNOWLEDGE OF THE NASA AND CONTRACTOR COMMUNITY AND PROVIDE ABILITY TO MAKE COST EFFECTIVE TRADE STUDIES FOR LIFE OF THE SSF PROGRAM
- EDAP DEPENDS ON DISCIPLINE COMMUNITY FOR TECHNICAL INPUT AND OVERSIGHT--IT IS ONLY AS GOOD AS THE MODELS IT CONTAINS

## ATTACHMENT

### WORKSHOP RECOMMENDATIONS

- IMPLEMENTATION PLAN:

- ACCOUNT FOR NEAR TERM AND LONG TERM NEEDS

- SET UP EDAP PROGRAM AND BEGIN PHASE 1 OF EWB IMMEDIATELY

- START WITH CURRENT FUNDING LEVELS AVAILABLE

- PHASE 1 EWB WILL INCLUDE TESTING OF INHERITED SOFTWARE, INTEGRATION OF CURRENT SSF APPROVED MODELS, CREATION OF DETAILED SOFTWARE DEVELOPMENT PLAN FOR PHASE 2, ESTABLISHMENT OF PROJECT STRUCTURE

- PHASE 2 EWB BUILDS A SYSTEM ARCHITECTURE THAT ALLOWS INCREMENTAL DELIVERY OF AN INCREASINGLY MORE CAPABLE PRODUCT

## RECOMMENDATIONS (CONT)

- STANDARDS FOR ARCHITECTURE, INTERFACES AND SOFTWARE OF EWB  
SYSTEM / MODELS:

- USE OBJECT ORIENTED PROGRAMMING (OOP) TECHNIQUES FOR ALL NEW  
CODE

- INHERIT EXISTING CODE BY WRAPPING

- USE C++ CONSISTENT WITH AT&T STANDARD FOR SYSTEM BUSS AND  
INTERFACES

- UNIX IS OPERATING SYSTEM OF CHOICE FOR FINAL PHASE 2 PRODUCT--ZENIX  
MAY BE USED FOR PHASE 1

- ANSI STD FORTRAN FOR MODELS/QUICK-LOOK TOOLS (OBJECT ORIENTED  
PASCHAL MAY BE USED ) -- STANDARD INTERFACE TO SYSTEM REQUIRED

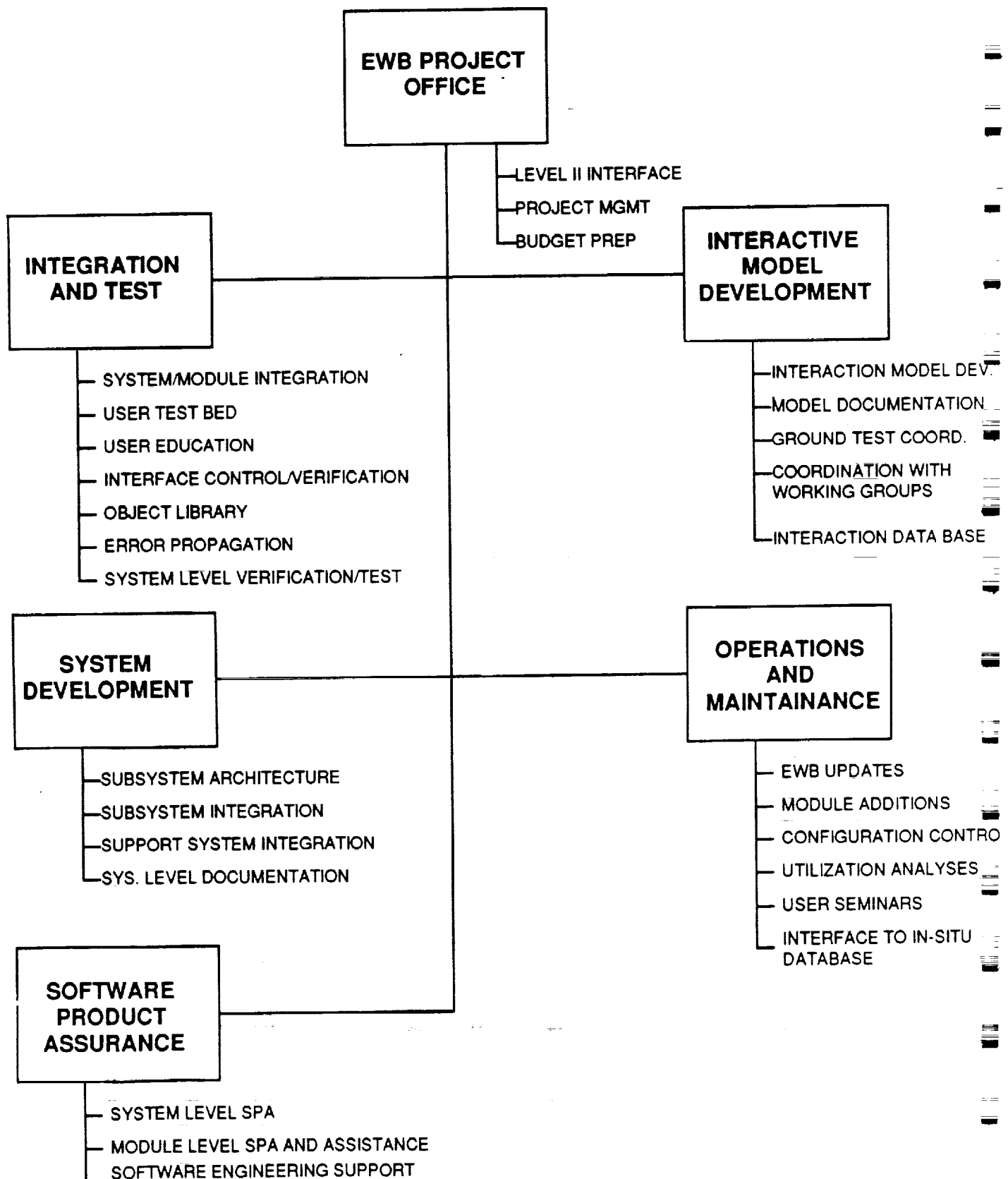
## **STANDARDS RECOMMENDATIONS (CONT)**

- OPERATING SYSTEM UNIQUE CALLS WILL BE IN SEPARATE OBJECTS ( SEPARATE MACHINE DEPENDENT CODE)**
- SOFTWARE MUST SUPPORT STRICT CONFIGURATION CONTROL AND PRIVATE / PUBLIC CAPABILITY**
- PARAMETERS SET TO DEFAULT VALUES WILL BE FLAGGED**
- NO HARD CODED INPUT DATA ALLOWED**
- GEOMETRY, GRIDS, I/O SUPPLIED BY SYSTEM MUST BE IN CONSISTENT UNITS**
- PARAMETERS MUST INCLUDE UNITS (DEFAULT IS MKS)**

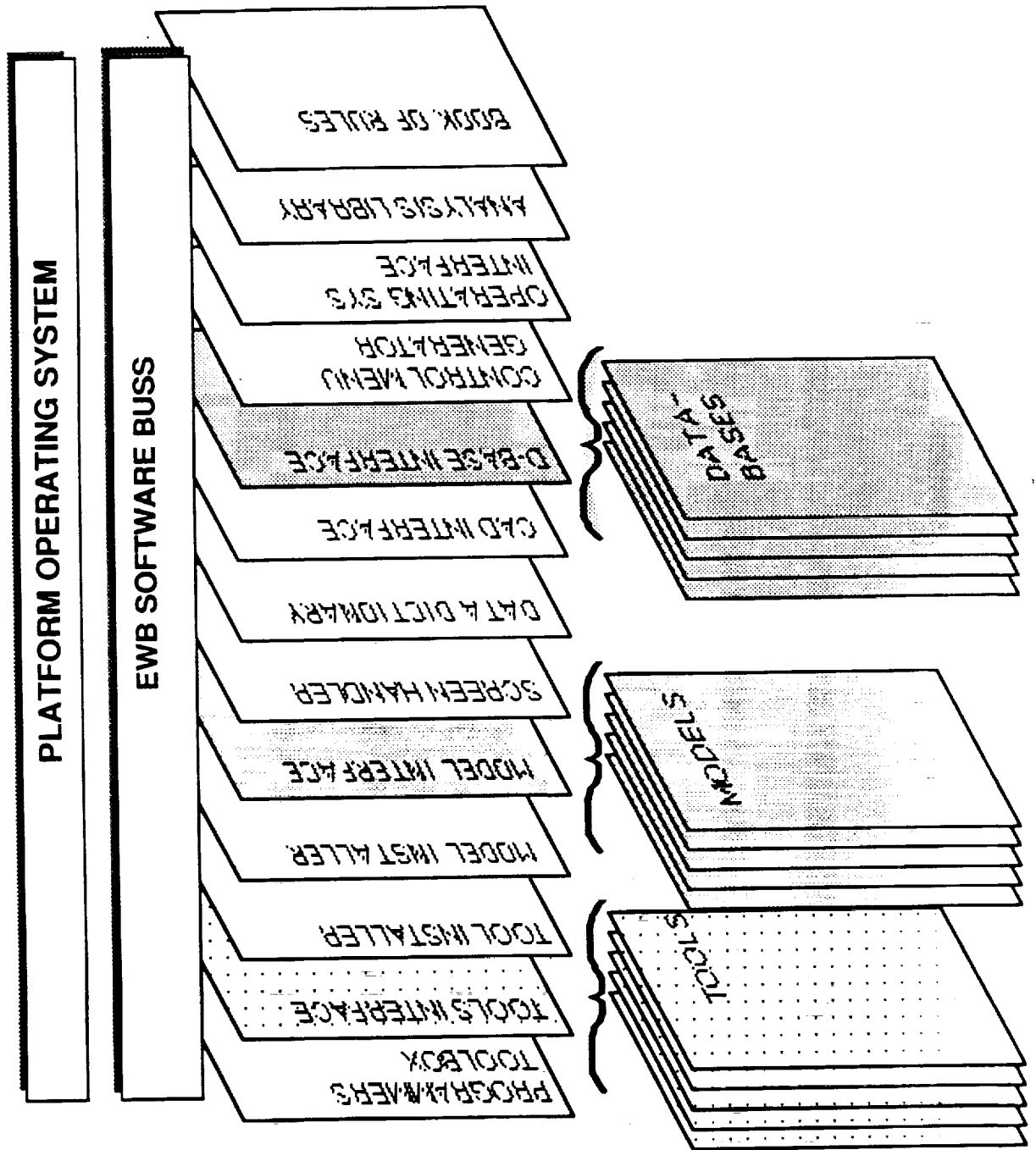
## **RECOMMENDATIONS (CONT)**

- **EWB SYSTEM UTILITIES PROVIDE FUNCTIONS TO MINIMIZE DEVELOPMENT TIME:**
  - DEVELOPERS TOOLBOX FOR TESTING MODELS PRIOR TO INTEGRATION
  - GRID TOOLS--CARTESIAN AND LOCALLY CARTESIAN (WITH INTERPOLATION)
  - (TBS) COORDINATE SYSTEMS FOR CALCULATION AND TRANSFORMATION
  - SSF GEOMETRY MODELS: BOUNDARY SURFACE; THERMAL; MASS; EMC; OPTICAL; AND EFFLUENT REPRESENTATIONS (A SHUTTLE DOCKING SIMULATION ALSO NEEDED)
  - SOFTWARE FOR GENERATION AND MOVEMENT OF SIMPLE OBJECTS
  - SCREEN INTERFACE UTILITIES (MENU, HELP, ETC.)
  - DATA DICTIONARY (A MODEL, TOOL AND DATABASE DICTIONARY)
  - TERMINAL EMULATION AND GRAPHICAL OUTPUT UTILITIES

## ENVIRONMENT WORKBENCH-WORK BREAKDOWN STRUCTURE



# EWB ARCHITECTURE



## **RECOMMENDATIONS (CONT)**

- **DEVELOP SOFTWARE STANDARDS HANDBOOK (PHASE 1):**
  - HARDWARE / SOFTWARE ENVIRONMENT DESCRIPTION**
  - USER, MODULE, GRAPHICS, DATABASE INTERFACE DESCRIPTIONS**
  - MODULE DEVELOPMENT AND REVIEW PROCEDURES AND GUIDELINES**
  - SOFTWARE INTEGRATION AND TEST PROCEDURES**
  - CONFIGURATION MANAGEMENT TECHNIQUES**
  - GUIDELINES FOR INCORPORATION / CONTROL OF EXISTING CODES**



## **RECOMMENDATIONS (CONT)**

- **SOFTWARE PRODUCT ASSURANCE (SPA):**

- SPA MUST RECOGNIZE RELATIVE CRITICALITY OF DIFFERENT MODELS AND TAILOR REQUIREMENTS TO CLASS

- SPA PROCEDURES IN LINE WITH SMAP GUIDELINES

- TWO LEVELS OF SPA MUST BE RECOGNIZED--SPA AT LEVEL II EDAP AND SPA AT THE POINT OF EWB SOFTWARE IMPLEMENTATION

- **CODE AUTHORS, WORKING GROUPS, EWB PROJECT SHARE RESPONSIBILITY AND COMMITMENT TO IMPLEMENT SPA**

## RECOMMENDATIONS (CONT)

- EFFECTS ANALYSIS:
- NATURAL ENVIRONMENTS, INDUCED ENVIRONMENTS, PHYSICAL PROCESS AND SYSTEM/SUBSYSTEM EFFECTS MODELS STUDIED TO FIND CRITICAL MISSING PIECES
- MOST MISSING PIECES IN EFFECTS MODELS--DATA AVAILABLE BUT NOT TIED INTO PROGRAM
- FIND, SORT, AND ASSEMBLE MISSING DATABASES DURING PHASE 1 EWB
- RESEARCH MODELS IDENTIFIED THAT WILL BE TRANSITIONED TO ENGINEERING DOMAIN
- CREATE MODEL DEVELOPMENT AND INTEGRATION PLAN THAT PARALLELS THE EFFORTS OF THE WORKBENCH SYSTEM SOFTWARE. MODELS CAN BE USED STAND-ALONE, THEN INTEGRATED

Scope of Work

- 1) Update Space Station Freedom model configuration to accurately reflect present configuration.  
Compare to JSC configuration.
- 2) Run a test case with the updated configuration of Space Station Freedom using MSIS neutral atmosphere model results for input.  
Generate a set of isodensity contours for neutral density environment.  
Establish that the geometric factors used are correct and not in conflict with other related models.
- 3) Document the configuration and test run results in a report.
- 4) Present results of study at contamination workshop.

## Geometry Update

- 1) Space Station Freedom geometry updated to the configuration described by NASA document "Level II Stage Configuration Drawings Assembly Sequence November 14, 1989" which is dated January 19, 1990.

JSC is using the same document for Space Station geometry modeling.

- 2) Dimensional changes to solar arrays, power radiators, thermal radiators, and rotating structural members.
- 3) Added a structure within the truss to represent the utility tray because it may be a significant structure in terms of outgassing and leakage due to coolant leaks and electrical connector and cable outgassing.

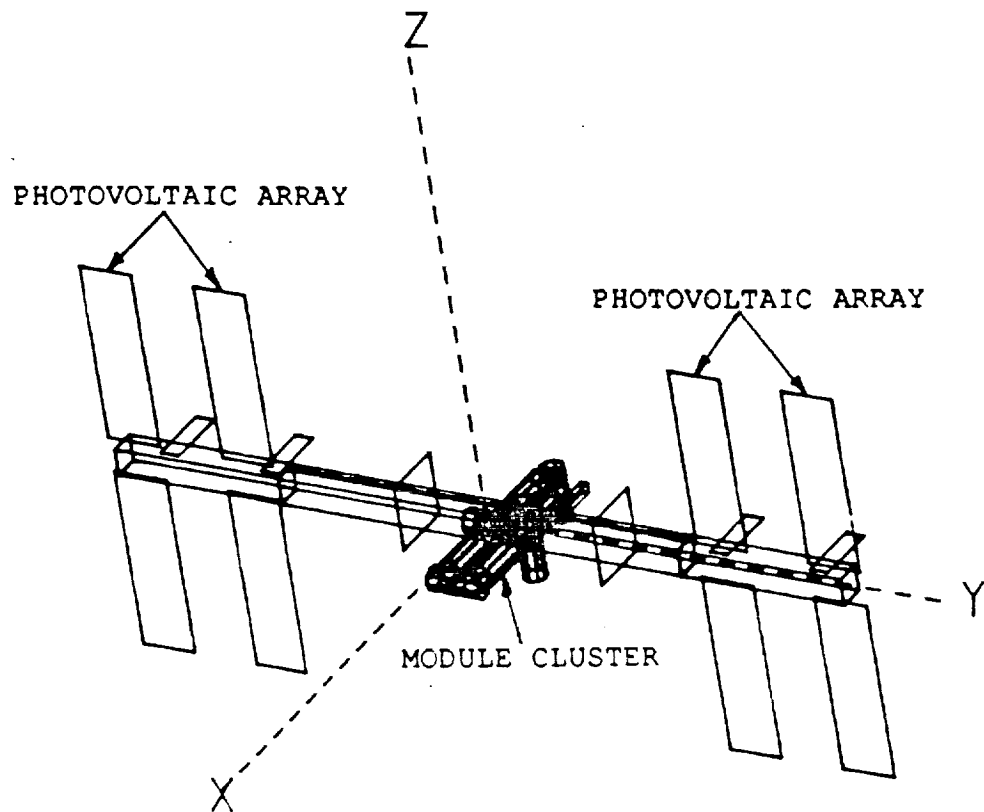


FIGURE 2.1 SPACE STATION CONFIGURATION, THREE-DIMENSIONAL VIEW

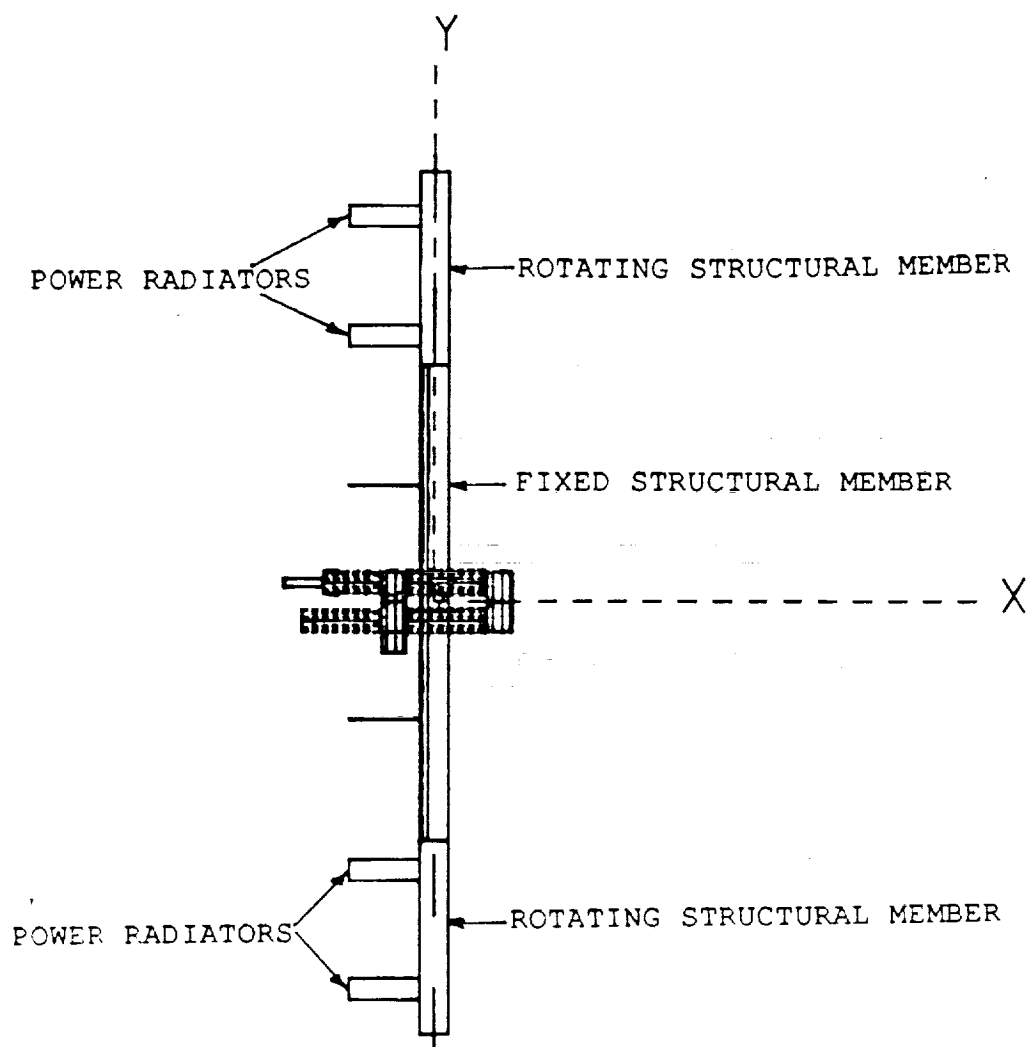


FIGURE 2.2 SPACE STATION CONFIGURATION

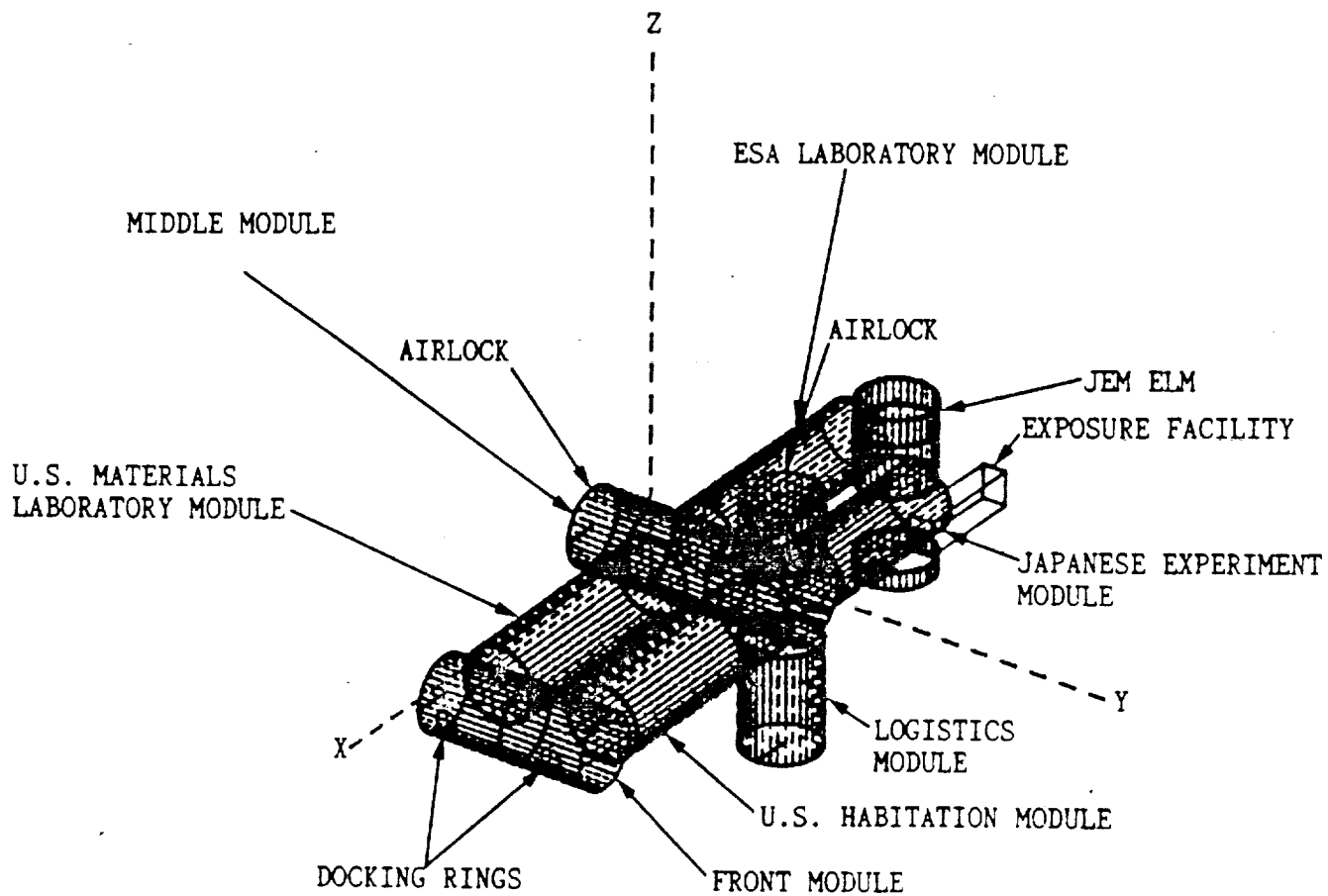


FIGURE 2.3 MODULE CLUSTER, THREE-DIMENSIONAL VIEW

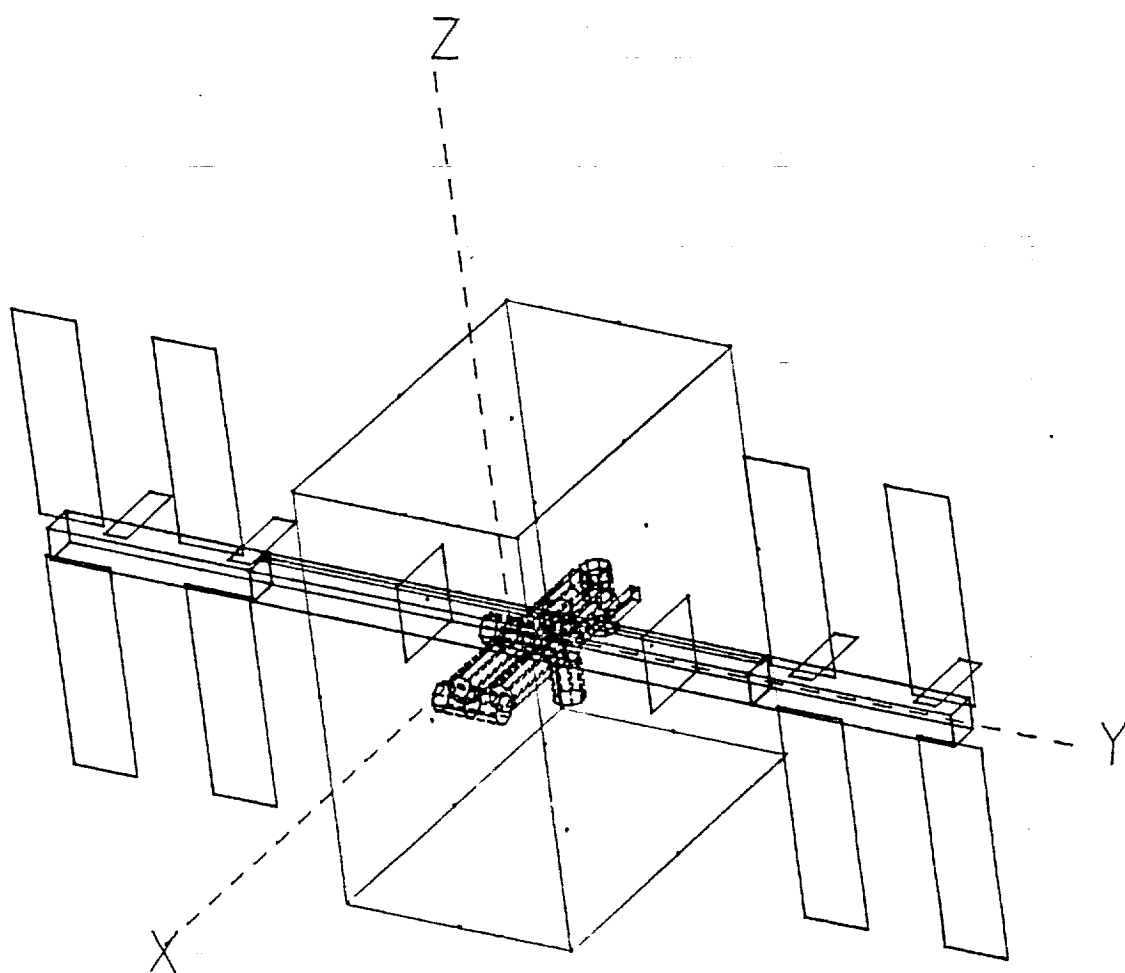
## Source Update

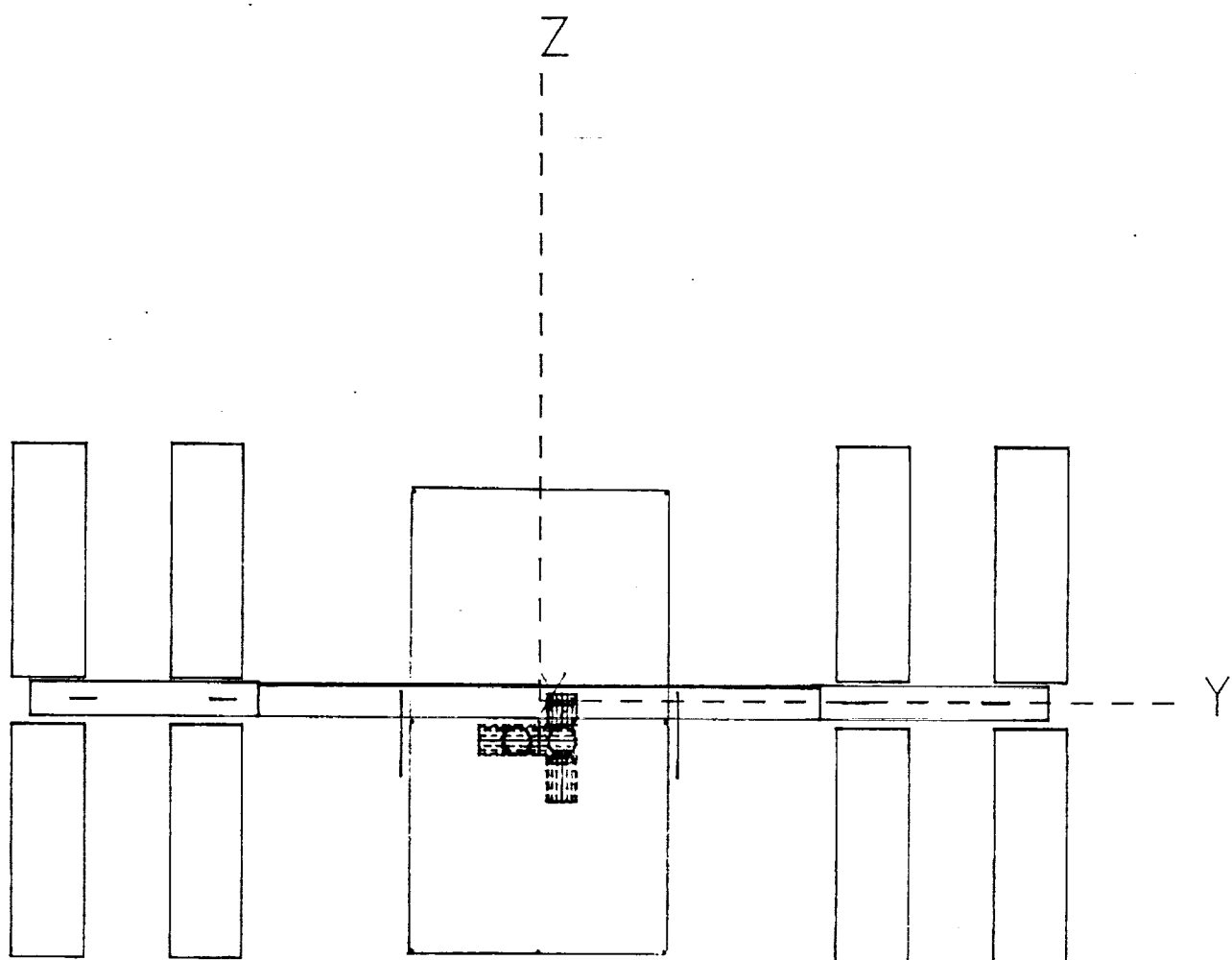
Source	Type	Constituents	Rate (g cm <sup>-2</sup> s <sup>-1</sup> ) (Mol. cm <sup>-2</sup> s <sup>-1</sup> )
Module Surfaces	Outgassing	Mean Mol. Wt.=60	1x10 <sup>-11</sup> 1x10 <sup>11</sup>
Solar Panels	Outgassing	Mean Mol. Wt.=60	5x10 <sup>-10</sup> 5x10 <sup>12</sup>
JEM	Outgassing	Mean Mol. Wt.=60	1x10 <sup>-11</sup> 1x10 <sup>11</sup>
Radiators	Outgassing	Mean Mol. Wt.=60	1x10 <sup>-11</sup> 1x10 <sup>11</sup>
Utility Tray	Outgassing	Mean Mol. Wt.=60	8x10 <sup>-10</sup> 8x10 <sup>12</sup>
Utility Tray	Leakage	Mean Mol. Wt.=60	2x10 <sup>-10</sup> 4x10 <sup>12</sup>
ECLSS Vent	Vent	CO <sub>2</sub>	.046 g s <sup>-1</sup> 6.5x10 <sup>20</sup> Mol. s <sup>-1</sup>
Inactive Seals Type 1	Leakage	75% N <sub>2</sub> , 22% O <sub>2</sub> 2% H <sub>2</sub> O, 1% CO <sub>2</sub>	.004 g s <sup>-1</sup>
Inactive Seals Type 2	Leakage	"	.005 g s <sup>-1</sup>
Inactive Seals Type 3	Leakage	"	.006 g s <sup>-1</sup>
Active Seal	Leakage	"	.013 g s <sup>-1</sup>
Air Lock	Leakage	"	.001 g s <sup>-1</sup>
Docking Ring	Leakage	"	.016 g s <sup>-1</sup>



## Model Test Case

- 1) Used newest version of the Integrated Spacecraft Environments Model (ISEM) to model the neutral molecular environment for Space Station.
- 2) All of the previously listed sources were activated. The modeled environment represents the neutral molecular environment during quiescent periods. Sources not activated in the test case include the resistojet, the RCS engines, airlock blowdown, and the experiment vent for internal payloads. These sources as well as others such as Shuttle docking and EVA's can be addressed by ISEM but were not included in this study.
- 3) Environmental Control Life Support System (ECLSS) vent was located on the bottom of the US Lab Module modeled as a sonic orifice with a rate equivalent to 2.2 pounds of CO<sub>2</sub> per man per day. A crew of four was assumed in the modeling test case.
- 4) The modeling volume for the test case was chosen to compute the neutral environment in proximity of the module cluster. Molecular sources outside the modeling volume are still accounted for in the modeling computations.

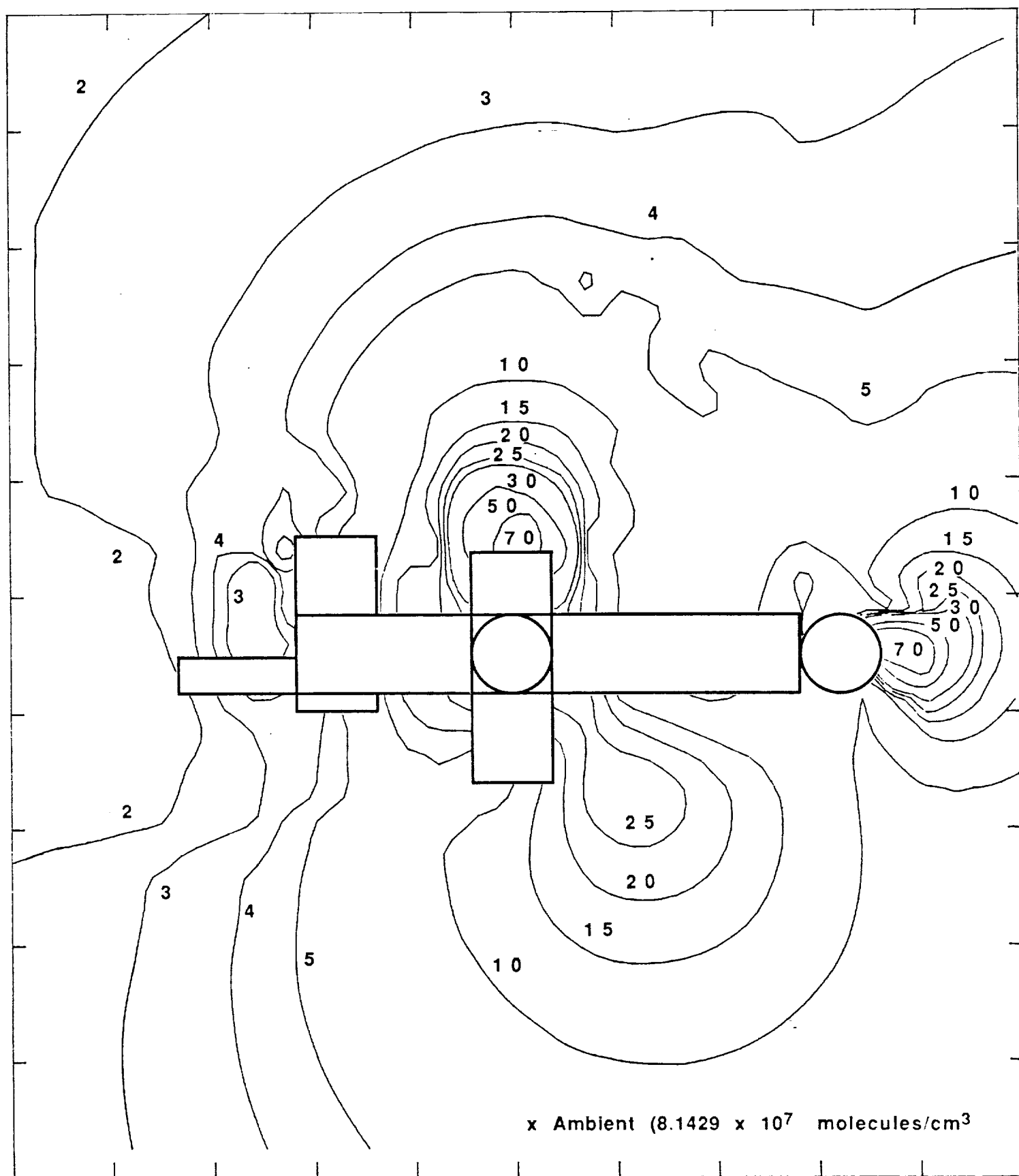




## Modeling Results

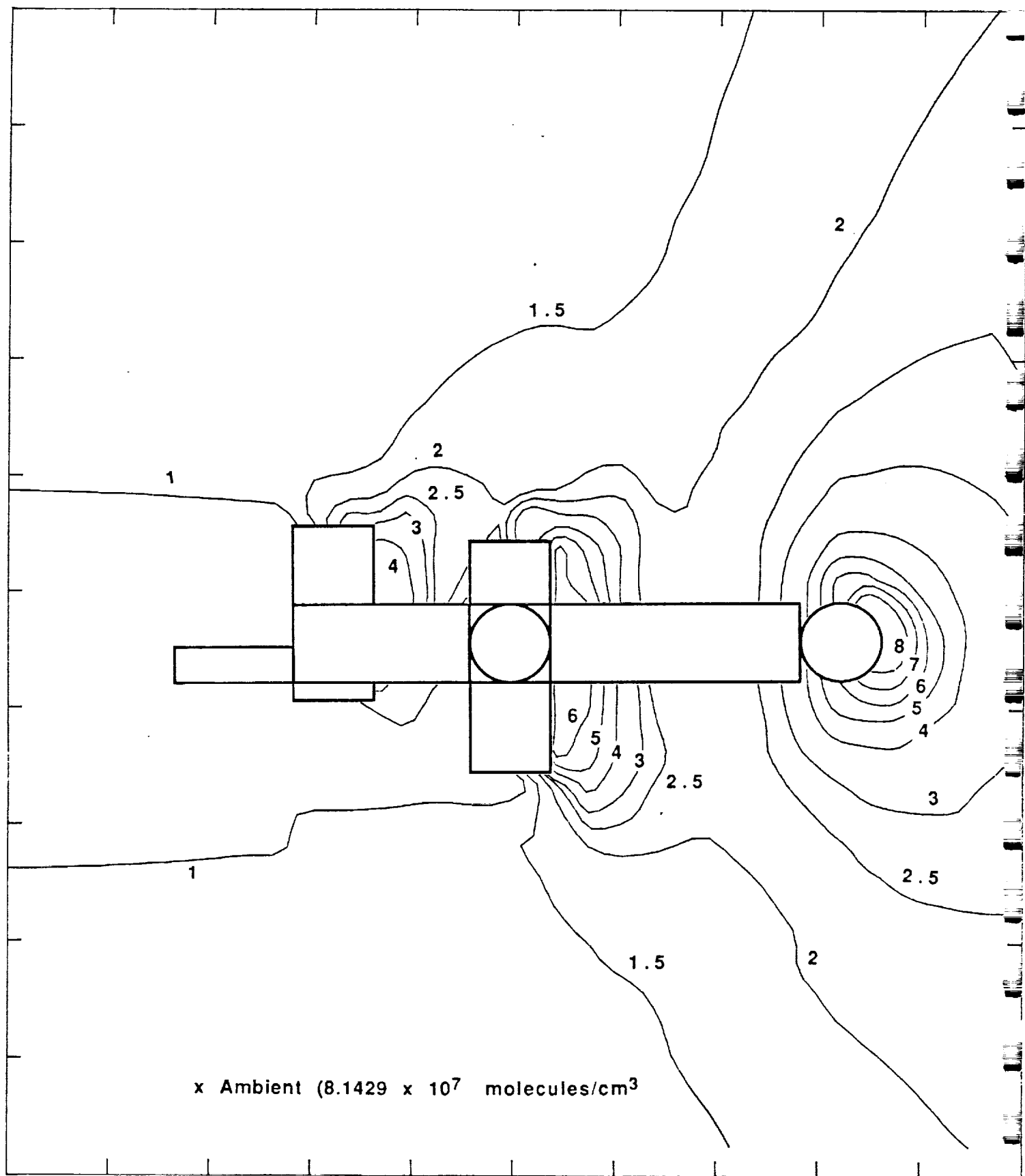
- 1) Molecular species tracked include:
  - ambient O, N<sub>2</sub>, and N
  - surface reemitted ambient O, N<sub>2</sub>, and N
  - two organic species of 30 amu and 60 amu
  - leaked N<sub>2</sub>, O<sub>2</sub>, H<sub>2</sub>O, and CO<sub>2</sub>
  - vented CO<sub>2</sub>
  - scattered (collided) portions of each of the above species
- 2) 3-D density matrix containing the density of each tracked species at 18,734 locations in the modeling volume. Planes of density values extracted from this matrix were used to generate the isodensity plots. The density matrix is also used to compute number column densities along any line-of-sight through the modeling volume.
- 3) 3-D matrix of density weighted average vector velocities for each tracked species at each of the 18,734 locations.
- 4) Incident flux of each tracked species to 39 points, each with a different viewing direction. All of the 39 points used in this run were given a hemispherical ( $2\pi$ ) field-of-view. The flux data was used to generate the flux versus viewing direction plots.

# TOTAL DENSITY X-Z PLANE AT Y=400



CONTOUR FROM 2.0000 TO 70.000 CONTOUR INTERVAL OF IRREGULAR  
 X INTERVAL= 560.00 Y INTERVAL= 660.00

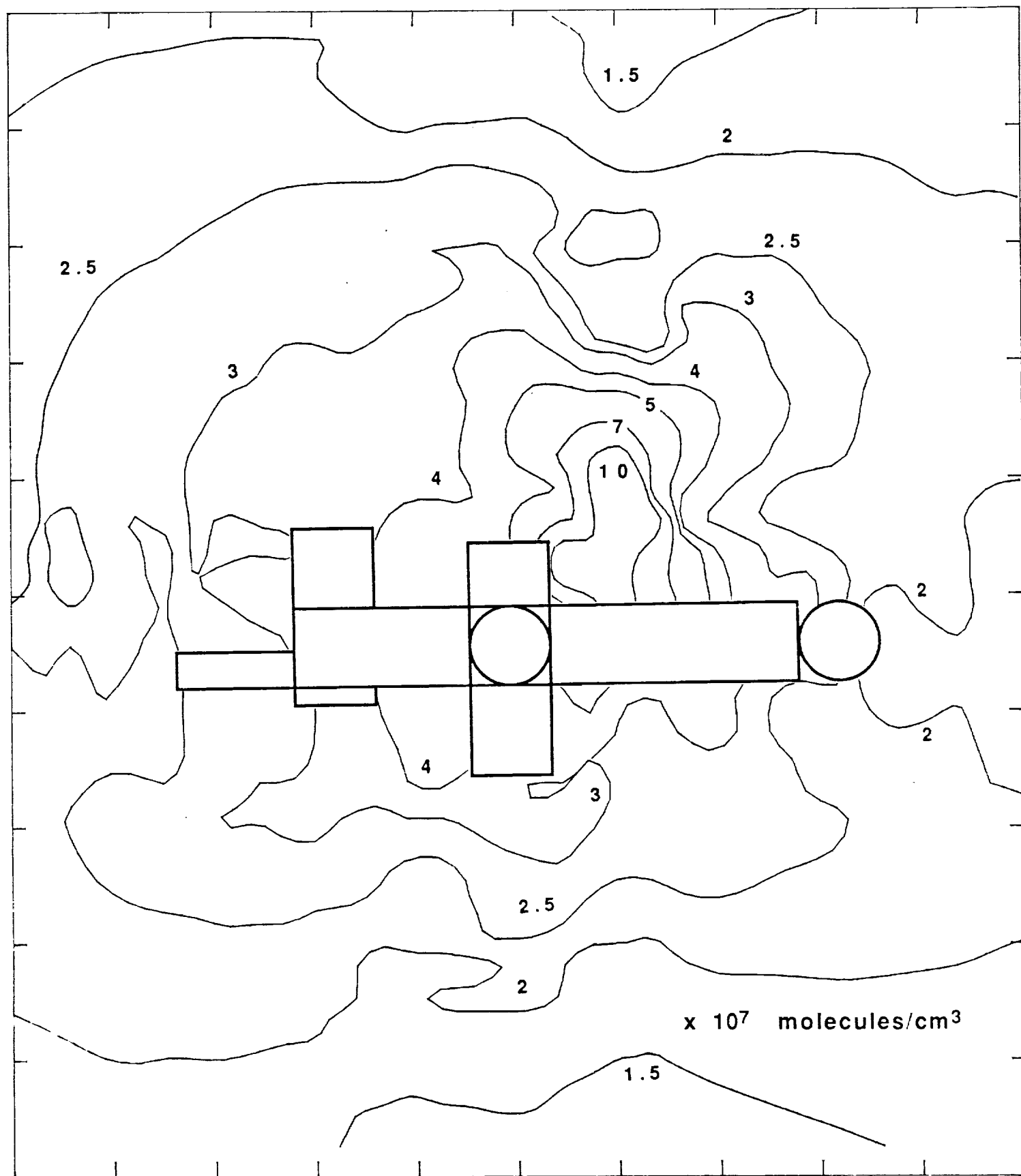
# INDUCED AMBIENT DENSITY X-Z PLANE AT Y=400 -



x Ambient ( $8.1429 \times 10^7$  molecules/cm<sup>3</sup>)

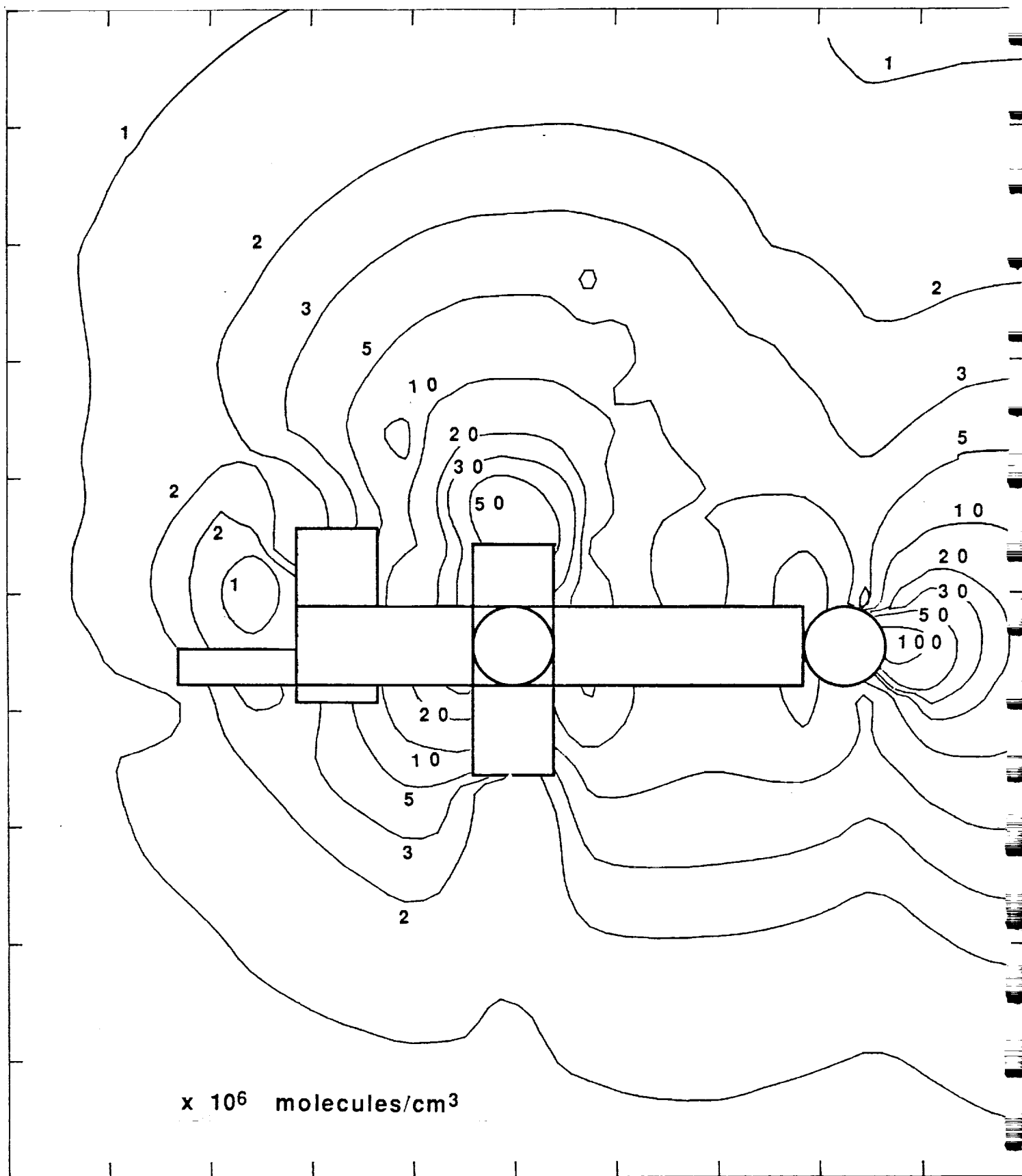
CONTOUR FROM 1.0000 TO 8.0000 CONTOUR INTERVAL OF IRREGULAR  
X INTERVAL= 560.00 Y INTERVAL= 660.00

# DENSITY OF ORGANICS X-Z PLANE AT Y=400



CONTOUR FROM 0.15000E+08 TO 0.10000E+09 CONTOUR INTERVAL OF IRREGULAR  
 X INTERVAL= 560.00 Y INTERVAL= 660.00

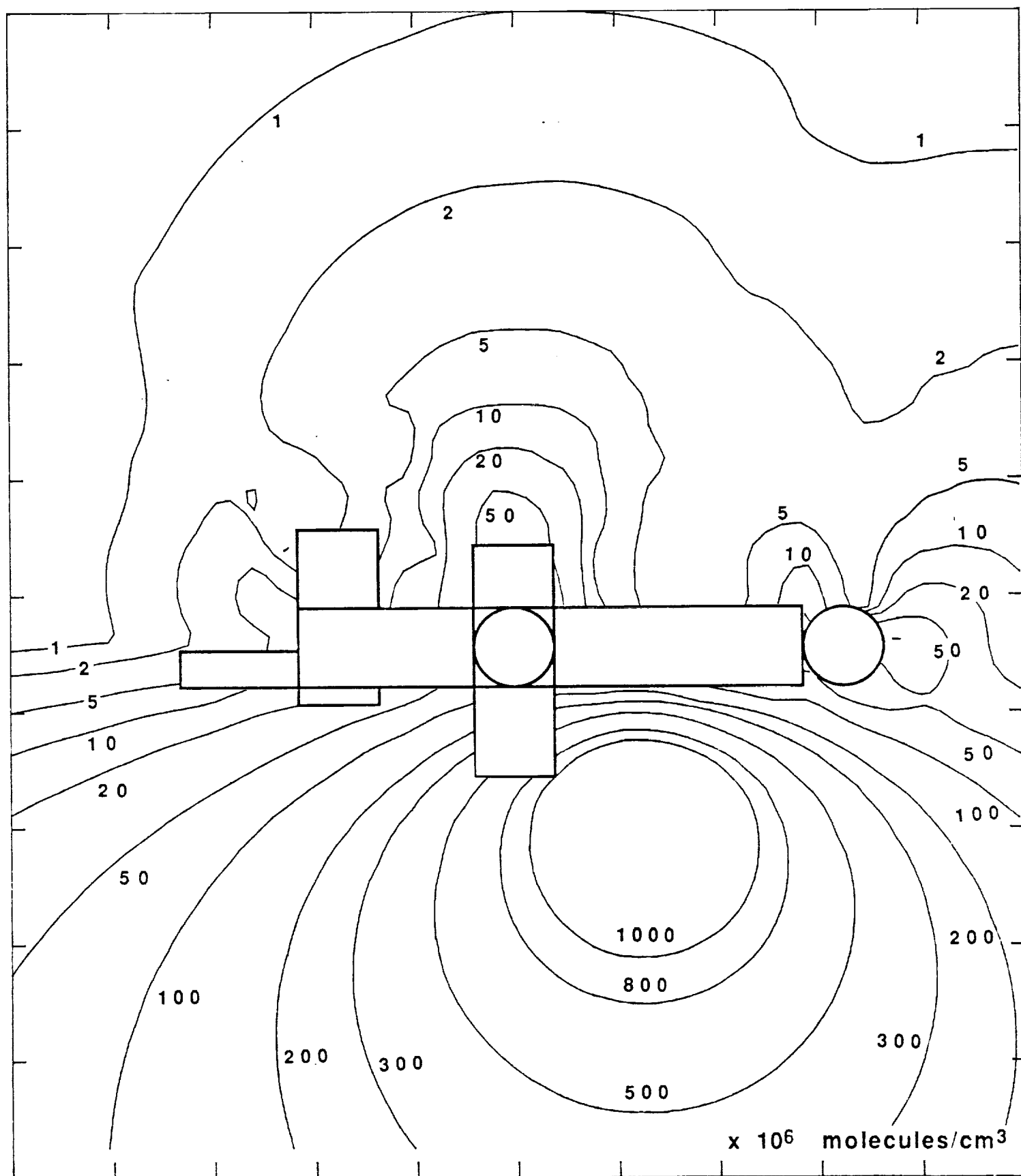
# DENSITY OF H2O X-Z PLANE AT Y=400



CONTOUR FROM 0.10000E+07 TO 0.10000E+09 CONTOUR INTERVAL OF IRREGULAR  
X INTERVAL= 560.00 Y INTERVAL= 660.00



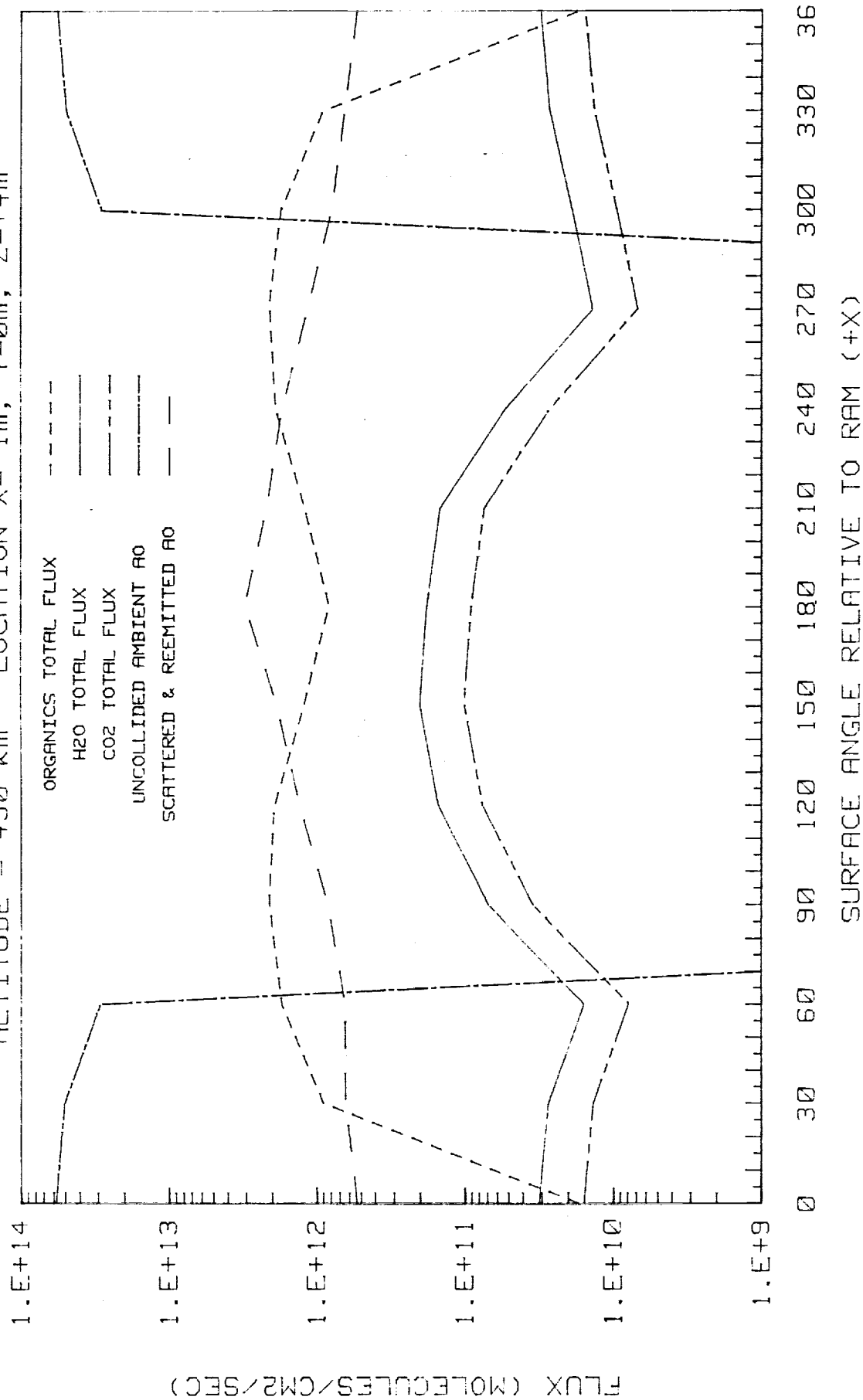
# DENSITY OF CO2 X-Z PLANE AT Y=400



CONTOUR FROM 0.10000E+07 TO 0.10000E+10 CONTOUR INTERVAL OF IRREGULAR  
 X INTERVAL= 560.00 Y INTERVAL= 660.00

# SELECTED SPECIES FLUX AS A FUNCTION OF ANGLE

ALTITUDE = 450 km LOCATION X=-1m, Y=0m, Z=+4m

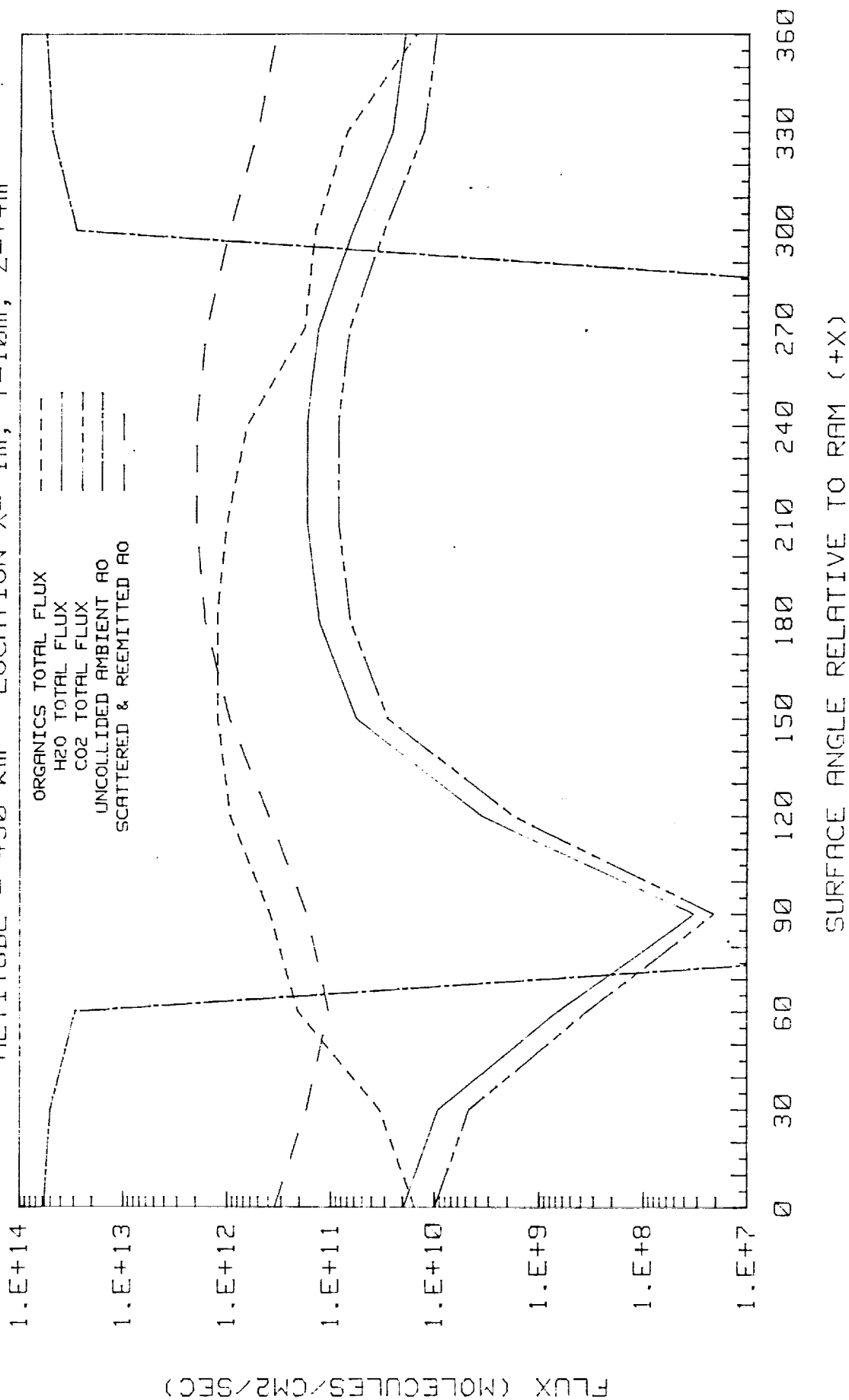


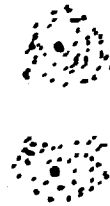
## Conclusions

- 1) ISEM was relatively easy to update to current (and future) configurations.
- 2) Solid angle computations were checked and are correct.
- 3) As a tool, ISEM can be used to analyze directly, or as a starting point for a number of future studies, including:
  - Vent location impact studies
  - Deposition studies on critical surfaces such as solar panels and radiators
  - Glow mechanism studies (currently being worked with Dr. Doug Torr under an APL study)
    - Ultimately glow prediction
    - Ionization production and transport
    - Sputtering product transport

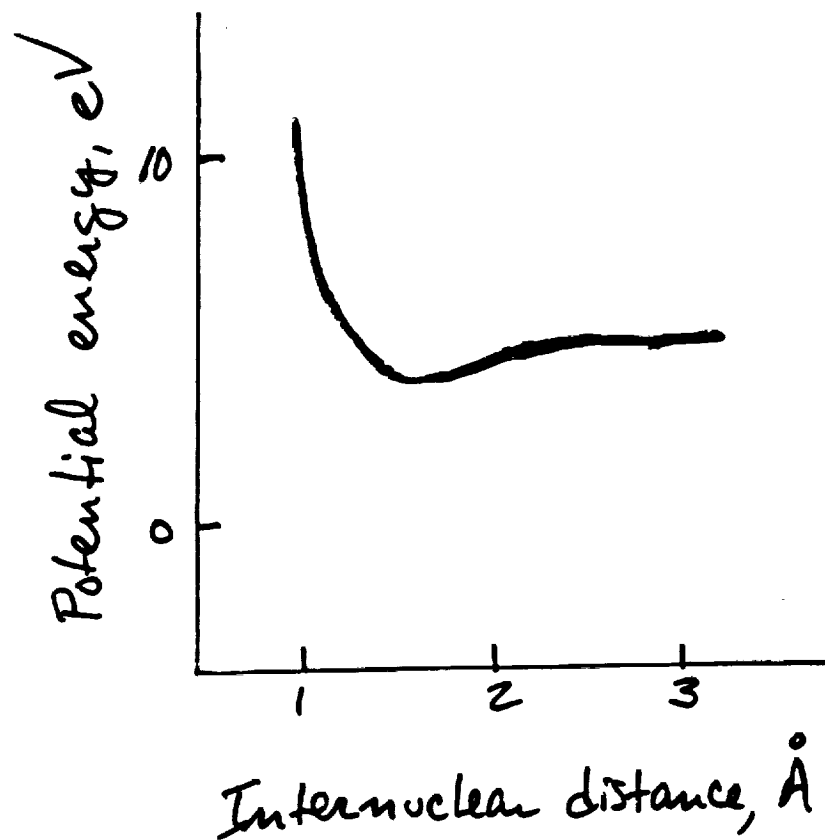
# SELECTED SPECIES FLUX AS A FUNCTION OF ANGLE

ALTITUDE = 450 km LOCATION X=-1m, Y=10m, Z=+4m

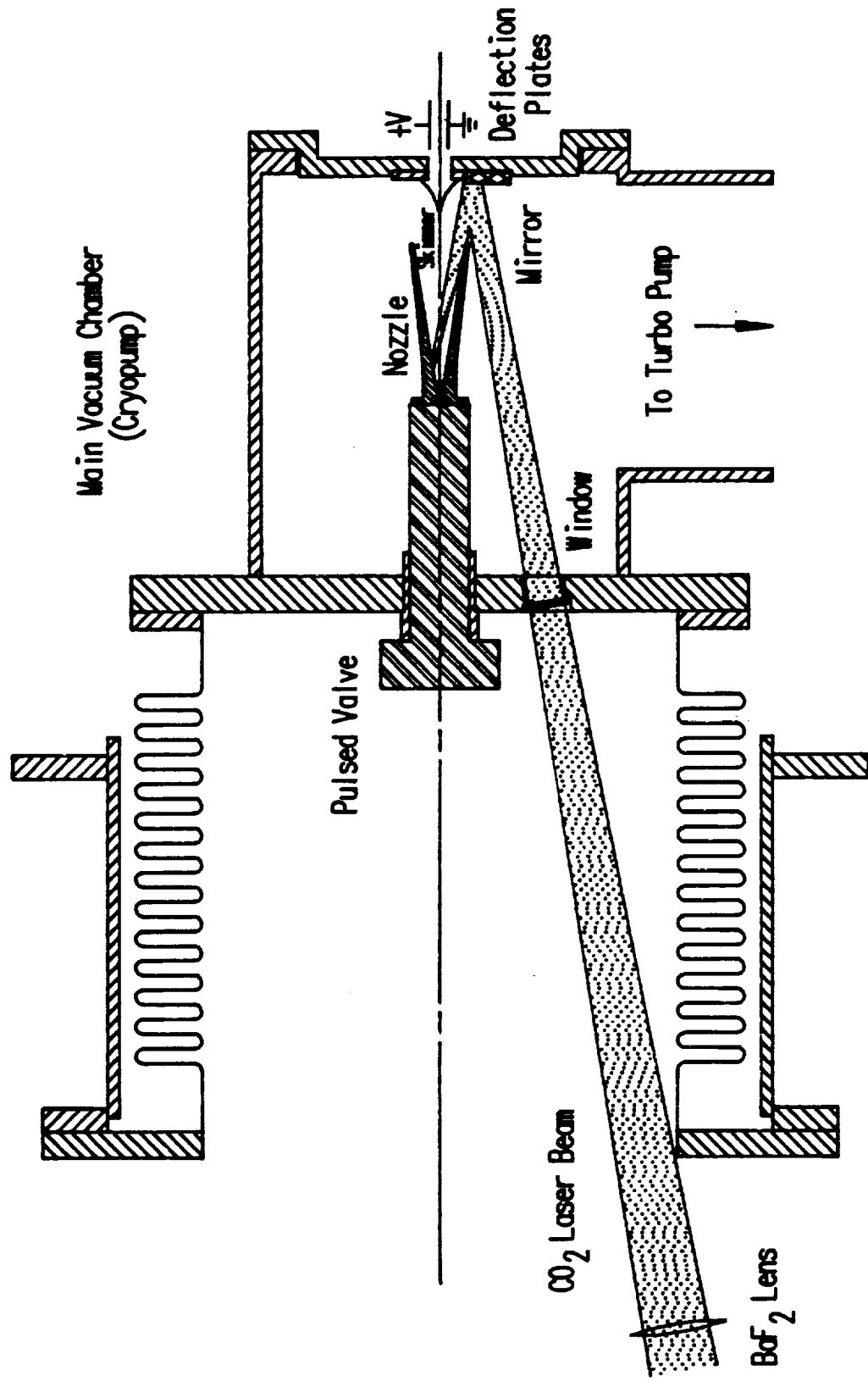




ORIGINAL PAGE IS  
OF POOR QUALITY



# 0 Atom Source Sectional View



# Differential Scattering Performance

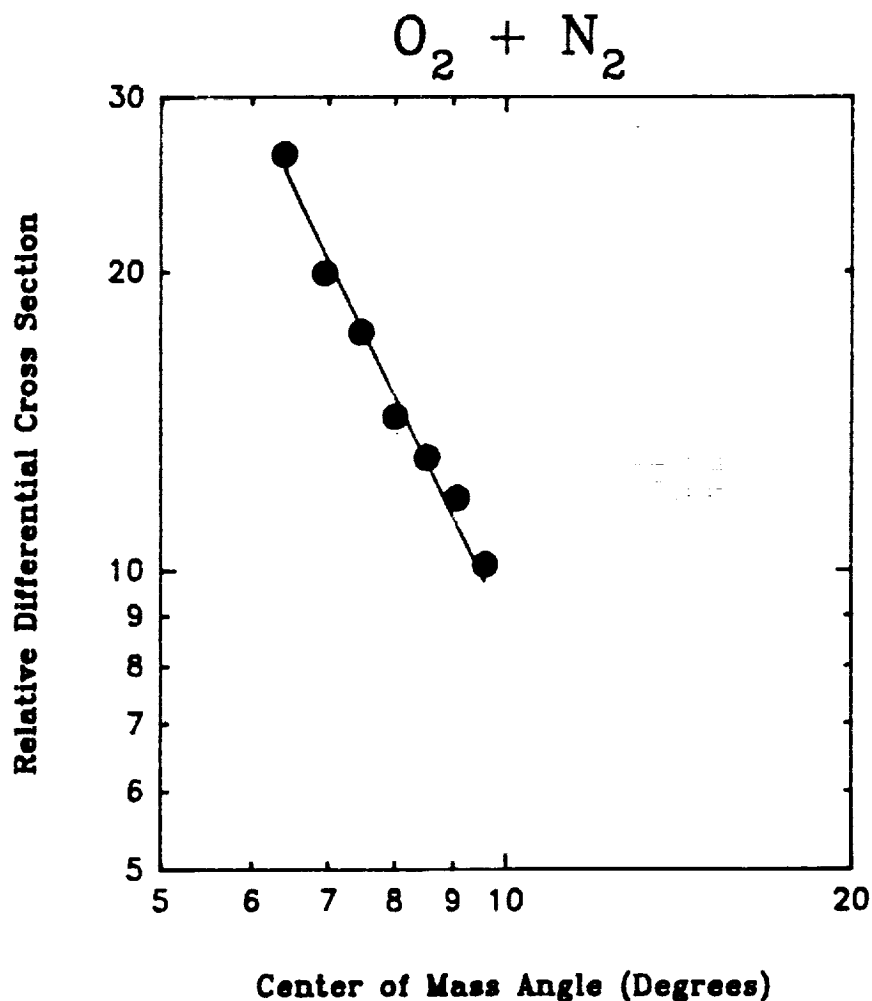
\* Test Case: Thermal Energy  $O_2 + N_2$

\* Classical Scattering Theory Predicts

$$I(\theta) = C \theta^{-7/3} \text{ for small angles}$$

\* Graph Shows Data and Least Squares Fit

\* Experimental Value of Exponent is  
 $-2.37 \pm .14$

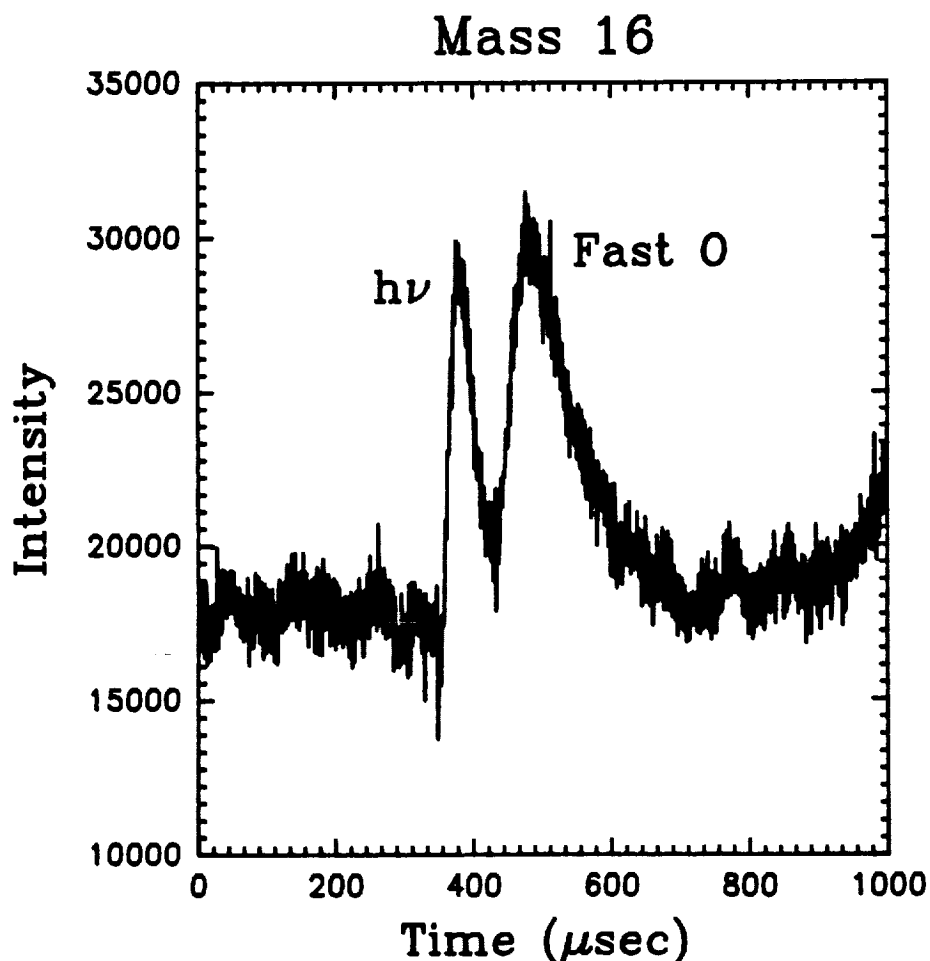


~~CONFIDENTIAL~~



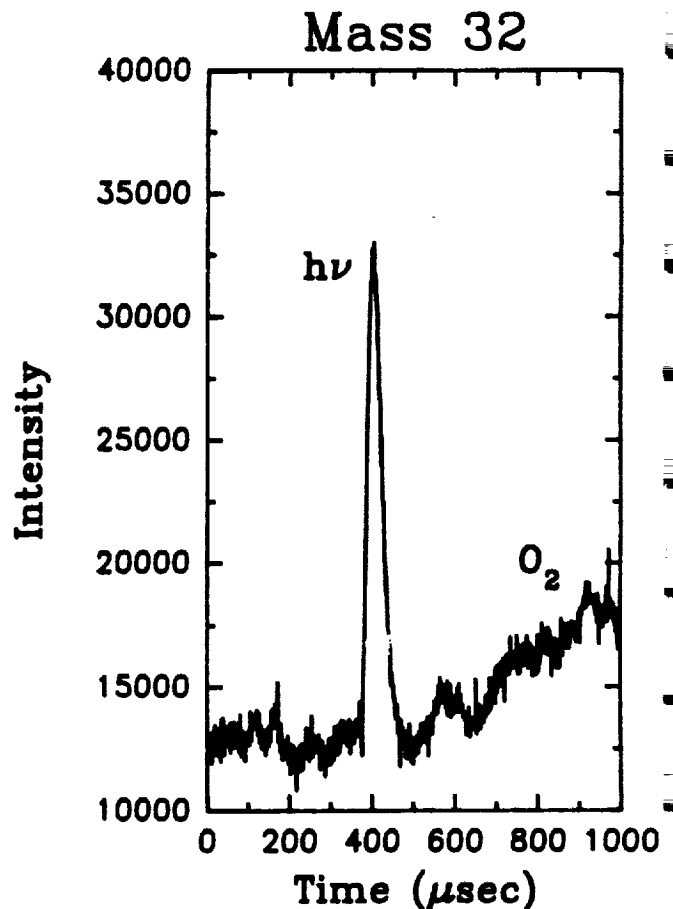
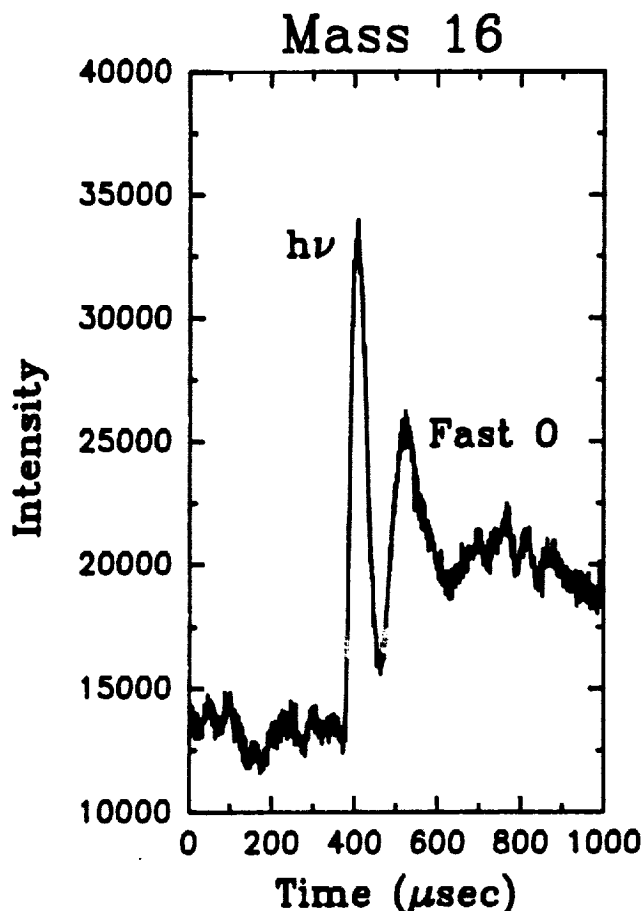
# O Atom Velocity Measurement

- \* First Peak due to Photons Striking the Detector
- \* Second Peak due to Fast O Atoms
- \* Assume Time Between Peaks is the Time of Flight for the O Atoms
- \* Velocity for this Measurement is 5.2 km/sec



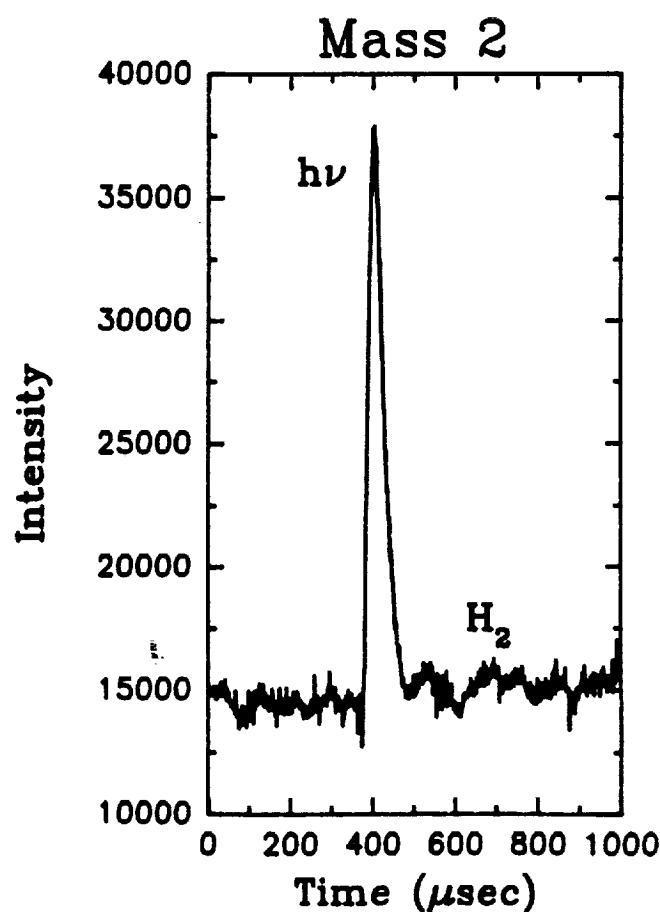
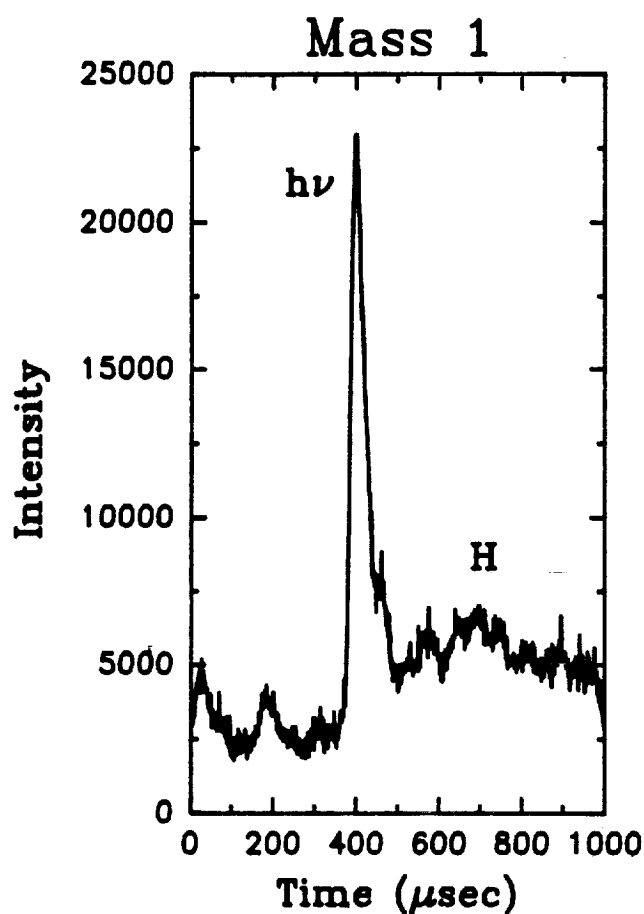
## O Atom/O<sub>2</sub> Molecule Ratio

- \* Ratio of O Atoms to O<sub>2</sub> Molecules is > 4:1
- \* Velocity of O Atoms is 6.2 km/sec
- \* Some Slower O Atoms and O<sub>2</sub> Molecules are Evident



# Fast H Atom & H<sub>2</sub> Molecule Impurities

- \* Fast H Atoms or H<sub>2</sub> Molecules Are Not Evident
- \* Estimate < 10% H or H<sub>2</sub> in Beam
- \* Some Slower H Atoms and H<sub>2</sub> Molecules are Evident



# Energetic Oxygen Atom Source

- Velocity Depends on Laser Intensity  
and Amount of Gas
- Velocity Range = 3 to 11 km/sec
- Oxygen Beam Composition
  - $O > 80\%$
  - $O_2^+ < 20\%$
  - $O^+ < 1\%$
- Ions Readily Removed With Parallel  
Plate Deflectors

# Future Directions

- Differential Scattering Cross Section  
 $O(5\text{ eV}) + N_2$
- Surface Scattering of 5 eV O by  
 $Al_2O_3$ ,  $SiO_2$ , etc.
  - Sticking Coefficients
  - Reaction Products
  - Temperature Dependence
- Charge Exchange Cross Sections
  - $O^+ + H_2O \rightarrow H_2O^+ + O$
  - $O^+ + N_2 \rightarrow N_2^+ + O$
  - $O^+ + N_2 \rightarrow NO^+ + N$

# Summary

A Unique Facility Has Been Developed  
for Addressing Many of the Important  
Issues Related to the Space Station

Induced External Environment.

Preliminary Assessments are  
Encouraging for Future Work.

# **INDUCED EMISSIONS**

## **STUDIES UNDERWAY:**

1. MODELING OF VEHICLE GLOW
2. CONTINUED REDUCTION OF GLOW DATA

## **CURRENT MODELING FOCUS:**

ISO AND S3-4 FAR UV GLOW

- DEVELOPMENT OF THEORETICAL MODELS
- TESTING OF MODELS
- DEVELOPMENT OF MODELS OF BACKGROUND  
TERRESTRIAL EMISSIONS

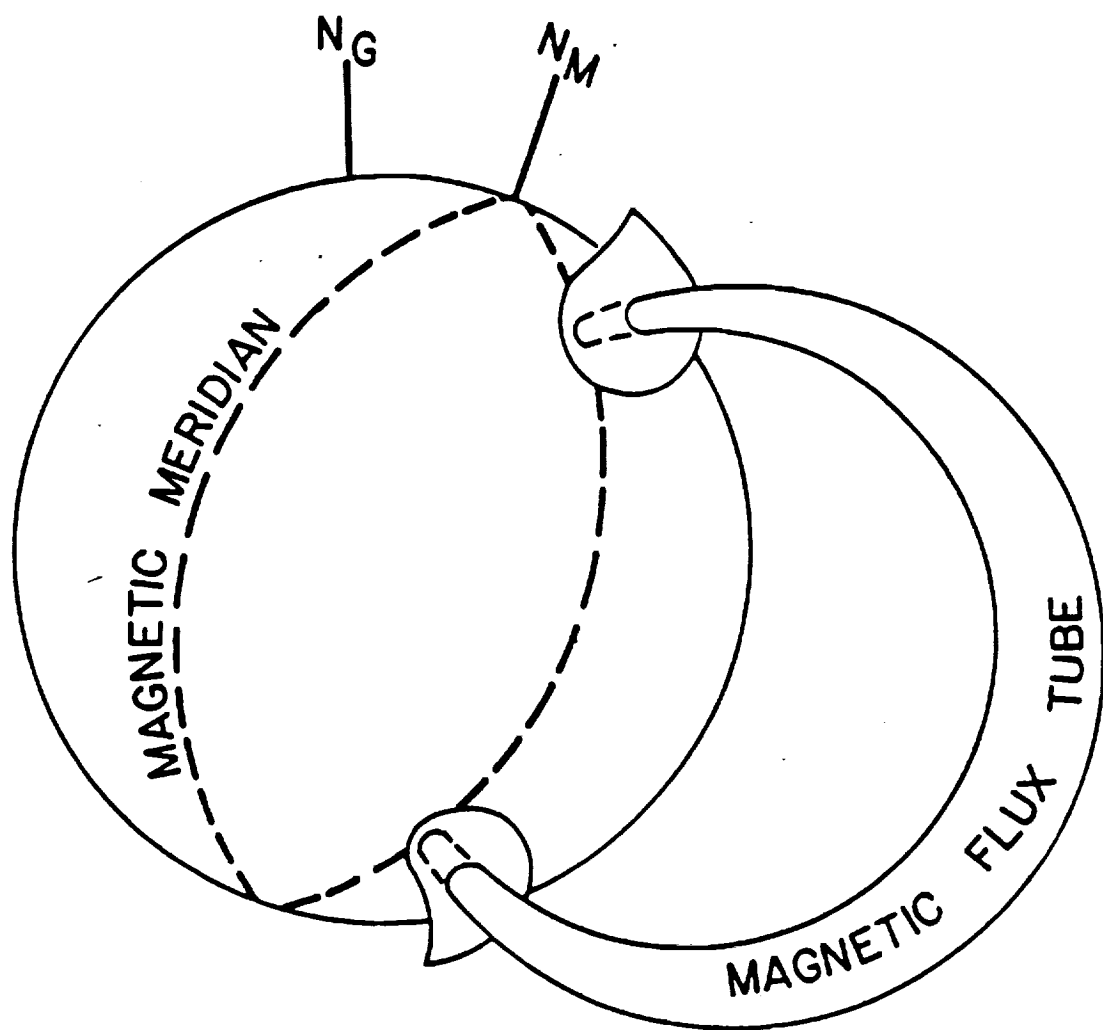
## **CURRENT GLOW DATA BEING UTILIZED:**

SPACELAB 1 ISO DATA

S3-4 DATA







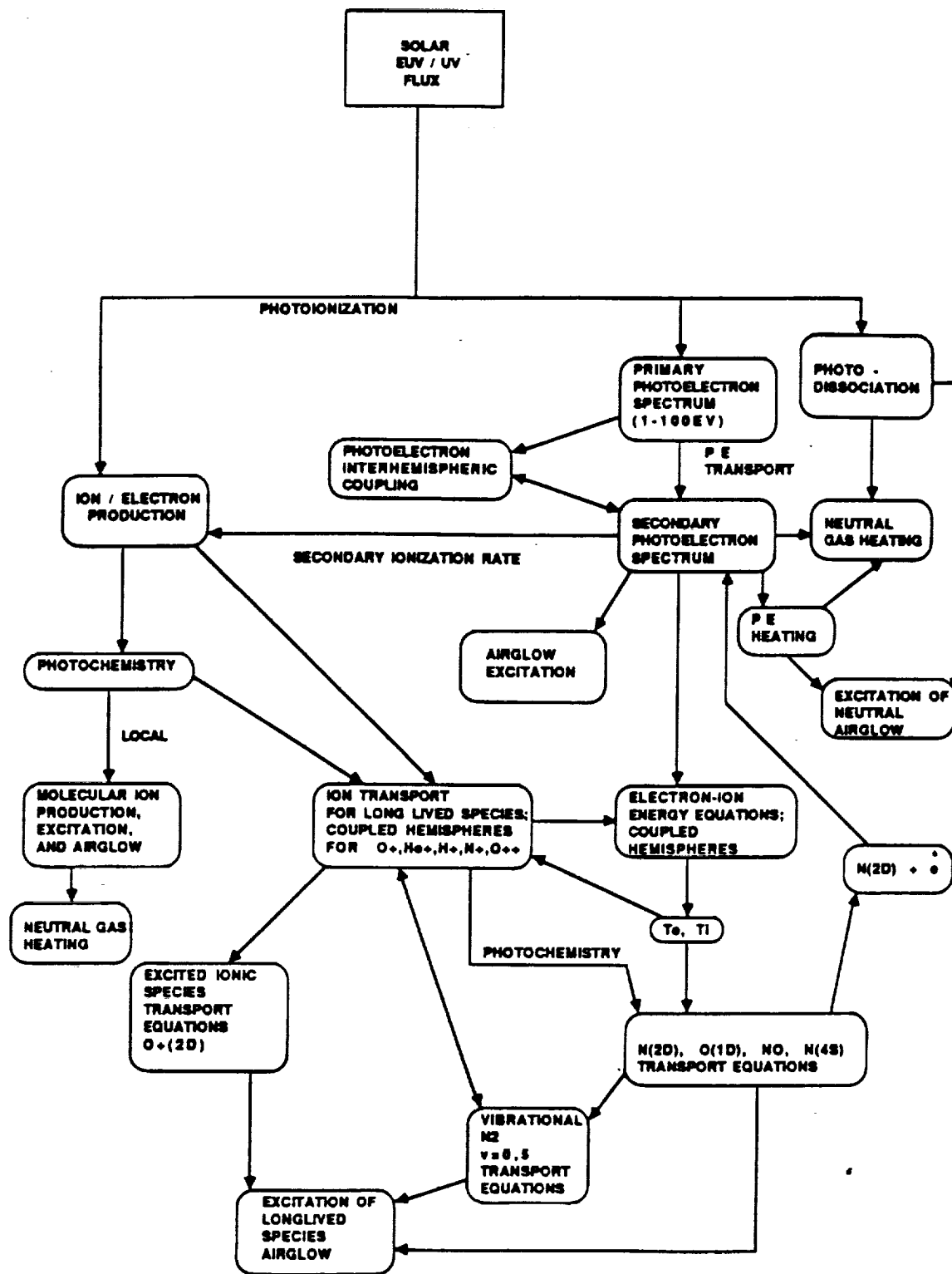
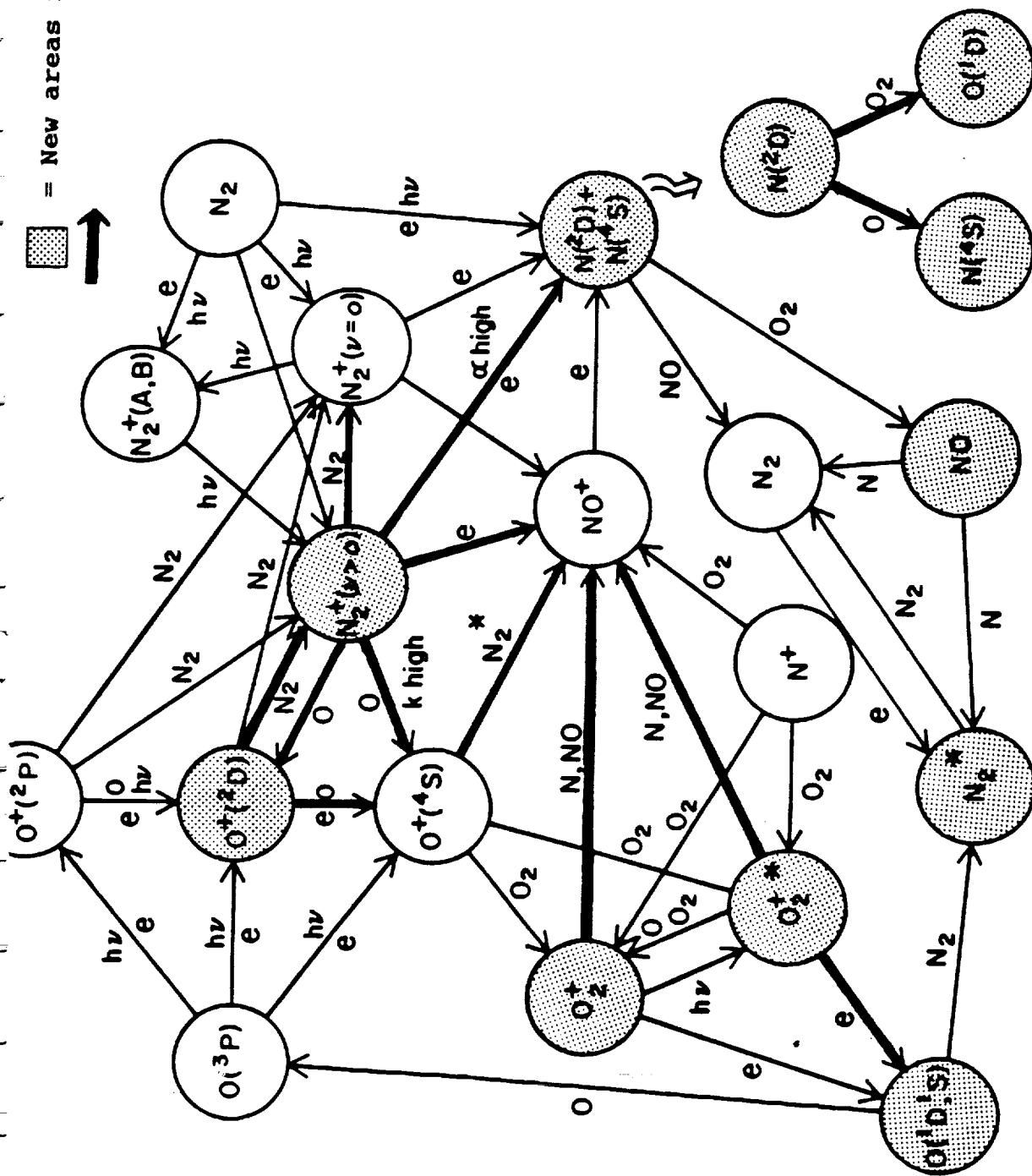



FIGURE 3c

C4



Schematic of the thermospheric and ionospheric chemistry to be studied

## FAR UV GLOW CHARACTERISTICS

### SPACELAB 1:

NIGHT AT 250 KM

VERY BRIGHT:

> 50 R/A PEAK

INTEGRATED INTENSITY:

~ 5kR

PSEUDO CONTINUUM:

COMPOSITE SPECTRUM

N<sub>2</sub>: LBH, VK

NO  $\epsilon$ ,  $\delta$ ,  $\gamma$

WEAKEST IN RAM

VIBRATIONAL DISTRIBUTION: PEAKS AT  $V = 0$

DECREASING TO 0 AT  $V = 6$

### S3-4 SATELLITE:

NIGHT

SPECTRALLY PURE LBH < IR AT 250 KM

ALTITUDE DEPENDENCE  $[N_2]^3$  OR  $[N_2]^2 [O]$

VIBRATIONAL DISTRIBUTION: SIMILAR TO SL1

MODELS: 1. SWENSON/MEYEROTT

2. TORR

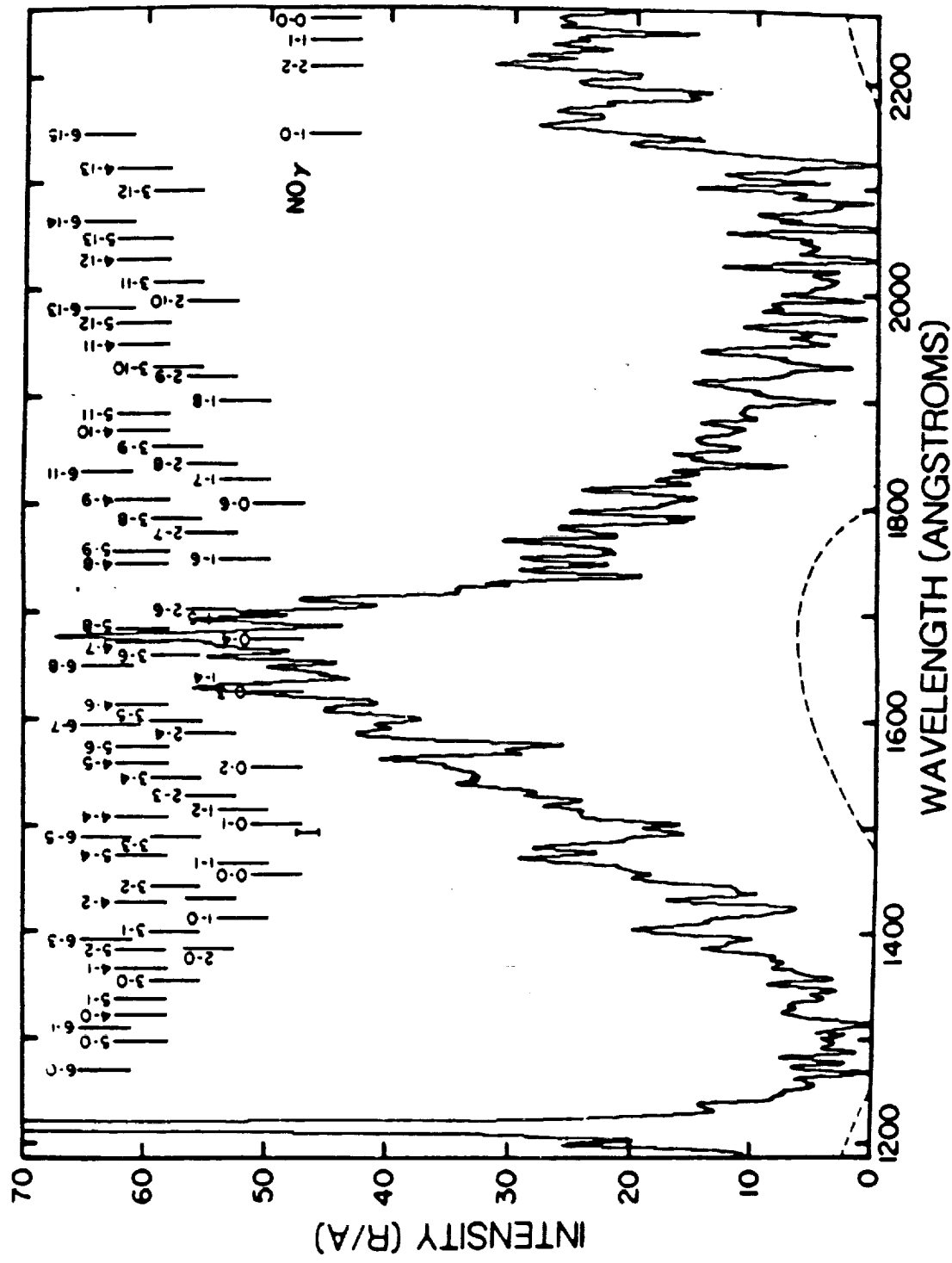
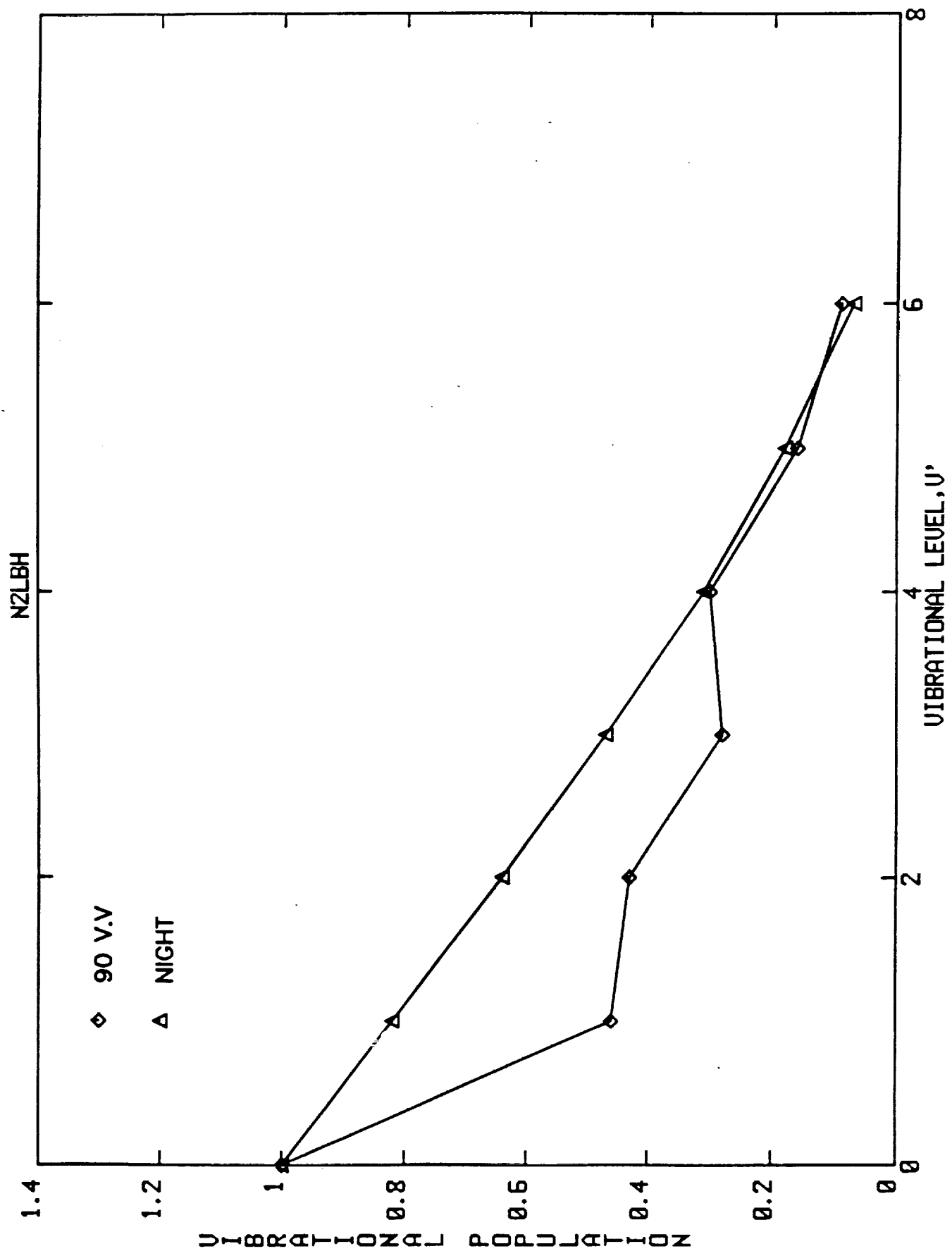


Fig. 5. Spectrum measured at night at southern mid-latitudes (trace 4 in Figure 1). These data were obtained on December 5, 1983, at 0500 UT.



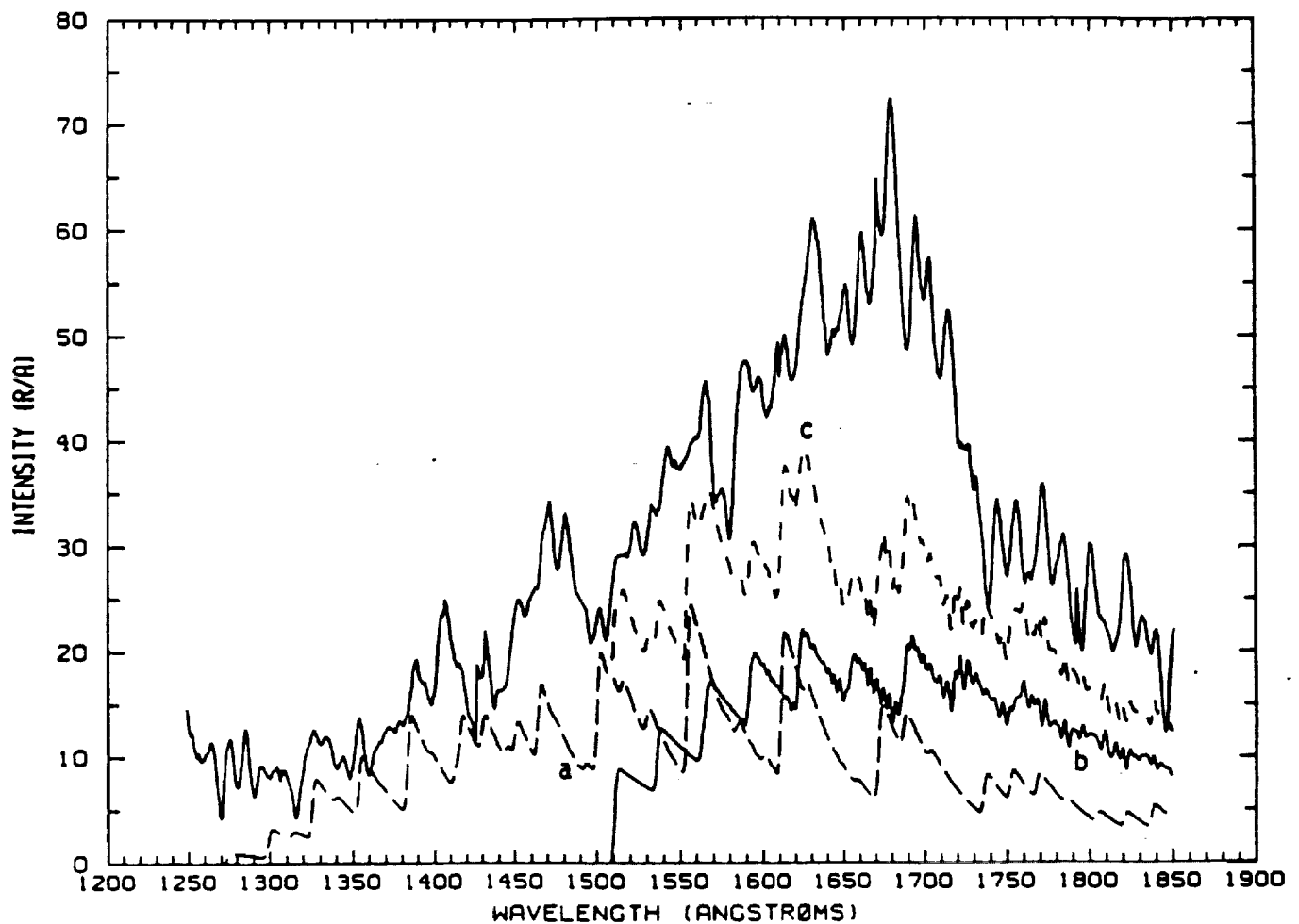


Fig. 2. An example of the vacuum ultraviolet spectrum observed on Spacelab 1 at 250 km on December 5, 1983 at  $130^{\circ}$  W, at 21 hours local time, solar zenith angle =  $107^{\circ}$ , at mid-latitudes. A mirror was used to view the  $90^{\circ}$  direction across the Y-wing of the Shuttle. Curves a and b are synthetic spectra of the  $N_2$  Lyman-Birge-Hopfield and Vegard Kaplan band systems respectively. Curve c shows a composite spectrum of these two systems.

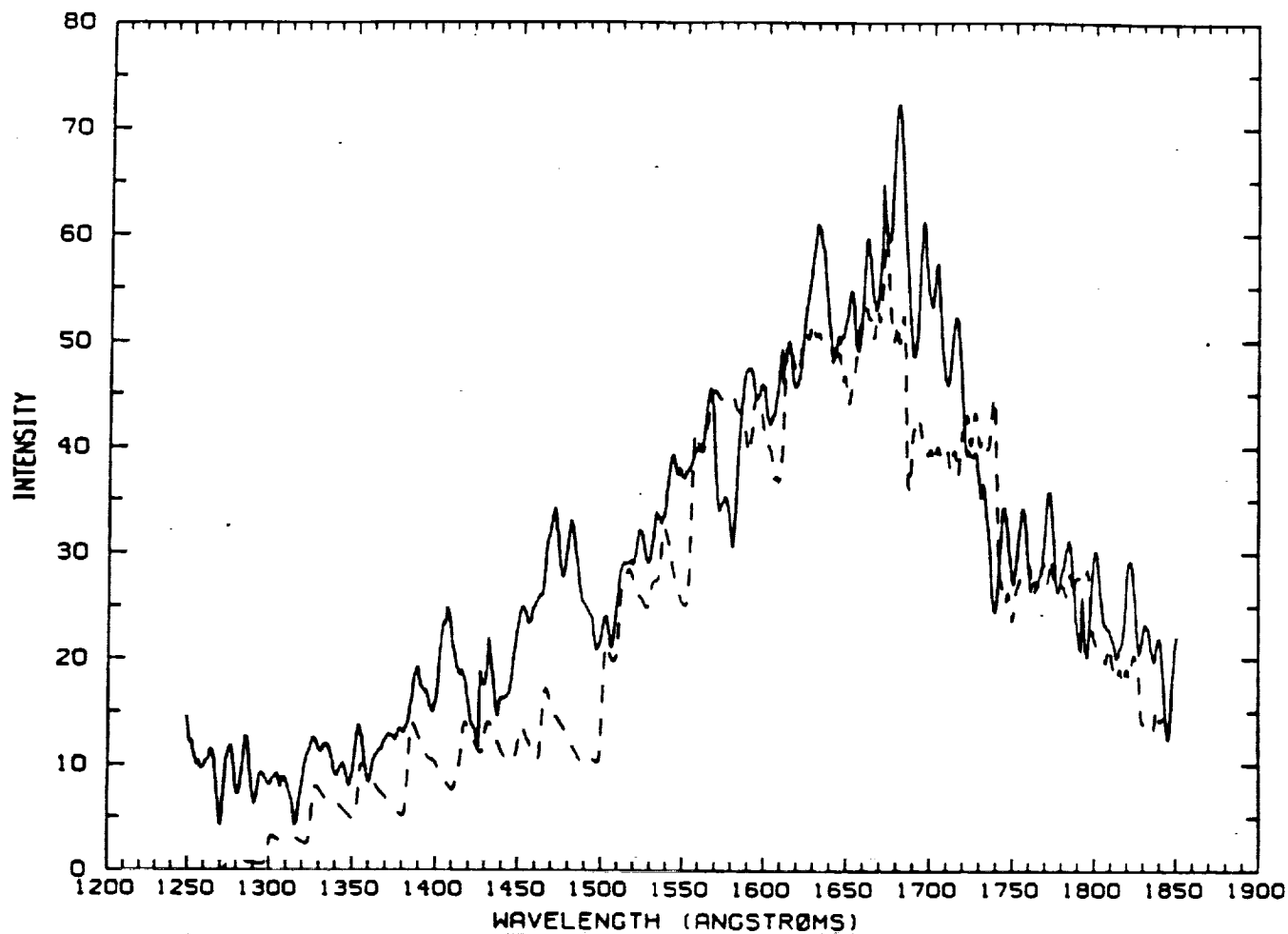


Figure 5: A comparison of the observations shown in Figure 2 with a composite synthetic spectrum comprising the N<sub>2</sub>, LBH, VK and NO  $\epsilon$  and  $\delta$  bands.



## ESSENCE OF ALL MODELS:

ENERGY SOURCE FOR REACHING FUV EXCITATION STATES:

SURFACE RECOMBINATION  
KOFISKY (1988)

EG       $N + N \rightarrow N_2^* \Rightarrow FUV$

$N + O \rightarrow NO^* \Rightarrow FUV$

$O + O \rightarrow O_2^* \Rightarrow$

COULD BE SOURCES OF SURFACE OR VOLUME GLOWS

DEPENDING ON THE RADIATIVE LIFETIME OF THE EXCITED  
PRODUCT.

THIS GENERIC MECHANISM COULD GENERATE GLOW FROM  
THE EUV TO NEAR IR

NOTE:      EUV CAN ARISE IF ONE OF THE RECOMBINING  
PARTNERS HAS RAM ENERGY  
(MEYEROTT AND SWENSON PSS 1990)

FOR LBH GLOW N-N RECOMBINATION YIELDS A SURFACE  
GLOW (~2.2CM)

## **WHAT KIND OF GLOWS HAVE BEEN OBSERVED?**

### **SPACELAB 1:**

#### **AIRPLANE MODE**

IN THE **AIRPLANE MODE** ISO IS SHIELDED FROM RAM  
FLUXES BY THE SL MODULE AND AFT BULKHEAD

**CAN ONLY SEE VOLUME GLOW**

### **OTHER SHUTTLE ORIENTATIONS:**

**SURFACE AND VOLUME GLOW**

∴ RAM GLOW: SURFACE AND OR VOLUME

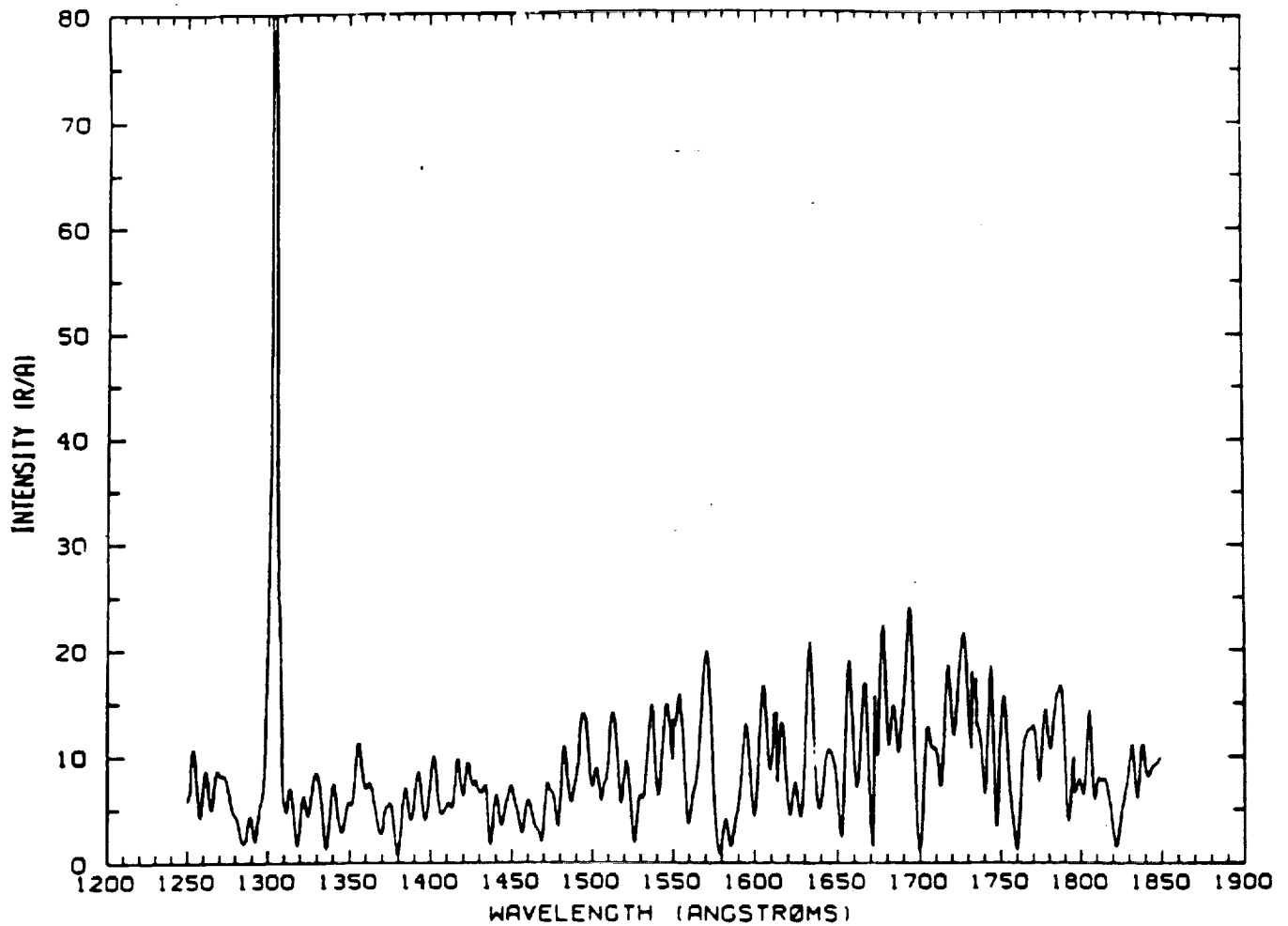


Figure 6: The ram VUV spectrum observed on Spacelab 1 on December 7. The spectra were taken under similar geophysical conditions to those shown in Figure 4, except that the local time was -04 hours which corresponds to twilight conditions.

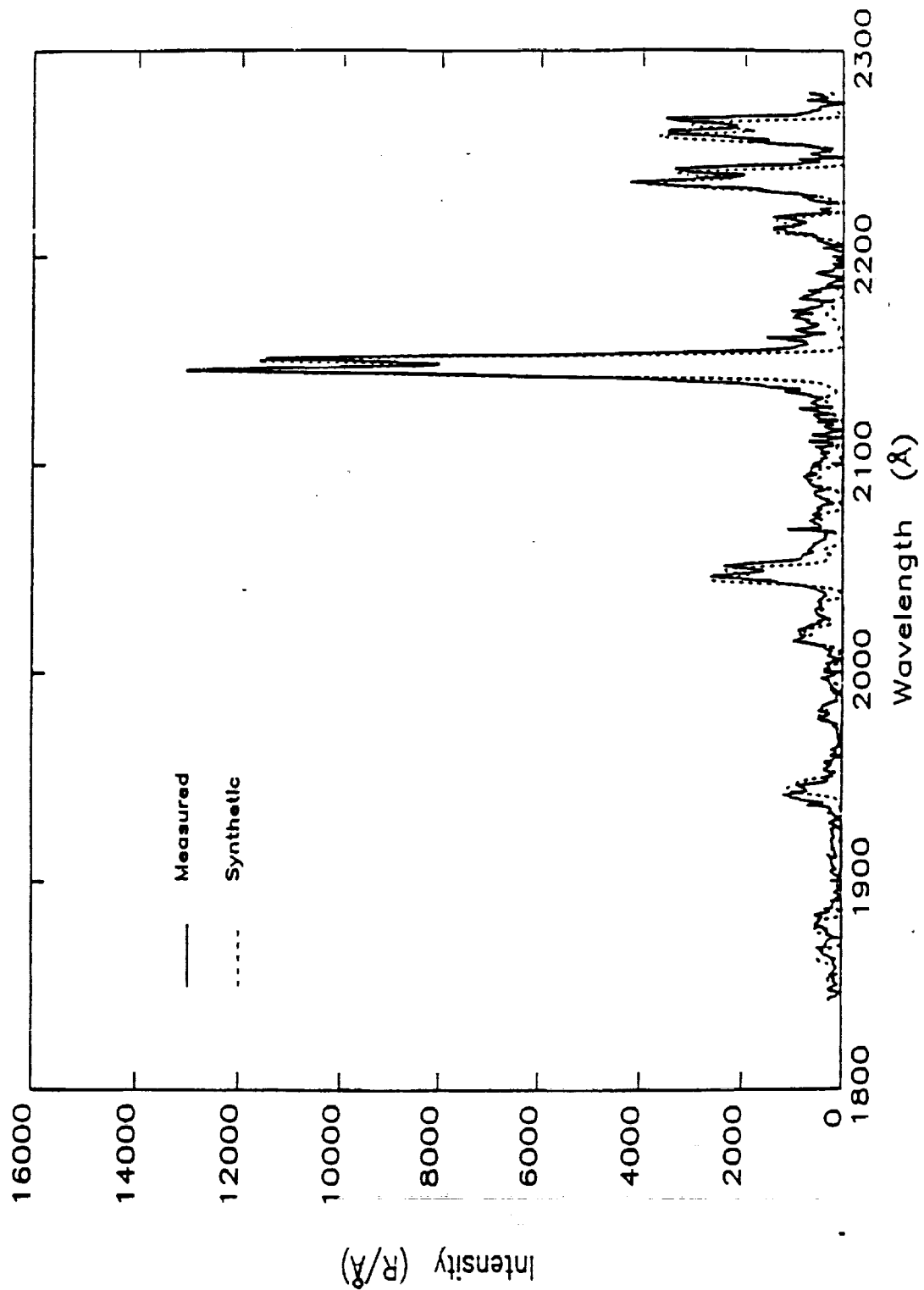
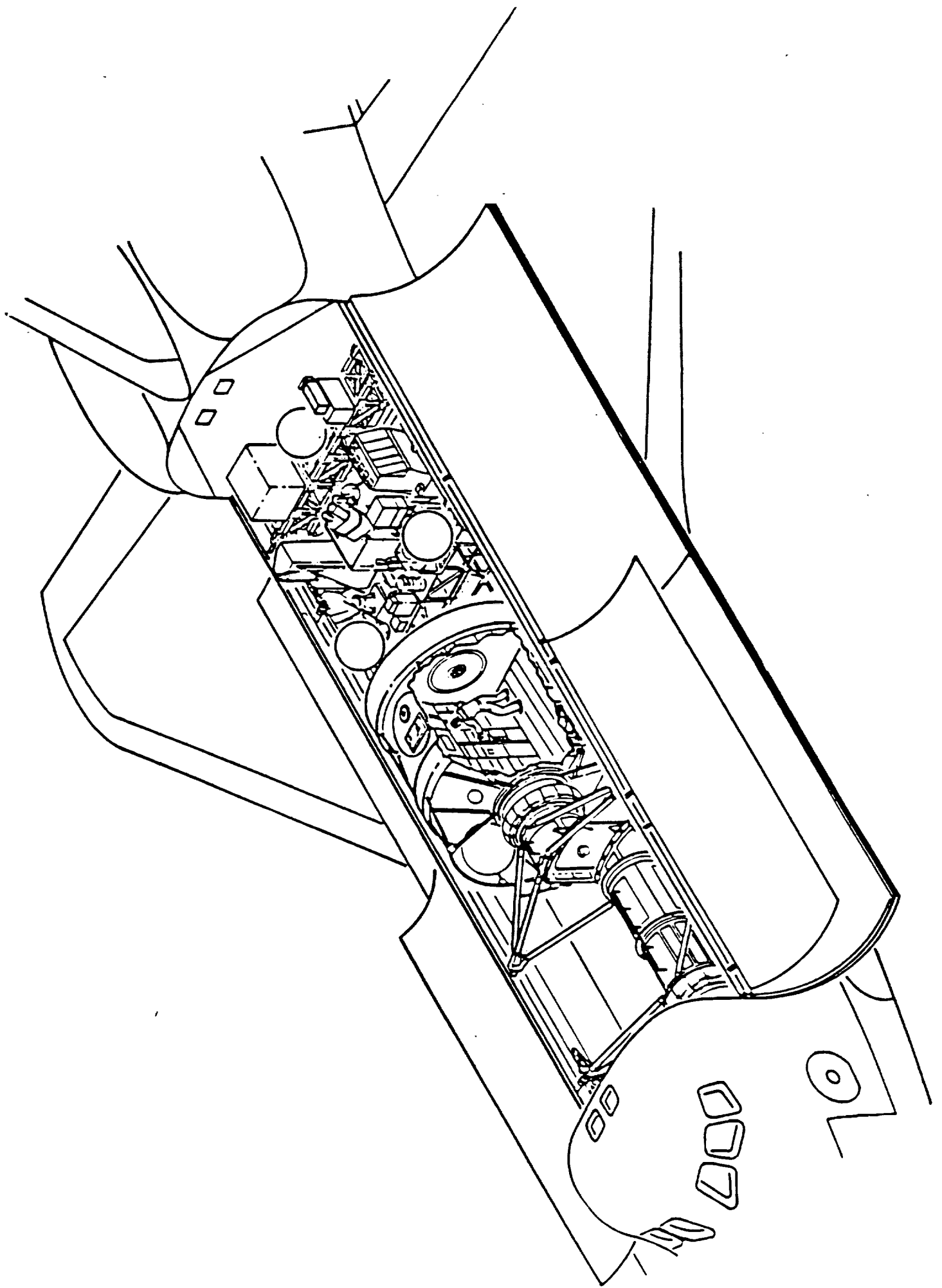


Figure 5-4 Comparison of Data and Synthetic Fit at 96 km



**S3-4:**

VERY HIGHLY CLASSIFIED MISSION

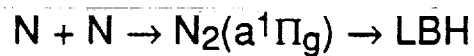
NO INFORMATION ON S/C OR INSTRUMENT GEOMETRIES

**OPINIONS:**

BOB HUFFMAN: CANT RULE OUT RAM SOURCES

BOB CONWAY: CANT RULE OUT RAM SOURCES

**SIMPLEST MODEL FOR S3-4 LBH GLOW:**



**PROBLEMS:**

1. WHERE DOES THE N COME FROM
2. WHAT ABOUT THE VIBRATIONAL DISTRIBUTION

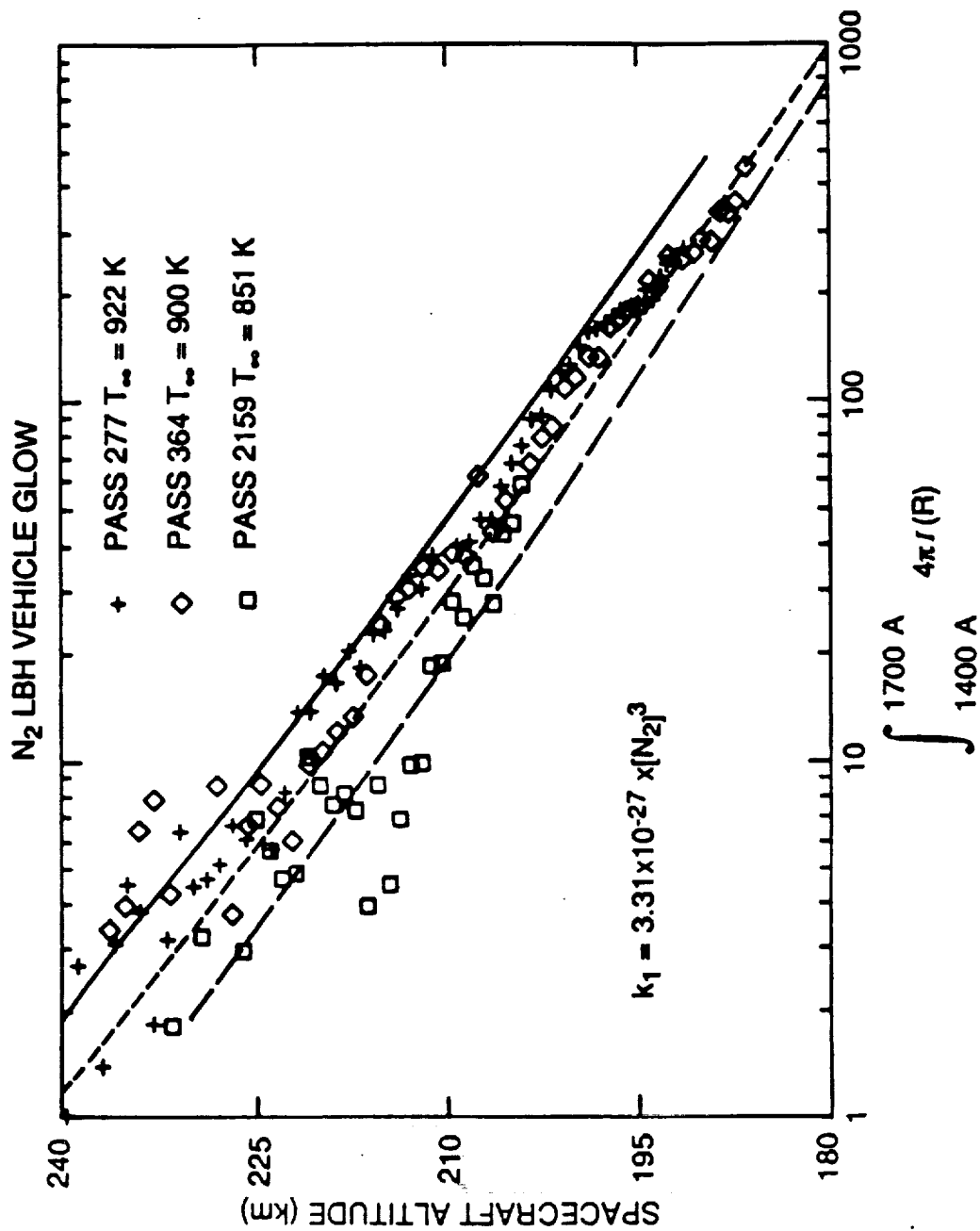


Figure 3: Observations of the N<sub>2</sub> LBH glow reported by Conway et al. (1987) for the S3-4 spacecraft.

## SOURCES OF N:

AMBIENT ALONE IS INSUFFICIENT

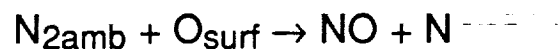
### SWENSON AND MEYEROTT

#### 1. GAS PHASE SOURCE



RAM VELOCITY  $\rightarrow$  EXOTHERMICITY

#### 2. SURFACE VERSION OF 1 RIDEAL REACTIONS



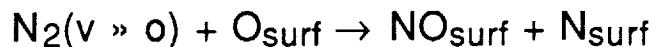
RAM VELOCITY  $\rightarrow$  EXOTHERMICITY

### TORR



VIBRATIONAL ENERGY  $\rightarrow$  EXOTHERMICITY

$\Rightarrow$  LANGMUIR - HINSHELWOOD REACTION





## **GLOW CHARACTERISTICS TO BE EXPLAINED:**

1. INTENSITY
2. SPECTRAL CHARACTER
3. VIBRATIONAL DISTRIBUTION
4. ALTITUDE DEPENDENCE
5. ANGULAR DEPENDENCE

## **SURFACE GLOWS:**

1. ALTITUDE DEPENDENCE DEPENDS ON DETAILS  
OF PROCESSES THAT OCCUR  
SCALE HEIGHT FOR SOURCE OF N ( $Q(N)$ )

## **RIDEAL REACTIONS:**

$$Q(N) \propto [O][N_2] \quad (\text{ambient})$$

## **LOSS OF N:**

ASSUME DESORPTION AND RECOMBINATION

$$L(N) = J_1 N_{\text{surf}} + k_1 [N_{\text{surf}}] [N_{\text{surf}}]$$

IF DESORPTION » RECOMBINATION

$$L(N) = J_1 N_{\text{surf}}$$

$J_1$  = DESORPTION FREQUENCY

**IN STEADY STATE:**

PRODUCTION = LOSS

$$Q(N) = L(N)$$

$$k_2 [O][N_2] = J_1 [N_{\text{surf}}]$$

$$[N_{\text{surf}}] = \frac{k_2}{J_1} [O][N_2]$$

N RECOMBINATION RATE  $\propto [N]^2 [O]^2$

$$Q(N_2)^* \propto [O]^2 [N_2]^2$$

$I_{\text{LBH}} \propto [O]^2 [N_2]^2$
--

DOES NOT MATCH S3-4 OBSERVATIONS

## LANGMUIR - HINSHELWOOD REACTION



$$Q(\text{N}) = k_2[\text{N}_2(\nu)_{\text{surf}}] - [\text{O}]_{\text{surf}}$$

$\text{N}_2(\nu)_{\text{surf}}$

$$Q(\text{N}_2(\nu)) = L(\text{N}_2(\nu))$$

RAM FLUX SOURCE = DESORPTION + DESTRUCTION BY  $\text{O}_{\text{surf}}$

$$\varepsilon_1 F(\text{N}_2) = (k_3[\text{O}_{\text{surf}}] + J_2) [\text{N}_2(\nu)_{\text{surf}}]$$

IF DESORPTION DOMINATES

$$[\text{N}_2(\nu)_{\text{surf}}] = \frac{\varepsilon_1(\text{N}_2)}{J_1} \propto [\text{N}_2]$$

$[\text{N}_2(\nu)_{\text{surf}}] \propto [\text{N}_2]$
--

$O_{surf}$ :

SOURCE



ASSUME

$O_{surf} - O_{surf}$  Recombination is  
the major loss process



$$Q(O_{surf}) = L(O_{surf})$$

$$\varepsilon_2 F(O) = k_4 [O_{surf}]^2$$

$$[O_{surf}] = \left[ \frac{\varepsilon_2}{k_4} F(O) \right]^{1/2}$$

$$[O_{surf}] \propto [O]^{1/2}$$

RECALL

$$Q(N) \propto [N_{2\text{surf}}] [O_{\text{surf}}]$$

$$\propto [N_2][O]^{1/2}$$

$$Q(N) = J_2[N]$$

$$[N] = \frac{Q(N)}{J_2}$$

$$N_2^* \propto [N]^2 \propto \left(\frac{Q}{J_2}\right)^2$$

$$N_2^* \propto N_2^2 [O]$$

MATCHES S3-4 OBSERVATIONS

SUGGESTS THE LANGMUIR-HINSHELWOOD PROCESS

IS THE MORE LIKELY CANDIDATE TO EXPLAIN

S3-4 GLOW

## SUMMARY OF MODEL RESULTS FOR S3-4

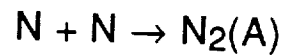
1. INTENSITY:  $\sim 10^{-6}$  INCIDENT AMBIENT FLUX
2. SPECTRAL CHARACTER: PURE LBH  
 $\sim 100\%$   
(IF  $N + N \rightarrow N_2(a^1\Pi_g)$ )
3. VIBRATIONAL DISTRIBUTION: SURFACE RELAXATION
4. ALTITUDE DEPENDENCE:  $[N_2]^2[O]$
5. ANGULAR DEPENDENCE: NOT MEASURED

## SHUTTLE FUV GLOW MODEL

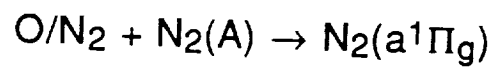
MUST BE A VOLUME GLOW

THEREFORE SOURCE IS GAS PHASE

HYPOTHESIS:



$\text{N}_2(\text{A})$  DESORBS INTO GAS CLOUD



$\Rightarrow$  LBH

AND



$\Rightarrow$  VK

NOTE: THE ELECTRONIC PRODUCTS OF SURFACE N-N  
RECOMBINATION DEPEND~~8~~ CRITICALLY ON THE  
SURFACE CATALYST

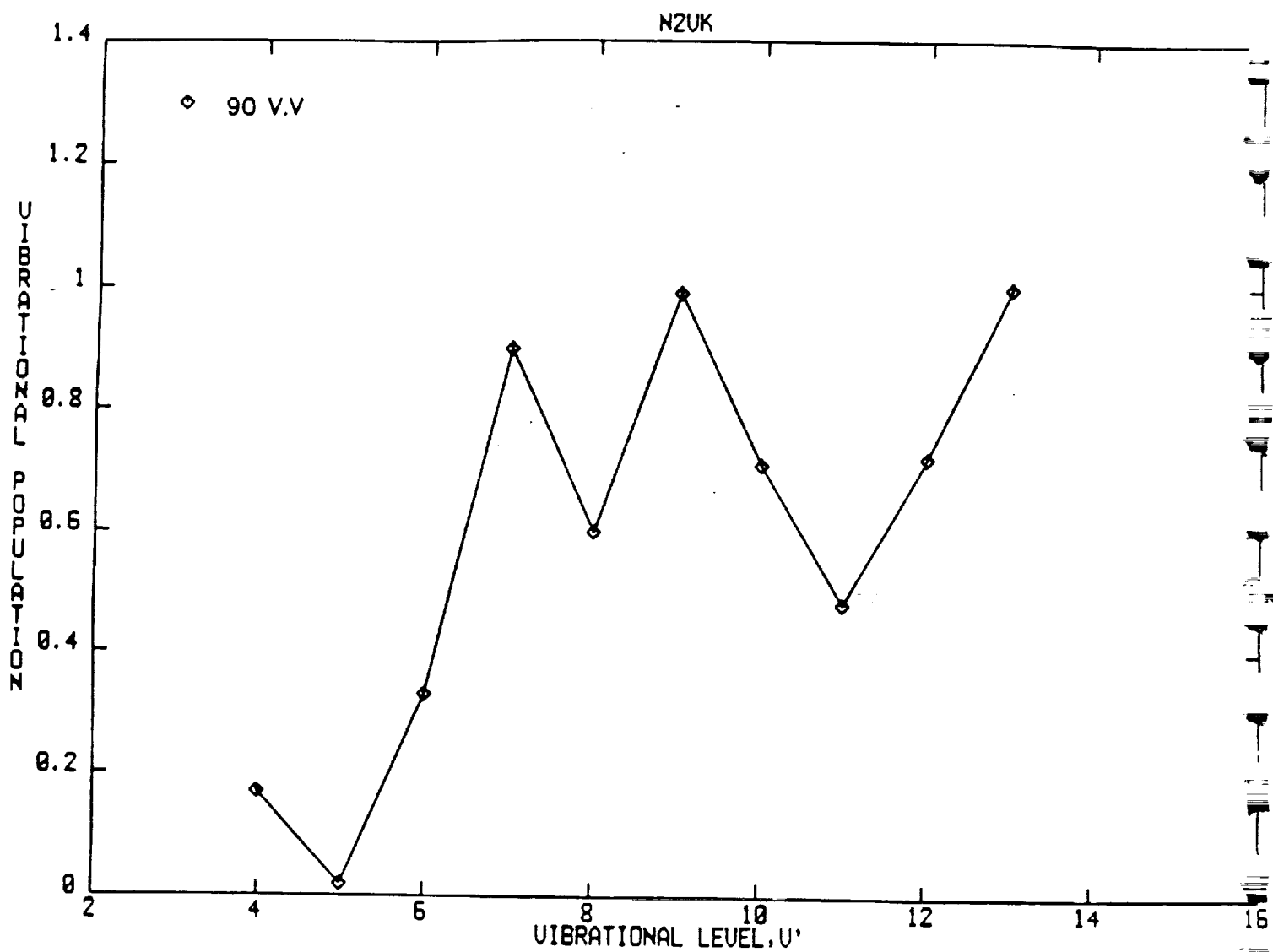


Figure 8: The  $N_2(A^3\Sigma_u^+)$  vibrational distribution required to produce the synthetic spectral fit shown in Figure 4. The results are normalized to unity at the peak value.



## LBH GLOW

LBH VOLUME EMISSION RATE:

$$\eta_{LBH} = (\sigma_{N_2} F(N_2) + \sigma_O F(O)) [N_2(A)]$$

WHERE THE  $N_2(A)$  DISTRIBUTION IN THE GAS CLOUD  
IS GIVEN BY

$$[N_2(A)] = [N_2(A)_{surf}] \frac{G_{surf}}{G} e^{-\tau'}$$

$G_{surf}/G$  CHARACTERIZES RADICAL OUTFLOW EFFECTS

$\tau' \Rightarrow$  COLLISIONAL ATTENUATION

- INFLOWING  $N_2$  AND O TO SURFACE
- OUTFLOWING  $N_2(A)$

$$\Rightarrow \eta_{LBH} = \sigma F[N_2(A)_{surf}] e^{-\tau}$$

WHERE

$$\tau = \tau' + \tau''$$

$\tau'' \Rightarrow$  COLLISIONAL ATTENUATION OF O AND  $N_2$

PRIOR TO EXCITATION OF  $N_2(A)$  TO  $N_2(a)$

FINALLY THE LBH INTENSITY IS FOUND

$$I_{LBH} = (\eta_{LBH,surf}) G_{surf} \int_{surf}^{\infty} \frac{e^{-\tau}}{G} ds$$

WHICH YIELDS FOR N<sub>2</sub> COLLISIONS

1) FOR NO ATTENUATION

$$I_{LBH} \propto [N_2]^3 [O] \text{ AT } \sim 400 \text{ km}$$

2) MODERATE ATTENUATION BETWEEN 200 - 240 km

$$I_{LBH} \propto \sim [N_2]^3$$

3) INCREASED ATTENUATION BETWEEN 160 - 180 km

$$I_{LBH} \propto \sim [N_2]^2 [O]$$

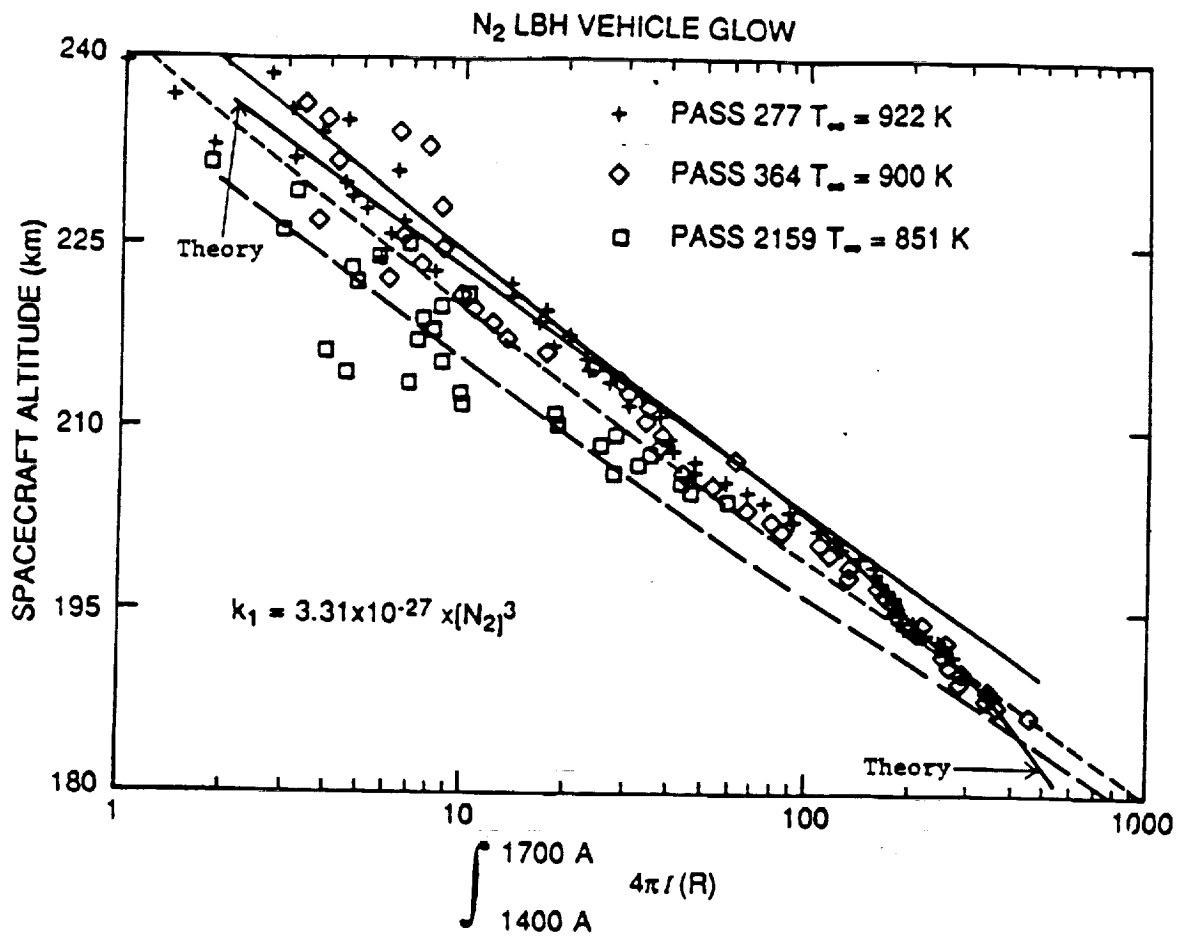
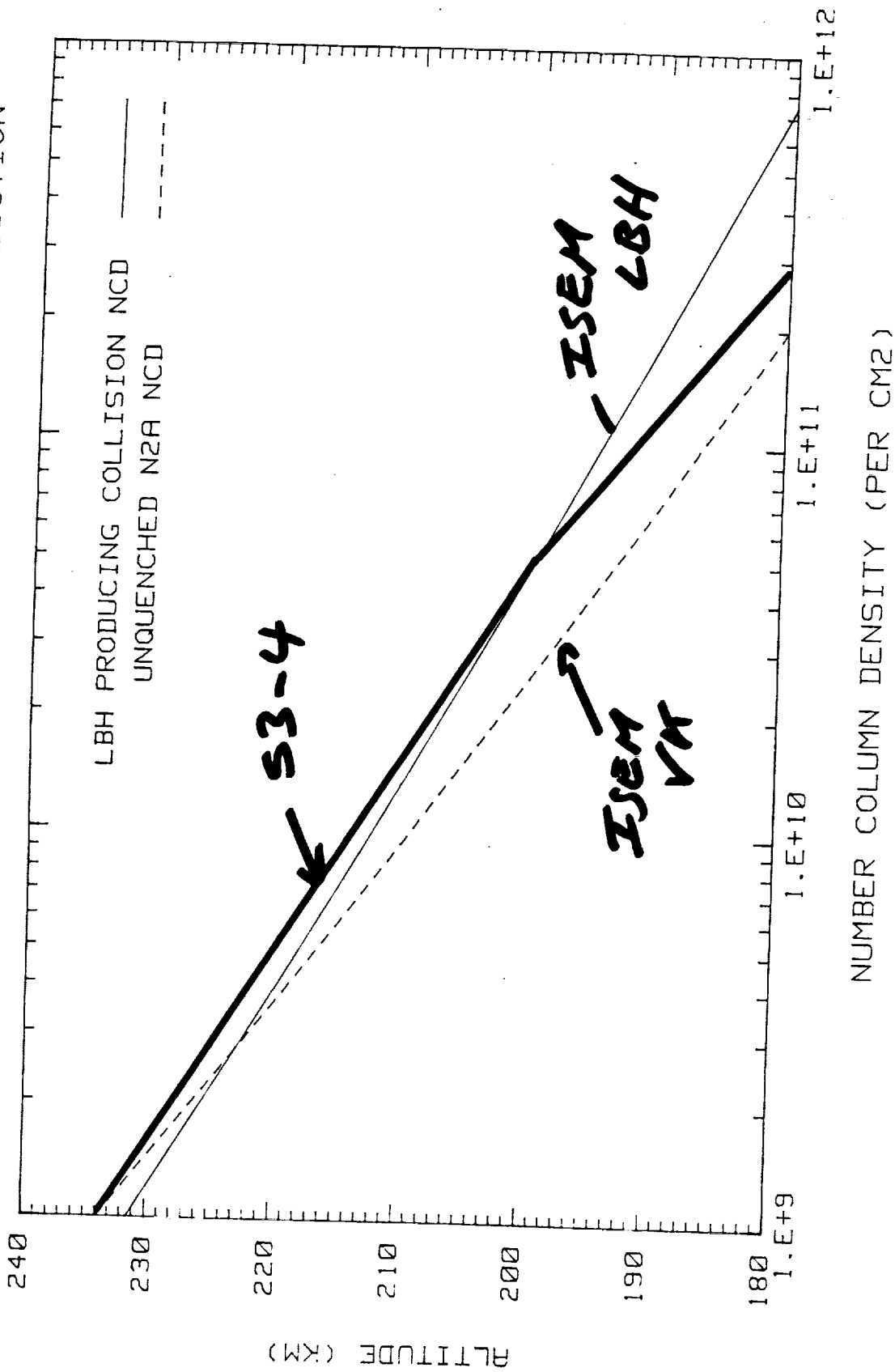


Figure 11: Comparison of estimated theoretical intensities based on the model results given Section 3.1.3.4 with the S3-4 observations of LBH glow as a function of altitude.

# NUMBER COLUMN DENSITIES FOR LBH AND VK PRODUCTION



## ANGULAR DEPENDENCE OF THE SHUTTLE FUV GLOW

$$I \propto I_0 e^{-\tau(\theta)}$$

WHERE  $\theta$  = ANGLE WITH RESPECT TO RAM

$$\tau(90^\circ) \approx 0.1 \tau(\text{ram})$$

$$e^{-\tau(\text{RAM})} \gg e^{-\tau(90^\circ)}$$

$$\frac{I(\text{RAM})}{I(90^\circ)} = \text{EXP} [-(\tau(\text{RAM}) - \tau(90^\circ))]$$

$$\approx \text{EXP} (-\tau(\text{RAM}))$$

$$\text{ISEM} \Rightarrow \tau(\text{RAM}) \approx 1.2$$

$$\Rightarrow \frac{I(\text{RAM})}{I(90^\circ)} \approx 1/3$$

$$\text{ISO DATA} \Rightarrow \sim 1/4$$

## SUMMARY FOR SHUTTLE GLOW MODEL

1. INTENSITY: MATCHES IF ALL PROCESSES  
ARE VERY EFFICIENT
2. SPECTRAL CHARACTER: INCLUDES LBH + VK
3. VIBRATIONAL DISTRIBUTION: NOT PREDICTED
4. ANGULAR DEPENDENCE:  $I(\text{RAM}) < I(90^\circ)$  FOR SL1  
FOR AIRPLANE MODE

# Atomic Oxygen Studies at PPPL

J.W. Cuthbertson,  
W.D. Langer, and R.W. Motley

Princeton University  
Plasma Physics Laboratory

and

J.A. Vaughn  
R.C. Linton, M.R. Carruth, A.F. Whitaker  
NASA Marshall Space Flight Center

1/29/1991

Low energy neutral beam sources are needed for laboratory study of atomic oxygen interaction with materials in Low Earth Orbit

- Degradation of surface materials
- Spacecraft glow phenomenon

Low energy neutral beams of 1–50 eV are also useful for studying a number of other processes:

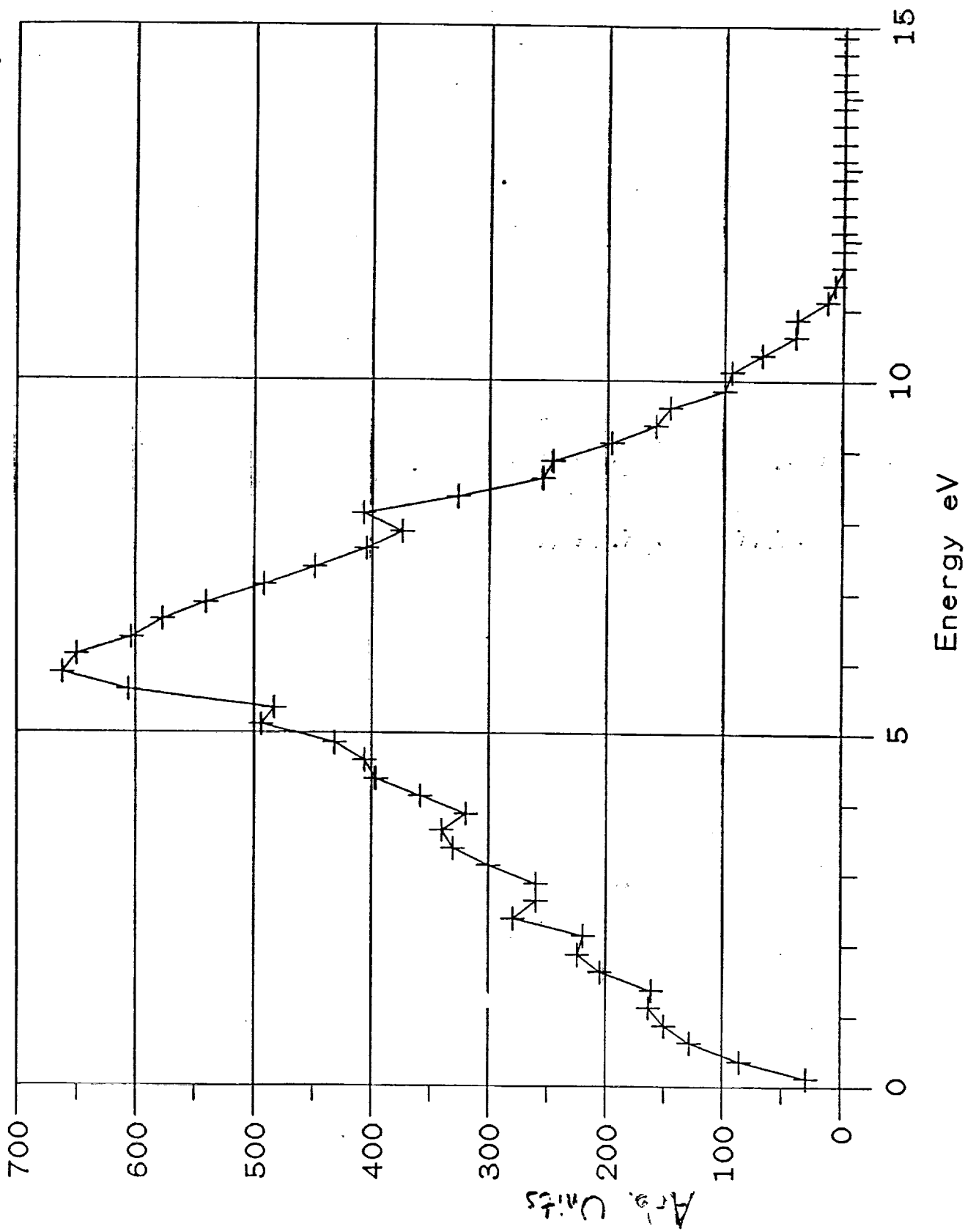
- atom-surface interactions
- atomic scattering
- gas phase “hot atom” chemical reactions
- materials modification/processing



Reflection of particles is predicted using TRIM code which follows trajectories of incident particles as they collide with atoms in the surface material. Reflection efficiency and reflected energy spectrum depend on:

- Incident energy
- Relative mass of incident and target atom
- Binding forces between atoms
- Surface roughness
- Surface impurities

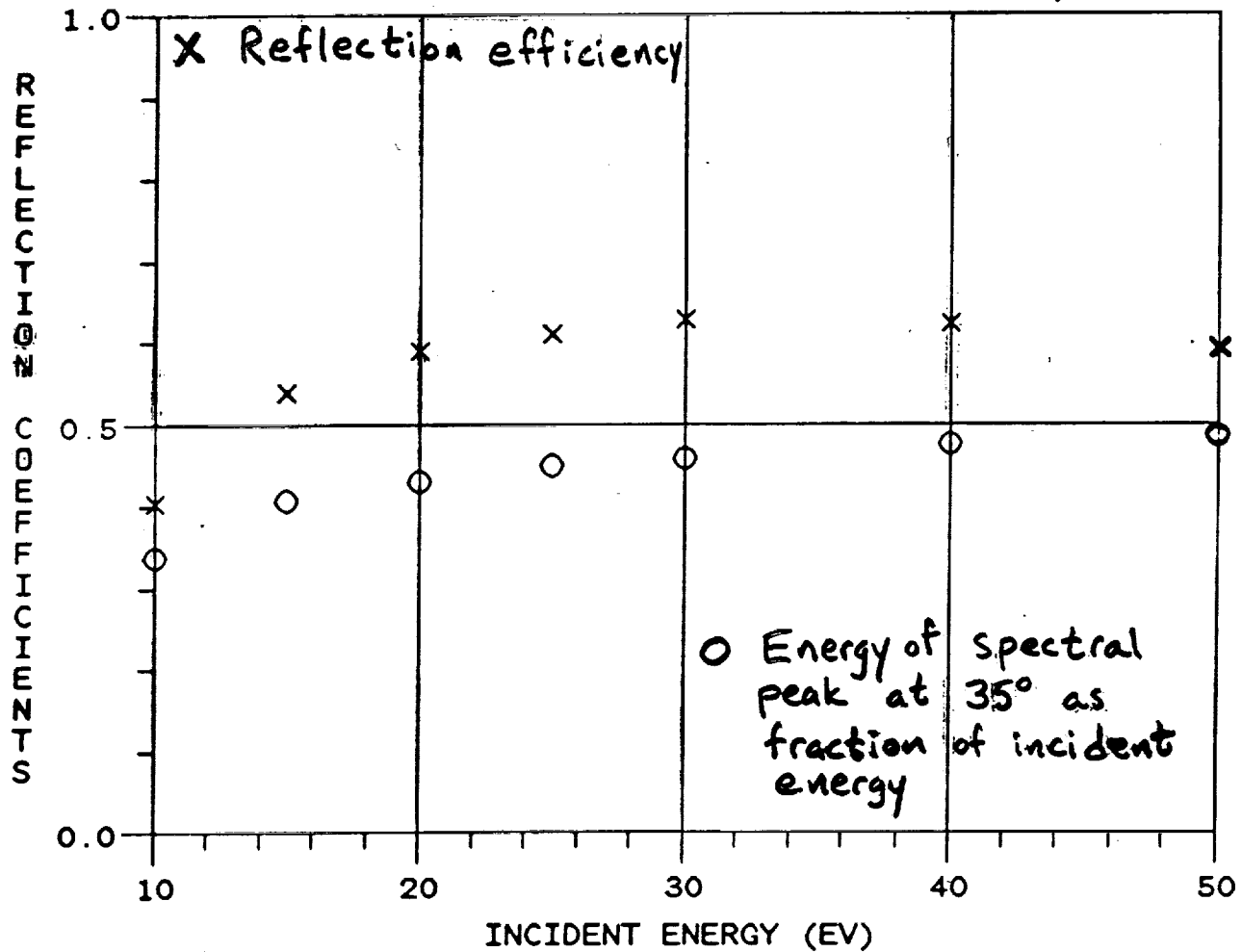
○ Predicted Reflected Spectrum for 15 eV  $O^+$  incident on Mo  
o3omo515 8-42 15. eV theta= 0.0-- 90. (All solid angles)



## General results of TRIM calculations:

- Reflection is efficient for large mass ratios
- Angular distribution of reflected neutrals is approximately  $\cos \theta$  about the normal to the surface
- Energy spectrum peaked about a characteristic fraction of incident energy
- Energy spread of a few eV

# TRIM Results for Oxygen incident on Molybdenum



## Example TRIM Results

Viewing spectrum 35° from normal

Oxygen on Molybdenum at 30 eV:

Reflection efficiency 63%

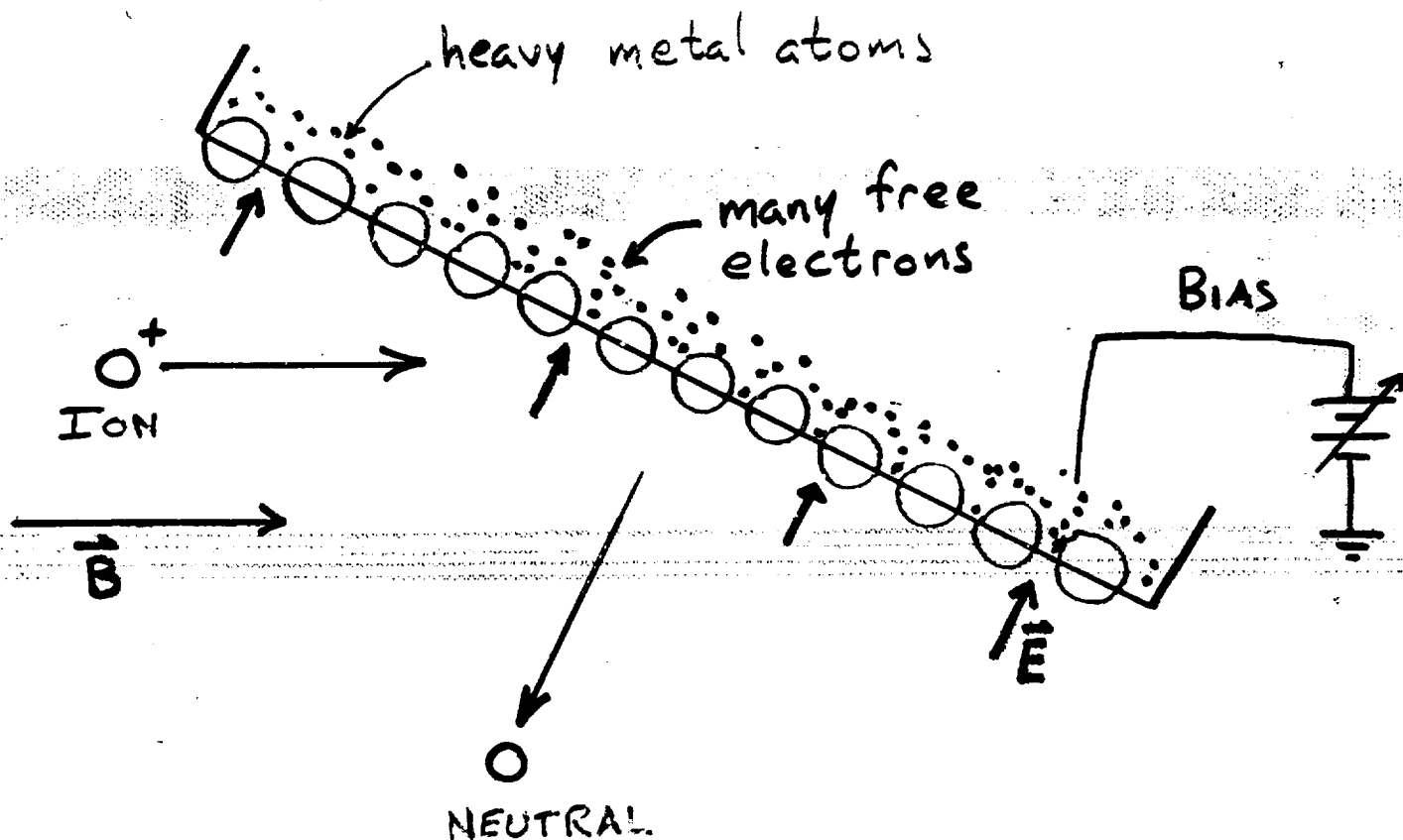
Energy spectrum peak at 13.8 eV,

$$E_{ref}/E_{inc} = 0.46$$

Compare with energy expected from single elastic scatter:

$$E_{ref}/E_{inc} = \frac{[m_1^2 + m_2^2 + 2m_1m_2\cos\theta_{CM}]}{(m_1 + m_2)^2} = 0.54$$

# Acceleration and Neutralization



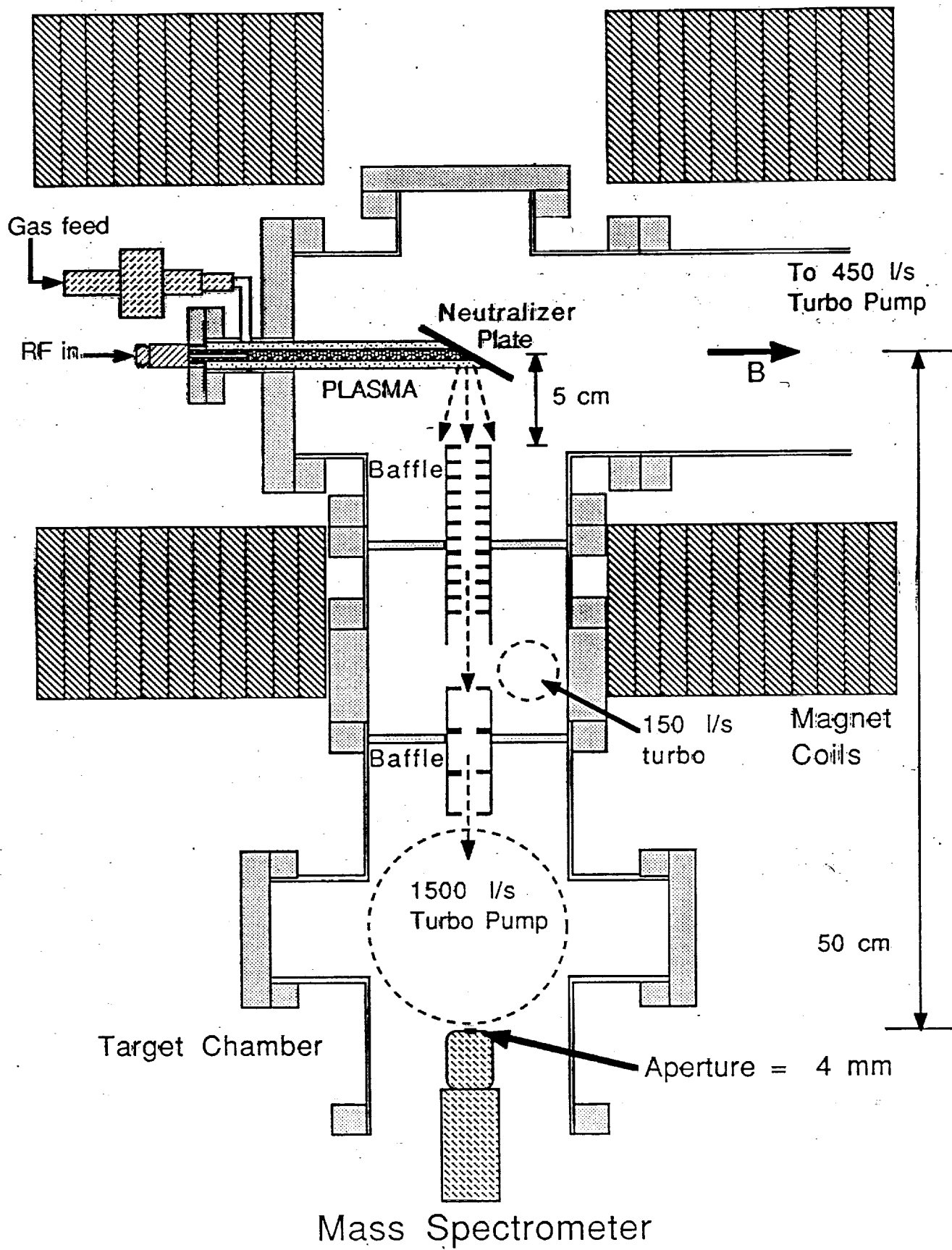
Reflection from metal surface biased negative with respect to plasma potential

- For large mass difference, most incident ions reflect as neutrals retaining large fraction of incident K.E.
- Reflected with approximately  $\cos \theta$  distribution about surface normal, forming diverging superthermal neutral beam.

The interaction of the plasma ions with the metal surface is itself a process of fundamental interest. Some of the processes which may occur are:

★ Reflection

- Adsorption
- Surface catalyzed chemical reaction
- Implantation
- Sputtering



34

## Operating Characteristics

Neutralizer can be biased from -50 to +15 V relative to ground, added to positive plasma space potential gives incident ion energies from about 10 to > 60 eV.

Sustained ion current to the plate of 4 A in  $O^+$  or  $Ar^+$ . Using predicted reflection efficiency for O this gives:

$$O \text{ flux} > 5 \times 10^{16} cm^{-2} s^{-1}$$

at usual target position about 9 cm from neutralizer.

Plasma emission spectra show virtually complete dissociation in oxygen plasma: ions are  $O^+$  rather than  $O_2^+$ . This is crucial since we desire a beam of atomic O.



## System Performance

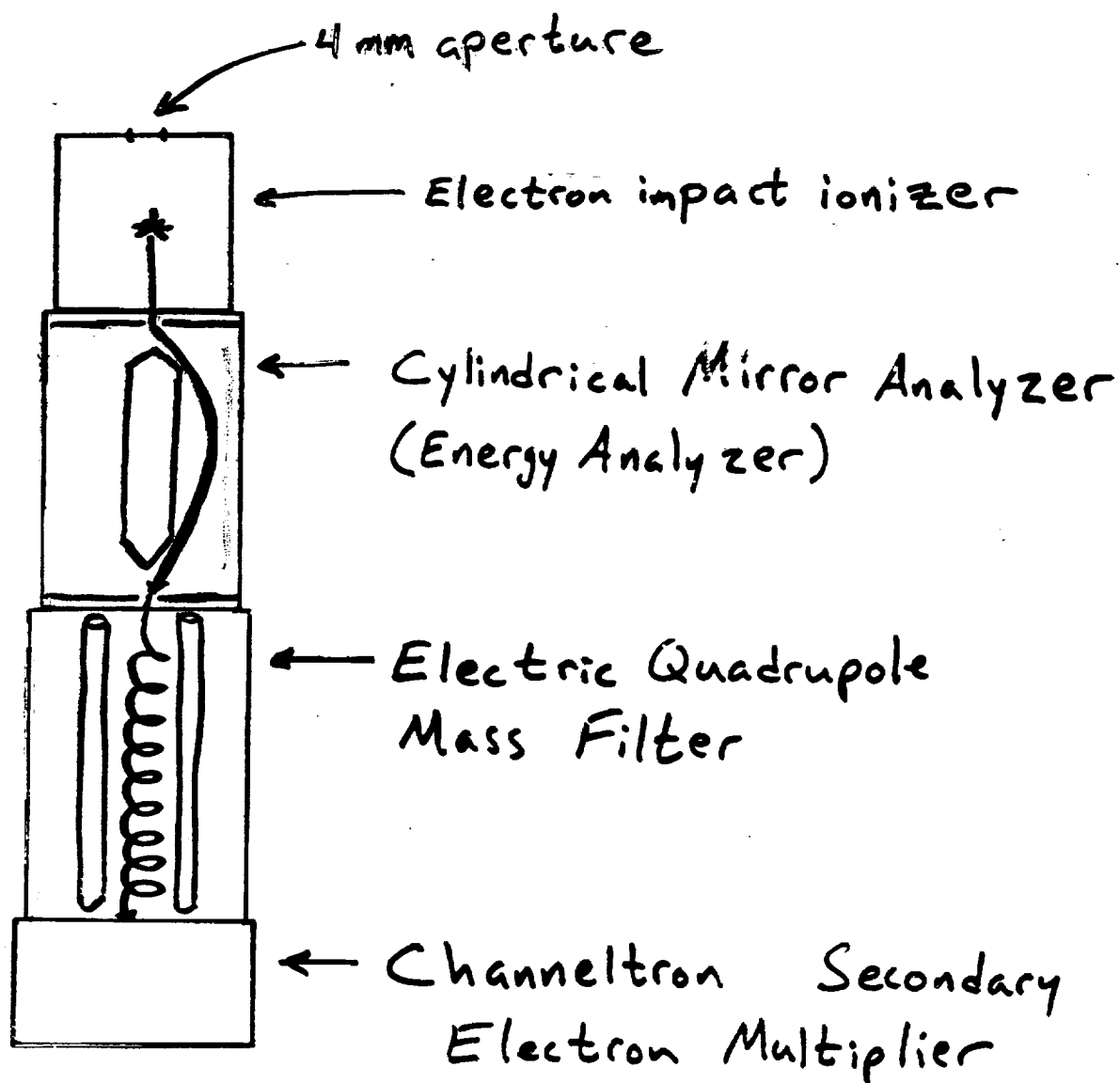
- Duty cycle of present source 10%, limited by heating of coax center conductor
- New, actively cooled Ni-plated Ti coaxial source completed and operated, with 7 A ion current at 40% duty cycle achieved so far. Plasma and beams produced by new plasma source must be characterized.
- Operation in 100% oxygen
- Stable and reliable operation over long run times
- Survival time of coax exciter  $> 100$  hours in O plasma

## Neutral Beam Measurements

Measurements of the neutral beam flux for atomic oxygen beams have been made with catalytic probes and are reported in a separate paper\*. Measurements support the theoretically expected flux levels.

Direct measurements of neutral beam energy spectra have been made using energy analyzing quadrupole mass spectrometer.

\*Vaughn et al. Paper 6-4



Schematic of VG SXP-600 Energy Analyzing  
Quadrupole Mass Spectrometer

## Beam Energy Spectrum Measurement

Ion species: Ar, Kr, Ne, O and some N

Inert species easier to analyze because:

1. Argon has high ionization cross-section
2. Heavier mass gives lower velocity
3. Molecular gases suffer interference from dissociation

Reflecting species: Mo, Ta, Au, Al, steel

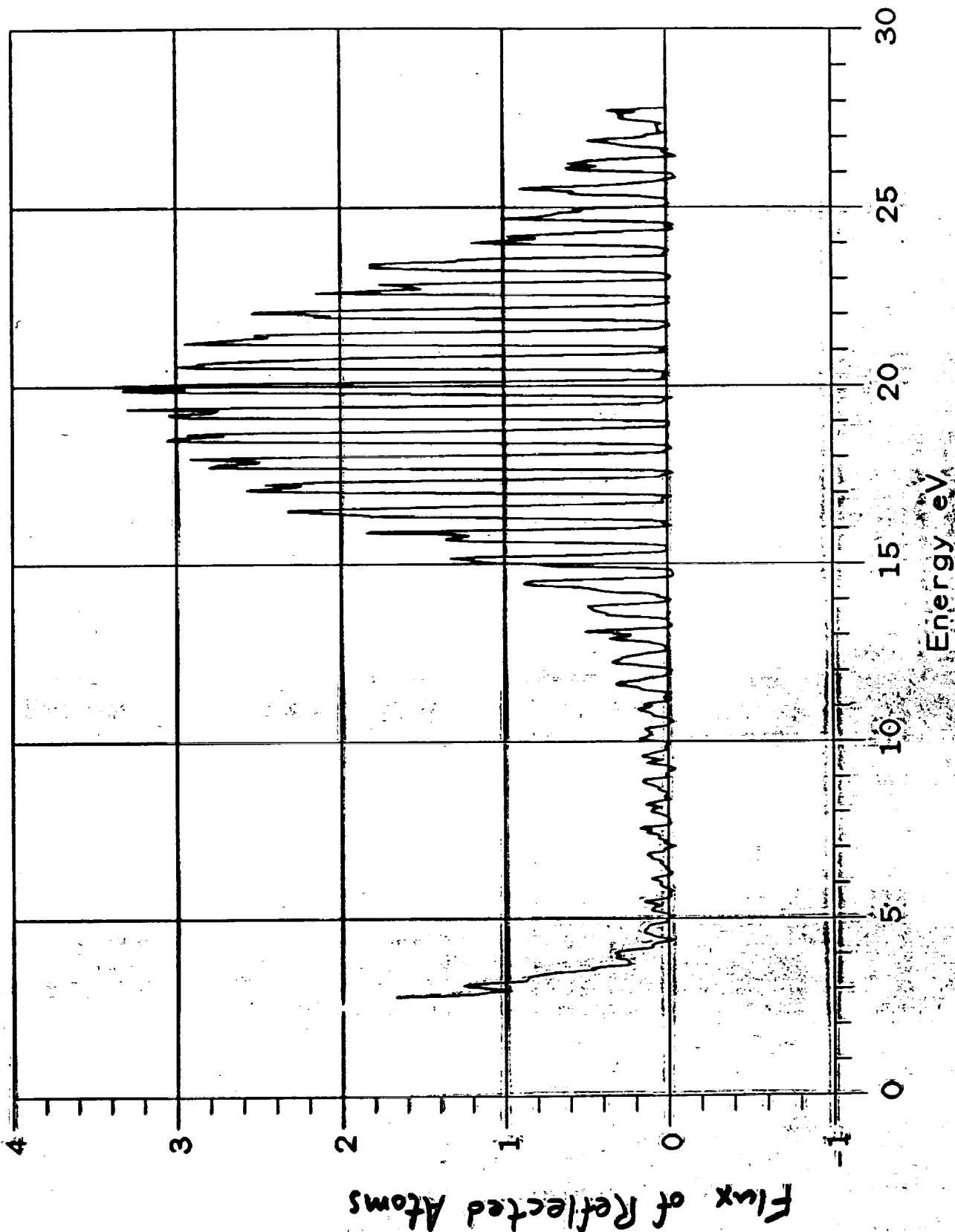
Bias voltage: -30 to + 10V, corresponding to 15 to 50 V accelerating potential

# Energy of Argon reflected from Tantalum

$\times 10^{-11}$

ar1026a.asc

# 3



ORIGINAL PAGE IS  
OF POOR QUALITY

Observed energy spectra of reflected beams exhibit the expected (relative) dependence on mass ratio, incident ion energy (i.e. bias voltage on neutralizer), and reflection angle.

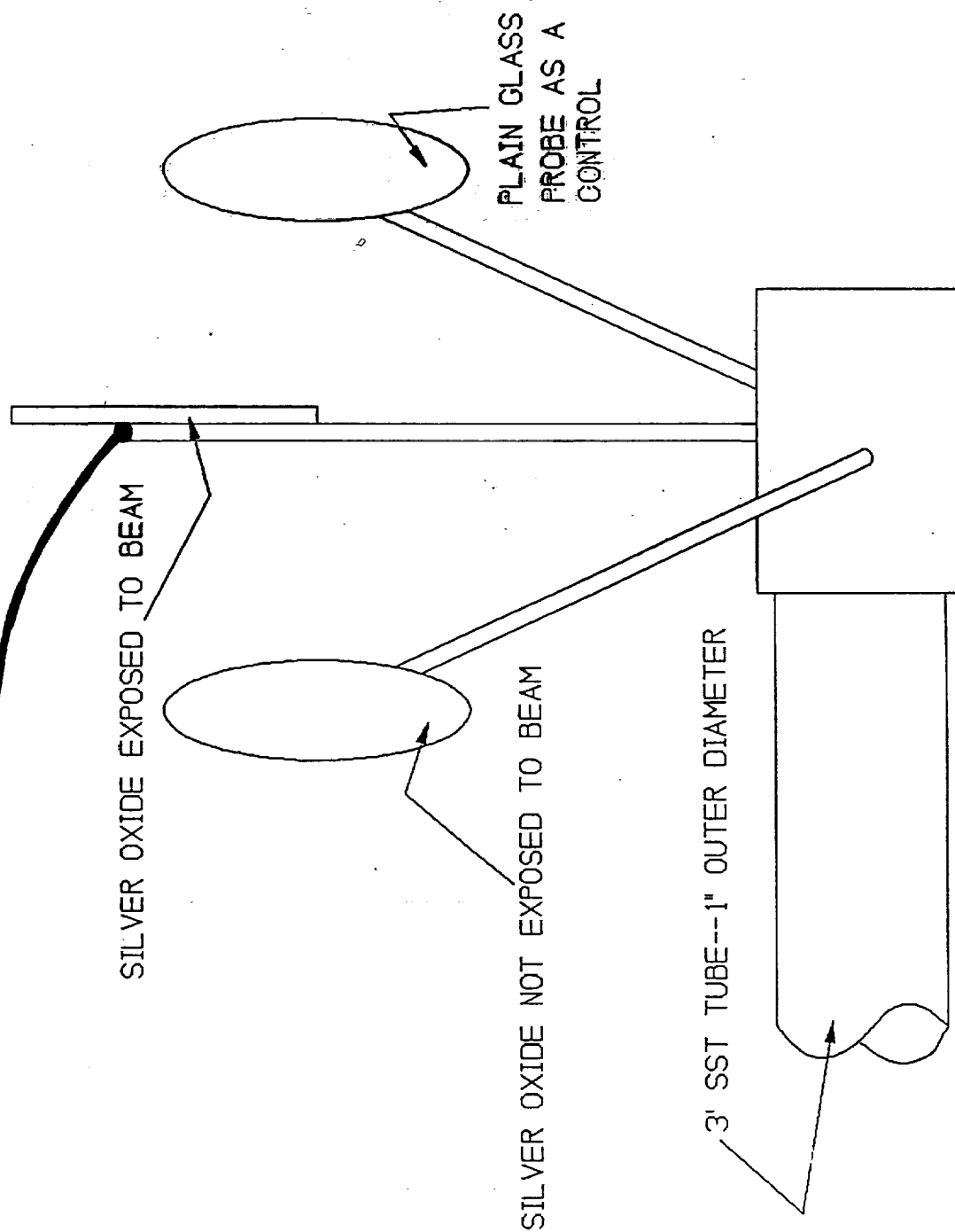
Incident ion mass: Energy of peak (as fraction of incident energy) lowest for Kr, higher for Ar, highest for Ne and O

Target atomic mass: Energy retained by reflected atoms highest for Ta, lower for Mo, steel, Al.

Incident energy: Energy peak of spectrum can be changed by changing bias voltage on neutralizer.

Reflection angle: Energy higher for atoms reflected  $65^\circ$  from normal than for  $45^\circ$ .

# Thermocouple



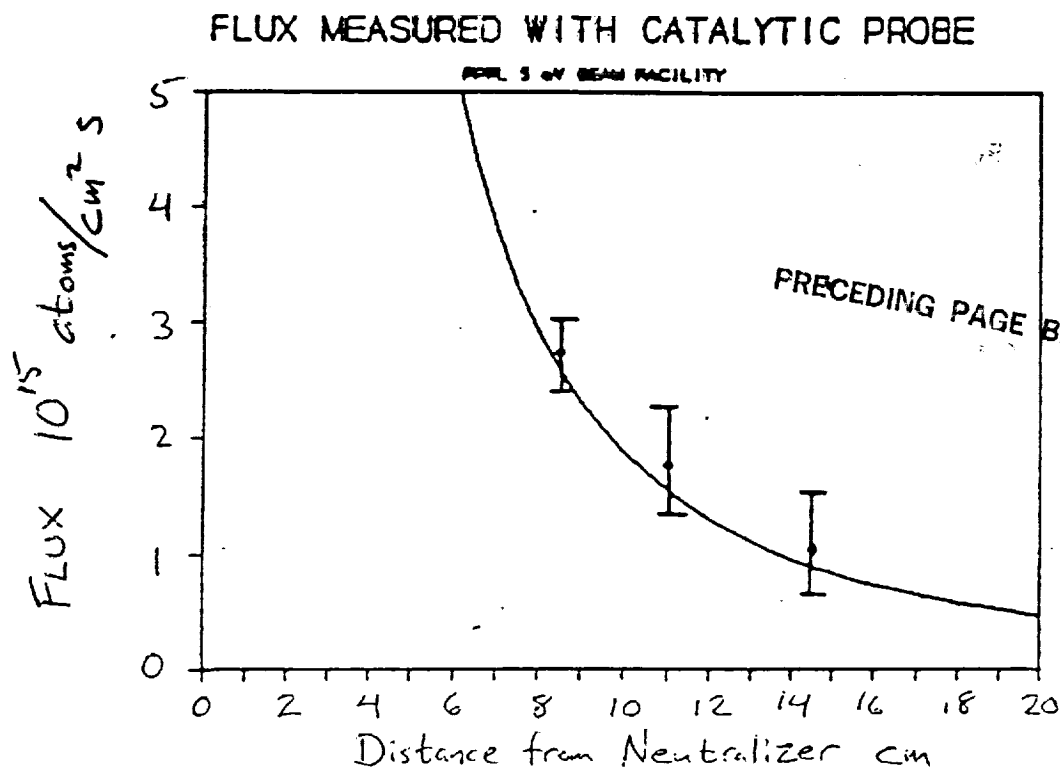
## Catalytic Probe

Recombination of oxygen atoms on surface of silver oxide catalyst (5.2 eV per molecule) causes temperature of probe to increase. Non-catalytic (glass) control probe used to account for heating of probe by inelastic impacts of the beam atoms and radiation from plasma.

$$\text{flux} = \frac{1.4 \times 10^7}{n} [e_p(T_p^4 - T_w^4) - e_g(T_g^4 - T_w^4)] \text{cm}^{-2} \text{s}^{-1}$$

$e$  = relative emissivity

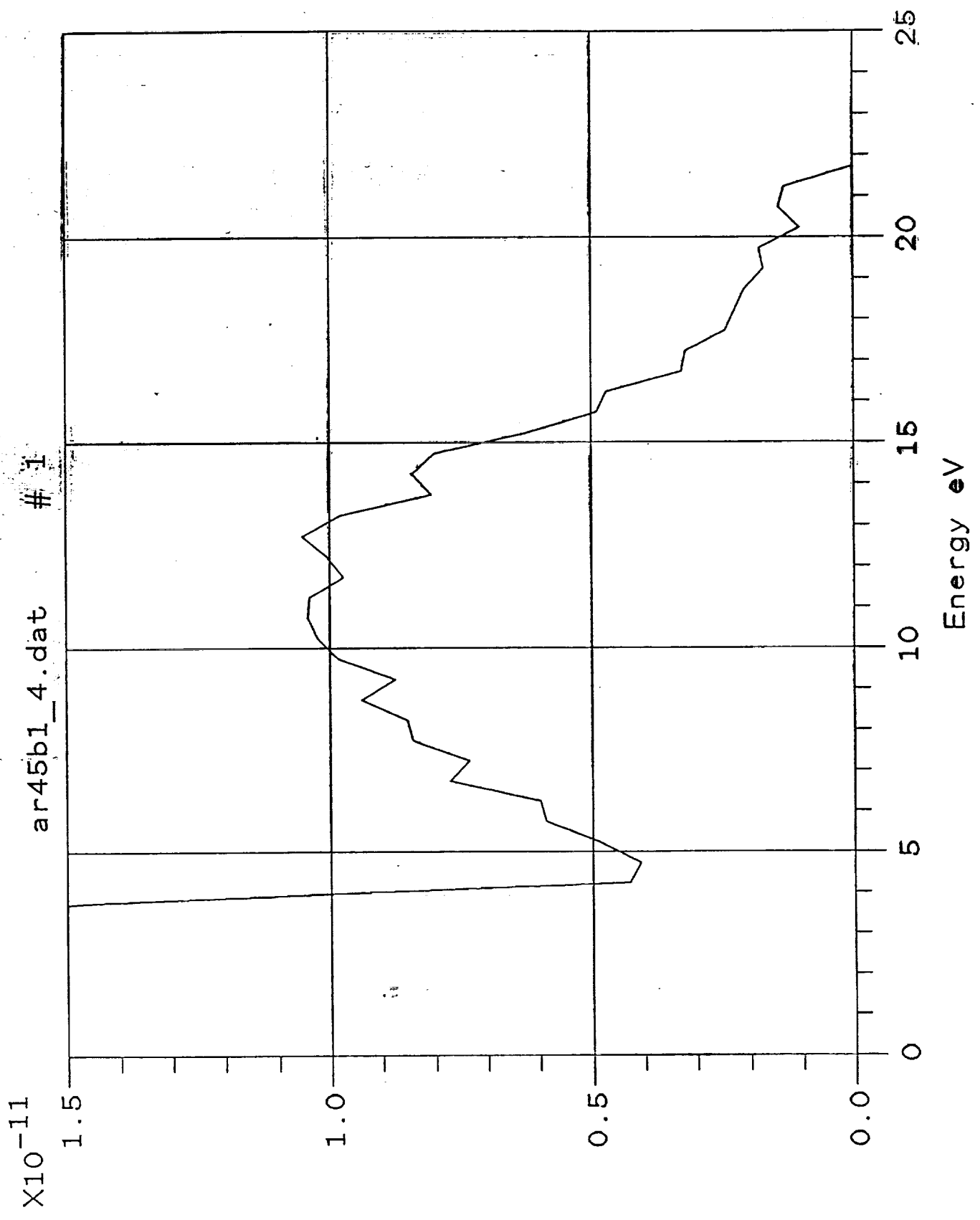
where  $n$  is recombination coefficient,  $n \approx 0.5$ .





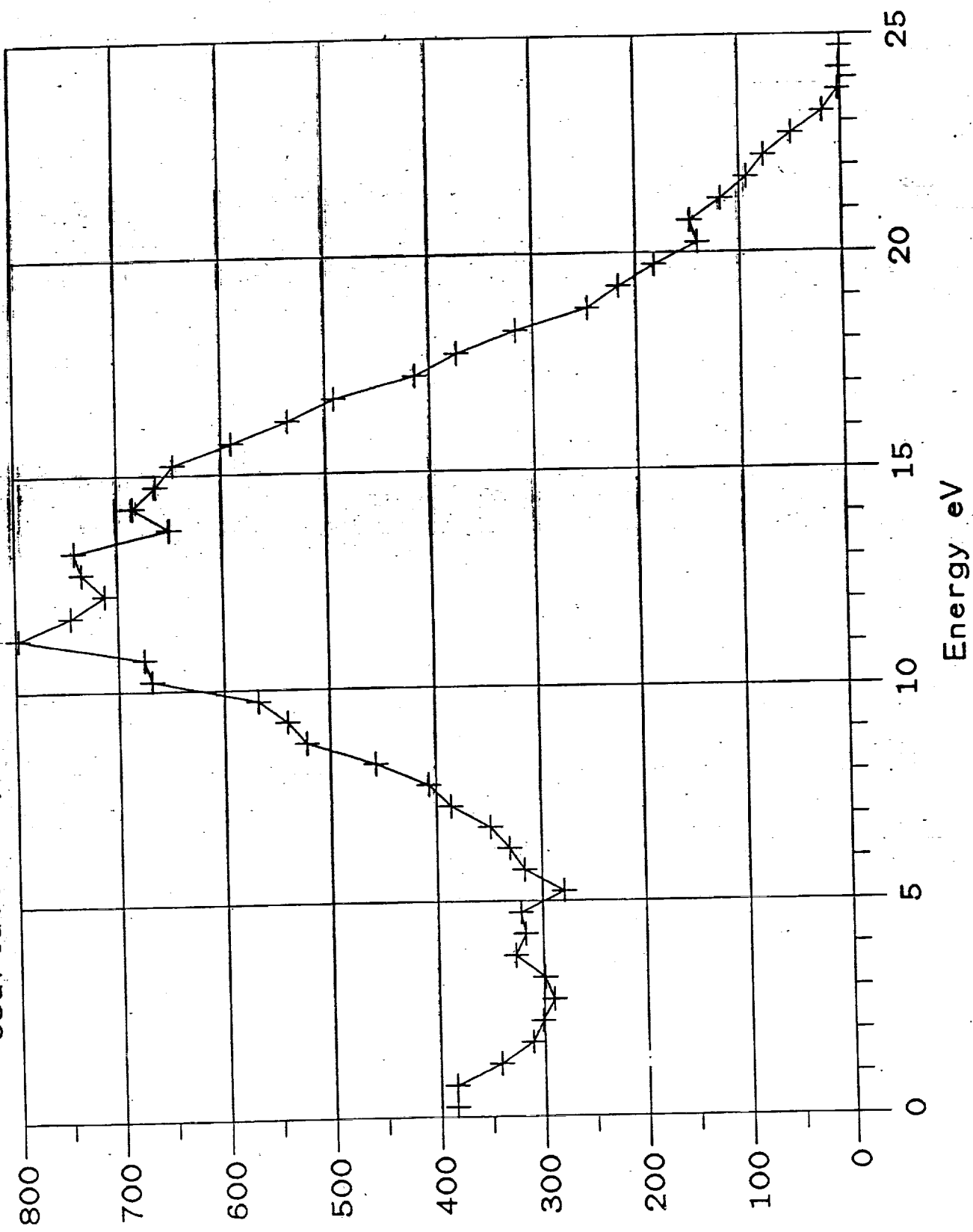
$\Delta V \approx 32$

Argon on Ta

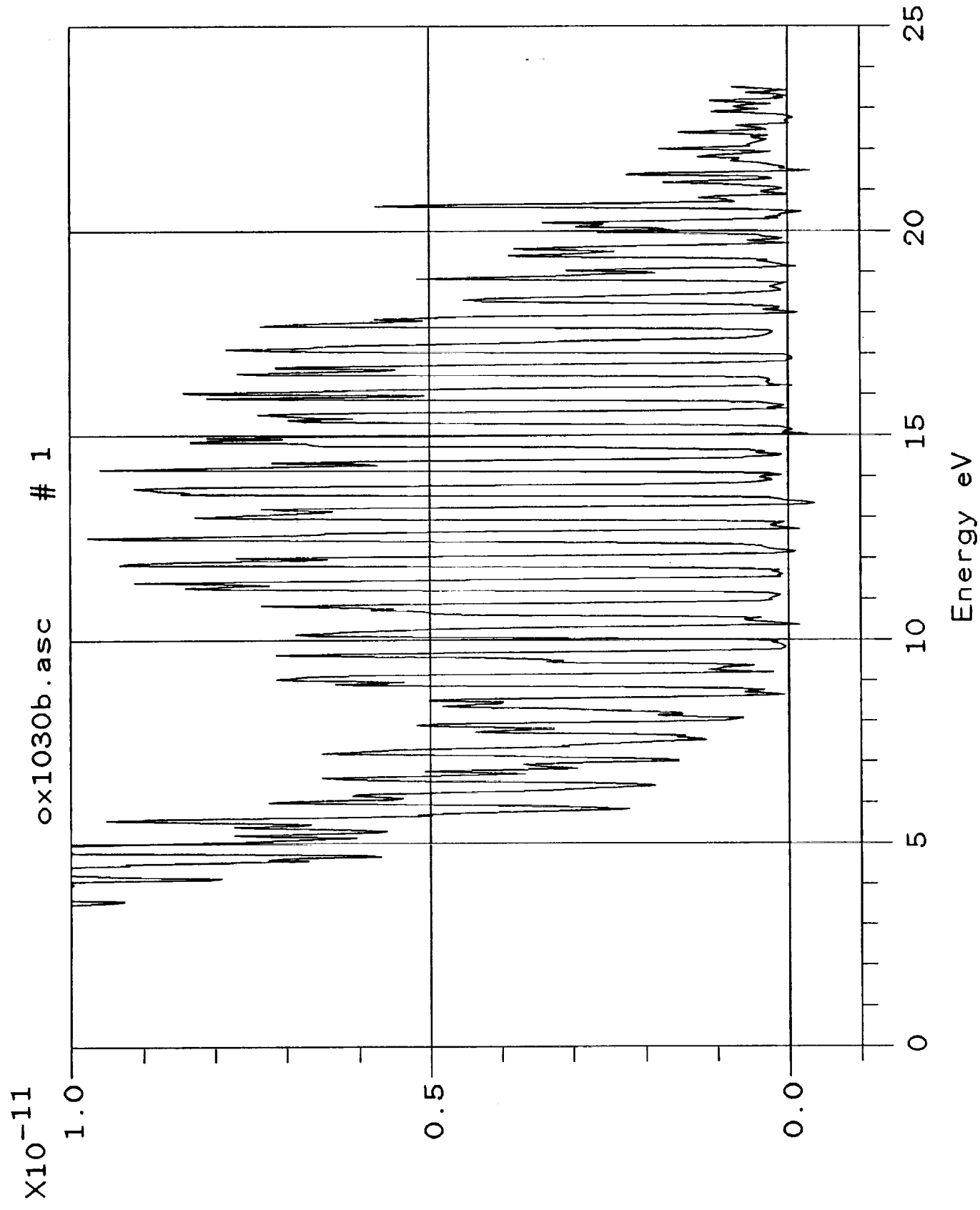


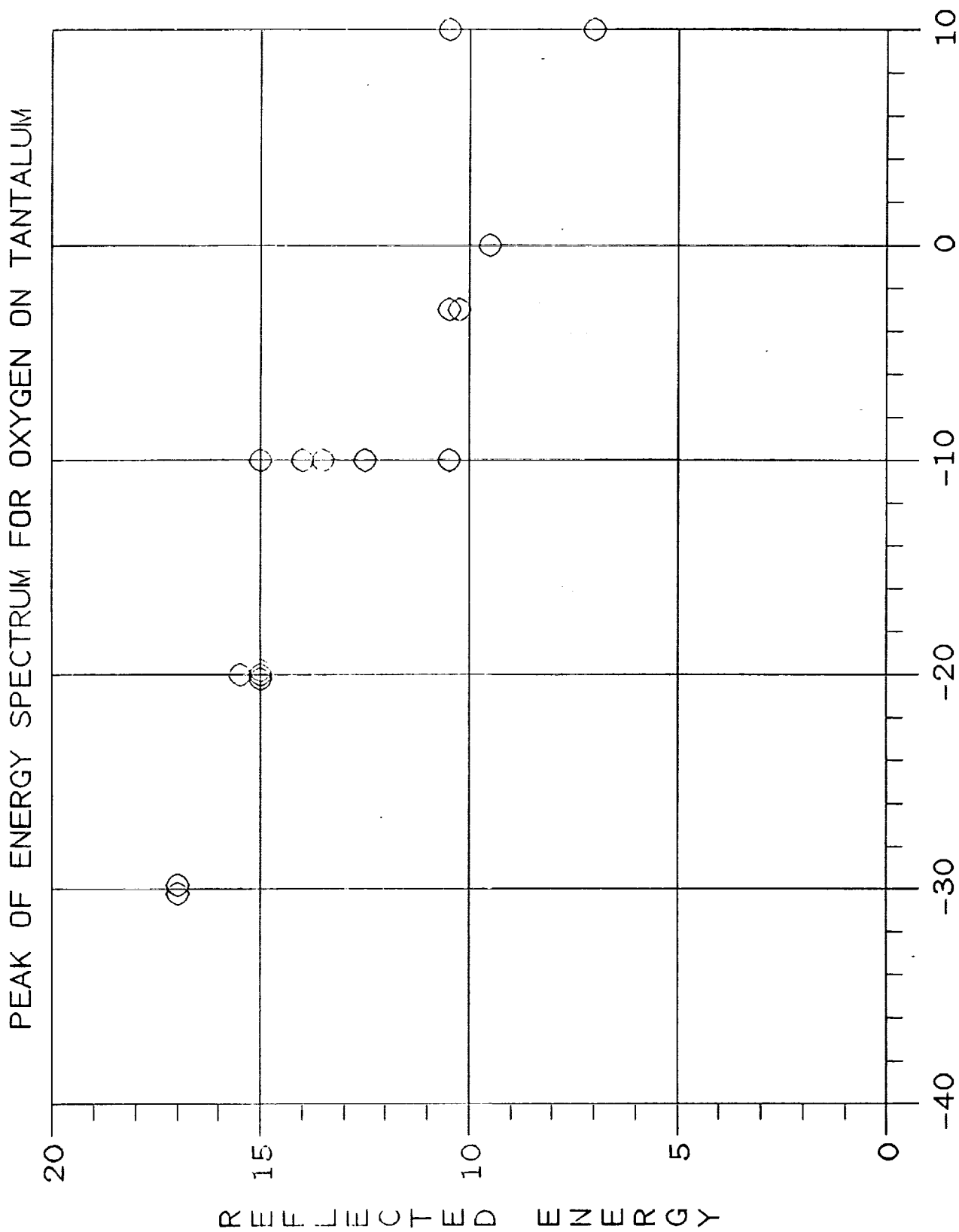
# TRIM Predicted Spectrum for Argon on Lanthanum at 30 eV

o3arta05 18->73 eV theta= 0.0-- 90. (all solid angles)



Oxygen, reflected from  $\alpha$   $\Delta V \approx 40^\circ$

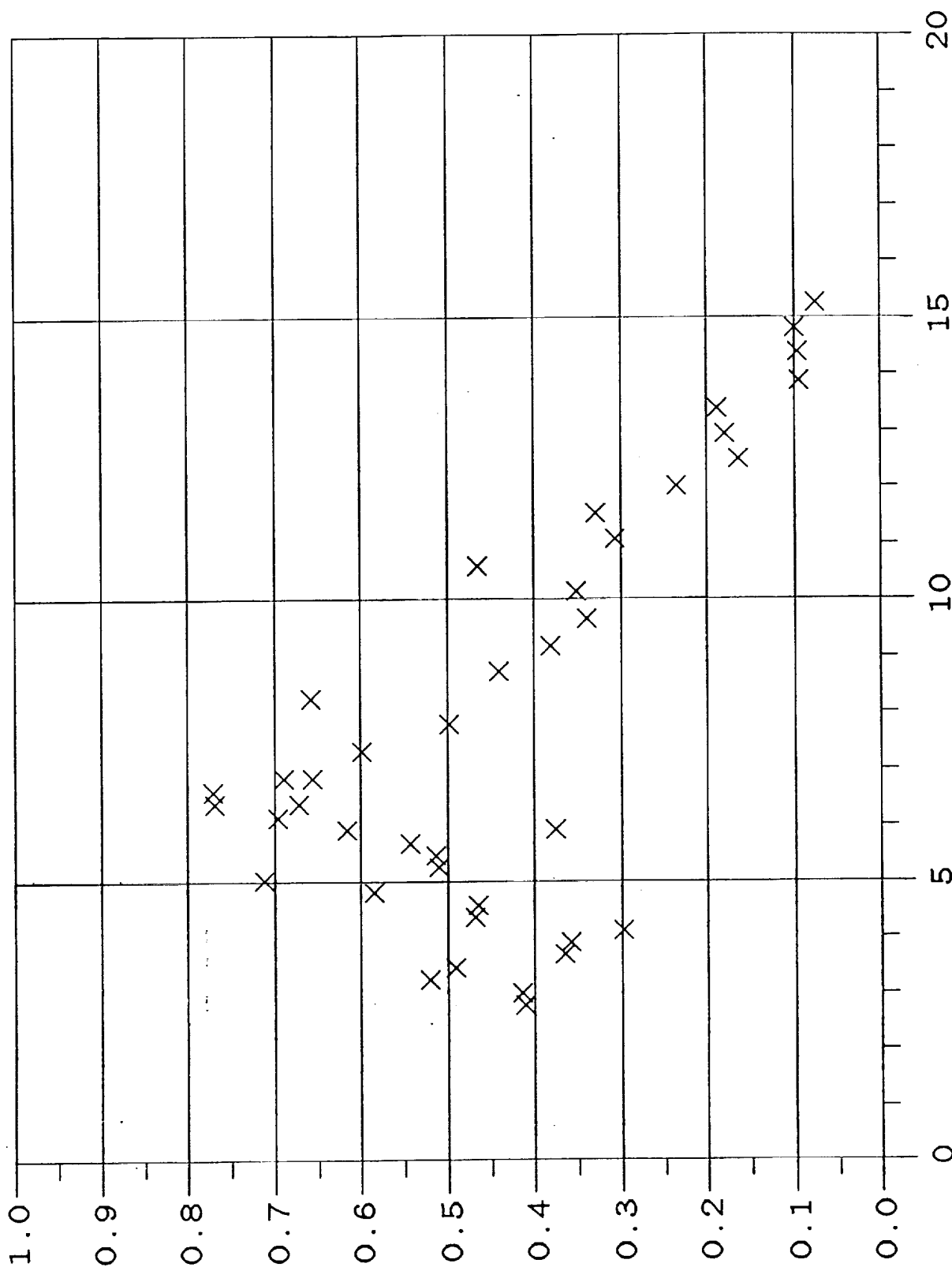




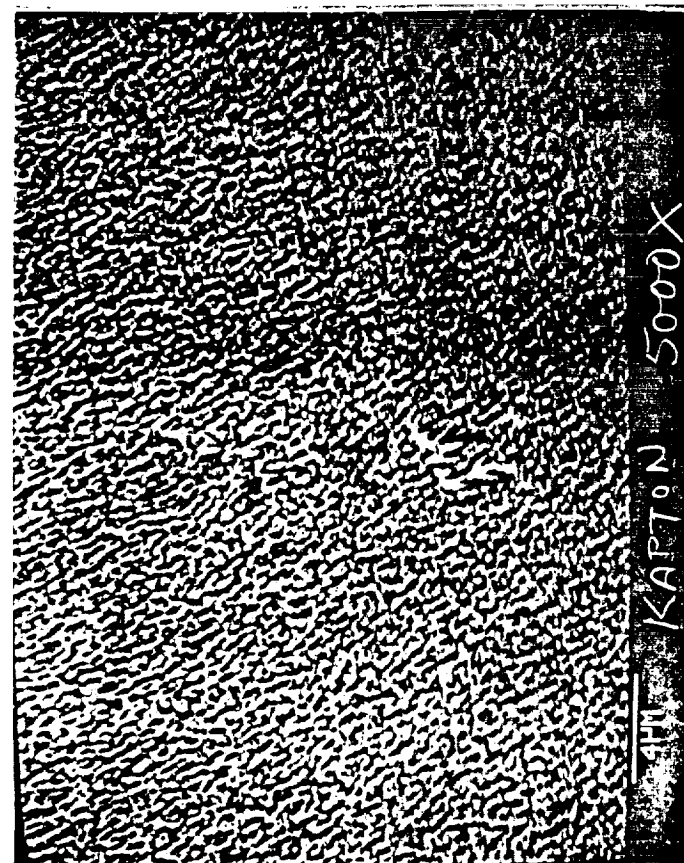
Oxygen reflected from Mo

$\times 10^{-11}$

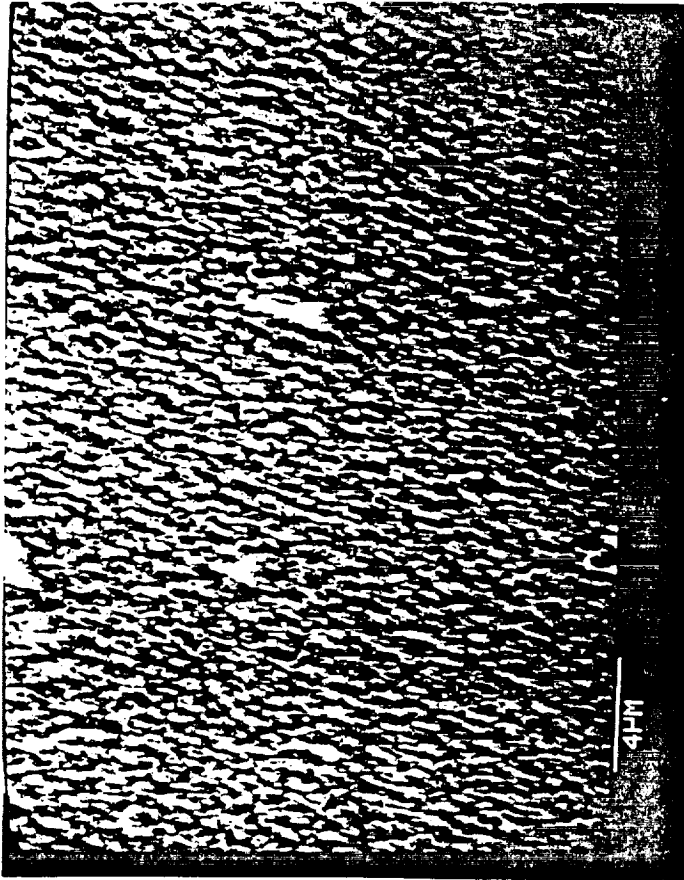
OX820F.ASC #2&# 3



Material	Measurements	Comments
Kapton (polyimide insulator)	Mass loss by erosion Scanning Electron Microscopy	"Standard" material, erosion rates calibrated in space
Black Kapton (polyimide + graphite)	Resistance change by erosion SEM of surface morphology	
Silver foil	Oxidation rate (Oxide layer thickness)	
Osmium (thin film)	Erosion rate	
Polyethylene	Mass loss by erosion	erosion rates calibrated in space
Z-306 Paint	Mass loss by erosion	Spacecraft thermal control paint
S13GLO Paint	Optical property changes	"
Z-302 Paint	(Absorptivity & emissivity)	"
A-276 Paint		"
SiOx on Kapton	Mass loss	Candidate protective coating
Lexan polycarbonate	Mass loss and directionality of etching	
Magnesium Fluoride film	Optical property changes	Protective coating on Hubble Space Telescope mirror
Silver/FEP Teflon	SEM of surface morphology	Reflective thermal control material, compared to LDEF
Silver Connectors	Oxidation rate Effect of cycling	INTELSAT solar cell interconnects
Si and SiC	Mass and thickness loss	
Rhodium Mirror Iridium Mirror	Optical property changes (VUV reflection)	Candidate materials for AXAF satellite x-ray mirrors

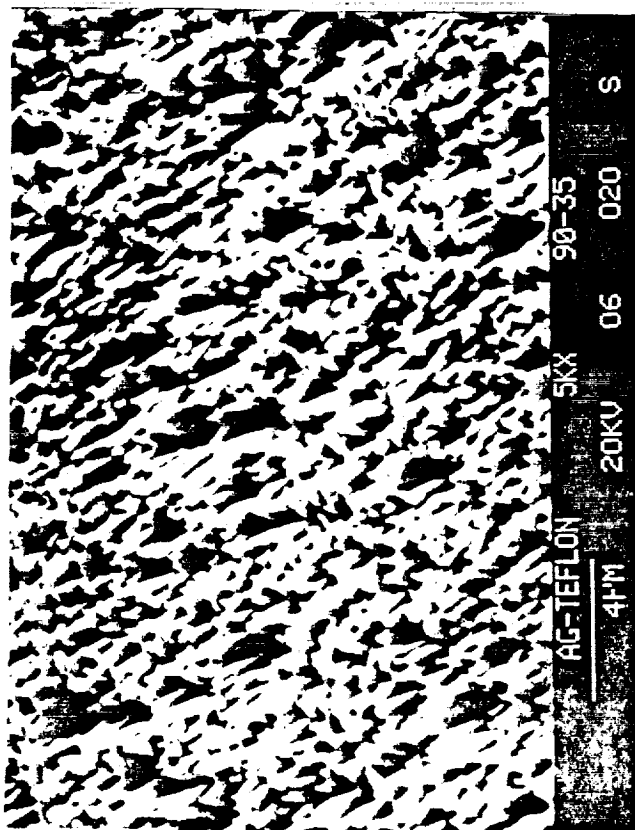


2 mil KAPTON EXPOSED TO A NEUTRAL  
ATOMIC OXYGEN BEAM AT PPPL .  
( FLUENCE  $2 \times 10^{19}$  ) (5000X)

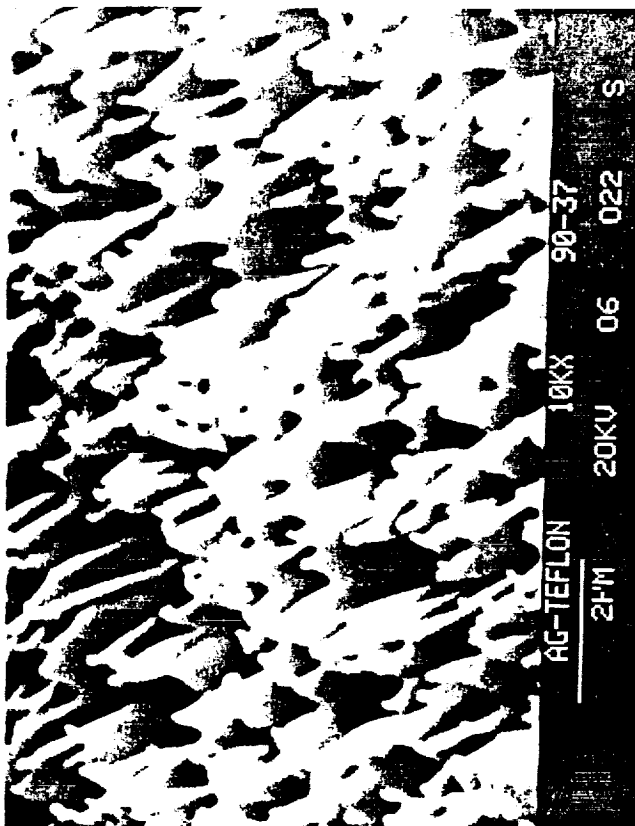


2 mil KAPTON EXPOSED DURING  
STS-8 . ( FLUENCE  $3 \times 10^{20}$  )  
(5000X)

ORIGINAL PAGE IS  
OF POOR QUALITY



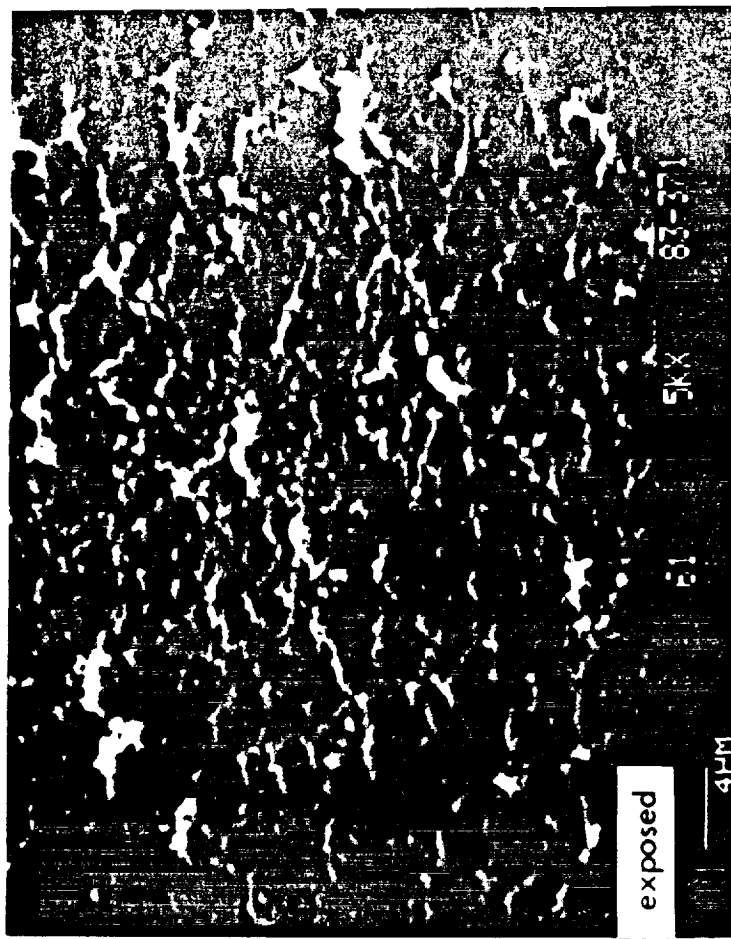
SILVER-TEFLON EXPOSED TO A NEUTRAL  
ATOMIC OXYGEN BEAM AT PPPL.  
(FLUENCE  $\times 10^{20}$  atoms/cm<sup>2</sup>) (5000X)



SILVER-TEFLON EXPOSED TO A NEUTRAL  
ATOMIC OXYGEN BEAM AT PPPL.  
(FLUENCE  $\times 10^{20}$  atoms/cm<sup>2</sup>) (10,000X)

ORIGINAL PAGE IS  
OF POOR QUALITY



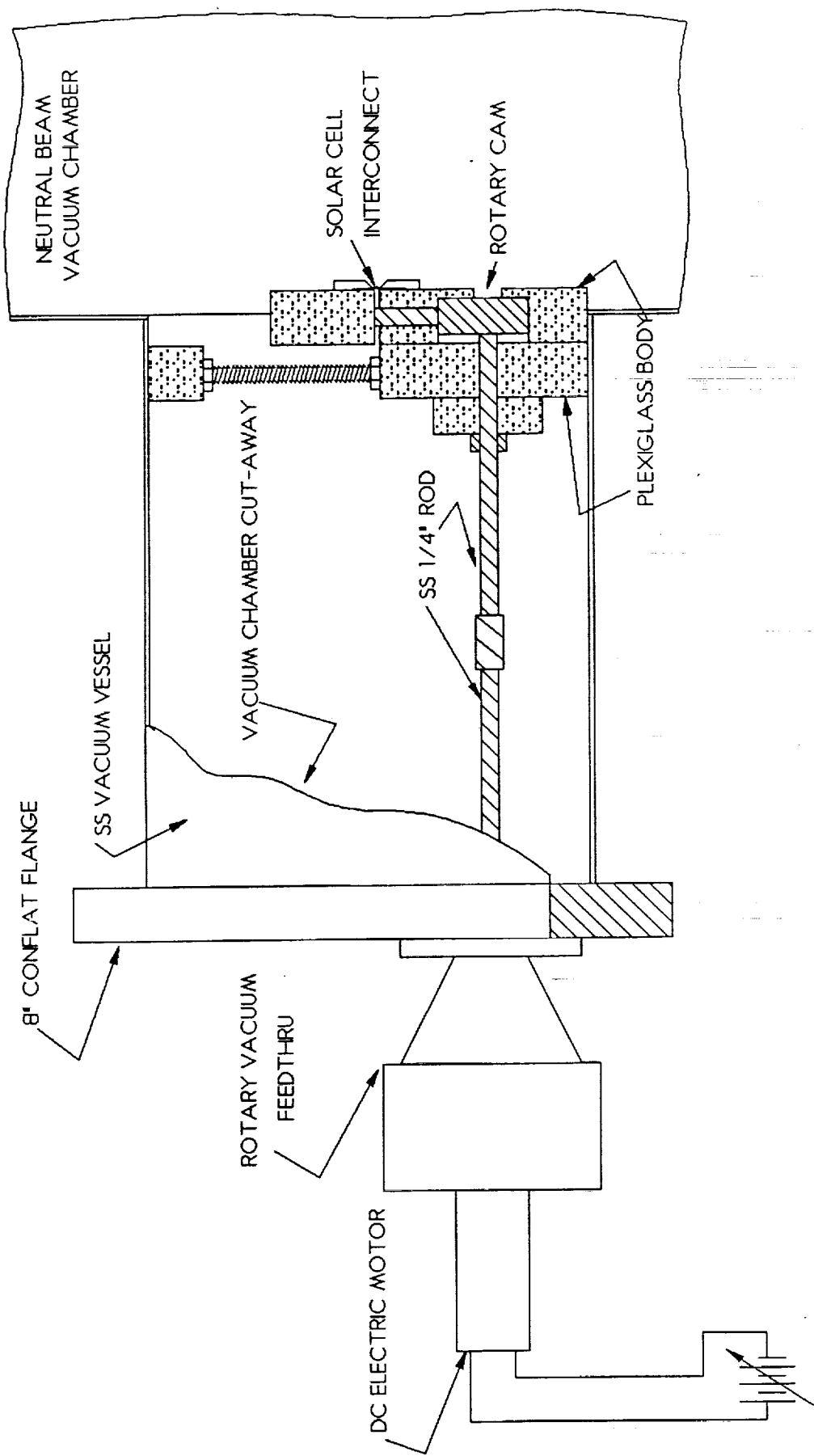


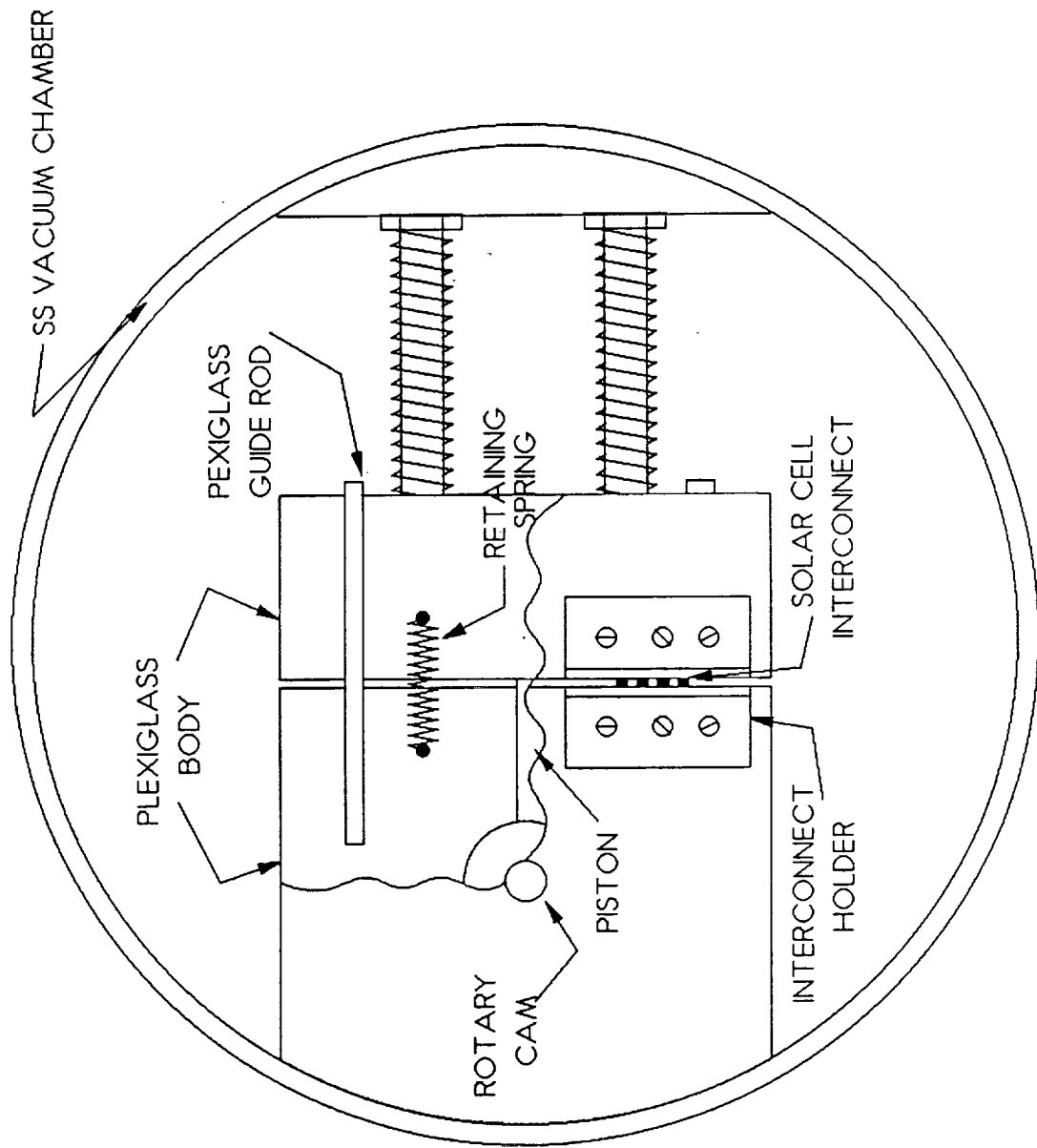
BLACK KAPTON EXPOSED DURING  
STS-5. ( FLUENCE  $3 \times 10^{20}$ )  
(5000X)



BLACK KAPTON EXPOSED AT PPPL  
9 cm FROM NEUTRALIZER. (5000X)

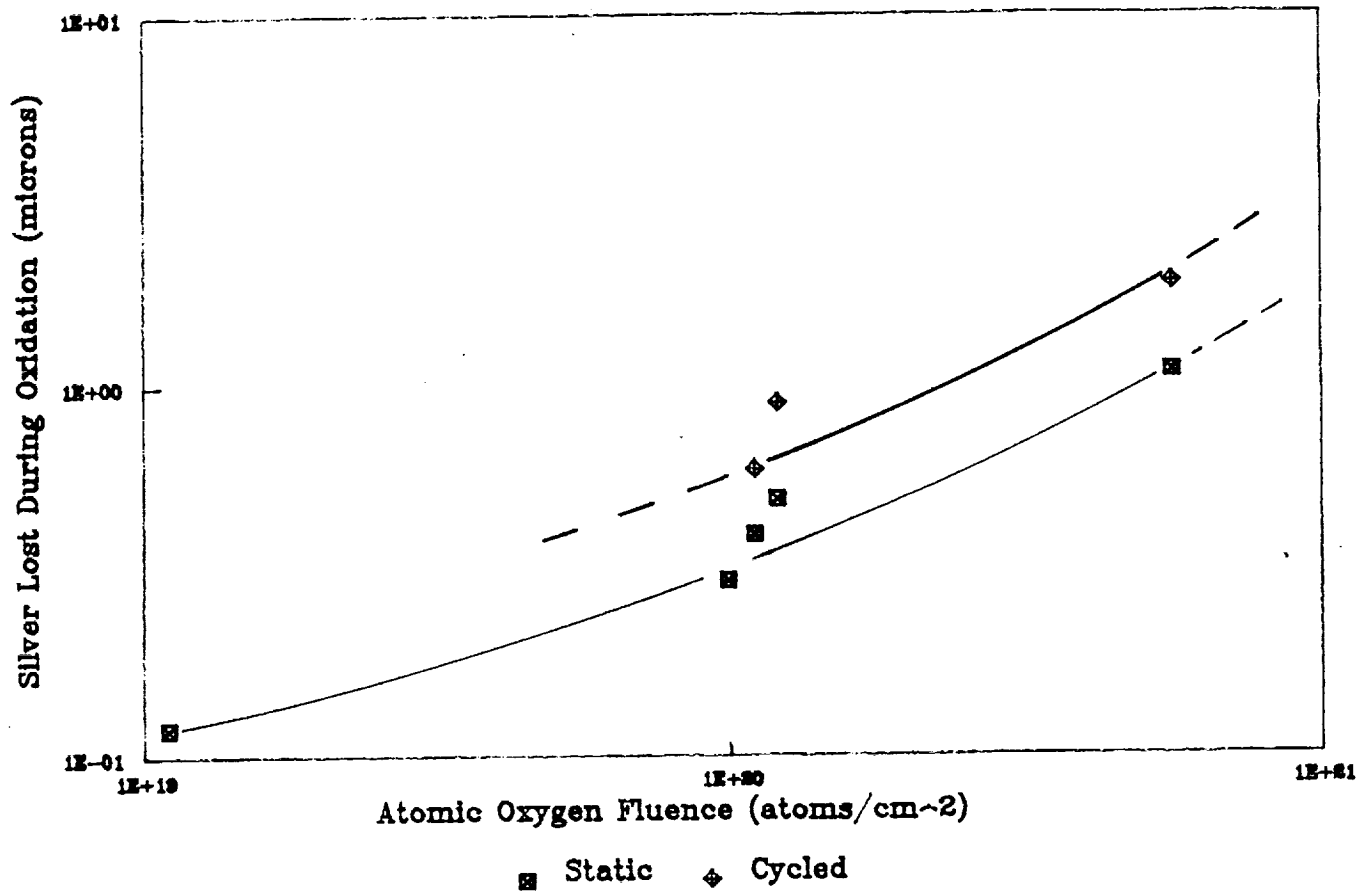
ORIGINAL PAGE IS  
OF POOR QUALITY





# Silver Erosion In Atomic Oxygen

## Effect of Simulated Thermal Cycling



## Future Plans

- Improve analysis of atomic Oxygen beam spectra, perhaps using time-of-flight
- Measure spectra for reflection of H and He
- Characterize large-bore, higher power RF exciter. Goal is 1.5 kW continuous power (100% duty cycle), giving  $10^{21} \text{cm}^{-2}$  fluence in six hours.
- Measure UV flux in source
- Developing spectroscopic experiments to study spacecraft glow phenomenon.

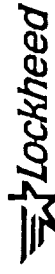
## Advantages for Glow Spectroscopy

- High flux: surface glows have been measured using fluxes  $\sim 10^{13}$  atoms/cm<sup>2</sup>s. Our current source can provide  $2.5 \times 10^{15}$  atoms/cm<sup>2</sup>s peak flux ( $3 \times 10^{14}$  avg.) on target at spectroscopy port (40 cm from source). New high power source can provide  $> 1.7 \times 10^{15}$  avg. flux.
- Uniform illumination of large target area allows for large light collection volume.
- Not restricted to O; can make beams of other reactive or inert species.
- Capability for multiple energetic bombarding species, e.g. oxygen plus nitrogen, as occurs in LEO.

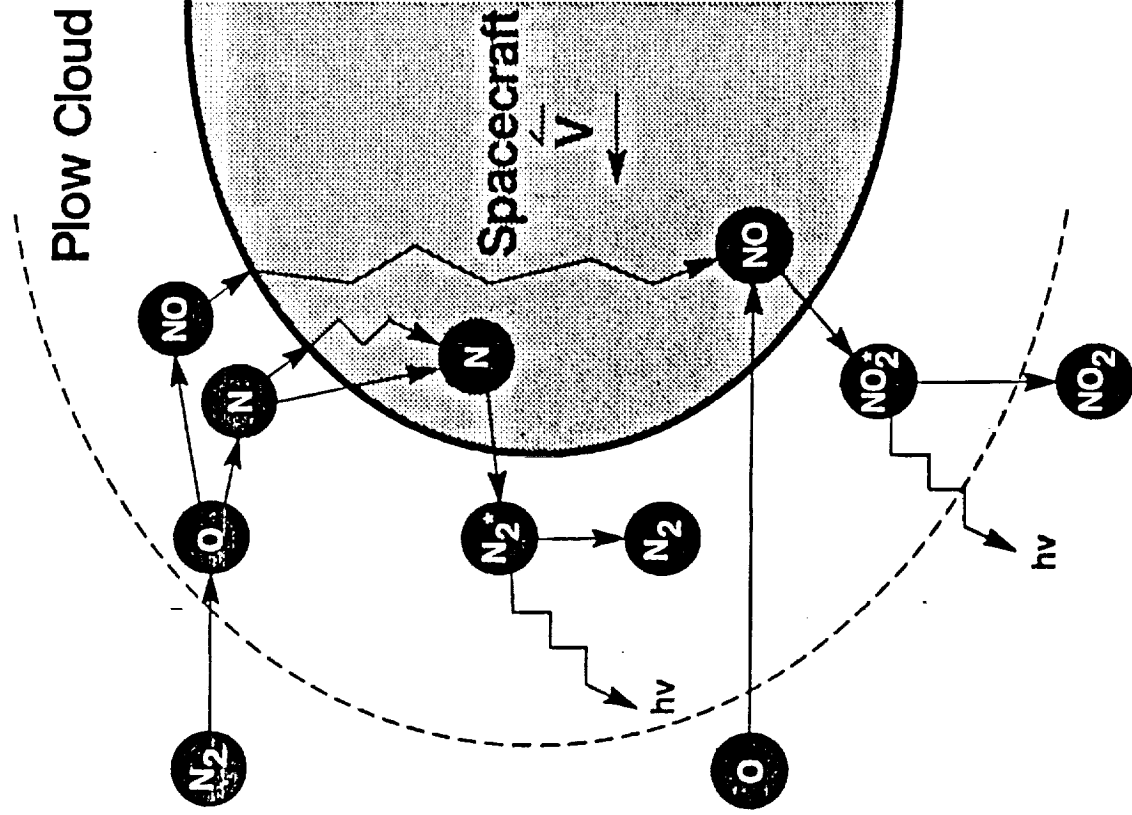
# OUTREACH

## EXPERIMENTAL INVESTIGATION OF SPACECRAFT GLOW

S.B. Mende

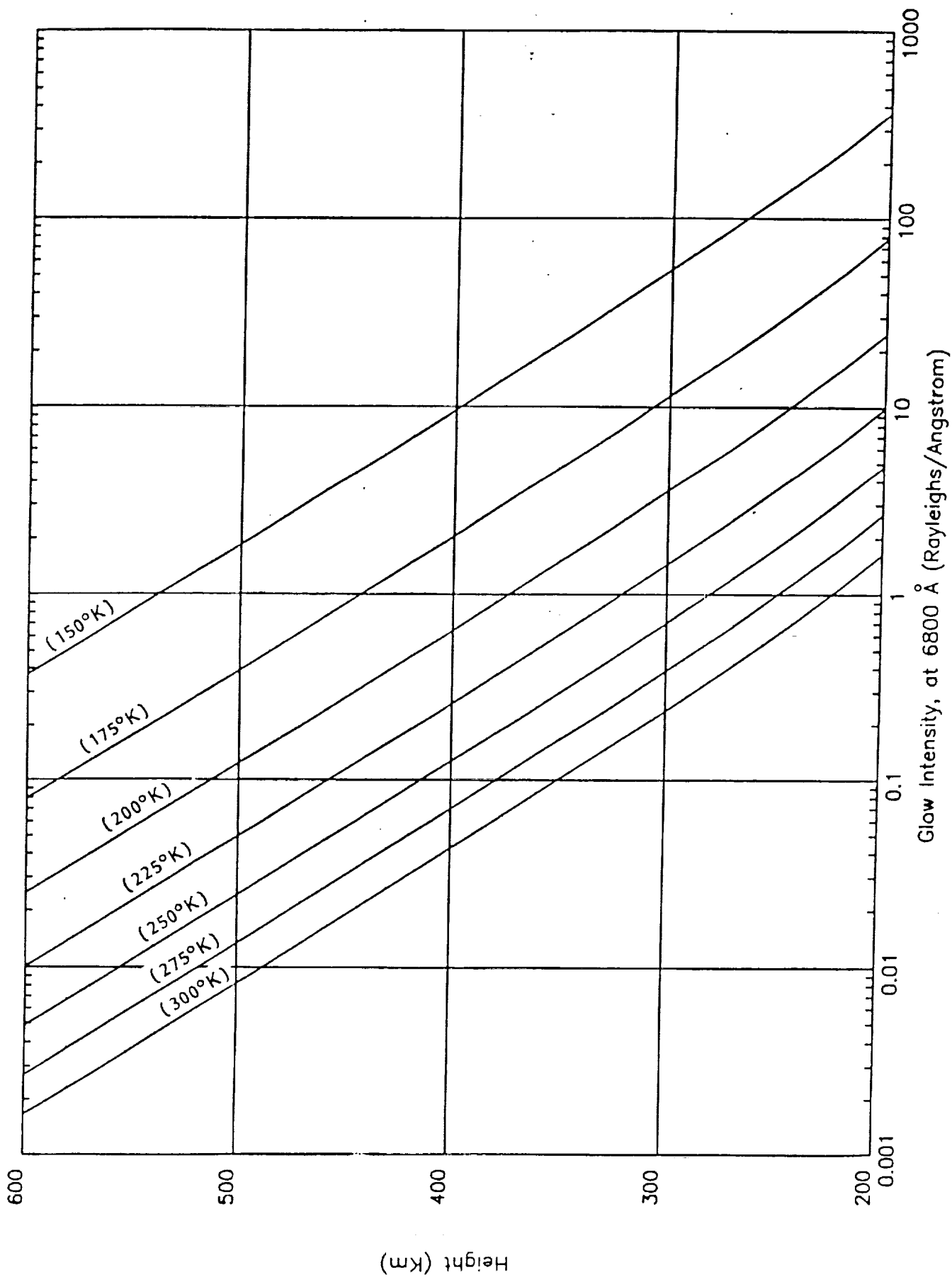


Jan 31, 1991

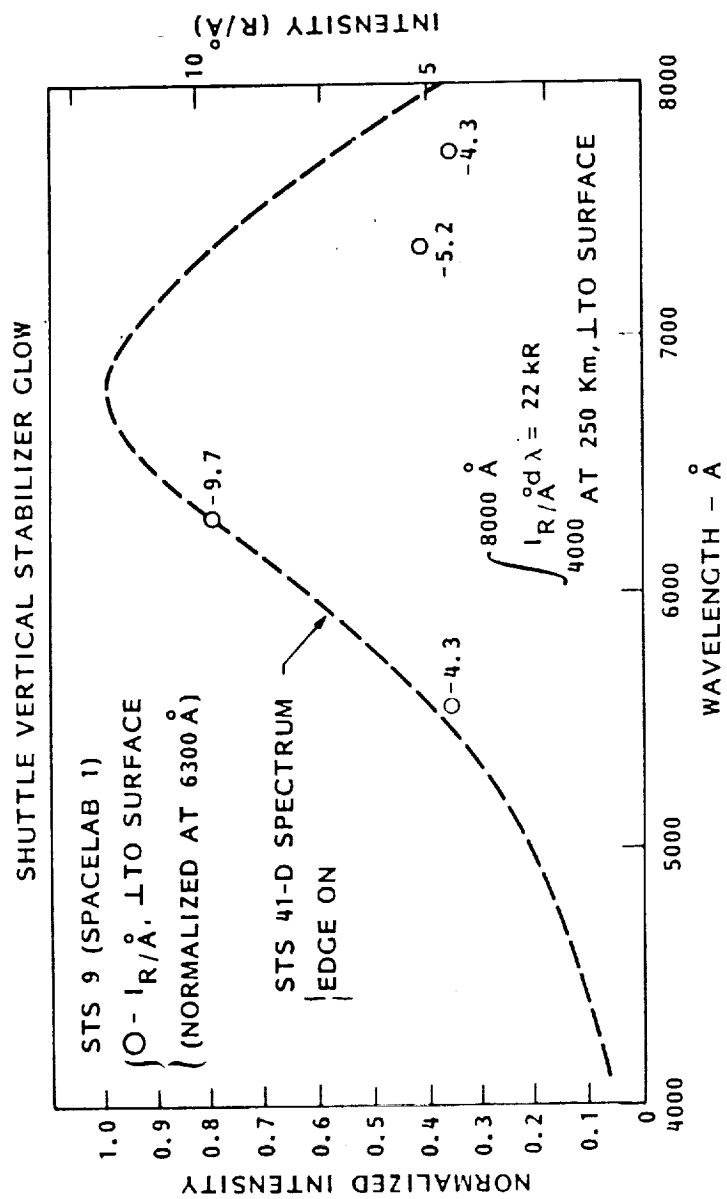


### Spacecraft-Atmospheric Interaction

The top of the figure shows atmospheric  $N_2$  interacting with rebounding O and atom exchanging to form N and NO. The N is shown to contact N which has been deposited on the surface, and to recombine to form  $N_2^*$ . This excited state leads to  $N_2$  LBH emission which is predicted to be responsible for the low-altitude glow seen on the S3-4 satellite. The bottom of the figure illustrates atmospheric O impinging on NO which is weakly bound to the surface. The surface recombination will lead to  $NO_2^*$  and has been proposed as being responsible for the "red" shuttle glow.







S.B.Mende

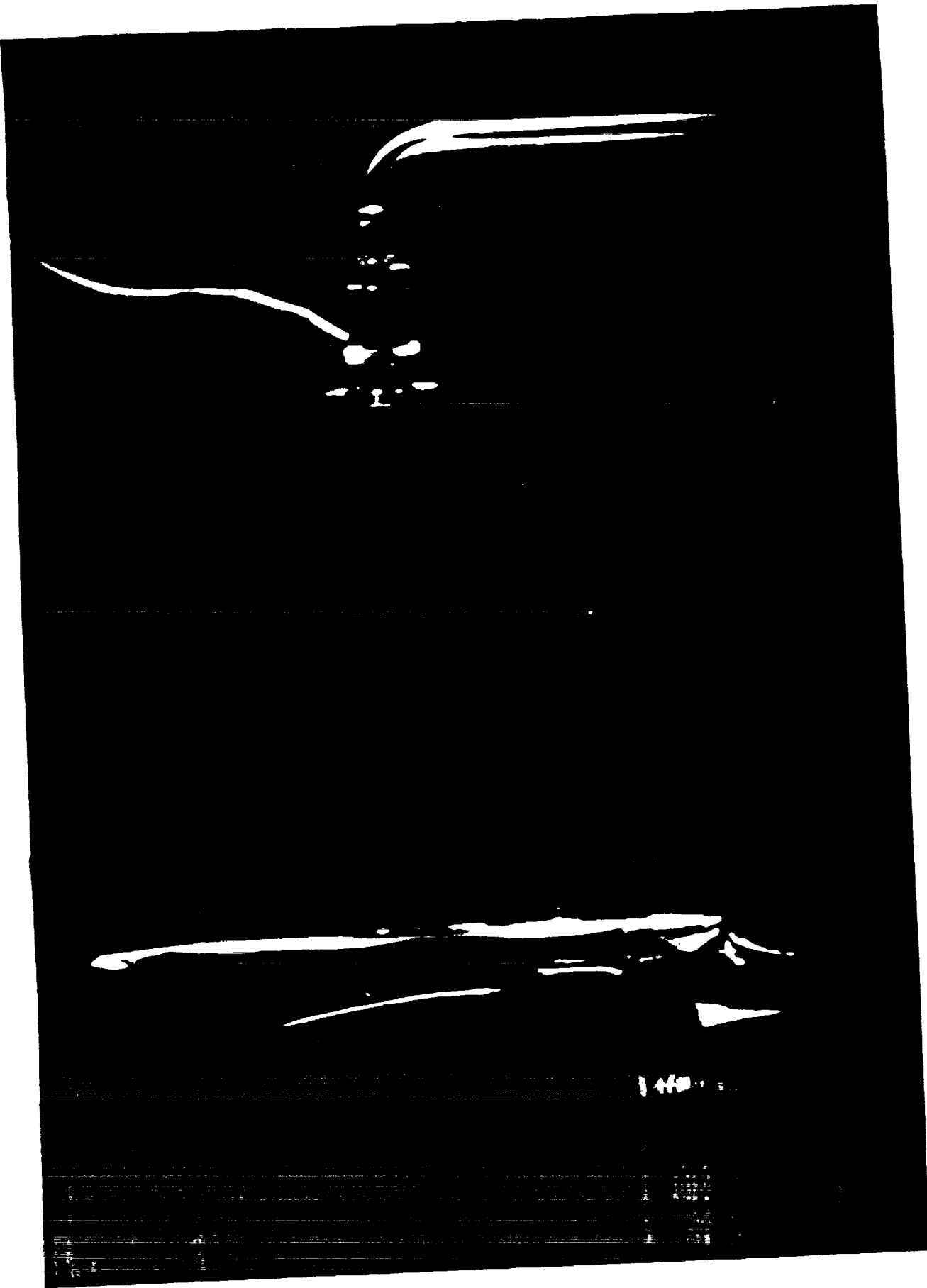


Figure 2

ORIGINAL PAGE IS  
OF POOR QUALITY

ORIGINAL PAGE  
BLACK AND WHITE PHOTOGRAPH

# Glow Spectra, Raw and Spectrally Corrected

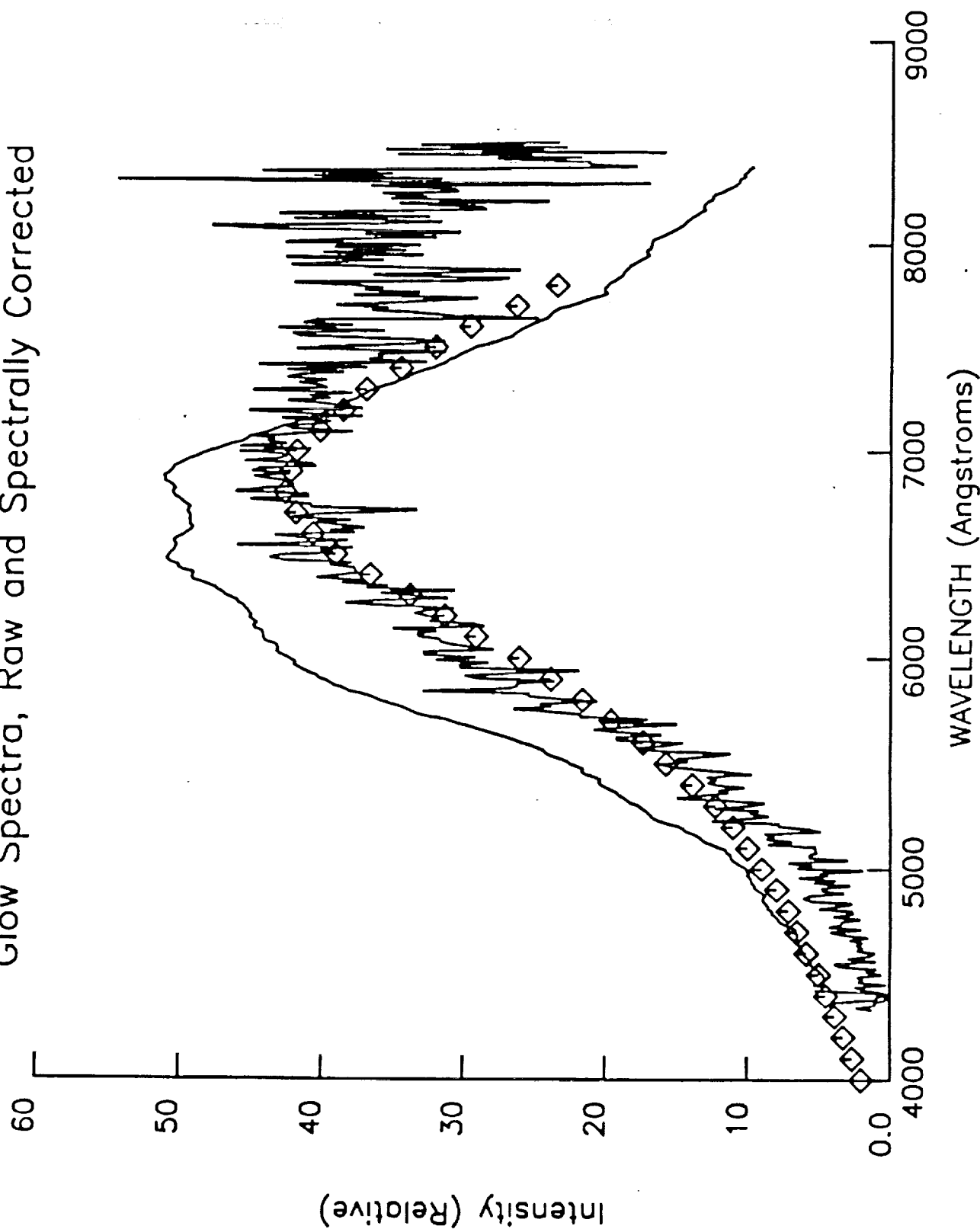
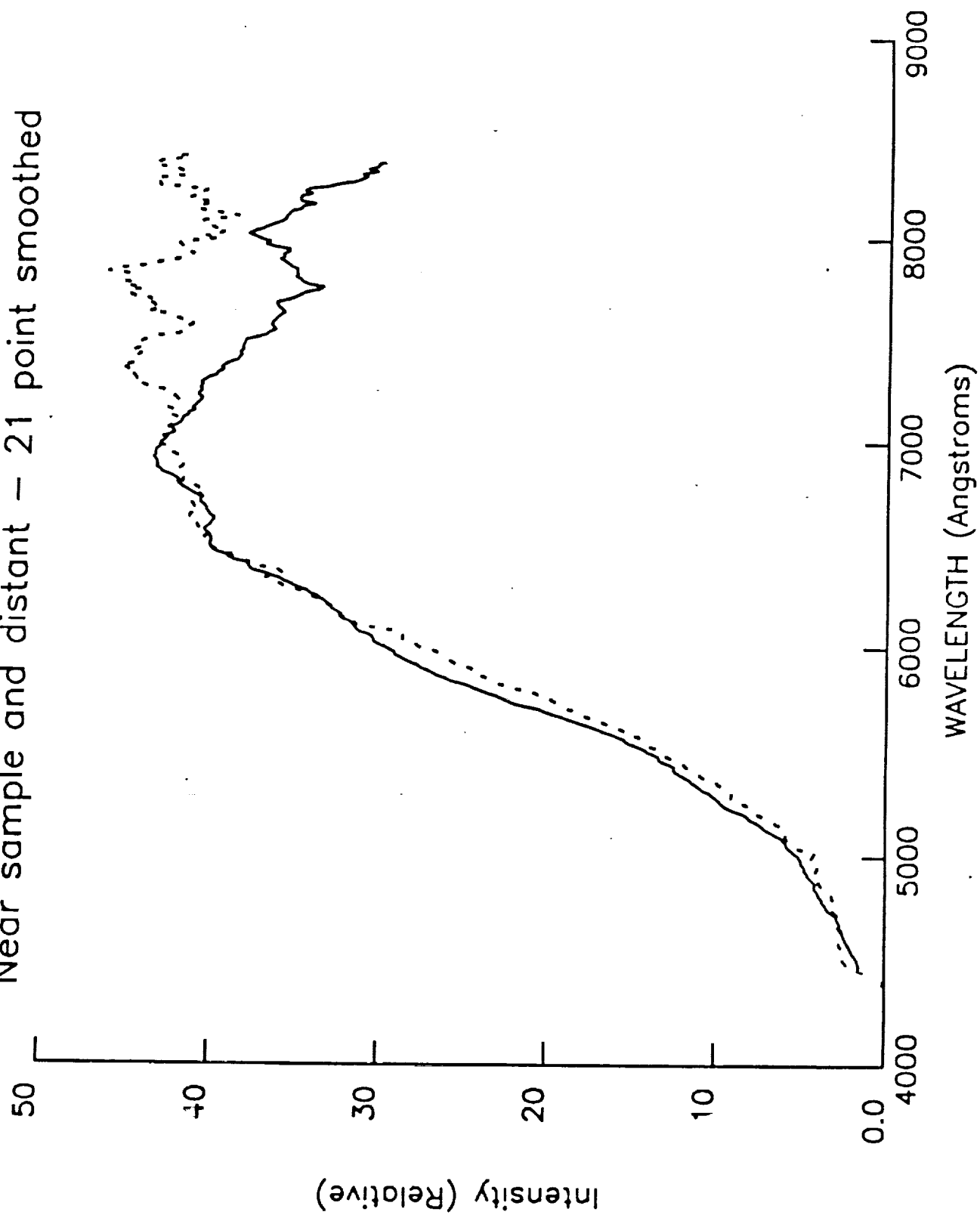
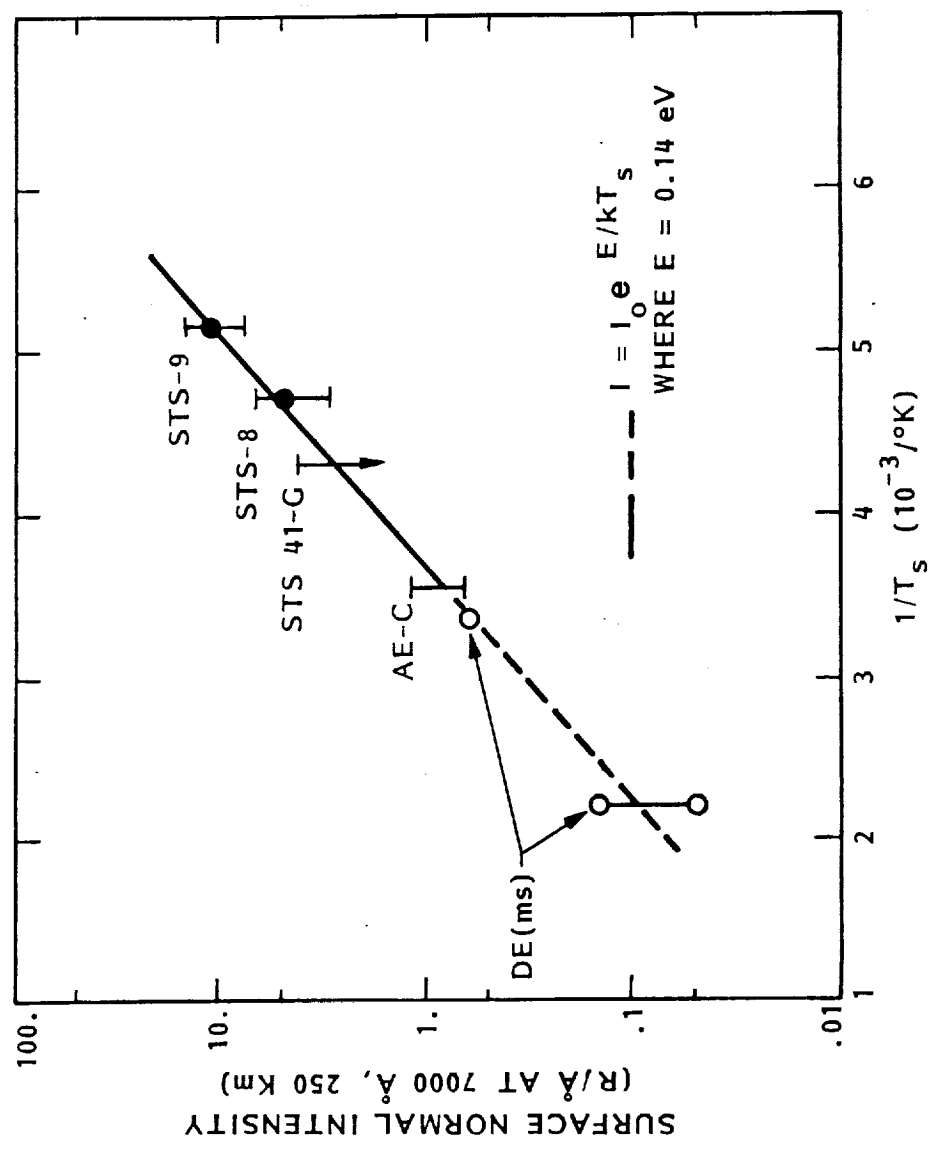


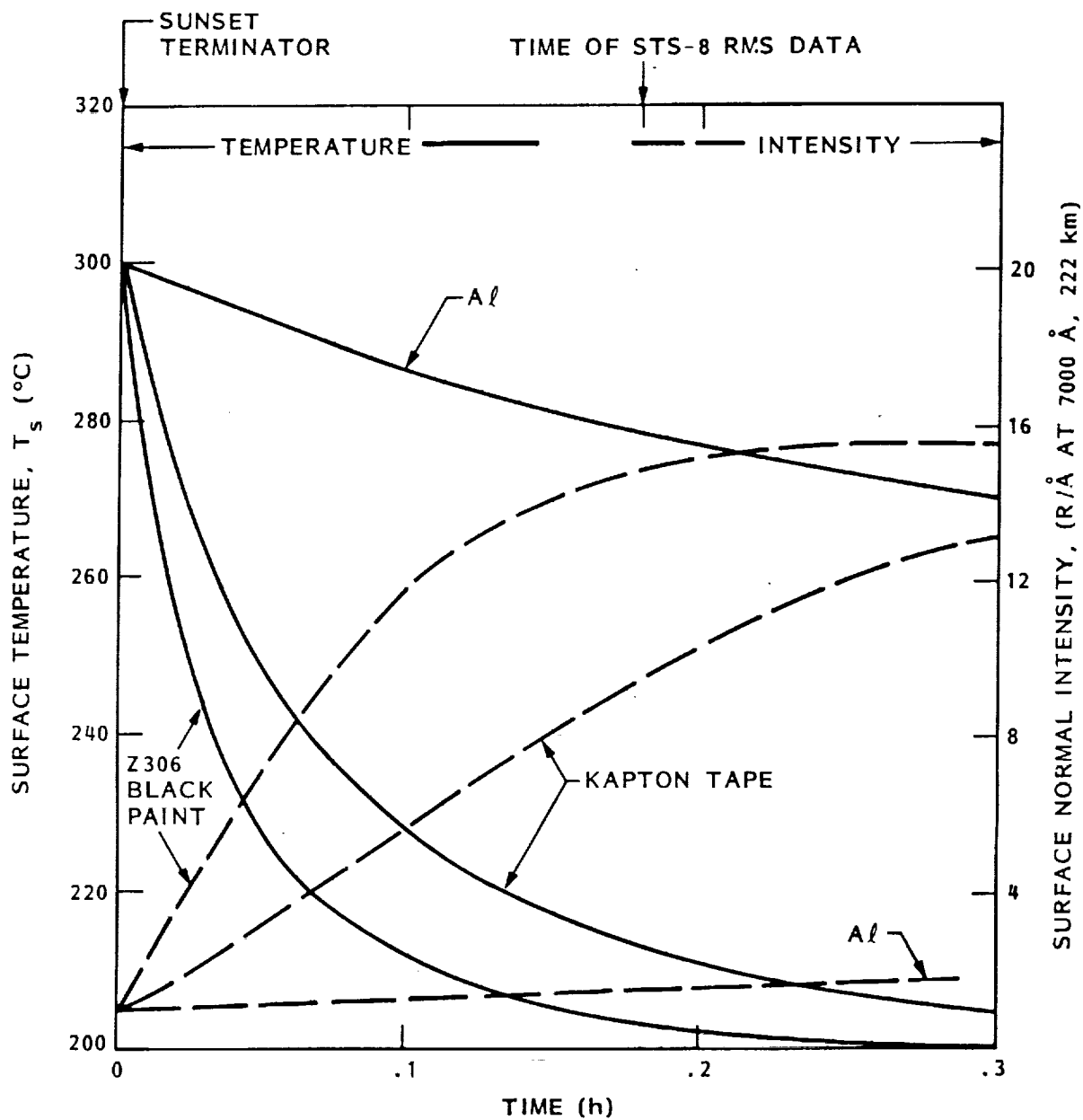
Figure 7b

Near sample and distant - 21 point smoothed



S. B. Menzel

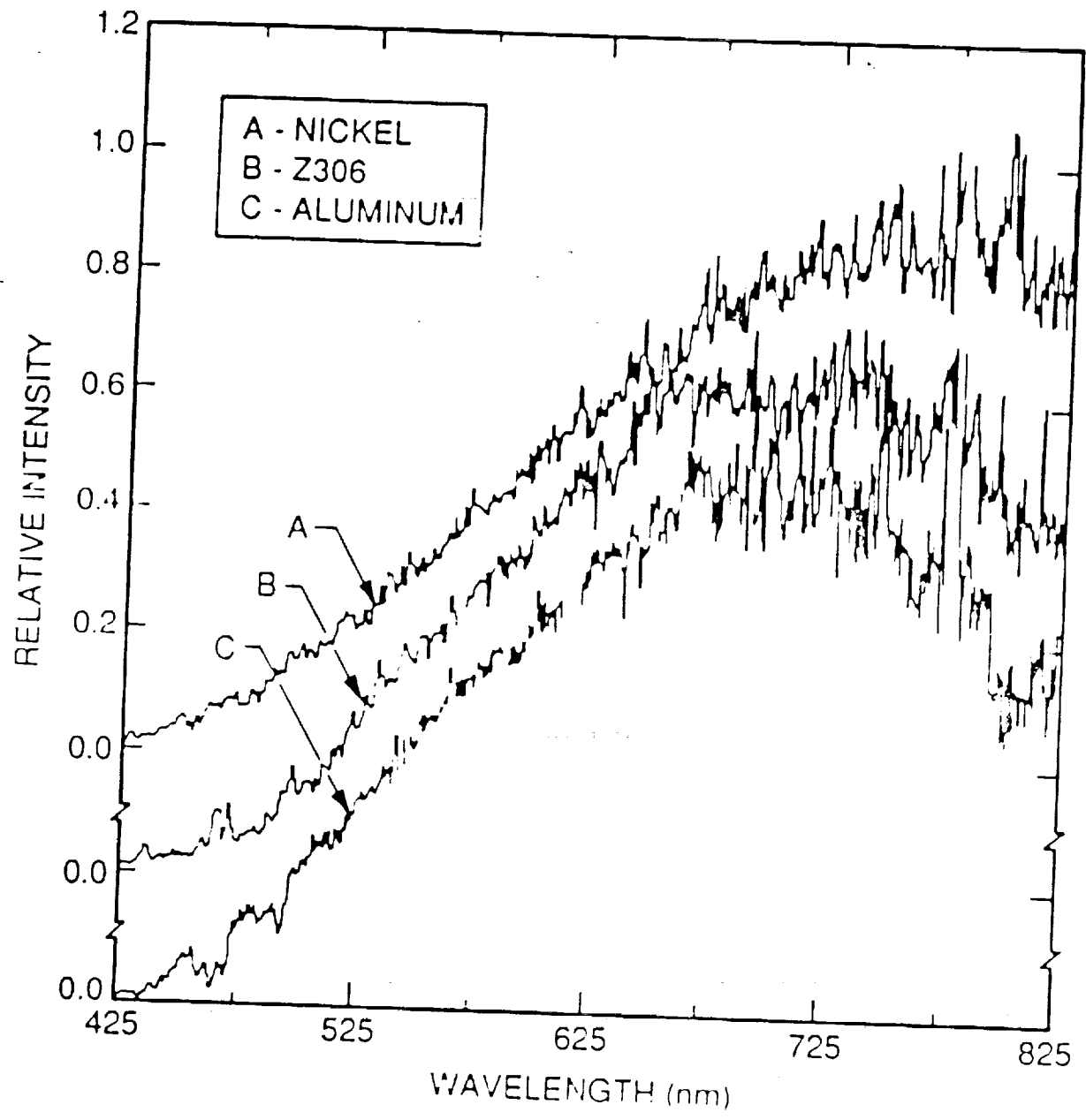


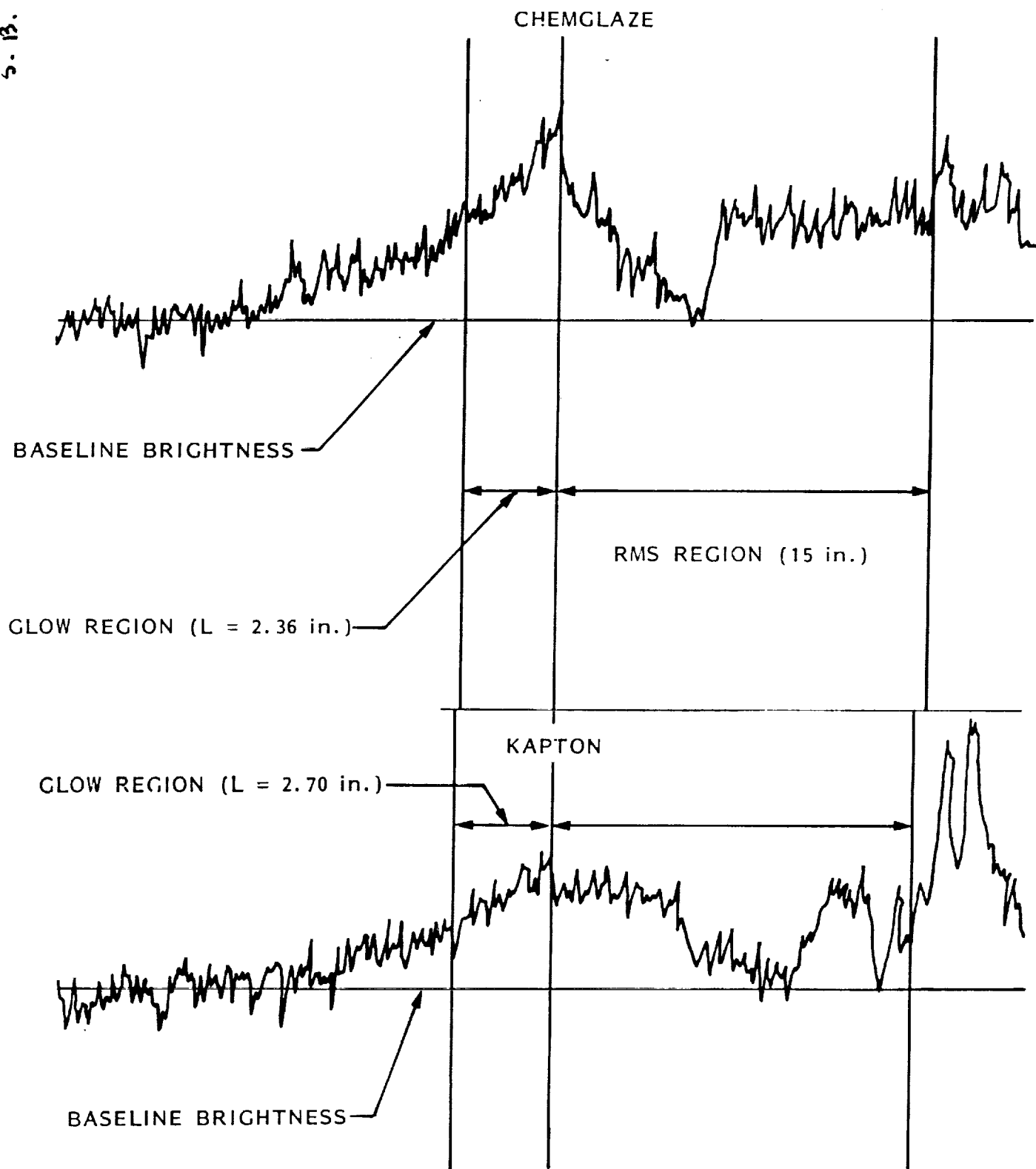


S. B. Mende

# Shuttle Glow

1883







ORIGINAL PAGE  
BLACK AND WHITE PHOTOGRAPH

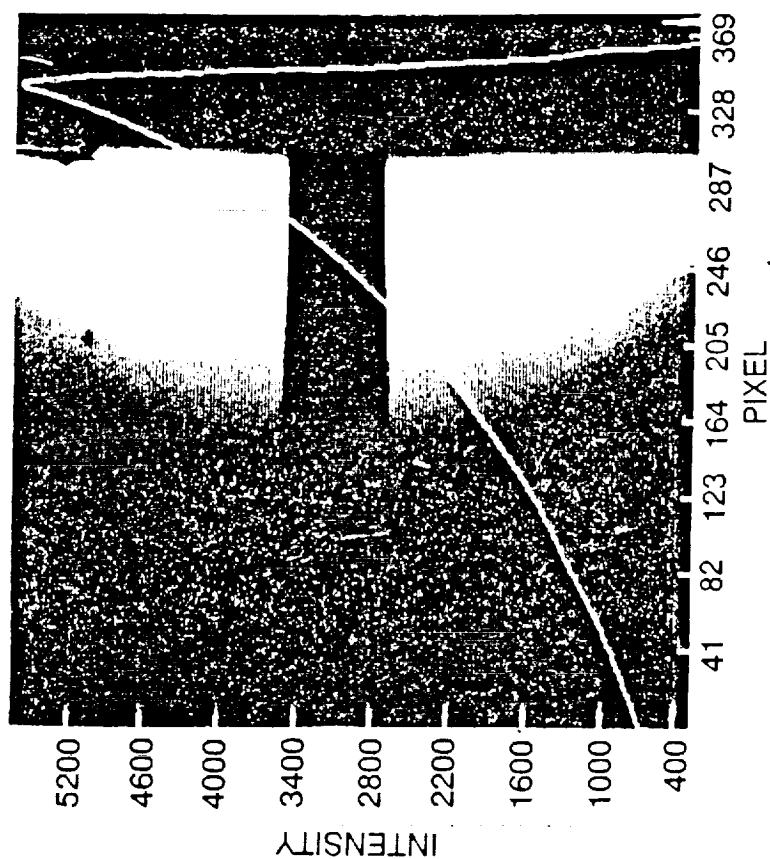
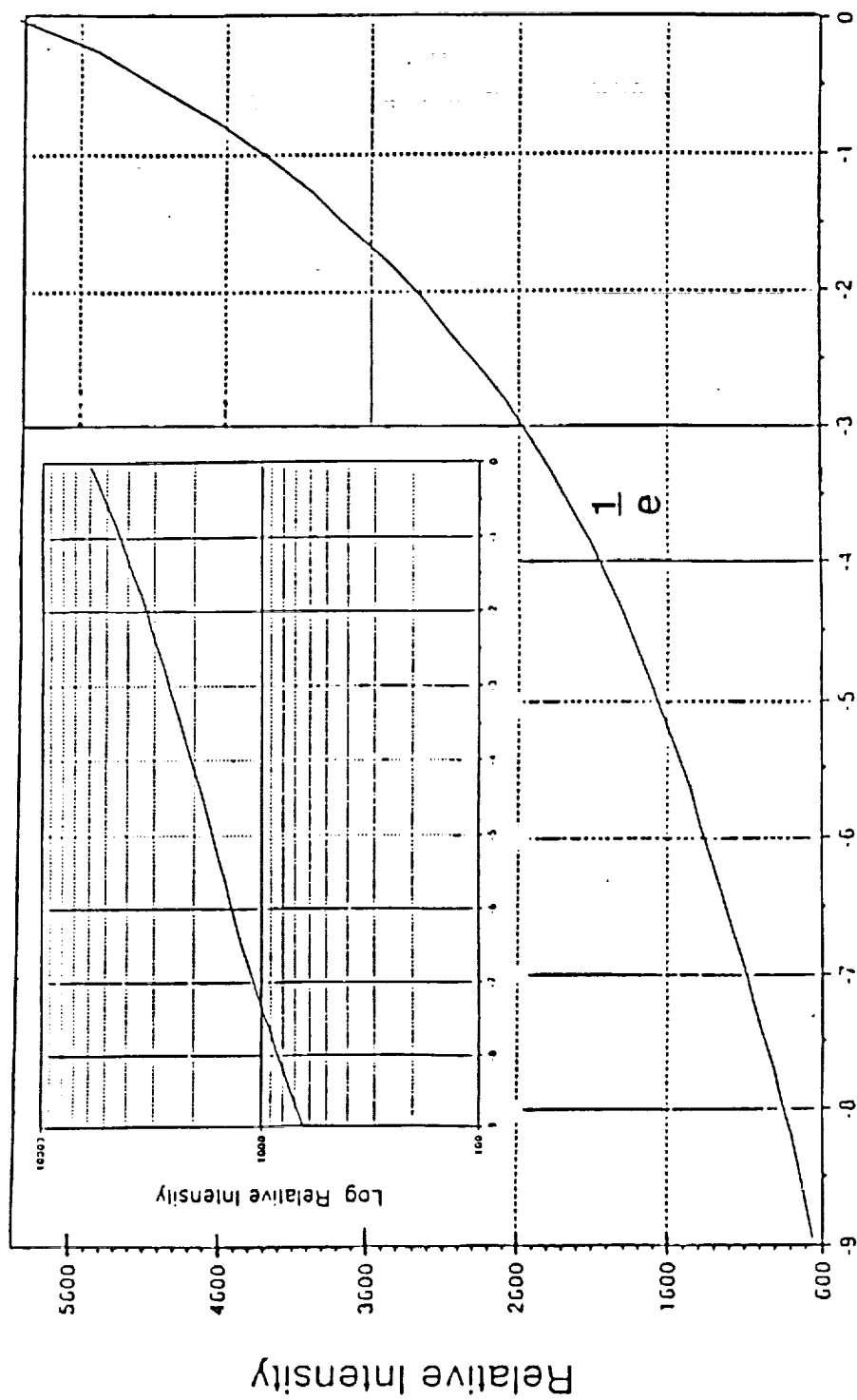


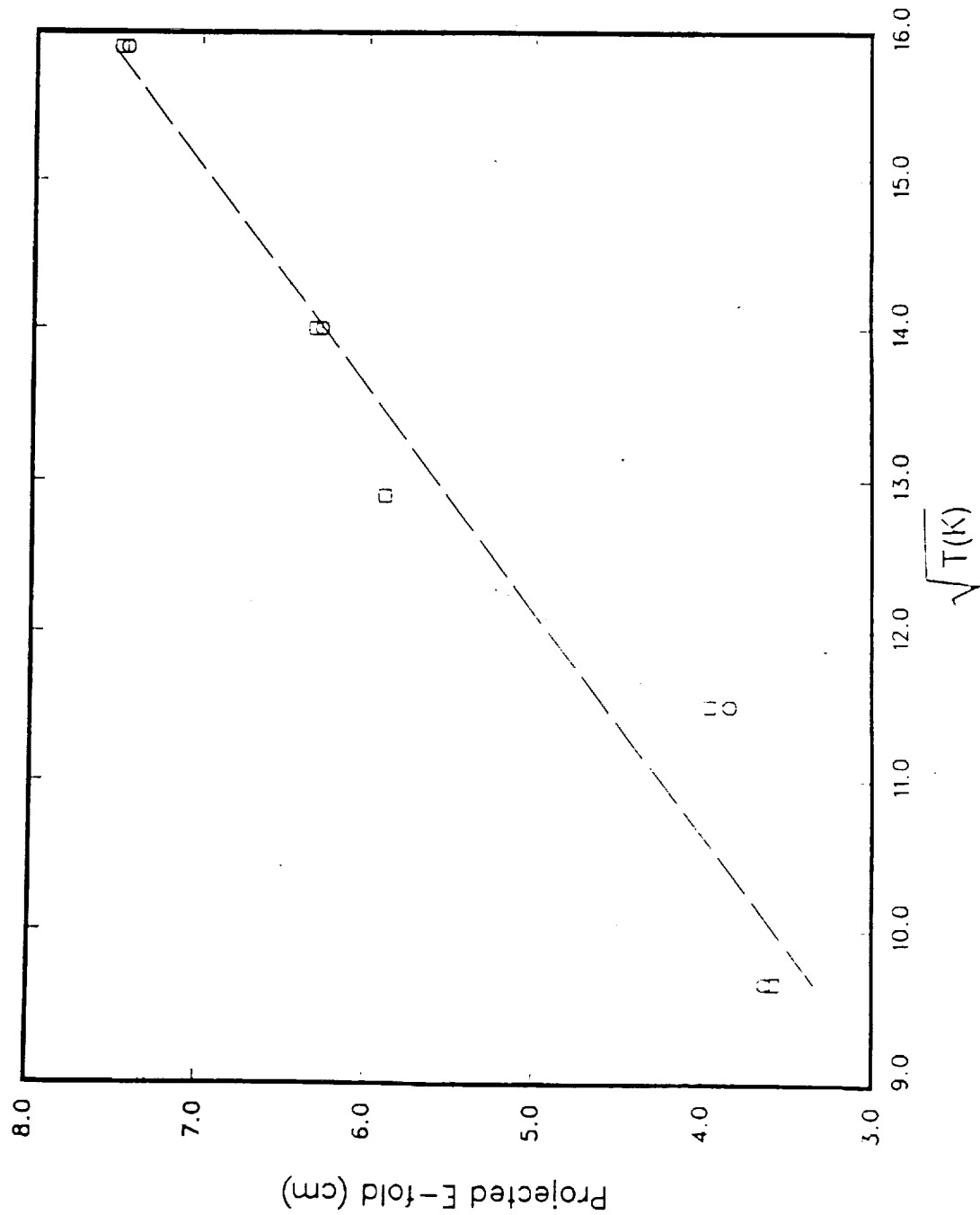
Figure 4

ORIGINAL PAGE IS  
OF POOR QUALITY

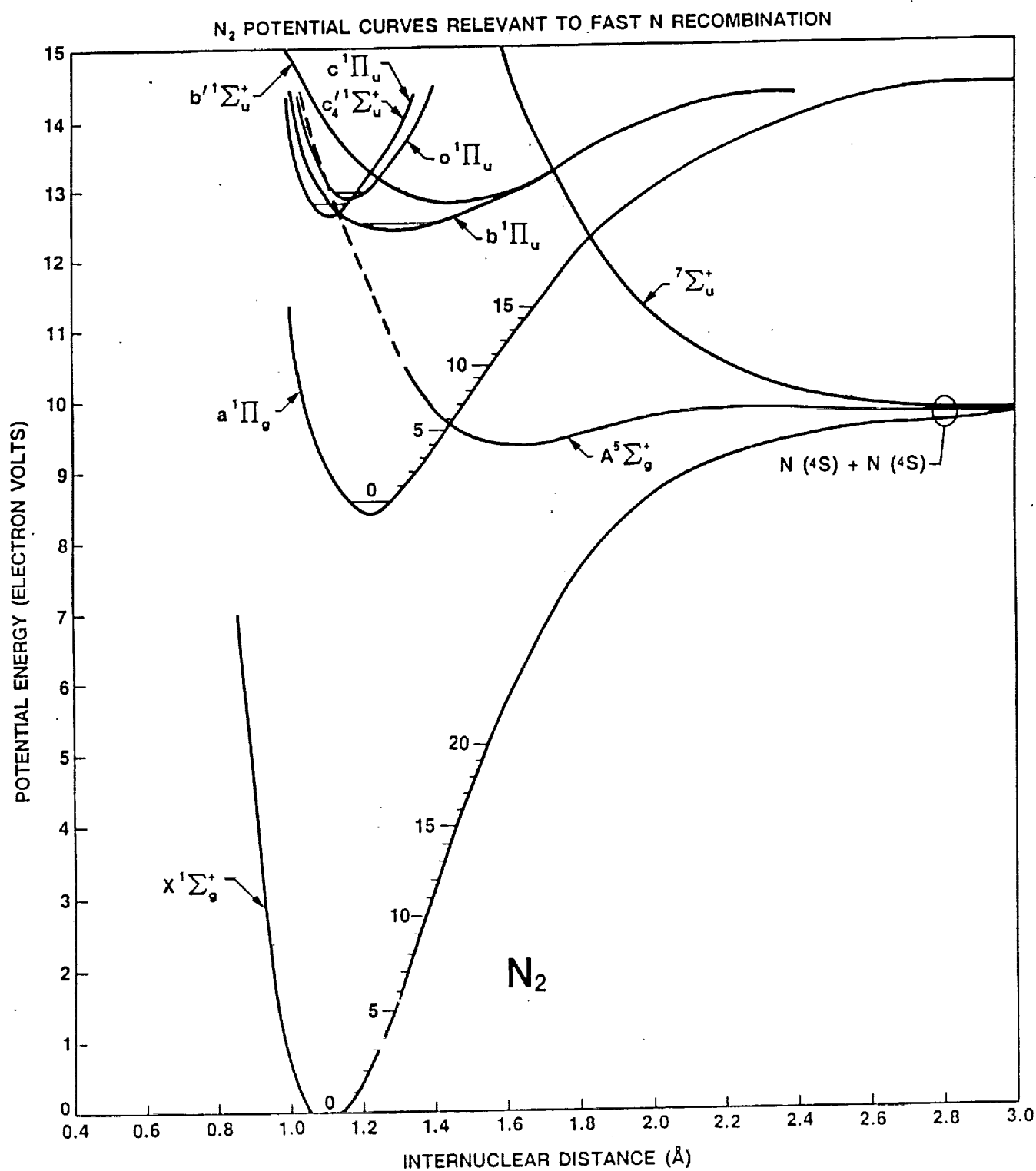


Distance from plate in cm.

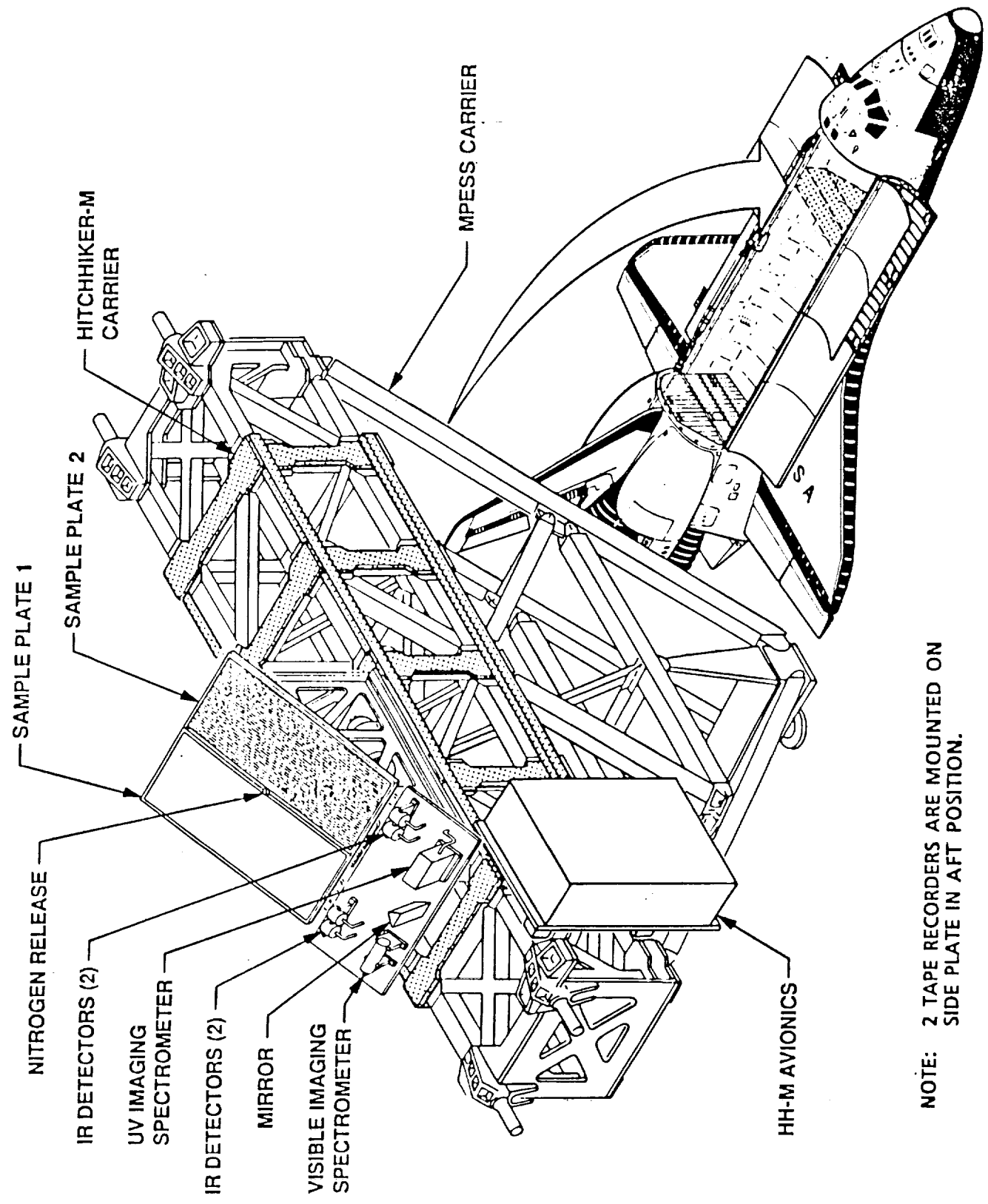
Figure 5



S. B. Mende




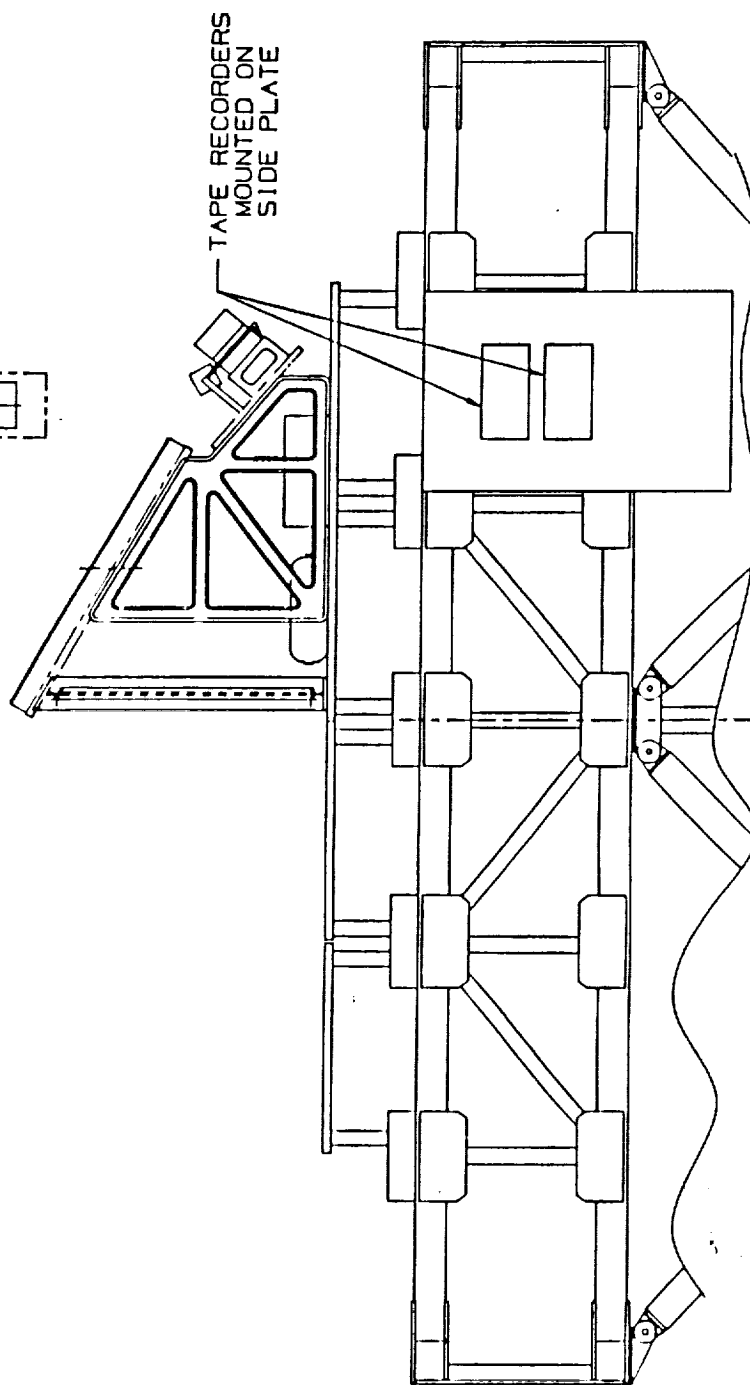
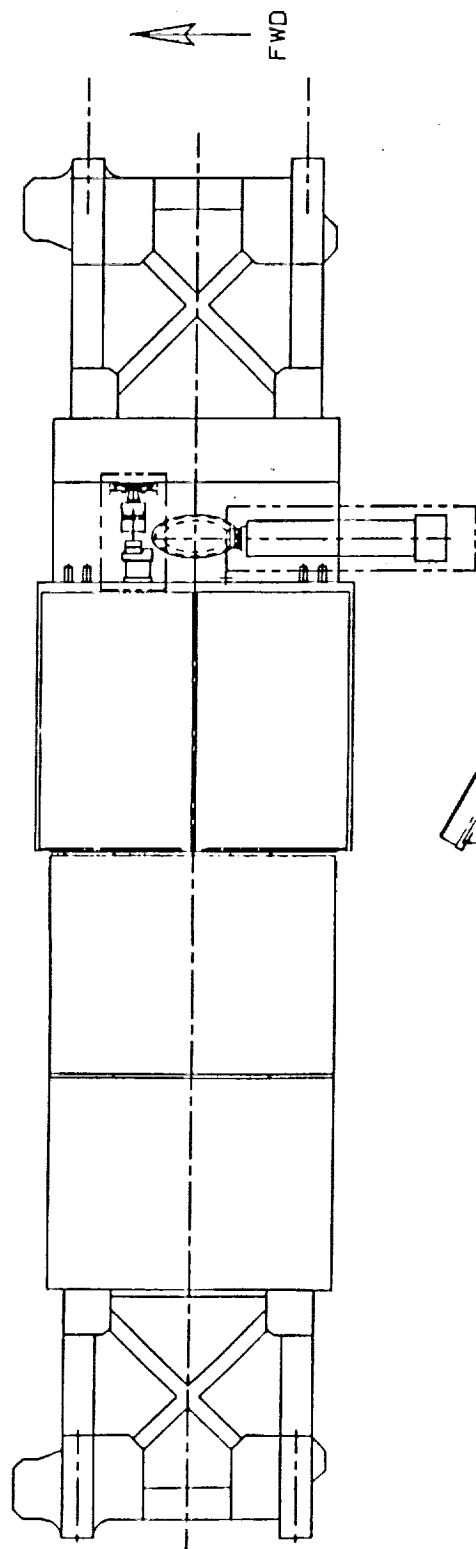
# EXPERIMENTAL INVESTIGATION OF SPACECRAFT GLOW



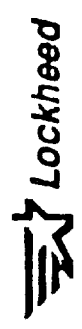
NOTE: 2 TAPE RECORDERS ARE MOUNTED ON  
SIDE PLATE IN AFT POSITION.

S. B. Hende

 <b>Lockheed</b>	<b>Experimental Investigation of Spacecraft Glow</b>	<b>Preliminary Design Review</b>
		SAM CHOUDHARY
		3/5/91



S. B. Mende

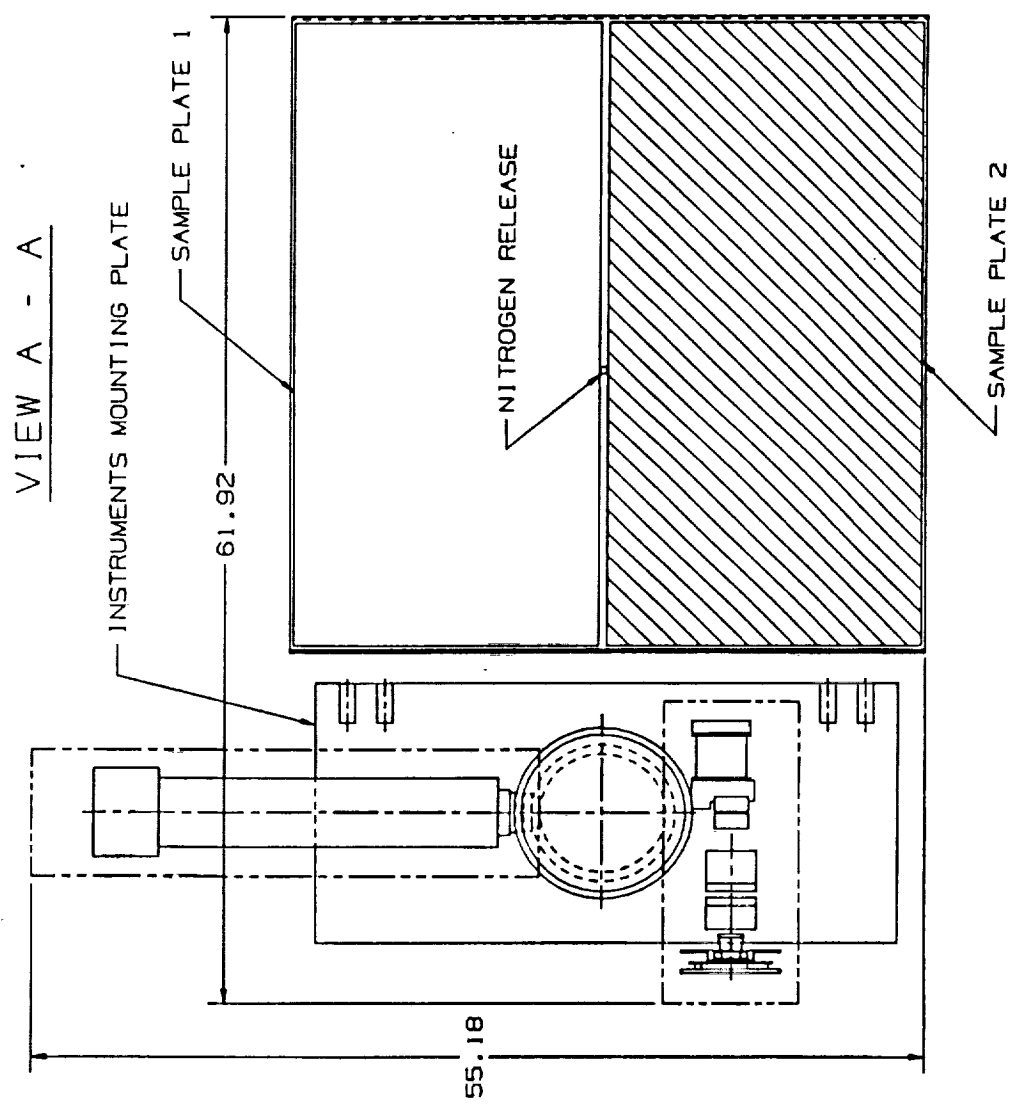


Experimental Investigation of Spacecraft Glow

Preliminary Design Review

SAM CHOUDHARY

3/5/91



SAMPLE CARRIER ASSY  
EISG EXPERIMENT

# **Surface Glow Mechanisms in Space**

## **"Particle-Solid Aeronomy"**

**Royal G. Albridge, Alan V. Barnes  
and Norman Tolk**

*Center for Molecular and Atomic Studies at Surfaces  
Department of Physics and Astronomy  
Vanderbilt University  
Nashville, Tennessee 37235 U.S.A.*





*Cmass...*

## **SURFACE GLOW MECHANISMS**

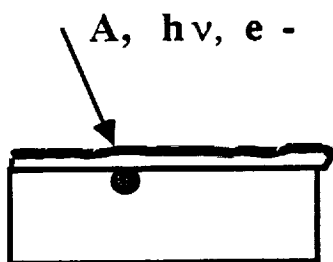
- **TEMPERATURE DEPENDENCE**
- **INFLUENCE OF DEFECTS**
- **SELECTIVE DESORPTION  
OF HOT MOLECULES**
- **COMPARISON OF LOW-ENERGY  
NITROGEN ION AND NEUTRAL  
BOMBARDMENT**



Vanderbilt University

# PARTICLE AND PHOTON INTERACTIONS WITH SURFACES

## Identification of ENERGY PATHWAYS; ELECTRONIC PROCESSES



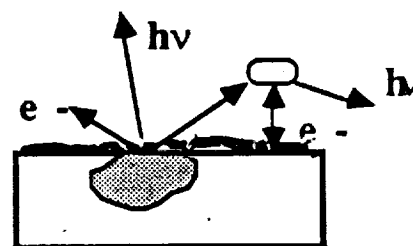
### EXCITATION

- One Hole
- Two Holes
- Exciton
- Defect
- Electronic excitations



### PARTITIONING

- Desorption-DIET
- Luminescence
- Charge Separation
- Dissociation
- Bond-Making
- Defects
- Momentum
- Thermal



### FINAL STATES

- Emitted Particles
- Surface
- Bulk

## ISSUES with regard to ENERGY PATHWAYS

- What is the role of TEMPORAL and SPATIAL LOCALIZATION?
- What is the effect of DOPANTS, DEFECTS and OVERLAYERS?
- What is the effect of SUBSTRATE TEMPERATURE?
- By changing the SURFACE or BULK ELECTRONIC STRUCTURE is it possible to significantly alter the ENERGY PATHWAY?

Center for Atomic and Molecular Physics at Surfaces

# ENERGY-SURFACE INTERACTION RESEARCH AT VANDERBILT

## VANDERBILT FACILITIES:

### --Photon Sources

- CW and Pulsed Lasers
- Vanderbilt FREE-ELECTRON LASER (FEL) X-ray
- Vanderbilt/SRC Beamline, Madison, WI

### --Electron-Beam Sources

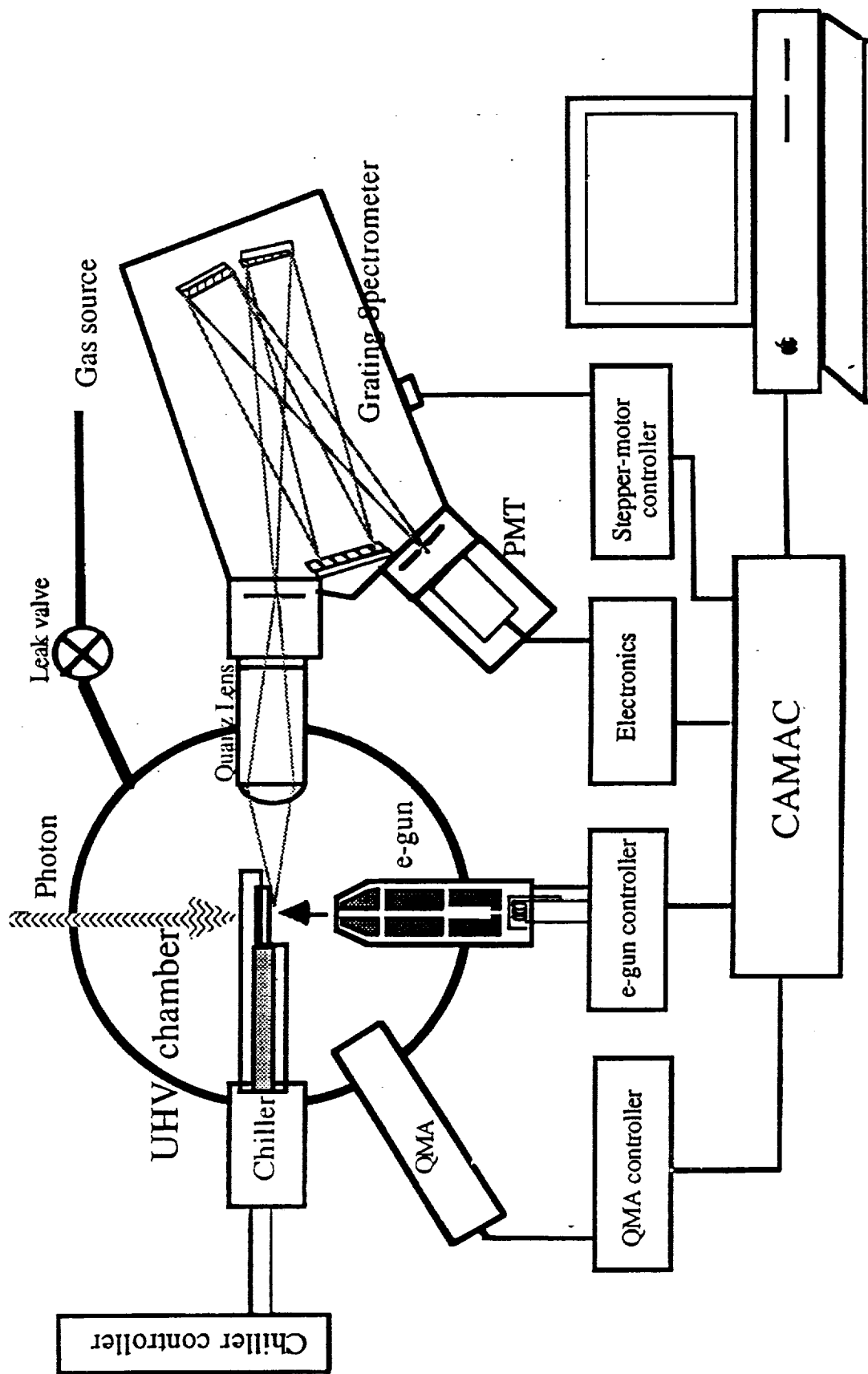
- 10 eV to 1 keV low-Energy Source
  - 40 MeV FEL Source
- X-Ray  
Simulation**

### --Ion and Neutral Atomic and Molecular Beam Sources

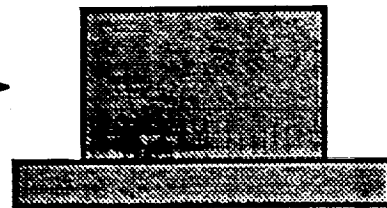
- Neutral Atomic O and Molecular N<sub>2</sub> Grazing Inc. Source
- Universal Ion Sources, 5 eV to 300 keV



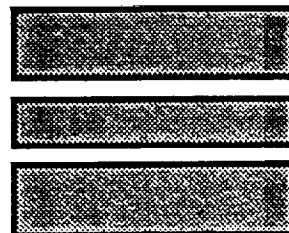
# Experimental Setup



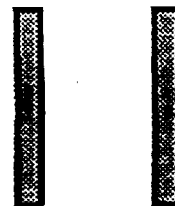
**COLUTRON ION SOURCE** →



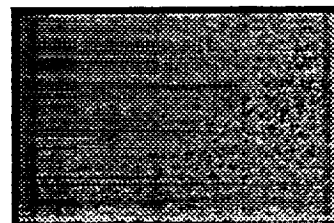
**ELECTROSTATIC LENS** →



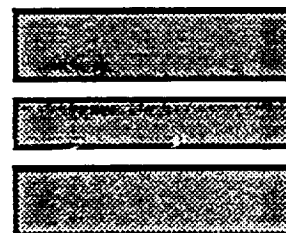
**DEFLECTION PLATES** →



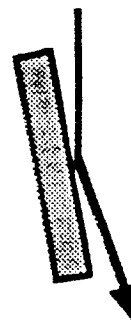
**WIEN FILTER** →



**DECELERATOR** →



**NICKEL CRYATAL** →



**TARGET** →



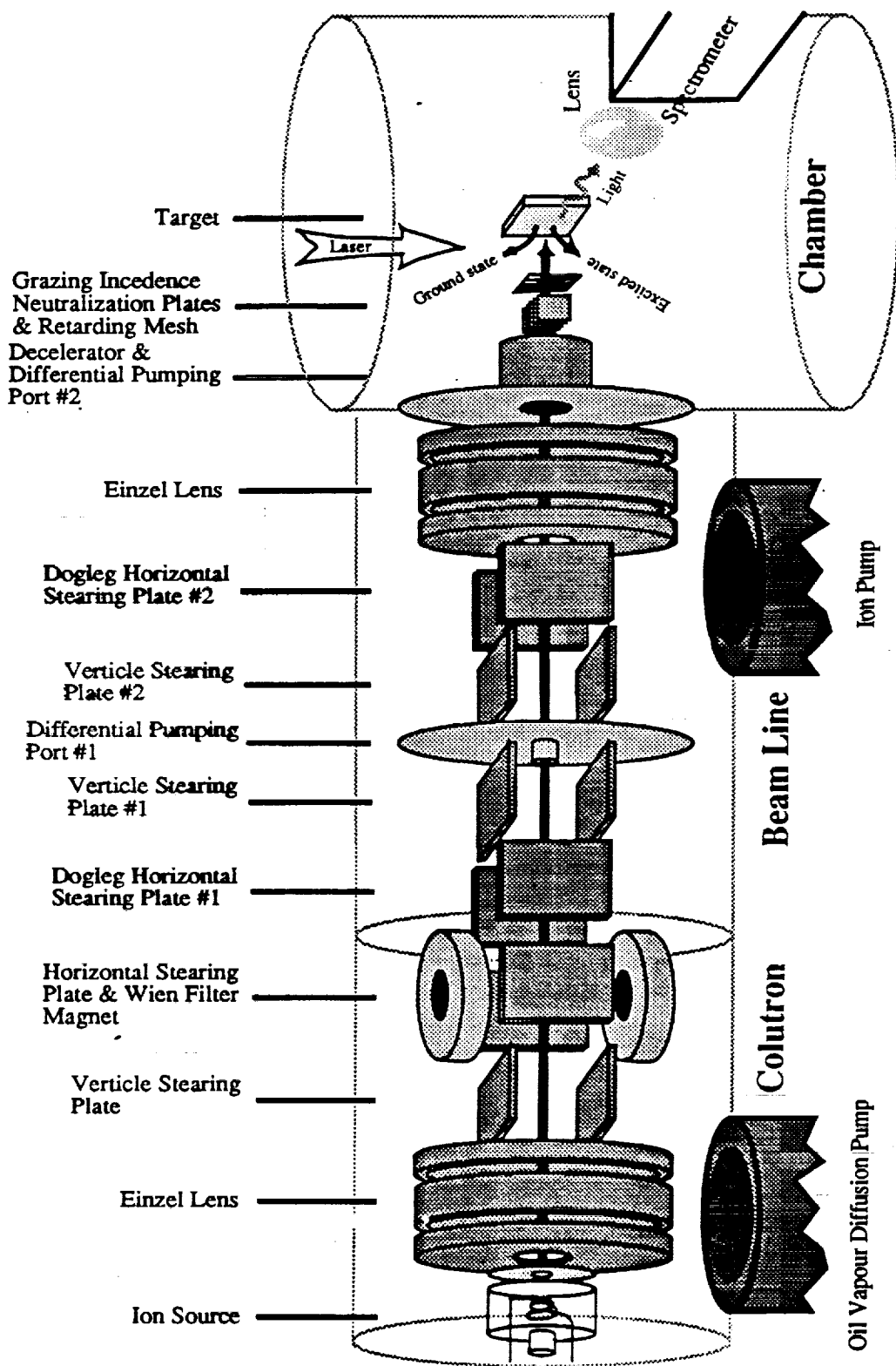
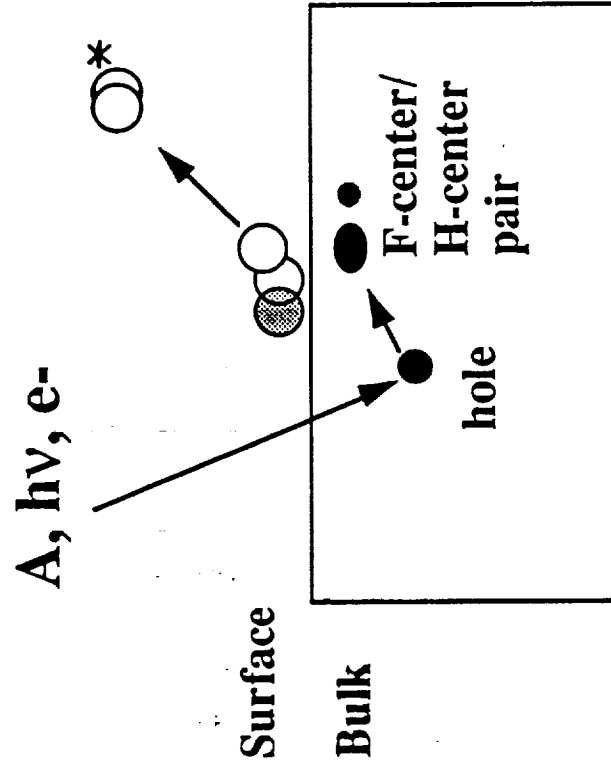


Figure 1

**Low Energy Neutral Source**  
Under Construction at Vanderbilt University

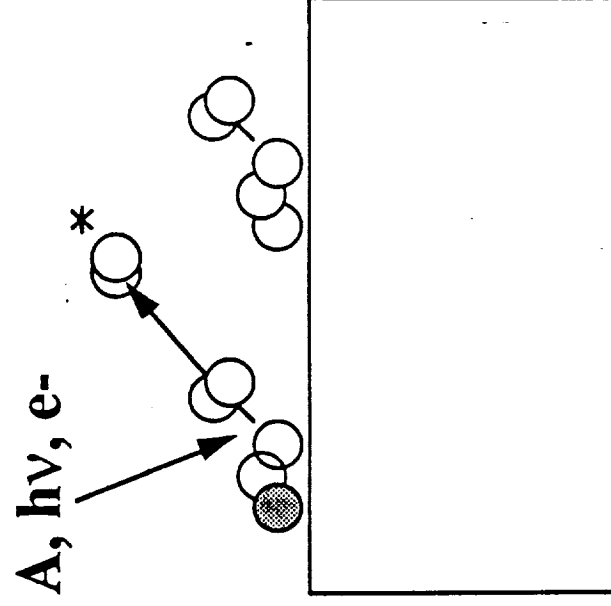
*Cmass...*

## ELECTRONICALLY STIMULATED DESORPTION MECHANISMS



I

**DEFECT MEDIATED  
DESORPTION  
(GLOW AND EROSION)**



II

**DIRECT SURFACE BOND-  
BREAKING  
(GLOW AND EROSION)**



Vanderbilt University

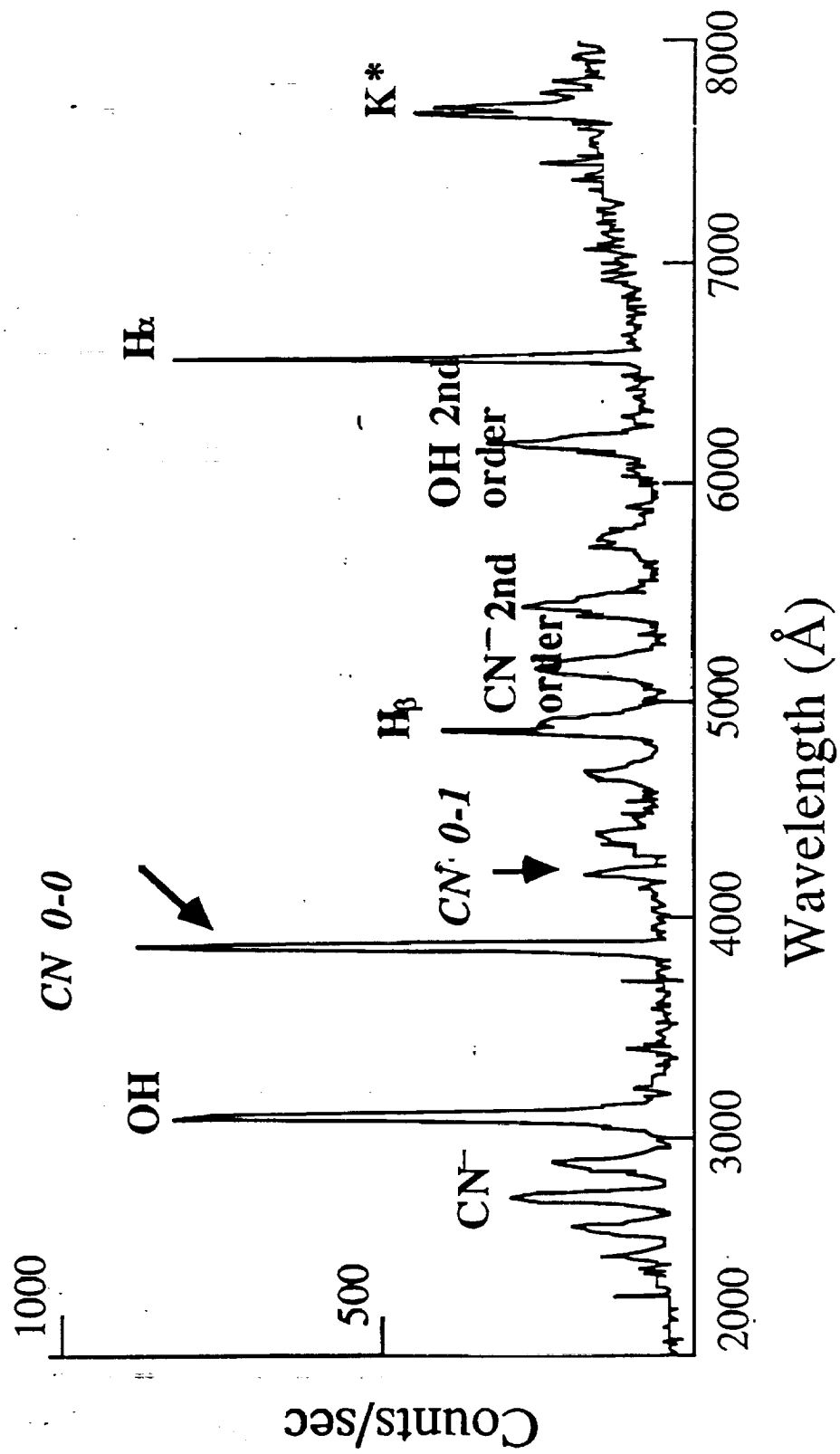
# **Optical Emmission (Glow) on Cool Surfaces in a Space Environment**

**N.H. Tolk, R.G. Albridge, A.V. Barnes,  
S. Espy, M. Riehl-Chudoba, J. Qi, and J. Xu**  
Center for Atomic and Molecular Physics at Surfaces  
Department of Physics and Astronomy  
Vanderbilt University  
Nashville, TN

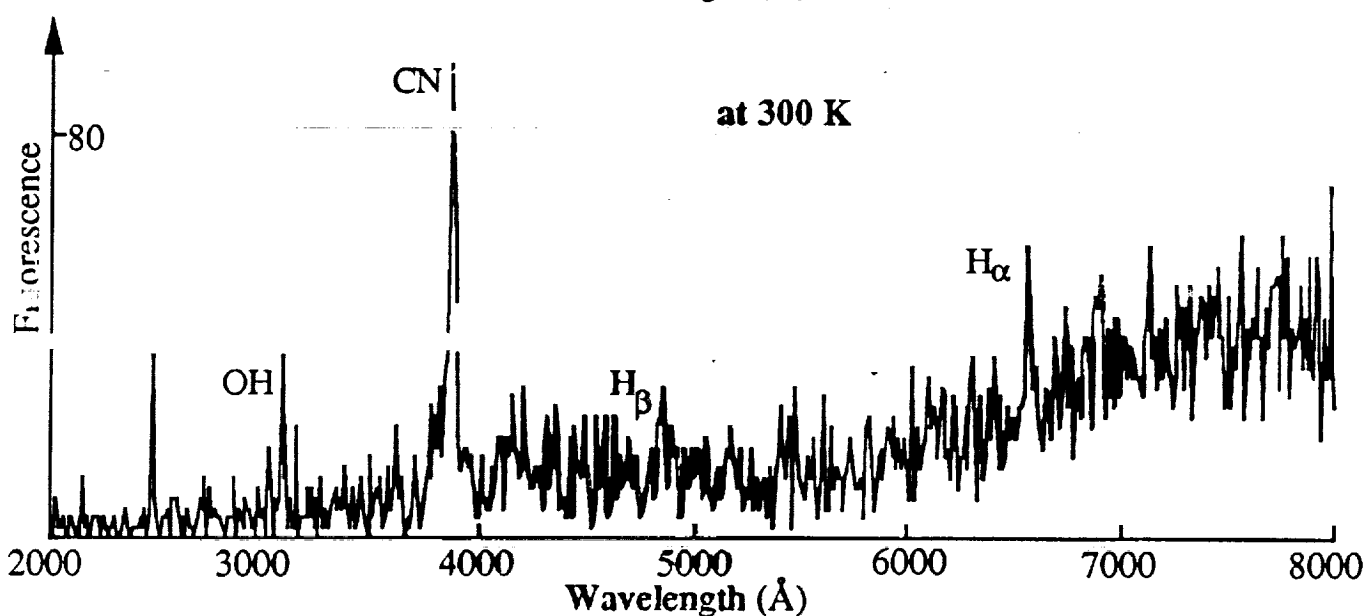
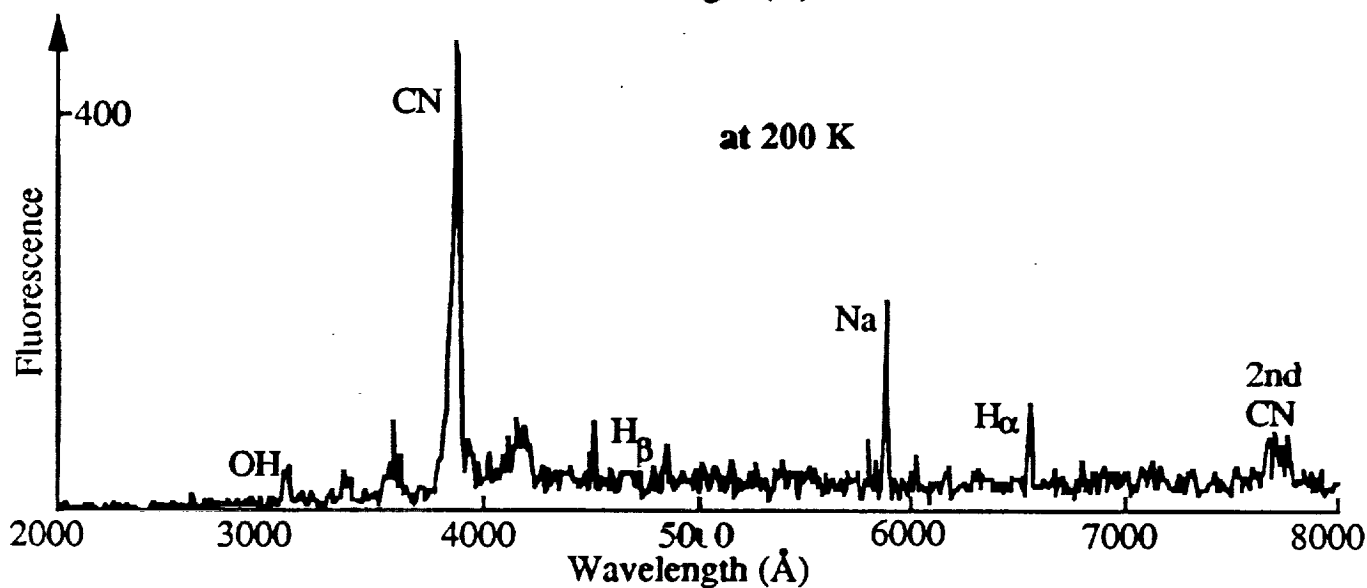
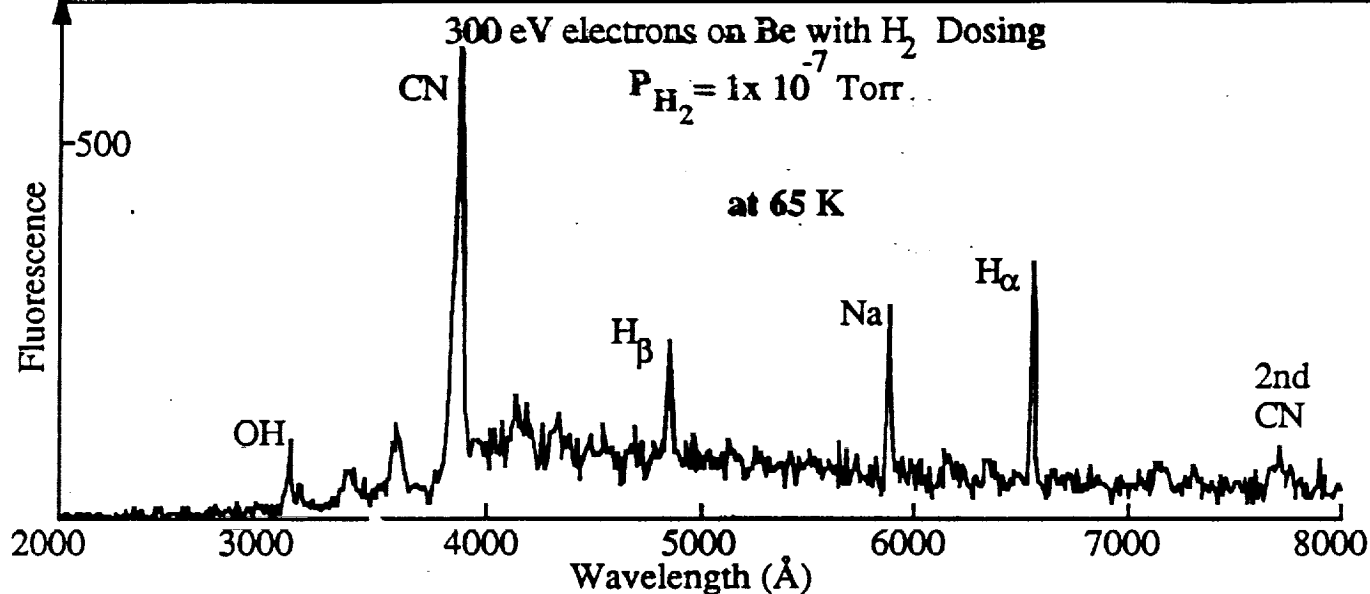


**Vanderbilt University**



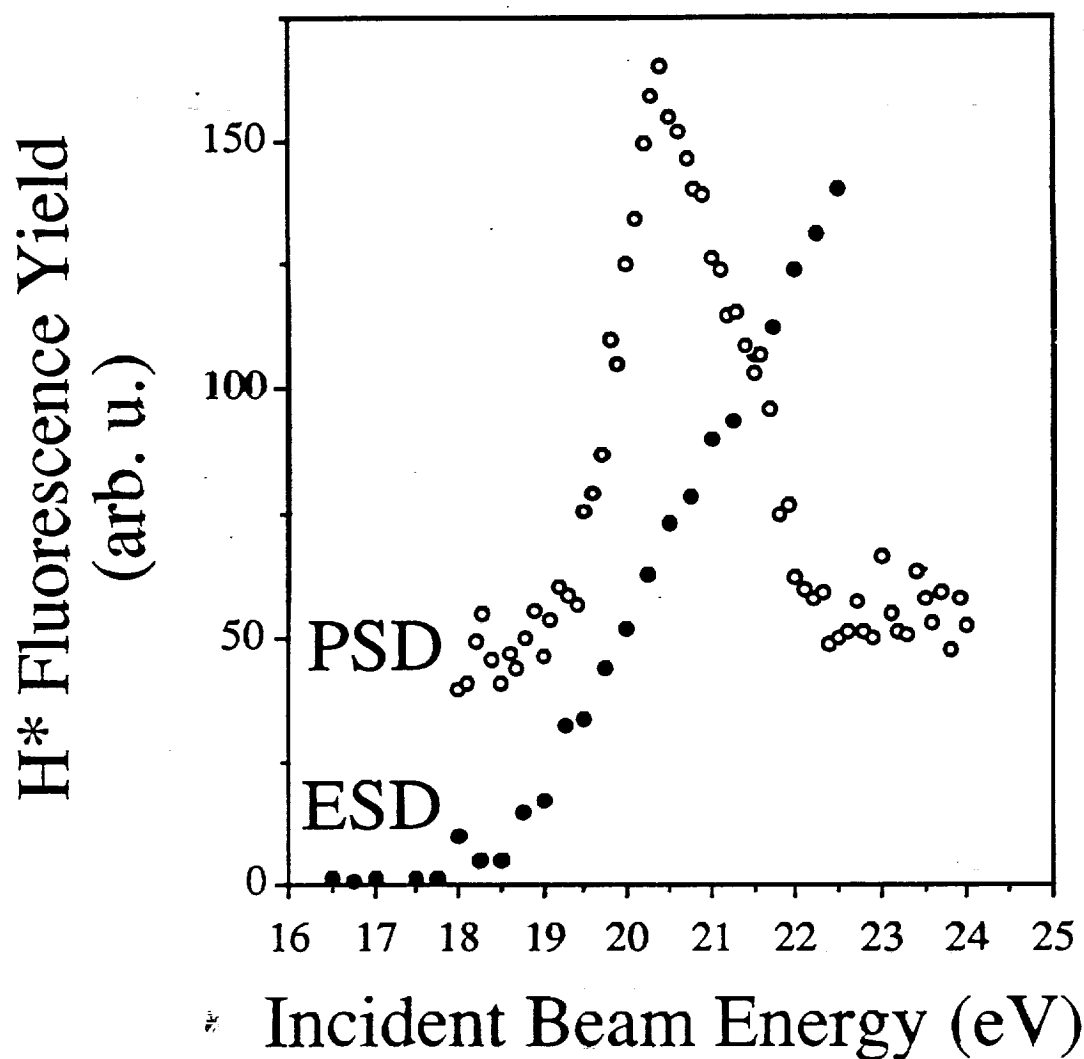


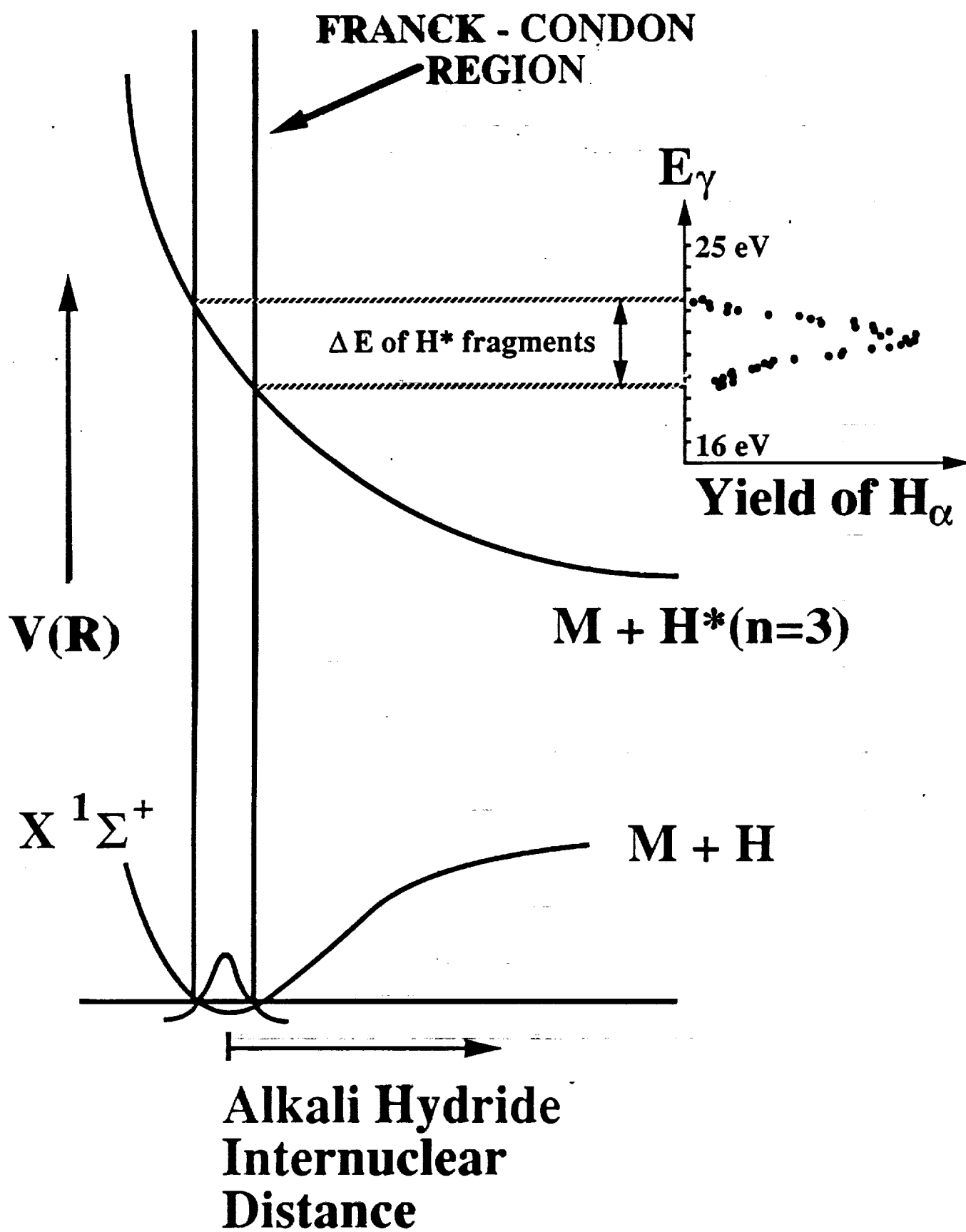
● Glow is significantly brighter at lower temperatures.



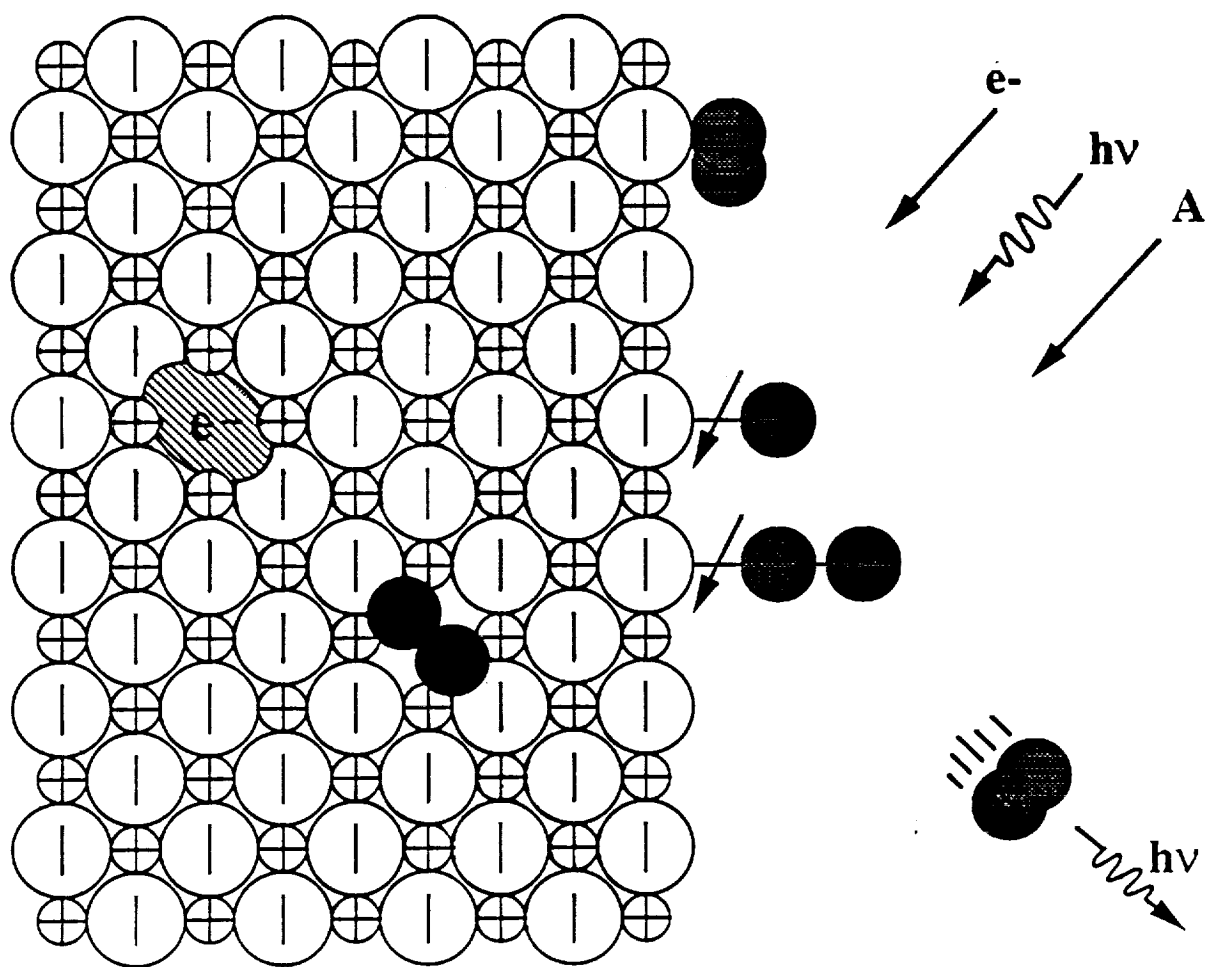
# Comparison of Electron and Photon Energy Dependent Yields of $H^*$ from KCl

**Surface Bond breaking**

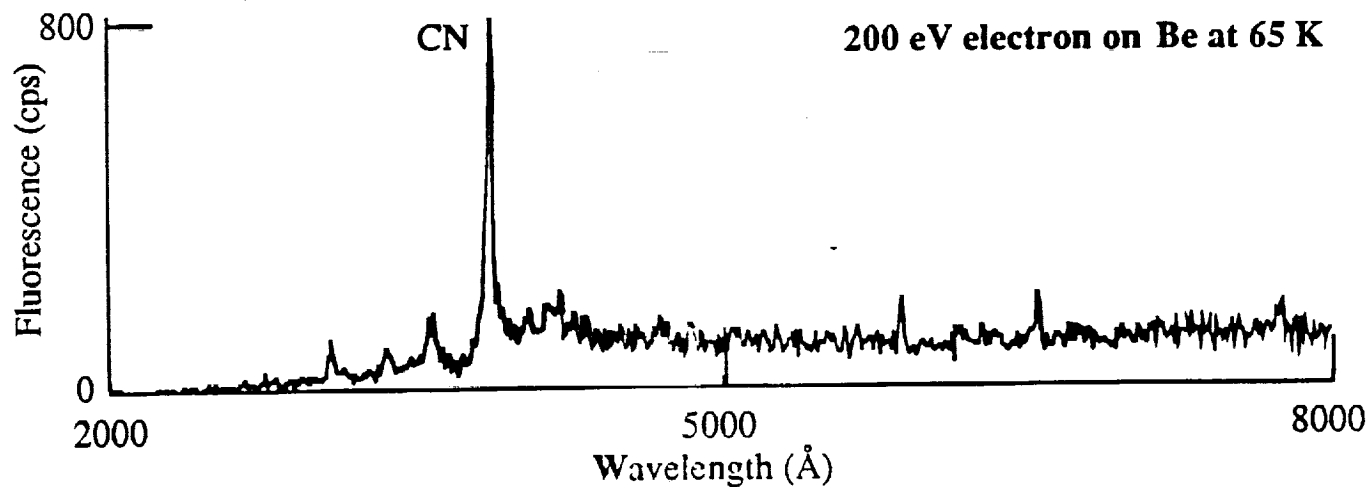
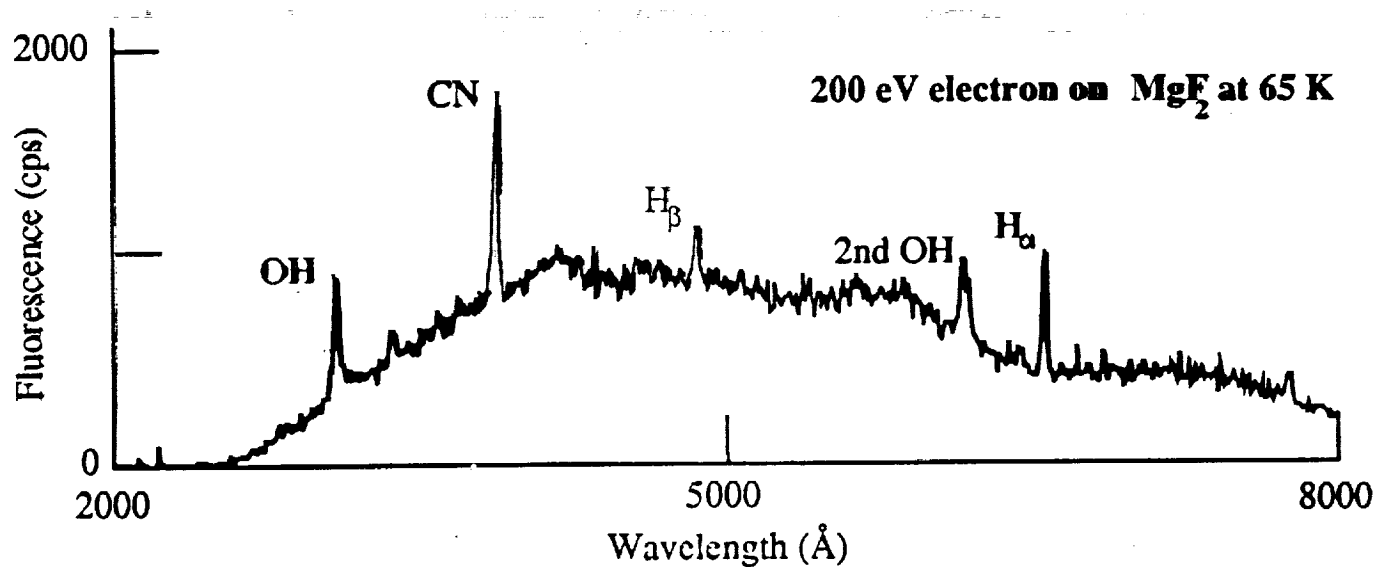
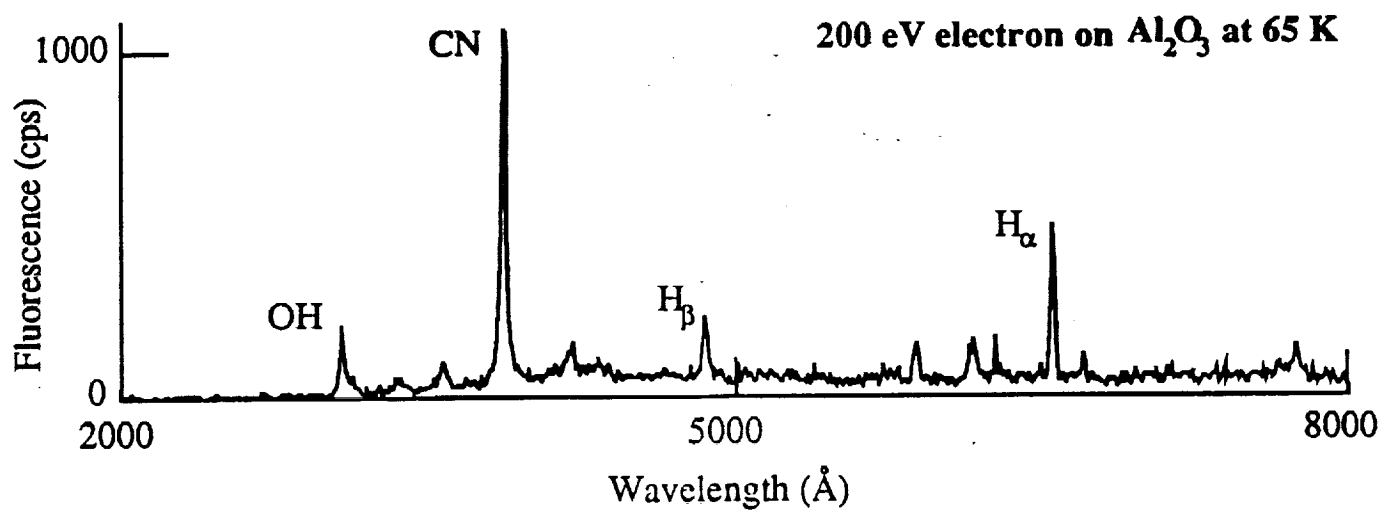




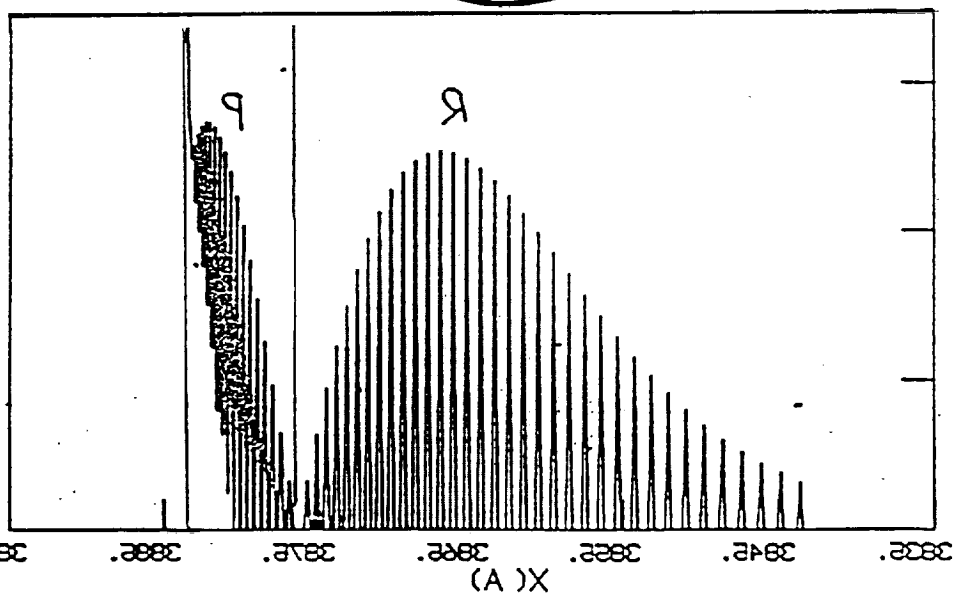
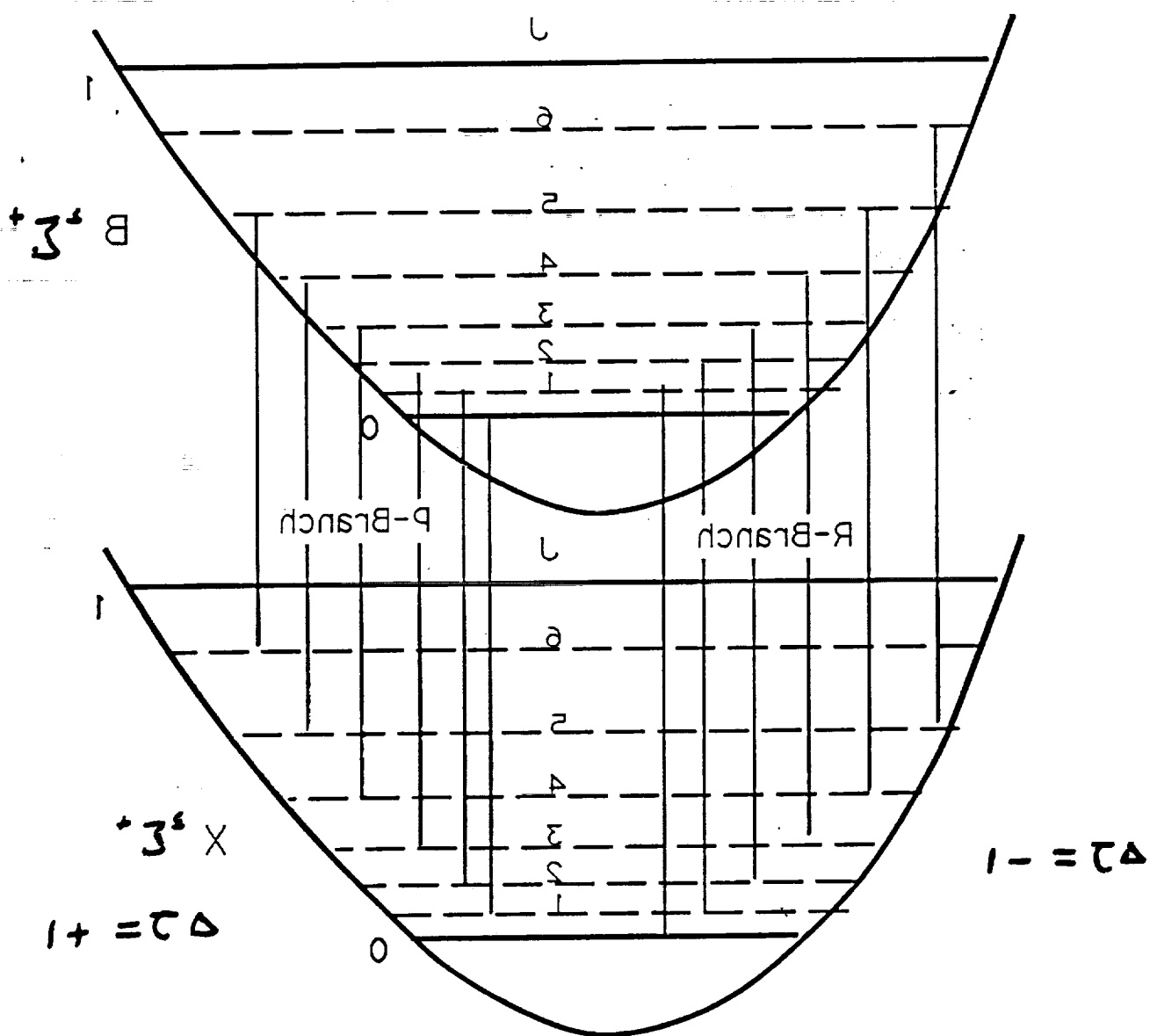
## Direct Surface Molecular Bond Breaking



**Air dosing**  
( $p_{\text{Air}} = 1.0 \cdot 10^{-7}$  mbar)



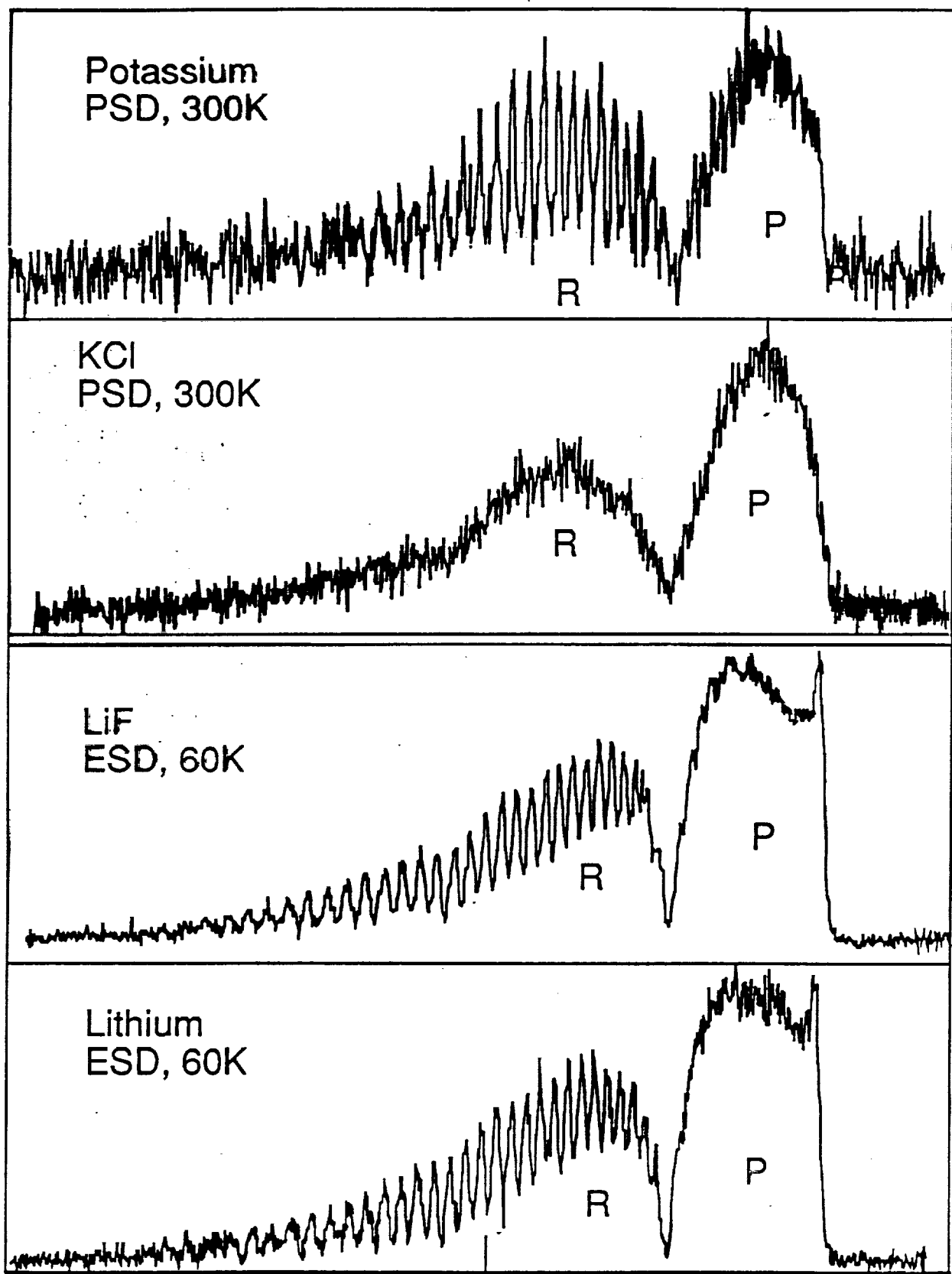
# [Measurements of Rotational Energy Distribution] Distribution of R and P Branches



ORIGINAL PAGE IS  
 OF POOR QUALITY

Each line represents one or more lines.

FLUORESCENCE YIELD (ARB. UNITS)



3840

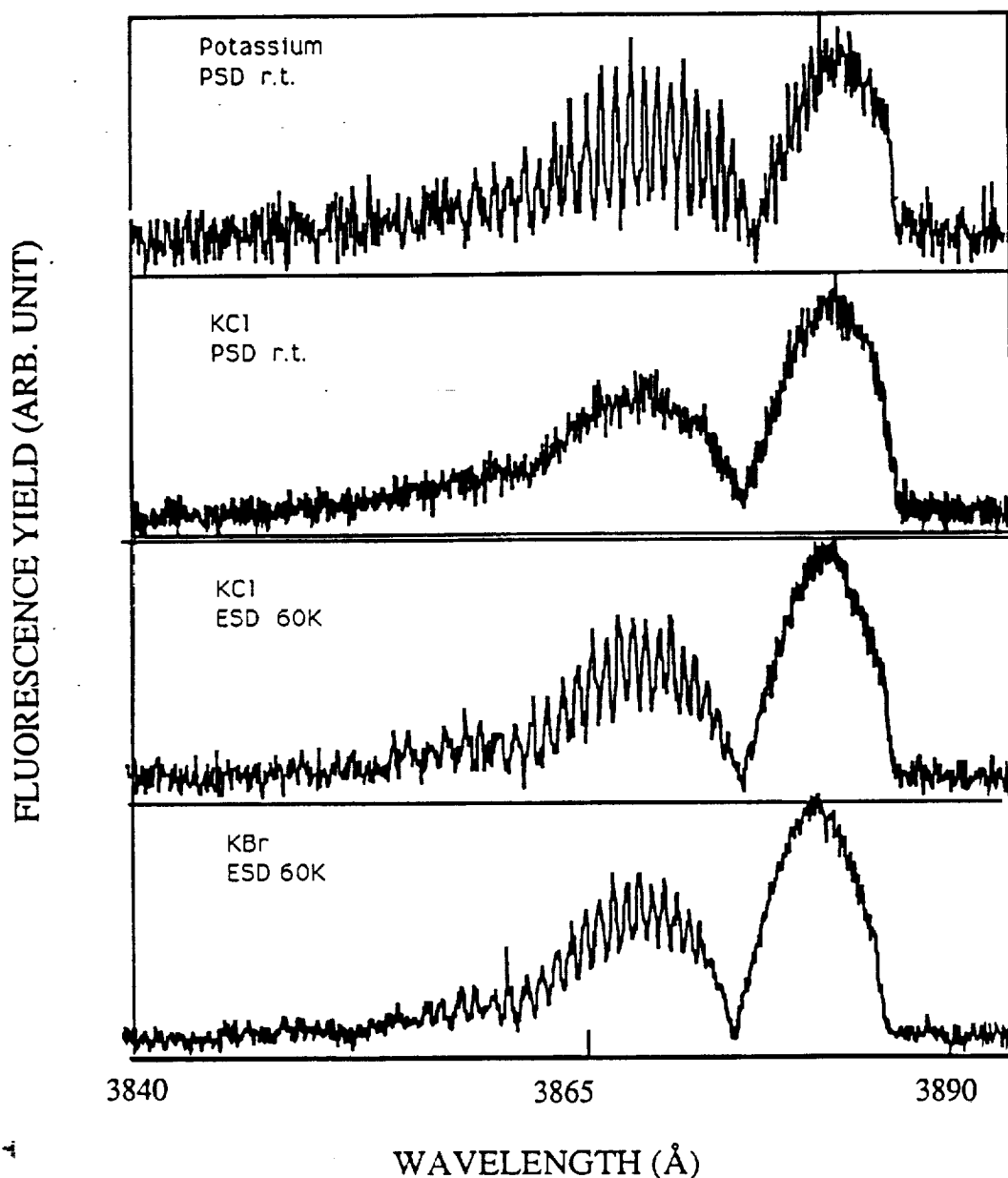
3865

3890-

WAVELENGTH (Å)



# Rotational distribution of desorbed CN\* from potassium related surfaces



Rotational Distributions are about same for potassium related substrates,

Independent of {

- 1. Halide
- 2. temperature
- 3. radiation source

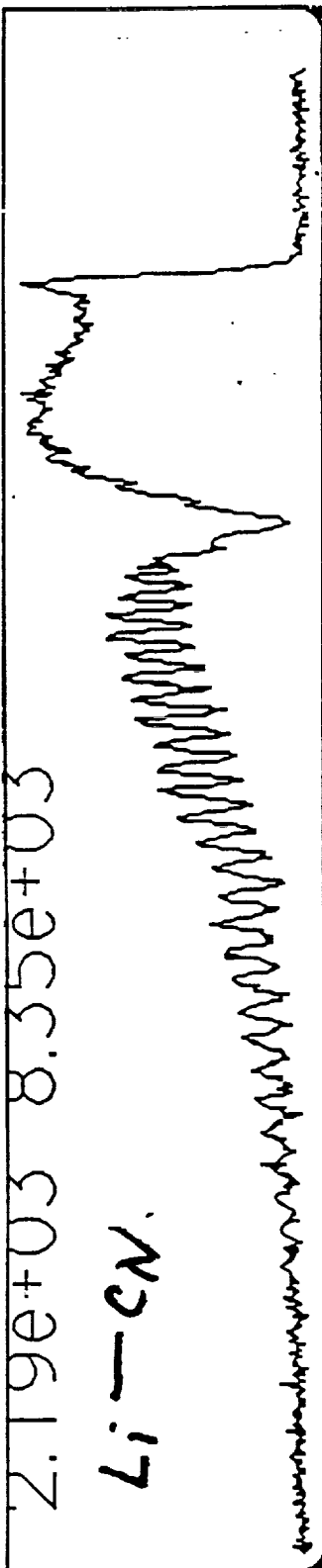
ORIGINAL PAGE IS  
OF POOR QUALITY

60 K e + LiF

051990.01

2.19e+03 8.35e+03

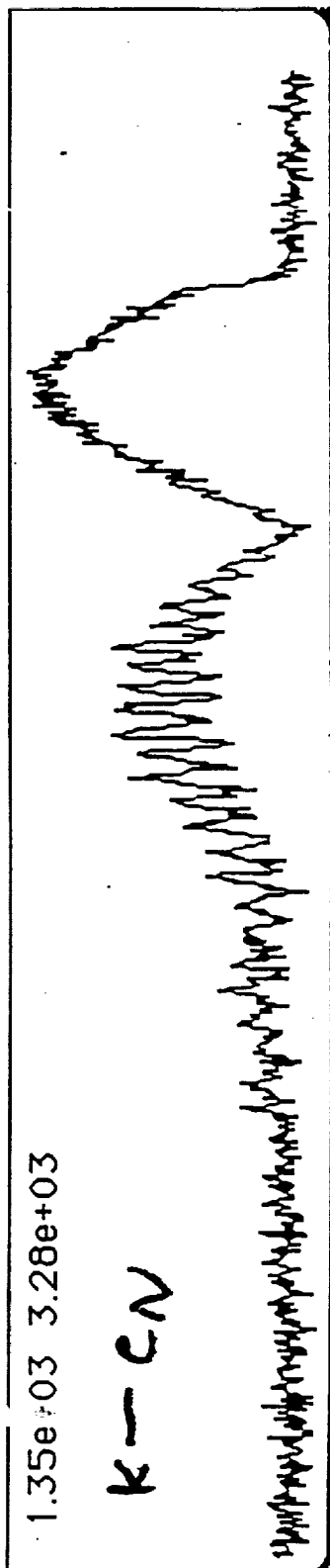
Li-CN



052390.01 KCl

1.35e+03 3.28e+03

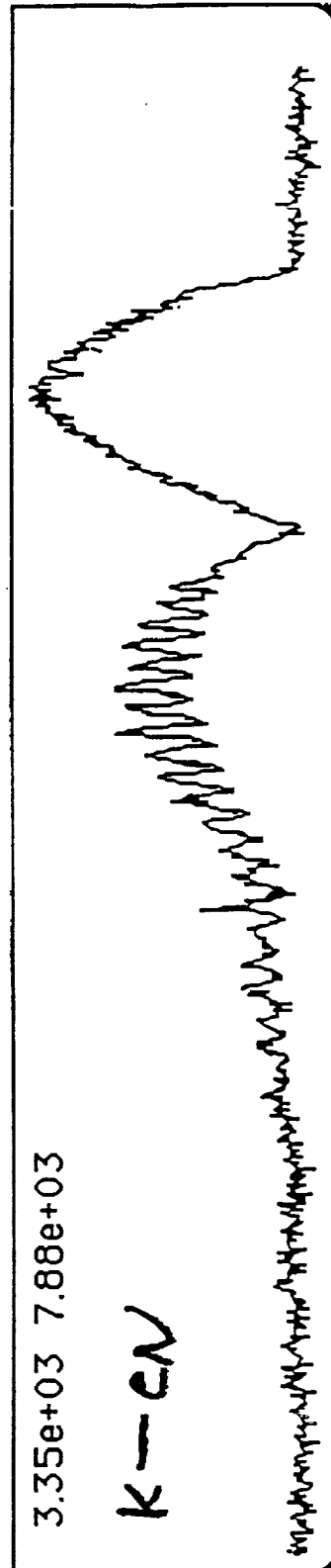
K-CN



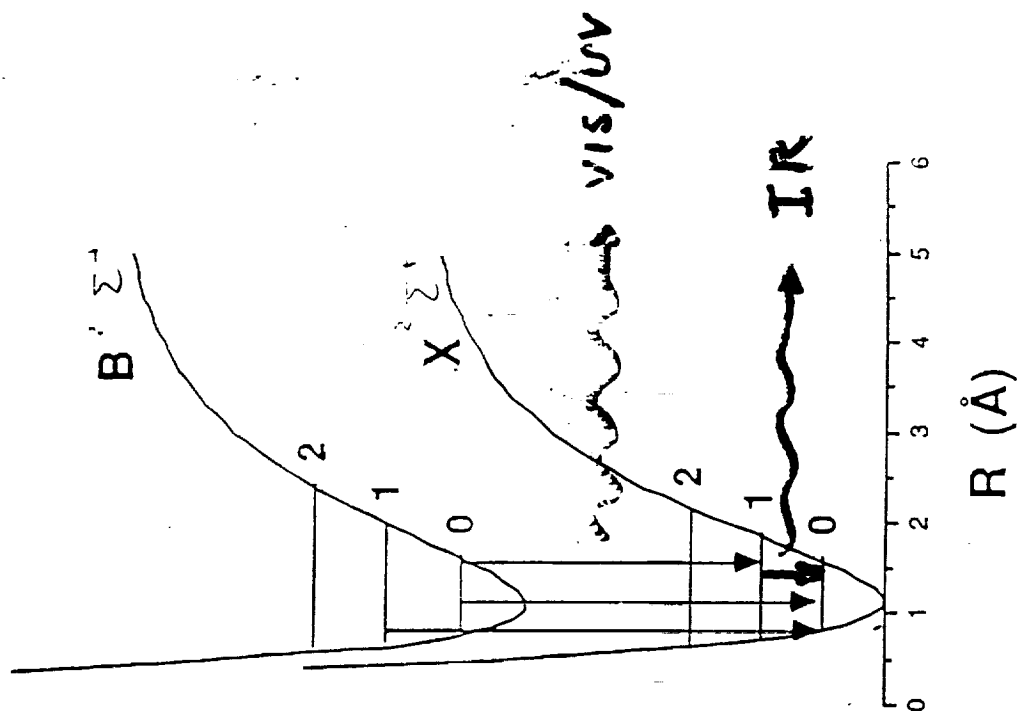
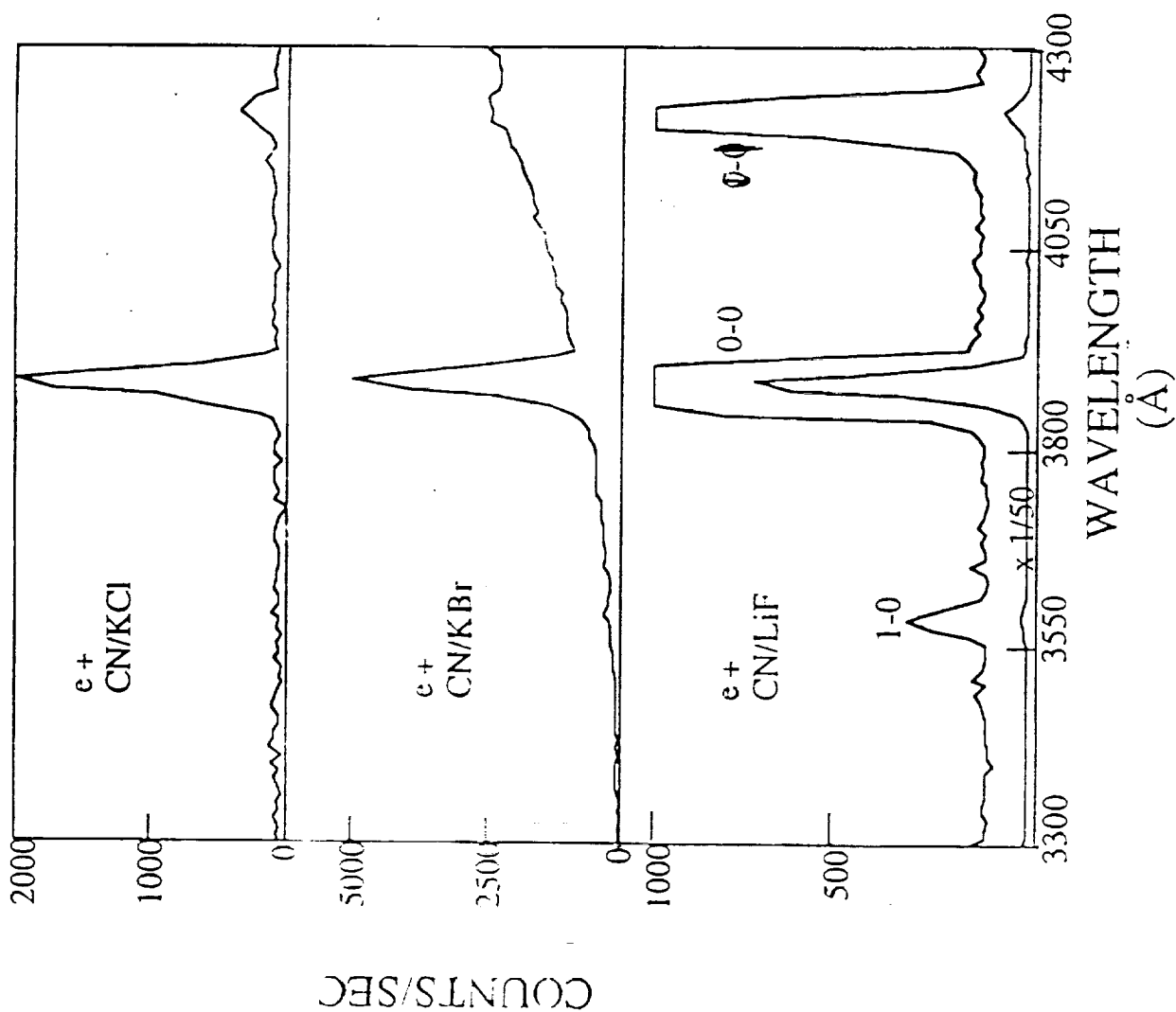
052290.01 KBr

3.35e+03 7.88e+03

K-CN



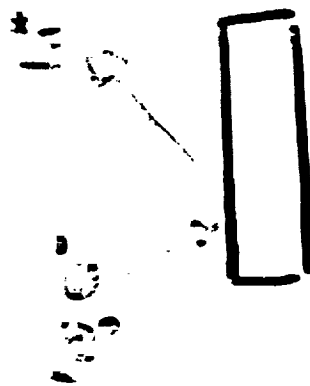
# Identification of CN\* Desorption



ORIGINAL PAGE IS  
OF POOR QUALITY

# New Mechanism for the Production of Excited Alkali Atoms by Photon Bombardment of Alkali Halide Crystals

Dengfa Liu, Alan V Barnes, and Norman H. Tolk  
*Department of Physics and Astronomy, Vanderbilt University*  
Nashville, Tennessee, USA 37235



Indirect!

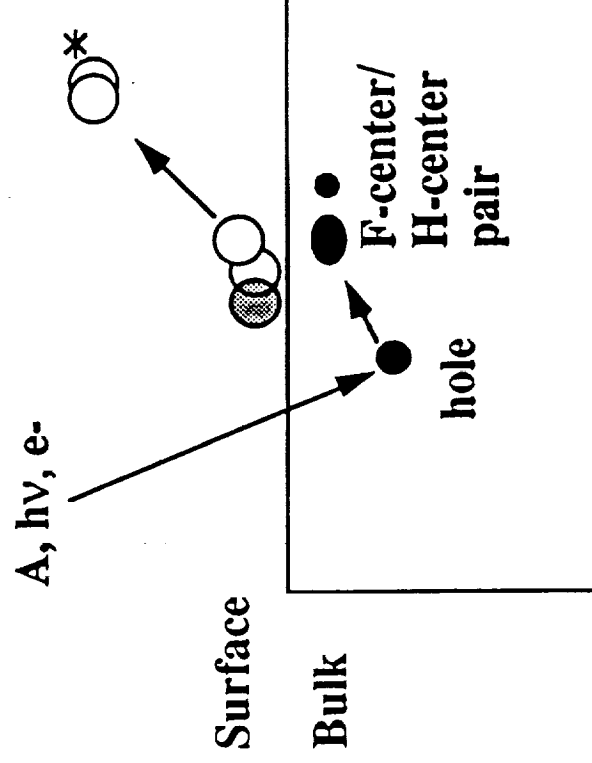
ORIGINAL PAGE IS  
OF POOR QUALITY

*Cmass...*

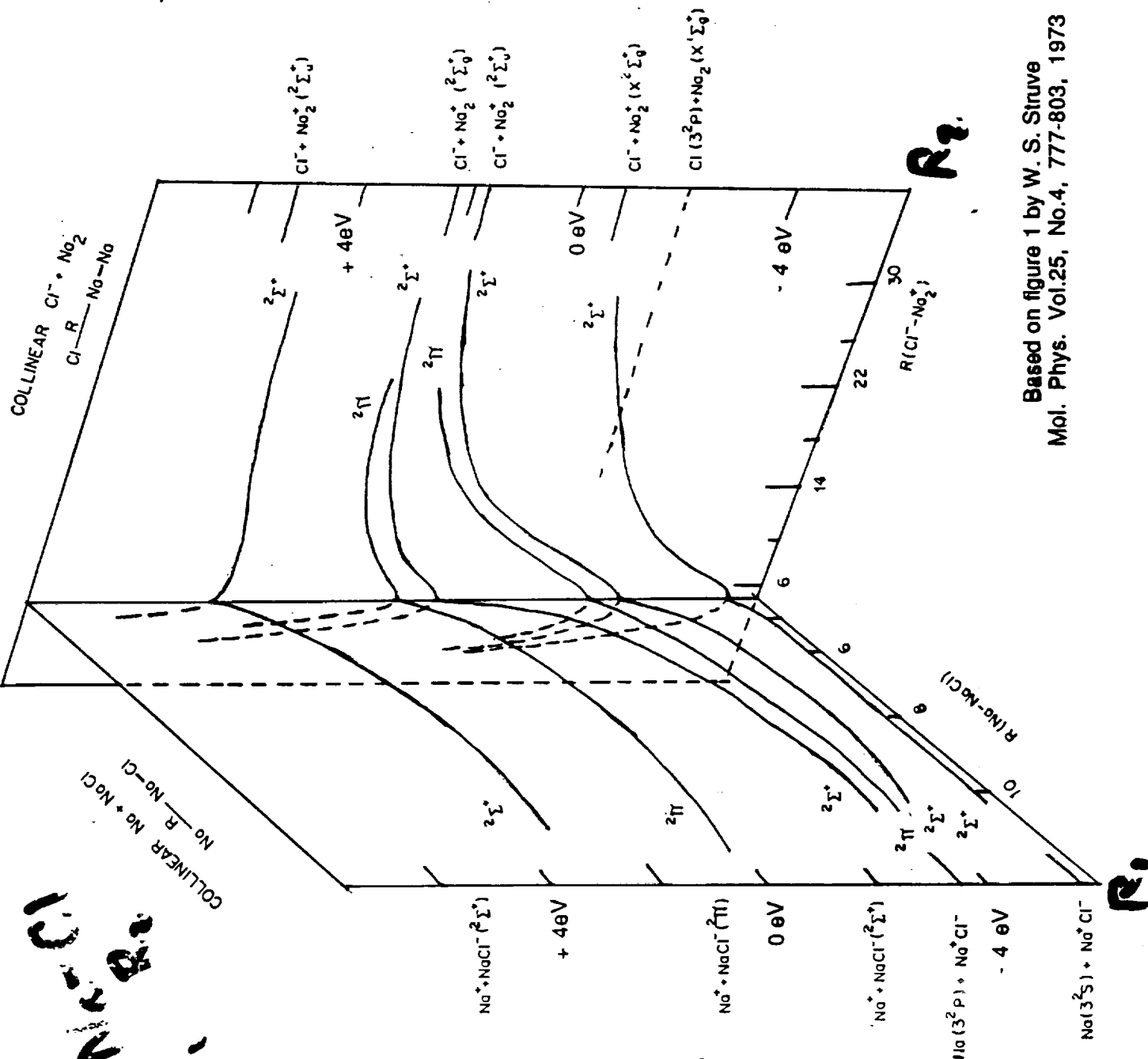
**GAS PHASE REACTION RESULTING  
IN  
ATOM EJECTED IN EXCITED STATE**



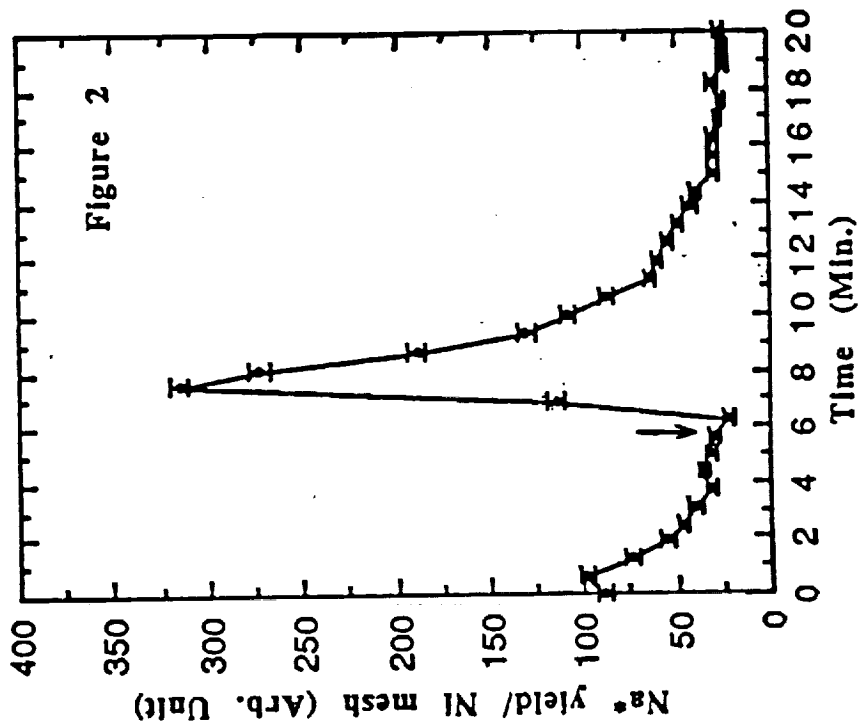
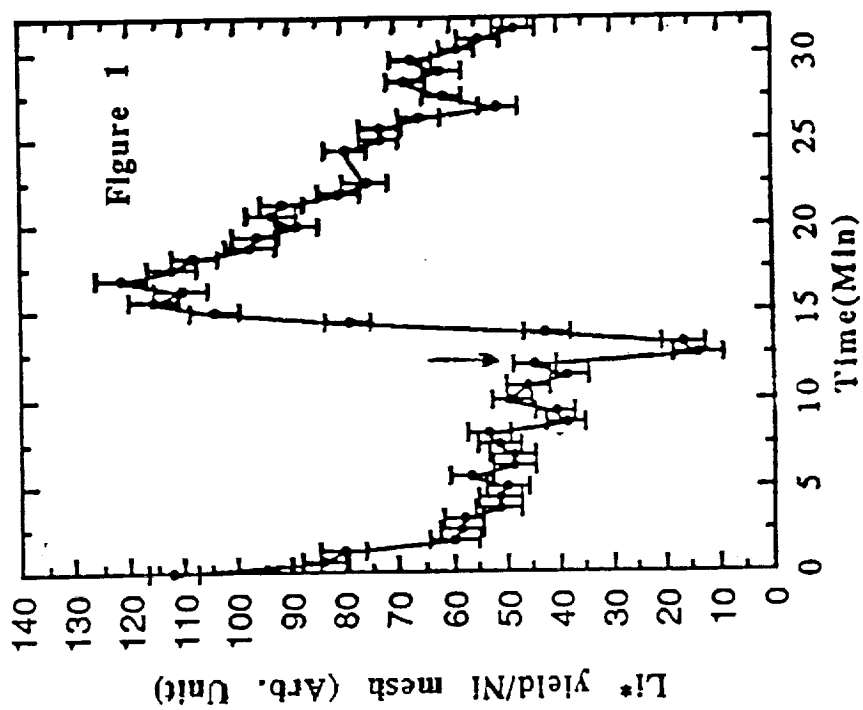
***WE HAVE SHOWN THE SAME THING APPLIES  
FOR THE SURFACE REACTION***



Vanderbilt University



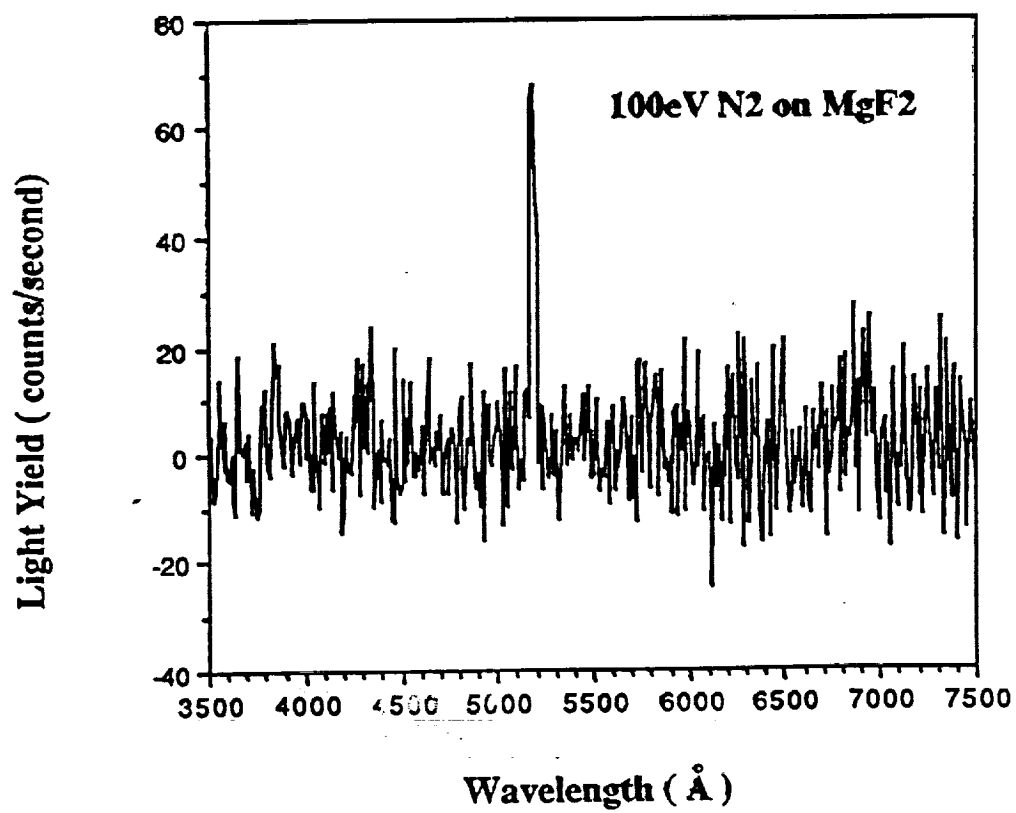
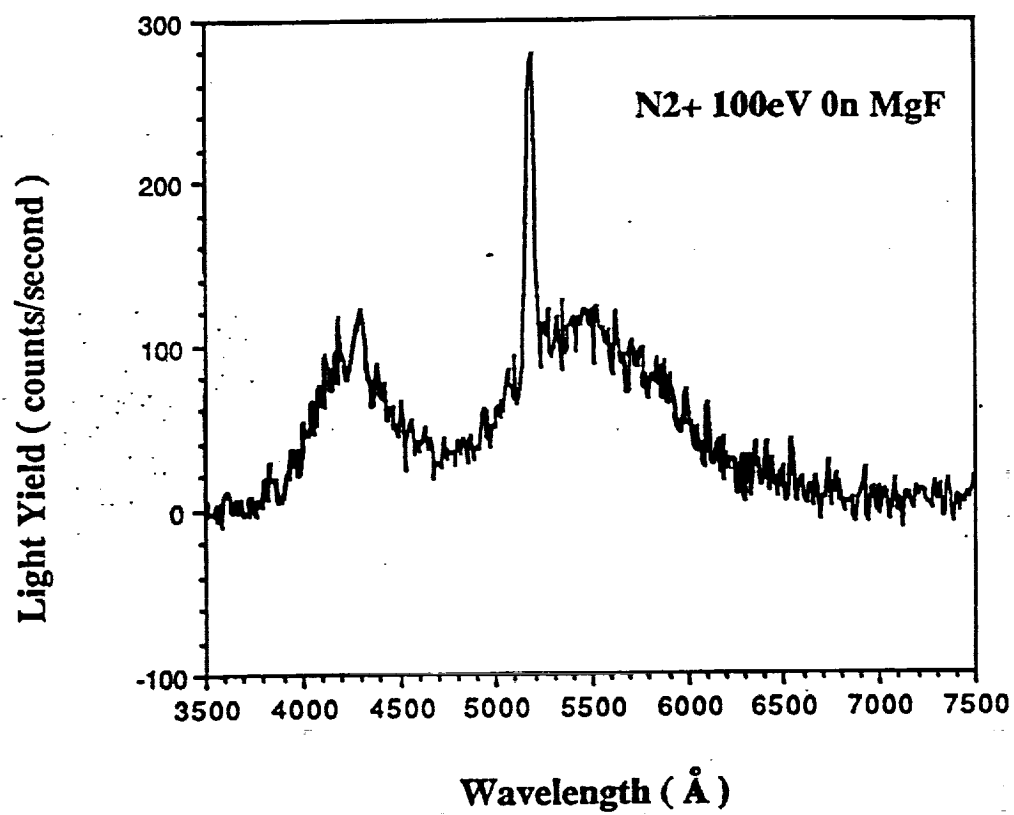
Based on figure 1 by W. S. Struve  
Mol. Phys. Vol.25, No.4, 777-803, 1973



ORIGINAL PAGE IS  
OF POOR QUALITY

Li\* yield to LiF (Fig. 1) and Na\* (Fig. 2)

The readings last about 10 seconds.



ORIGINAL PAGE IS  
OF POOR QUALITY



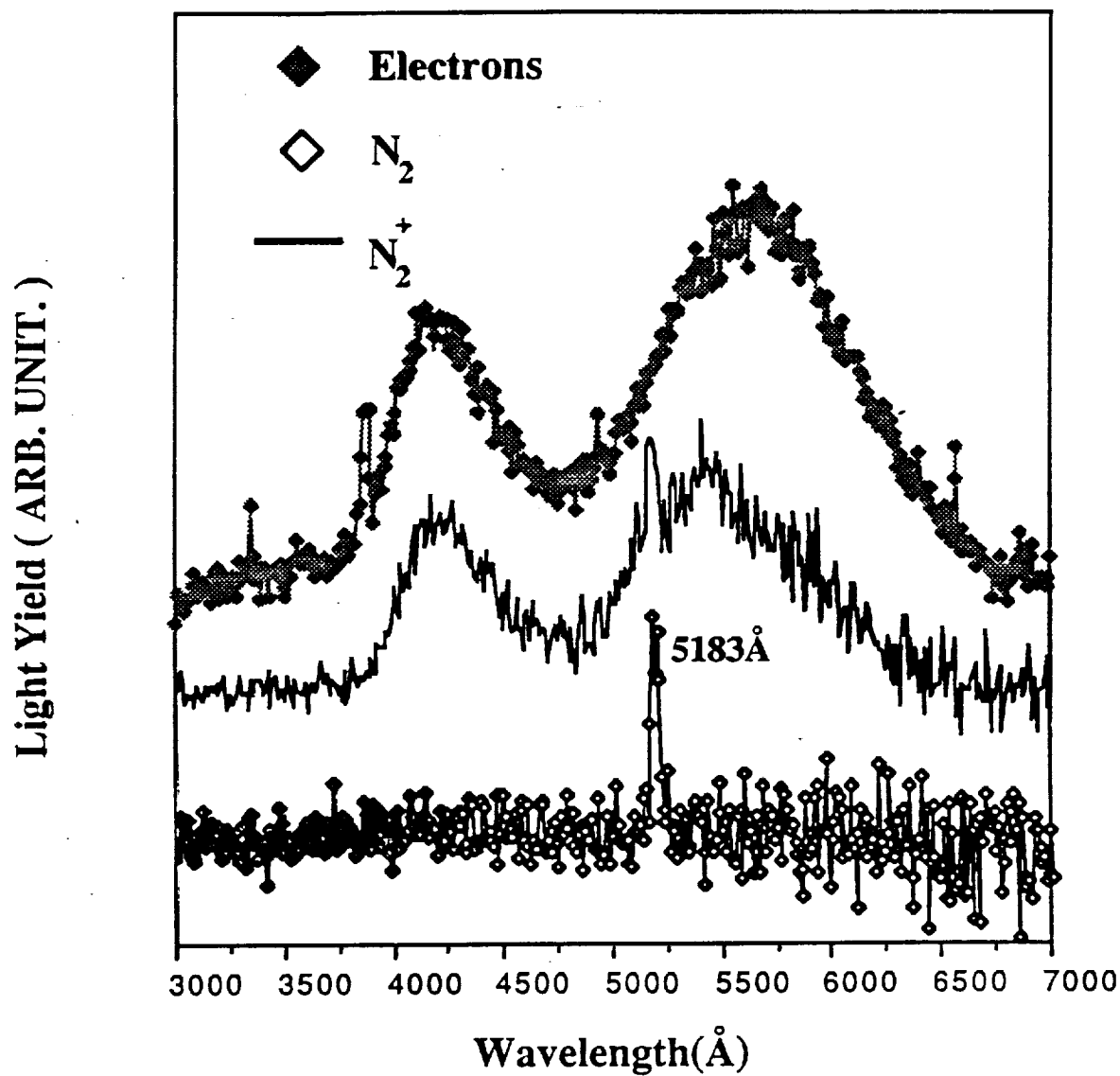


Fig 4.

Net Creation

ORIGINAL PAGE IS  
OF POOR QUALITY



8. **APPENDIX D**

UVI Science Team Meeting  
Park City, Utah  
August 15-16, 1990



# UVI SCIENCE TEAM MEETING

Park City, Utah  
15, 16 August 1990

## ATTENDEES

Joe Ajello  
Ken Clark  
Bob Clauer  
Glynn Germany  
George Parks  
Jim Spann  
Doug Torr  
Marsha Torr

**ULTRAVIOLET IMAGING TEAM MEETING  
PARK CITY, AUGUST 15-16, 1990**

**REVISED PRELIMINARY AGENDA (8/6/90)**

**WEDNESDAY: AUGUST 15, 1990**

9:00am	INTRODUCTION Instrument Overview Project Status Objectives of Meeting	M. Torr
10:00am	Discussion	All
10:30am	Break	
11:00am	Strawman Mission Observing Sequences	M. Torr
11:30am	Discussion	All
12:00noon	Lunch	
1:30pm	REVIEW OF SCIENCE OBJECTIVES  What Should We Be Doing in 1993.	G. Parks
2:15pm	Discussion	All
2:45pm	More of What We Should Be Doing in 1993.	P. Banks
3:30pm	Break	
4:00pm	Discussion	All
4:30pm	What We Should Be Doing in 1993	J. Ajello/ B.Tsurutani
5:15pm	Adjourn for Day	

**THURSDAY: AUGUST 16, 1990**

8:30am	Review of Science Objectives continued Imaging Science for 1993	K. Clark
9:15	ANALYSIS TOOLS Overview	M.Torr
9:30am	Energy Deposition Code/ Energy Flux Extraction	D. Torr
10:00am	Characteristic Energy Extraction	G. Germany
10:30am	Break	
10:45am	Signal Extraction: Part I	D. Torr
11:00am	Use Of "Snakes" to Extract Auroral Oval	R. Clauer
12:00noon	Lunch	
1:30pm	LBH and NI Cross Sections	J. Ajello
2:00pm	Field Line Mapping	R. Clauer
2:30pm	Discussion	All
2:45pm	Revised Data Analysis Plan	M.Torr
3:15pm	Summary - action items - other business - next meeting	
4:00pm	Adjourn Meeting	

# INTRODUCTION

Instrument Overview  
Project Status  
Objectives of Meeting

Marsha Torr

9:00      15 August



## ULTRAVIOLET IMAGER

### GLOBAL GEOSPACE SCIENCE/POLAR S/C MISSION SUMMARY:

LAUNCH: JUNE 1993

DELIVERY OF INSTRUMENTS TO GE ASTRO: JAN-FEB 1992

DELTA-TYPE LAUNCH VEHICLE

2 YEAR NOMINAL MISSION LIFE TIME

11 INSTRUMENTS MAKE UP PAYLOAD

3 INSTRUMENTS LOCATED ON SINGLE AXIS DESPUN  
PLATFORM

CDR's COMPLETE ON MOST INSTRUMENTS

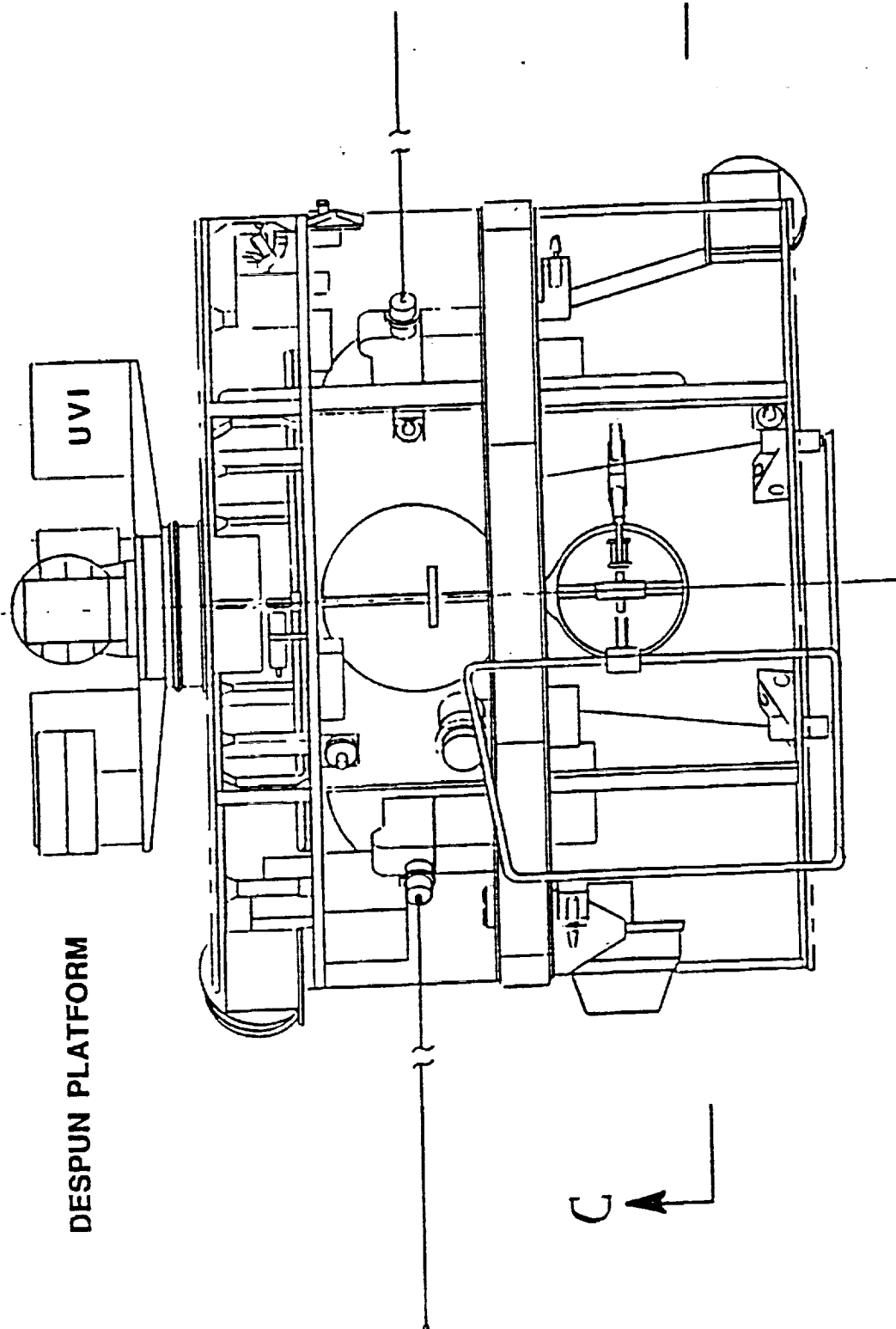
SPACECRAFT CDR SCHEDULED FOR AUGUST 28-30, 1990

PROJECT AS A WHOLE APPEARS TO BE PROGRESSING WELL

Z

DESPUN PLATFORM

UVI



C A

POLAR SPACECRAFT

## ULTRAVIOLET IMAGER: 8/15-16/90

### STATUS OF ULTRAVIOLET IMAGER DESIGN:

ALL ASPECTS OF MECHANICAL DESIGN ARE COMPLETE AND ARE MACHINED, IN THE SHOP OR BEING PREPARED FOR THE SHOP FOR ENGINEERING MODEL

DETECTOR BOARDS ARE COMPLETE AND ENGINEERING MODEL DETECTOR IS BEING ASSEMBLED

ALL MIRRORS FOR E.M. ARE FABRICATED AND TESTED

ALL FILTER DESIGNS ARE FABRICATED AND EVALUATED

7 OF THE 9 DISTINCT ELECTRONICS BOARDS ARE DESIGNED AND SEVERAL ARE BUILT AND TESTED

THE GSE IS DESIGNED, THE SOFTWARE IS LARGELY COMPLETE, AND THE S/C SIMULATOR IS PROTOTYPED

CDR HELD AT MSFC: JULY 2-6, 1990

CDR HELD AT GSFC: JULY 11-13, 1990

BOTH WENT VERY WELL

## **ULTRAVIOLET IMAGER - SCIENTIFIC OBJECTIVES**

**TO PROVIDE GLOBAL COHERENT INFORMATION ON:**

- \* THE TOTAL PARTICLE ENERGY INFLUX INTO THE ATMOSPHERE**
- \* THE SPATIAL AND TEMPORAL MORPHOLOGY OF THE AURORA**
- \* AN ESTIMATE OF THE CHARACTERISTIC ENERGY OF THE PRECIPITATING PARTICLES**
- \* CORRELATION OF AUROREAL/POLAR CAP REGIMES WITH OTHER ISTP ELEMENTS IN RELATED PARTS OF THE MAGNETOSPHERE**

## **ULTRAVIOLET IMAGER - INSTRUMENT REQUIREMENTS**

FAST OPTICS (f/3) WITH GOOD SPATIAL RESOLUTION  
(25km from 9Re)

2-D IMAGING OVER RELATIVELY LARGE FIELD OF VIEW ( $8^{\circ}$ )

LARGE DYNAMIC RANGE ( $10^3$  instantaneous over  $10^5$ )  
(10R to 1MR)

ABILITY TO OBSERVE DAY OR NIGHT SIDE (VUV/CsI)

VERY GOOD SCATTERED LIGHT REJECTION  
(particularly in field)

ABILITY TO SPECTRALLY SEPARATE NEARBY BRIGHT LINES

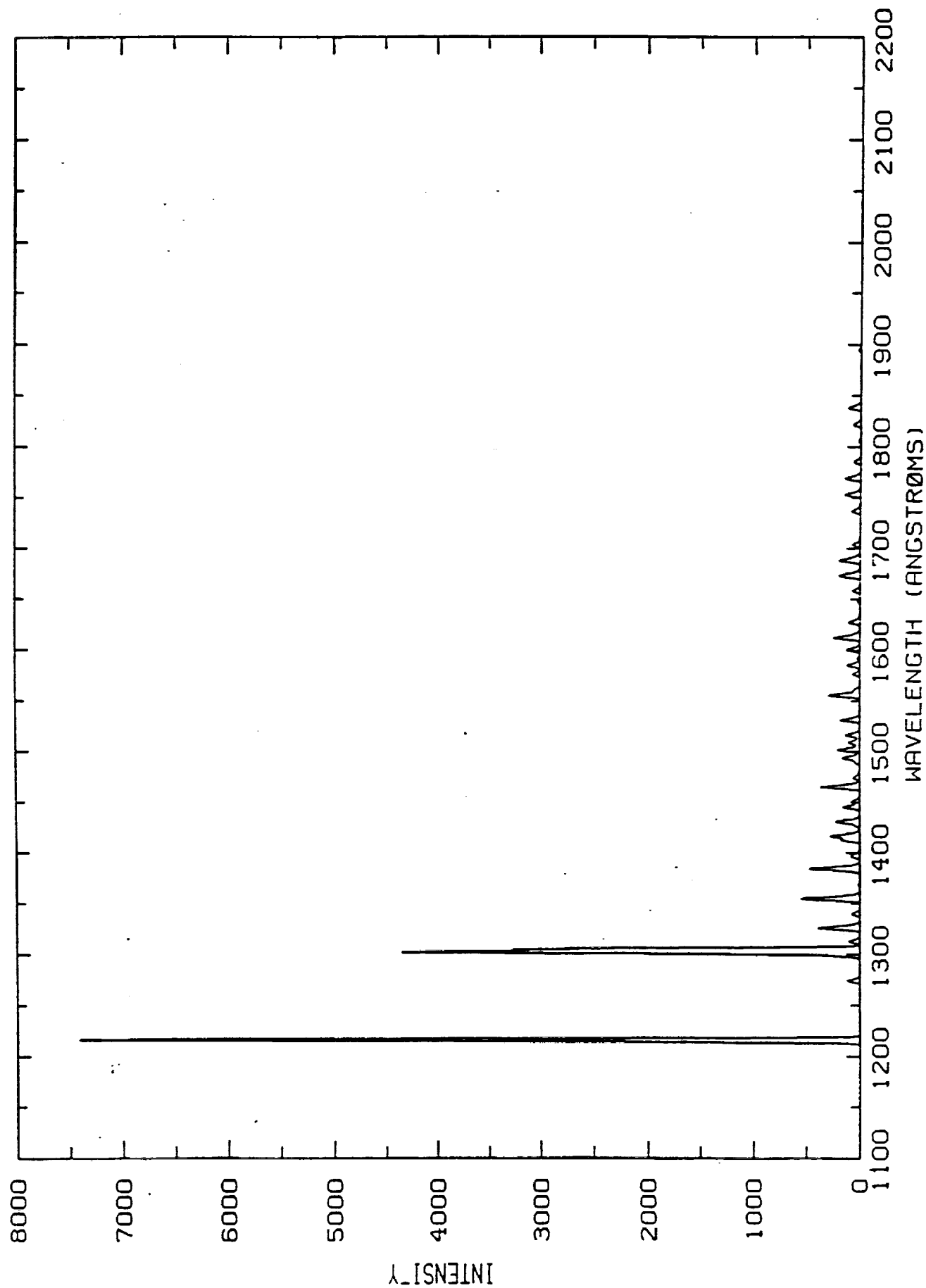
COOL CCDs TO  $<-55^{\circ}\text{C}$  USING PASSIVE TECHNIQUES

ON-ORBIT DAT COMPRESSION FROM  
1.6Mbits/FRAME TO 12kbps

NOMINAL MISSION LIFETIME OF 3 YEARS

ABILITY TO SURVIVE A MISSION RADIATION DOSE OF 300Krad

N2. ØI. NI. HI



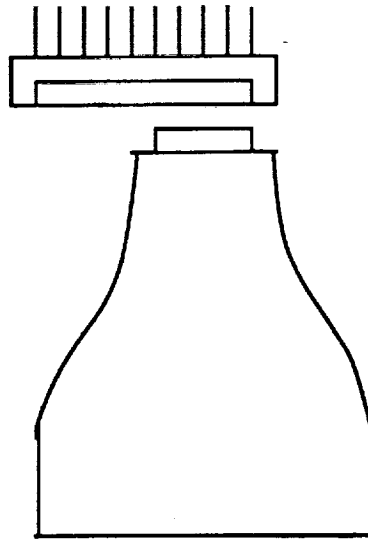
DETECTOR SUMMARY:

INTENSIFIED - CCD DETECTOR SYSTEM

- ITT Generation II Proximity Focussed Image Intensifier
- Thomson CSF 7866 frame transfer CCD
- fiber optic taper (2.74:1)

Represents a refinement of a 15 year continuing evolution of these systems which we have largely pioneered:

- original prototypes built in 1977-1980
- 1 system built for ground based observations of airglow (1982-1983)
- 5 systems flown on Spacelab 1 (1983)
- 2 systems flown on high altitude balloons (1983 and 1986)
- 5 systems built to fly on EOM-1 - due to Challenger used in extended program from McDonald Observatory (1987-1988)
- 1 system built for space prototype and used to observe rocket chemical releases (1989)
- 5 systems built for ATLAS-1 mission to fly next summer (1991)



FIBER OPTIC TAPER      CCD

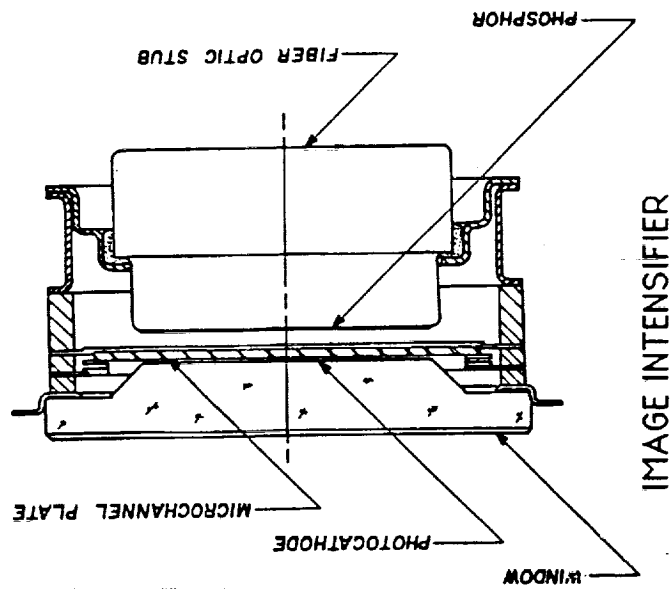
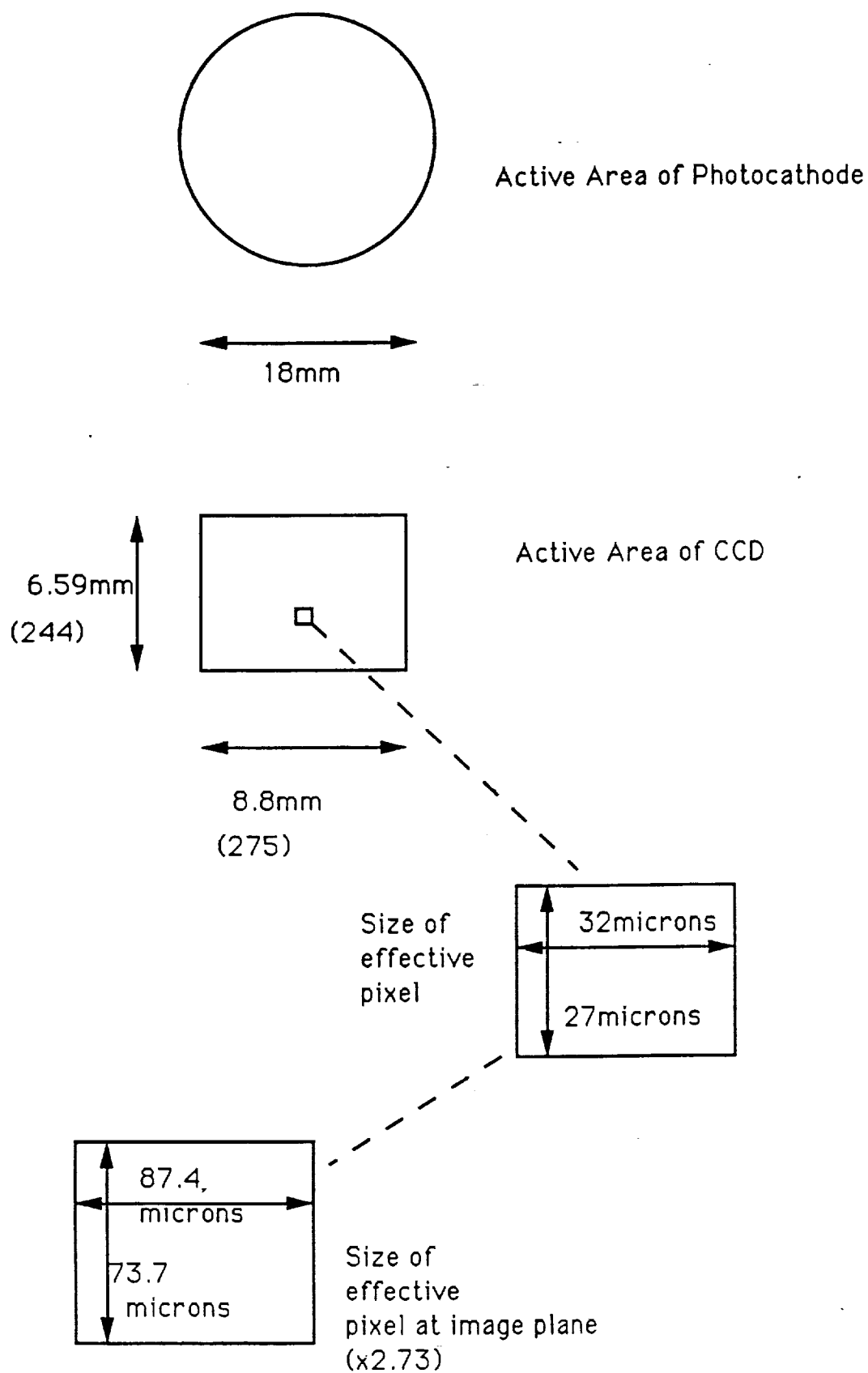


IMAGE INTENSIFIER



# PARAMETERS IN MAPPING OF PHOTOCATHODE TO CCD



## SUMMARY OF UVI SENSITIVITY

$$\text{Sensitivity (counts/sec/R)} = 10^6 \cdot (A \Omega/4 \pi) \cdot R_m(\lambda)^3 \cdot F_R(\lambda) \cdot F_T(\lambda) \cdot Q_e(\lambda)$$

where:

$$A = 14.5 \text{ cm}^2$$

$$\Omega = 2.0\text{E-}2$$

$$\text{so } 10^6 \cdot (A \Omega/4 \pi) = 23077$$

and typical values of the other parameters are as follows (detailed wavelength dependencies shown separately):

$$R_m = 0.8$$

$$R_m^3 = 0.51$$

$$F_R = 0.8$$

$$F_T = 0.3$$

$$Q_e = 0.05$$

so that a "typical" value for  $R_m^3 \cdot F_R \cdot F_T \cdot Q_e = .006$

Sensitivity continued:

Using these values to illustrate the calculation:

$$S = 138 \text{ counts/sec/R}$$

$$\text{or} \quad = 4140 \text{ counts/30 sec integration period/R}$$

Now to determine the sensitivity per pixel:

$$\text{Area of Intensifier} = \pi.9^2 = 254.5 \text{ mm}^2$$

$$\begin{aligned} \text{Area of intensifier at CCD} &= 254.5/(2.73^{**2}) \\ &= 34.14 \text{ mm}^2 \end{aligned}$$

$$\text{Area of CCD} = 8.8 * 6.59 = 57.92$$

$$\begin{aligned} \text{Therefore, number of pixels used} &= 34.14/57.92 \text{ (244 . 275)} \\ &= 0.589 \cdot 67100 \\ &= 39522 \end{aligned}$$

$$\text{therefore} \quad \text{Spix} = 4140/39522 = 0.1 \text{ counts/30sec/R}$$

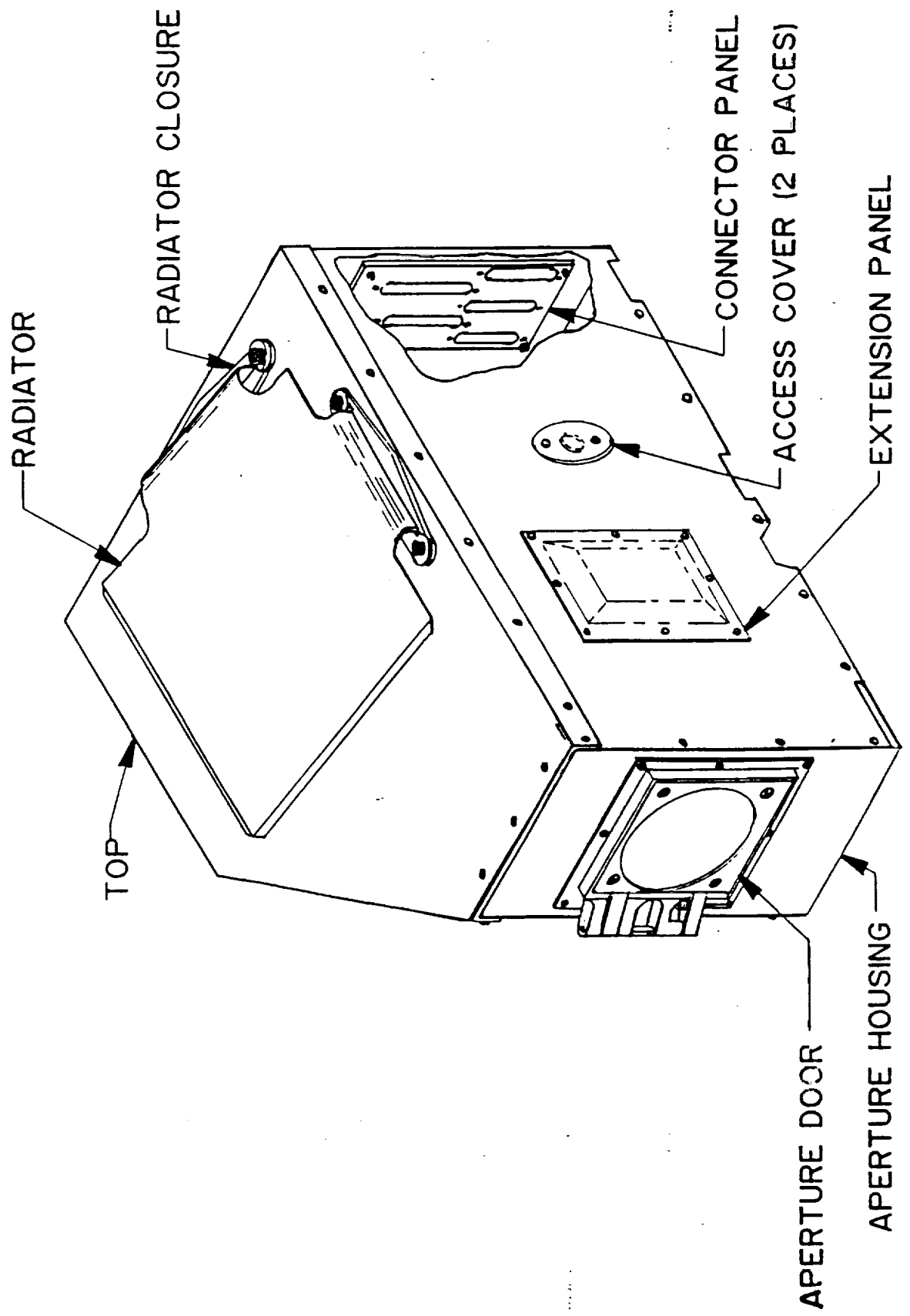
Sensitivity continued:

From this we can determine the noise equivalent signal:

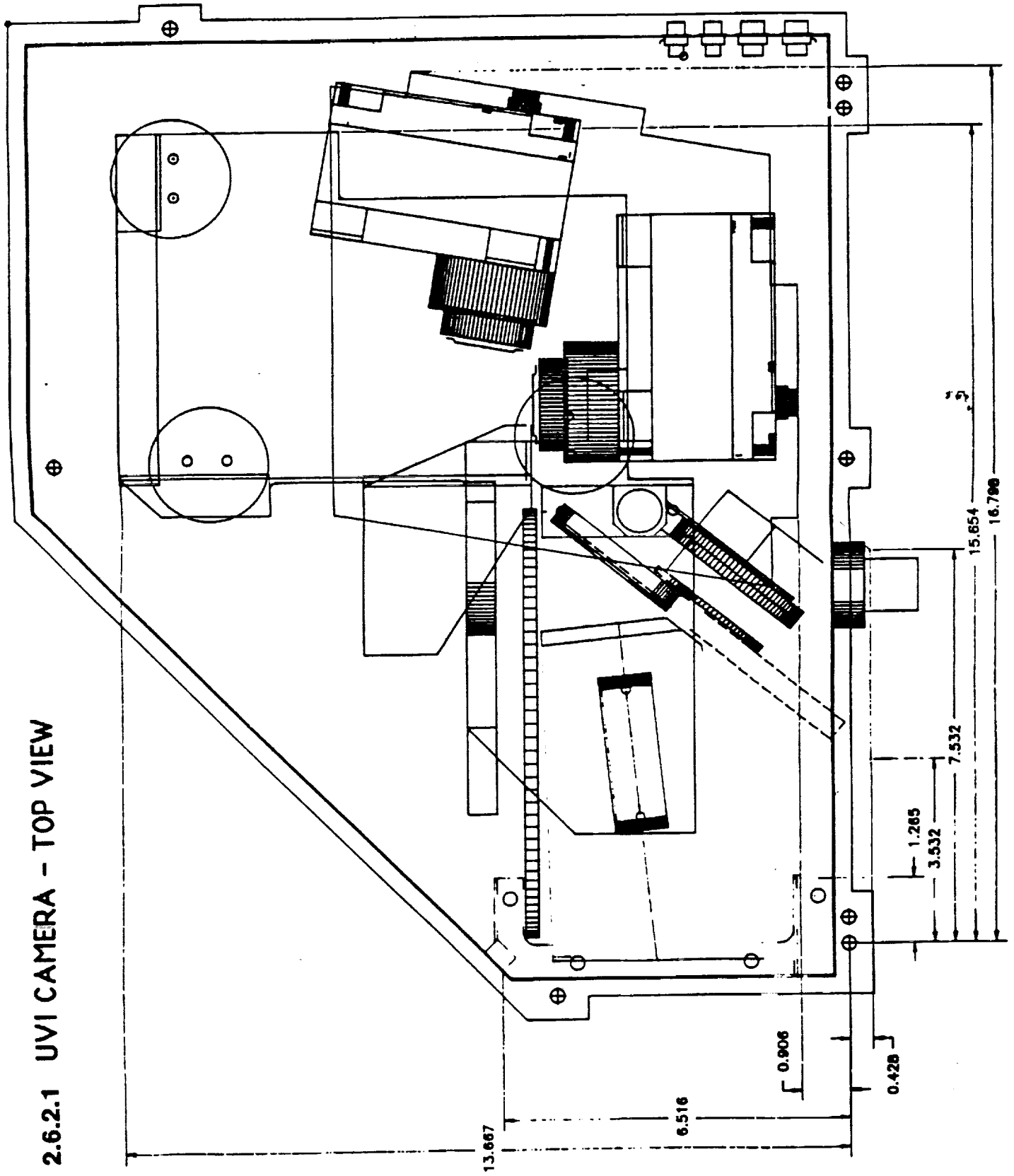
$$NES = 10 \text{ Rayleighs/pixel/30 sec}$$

# UVI CAMERA HOUSING ASSY

## —OVERVIEW—

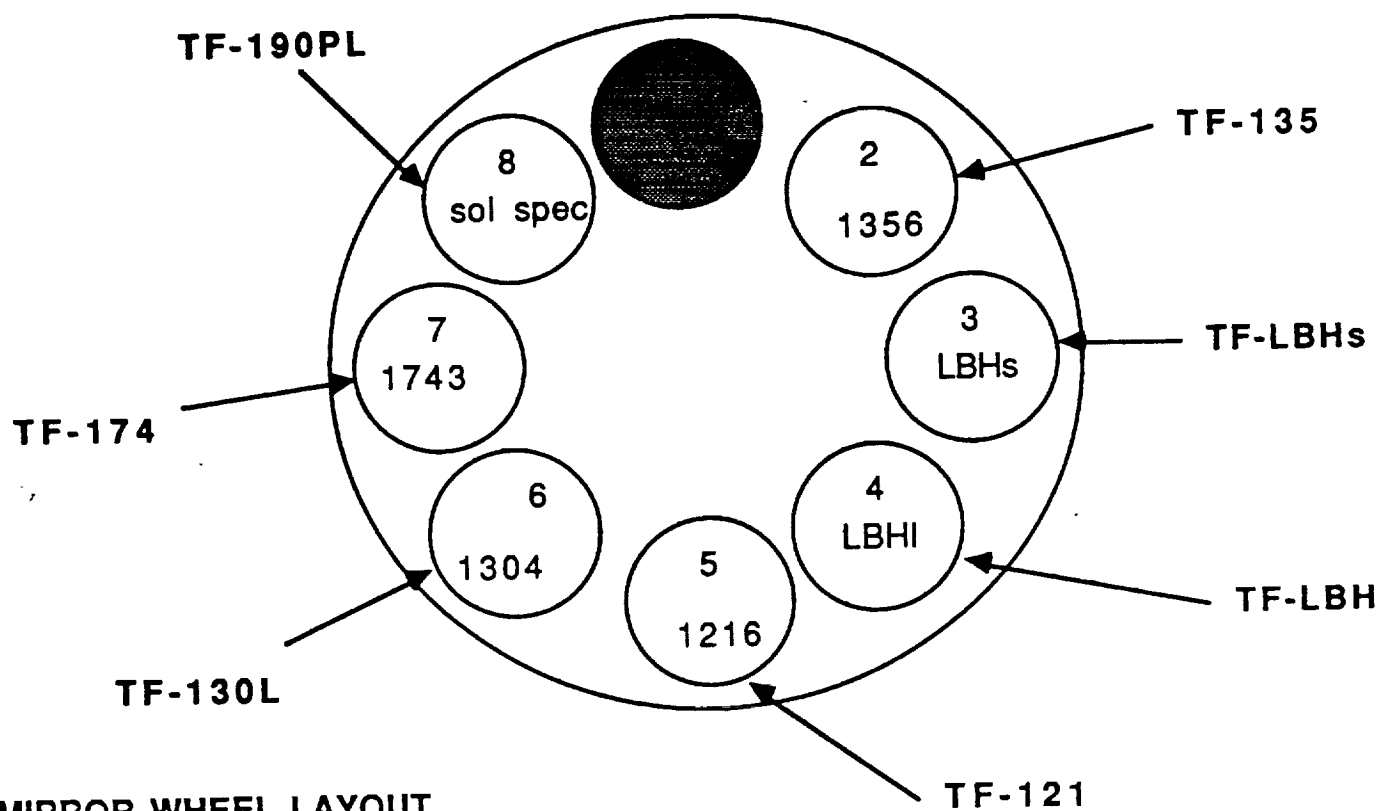


# 2.6.2.1 UVI CAMERA - TOP VIEW

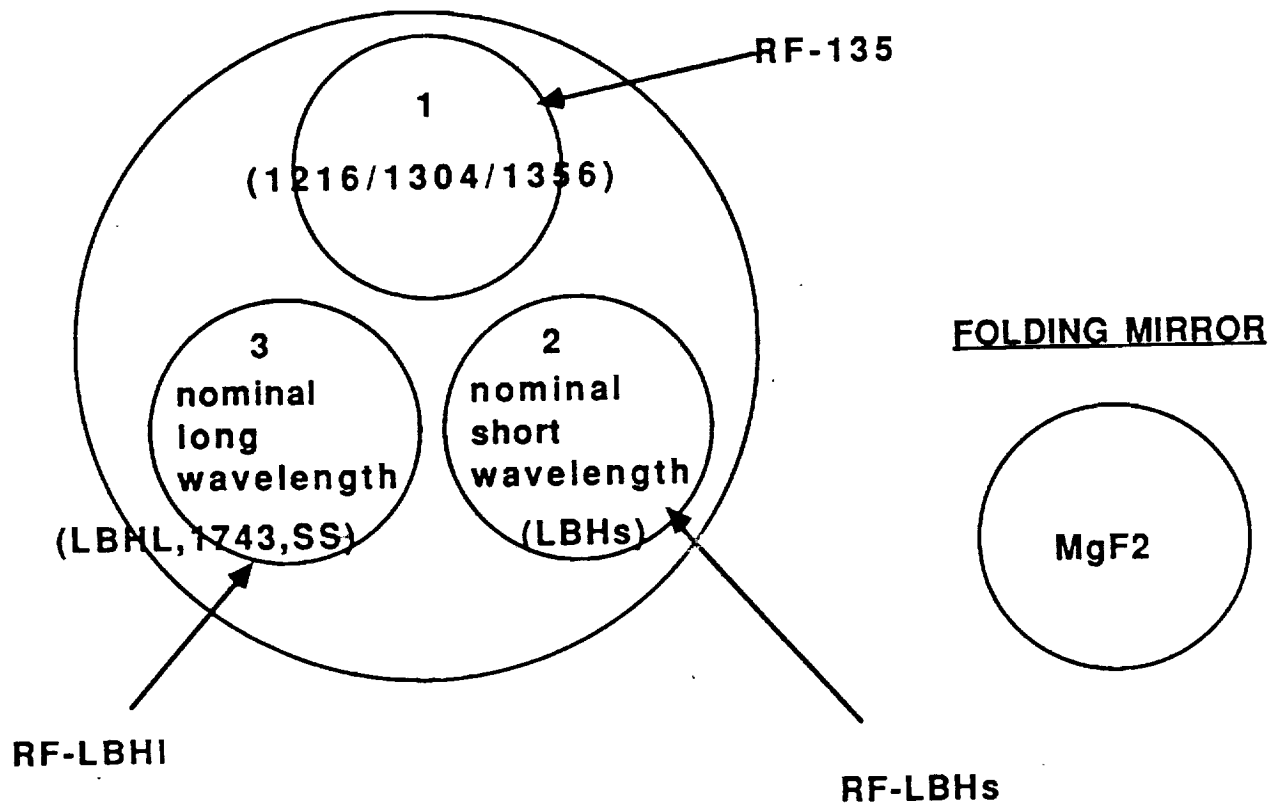


## UVI FILTER WHEEL LAYOUT

Date: 6/18/90



## MIRROR WHEEL LAYOUT



# STRAWMAN OBSERVING SEQUENCES

Marsha Torr

11:00      15 August



REV DATE: 8/9/90

**UVI ORBITAL**  
**SEQUENCE PLANNING**

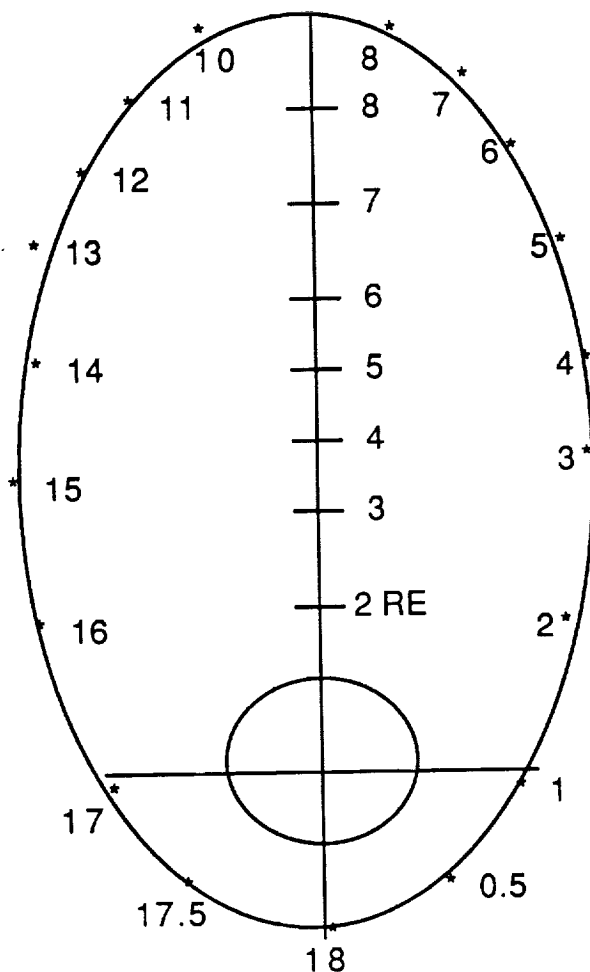
ISTP/POLAR ORBIT:  
2RE X 9RE  
18 HOURS

1) HOURS 4:30 - 13:30  
(COUNTERCLOCKWISE):  
GLOBAL AURORAL MODE -  
OPTICAL AXIS AT MAGNETIC POLE

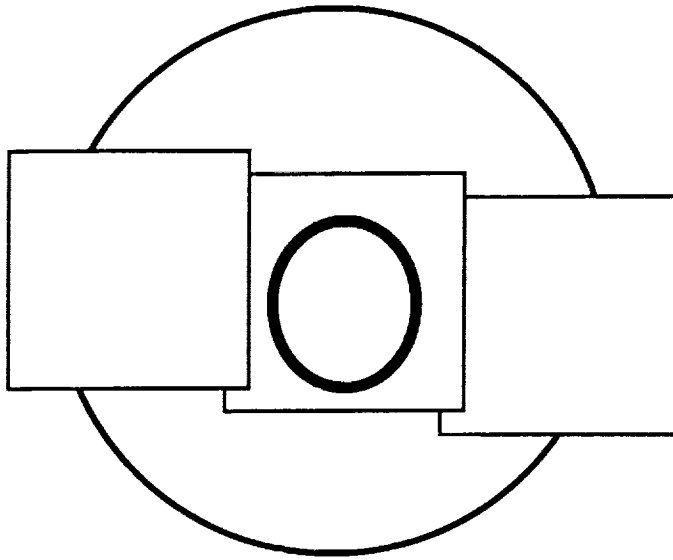
2) HOURS 3-4:30 AND 13:30 - 15  
REGION SPECIFIC STUDY  
PLATFORM OFFSET ANGLE  
BETWEEN 0 AND 9.6 DEGREES

3) HOURS 1-3 AND 15-17:  
HIGH RESOLUTION AURORAL  
DETAIL. ALSO, THE STELLAR  
POINTING TO CALIBRATE  
THE DESPUN PLATFORM COULD  
BE DONE IN THESE TWO WINDOWS

4) HOURS 17 - 1: OFF LIMB VIEWING  
RANGE OF OFFSET IS 28-35 DEGRE  
STEP PLATFORM ~1DEGREE /8MIN



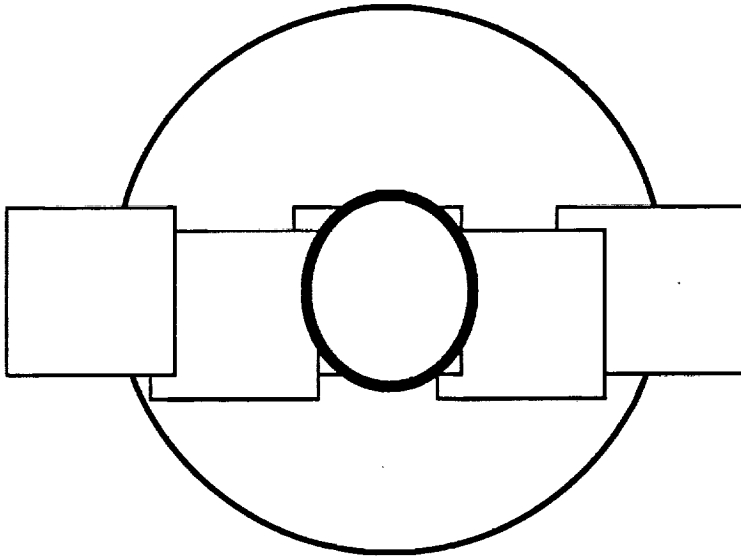
FROM 9Re



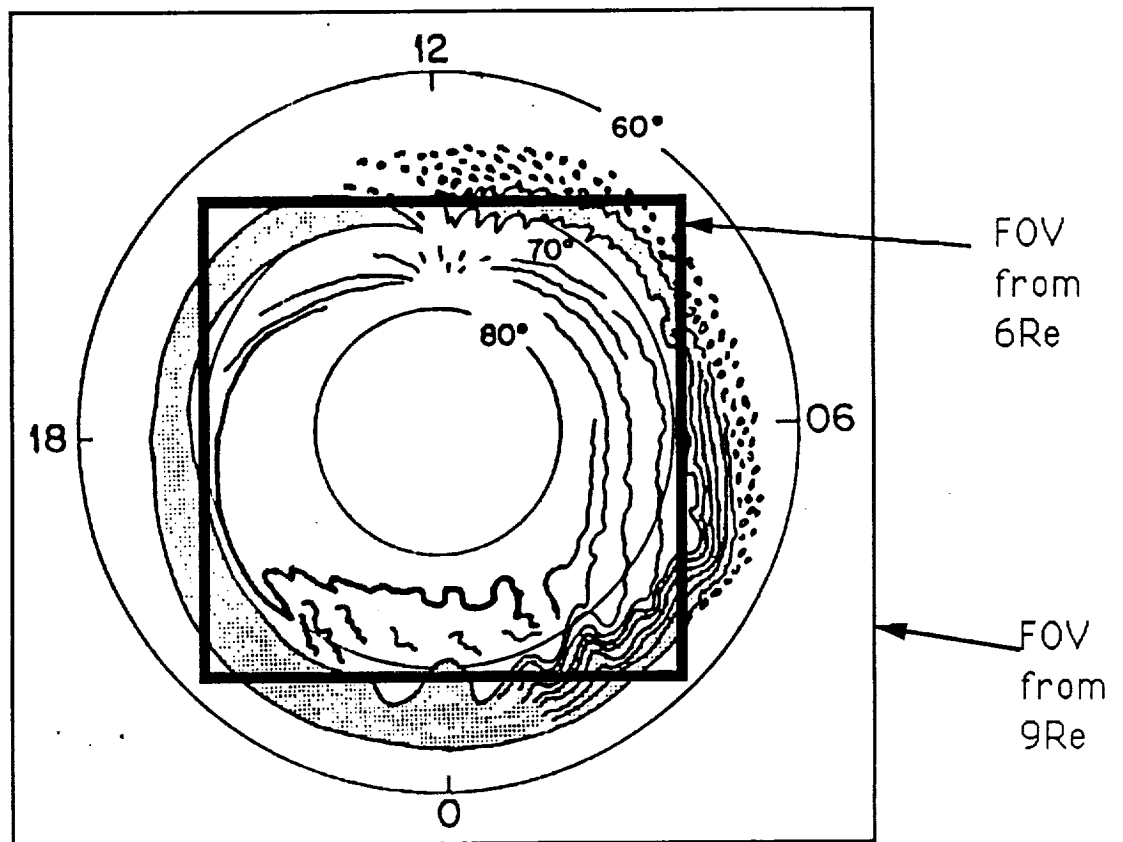
fov's displaced  
for clarity

platform offset angle=6.4 degrees

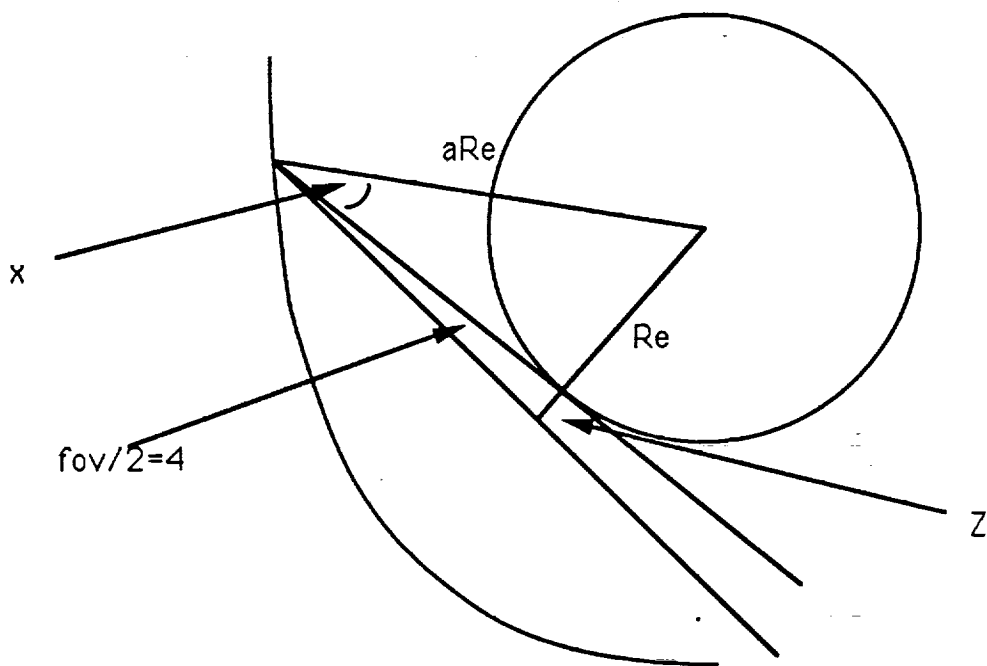
FROM 6 Re



OFFSET ANGLES FOR POSITIONS SHOWN  
ARE 0, 4.8, AND 9.6 DEGREES



TYPICAL AURORAL OVAL WITH 8 x 8 degree FIELD OF VIEW  
FROM 6Re and from 9Re APPOGEE



$$\text{fov} = 2Z = 2Re \cdot \sin 4 \cdot \text{SQRT}(a \cdot a - 1)$$

$$\text{for } a=1.5 \quad \text{fov} = 998\text{km}$$

over ~220 pixels

→ ~ 4.5km/pixel

# **ULTRAVIOLET IMAGER**

## **MISSION OPERATIONS**

**A PRELIMINARY SUMMARY OF TYPICAL OPERATIONS  
DURING VARIOUS MISSION PHASES**

**DATE PREPARED: 6/20/90**

### 3. NORMAL OPERATIONS

#### 3.1 Introduction:

The UVI has 5 typical observing modes, distributed about the orbit as illustrated in the attached figure. In addition the UVI has a startup and shut down sequence. The startup sequence must be run whenever the instrument has been powered off. The shut down sequence must be run whenever the instrument will be idle for lengthy periods of time. The main modes are summarized as follows:

MODE	DESCRIPTION
1)STARTUP	Brings the instrument up from a powered off condition. It assume that the aperture door was left open.
2)SHUTDOWN	Places the instrument in a powered down condition but with the aperture door open.
3) GLOBAL	Full global images of the aurora taken during the 9 hours centered on apogee.
4) REGION	This focusses on selected regions of auroral interest, such as the dawn, dusk, noon, midnight or polar cap sectors. For this co-ordination with the stepping of despun platform is required. A specific and predetermined offset angle between 0 and 9.6 degrees will be required.
5)CLOSEUP	High spatial resolution auroral detail.
6)LIMB	Limb viewing mode. This requires off-set pointing of the despun platform to view the aurora edge on. (see attached figure).

## 7)HIRES

Higher temporal resolution images taken with a smaller portion of the detector used for the miniframe mode.

Below are given typical observing sequence command tables for each of these primary modes, together with power profiles.

### 3.1 STARTUP

This sequence must be run whenever the instrument is turned on from a powered off condition, with the exception of the initial turn on and checkout sequence.

COMMAND	COMMENTS
POWER A ON	
POWER HEAT ON	Backup channel B may be selected on occasion.
SET TEMP1 22.0	
SET TEMP2 22.0	Four different temperature set points can be selected.
SET TEMP3 22.0	
SET TEMP4 22.0	
INIT FIL WHL	
INIT MIR WHL	
INIT FOLD A	
EN HVPS	

### **3.2 SHUTDOWN**

This sequence turns off power to the instrument. The aperture door is left open, but the shutter is closed and all high voltage is disabled. All 28V to the instrument is disabled.

COMMAND	COMMENTS
SET GAIN 0	
DIS HVPS	
INIT FIL WHL	
INIT MIR WHL	
POWER HEAT OFF	
POWER A OFF	



### 3.3 GLOBAL OBSERVING SEQUENCE

This is a basic sequence to gather full auroral images from beyond 6Re. The sequence is intended to obtain images down to 100R in intensity and gathers data using all filters so that all ratio information is available with full correction for contaminant emissions.

COMMAND	COMMENTS
SET GAIN 4	
LOOP 1 12	
POS MIR WHL 1	
REC 3	Background
POS FIL WHL 2	
REC 3	1356
POS MIR WHL 2	
POS FIL WHL 3	
REC 3	LBHs
POS MIR WHL 3	
POS FIL WHL 4	
REC 3	LBHI
POS MIR WHL 2	
POS FIL WHL 5	
REC 2	1216
POS FIL WHL 6	
REC 1	1304
POS MIR WHL 3	
POS FIL WHL 7	
REC 1	sol spec
1 POS FIL WHL 1	end of loop

### 3.4 SPECIFIC REGION/PLATFORM OFFSET SEQUENCE

This sequence is run for spacecraft distances of 4 to 6 Re. The despun platform is offset to a predetermined offset angle from nadir. The angle will lie between 0 and 10degrees. The images are obtained for a specific region such as the dawn sector or the polar cap.

#### COMMAND

#### COMMENTS

**Position Platform to Specified Angle**  
Standby for YY minutes during platform step.

RECXX

LOOP 16

POS MIR WHL 1

REC3

POS FIL WHL 2

REC3

POS MIR WHL 2

POS FIL WHL 3

REC3

POS MIR WHL 3

POS FIL WHL 4

REC3

POS MIR WHL 2

POS FIL WHL 5

REC2

POS FIL WHL 6

REC1

POS MIR WHL 3

POS FIL WHL 7

REC1

POS FIL WHL 1

1

Background

1356

LBHs

LBHI

1216

1304

sol spec  
end of loop

### 3.7 LIMB VIEWING/ PLATFORM OFFSET SEQUENCE

This mode will be used approximately 25% of the time as the spacecraft passes around perigee.  
(1 hour on either side of perigee.)

COMMAND	COMMENTS
SET GAIN 4	Position Platform to 29 degrees off nadir (perigee side)
LOOP 1 5	
POS MIR WHL 1	
REC 3	
POS FIL WHL 2	Background
REC 3	
POS MIR WHL 2	
POS FIL WHL 3	
REC 3	LBHs
POS MIR WHL 3	
POS FIL WHL 4	
REC 3	
POS MIR WHL 2	LBHI
POS FIL WHL 5	
REC 2	
POS FIL WHL 6	
REC 1	1216
POS FIL WHL 1	
	1304
1 REC xx	Step Platform by 1 degree Record background for XX frames while platform steps

### 3.8 HIGH TEMPORAL RESOLUTION SEQUENCE

This sequence uses the miniframe (STAR pointing) mode, to obtain high (1.5 second) temporal resolution images of small spatial segments of the aurora. It will sometimes be used with a despun platform offset.

This sequence obtains sequential images at one wavelength only.

COMMAND	COMMENTS
SEL STAR	
POS FIL WHL 1	Selects miniframe mode for instrument.
SET GAIN 5	
REC 10	Background
POS MIR WHL 2	
POS FIL WHL 3	Monochromatic images
REC 2400	
POS FIL WHL 1	Background.
REC 10	
SET GAIN 0	

### 5. STAR POINTING MODE (Miniframe)

This sequence is used to obtain information on the pointing accuracy/stability of the despun platform. The despun platform is rotated so as to place the field of view of the instrument on a known star. The detector is read out 4 times per spin (1.5sec) but only a portion of the full image (a miniframe) is digitized and transmitted.

COMMAND	COMMENTS
SEL STAR	
POS FIL WHL 1	Selects miniframe mode for instrument.
SET GAIN 5	
REC 5	Obtains 5 frames of background.
POS MIR WHL 2	Wavelength selection is for 1400 - 1600A
POS FIL WHL 3	range, equivalent to that used for LBHs.
REC 400	Records 400 1.5 sec frames or as long as stellar pointing is maintained.
SET GAIN 0	
POS FIL WHL 1	

## STAR POINTING MODE

ASSUMPTION: DATA RATE ALLOCATION MUST REMAIN THE SAME (12kbps)

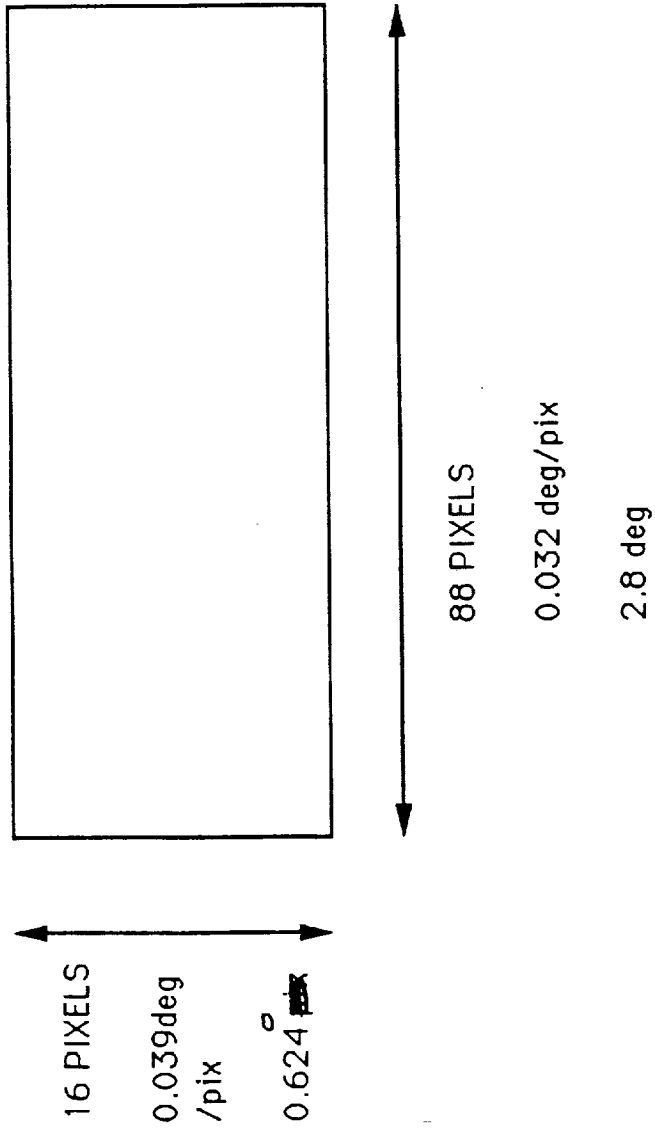
Under this assumption, there are various miniframe options.  
For example:

MINIFRAME RATE	PIXEL ARRAY	ANGULAR RANGE (deg)
1.5 sec	38 x 38	1.2 x 1.48
1.0 sec	30 x 30	0.96 x 1.17
0.5 sec	22 x 22	0.70 x 0.86

NOTE: The 1.5second option gives us 4 samples per rotation and  
allows the largest area in which to work.

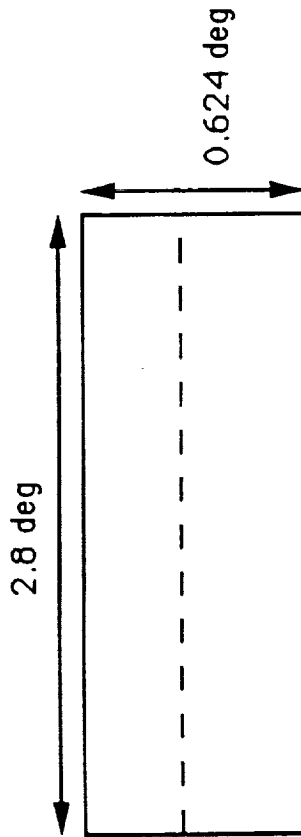
HOWEVER, FOR THESE PURPOSES A RECTANGULAR MINIFRAME WOULD BE  
MORE DESIRABLE

RECTANGULAR MINIFRAME

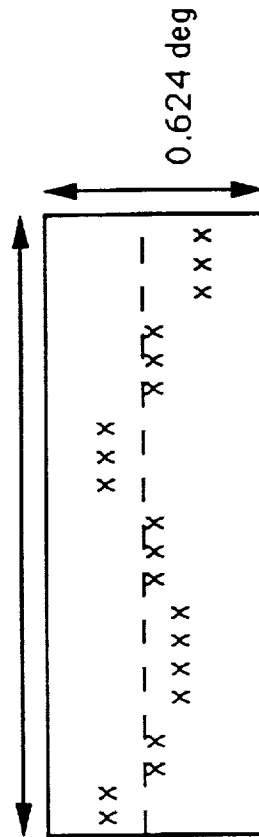


## ANTICIPATED DISPLAYS

1) GENERATE GRID WITH PROJECTED  
STAR TRACK



2) GENERATE NRT LOCUS OF STAR  
LOCATION FROM FRAME TO FRAME  
POSITION



3) OVERLAY ON PREDICTED GRID

FROM THE DIFFERENCE BETWEEN THE PREDICTED AND THE MEASURED  
DETERMINE PITCH AND ROLL ERRORS, AND JITTER



GGS PROGRAM REVIEW

George Parks

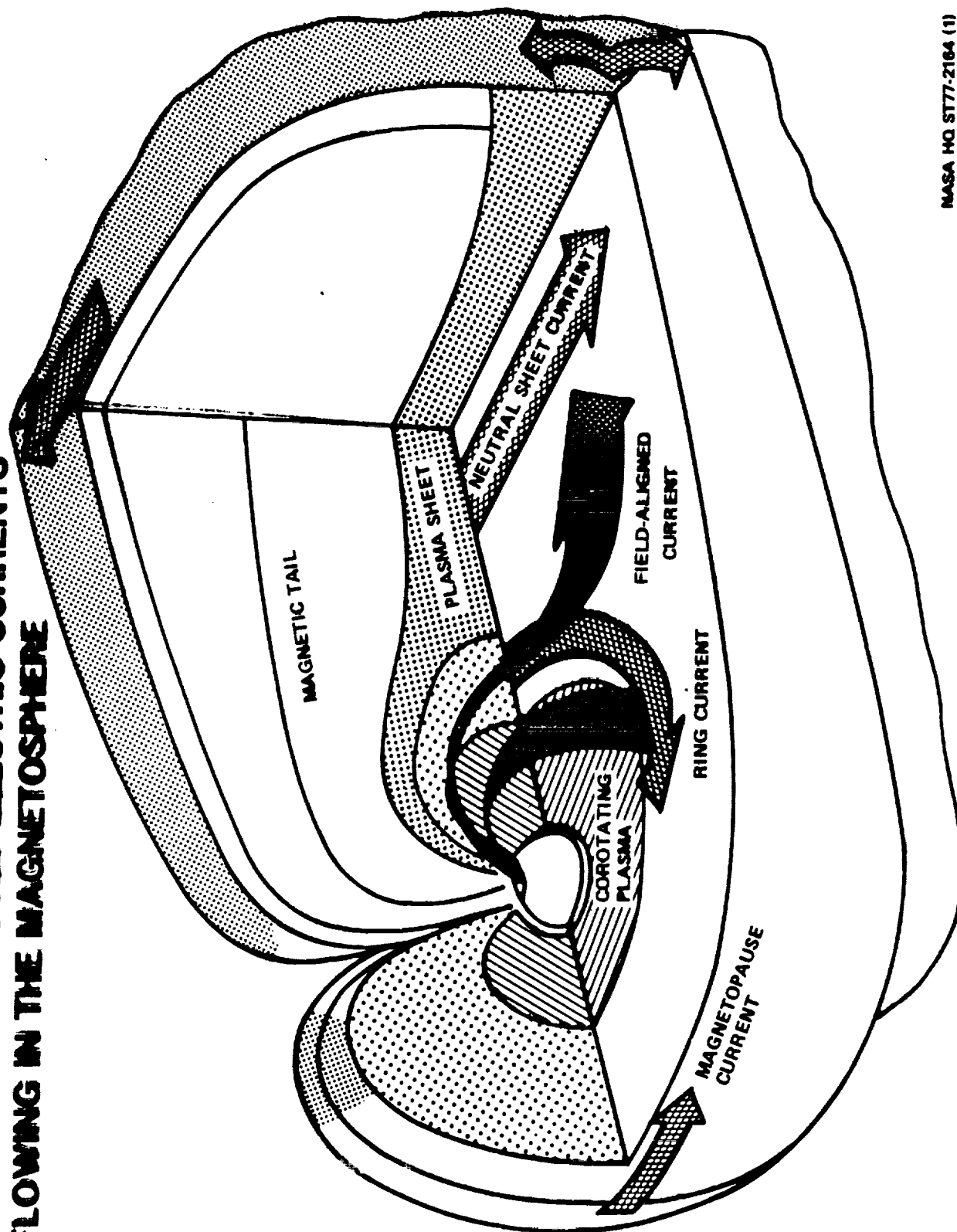
1:30 15 August

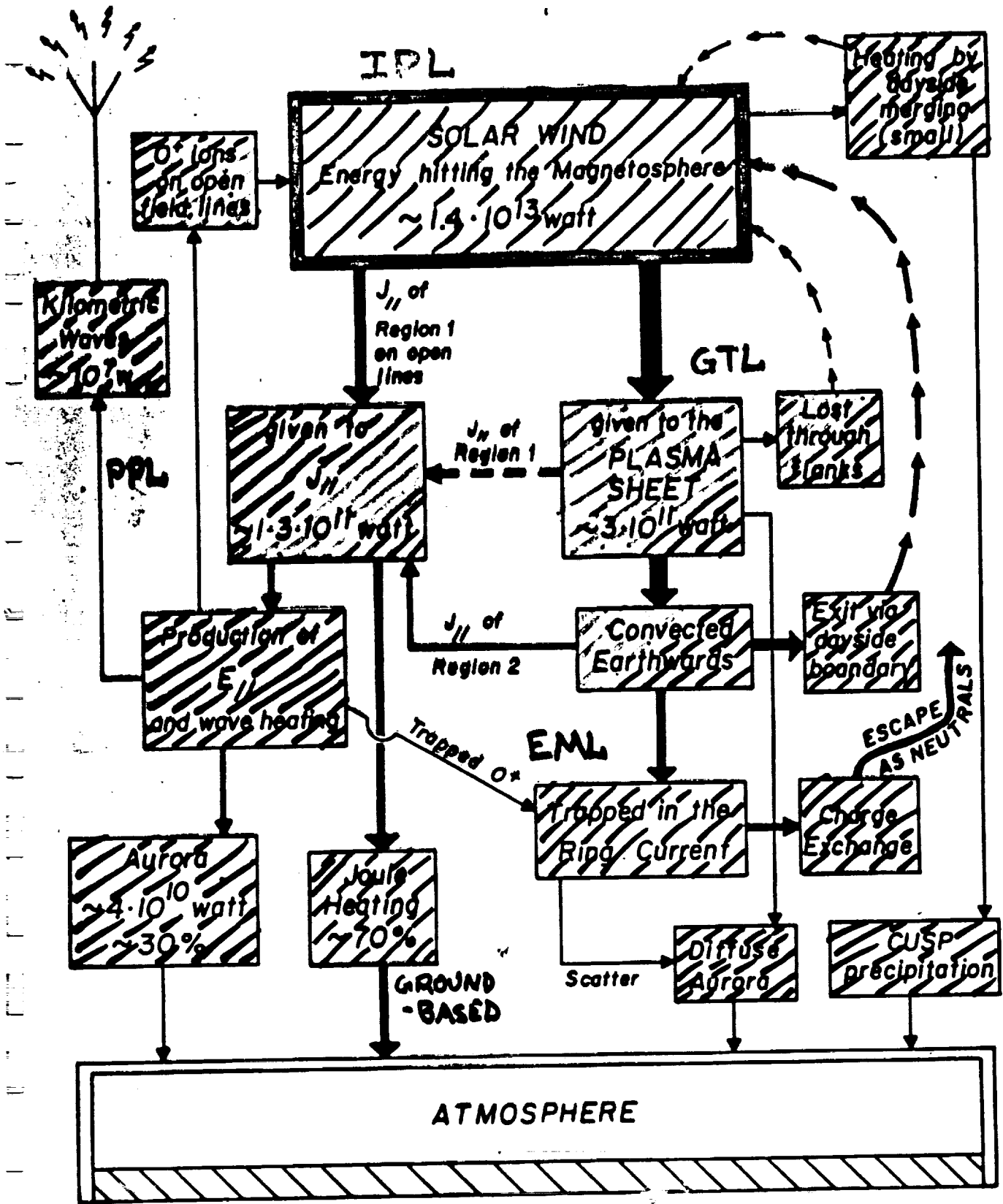
- \* FIRST COORDINATED GEOSPACE MEASUREMENTS  
IN KEY PLASMA SOURCE AND STORAGE REGIONS
- \* FIRST MULTI-SPECTRAL GLOBAL AURORAL  
IMAGING
- \* FIRST COMPREHENSIVE MULTI-POINT STUDY OF  
MAGNETOSPHERIC RESPONSE TO SOLAR WIND
- \* FIRST APPLICATION AND TEST OF  
QUANTITATIVE GEOSPACE MODELS

## CRITICAL PROBLEMS OF MAGNETOSPHERIC PHYSICS

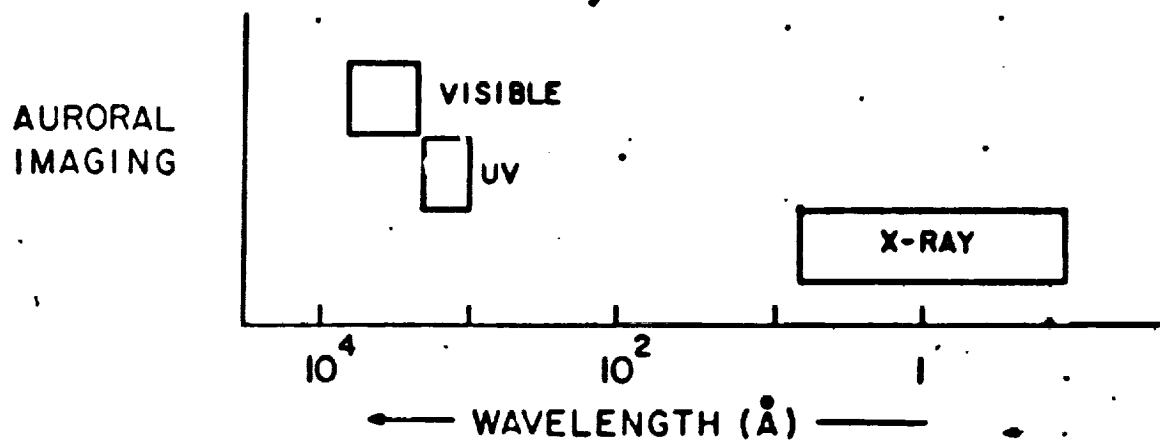
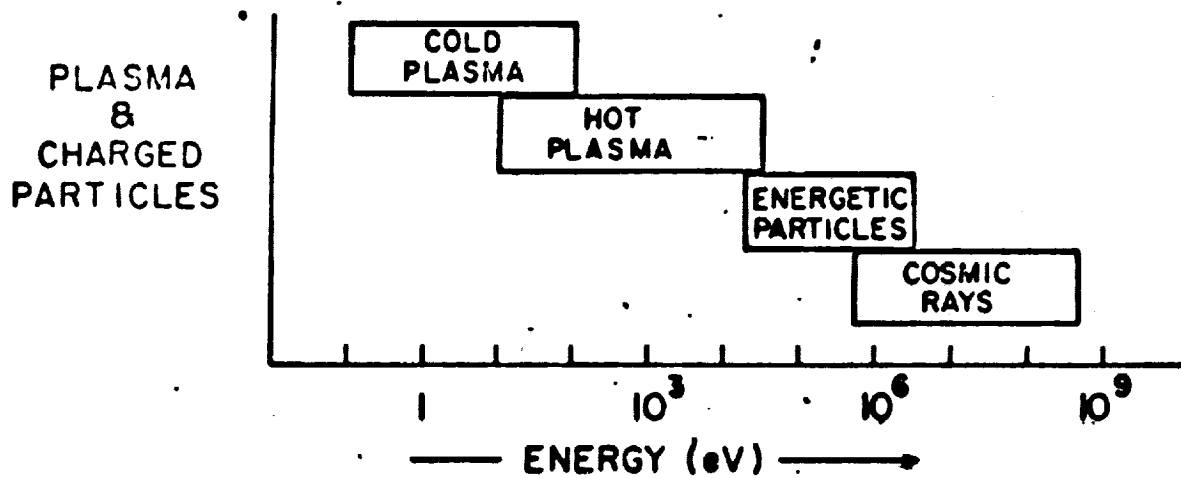
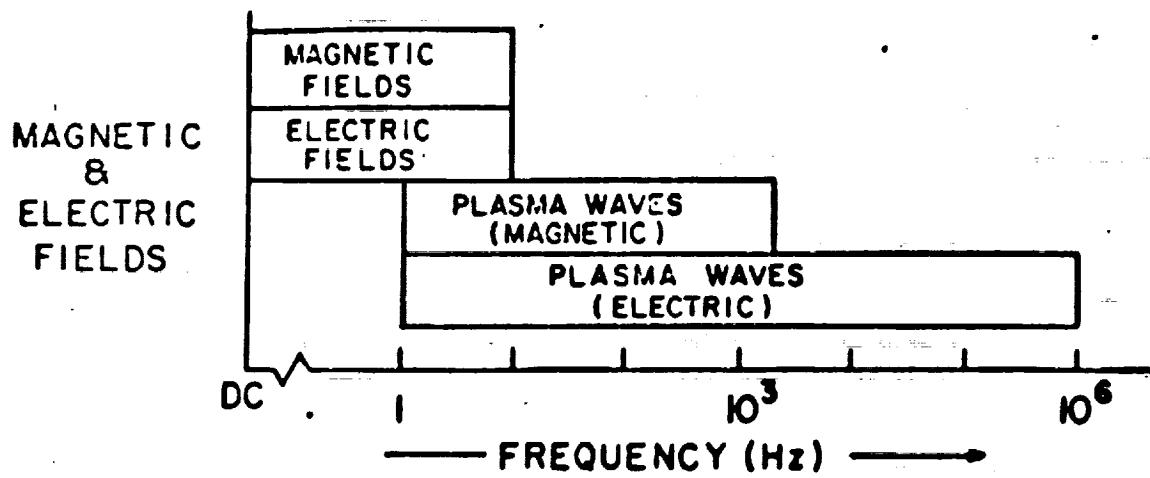
1. How does solar wind couple energy to magnetosphere?
2. How does solar wind couple plasma to magnetosphere?
3. How does tail dissipate stored magnetic energy to create substorms?
4. How does magnetosphere couple with atmosphere and ionosphere?

# SOLAR WIND- INDUCED ELECTRIC CURRENTS FLOWING IN THE MAGNETOSPHERE





# PARTICLES, FIELDS, AND IMAGING COVERAGE



ORIGINAL PAGE IS  
OF POOR QUALITY

## Typical Parameters

$$\left. \begin{array}{l} R_{pt} \gtrsim 100 \text{ km} \\ T_i \sim 1 \text{ sec} \end{array} \right\} \text{ outer magnetosphere}$$

UV imager resolution  $\sim 30 \text{ km}$   
 $\Leftrightarrow \sim 6000 \text{ km @ } 6-7 R_e$

resol.  $\sim 4.5 \text{ km} \Leftrightarrow 1 R_{pt} @ 6 R_e$

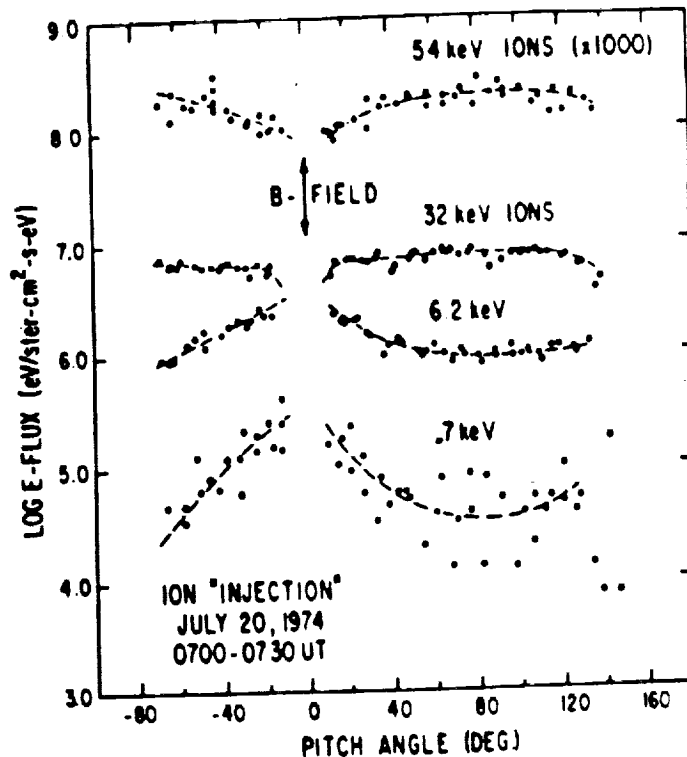
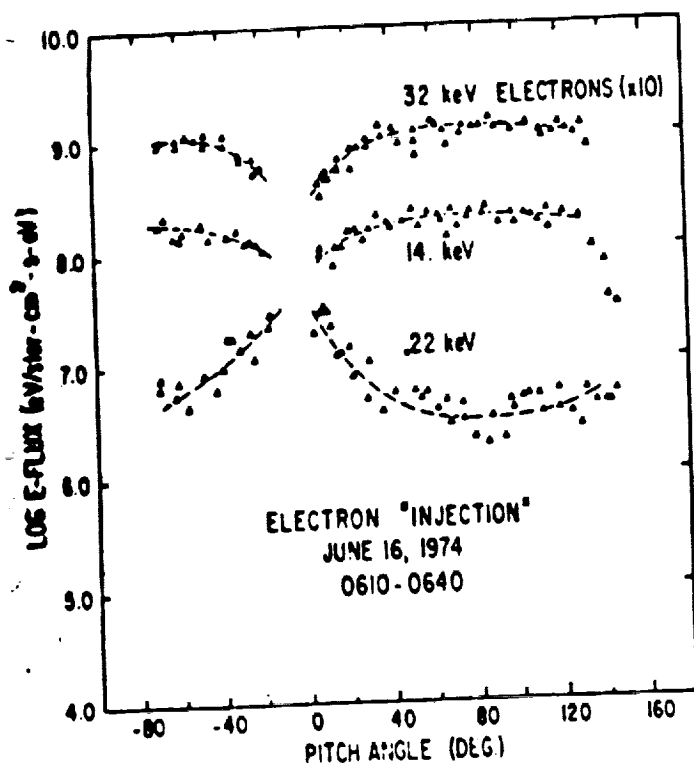


Figure 1c: Electron and ion pitch-angle distributions during an injection event. Note that the pitch-angle distribution is strongly energy dependent. Low-energy component is field-aligned (Mauk and McIlwain, 1975)

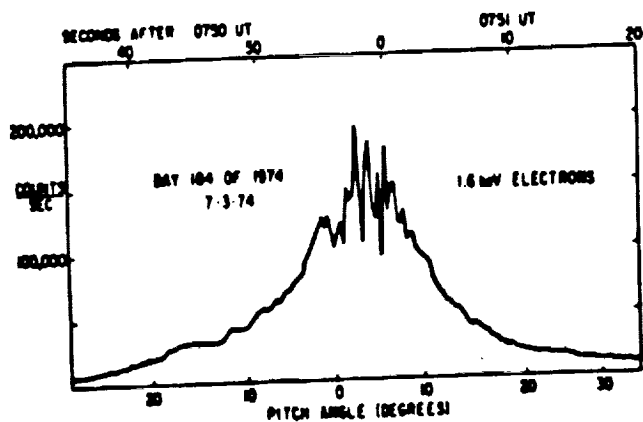


Figure 1d: Fluctuations within an electron beam observed within the narrow range of pitch-angles near the direction of local B (McIlwain, 1975).

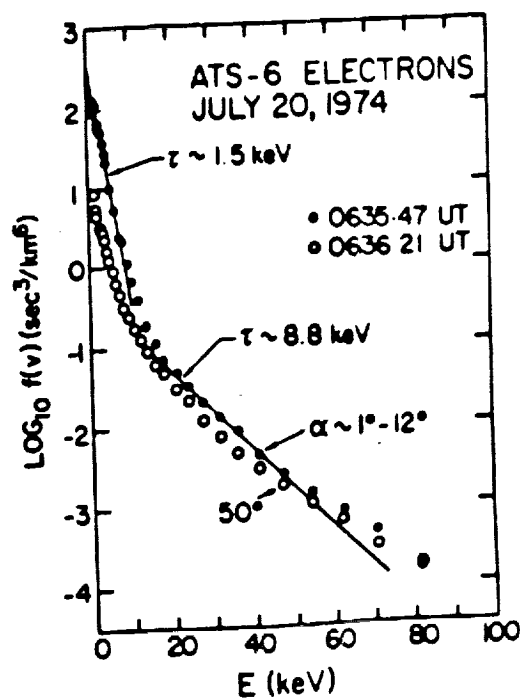


Figure 1e: Distribution function of electrons at injection. Note the presence of two quasi-Maxwellian components (Parks et al, 1979a).



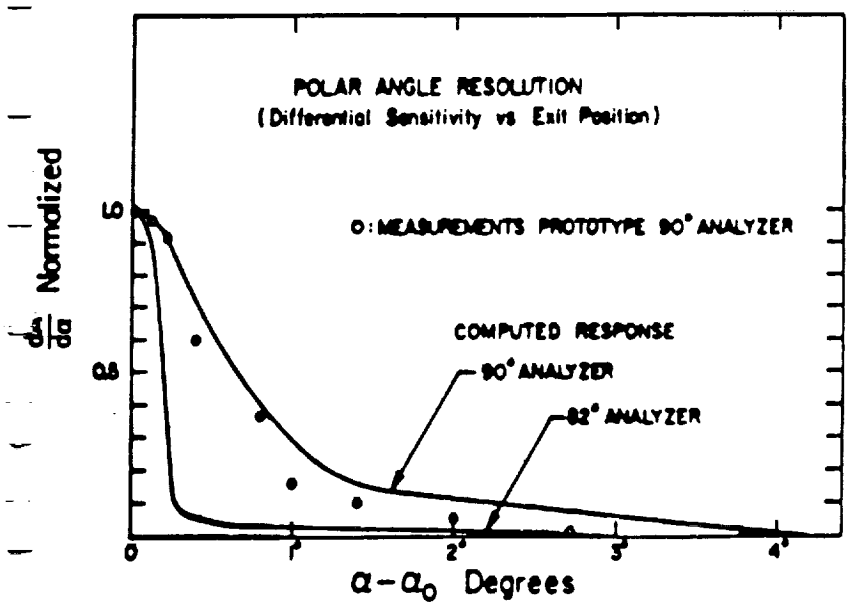
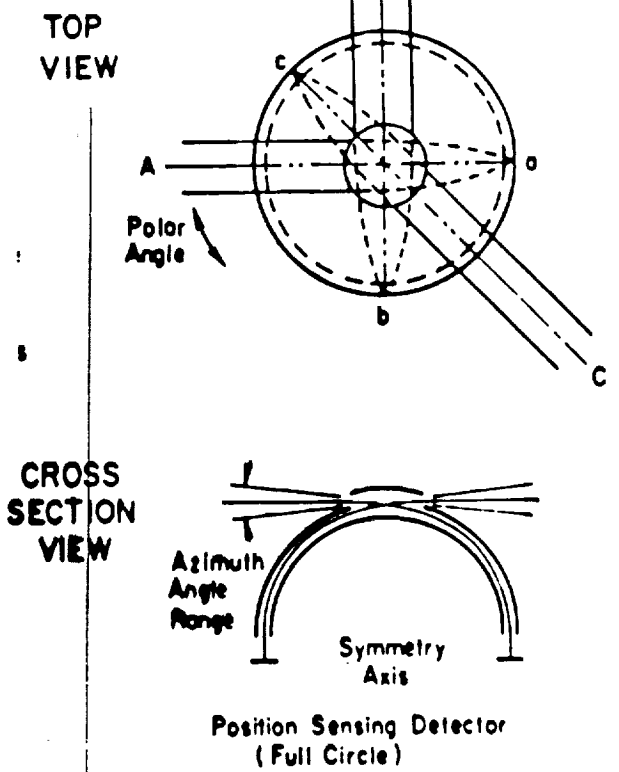


Fig. 4C. Polar angle response deconvoluted from Fig. 4A using the finite width of the source (measured and computed). Better than 1° resolution (FWHM) is realizable.



SYMMETRICAL QUADRASPHER

Fig. 3A. Theoretical particle orbits within the normal quadrasphere analyzer and our proposed new symmetrical quadrasphere analyzer. Note the loss of focusing with the normal quadrasphere for non-zero incidence angles.

$$FOV = 2\pi + \frac{spin}{2} = 4\pi$$

$E^+ \sim 3eV - 40keV$

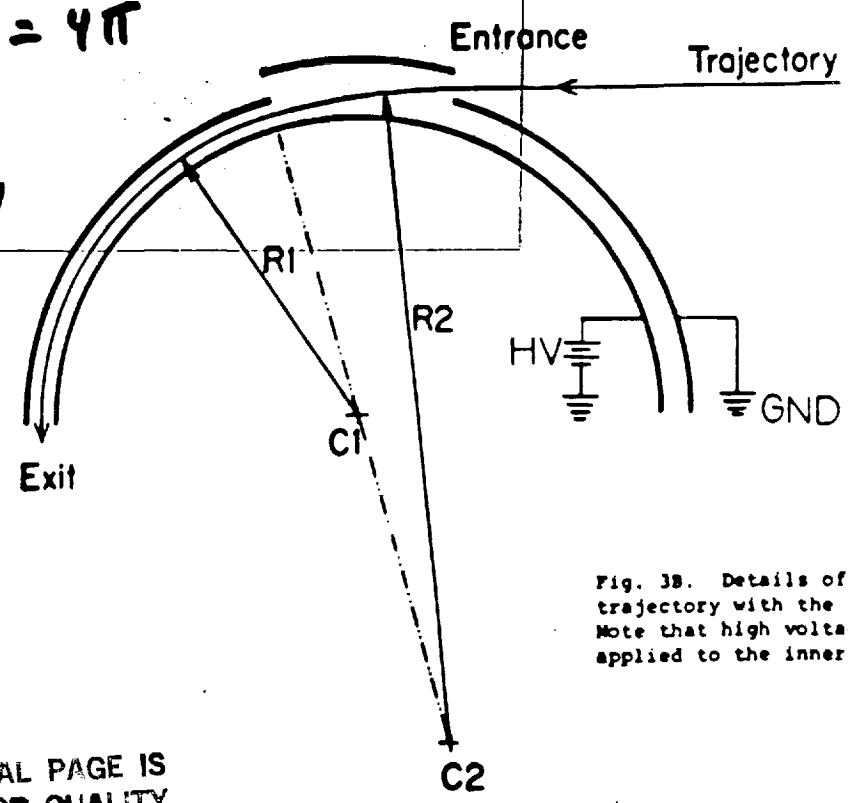


Fig. 3B. Details of particle trajectory with the new analyzer. Note that high voltage is only applied to the inner plate.

ORIGINAL PAGE IS  
OF POOR QUALITY



ORIGINAL PAGE IS  
OF POOR QUALITY

## GLOBAL GEOSPACE SCIENCE PROGRAMME

George Parks\*, Stanley Shawhan, Michael Calabrese and Joseph Alexander.  
National Aeronautics and Space Administration Office of Space Science and Applications Washington, DC 20546 USA.

The Global Geospace Science (GGS) Programme is an element of the International Solar Terrestrial Physics (ISTP) Programme dedicated to study the global plasma dynamics of the solar-terrestrial environment. The participants in the GGS Programme are the European Space Agency (ESA), the Japanese Institute of Space and Astronautical Science (ISAS), the US Department of Defense (DoD), and the National Aeronautics and Space Administration (NASA). Coordinated measurements are being planned by five spacecraft from strategic regions of space: WIND and POLAR are NASA spacecraft, GEOTAIL is a joint ISAS/NASA mission, the Combined Release and Radiation Effects Satellite (CRRES) is a DoD/NASA mission, and CLUSTER Equatorial Science Phase (ESP) spacecraft is a ESA/NASA mission. WIND will measure the solar wind forcing function, GEOTAIL will investigate the plasma dynamics of the geomagnetic tail, CLUSTER-ESP will observe entry and boundary layer particles near the dayside magnetopause and will investigate the physics of aurora in the near-earth neutral line region on the nightside, and CRRES will measure the ring current particles inside six earth radii (Re). Ground based observations and theory and modeling investigations are important ingredients of the GGS Programme. One of the scientific goals of the GGS Programme is to use the combined data set from these spacecraft and construct quantitative models to describe how the solar wind mass, momentum, and energy are transported across the boundaries, stored and energized in the magnetosphere, and subsequently dissipated into the earth's atmosphere.

### I. INTRODUCTION

The article by S. M. Krimigis (this issue) has shown that solar flares, magnetic storms, and the global terrestrial aurora are examples of cosmic plasmas in action in our solar system. These phenomena are produced by a dynamic and complex system of interacting plasmas, magnetic fields, and electrical currents. The space comprising the magnetized solar wind plasma plus the perturbations created in the heliosphere by the presence of the magnetic Earth and its plasma environment is called "geospace".

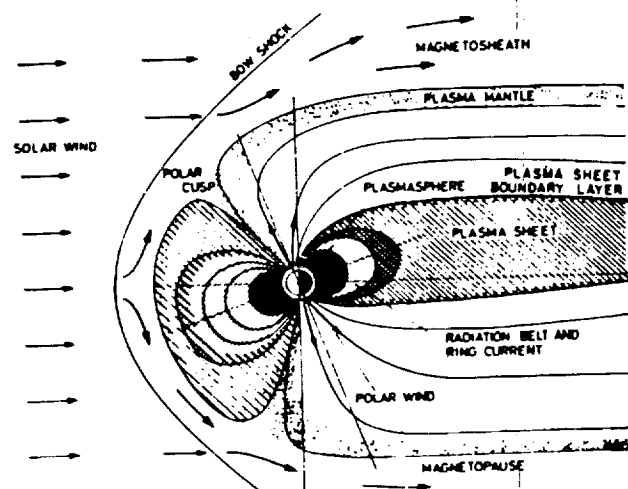
Intrinsic to the geospace system are two major plasma sources, the solar wind and the terrestrial ionosphere, and two major plasma storage regions, the geomagnetic tail and the near-earth equatorial plasmashield and ring current. These source and storage regions are interconnected by a complex network of transport processes which determine the highly interactive behaviour of the system as a whole, a system spanning millions of kilometers but with dynamic time scales as short as minutes.

Previously, the near-earth geospace has been explored and studied primarily as a system of independent component parts: the interplanetary region, the magnetosphere, the ionosphere and the upper atmosphere (Figure 1). From these early observations, we learned that geospace is a complex system in which these components are highly interactive. While previous programmes have advanced our understanding of these regions of geospace individually, an understanding of geospace as a whole requires a planned programme of simultaneous observations in key regions of geospace.

A co-operative world-wide effort has been planned under the International Solar-Terrestrial Physics (ISTP) Programme to study and develop quantitative understanding of the fundamental electrodynamic processes in our solar-terrestrial environment [1]. The participating organizations of ISTP are the Japanese Institute for Space and Astronautical Science (ISAS), the European Space Agency (ESA), the Department of Defense (DoD), and the National Aeronautics and Space Administration (NASA).

The ISTP Programme will be implemented by the Solar Terrestrial Science Programme (STSP), the Global Geospace

Fig. 1. Working definition of the major plasma regimes of Geospace.



\*Visiting Senior Scientist, On leave from the University of Washington, Seattle, WA 98195.

of good quality

# MAGNETOSPHERIC MODELS

George Parks

15 August

1000  
1000

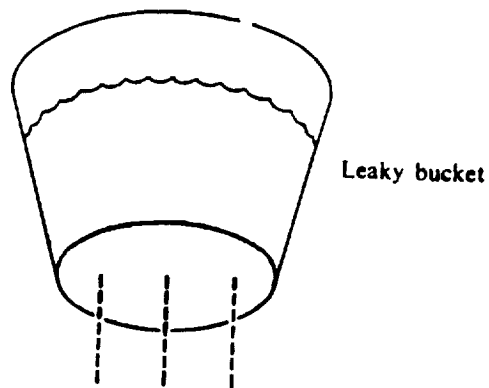
# PROBLEM

- SOLAR WIND INTERACTION  
WITH MAGNETIZED PLANETS

\* APPENDIX \*

ORIGINAL PAGE IS  
OF POOR QUALITY

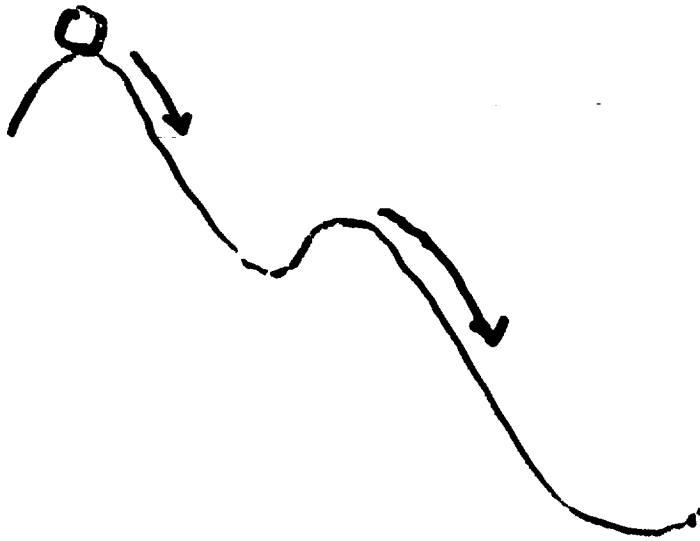
1960



1980

AURORA  $\equiv$  DISSIPATION OF  
SOLAR WIND ENERGY

# SUBSTORM $\equiv$ UNSTABLE PLASMA



Minimum  
Energy State

Theorem:

IDEAL MHD PLASMA, (constraints)

MINIMUM  $\equiv$  FORCE FREE ( $\vec{J} \times \vec{B} = 0$ )  
ENERGY  
STATE CONFIGURATION

Chandrasekhar / Wolfgar (1958)

LOW  $\beta$   
 $\sigma = \infty$

ORIGINAL PAGE IS  
OF POOR QUALITY



## Correct Approach

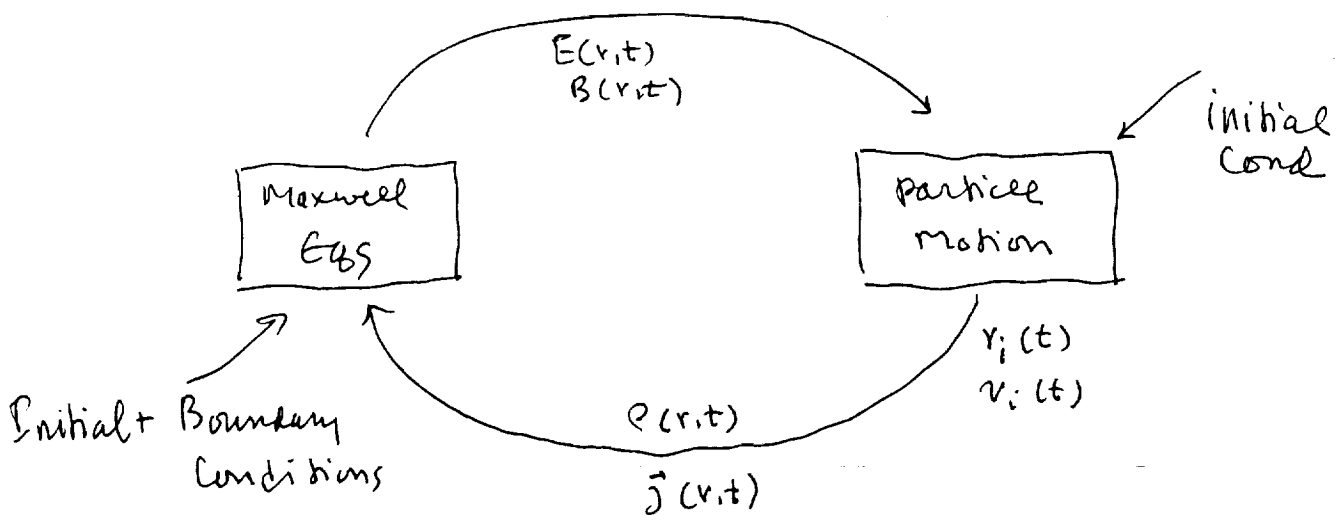
$$m_i \frac{d\vec{v}_i}{dt} = q_i (\vec{E} + \vec{v}_i \times \vec{B})$$

+

Maxwell Eqs. of Electrodynamics

$$i = 1 \rightarrow N$$

There are as many equations as particles.



- Space very large ~  $n \approx 1/cc$  Sun-Earth  $\sim 1.5 \times 10^{13} cm$
- density is low but dealing w/ long range force.

## STATISTICAL

Define  $f(\vec{r}, \vec{v}, t)$  in  $(\vec{r}, \vec{v})$  space

Use

$$\frac{df}{dt} = \frac{\partial f}{\partial t} + \dot{x}_i \frac{\partial f}{\partial x_i} + \dot{v}_i \frac{\partial f}{\partial v_i} = 0$$

For E&M force

$$\frac{\partial f}{\partial t} + \vec{v} \cdot \frac{\partial f}{\partial \vec{r}} + \frac{q}{m} (\vec{E} + \vec{v} \times \vec{B}) \cdot \frac{\partial f}{\partial \vec{v}} = 0$$

+

$$\nabla \cdot \vec{D} = n \int f d^3v$$

$$\nabla \times \vec{H} = n \int q \vec{v} f d^3v + \partial \vec{D} / \partial t$$

$$\nabla \times \vec{E} = -\partial \vec{B} / \partial t$$

$$\nabla \cdot \vec{B} = 0$$

## MHD DESCRIPTION

$$(1) \quad \partial \rho_m / \partial t + \nabla \cdot \rho_m \mathbf{U} = 0$$

$$(2) \quad \partial(\rho_m \mathbf{U}) / \partial t + \nabla \cdot \Pi = 0$$

where

$$\Pi_{ik} = \rho_m U_i U_k + p \delta_{ik} - \tau_{ik} - (H_i H_k - 1/2 H^2 \delta_{ik}) / 4\pi$$

$$(3) \quad \partial / \partial t (\rho U^2 / 2 + p\epsilon + H^2 / 8\pi) + \nabla \cdot \mathbf{q} = 0$$

where

$$\mathbf{q} = \rho \mathbf{U} (U^2 / 2 + w) - \mathbf{U} \cdot \boldsymbol{\tau} - \kappa \nabla T$$

$$w = \epsilon + p/\rho$$

+

(4) EM MAXWELL EQUATIONS

**APPLICATION RESTRICTIVE !**

(1) IGNORE VISCOSITY,

(2) INTRODUCING NEW DIMENSIONLESS VARIABLES,  $r^* = r / L$ ,  $t^* = t / T$ ,  $U^* = U / U_0$ ,  $p^* = p / p_0$ ,  $\bar{p}^* = p / p_0$ , and  $B^* = B / B_0$ .

EXAMINE MOMENTUM EQUATION (FOR IDEAL FLUID)

$$(M_A^2 / \delta) \partial \mathbf{U} / \partial t + M_A^2 (\mathbf{U} \cdot \nabla) \mathbf{U} = \beta^2 \nabla p / \rho_m + (\nabla \times \mathbf{B}) \times \mathbf{B} / \mu_0 \rho_m$$

WHERE

$$\delta = U_0 T / L$$

$$M_A = U_0 / U_A, \quad U_A^2 = B_0^2 / \mu_0 \rho_0 = (\text{Alfven velocity})^2$$

$$\beta^2 = p_0 / \rho_0 U_A^2$$

$$\frac{M_A^2}{\delta} \frac{\partial \vec{u}}{\partial t} + M_A^2 (\vec{u} \cdot \nabla) \vec{u} = \frac{\beta^2}{\rho_m} \nabla p + \frac{\vec{J} \times \vec{B}}{\rho_m}$$

IN THE IONOSPHERE,

$$M_A^2 \approx (1/1000)^2 = 10^{-6} \ll 1$$

AND

$$\beta^2 \approx (10^{-5})^2 \ll 1$$

SO FROM THE MOMENTUM EQUATION, WE SEE THAT THE  
MAGNETIC FIELD IN THE IONOSPHERE BECOMES FORCE-FREE

$$(\nabla \times \mathbf{B}) \times \mathbf{B} = \mathbf{J} \times \mathbf{B} = 0$$

THAT IS,  $\mathbf{J}$  IS PARALLEL TO THE DIRECTION OF  $\mathbf{B}$ .

So observations in the ionosphere  
consistent with MHD predictions.

FIELD ALIGNED CURRENTS/  
BOUNDARY STRUCTURES

George Parks

15 August

MAGNETOSPHERE SURROUNDING FIELD.

ALIGNED CURRENTS ( $\vec{S} \times \vec{E}$ ) etc

ORIGINAL PAGE IS  
OF POOR QUALITY

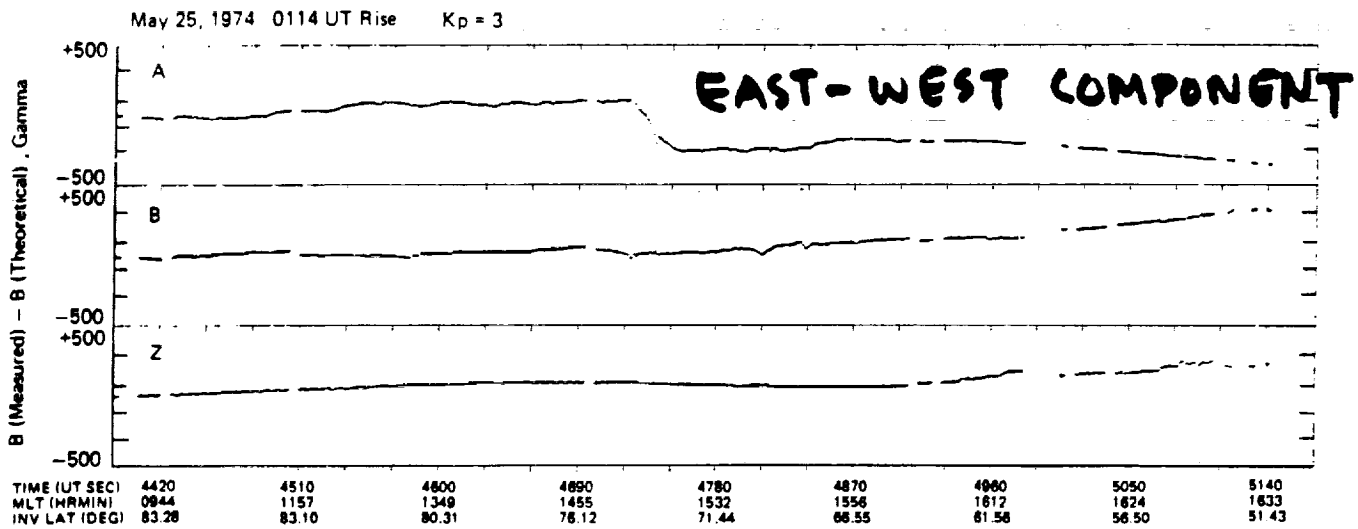


Fig. 1. Example of a steplike level shift in the output from the A magnetometer sensor, which is approximately in the dipole east-west direction, indicating a net upward current in the field-aligned current layer; a typical example observed in the afternoon.

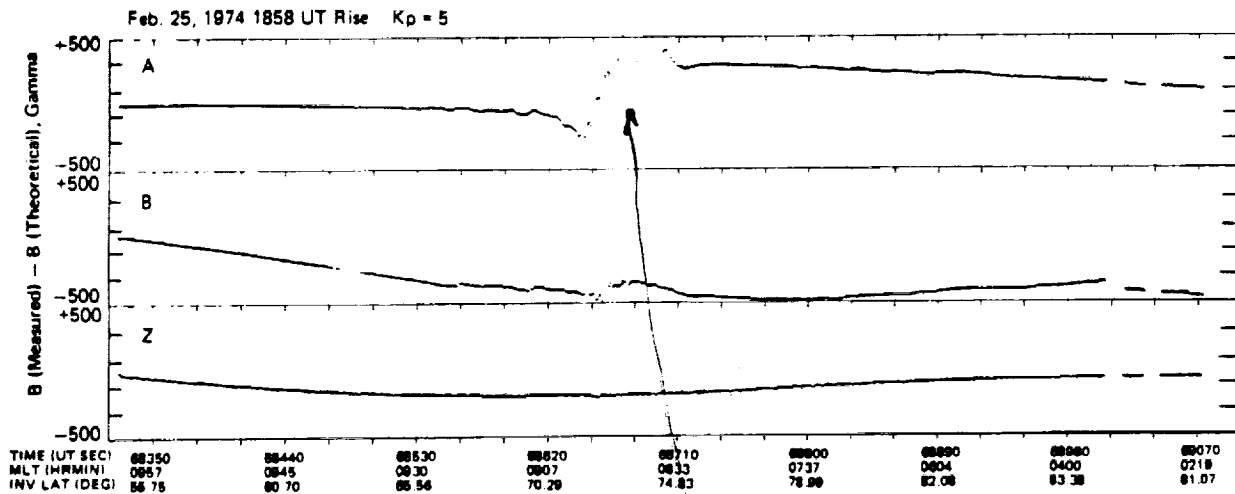
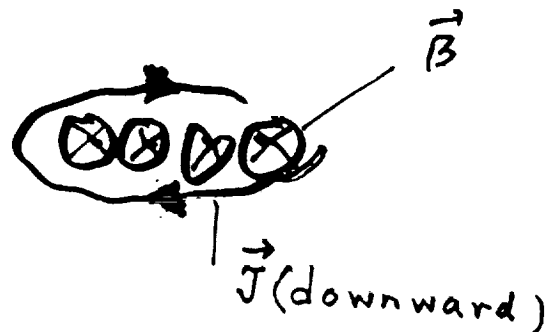


Fig. 2. Example of a level shift of large amplitude, indicating a net downward field-aligned current observed during a magnetically disturbed period.

ORIGINAL PAGE IS  
OF POOR QUALITY





February 10, 1973

80

75

70

Latitude (deg. N)

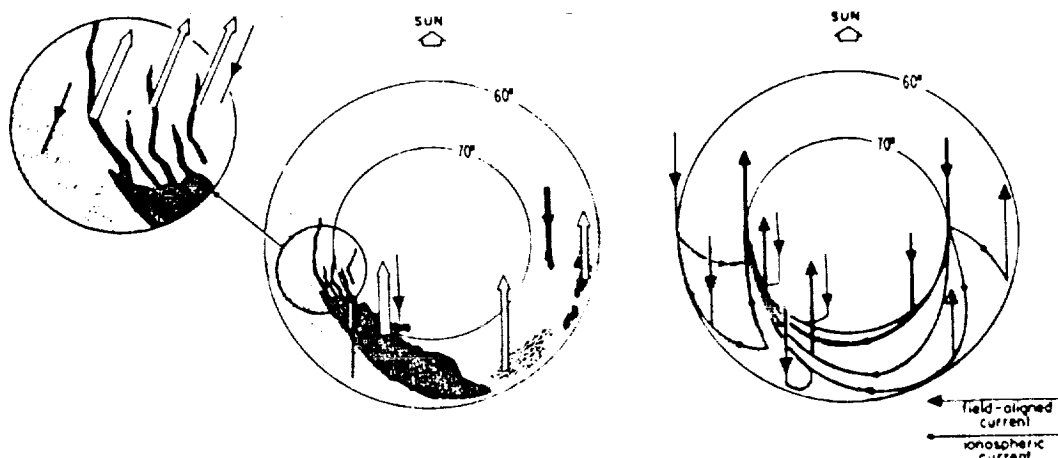
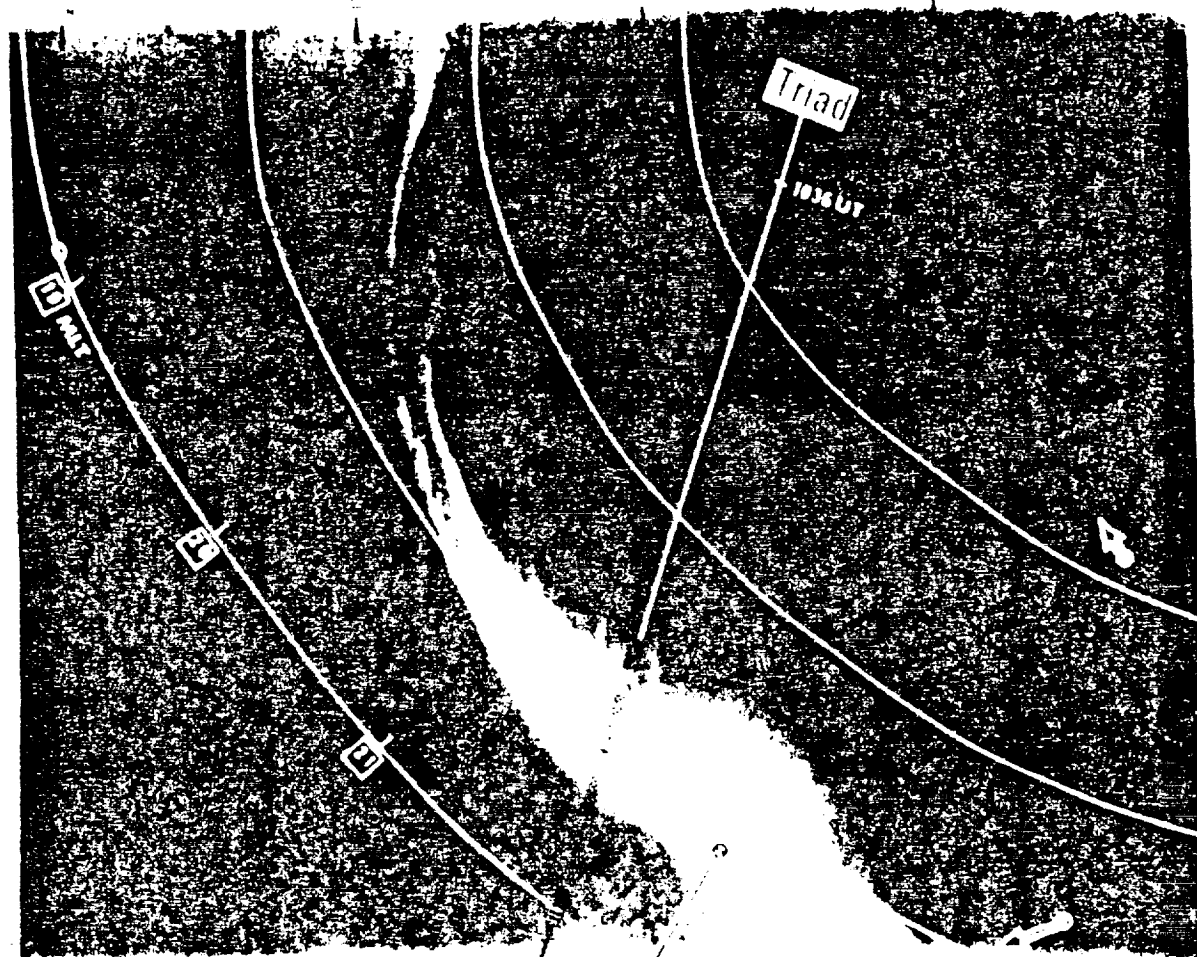
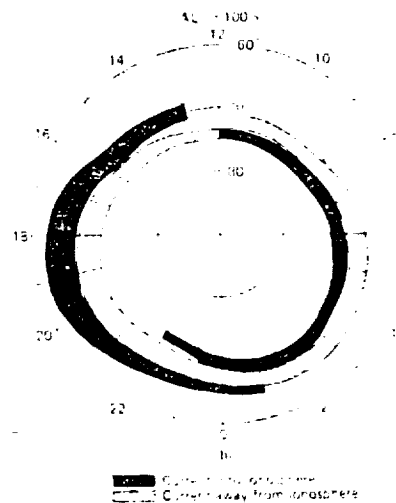
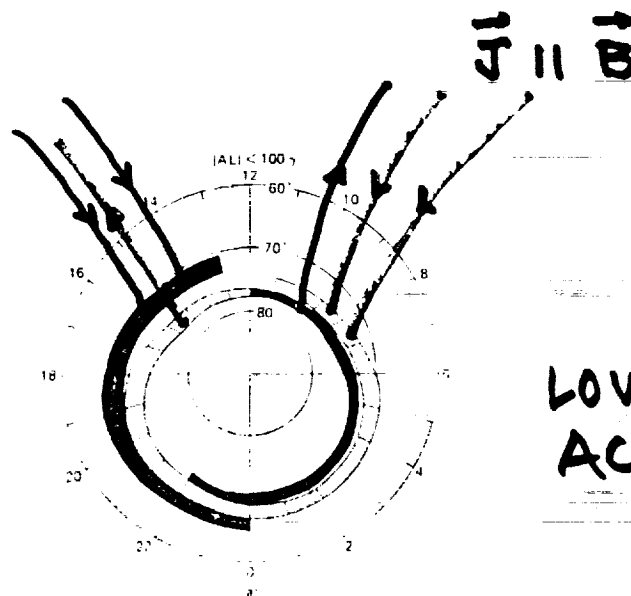


Fig. 8. Schematic diagram showing the relationship of the auroral electrojets and Birkeland currents with respect to the auroral distributions. Vertical arrows represent the Birkeland (upward and downward) currents (from Kamide and Rostoker, 1977; their Figure 16).

ORIGINAL PAGE IS  
OF POOR QUALITY



UCB BIDARCA

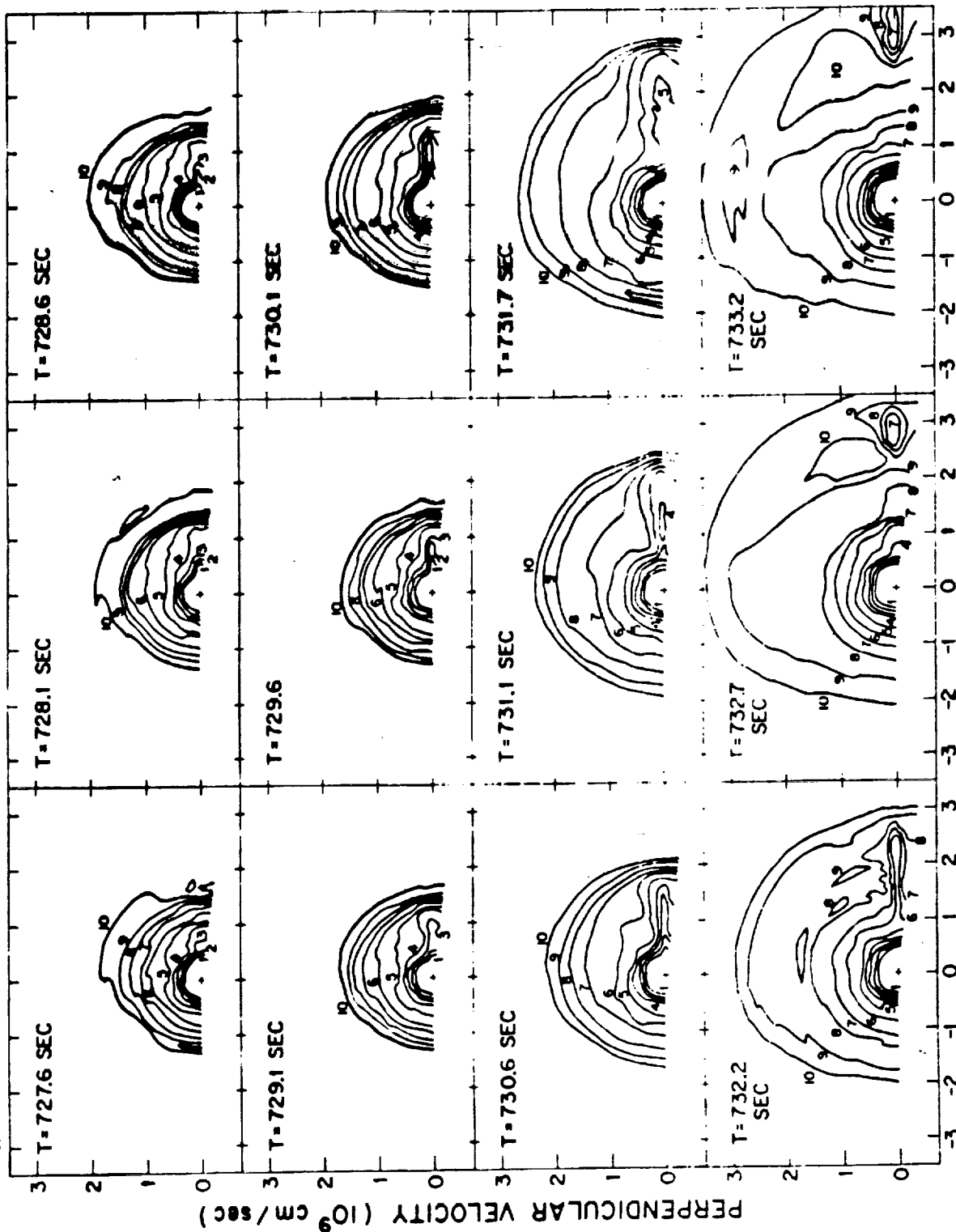
TERRIER MALEMUTE

7 FEBRUARY 1984

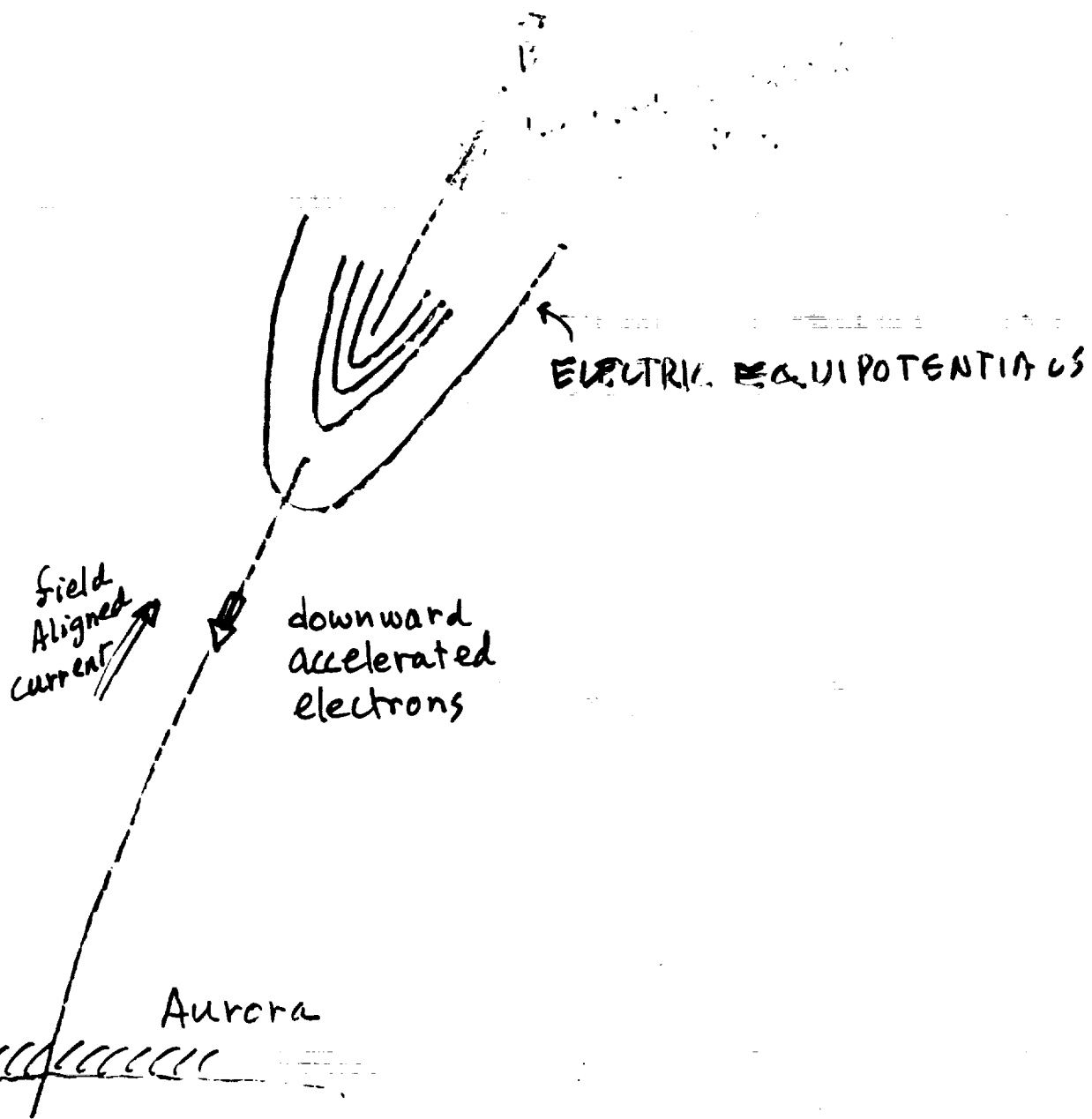
T=0 09:09:00 UT

LAUNCH 09:10:40 UT

ELECTRON DISTRIBUTION FUNCTION



ORIGINAL PAGE IS  
OF POOR QUALITY



Action Integral

$$\int p dq \approx \text{constant}$$

$$E_1 \frac{\sin^2 \alpha_1}{B_1} = (E_1 - \nabla \phi) \frac{\sin^2 \alpha_2}{B_2}$$



Source for diffuse and discrete auroral particle precipitation

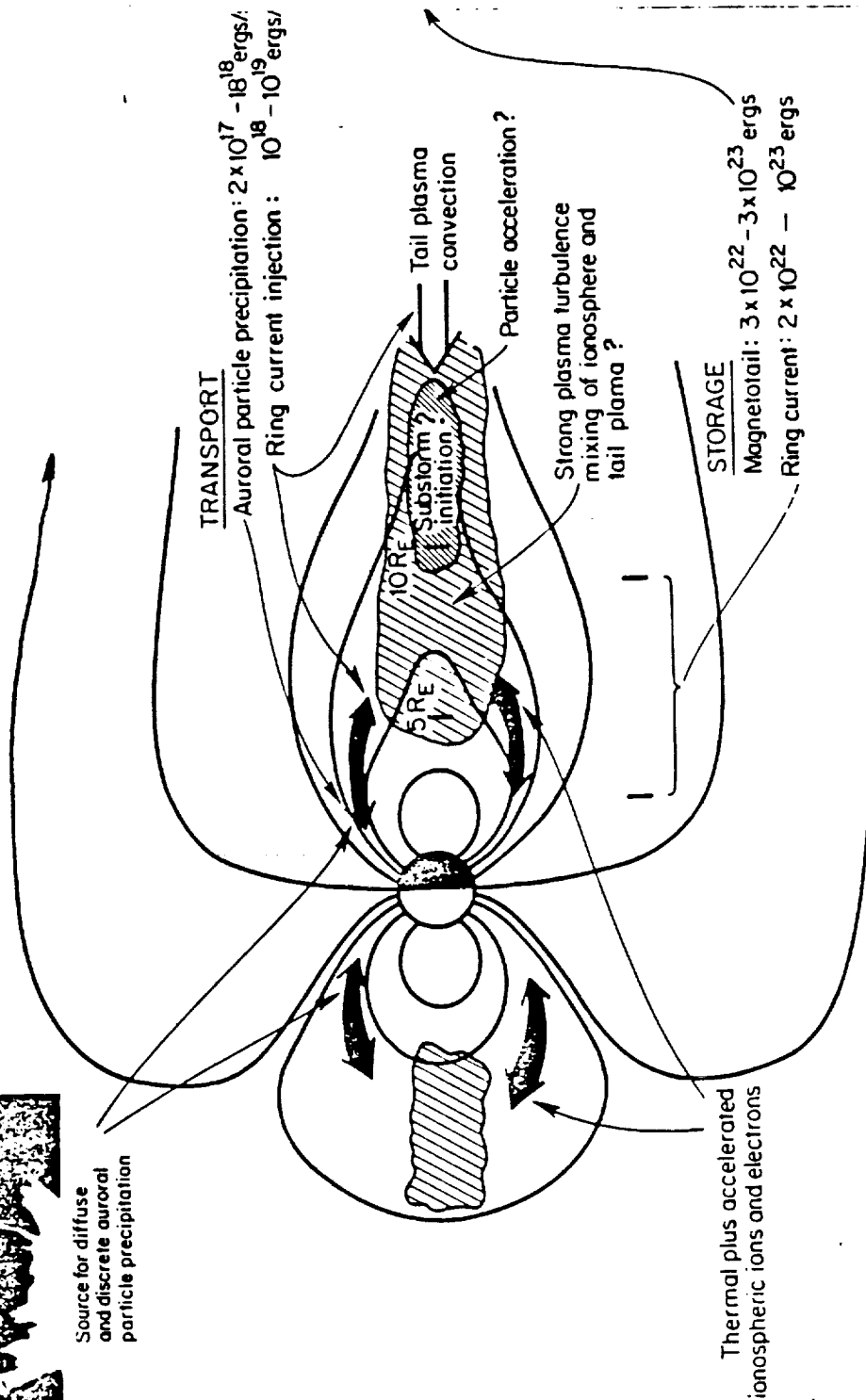
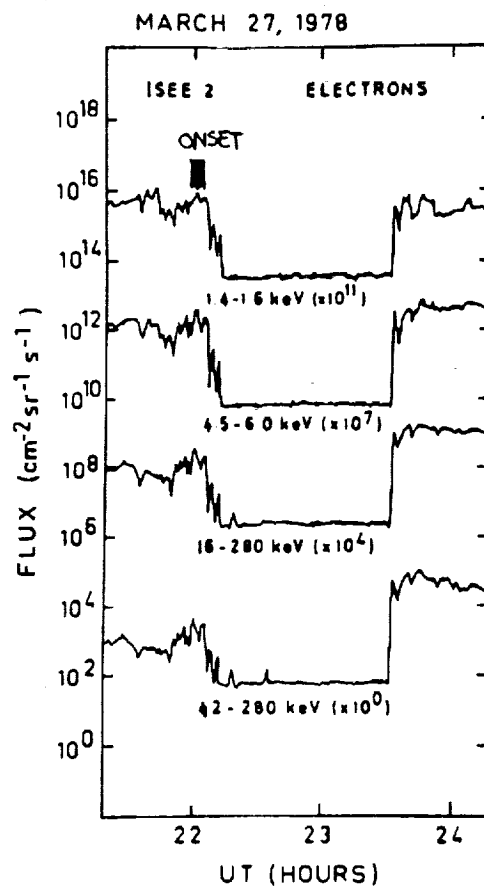
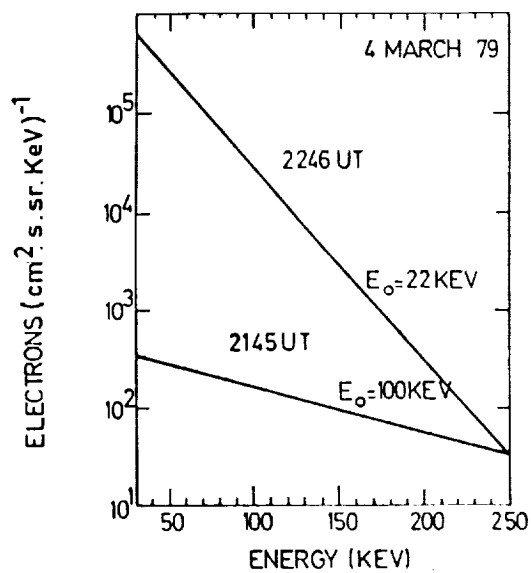
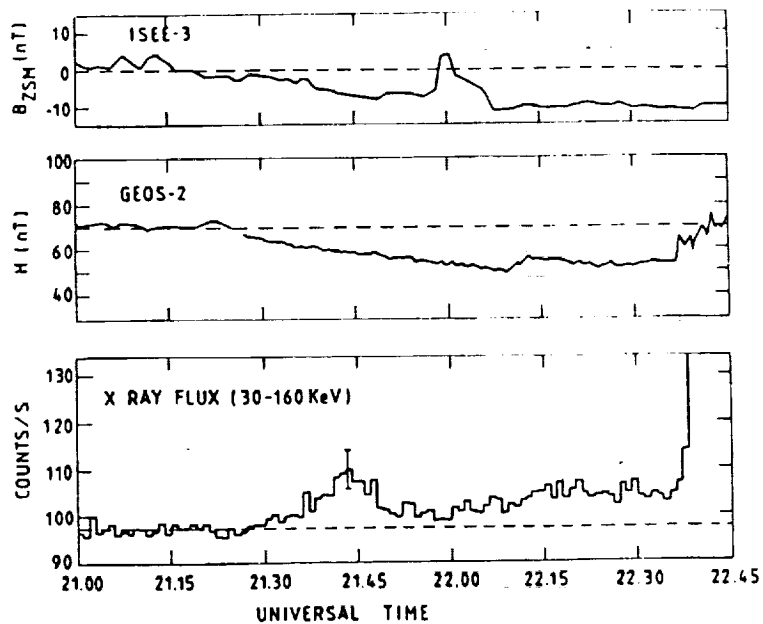


Fig. II-4: A schematic view of transport and storage questions involving the equatorial region of auroral magnetic fields that can be addressed by the ISTP/GJS program.



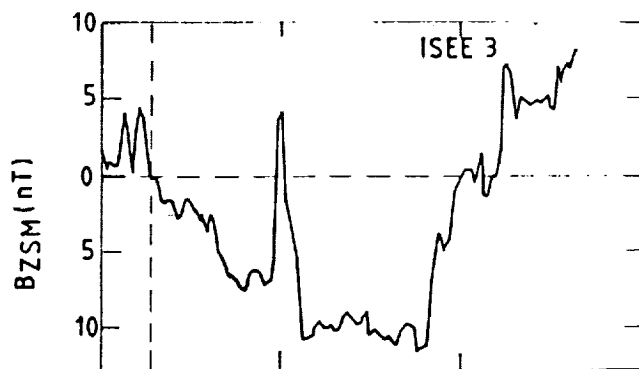
satellite at  
2.2  $R_e$  distance  
in the tail.

ORIGINAL PAGE IS  
OF POOR QUALITY

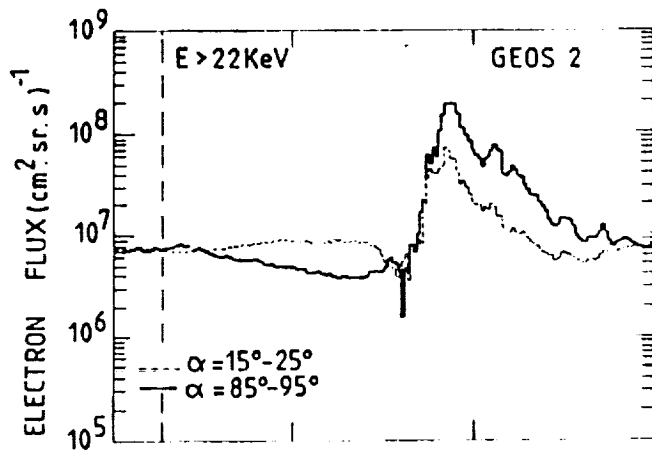


ORIGINAL PAGE IS  
OF POOR QUALITY

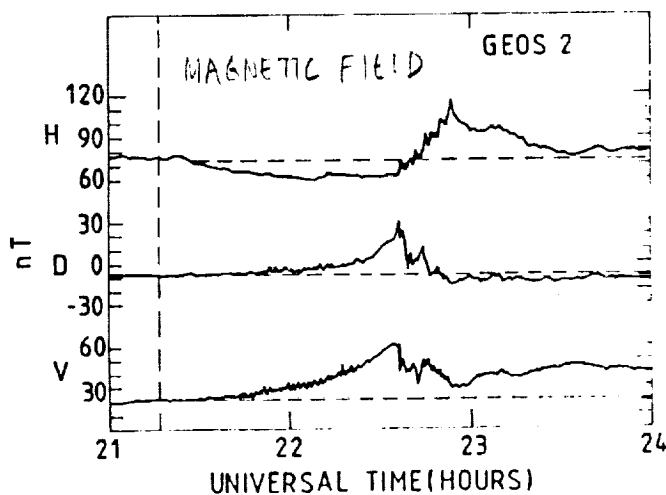
MARCH 4, 1979



SOLAR WIND  
MAGNETIC FIELD



INJECTION



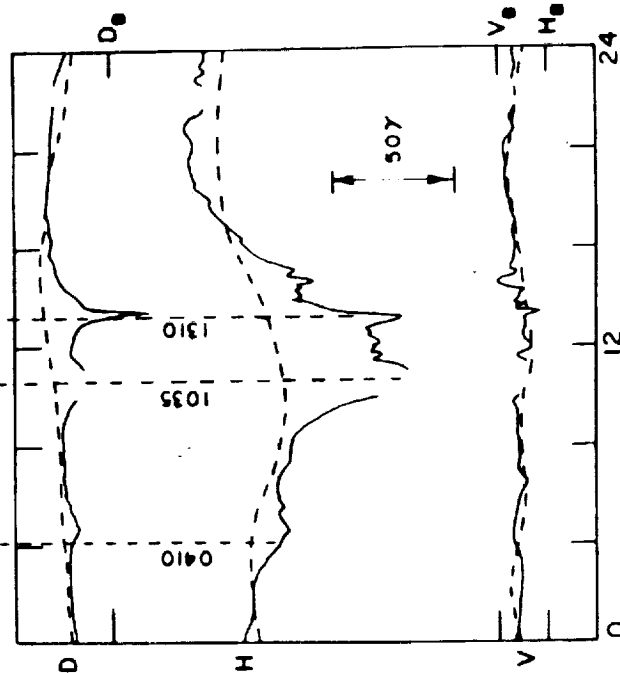
MAGNETIC FIELD  
(GEOS. ORBIT)

ORIGINAL PAGE IS  
OF POOR QUALITY



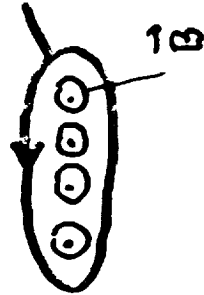
# GEOSTATIONARY ORBIT

POLAR  
SUBSTORM



U.T. (HOURS)

$$\nabla \times \vec{B} = \vec{J}$$



$\vec{J}$

D-component decrease  
flowing away from equator

## 1. ORBIT AND COORDINATE SYSTEM

The orbit of ATS and the two coordinate systems used in this paper are shown in Fig. 1. The orbit is circular at a distance of 3.6  $R_E$  with a period of 24 hours. When the satellite is launched, it will be in a point on the Earth's surface (135°W geographic longitude), which is always at the same universal time, 0000 UT.

The XYZ coordinate system is geocentric with the Z-axis parallel to the Earth's rotation axis. The X-axis is perpendicular to the Z-axis and lies in the plane containing the Sun and the rotation axis. The Y-axis completes the orthogonal system.

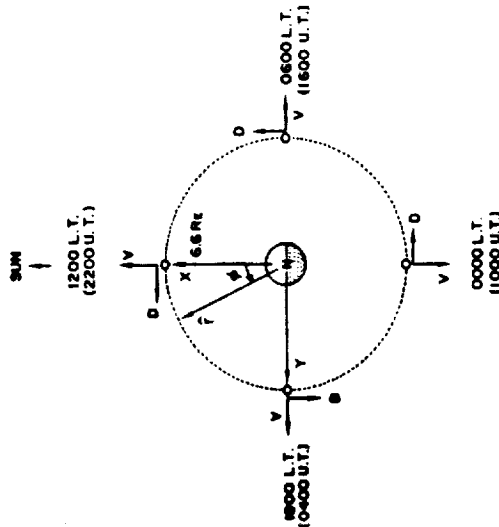


Figure 1. Orbit of ATS and the two coordinate systems used in this paper. The X-axis is perpendicular to the Z-axis and lies in the plane containing the Sun and the rotation axis. The Y-axis completes the orthogonal system.

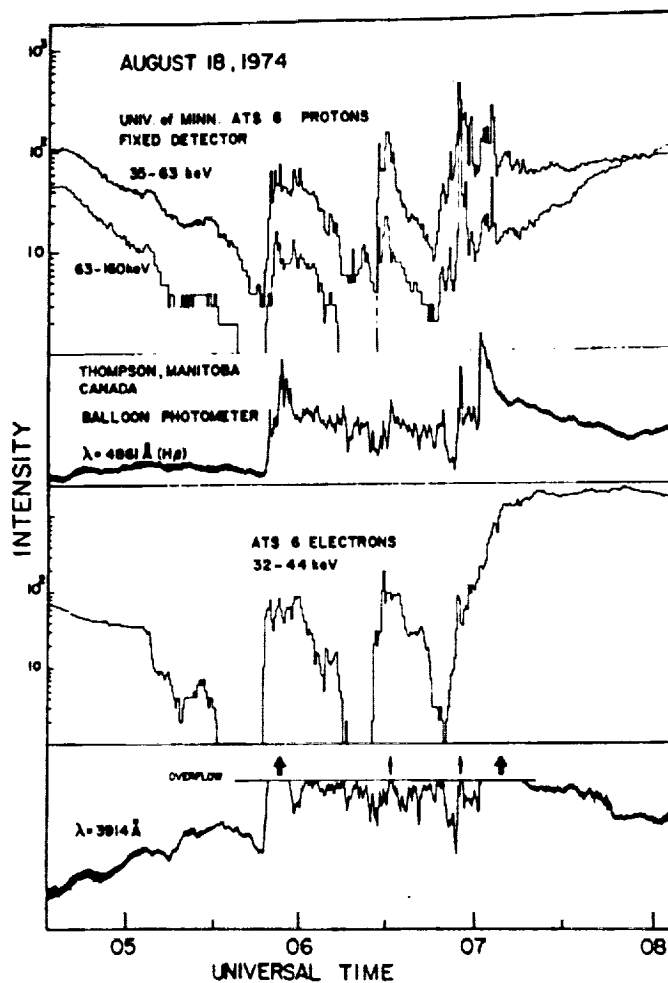
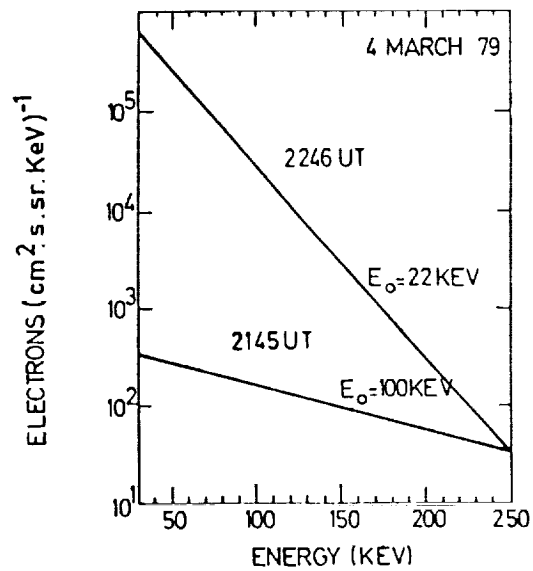
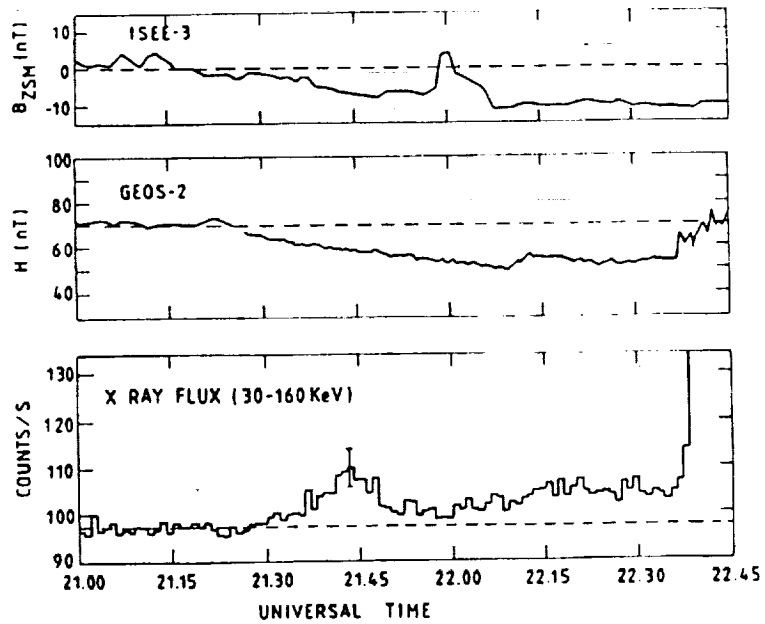


Fig. 1. Count rate time profile of equatorial particles (University of Minnesota detector) and auroral photometric emission data obtained from balloons.

ORIGINAL PAGE IS  
OF POOR QUALITY



ORIGINAL PAGE IS  
OF POOR QUALITY

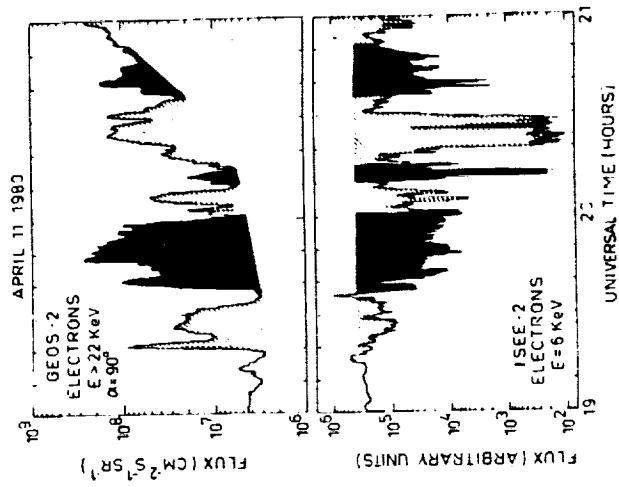
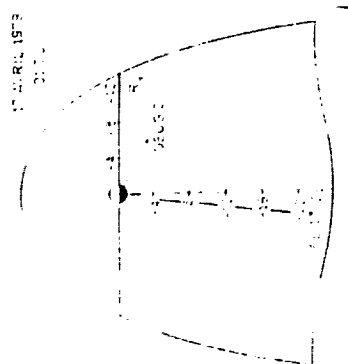
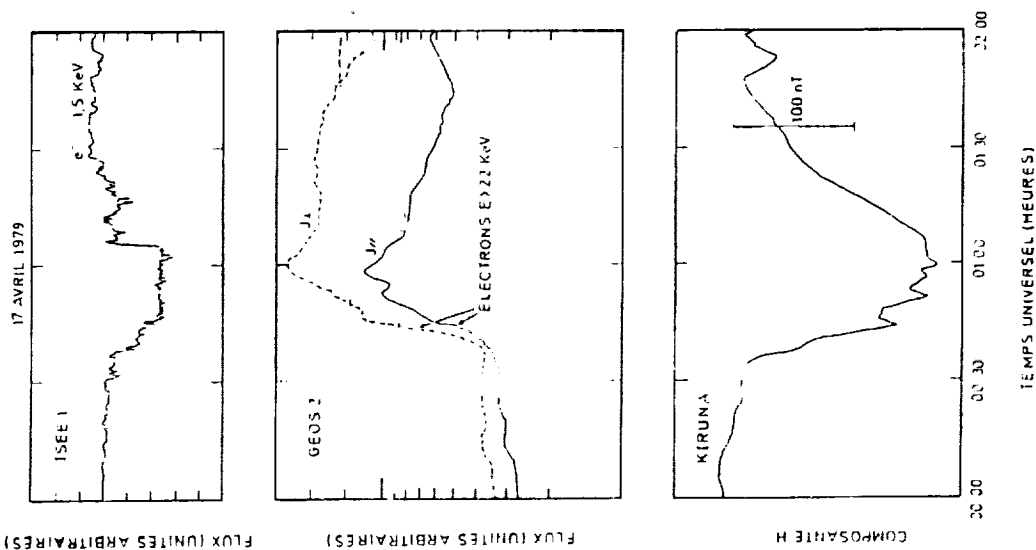


Figure 5. : High time resolution measurements from GEOS-2 and ISEE-2 during a multiple injection/thinning event on April 11, 1980.

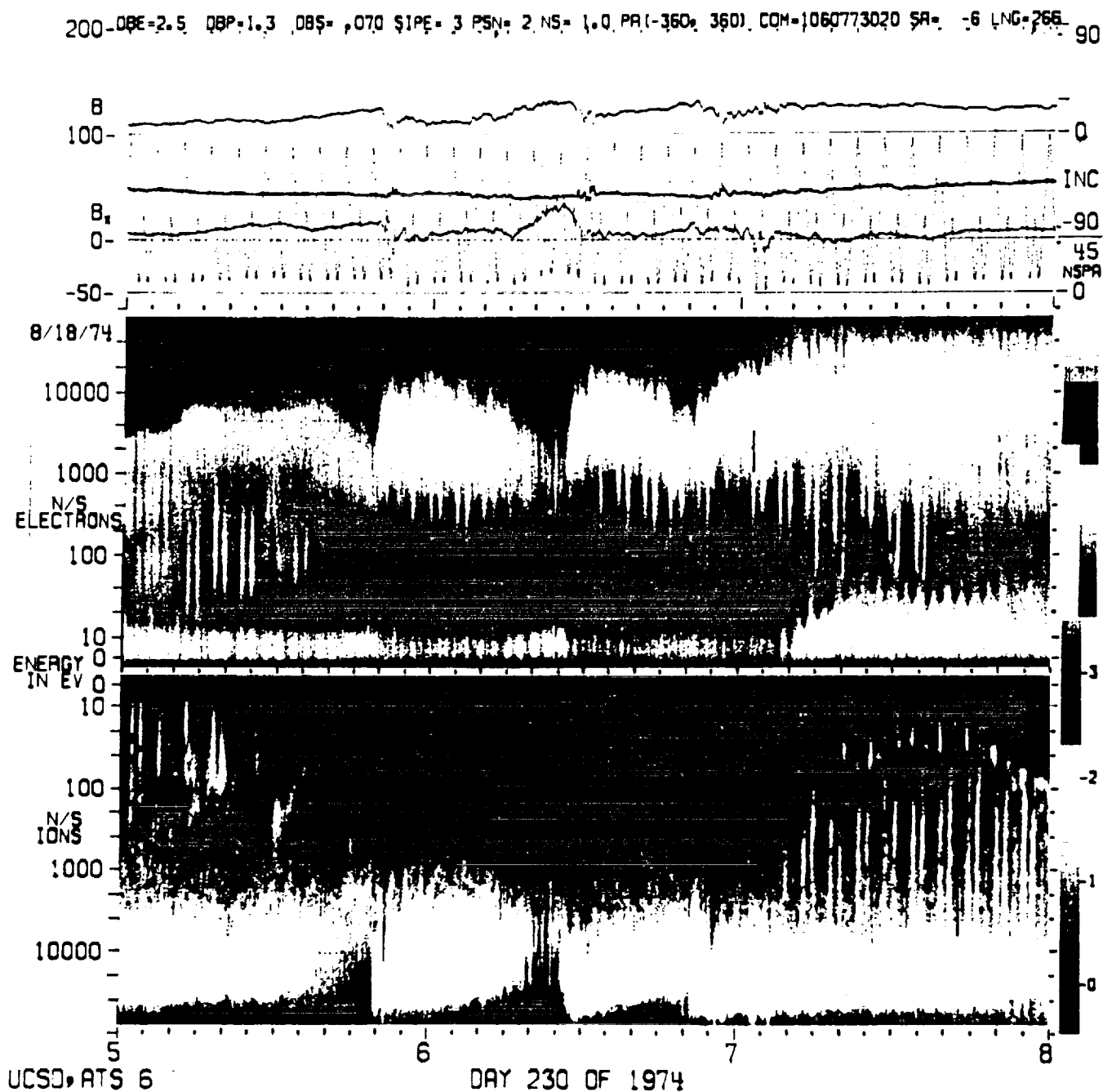


Fig. 2. Spectrogram of UCSD plasma data obtained by the north-south detector. The regular pattern of bright vertical lines is due to field-aligned particle fluxes.

ORIGINAL PAGE IS  
OF POOR QUALITY

IN THE OUTER MAGNETOSPHERE,

$$\beta \approx 0.1 - 1$$

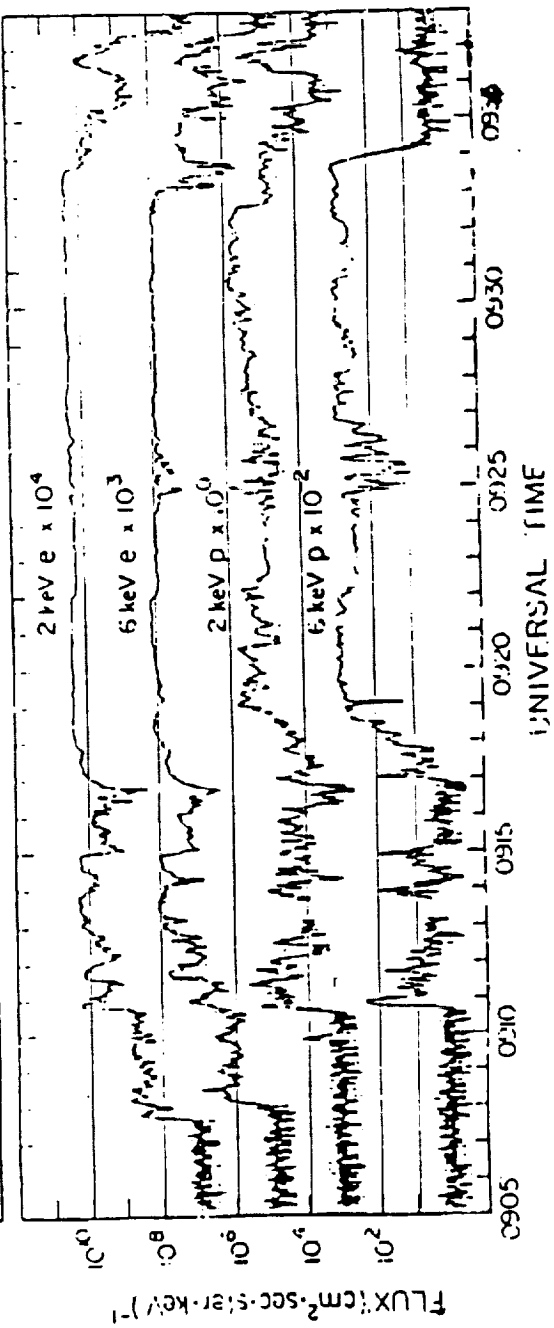
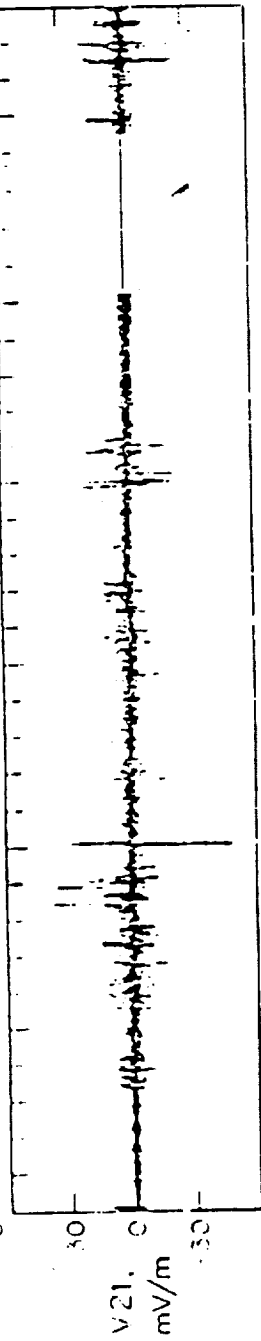
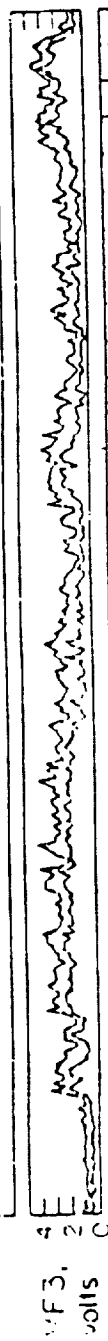
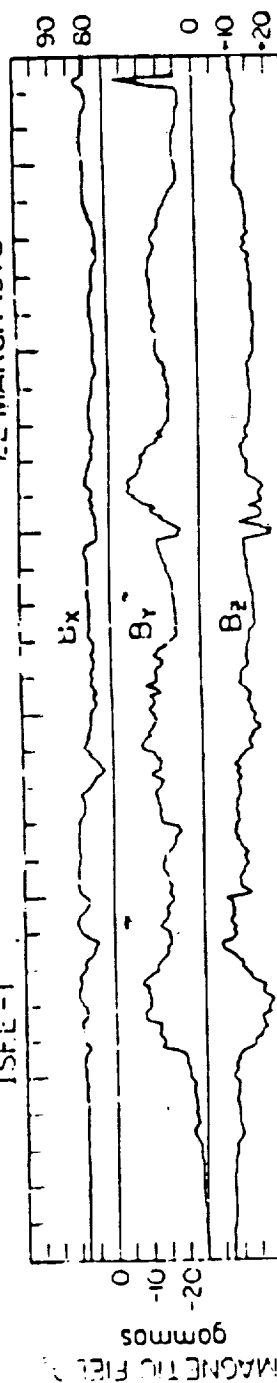
and

$$M_A \approx 0.1 - 0.5$$

HENCE, ONE EXPECTS IN GENERAL THERE IS DEPARTURE FROM THE  $\mathbf{J} \times \mathbf{B} = 0$  CONFIGURATION. NOTE, HOWEVER, THAT DURING DIPOLARIZATION, EVEN THE OUTER MAGNETOSPHERE MOMENTARILY ATTEMPTS TO ACHIEVE  $\mathbf{J} \times \mathbf{B} = 0$  CONFIGURATION. THIS IS BECAUSE  $\mathbf{J} \times \mathbf{B} = 0$  REPRESENTS AN MHD CONFIGURATION WITH MINIMUM ENERGY?

22 MARCH 1978

ISFE-1



ORIGINAL PAGE IS  
OF POOR QUALITY

MARCH 31, 1979  
ISEE-1

a → b | c → d →

46 eV

61 eV

87 eV

122 eV

180 eV

255 eV

359 eV

510 eV

724 eV

1 keV

1.46 keV

2 keV

2130

2200

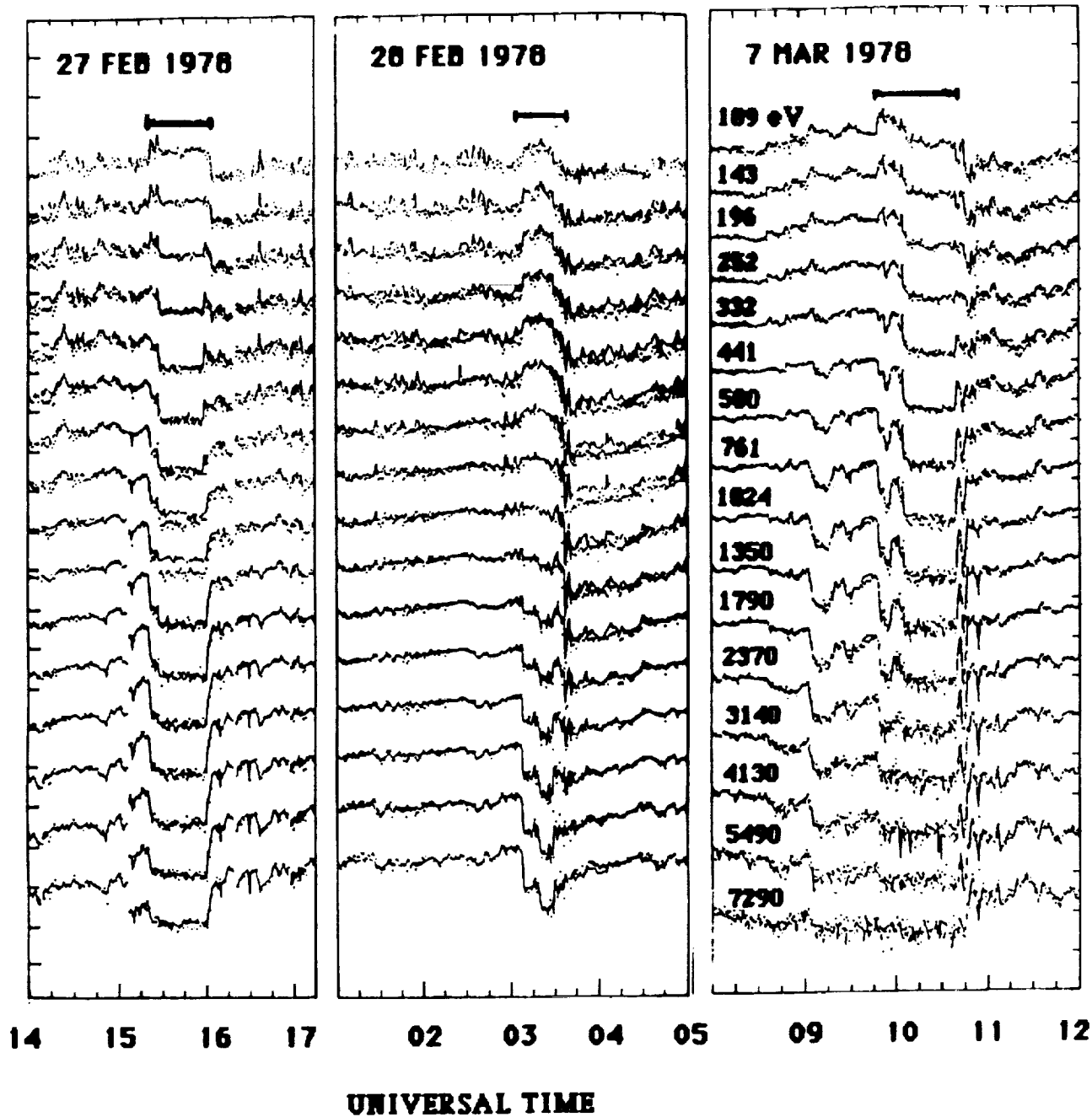
2300

2330

2400

UNIVERSAL TIME





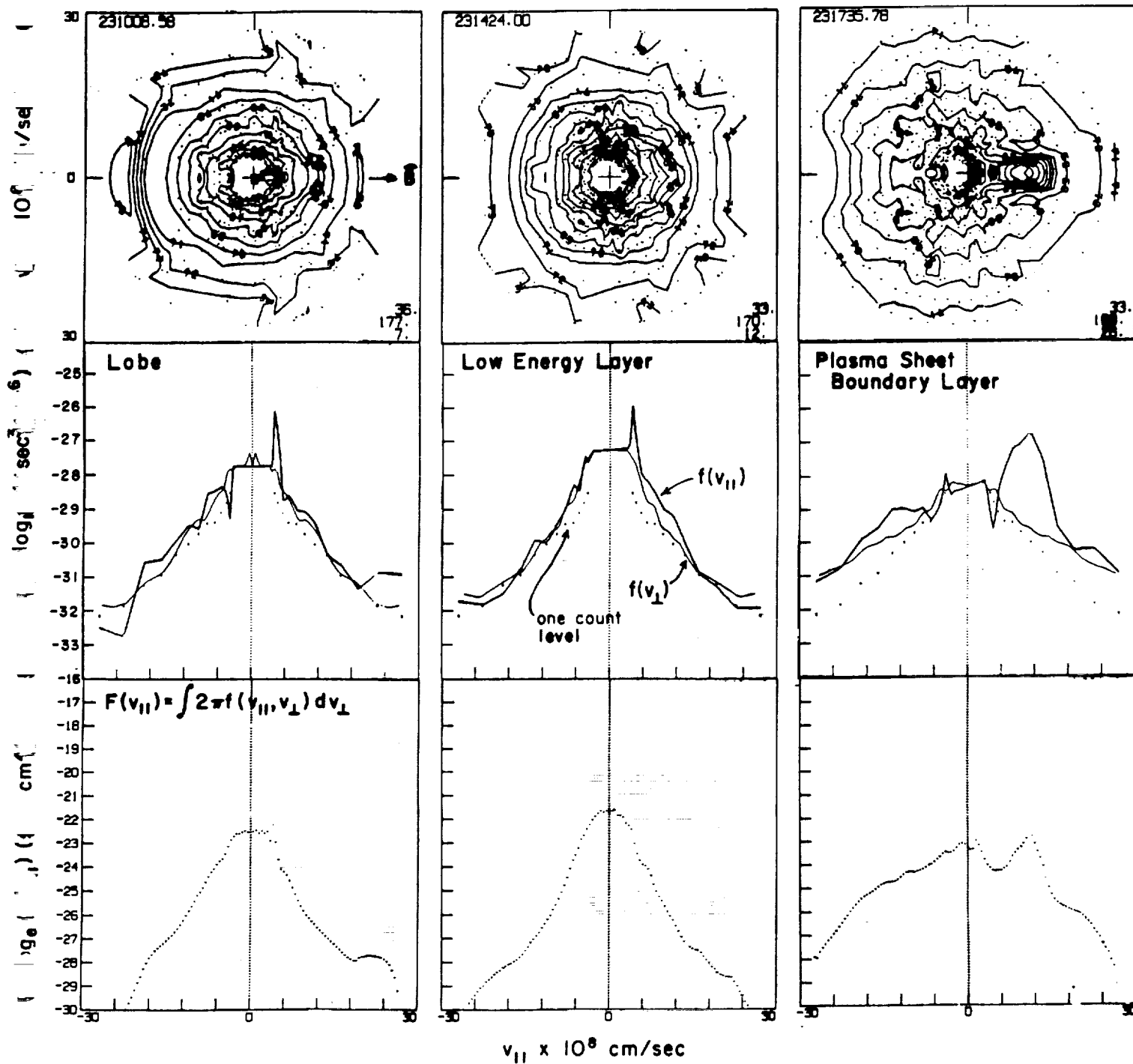
ORIGINAL PAGE IS  
OF POOR QUALITY

FLOW VELOCITIES  $\{U_1, U_2, U_3\}$  GIVEN in GSE  
COORDINATE SYSTEM.

WANT TO DETERMINE THE SENSE OF FLOW  
ABOUT THE AVERAGE MAGNETIC FIELD  
DIRECTION  $\langle B \rangle$ .

1. Calculate average  $B$  and associated unit  
vector  $b$ . Let  $b$  be along  $Z'$  direction.
2. Calculate perpendicular component of  $U$ ,  
 $U_{\perp} = U - (U \cdot b) b$
3. Define unit vectors  $X' = U_{\perp} / |U_{\perp}|$  and  $Y' =$   
 $b \times X'$
4. Calculate  $U'_{\perp}$  in coordinate frame  $X'$  and  $Y'$ .

$$f(v_{||}, v_{\perp})$$



ORIGINAL PAGE IS  
OF POOR QUALITY

19 APRIL 1978 ISEE-1

ELECTRONS 2 keV

6 keV

PROTONS 2 keV

6 keV

FLUX (ARB. UNITS)

FREQUENCY (kHz)

20

10

0

11 40

11 50

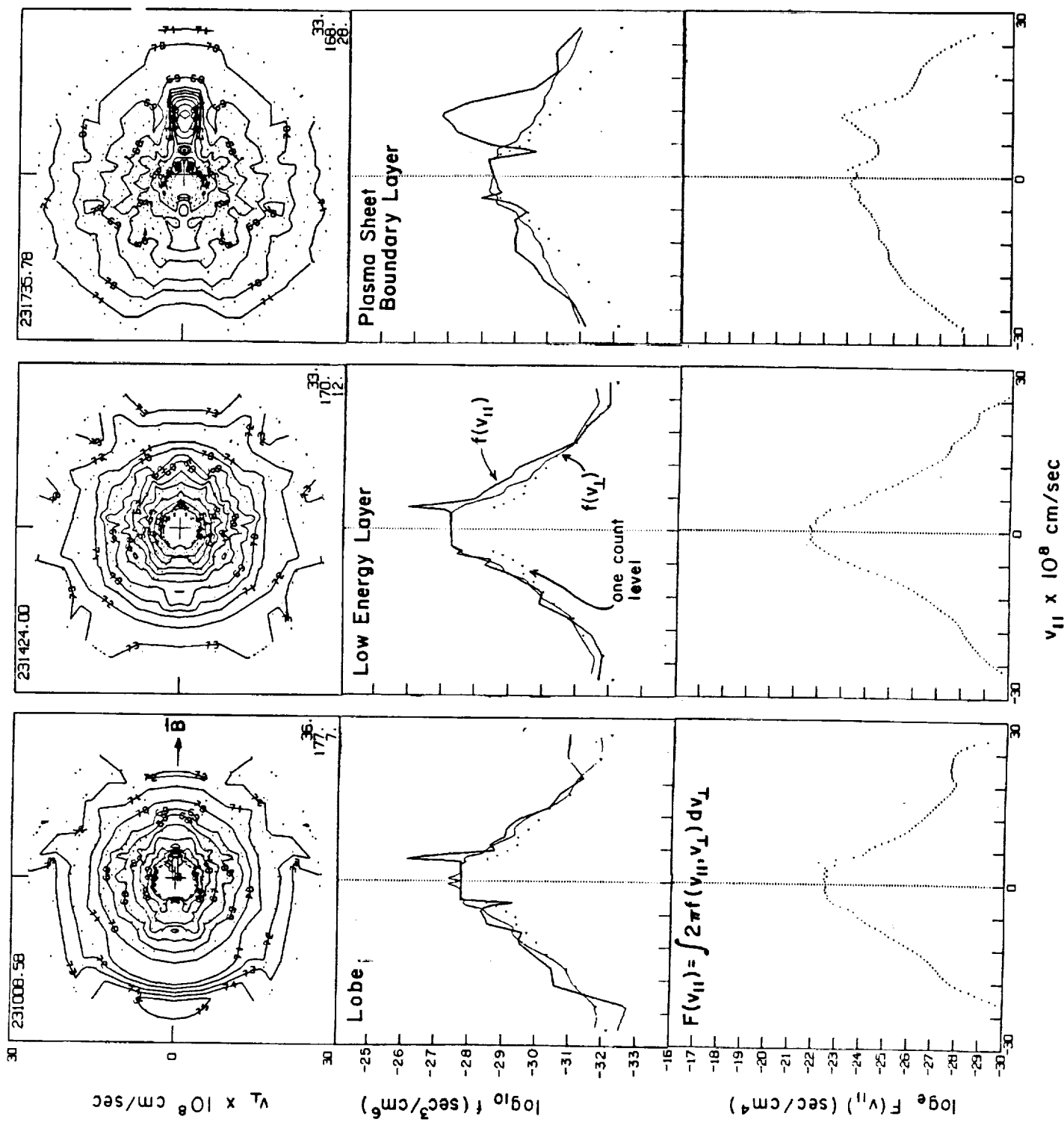
12 0

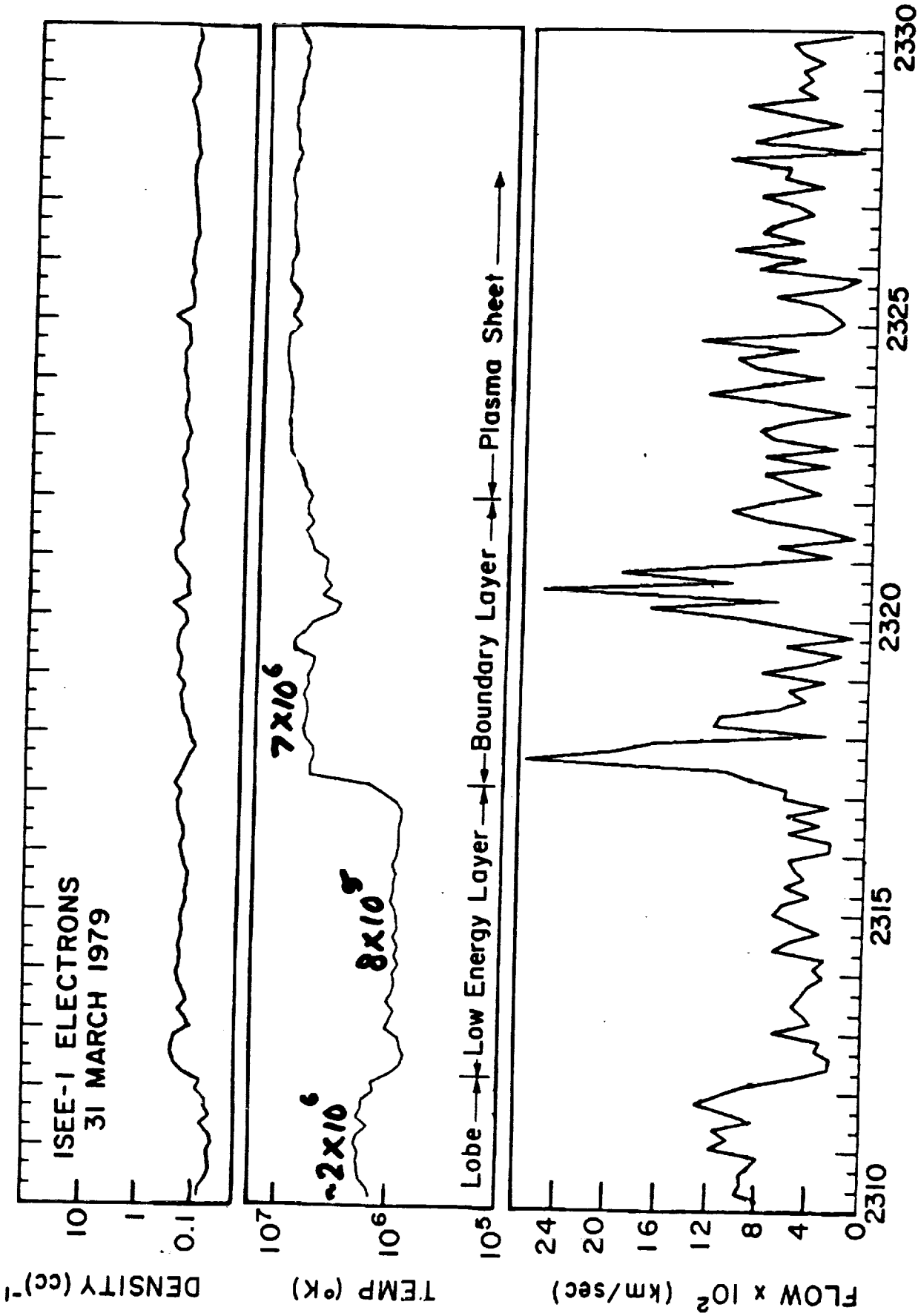
12 10

12 20

UNIVERSAL TIME

ORIGINAL PAGE IS  
OF POOR QUALITY





UVI CALIBRATION SOURCE

Joe Ajello

4:00 15 August





# Simple ultraviolet calibration source with reference spectra and its use with the Galileo orbiter ultraviolet spectrometer

J. M. Ajello, D. E. Shemansky, B. Franklin, J. Watkins, S. Srivastava, G. K. James, W. T. Simms, C. W. Hord, W. Pryor, W. McClintock, V. Argabright, and D. Hall

We have developed a simple compact electron impact laboratory source of UV radiation whose relative intensity as a function of wavelength has an accuracy traceable to the fundamental physical constants (transitions probabilities and excitation cross sections) for an atomic or molecular system. Using this laboratory source, calibrated optically thin vacuum ultraviolet (VUV) spectra have been obtained and synthetic spectral models developed for important molecular band systems of  $H_2$  and  $N_2$  and the  $n^1P^o$  Rydberg series of He. The model spectrum from  $H_2$  represents an extension of the molecular branching ratio technique to include spectral line intensities from more than one electronic upper state. The accuracy of the model fit to the VUV spectra of  $H_2$  and  $N_2$  is sufficient to predict the relative spectral intensity of the electron impact source and to serve as a primary calibration standard for VUV instrumentation in the 80–230-nm wavelength range. The model is applicable to VUV instrumentation with full width at half-maximum  $\geq 0.4$  nm. The present accuracy is 10% in the far ultraviolet (120–230 nm), 10% in the extreme ultraviolet (EUV) (90–120 nm), and 20% in the EUV (80–90 nm). The  $n^1P^o$  Rydberg series of He has been modeled to 10% accuracy and can be considered a primary calibration standard in the EUV (52.2–58.4 nm). A calibrated optically thin spectrum of Ar has been obtained at 0.5-nm resolution and 200-eV electron impact energy to 35% accuracy without benefit of models over the EUV spectral range of 50–95 nm. The Ar spectrum expands the ultimate range of the VUV relative calibration using this source with the four gases, He, Ar,  $H_2$ , and  $N_2$ , to 50–230 nm. The calibration of the Galileo orbiter ultraviolet spectrometer for the upcoming Jupiter mission has been demonstrated and compared to results from other methods.

## I. Introduction

Primary and secondary standards of absolute spectral radiance with uncertainties of  $<10\%$  in the vacuum ultraviolet (VUV) from 50 to 250 nm include the argon mini<sup>1</sup> and maxi<sup>2</sup> arcs, the synchrotron,<sup>3,4</sup> the deuterium lamp,<sup>5,6</sup> and the hydrogen arc discharge.<sup>2,7–9</sup> Prior to 1980 the argon mini arc was the only small compact

laboratory source available for general laboratory use below 170 nm with a short-wavelength cutoff of  $\sim 114$  nm, depending on window material. The small portable deuterium lamp has had its short-wavelength calibration edge brought down to 115 nm extending its wavelength range of applicability to include all wavelengths between 115 and 350 nm.<sup>5,6</sup> Both the argon mini arc and the deuterium lamp are calibrated against the hydrogen arc. The hydrogen arc is a primary standard of reference. This method is based on the assumption that the hydrogen plasma is in local thermodynamic equilibrium. The hydrogen arc is complicated and requires a 1200-V 100-A dc power supply.<sup>2</sup> To meet the lack of portable transfer standards in the far ultraviolet (FUV) the argon mini arc secondary standard was developed. A power supply of 1.2 kW is normally required. By contrast the principal power requirement for the simple electron source controller described here is the dc filament power supply of 2.5 V at 2 A. Degradation of optics from intense EUV radiation is absent. The uniformity of the source eliminates the need for field apertures as required in other

D. Hall and D. E. Shemansky are with University of Arizona, Lunar & Planetary Laboratory, Tucson, Arizona 85721; V. Argabright, W. McClintock, W. Pryor, and C. W. Hord are with University of Colorado, Department of Astrophysical, Planetary & Atmospheric Science, Laboratory for Atmospheric & Space Physics, Boulder, Colorado 80309; the other authors are with California Institute of Technology, Jet Propulsion Laboratory, Pasadena, California 91109.

Received 6 April 1987.

0003-6936/88/050890-25\$02.00/0.

© 1988 Optical Society of America

1. The first part of the document is a list of names and addresses of the members of the committee.

2. The second part of the document is a list of names and addresses of the members of the committee.

3. The third part of the document is a list of names and addresses of the members of the committee.

4. The fourth part of the document is a list of names and addresses of the members of the committee.

5. The fifth part of the document is a list of names and addresses of the members of the committee.

6. The sixth part of the document is a list of names and addresses of the members of the committee.

7. The seventh part of the document is a list of names and addresses of the members of the committee.

8. The eighth part of the document is a list of names and addresses of the members of the committee.

9. The ninth part of the document is a list of names and addresses of the members of the committee.

10. The tenth part of the document is a list of names and addresses of the members of the committee.

11. The eleventh part of the document is a list of names and addresses of the members of the committee.

12. The twelfth part of the document is a list of names and addresses of the members of the committee.

13. The thirteenth part of the document is a list of names and addresses of the members of the committee.

14. The fourteenth part of the document is a list of names and addresses of the members of the committee.

15. The fifteenth part of the document is a list of names and addresses of the members of the committee.

16. The sixteenth part of the document is a list of names and addresses of the members of the committee.

17. The seventeenth part of the document is a list of names and addresses of the members of the committee.

18. The eighteenth part of the document is a list of names and addresses of the members of the committee.

MAGNETOSPHERIC ENERGY FLOW

Bruce Tsuratani  
(Joe Ajello)

15 August

## MAIN ISSUE OF ISTP: ENERGY FLOW

- 1) FROM AURORAL ZONE UV OBSERVATIONS, CALCULATE ENERGY DEPOSITION INTO IONOSPHERE
  - a) Whole auroral oval
  - b) Near-midnight sector (to measure instantaneous particle injection)
- 2) Compare with interplanetary indices ( $L_o^2$   $VB^2 \sin^4 (\theta/2)$ ,  $p^{1/6} VB \sin^4 (\theta/2)$ ,  $p^{1/2} VB_z$ , etc.)
- 3) Compare with tail lobe/plasma sheet energy ( $B^2/8\pi \times A$ )

Most people believe the magnetosphere act as a "leaky bucket". Thus the energy injection from the solar wind (item 2) partially goes into tail storage (item 3) and partly into the ionosphere (item 1a, b). The time phasing is variable, depending on the level of geomagnetic activity? The auroral energy at local times other than near midnight (item 1a) is partly from the precipitation of energetic particles that have (gradient and curvature) drifted to other local times and is partly due to other processes causing the dayside aurora (cross-field diffusion, etc.). The energy associated with the latter process should be subtracted out.

## DECOUPLING OF AURORAL ZONE AND RING CURRENT ENERGIES

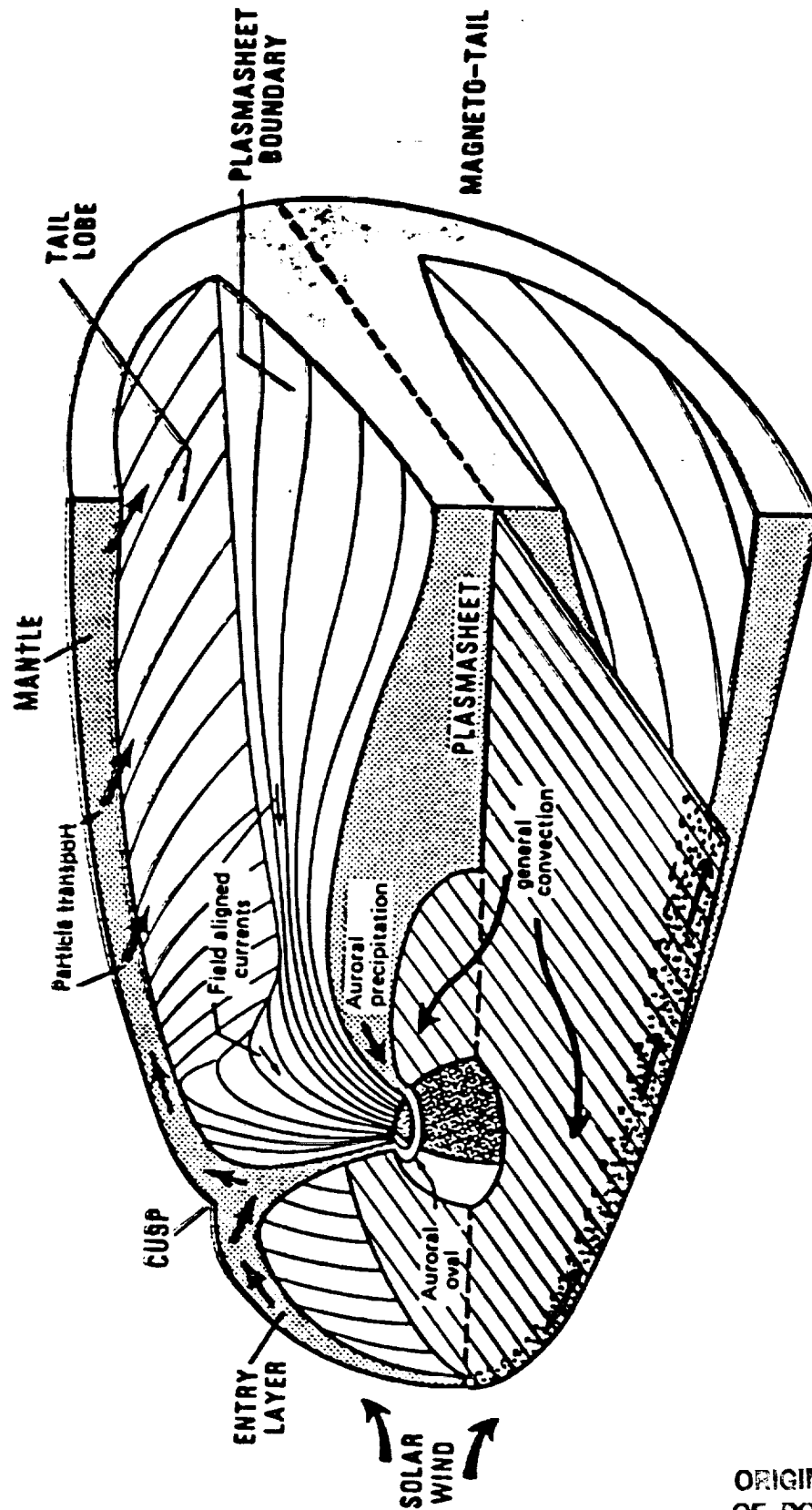
By comparing 2) and 1) (and by measuring the radiation belt energy), one should be able to determine what portion of the interplanetary energy is going into the auroral zone and how much into the ring current.

GROUND-BASED MEASUREMENTS OF  
FIELDS AND CURRENTS

Bob Clauer

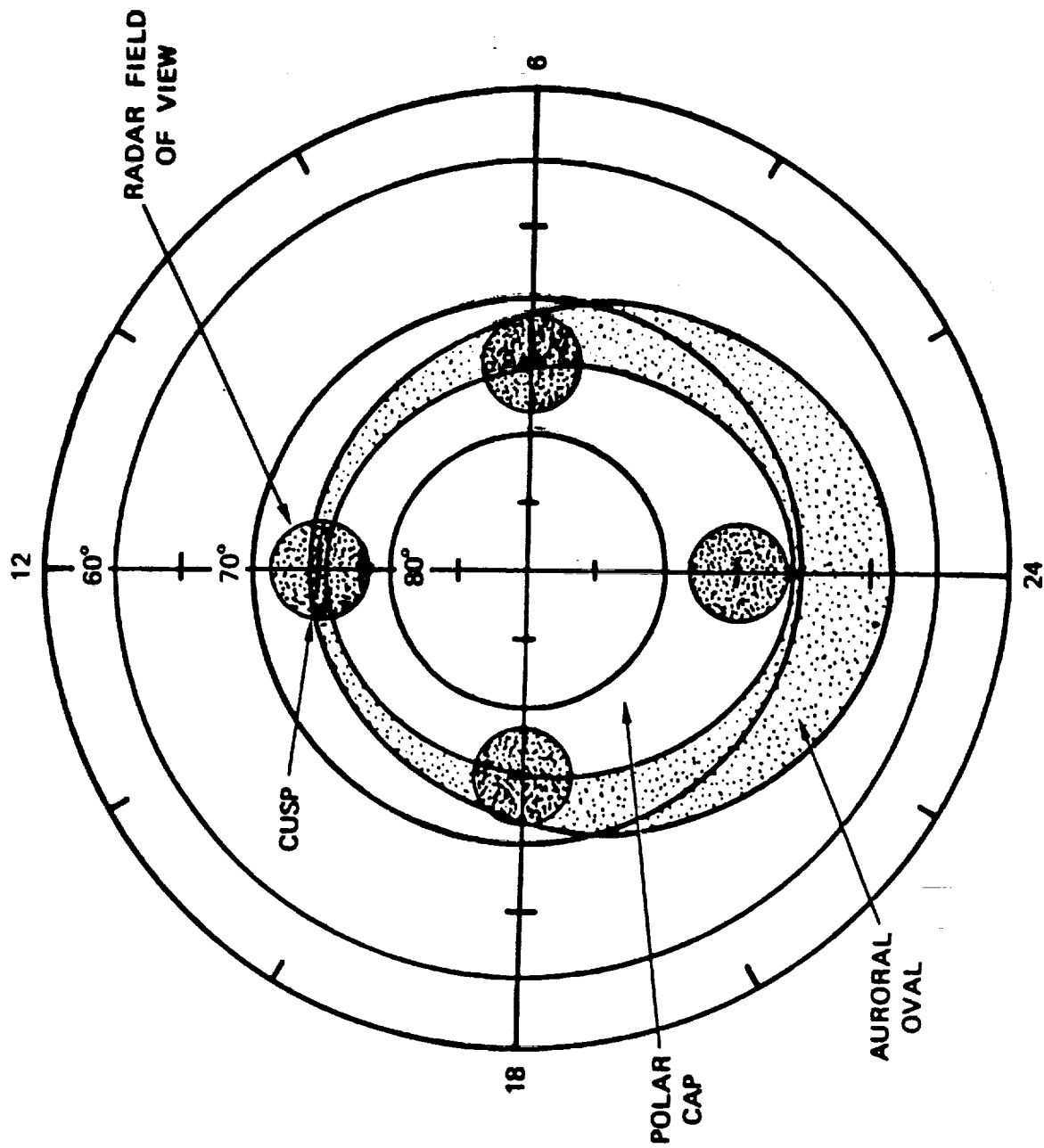
4:30 15 August

# CONNECTIONS BETWEEN THE MAGNETOSPHERE AND HIGH-LATITUDE IONOSPHERE

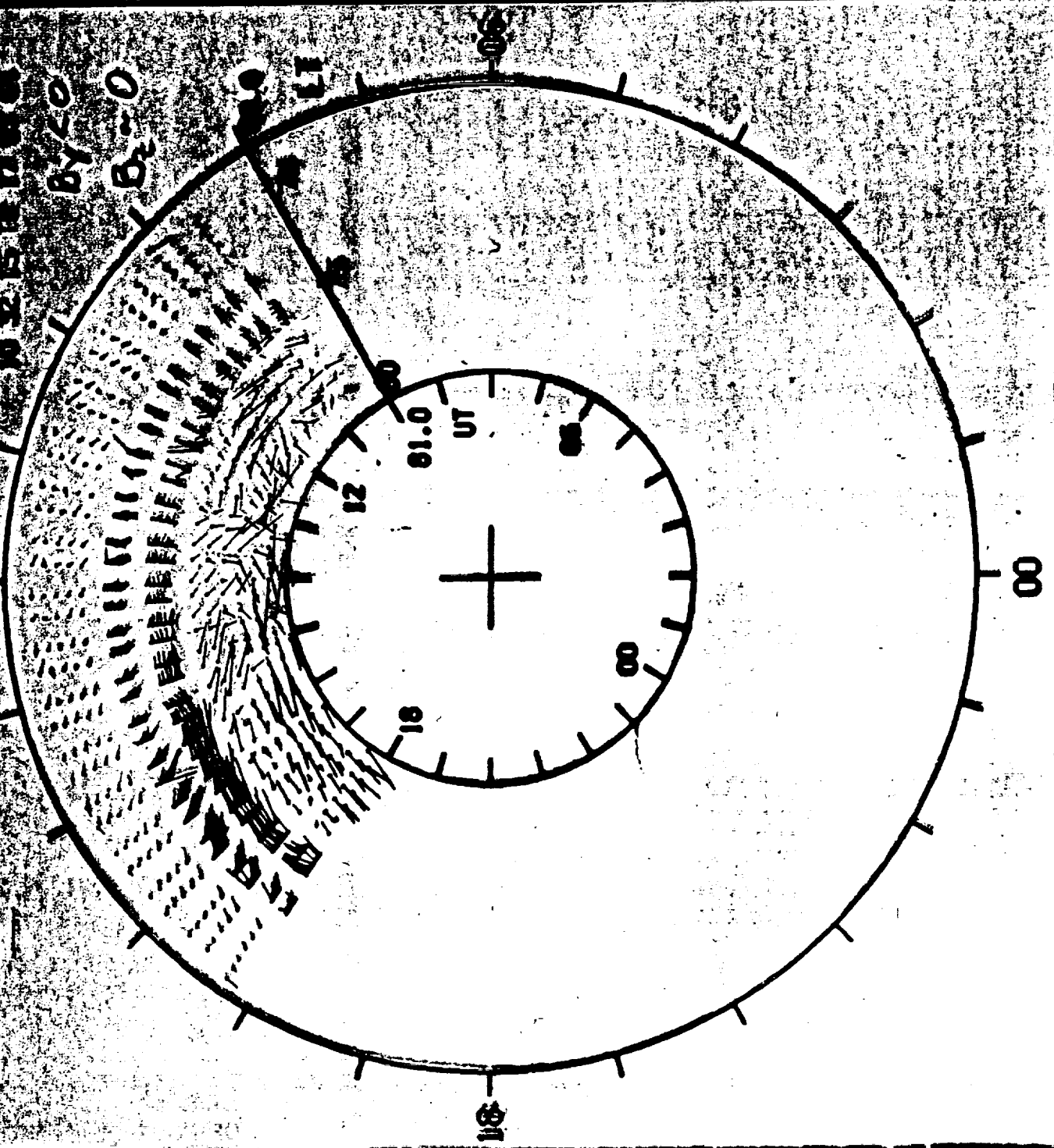


ORIGINAL PAGE IS  
OF POOR QUALITY

# THE SONDRESTROM RADAR IN RELATION TO THE AURORAL OVAL, CUSP, AND POLAR CAP

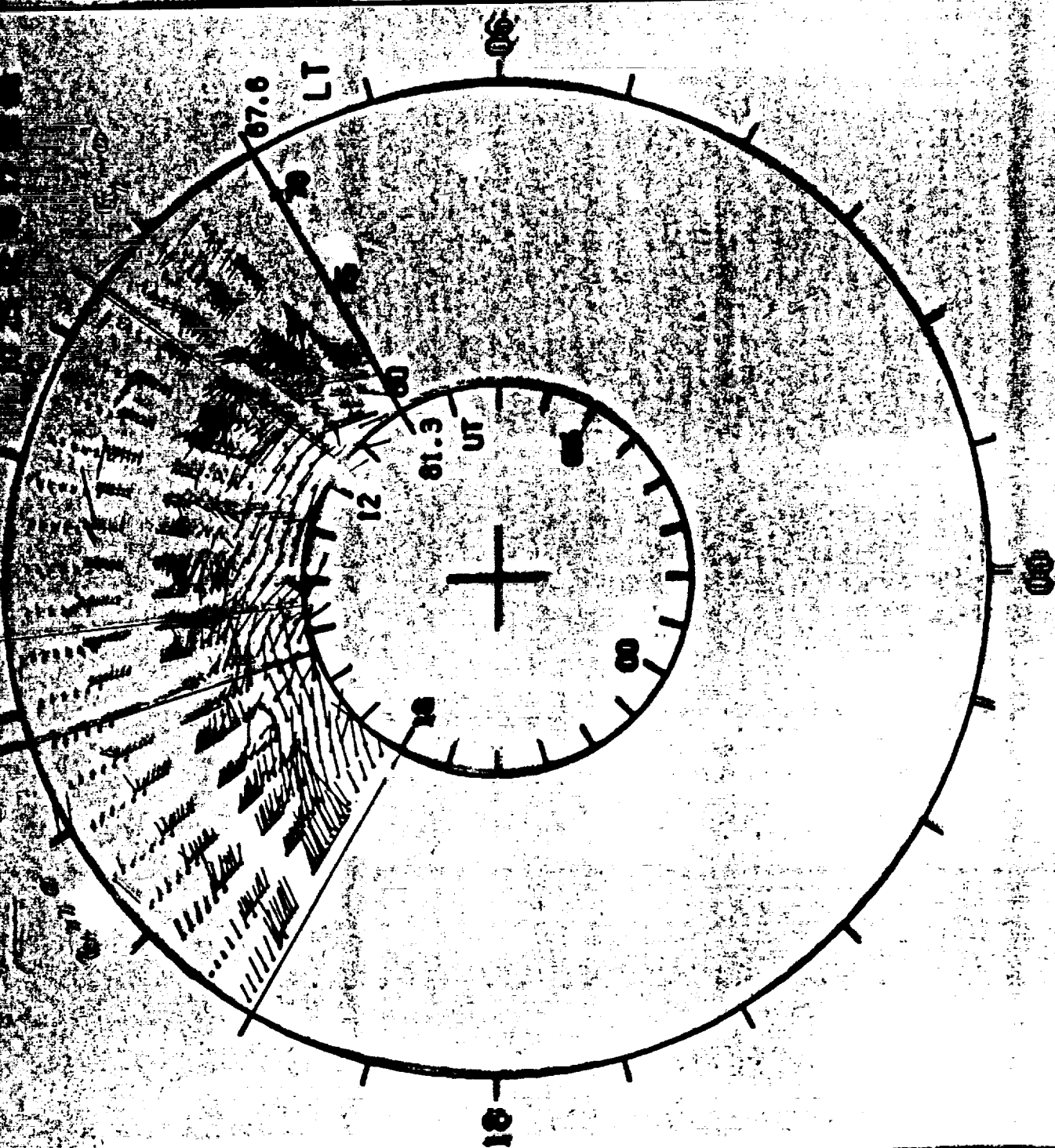




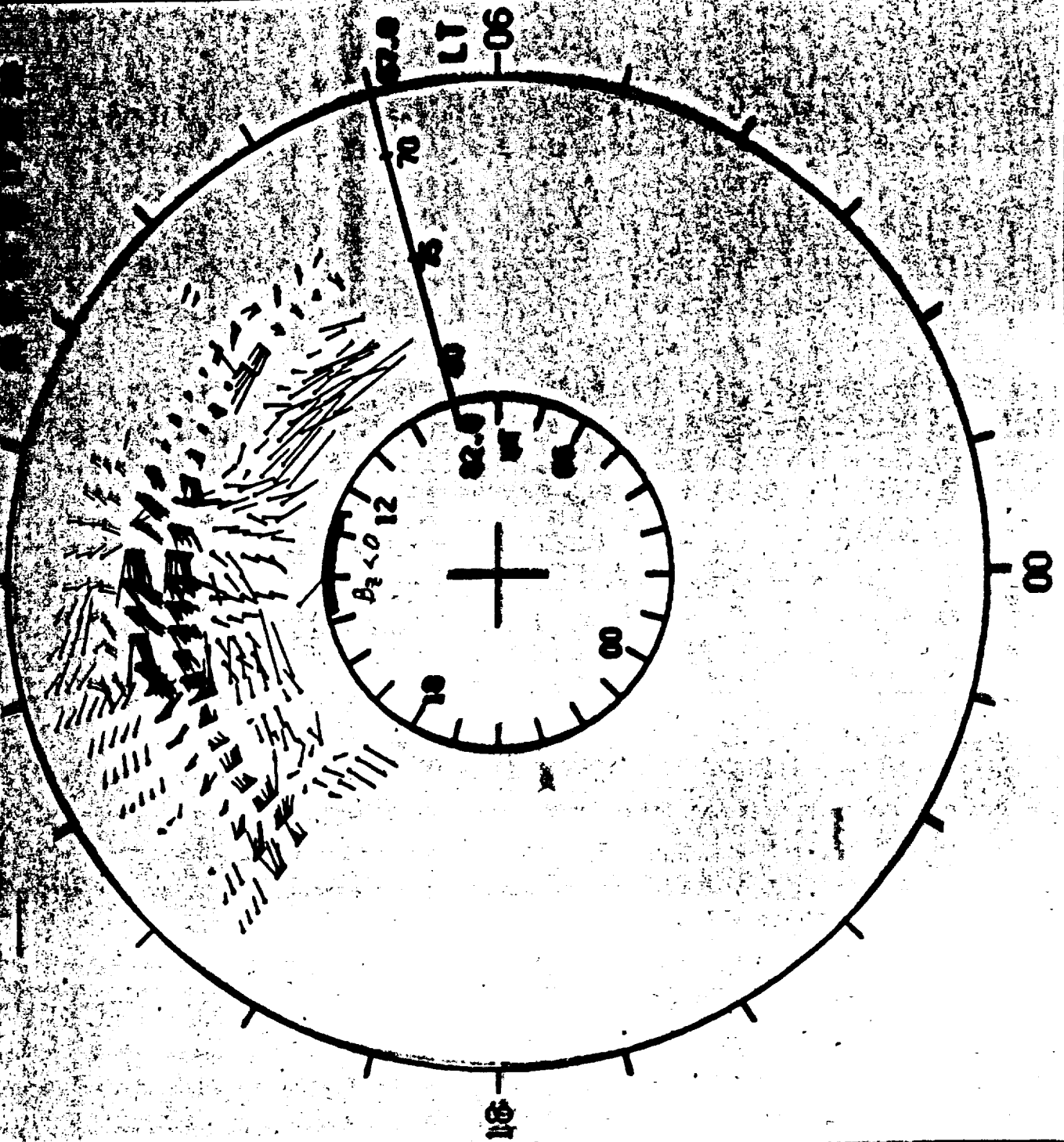


ORIGINAL PAGE IS  
OF POOR QUALITY

VELOCITY



ORIGINAL PAGE IS  
OF POOR QUALITY



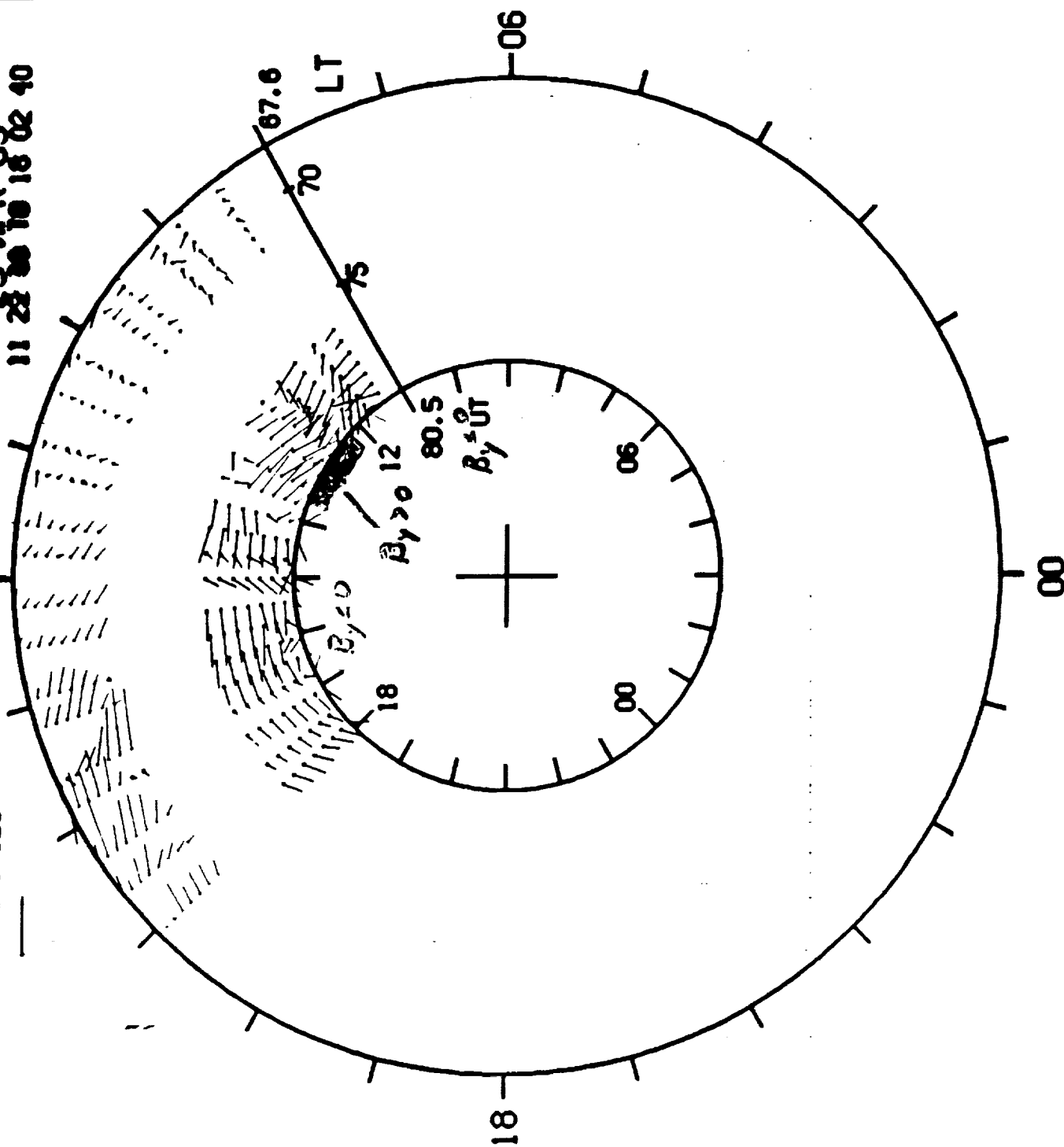
C-6

ORIGINAL PAGE IS  
OF POOR QUALITY

# VELOCITY

2000.0 METERS/SEC

25-APR-83  
11 22 33 18 02 40



ORIGINAL PAGE IS  
OF POOR QUALITY

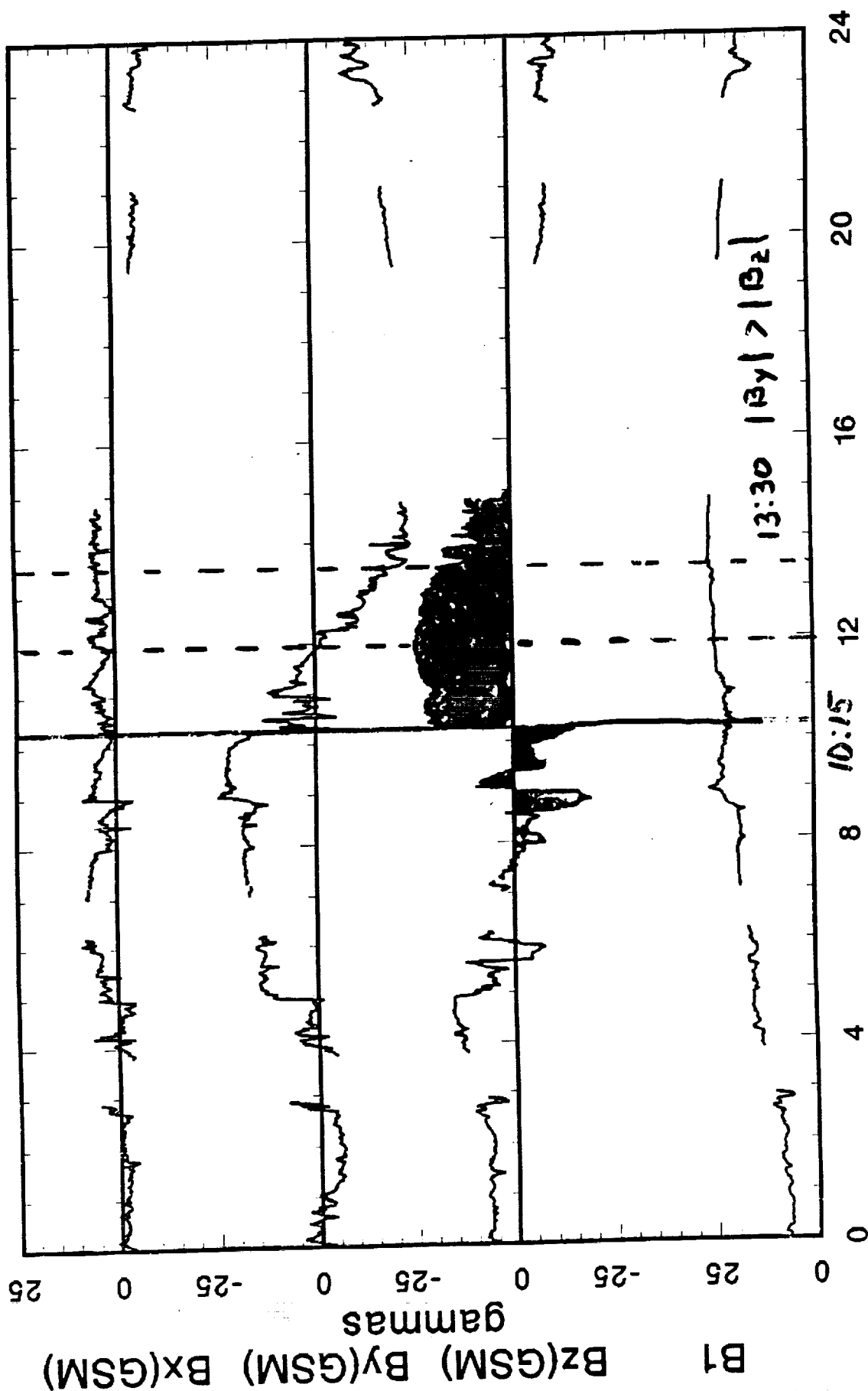
# IMP-8 MAGNETIC FIELD

23-JUL-83

00:00:00 TO 24:00:00

$V_{sw} \approx 400 \text{ km/sec}$

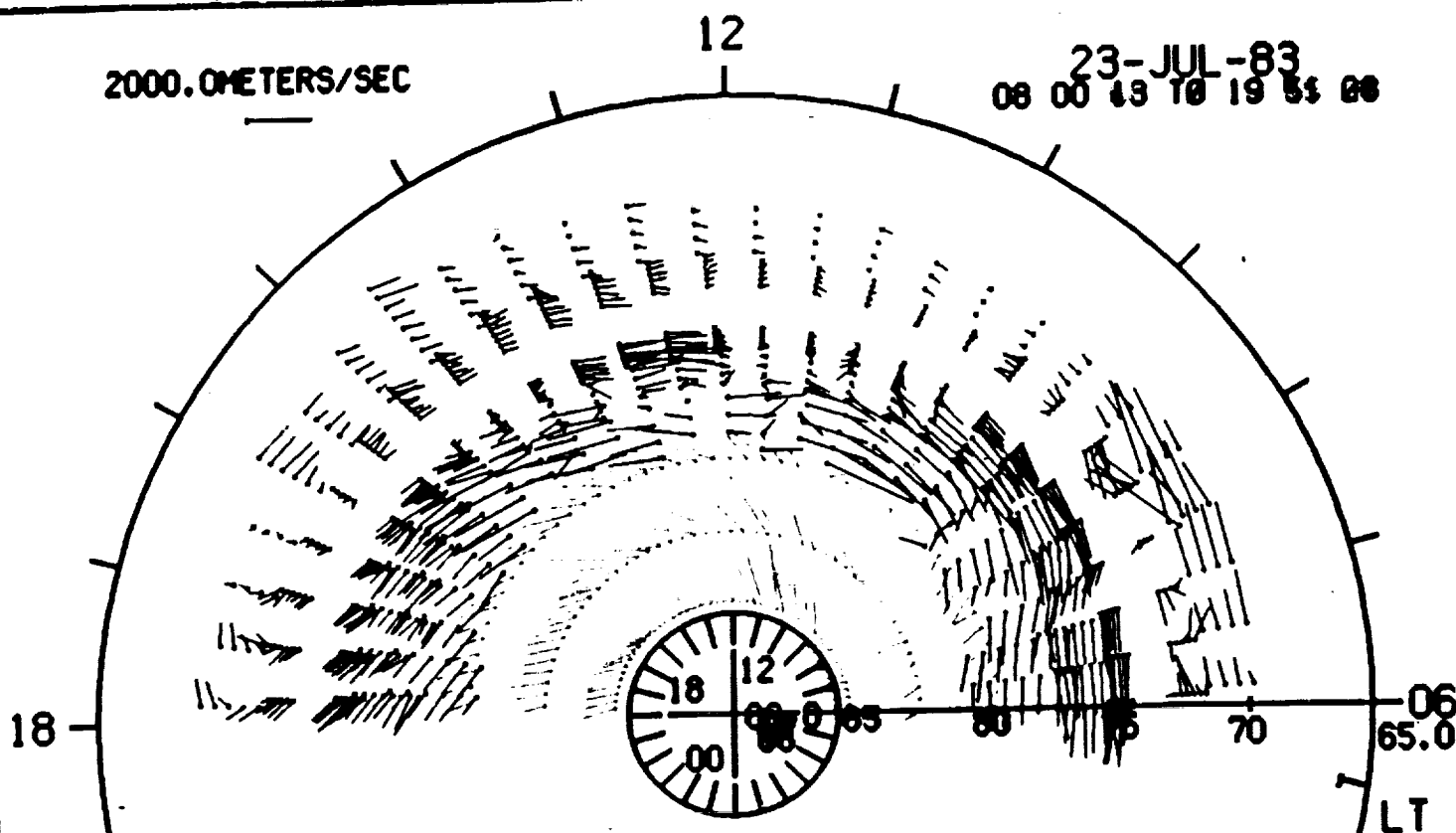
$\rho_{sw} \approx 10/\text{cm}^3$



# MEASURED ION VELOCITY

2000.0 METERS/SEC

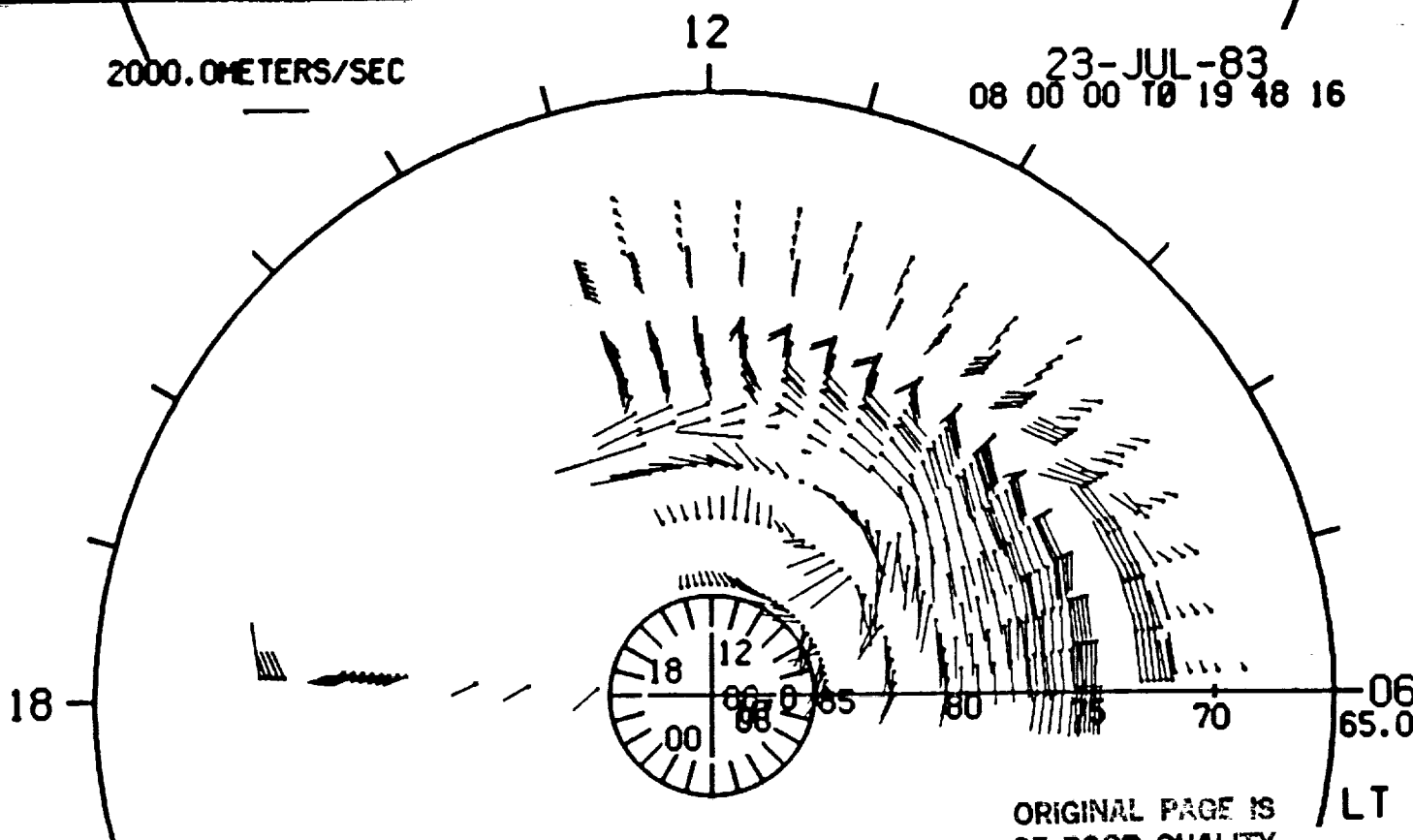
23-JUL-83  
08 00 49 10 19 51 00



# MODEL ION VELOCITY

2000.0 METERS/SEC

23-JUL-83  
08 00 00 10 19 48 16

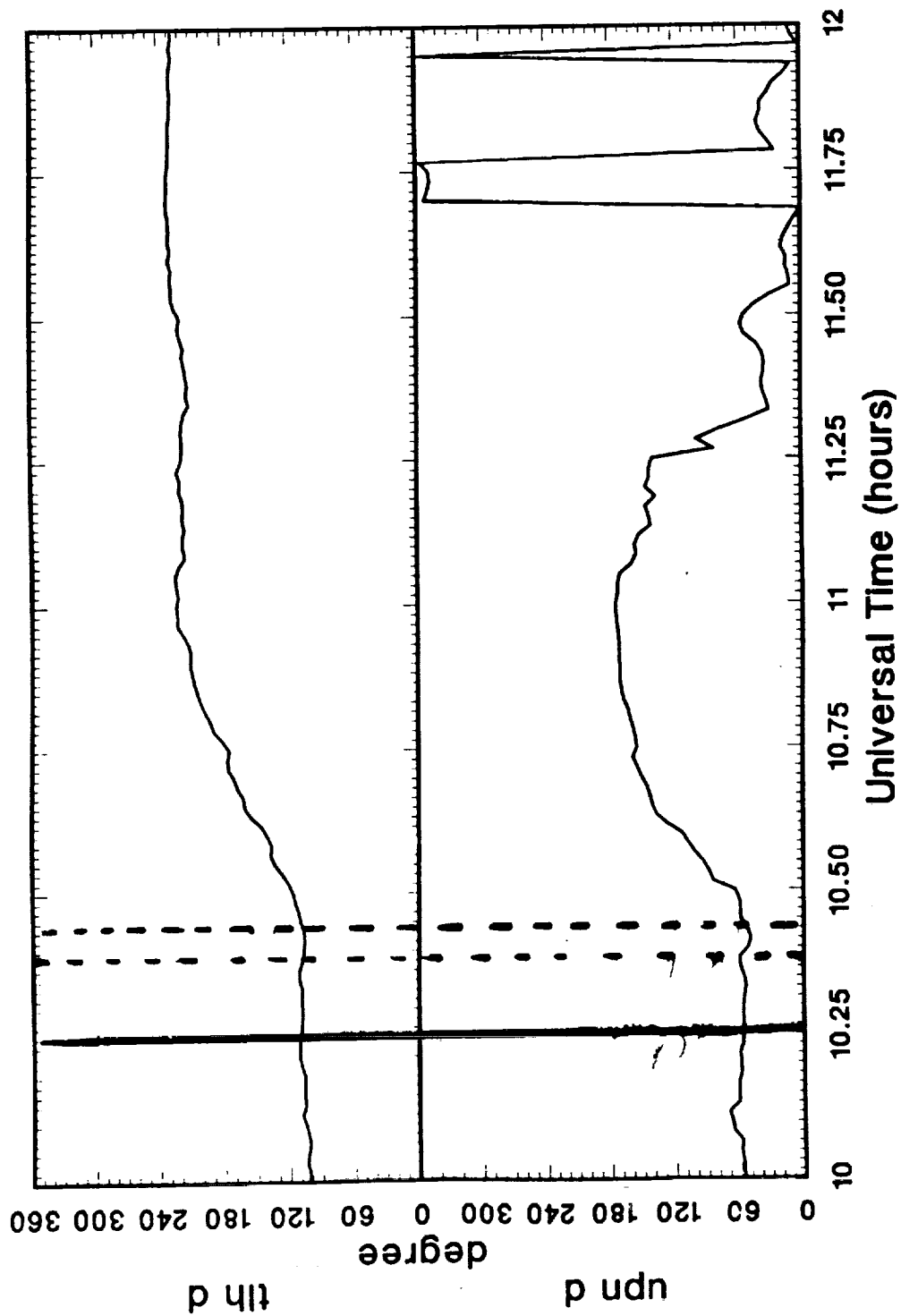


ORIGINAL PAGE IS  
OF POOR QUALITY

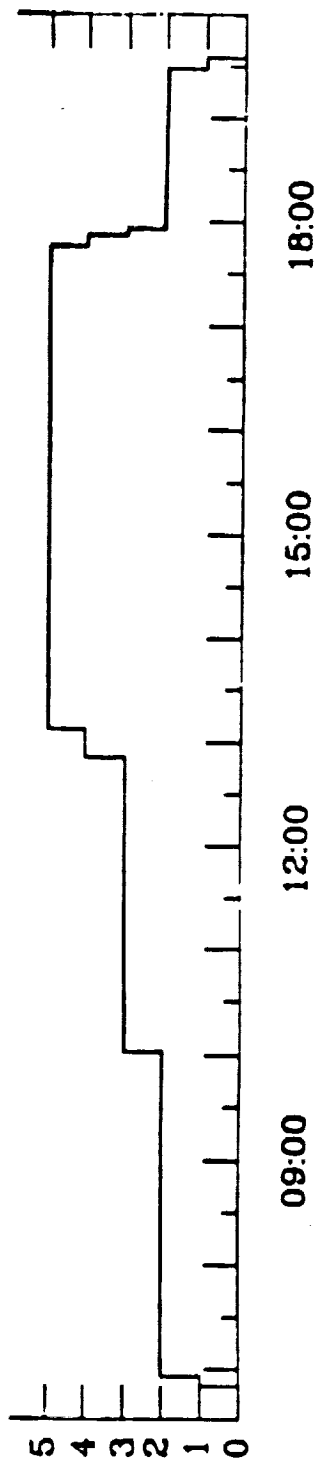
# greenland magnetometer data

23-JUL-83

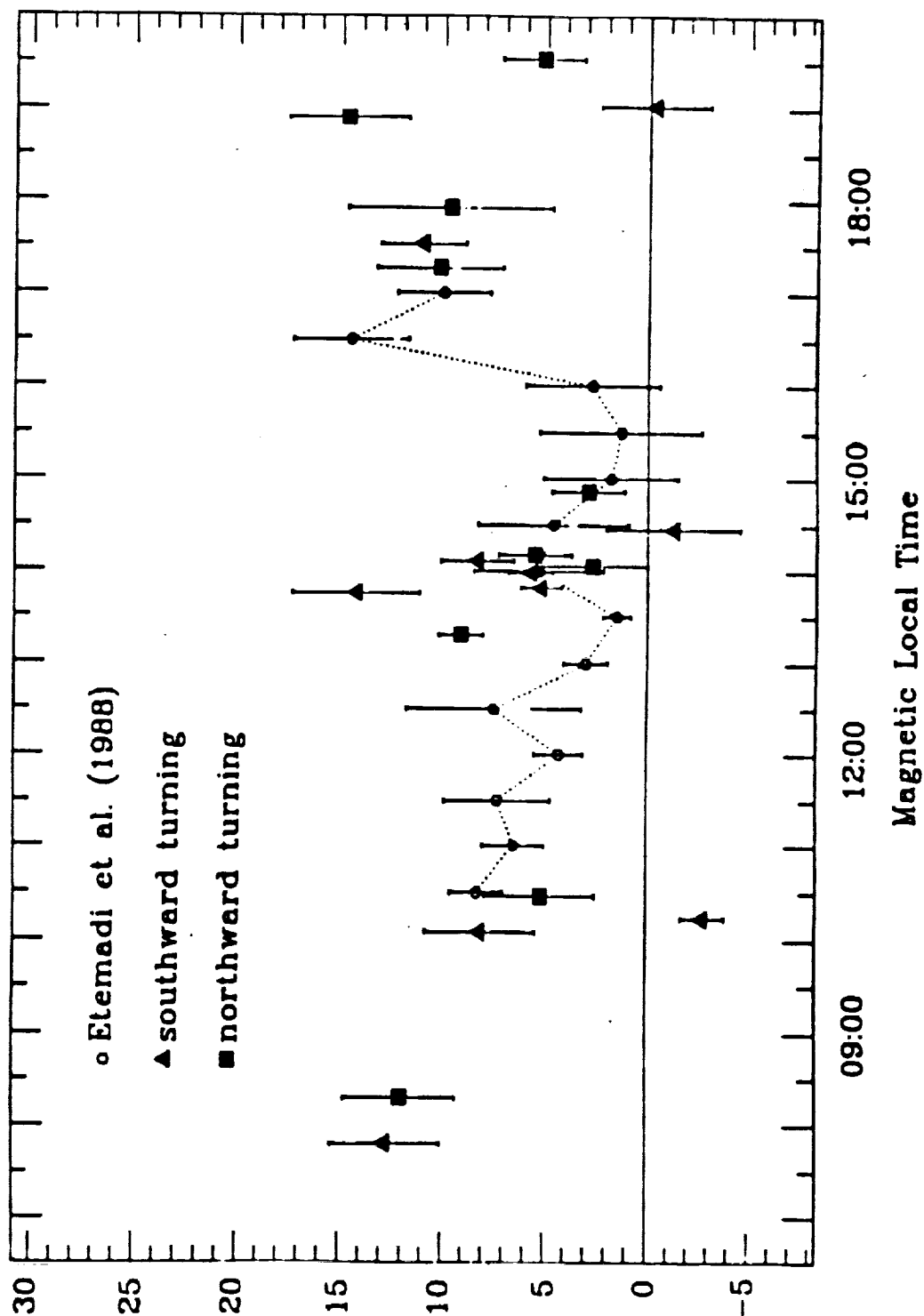
10:00:00 TO 12:00:00



Number of Expts.

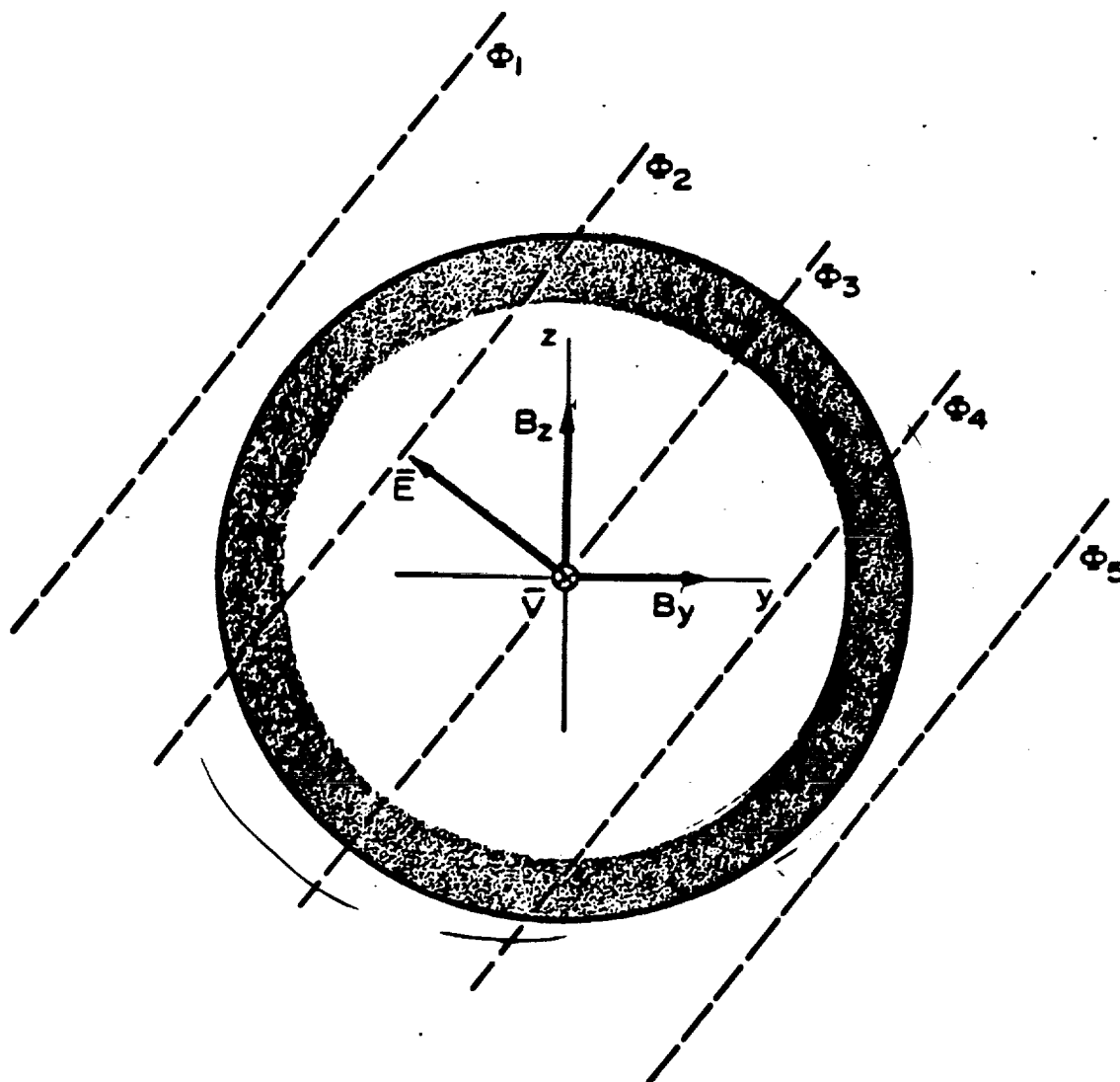


Ionospheric Response Time (min)



ORIGINAL PAGE IS  
OF POOR QUALITY





ORIGINAL PAGE IS  
OF POOR QUALITY

# Ionospheric Distribution of Field-Aligned Current

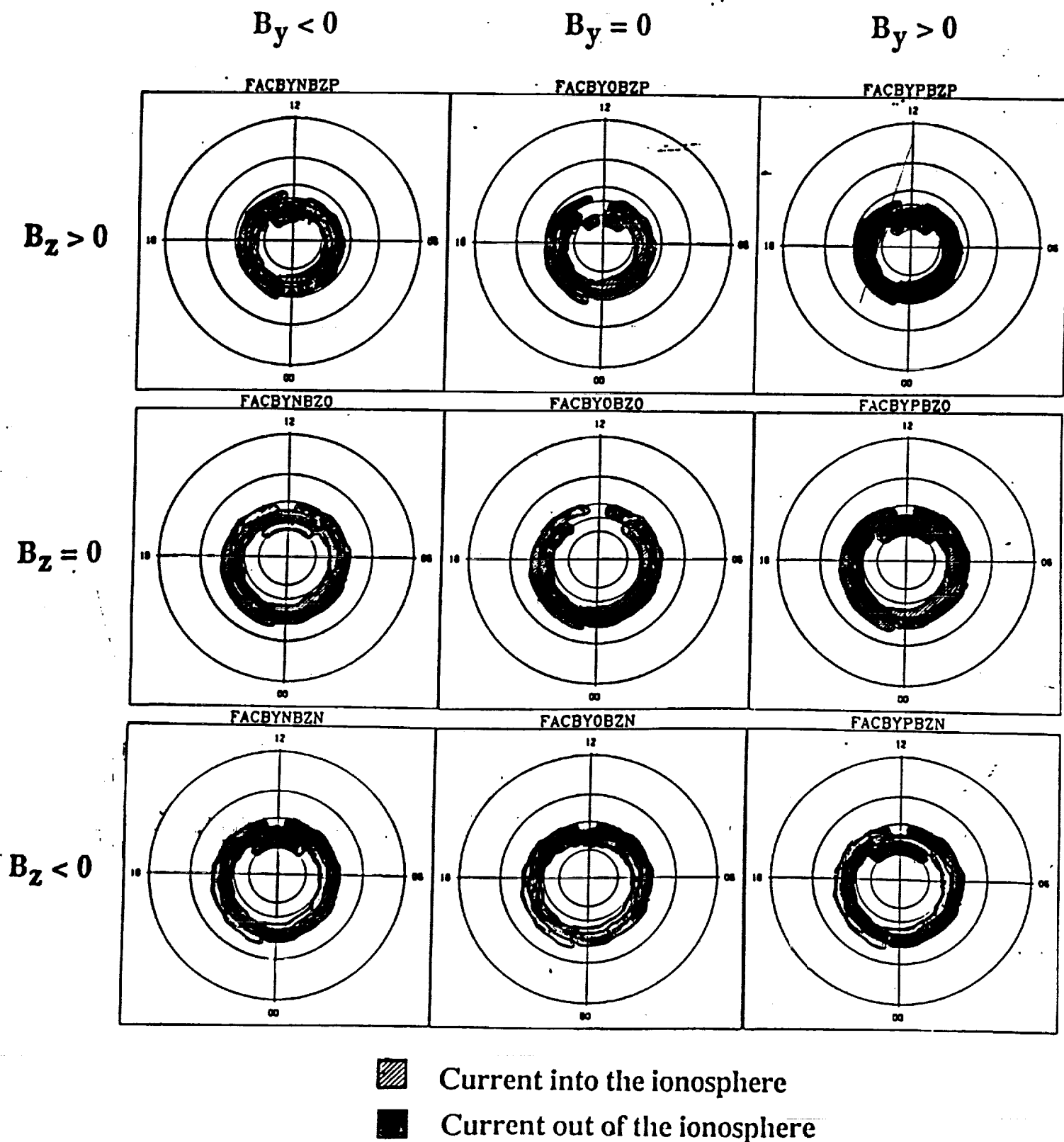
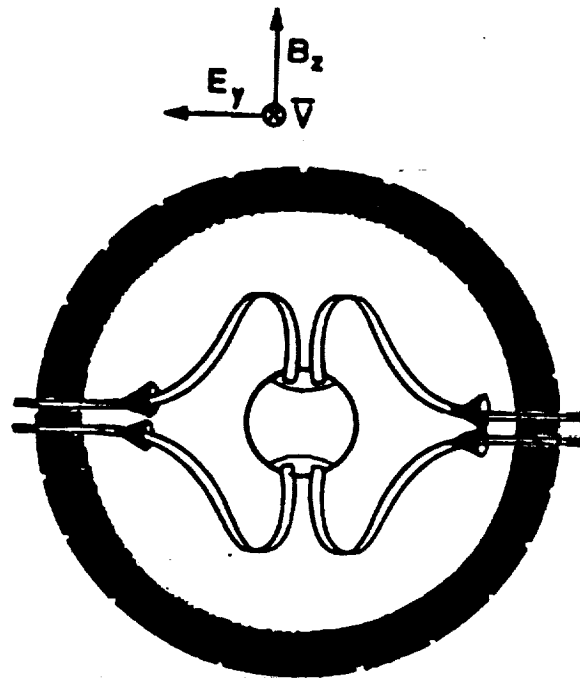
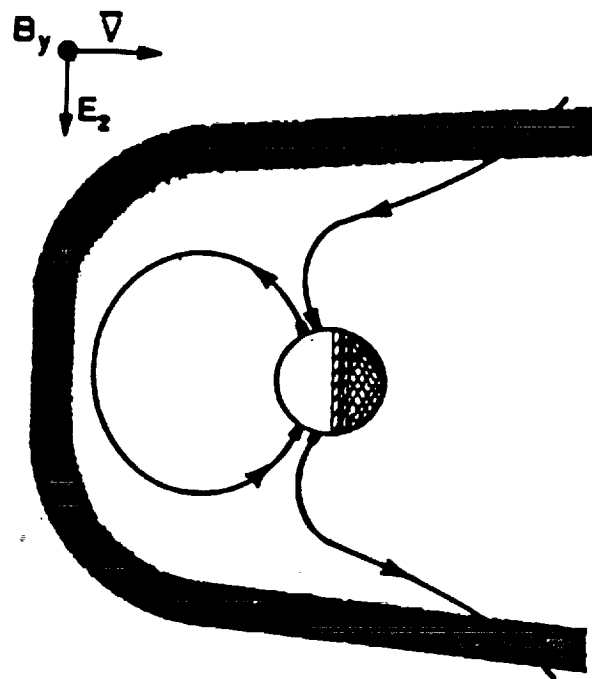


FIGURE 4



PANEL A



PANEL B

FIGURE 2

# Ionospheric Electric Potential Pattern

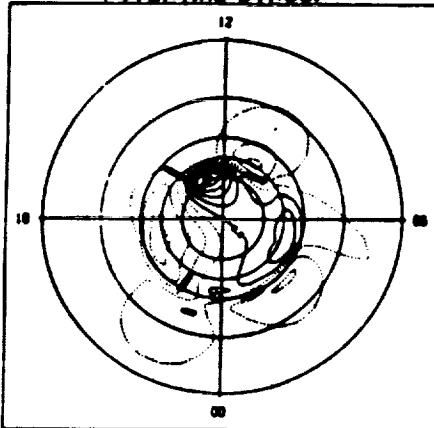
$B_y < 0$

$B_y = 0$

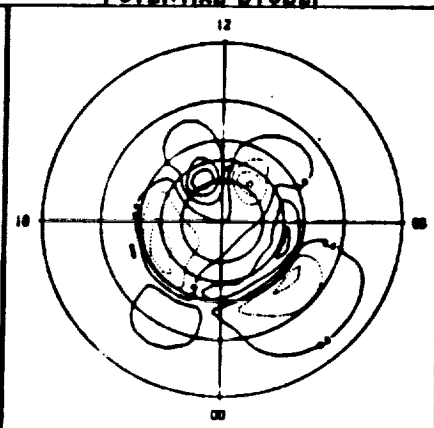
$B_y > 0$

$B_z > 0$

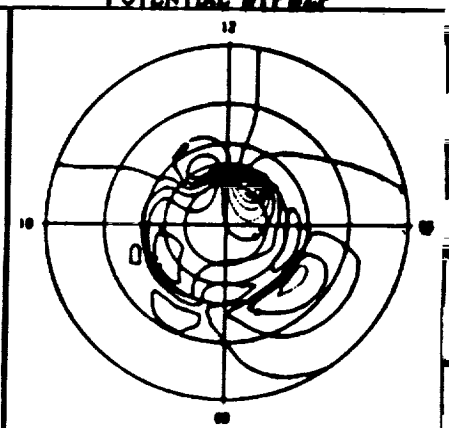
POTENTIAL BYNBZP



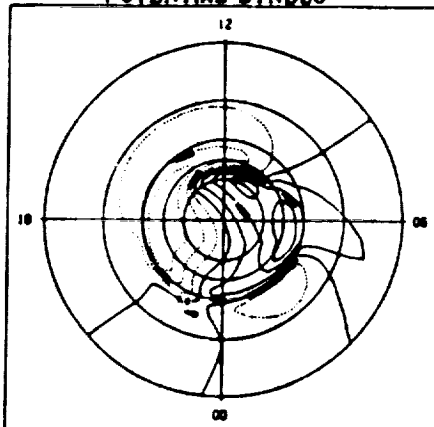
POTENTIAL BYOBZP



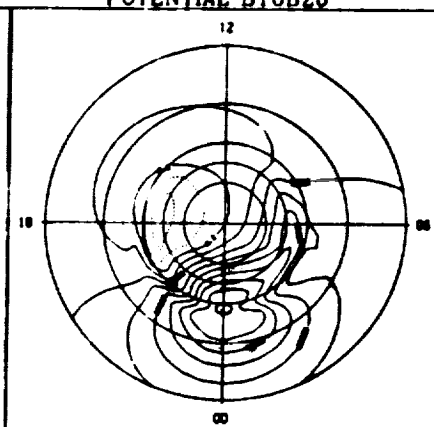
POTENTIAL BYPBZP



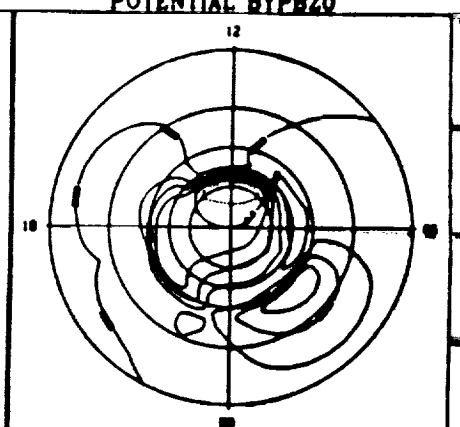
POTENTIAL BYNBZ0



POTENTIAL BYOBZ0

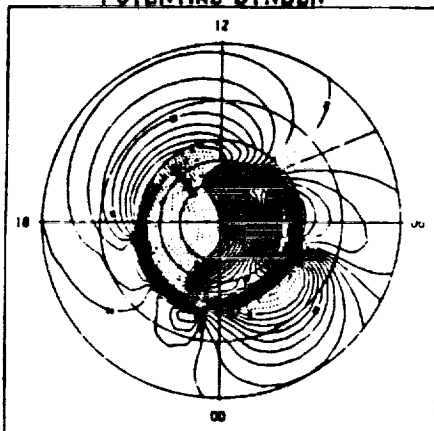


POTENTIAL BYPBZ0

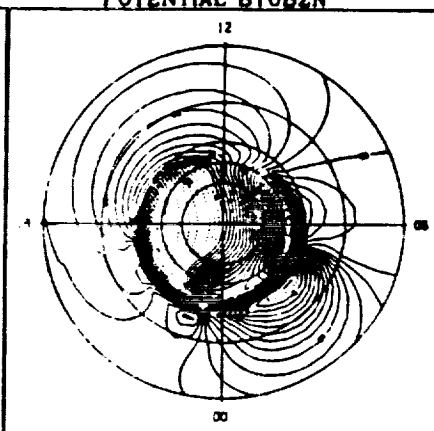


$B_z = 0$

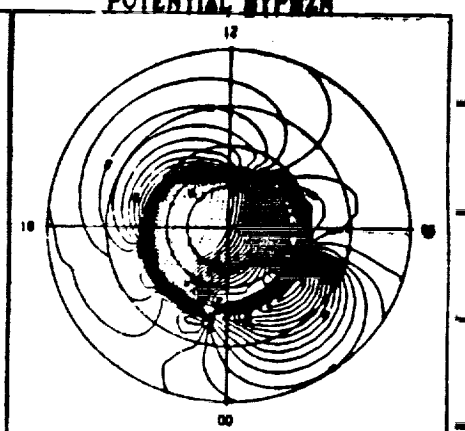
POTENTIAL BYNBZN



POTENTIAL BYOBZN

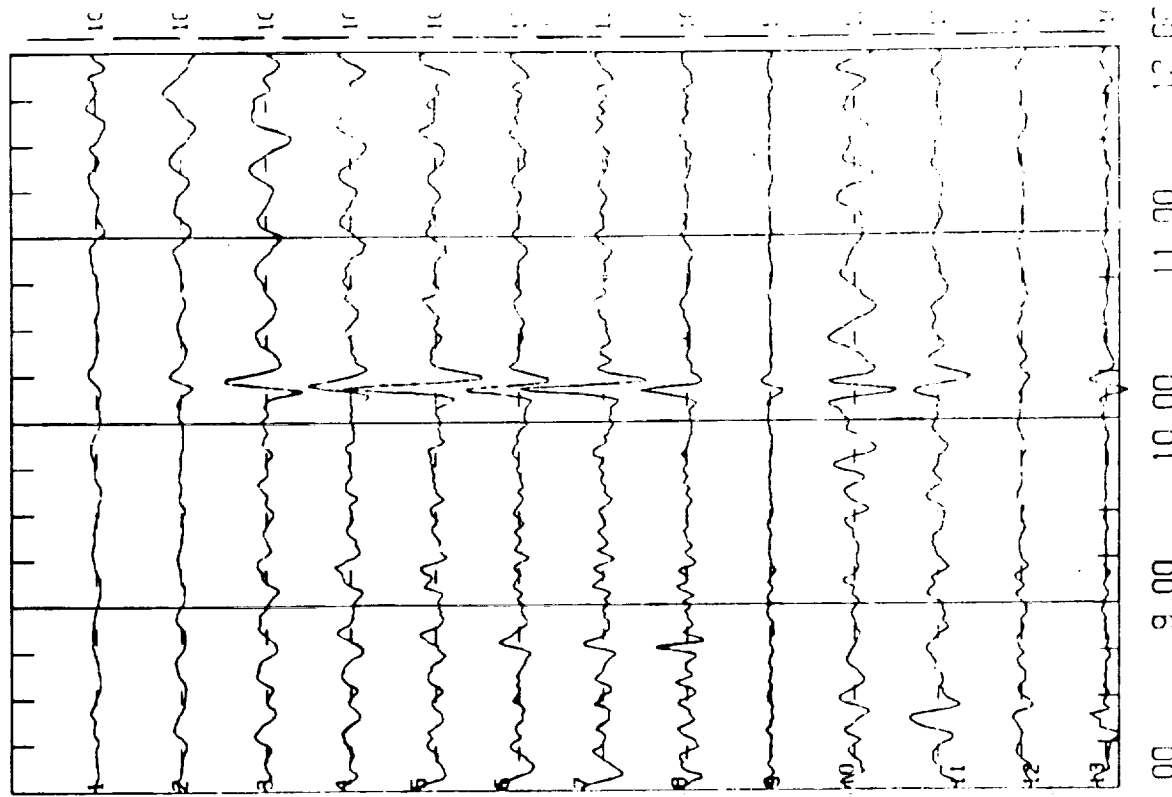


POTENTIAL BYPBZN

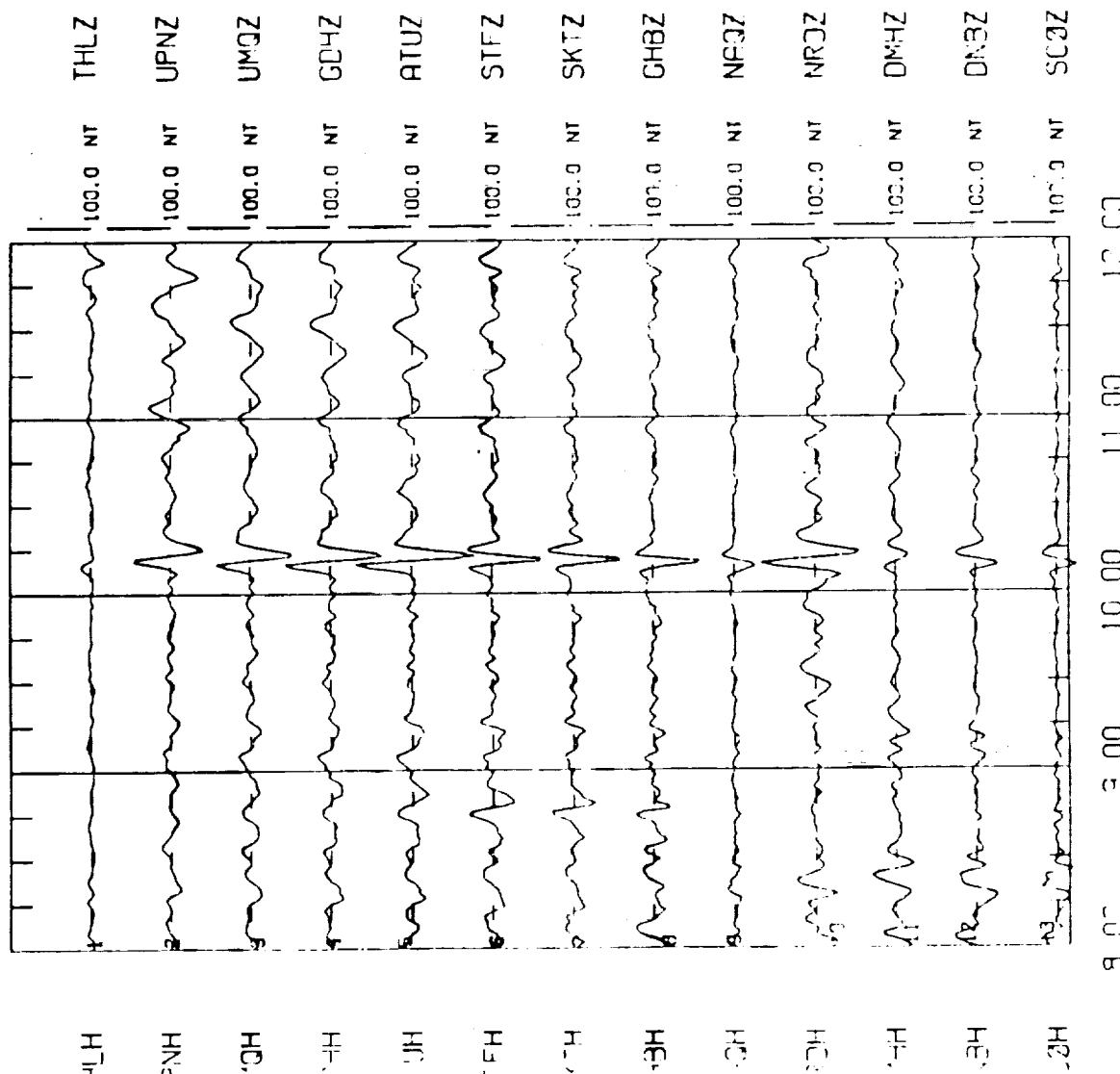


$B_z < 0$

# GREENLAND MAGNETOMETER CHAIN 86- 6-28



# GREENLAND MAGNETOMETER CHAIN 86- 6-28



ORIGINAL PAGE IS  
OF POOR QUALITY

UNIVERSAL TIME  
CRC. CHAG. GREENLAND GEZIMINI IL 179

27 APR 89 15

Figure 1

ORIGINAL PAGE IS  
OF POOR QUALITY

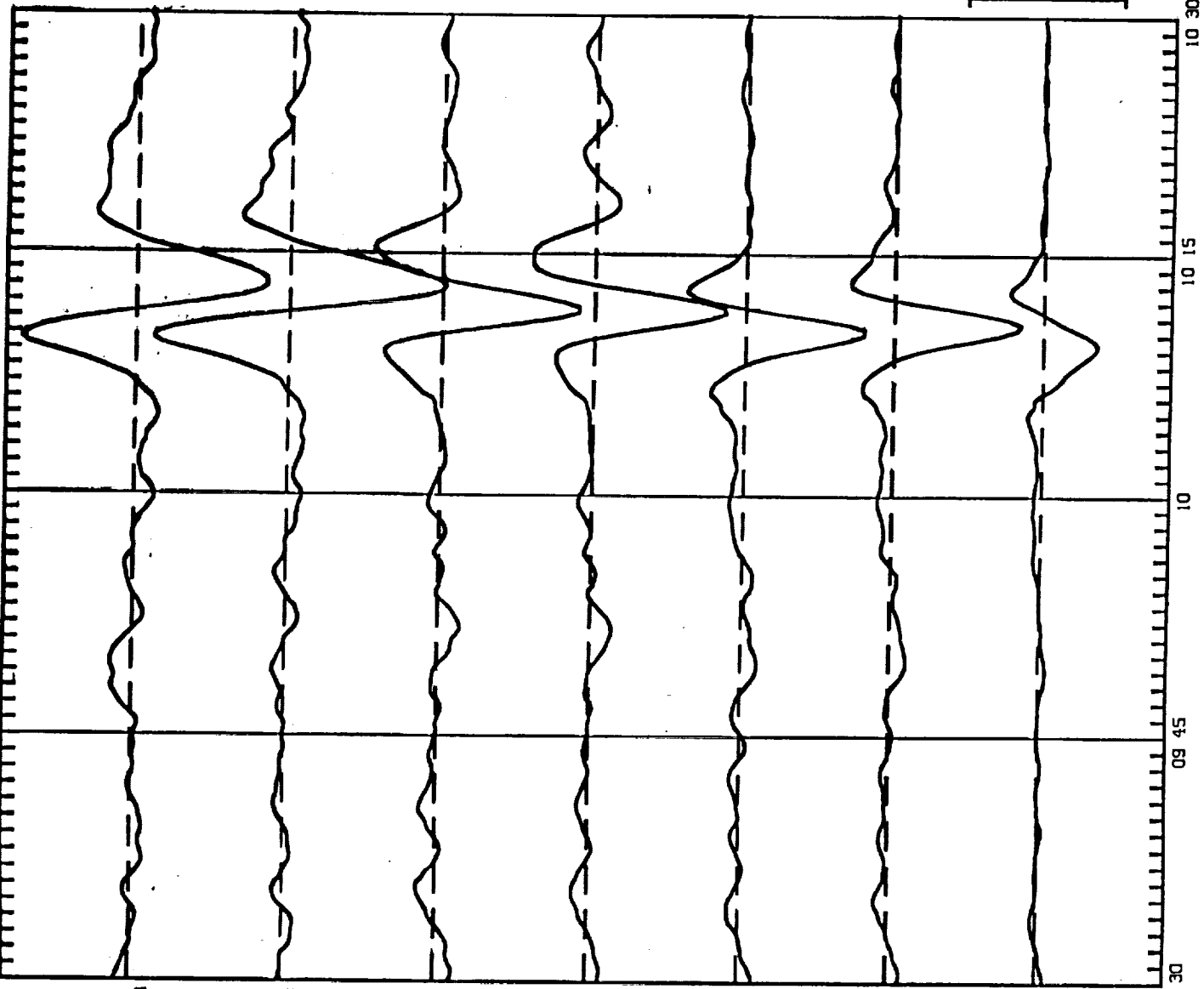
28 JAN 86 09 30 00  
28 JAN 86 10 30 00

13-NOV-87  
12 16 50

100  
UNITS/INCH

GREENLAND CHAIN 20 SEC DATA 30 MIN PERIOD HIGH PASS

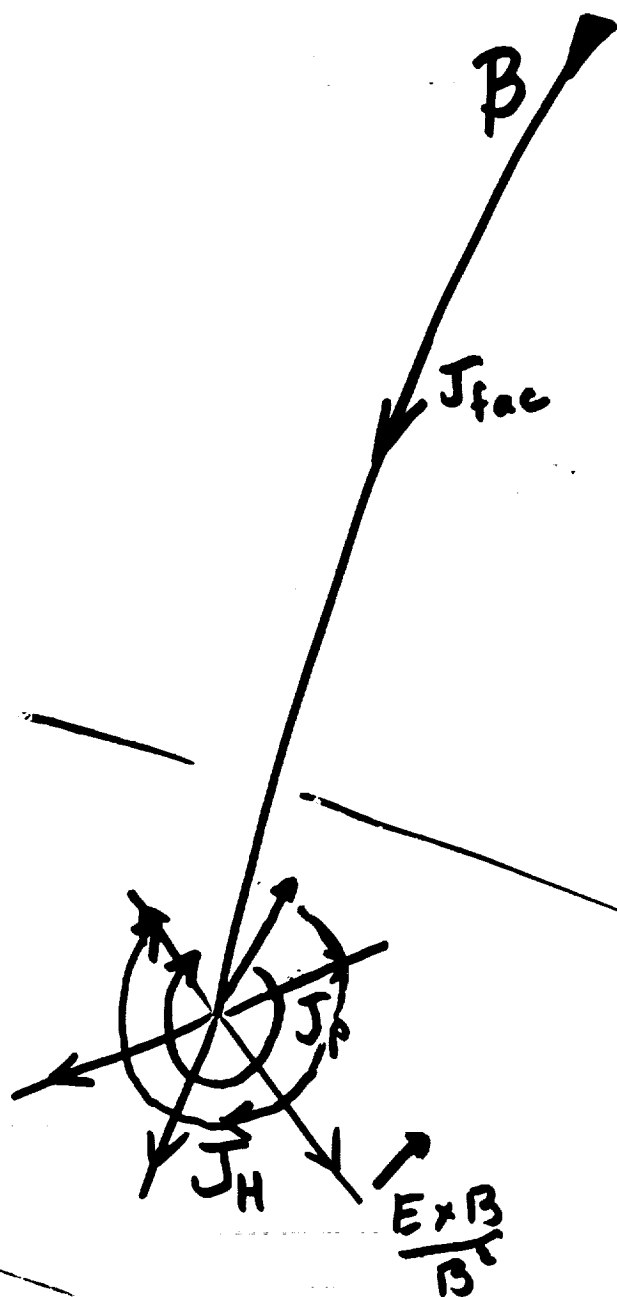
98062820SEC30MINHIGH



CDH<sup>0</sup>  
NT  
ATU<sup>0</sup>  
NT  
STF<sup>0</sup>  
NT  
SKT<sup>0</sup>  
NT  
DYB<sup>0</sup>  
NT  
CHB<sup>0</sup>  
NT  
NAB<sup>0</sup>  
NT

TIME IN HOURS

09 30 09 45 10 10 15 10 30



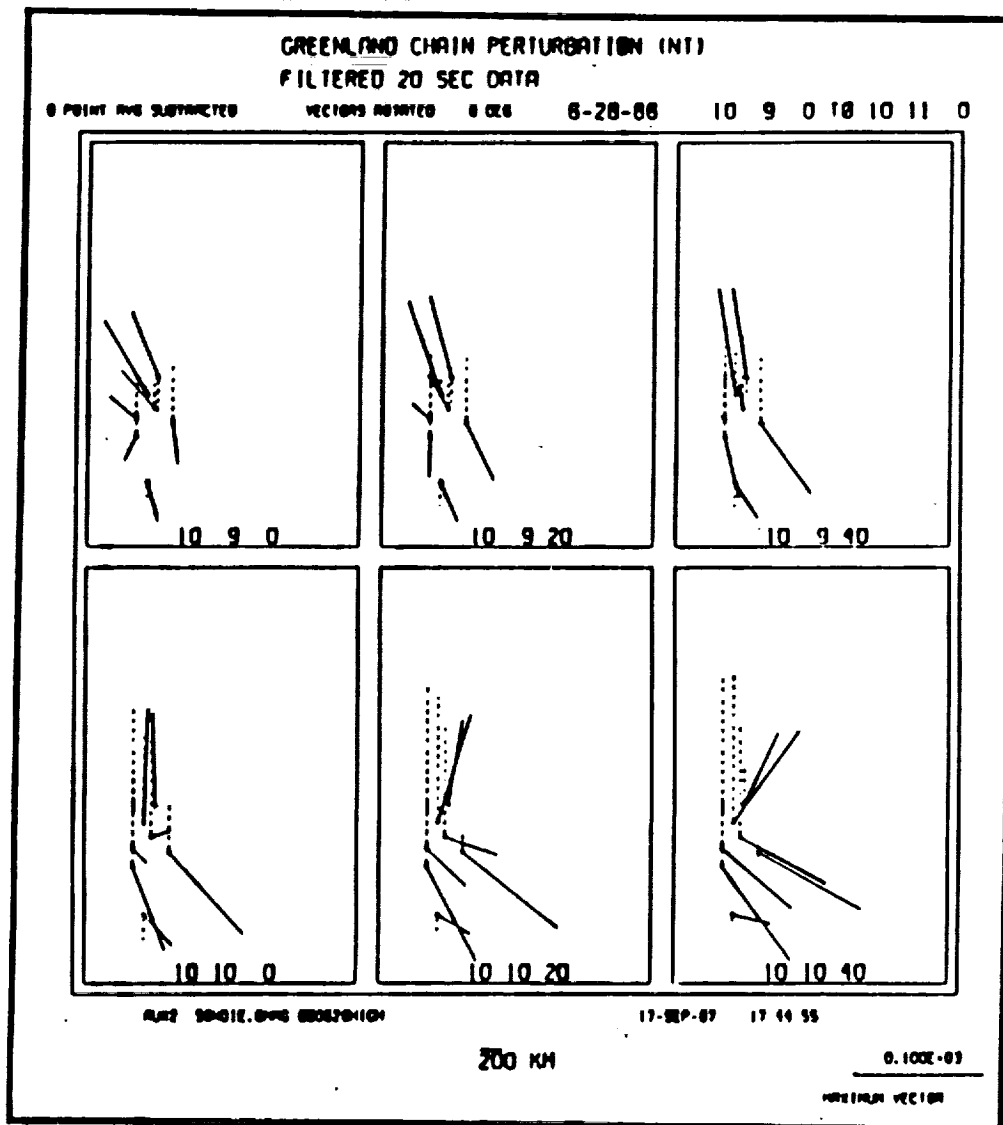
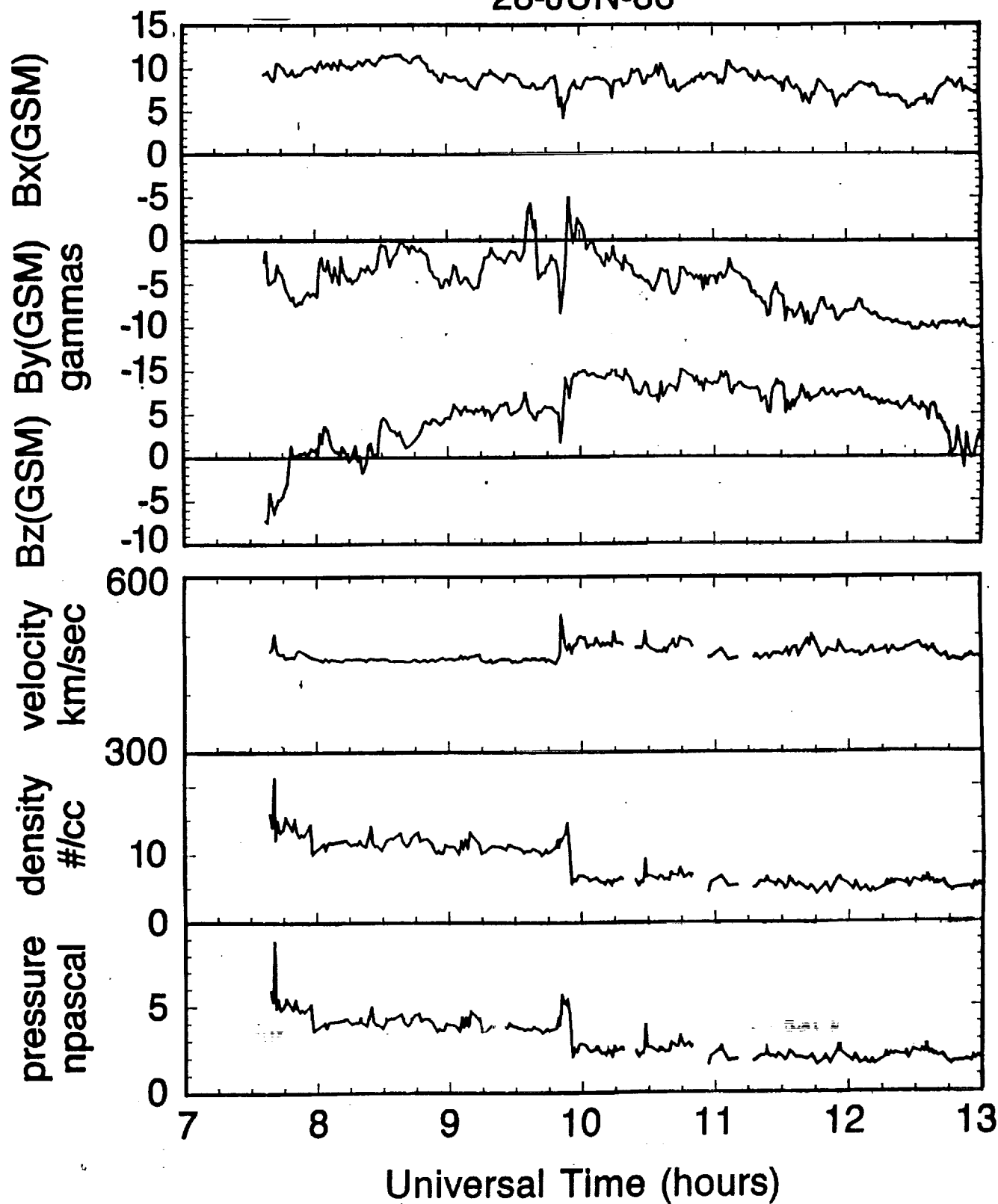


Figure 27: Magnetic perturbations are plotted in successive panels at the location of the corresponding station for the temporary array of observatories operated around Sondre Stromfjord, Greenland. This data is obtained at 20-second resolution so the time difference between each panel is 20 seconds. The total horizontal components of the magnetic perturbation are shown with a solid vector while the vertical component perturbations are shown with a vertical dashed line. At 10:08 UT, the disturbance approached the stations from the east causing a horizontal perturbation which points radially from a source position as well as a large vertical (dashed lines) perturbation. At 10:10 UT the disturbance is centered over the array of stations.



# IMP-8 PLASMA AND FIELD MEASUREMENTS

28-JUN-86



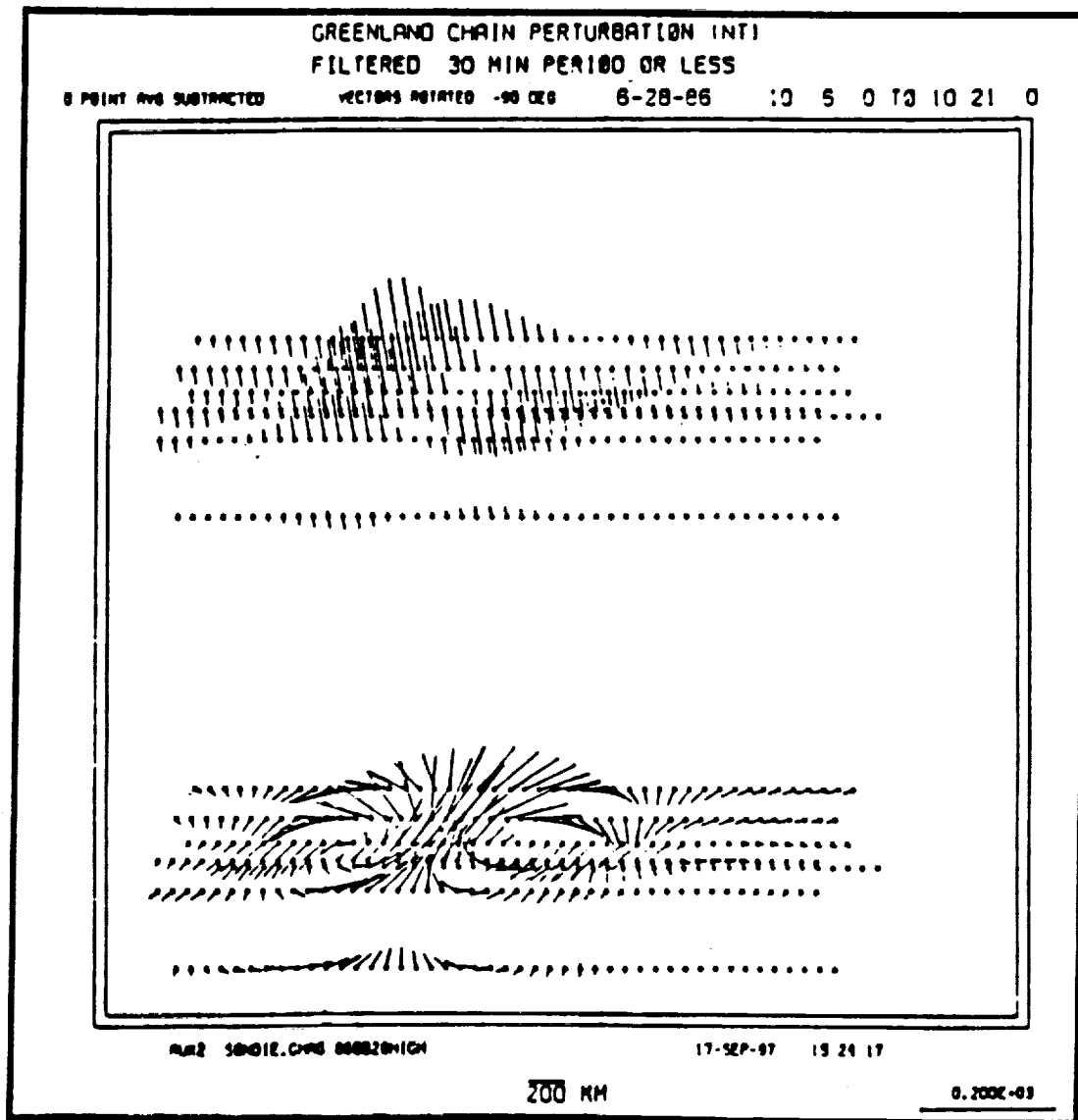
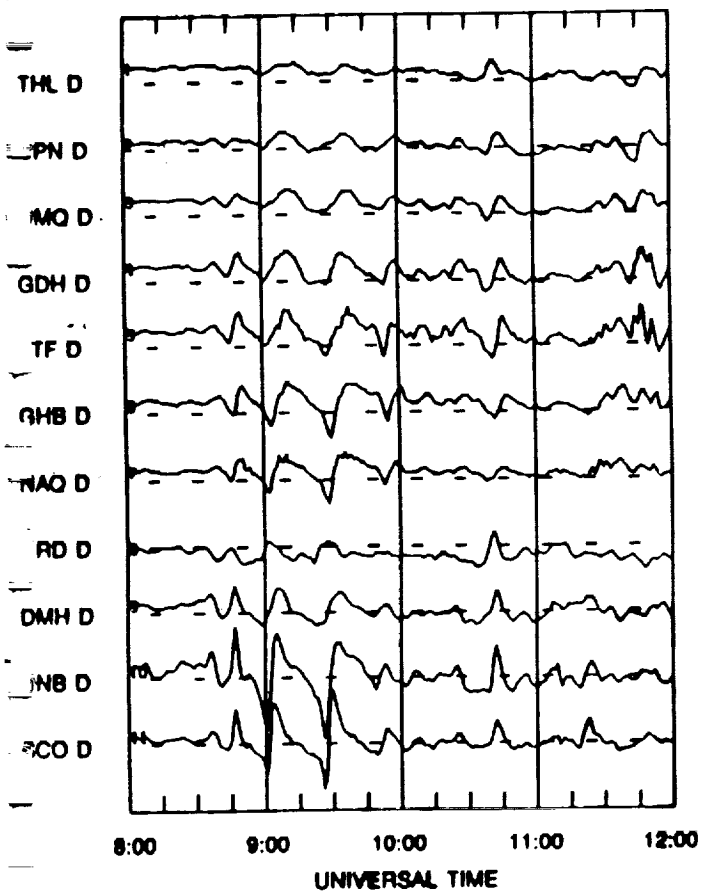


Figure 28: The magnetic perturbations in the vertical component (top) and horizontal component (bottom) from the array of 20-second stations for the interval 10:06 UT to 10:21 UT. The horizontal component has been rotated 90 degrees counter clockwise to show the equivalent ionospheric convection direction. We offset the station locations by 80 km for each set of 20 second data, corresponding to a velocity of about 4 km/sec. The resulting twin vortex pattern is indicative of a pair of oppositely directed field-aligned current filaments moving rapidly over the array of stations.

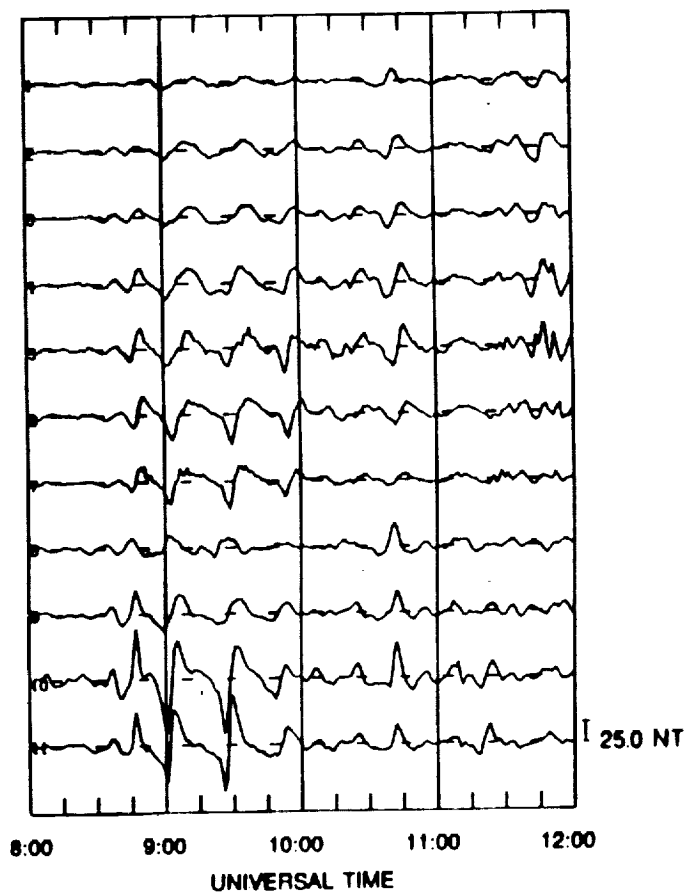
# UNFILTERED DATA

85-10-28



# FILTERED DATA

85-10-28

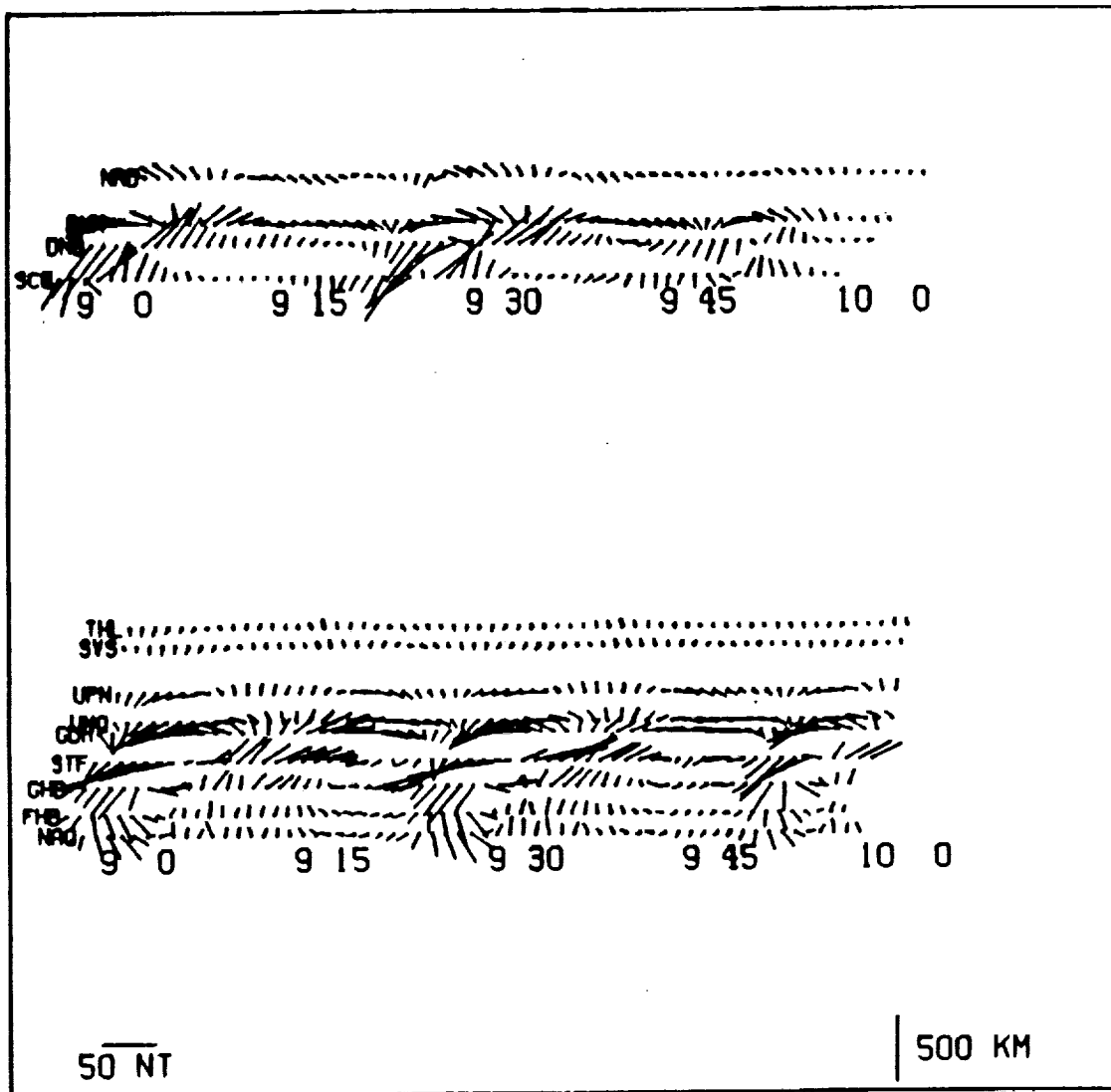


— PRECEDING PAGE BLANK NOT FILMED

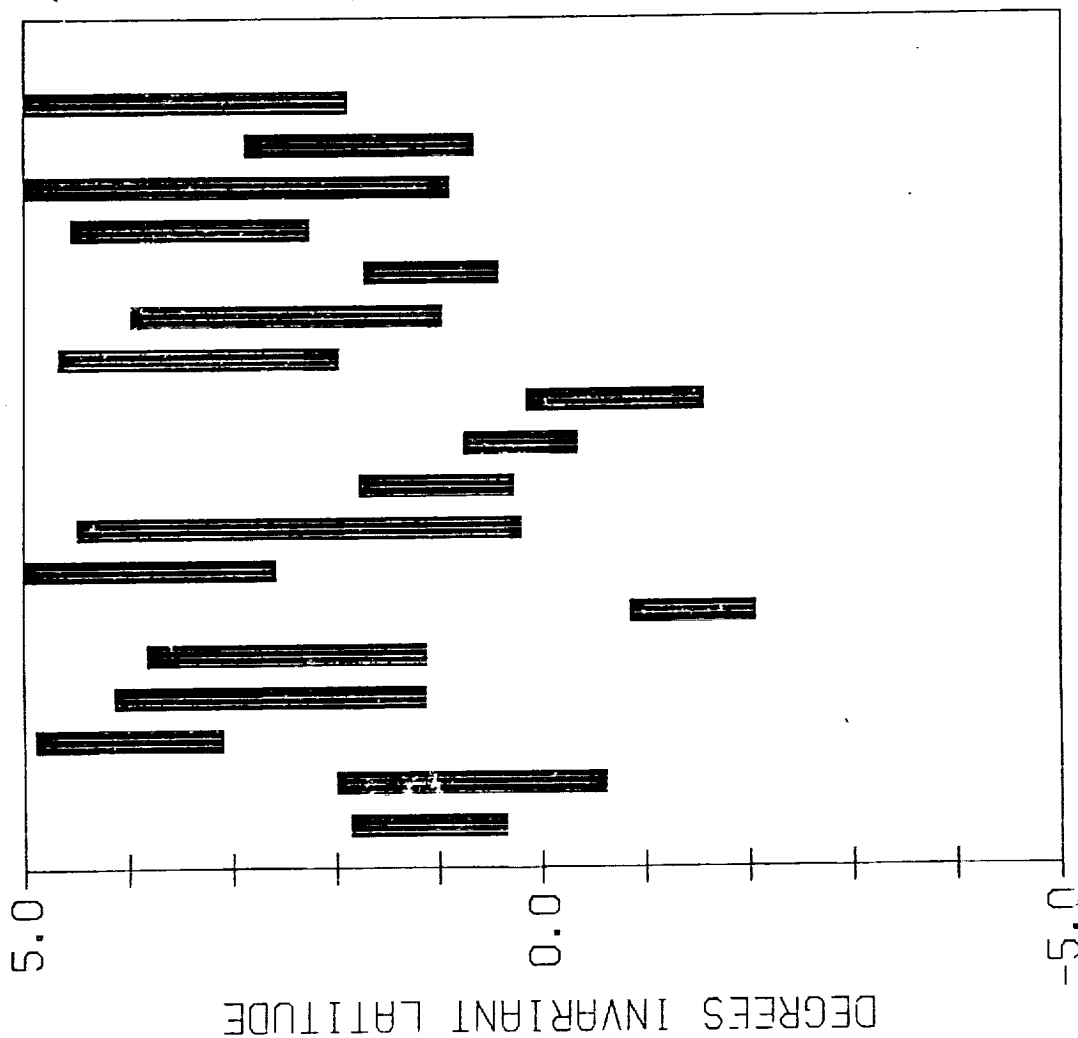
# IMPLIED CONVECTION

SPEED (KM/SEC) = 2.0

85 10 28



# LLBL LOCATION RELATIVE TO PULSATIØNS

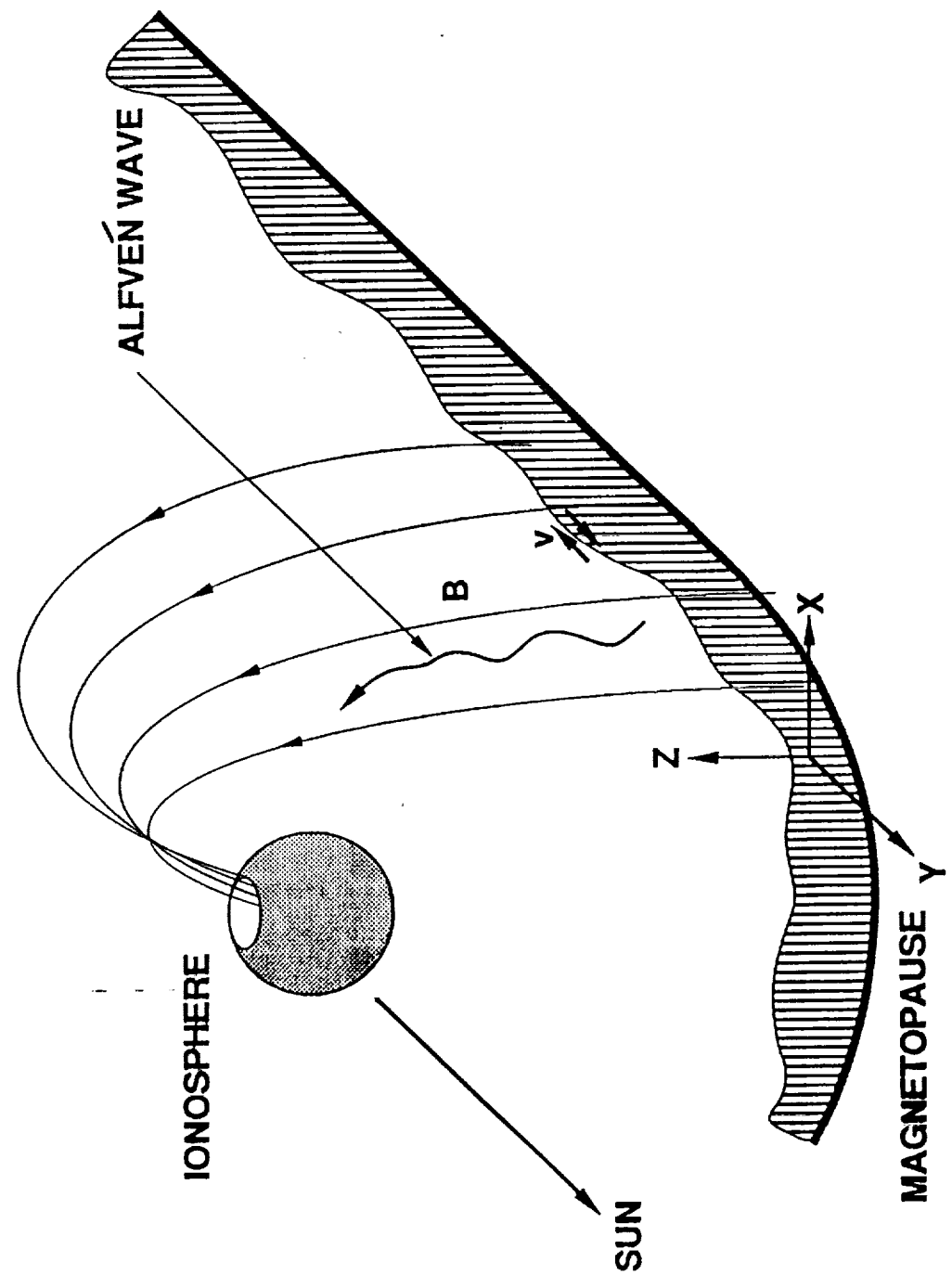


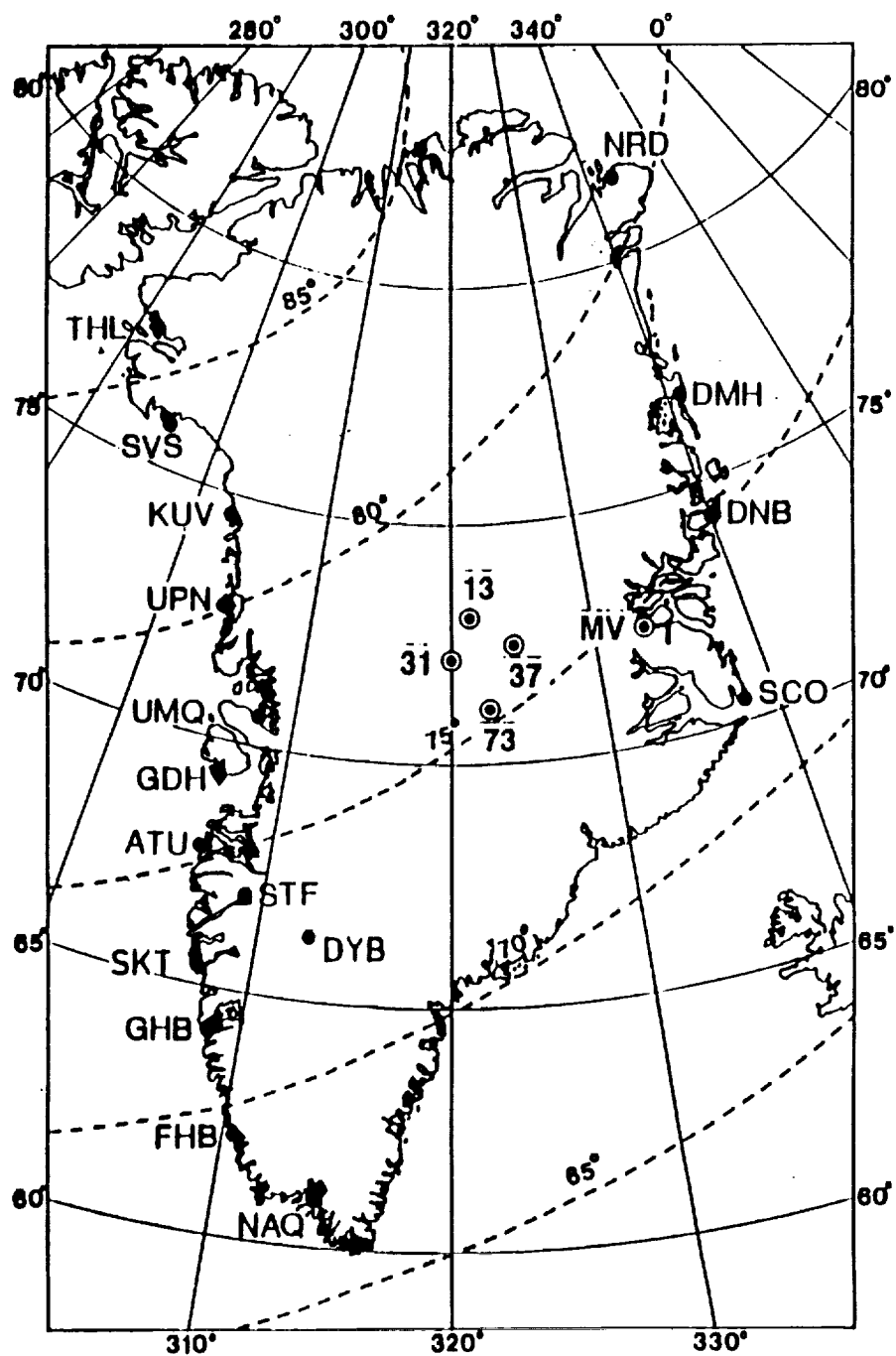
DATE OF DMSP PASS

DATA1 C°C. SØNDIE. I\*P DMSPGREENLAND.DAT



# COUPLING OF BOUNDARY LAYER TURBULENCE TO THE IONOSPHERE





## COMMENTS

Ken Clark

8:30 16 August



## Comments on futures.

Need much analysis money.

Keep informed on other imagers aloft

Auroras in post-max period,  
somewhat quiet. Great?

Excellent to use stable UV star  
continuum for calibrations.

Also to monitor growth of  
surface scattering.

N-S conjugacy: try by slew control  
Night and day.

Pulsations: look for by slew?

Extent, morphology.

Geotail image: (<sup>1216</sup>~~1216~~) Try by slew.

Slew for continuous earth view  
throughout orbit?

Look for "dark aurora" patches  
a la DMSP, equatorward.

Discrete auroras can be only 0.5 km thick,  
viewed  $\parallel B$ . Our view almost  
always slantwise. Correction  
geometry not simple.  
LBH long/short height displ.

Polar cap auroral forms: for us.

Magnetopause waves?

Consult polar mapping wind/temp.

Test prototype instrument vs. other  
photometers on aurora, subst.  
filters. A pre flight necessity.

Absolute calibrations of instr. necessary

- Position resolution, simultaneous  
strong/weak neighbors. Pinholes.
- Wavelength resolution. Ditto.
- Lab aurora mockup test image.

Monochromator?  $H_2$ ? Partial sph.  
(Other abs. cal. of detector by  
cascade photons)

Temp. sensors on board? Image corners  
Check radia. cooling at NASA?

ANALYSIS TOOLS

RDAF  
Key Parameters

Marsha Torr

9:00      16 August

## ULTRAVIOLET IMAGER: 8/15-16/90

### UVI DATA ANALYSIS SOFTWARE PRODUCTS:

#### 1) IMAGES -

CALIBRATED RECONSTRUCTED SPECTRAL  
IMAGES WITH BRIGHTNESS IN RAYLEIGHS

#### 2) KEY PARAMETERS -

SUMMARY PARAMETERS TO BE PRODUCED  
ROUTINELY BY CDHF USING OUR DELIVERABLE  
SOFTWARE TO BE STORED ON UNIFORM TIME  
INCREMENTS IN FILE AVAILABLE TO ALL  
INVESTIGATORS

#### 3) FULL SCALE DATA ANALYSIS

REDUCTION OF SPECTRAL IMAGES TO  
GEOPHYSICAL PARAMETERS AND MORE  
EXTENSIVE DATA SETS OF IMAGES DONE ON  
RDAF

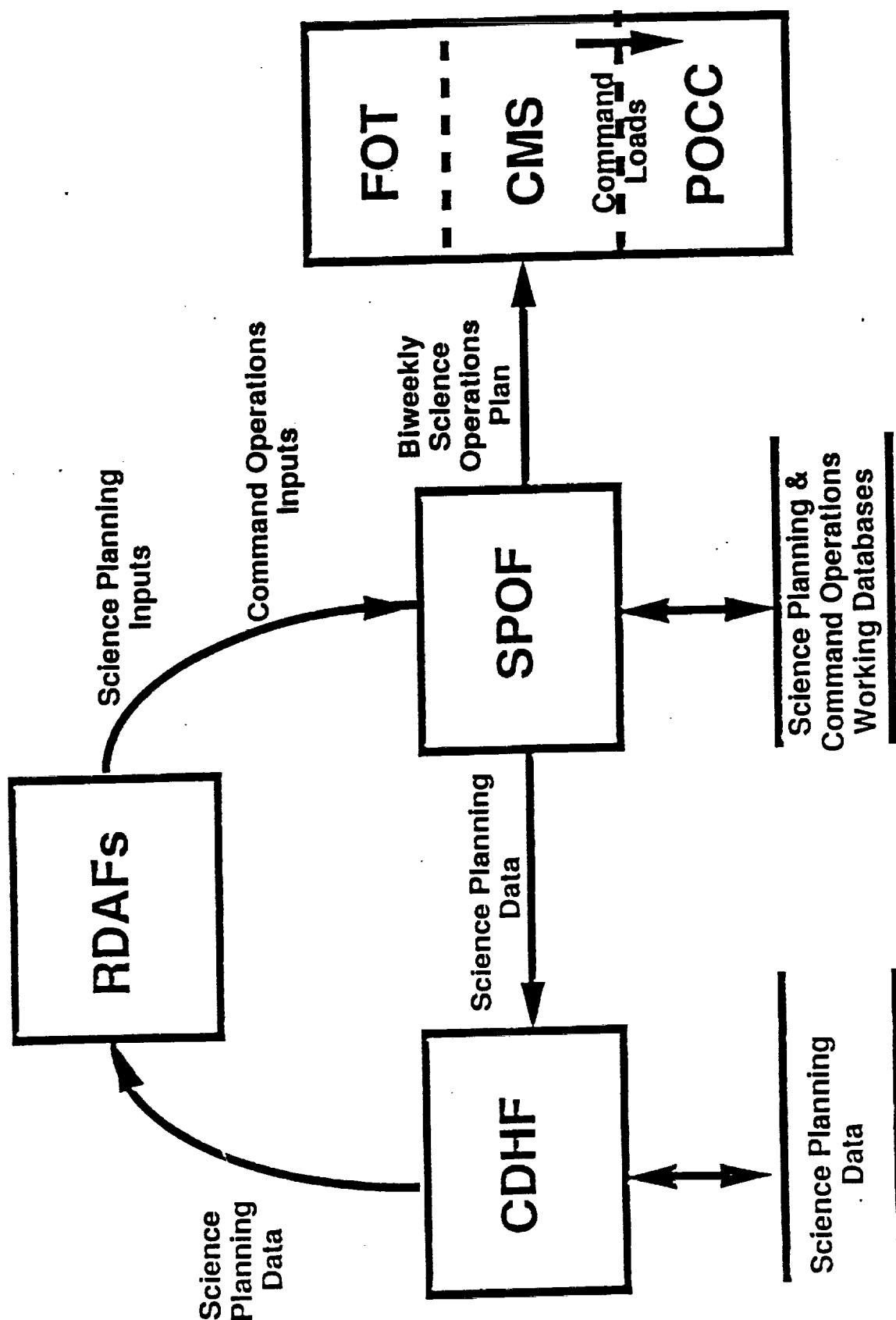
#### 4) MODELING STUDIES FOR COMPARISON WITH DATA

## ULTRAVIOLET IMAGER: 8/15-16/90

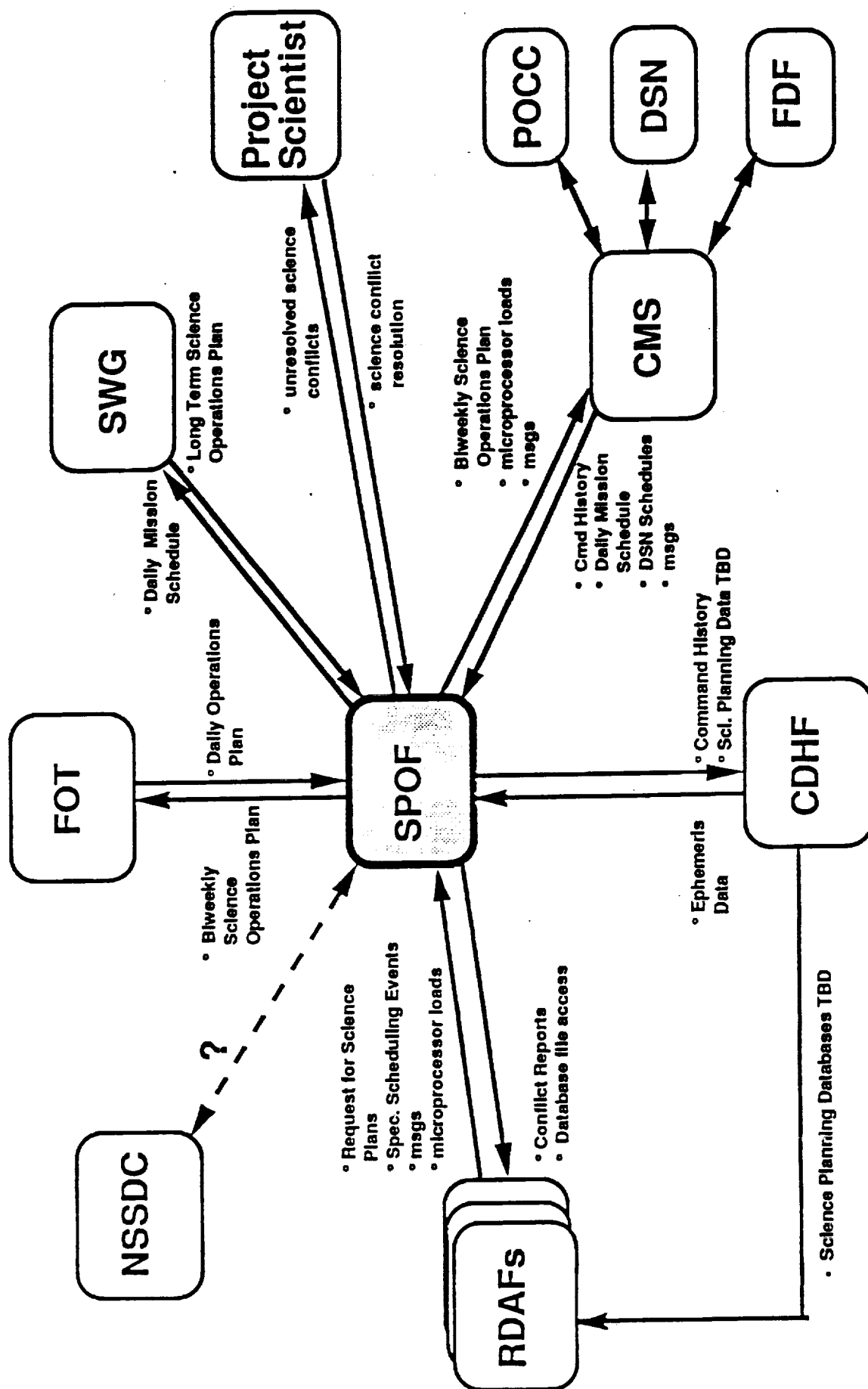
### KEY PARAMETERS:

- 1) TOTAL ELECTRON ENERGY INPUT
- 2) PARAMETERS TO INDICATE SIZE OF OVAL
  - MOST EQUATORWARD BOUNDARY
  - MOST POLEWARD BOUNDARY
- 3) TOTAL ENERGY INFLUX INTO POLAR CAP
- 4) TOTAL ENERGY INFLUX INTO OVAL
  - FOUR QUADRANTS (DAWN, DUSK, NOON, MIDNIGHT)
- 5) INDICATOR OF AVERAGE CHARACTERISTIC ENERGY IN SAME FOUR QUADRANTS
- 6) ACTIVITY INDICATOR
- 7) IMAGE EVERY 10 MINUTES

# GROUND SYSTEM OVERVIEW (SPOF PERSPECTIVE)



# GGG SPOF INTERFACES



ENERGY DEPOSITION CODE/  
ENERGY FLUX EXTRACTION

Doug Torr

9:30 16 August



## **APPLICATION OF THE ISTP IMAGES TO IONOSPHERIC GLOBAL MODELING**

**IONOSPHERIC GLOBAL MODELS REQUIRE THE FOLLOWING FUNDAMENTAL  
INPUT PARAMETERS:**

- SOLAR EUV FLUX**
- PRECIPITATED PARTICLE FLUX**
- NEUTRAL WINDS**
- CONVECTION ELECTRIC FIELDS**
- NEUTRAL THERMOSPHERE**

**GOOD MODELS EXIST FOR**

- THE SOLAR EUV FLUX**
- THE NEUTRAL THERMOSPHERE**

**GROUND-BASED TECHNIQUES CAN BE USED WITH MODELS TO  
INFER NEUTRAL WINDS**

**AURORAL IMAGING HAS THE POTENTIAL TO SIGNIFICANTLY  
CONSTRAIN MODELS OF**

- ELECTRON PRECIPITATION PATTERNS**
- CONVECTION ELECTRIC FIELDS**

## **GLOBAL ELECTRON PRECIPITATION PATTERN**

**THE PRECIPITATED ELECTRON FLUX CAN BE APPROXIMATELY  
CHARACTERIZED BY:**

- THE PRECIPITATED ENERGY FLUX**
- A CHARACTERISTIC ENERGY**

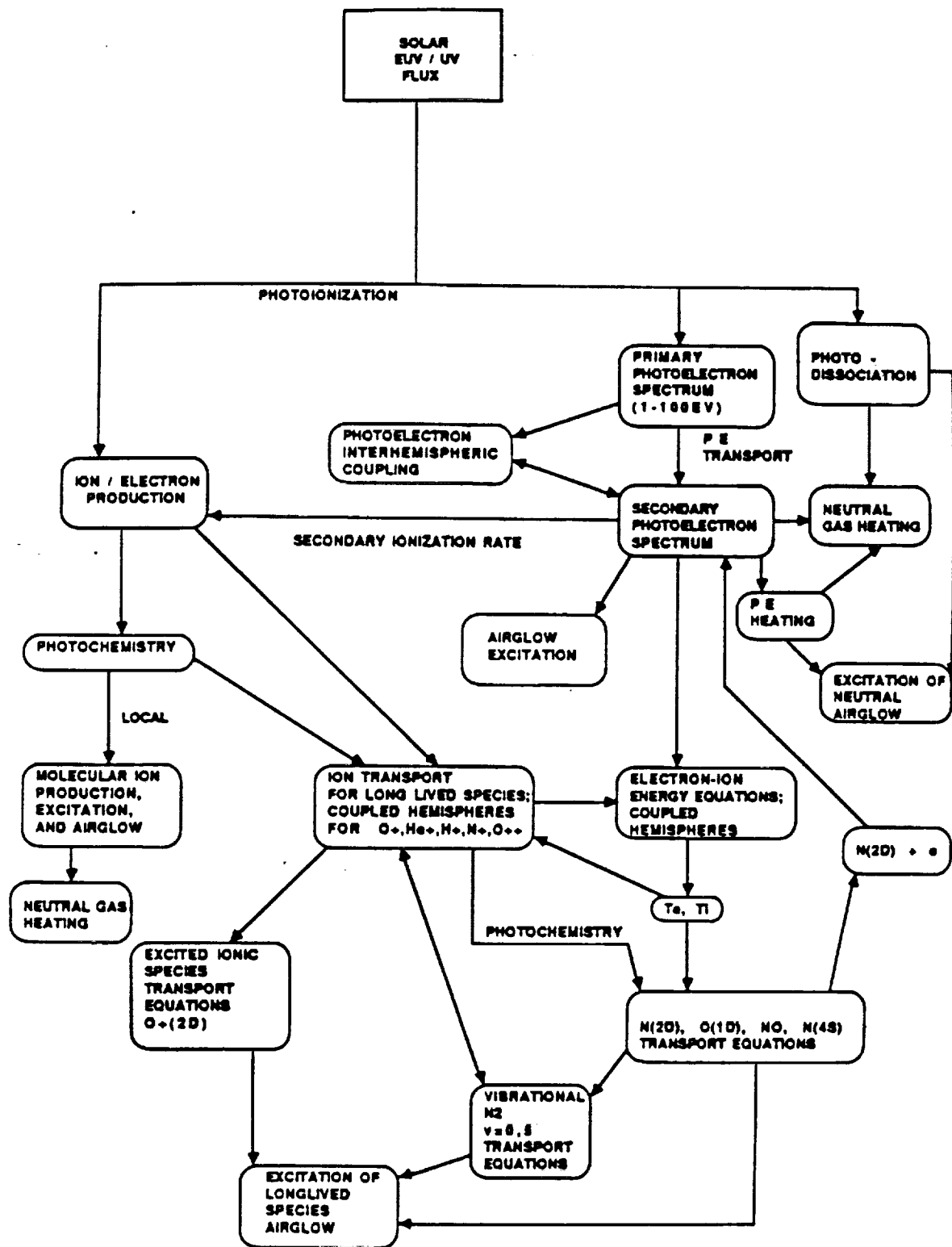
**OBSERVATIONS AND MODEL SIMULATIONS HAVE ESTABLISHED THAT:**

- THE PRECIPITATED ENERGY FLUX  $\propto$  AURORAL LUMINOSITY**
- THE CHARACTERISTIC ENERGY  $\propto$  LUMINOSITY RATIOS**

**$\Rightarrow$  ESTIMATE OF THE ENERGY SPECTRUM OF PRIMARIES**

**$\Rightarrow$  CORPUSCULAR IONIZATION RATE**

**$\Rightarrow$  IONOSPHERIC INTEGRATED CONDUCTIVITY**



FLIP model computational flow chart.

## **CONVECTION ELECTRIC FIELDS**

CURRENTLY LARGE SCALE POTENTIAL PATTERNS DESCRIBING IONOSPHERIC CONVECTION PATTERNS ARE ESTIMATED USING STATISTICAL MODELS FOR IONOSPHERIC ELECTRODYNAMICS.

THE RICHMOND-KAMIDE MODEL, FOR EXAMPLE, UTILIZES:

INCOHERENT SCATTER RADAR CONVECTION OBSERVATIONS

SATELLITE DIRECT FIELD OBSERVATIONS

GROUND AND SATELLITE MAGNETOMETER OBSERVATIONS

IONOSPHERIC ELECTRICAL CONDUCTANCE OBSERVATIONS

GROUND-BASED OBSERVATIONS OF IONOSPHERIC ELECTRODYNAMIC FEATURES ARE CAPABLE OF TRACKING RAPID CHANGES IN ELECTRIC FIELDS AND CURRENTS, CONDUCTIVITIES AND ASSOCIATED MAGNETIC PERTURBATIONS.

THE ELECTRODYNAMICS MODELS COMBINE THE DIFFERENT TYPES OF ELECTRODYNAMICAL DATA TO INFER HIGH-LATITUDE ELECTRIC POTENTIAL PATTERNS AS THEY EVOLVE IN TIME

SPATIAL COVERAGE IS LIMITED SO THAT MANY INSTRUMENTS WOULD BE NEEDED TO OBTAIN GLOBAL COVERAGE

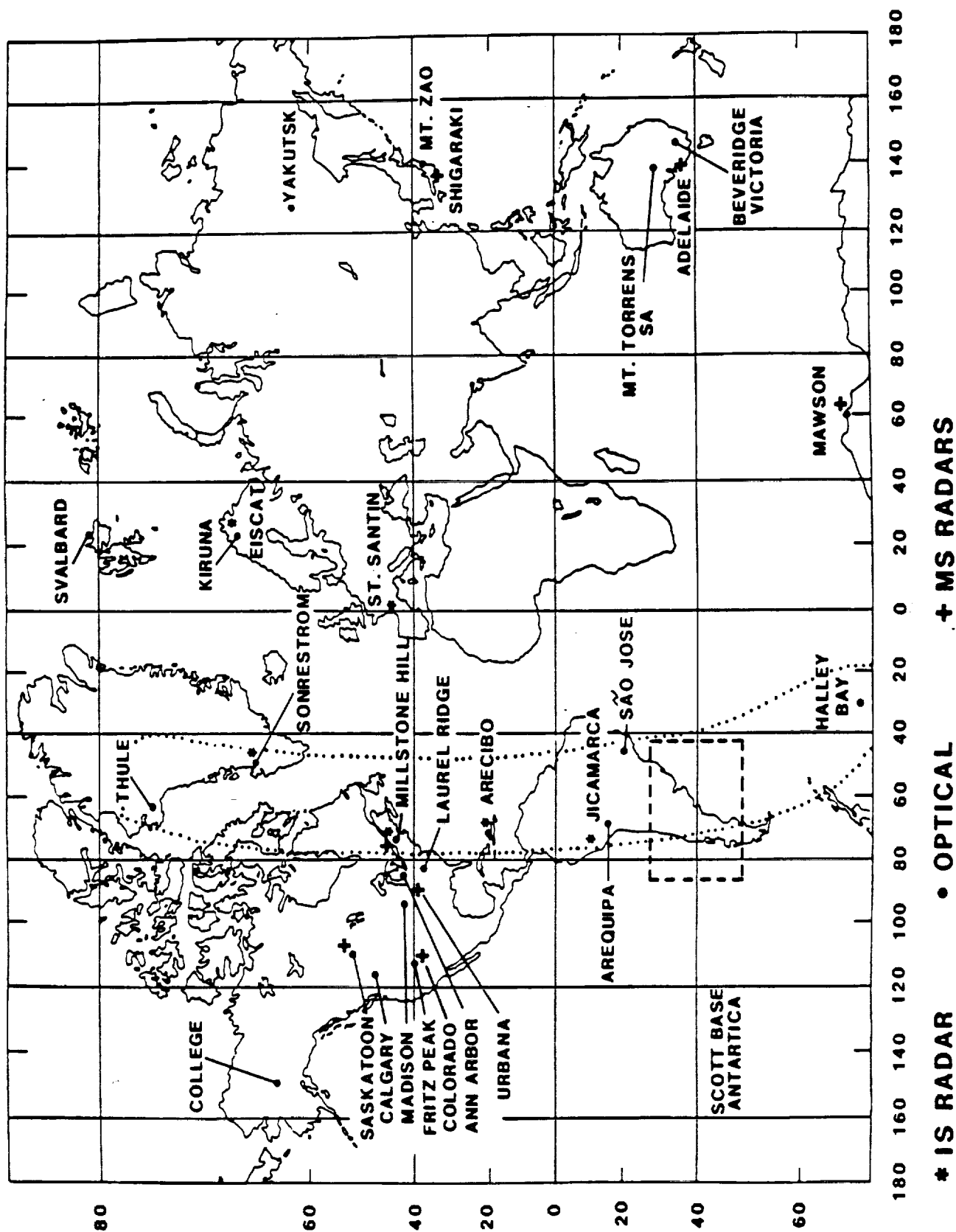


FIGURE 3.2 World wide distribution of Fabry Perot interferometer (IS) and MS radar sites, indicating present capabilities for coordinated measurements with global scale geographic coverage, as for example with the "pole-to-pole" longitudinal chain enclosed by the dotted line.

## **APPLICATION OF THE ISTP IMAGES TO IONOSPHERIC GLOBAL MODELING**

**IONOSPHERIC GLOBAL MODELS REQUIRE THE FOLLOWING FUNDAMENTAL  
INPUT PARAMETERS:**

- SOLAR EUV FLUX**
- PRECIPITATED PARTICLE FLUX**
- NEUTRAL WINDS**
- CONVECTION ELECTRIC FIELDS**
- NEUTRAL THERMOSPHERE**

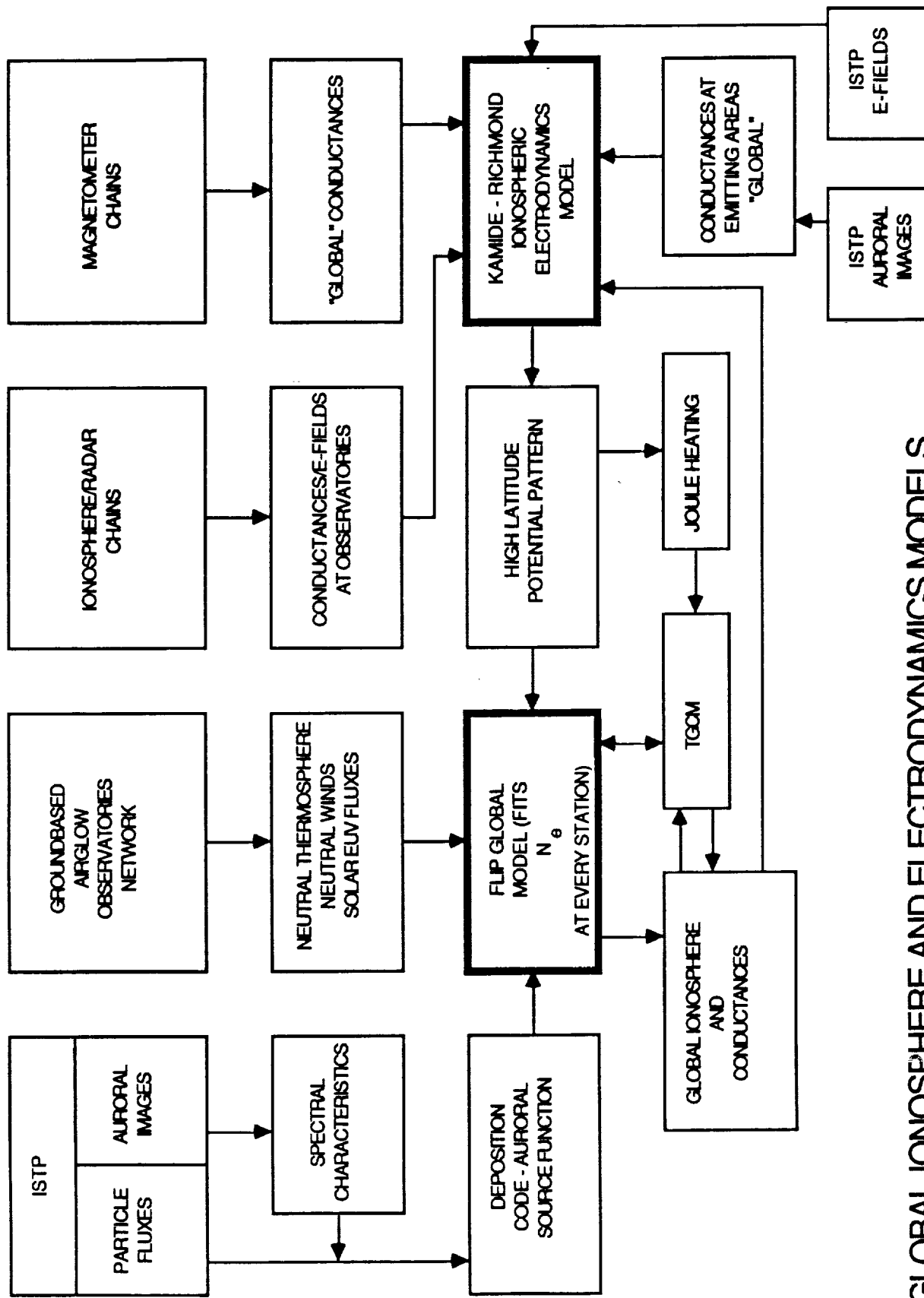
**GOOD MODELS EXIST FOR**

- THE SOLAR EUV FLUX**
- THE NEUTRAL THERMOSPHERE**

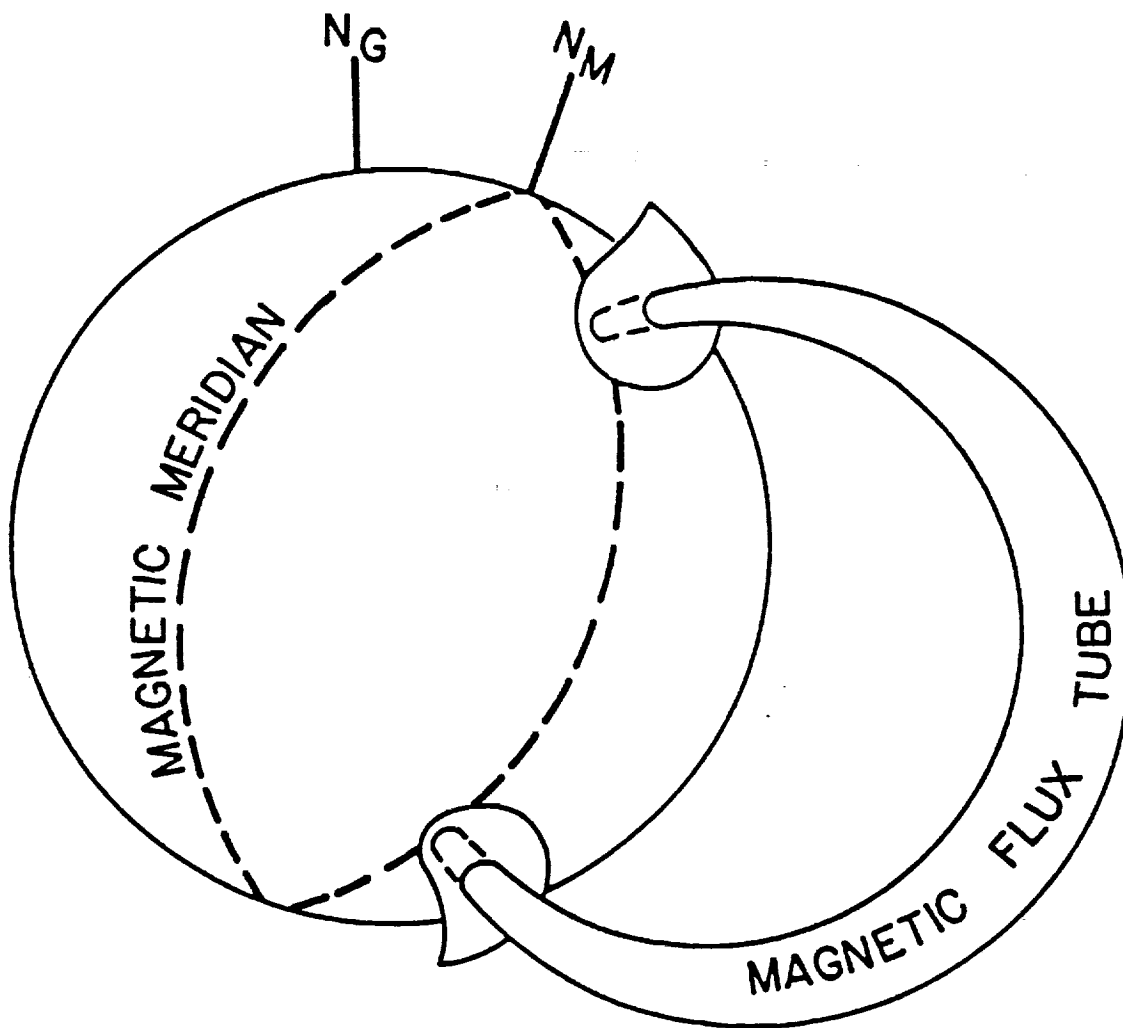
**GROUND-BASED TECHNIQUES CAN BE USED WITH MODELS TO  
INFER NEUTRAL WINDS**

**AURORAL IMAGING HAS THE POTENTIAL TO SIGNIFICANTLY  
CONSTRAIN MODELS OF**

- ELECTRON PRECIPITATION PATTERNS**
- CONVECTION ELECTRIC FIELDS**

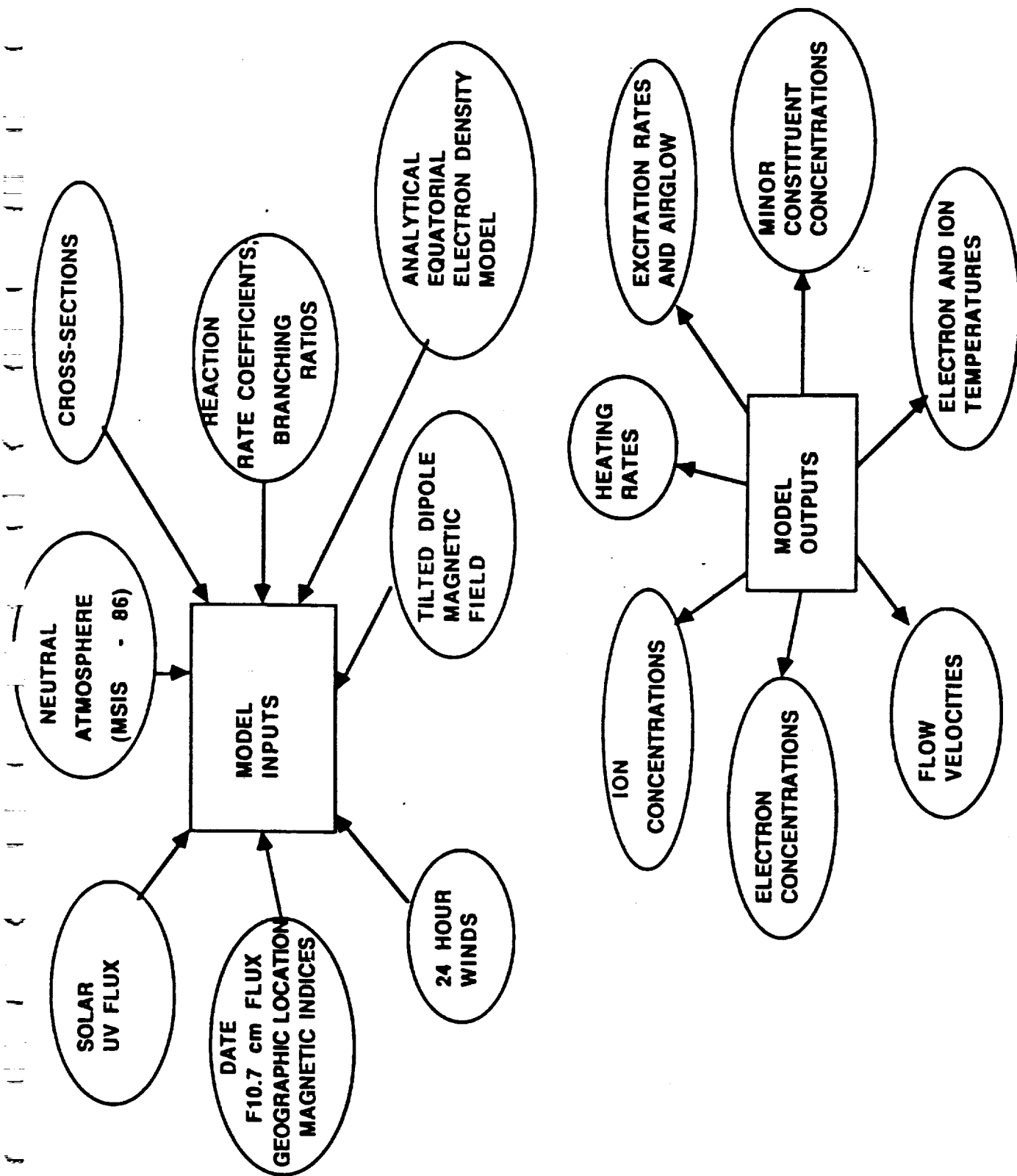


GLOBAL IONOSPHERE AND ELECTRODYNAMICS MODELS



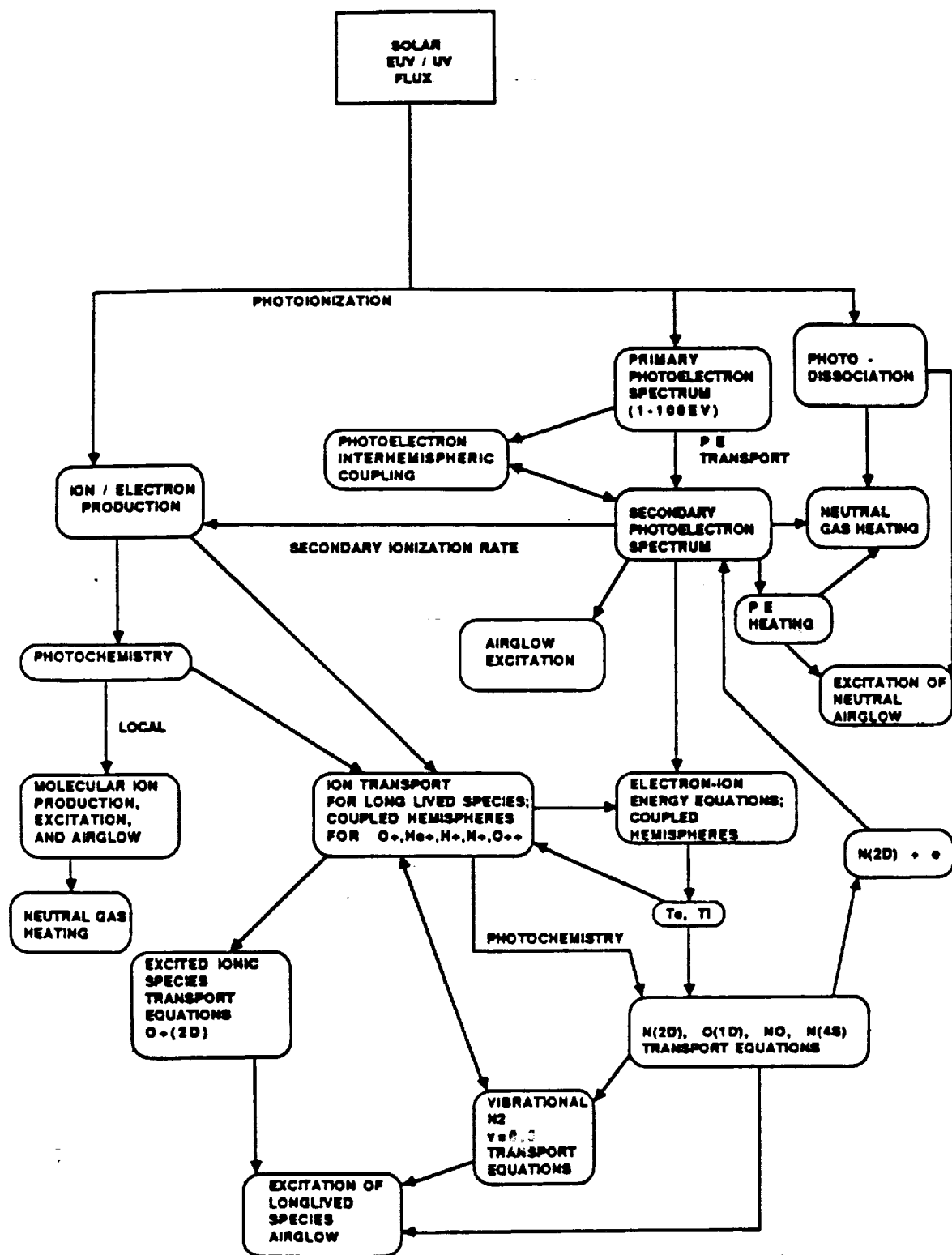
FLIP model tilted dipole geometry.





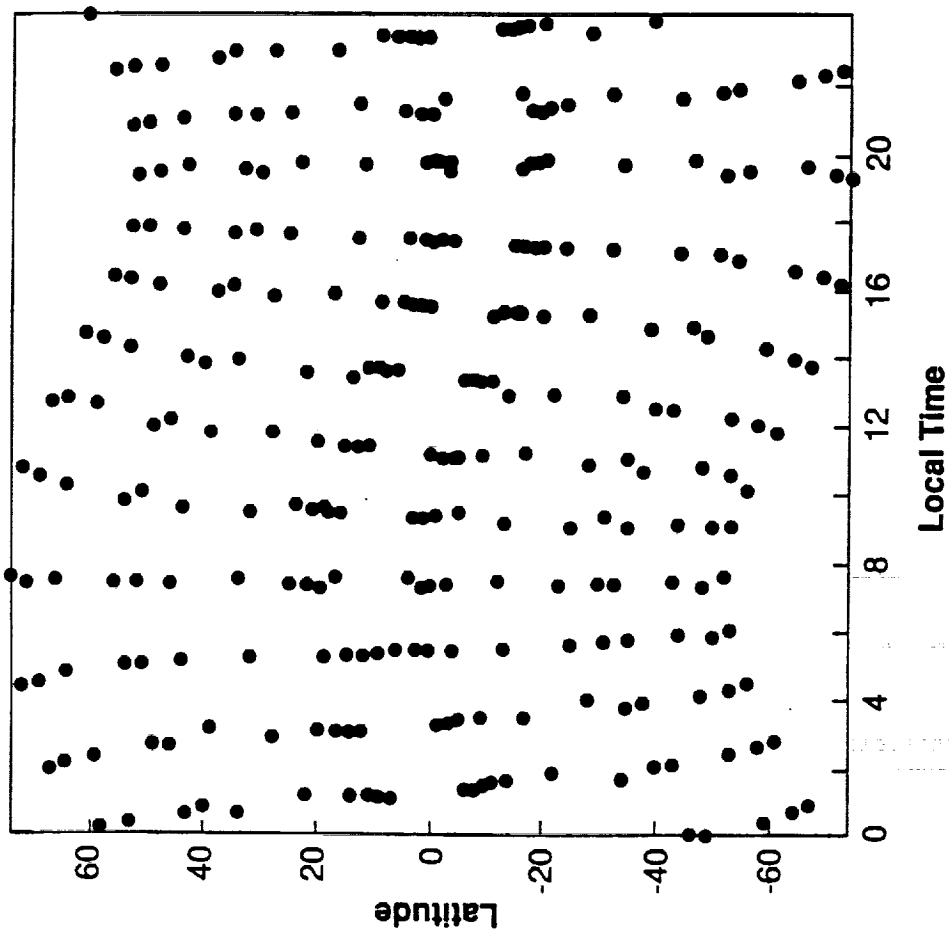
FLIP model inputs and outputs. An additional output not shown is the photoelectron flux.





ORIGINAL PAGE IS  
OF POOR QUALITY

FLIP model computational flow chart.



## FLIP ELECTRON DEPOSITION MODEL

WE NEED A VERY EFFICIENT CODE TO CALCULATE THE AURORAL IONIZATION RATE AS A FUNCTION OF ALTITUDE AT EVERY HIGH-LATITUDE PIXEL.

OUR MODEL IS BASED ON THE TWO-STREAM CODE OF NAGY AND BANKS (1970) WITH THE FOLLOWING CHANGES:

1. VARIABLE ENERGY GRID  
 $\Rightarrow 0 < E < 50 \text{ keV}$

2. VARIABLE ALTITUDE GRID

$\Delta h < 1 \text{ km}$  BELOW 20 km

$\Delta h > 50 \text{ km}$  ABOVE 500 km.

$\Rightarrow$  MANAGEABLE NO. OF GRID POINTS

3. INTRODUCE AN AVERAGE ENERGY LOSS PER IONIZATION / EXCITATION

$\Rightarrow$  NEED ONLY TOTAL EXCITATION AND IONIZATION CROSS-SECTIONS

$\Rightarrow$  ELIMINATES HUNDREDS OF CALCULATIONS 133

ENERGY LOSS: PARTITIONING INTO

ELECTRONIC, VIBRATIONAL STATES

eq. IONIZATION:

AVERAGE ENERGY OF DEGRADED PRIMARIES

$$= E_p - I - E_s$$

WHERE:

$E_p$  = ENERGY OF PRIMARY ELECTRON

$I$  = AVERAGE IONIZATION POTENTIAL

$E_s$  = AVERAGE SECONDARY ELECTRON ENERGY

eq.  $N_2$ : IONIZATION RESULTS FROM THE FORMATION OF THE X, A, B STATES OF  $N_2^+$  AND DISSOCIATION YIELDING  $N^+$ .

$$I(X, A, B) = 15.6, 16.8, 18.8 \text{ eV} \\ \text{RESPECTIVELY}$$

$$N^+ : \sim 37 \text{ eV.}$$

+ VIBRATIONAL ENERGY

+ KINETIC ENERGY - DISSOCIATION

CONSIDER A 100eV PRIMARY

		CROSS-SECTION
DISSOCIATION:	~20%	OF <del>ENERGY</del>
B STATE	10%	OF CROSS-SECTION
X STATE	35%	" "
A STATE	35%	" "

WITH THESE CROSS-SECTIONS AND  
IONIZATION POTENTIALS, THE AVERAGE  
IONIZATION POTENTIAL FOR A 100eV  
ON  $N_2$  IS ~20eV

CONSIDER A LOW ENERGY PRIMARY ELECTRON  
 $\bar{I}(N_2) = 15.6eV$  FOR THE X STATE

$\bar{I}(N_2)$  INCREASES TO ~16eV WHEN THE A  
STATE THRESHOLD IS REACHED

$\bar{I}(N_2)$  INCREASES TO 16.8 WHEN THE B STATE  
( $\sigma(10\%)$ ) IS REACHED

AT 30eV DISSOCIATION BECOMES IMPORTANT  
BY 50eV  $\bar{I}(N_2)$  INCREASES TO ~19eV  
INCREASING TO 20eV FOR HIGH ENERGIES

THE AVERAGE ENERGY LOSS DEPENDS  
ON SPECIES AND ENERGY

CALCULATION OF EMISSION RATES  
BECOMES A TWO-STAGE PROCESS.

- CALCULATION OF ELECTRON FLUX AS A  
FUNCTION OF ENERGY (WITH AVERAGE  
ENERGY LOSS, I.E. TOTAL CROSS-SECTIONS)
- CALCULATION OF EMISSIONS BY FOLDING  
THIS SPECTRUM WITH PARTIAL  
CROSS-SECTIONS.



## **GLOBAL ELECTRON PRECIPITATION PATTERN**

**THE PRECIPITATED ELECTRON FLUX CAN BE APPROXIMATELY CHARACTERIZED BY:**

- THE PRECIPITATED ENERGY FLUX**
- A CHARACTERISTIC ENERGY**

**OBSERVATIONS AND MODEL SIMULATIONS HAVE ESTABLISHED THAT:**

- THE PRECIPITATED ENERGY FLUX  $\propto$  AURORAL LUMINOSITY**
- THE CHARACTERISTIC ENERGY  $\propto$  LUMINOSITY RATIOS**

**$\Rightarrow$  ESTIMATE OF THE ENERGY SPECTRUM OF PRIMARIES**

**$\Rightarrow$  CORPUSCULAR IONIZATION RATE**

**$\Rightarrow$  IONOSPHERIC INTEGRATED CONDUCTIVITY**



## **CONVECTION ELECTRIC FIELDS**

**CURRENTLY LARGE SCALE POTENTIAL PATTERNS DESCRIBING IONOSPHERIC CONVECTION PATTERNS ARE ESTIMATED USING STATISTICAL MODELS FOR IONOSPHERIC ELECTRODYNAMICS.**

**THE RICHMOND-KAMIDE MODEL, FOR EXAMPLE, UTILIZES:**

**INCOHERENT SCATTER RADAR CONVECTION OBSERVATIONS**

**SATELLITE DIRECT FIELD OBSERVATIONS**

**GROUND AND SATELLITE MAGNETOMETER OBSERVATIONS**

**IONOSPHERIC ELECTRICAL CONDUCTANCE OBSERVATIONS**

**GROUND-BASED OBSERVATIONS OF IONOSPHERIC ELECTRODYNAMIC FEATURES ARE CAPABLE OF TRACKING RAPID CHANGES IN ELECTRIC FIELDS AND CURRENTS, CONDUCTIVITIES AND ASSOCIATED MAGNETIC PERTURBATIONS.**

**THE ELECTRODYNAMICS MODELS COMBINE THE DIFFERENT TYPES OF ELECTRODYNAMICAL DATA TO INFER HIGH-LATITUDE ELECTRIC POTENTIAL PATTERNS AS THEY EVOLVE IN TIME**

**SPATIAL COVERAGE IS LIMITED SO THAT MANY INSTRUMENTS WOULD BE NEEDED TO OBTAIN GLOBAL COVERAGE**

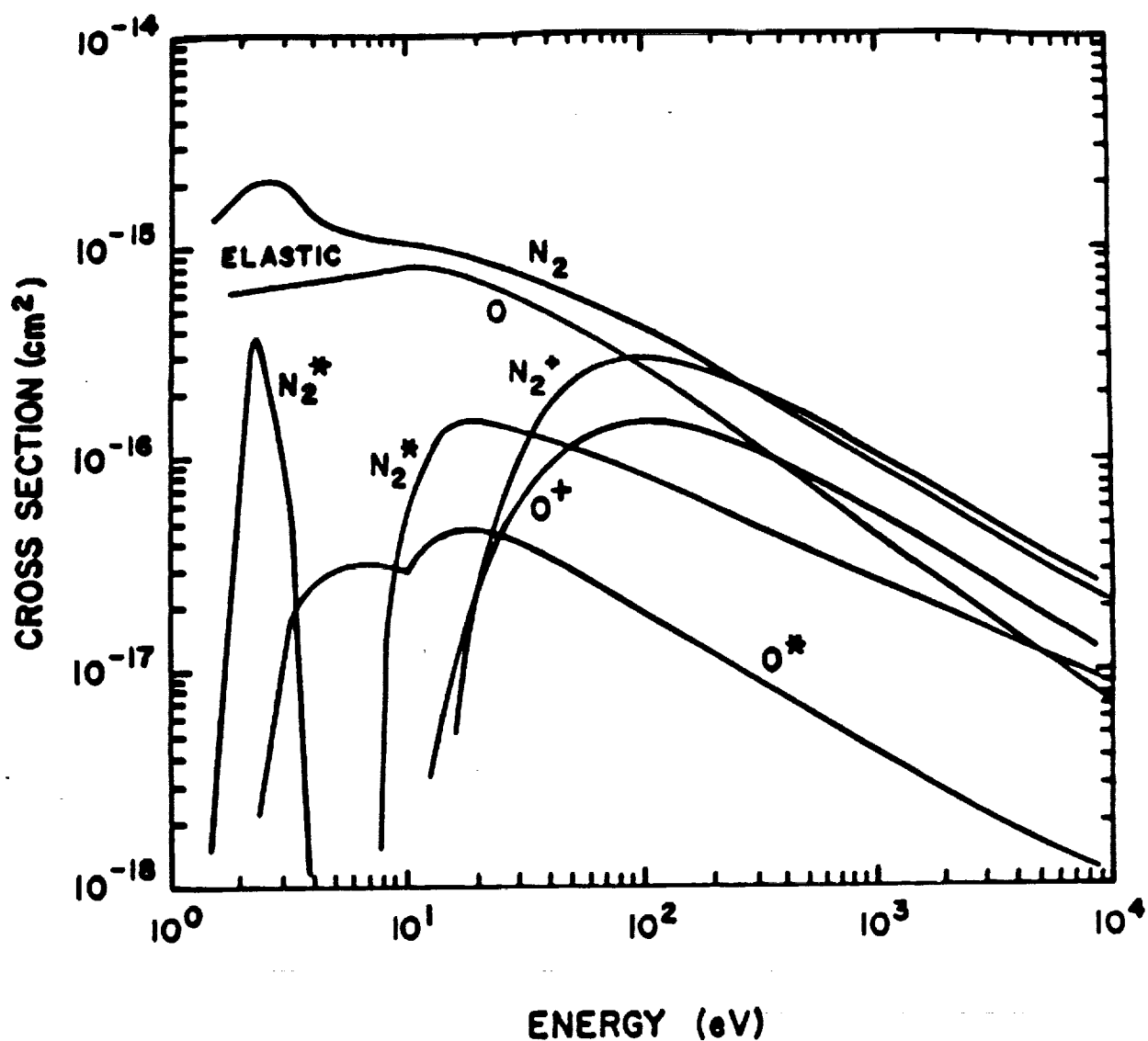


Figure 2: Total elastic, excitation, and ionization cross sections employed in the model. The ionization cross sections are indicated by a '+' while the excitation cross sections are indicated by a '\*'.

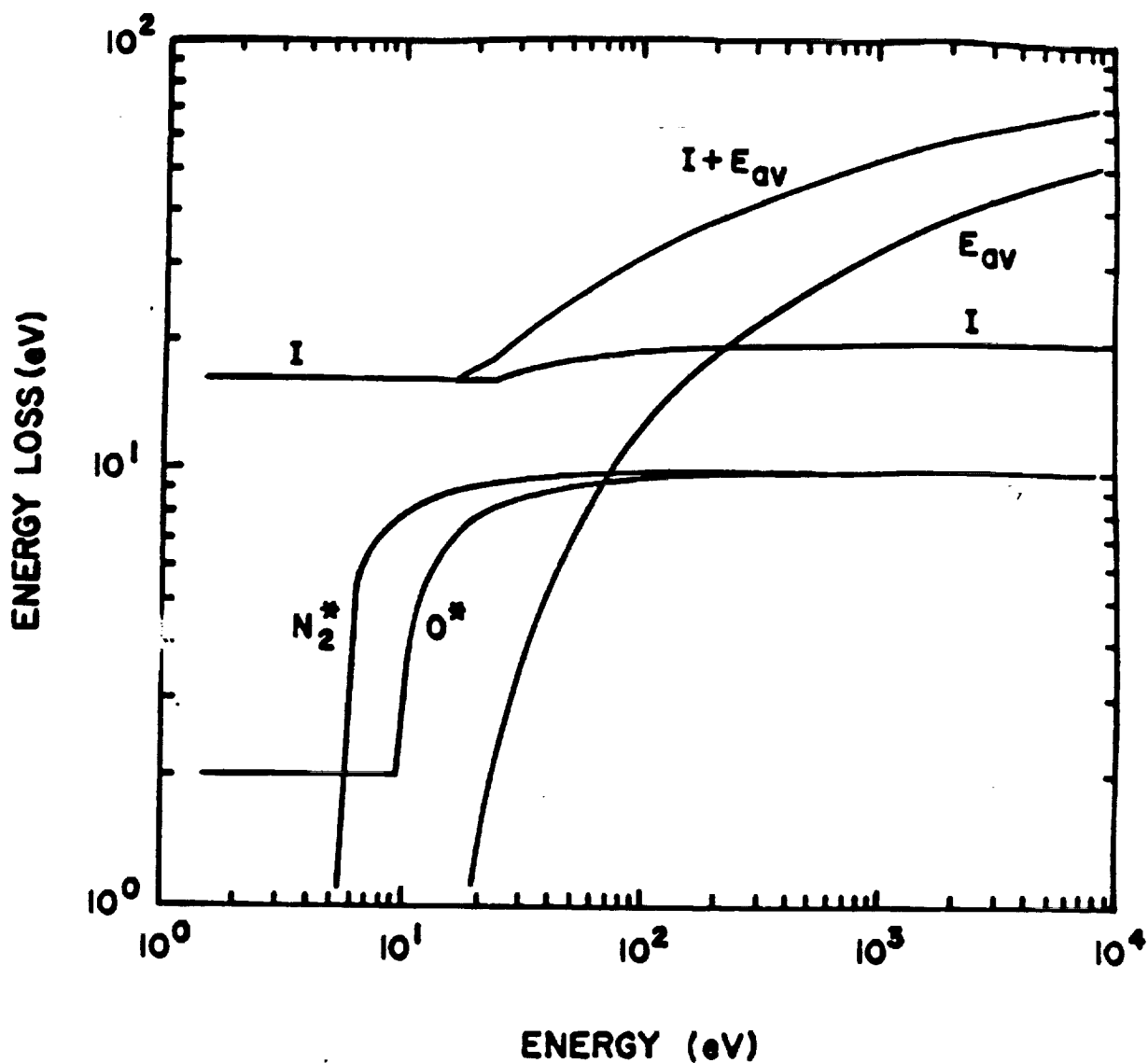


Figure 1: Average energy losses per collision and average secondary electron energies ( $E_{av}$ ) as a function of primary electron energy. The average ionization potential is labeled  $I$  and the total energy loss per ionization is labeled  $I + E_{av}$ . The average excitation potentials are indicated by a "\*" and the  $O_2$  excitation potential is set equal to that of  $N_2$ . Note that below 5 eV, the  $N_2$  excitation potential is set at 1 eV.

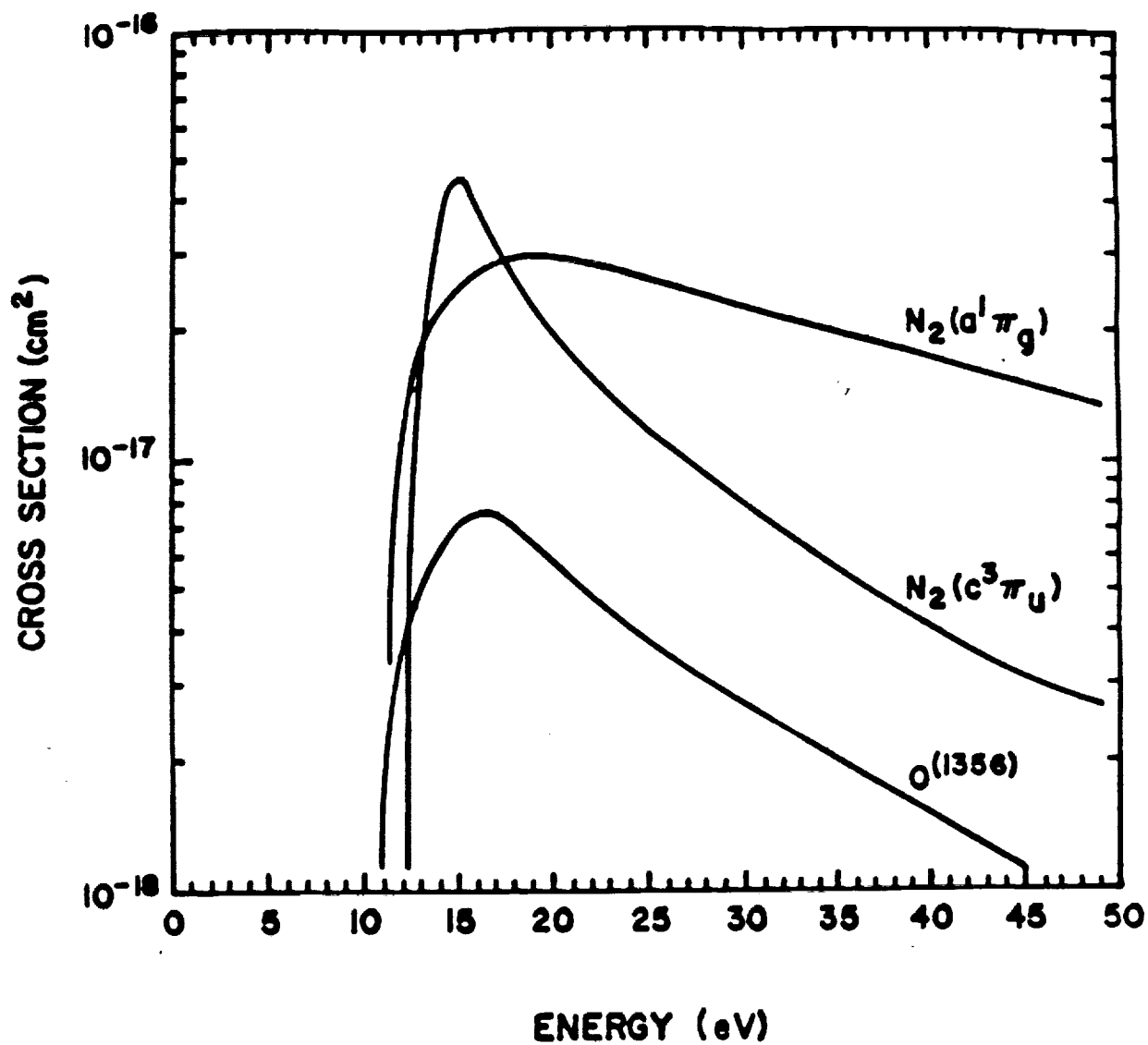


Figure 3: Cross sections for the three excited states giving rise to the emissions studied.

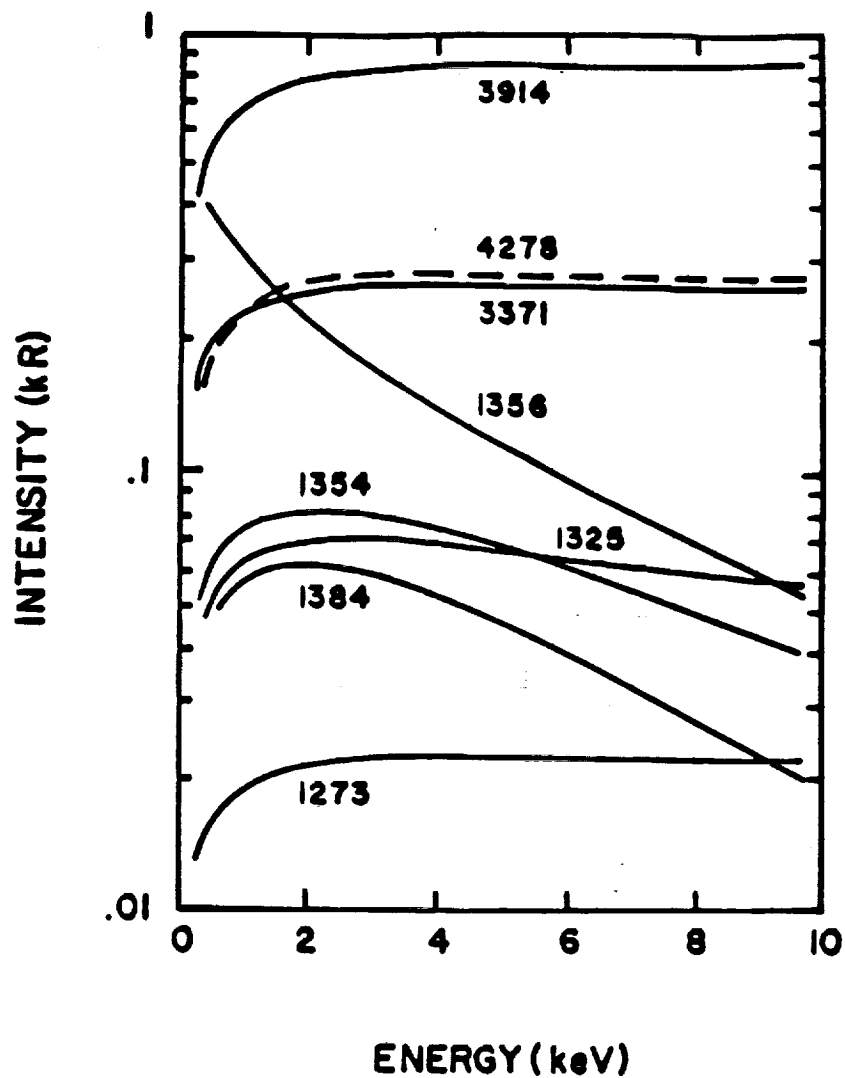
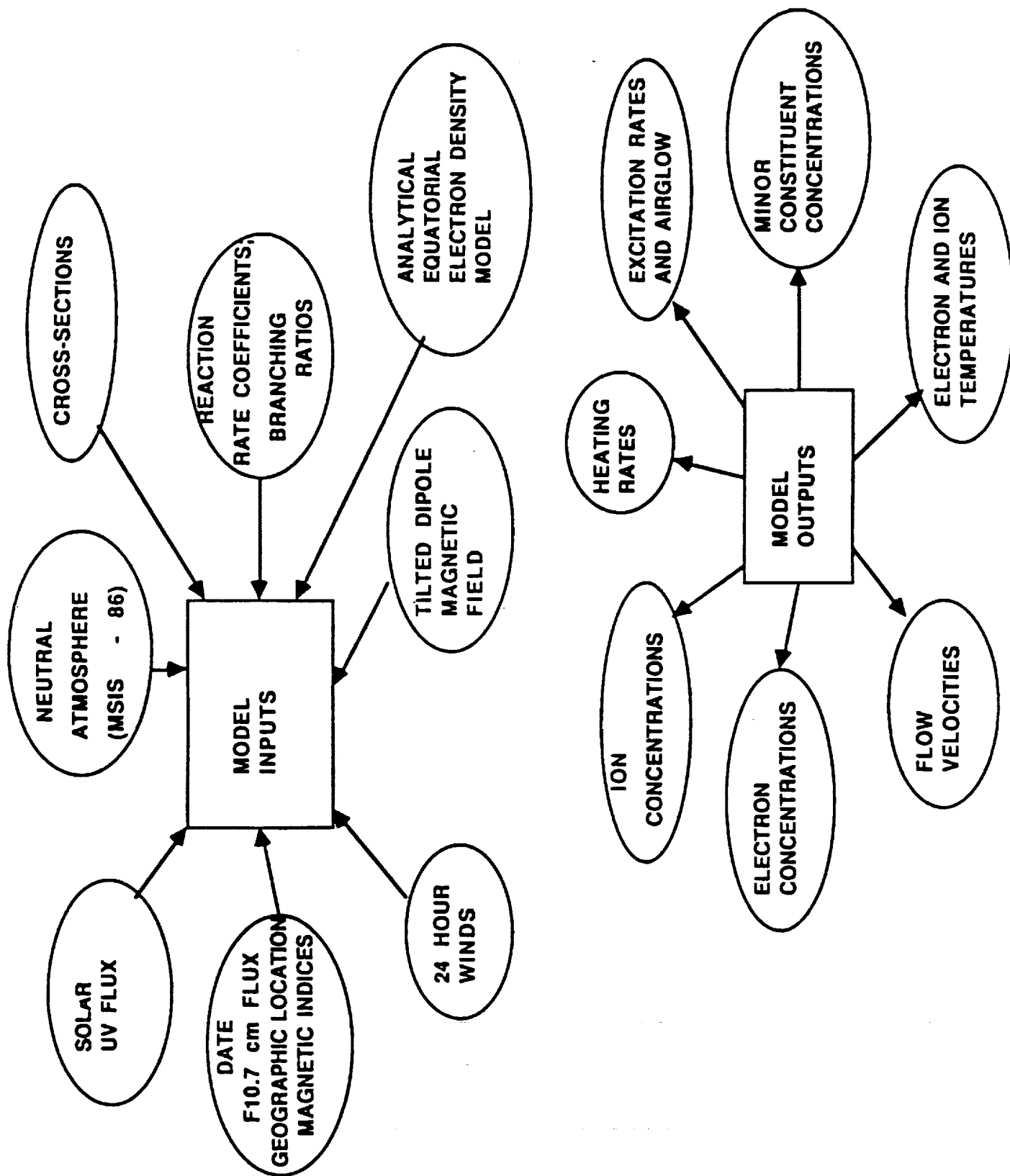


Figure 4: Calculated emission rates as a function of the characteristic energy for a Gaussian energy distribution with a total incident energy flux of  $1 \text{ erg cm}^{-2} \text{ s}^{-1}$ . When differences in cross sections are taken into account, there is excellent agreement with the calculations of Strickland *et al.* (1983) and Daniell and Strickland (1986).



FLIP model inputs and outputs. An additional output not shown is the photoelectron flux.



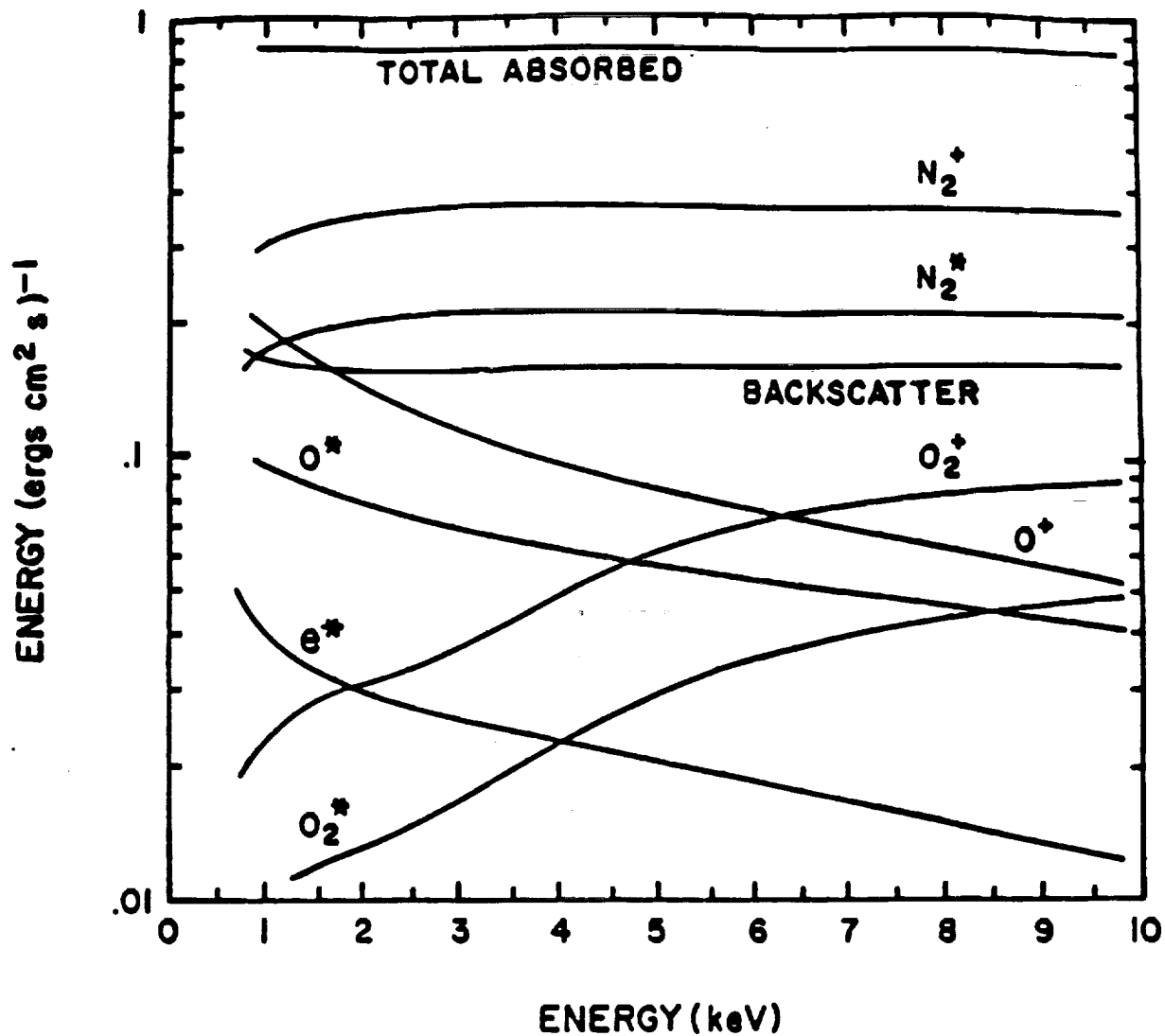


Figure 5: The initial partitioning of the incident  $1 \text{ erg cm}^{-2} \text{ s}^{-1}$  energy flux between ionization, excitation, thermal electron heating, and backscatter as a function of characteristic energy. The largest proportion of the energy ( $\sim 35\%$ ) goes initially into the ionization potential of the  $\text{N}_2^+$  while ( $\sim 20\%$ ) goes into  $\text{N}_2$  excitation. Only ( $\sim 16\%$ ) is backscattered out of the thermosphere. O is an important absorber of energy at the lowest energies while  $\text{O}_2$  becomes increasingly important as the characteristic energy increases.

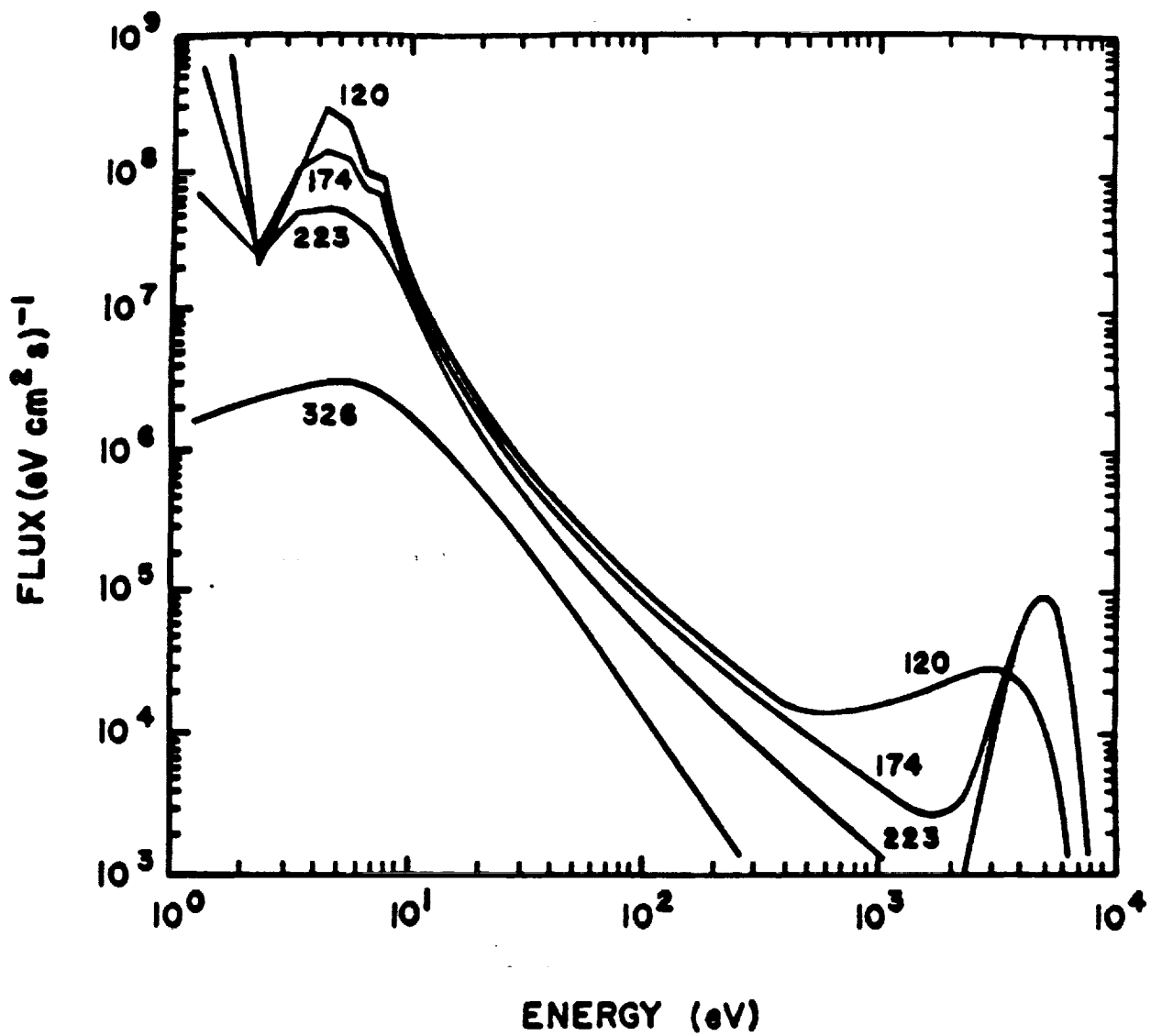


Figure 6: Downward moving electron flux spectra at several altitudes for a 5 keV Gaussian incident flux. The incident energy flux is  $1 \text{ erg cm}^{-2} \text{s}^{-1}$ .

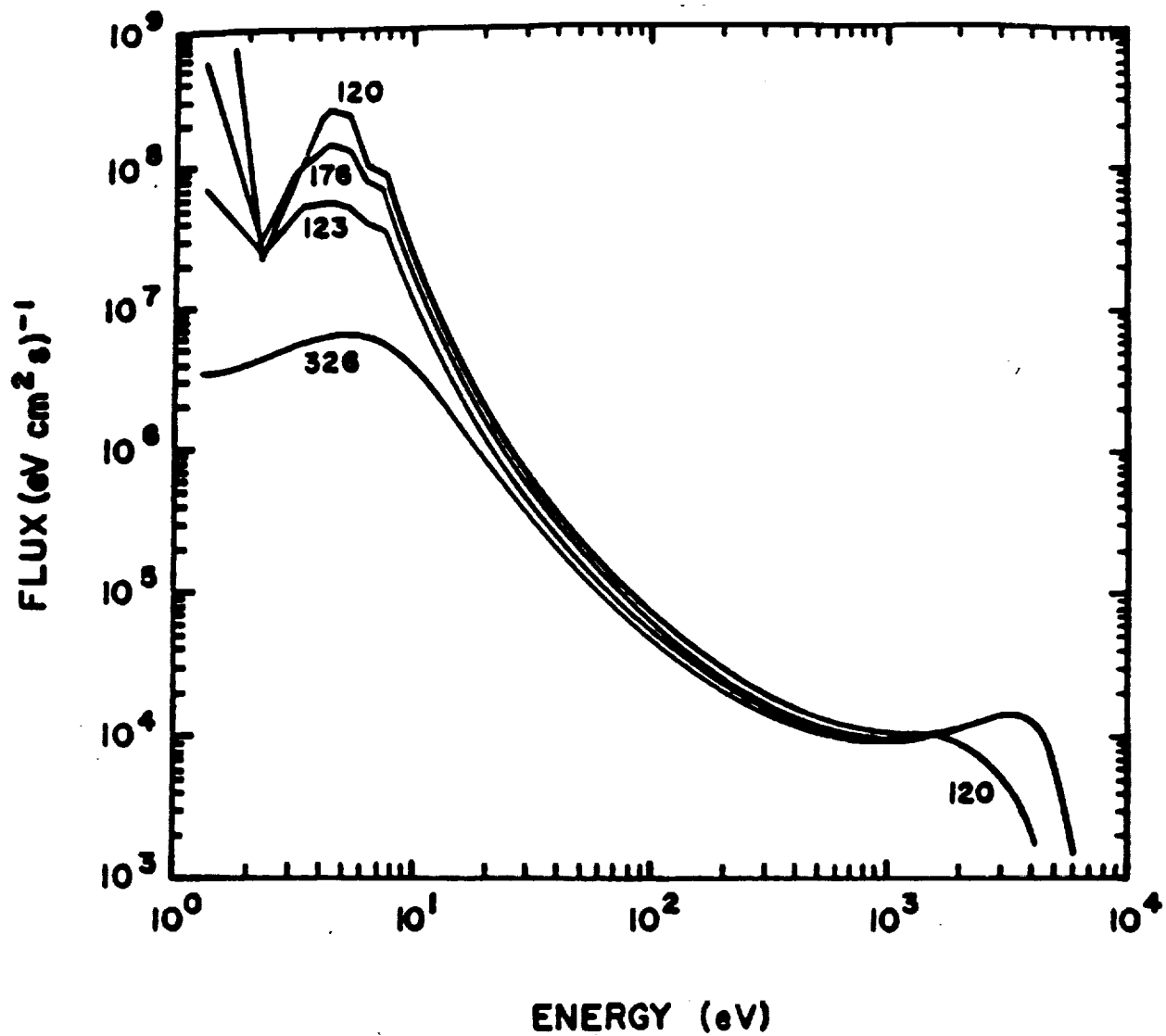
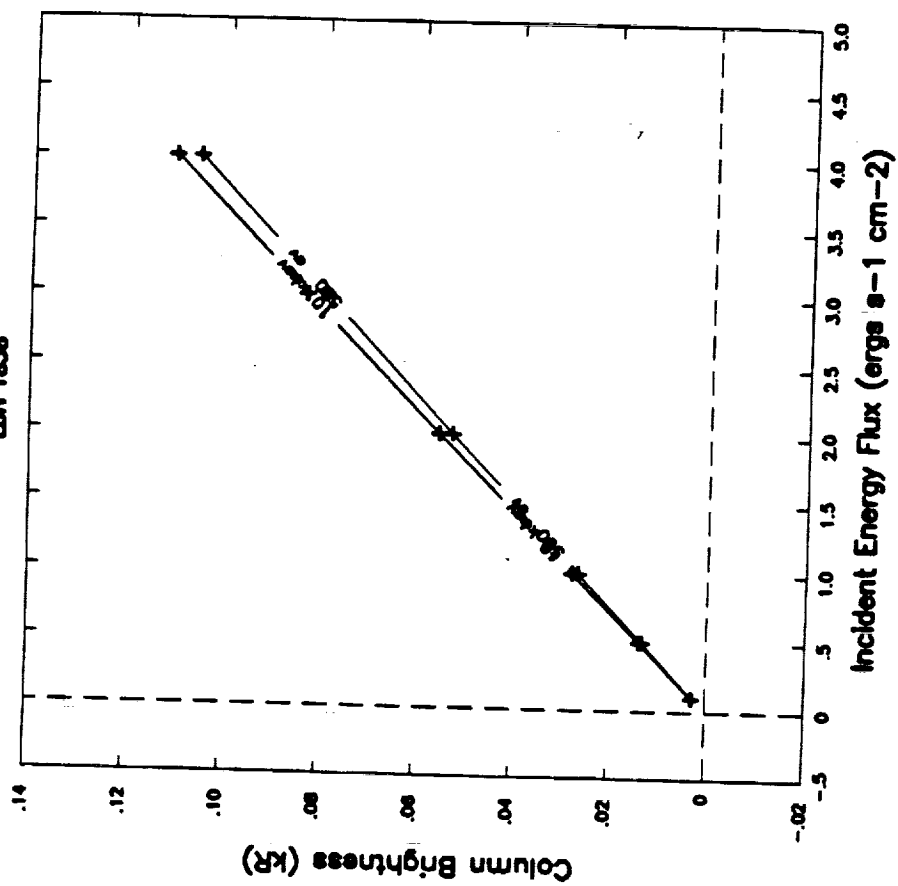


Figure 7: Upward moving electron flux spectra for the 5 keV Gaussian incident flux shown in Figure 6.

# Energy Flux Extraction

11 August 1960

LEH 1838



## STATUS OF MODELS

1. SUBSONIC FLIP MODEL DEVELOPED  
(INTERHEMISPHERIC IONOSPHERE-AIRCLOW MODEL)
2. SUPERSONIC PLASMA MODEL DEVELOPED  
(HYDRODYNAMIC OPEN FIELD-LINE MODEL)
3. AURORAL DEPOSITION CODE DEVELOPED.
4. CONVECTION MODEL TO BE DEVELOPED
5. INTEGRATION OF ABOVE MODELS TO BE DONE.

### FIRST TASK.

USE FLIP MODEL AND DEPOSITION CODE  
TO DERIVE A RELATIONSHIP BETWEEN  
AURORAL INTENSITIES AND RATIOS AND  
PEDERSEN AND HALL CONDUCTANCES.



ORIGINAL PAGE IS  
OF POOR QUALITY

## Auroral Modeling of the 3371 Å Emission Rate: Dependence on Characteristic Electron Energy

P. G. RICHARDS

Computer Science Department and Center for Space Plasma and Aeronomic Research  
University of Alabama in Huntsville

D. G. TORR

Physics Department and Center for Space Plasma and Aeronomic Research  
University of Alabama in Huntsville

We have developed an efficient two-stream auroral electron model to study the deposition of auroral energy and the dependence of auroral emission rates on characteristic energy. This model incorporates the concept of average energy loss to reduce the computation time. Our simple two-stream model produces integrated emission rates that are in excellent agreement with the much more complex multistream model of Strickland et al. (1983) but disagrees with a recent study by Rees and Lummerzheim (1989) that indicates that the  $N_2$  second positive emission rate is a strongly decreasing function of the characteristic energy of the precipitating flux. Our calculations reveal that a 10 keV electron will undergo approximately 160 ionizing collisions with an average energy loss per collision of 62 eV before thermalizing. The secondary electrons are created with an average energy of 42 eV. When all processes including the backscattered escape fluxes are taken into account, the average energy loss per electron-ion pair is 35 eV in good agreement with laboratory results.

### 1. INTRODUCTION

There is currently renewed interest in the use of auroral optical emission rates to deduce the characteristics of the precipitating particle fluxes, and ultimately, the global auroral energy input to the Earth's upper atmosphere. Images from the Dynamics Explorer satellite have been used by Rees et al. [1988] to calculate the energetic electron flux and its characteristic energy. Imaging instruments planned for the ISTP mission will monitor key UV emissions on a global scale for the express purpose of determining the global energy input.

Early work in determining auroral particle characteristics from emissions concentrated on the use of the ratios of atomic oxygen emission rates (6300 Å, 5577 Å) to molecular nitrogen ion emission rates (3914 Å, 4278 Å) to deduce the incident auroral spectrum [Rees and Luckey, 1974; Vallance Jones, 1975; Shepherd et al., 1980; Strickland et al., 1983]. The higher energy auroral electrons penetrate deeper into the thermosphere where the relative proportion of atomic oxygen is smaller. Thus the ratio of atomic to molecular emission rates decreases with increasing electron energy. Unfortunately, chemical processes play an important role in the atomic oxygen emissions and it is difficult to separate the effects caused by the characteristics of the auroral energy flux from the effects caused by changes in the atmospheric composition. Therefore, it would be useful to find an emission rate ratio that is sensitive to the auroral characteristics but which is not complicated by chemical factors.

Recently, Rees and Lummerzheim [1989] suggested that the ratio of the second positive to first negative emission rates could be used to determine the characteristic energy of the auroral electron flux. Using an auroral electron model developed by Lummerzheim et al. [1989], Rees and Lummerzheim [1989] found that the  $N_2$  second positive (3371 Å) emission rate decreases substantially with increasing characteristic energy of the auroral electrons while the  $N_2^+$  emission rates are almost constant. This ratio would be an attractive alternative to those used previously because it would be independent of atmospheric composition and both emissions are prompt, thus eliminating chemical effects. Unfortunately, the calculations of Rees and Lummerzheim [1989] are in conflict with the earlier calculations by Daniell and Strickland [1986] who found that the 3371 Å emission rate was nearly independent of the characteristic energy.

The experimental evidence also seems to be in conflict. Rees and Lummerzheim [1989] present data from high flying aircraft that support their theoretical calculations. On the other hand, Solomon [1989] presented data from the visible airglow instrument on the Atmosphere Explorer C satellite showing that the ratio of the  $N_2$  3371 Å to  $N_2^+$  4278 Å emission rates has only a small dependence on the characteristic energy, which can be accounted for by contamination of the 3371 Å second positive emission by the Vegard-Kaplan (0-9) band. The VAE data support the earlier calculations of Daniell and Strickland [1986] and Strickland et al. [1983]. Solomon was able to reproduce the observed ratios using his own two-stream auroral electron deposition code. We note that the experimental data presented by Solomon [1989] for the ratio of  $N_2$  3371 Å to  $N_2^+$  4278 Å is in excellent agreement with the ratio of  $N_2$  3371 Å to  $N_2^+$  3914 Å that was measured on a 1974 rocket flight by Sharp et al. [1979].

Copyright 1990 by the American Geophysical Union.





# CHARACTERISTIC ENERGY EXTRACTION

Glynn Germany

10:30 16 August

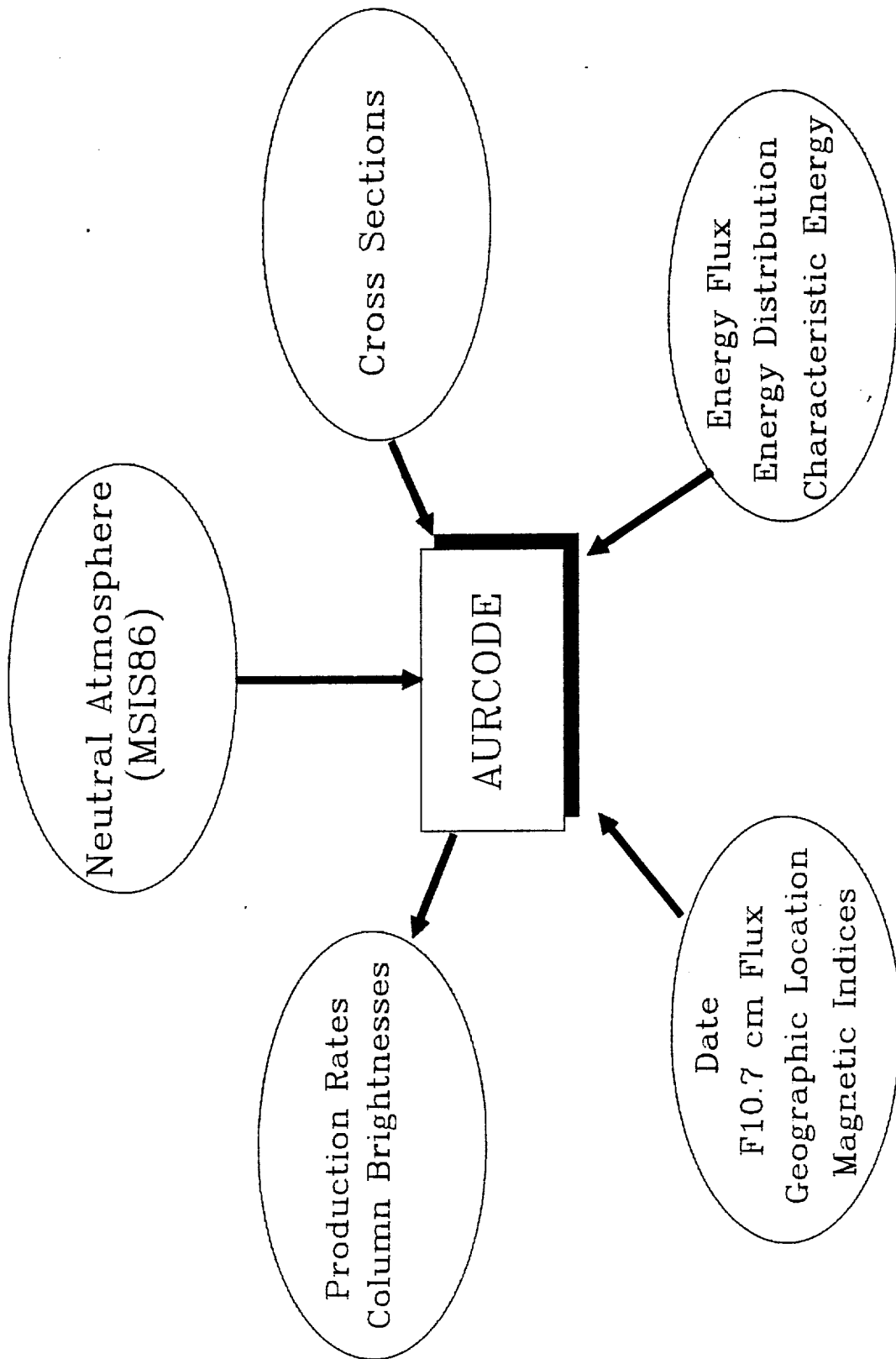
## CHARACTERISTIC ENERGY DETERMINATION

---

Use measured VUV intensity ratios  
to determine  $E_{\text{CHAR}}$ .

Lookup tables bypass need for  
extensive calculations.

Final result depends on quality of  
model & input parms.



## NEUTRAL ATMOSPHERIC STUDY

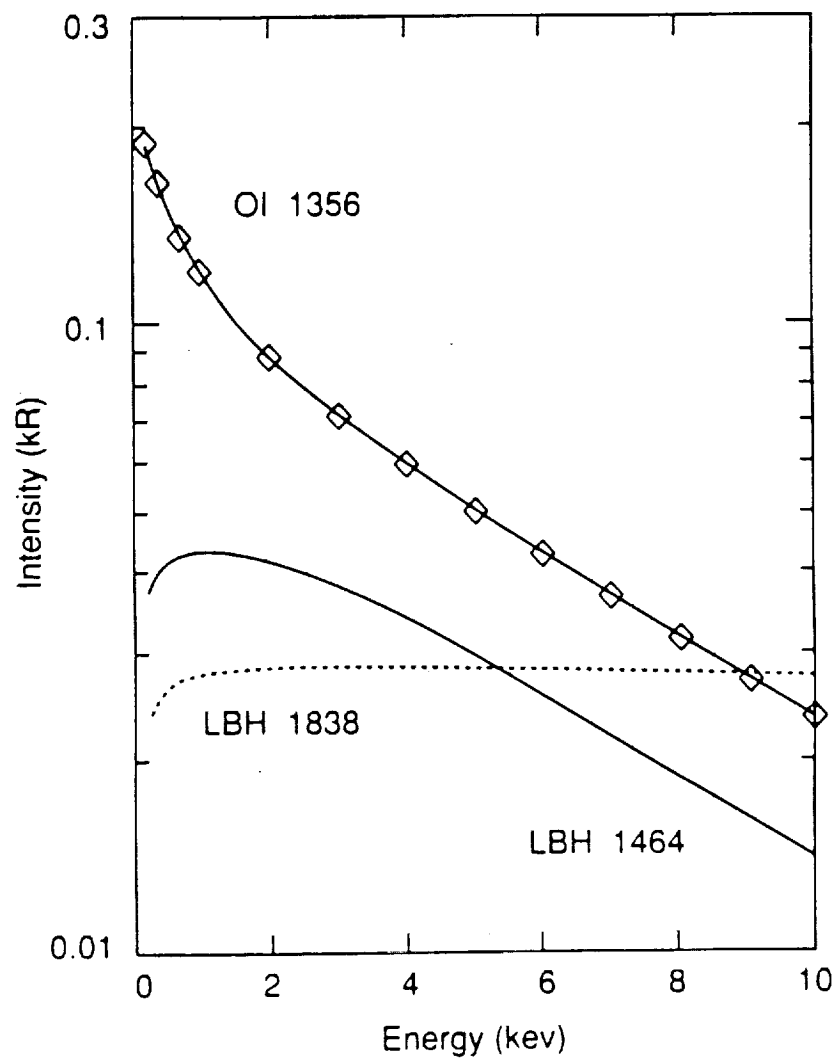
---

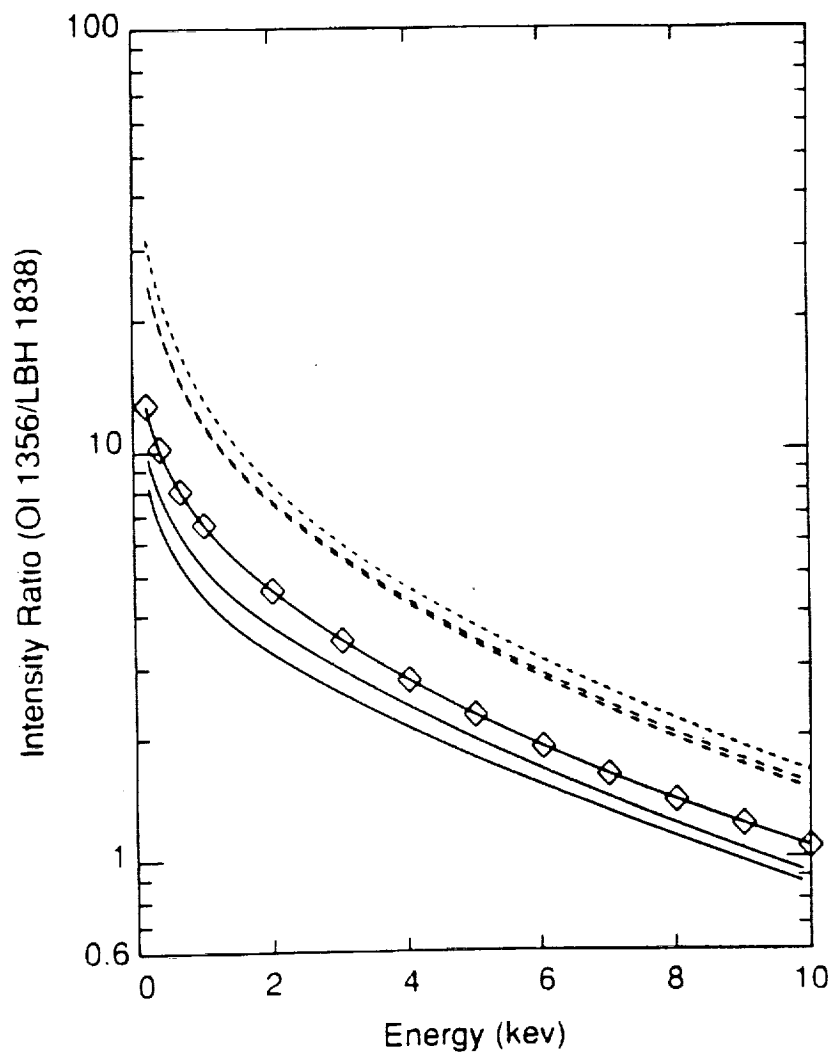
Modeled VUV auroral emissions:

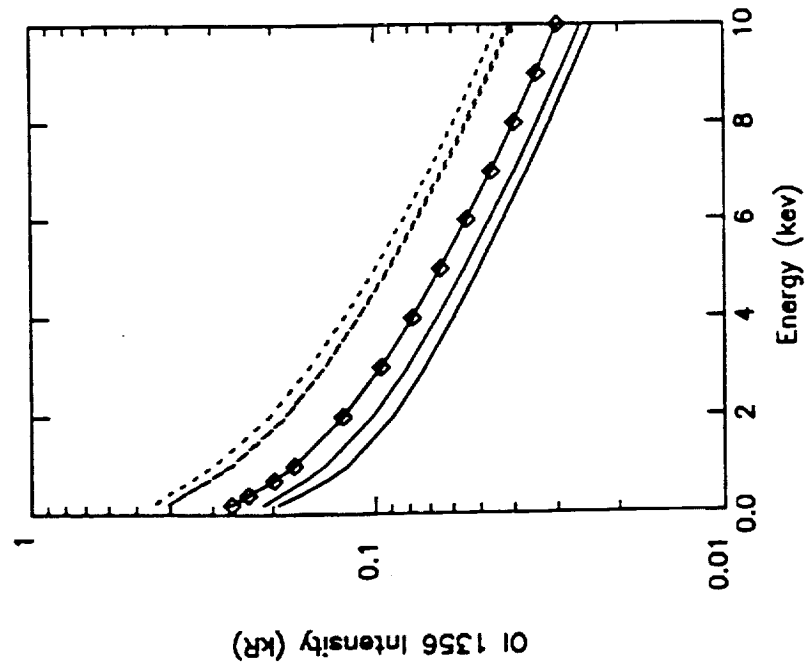
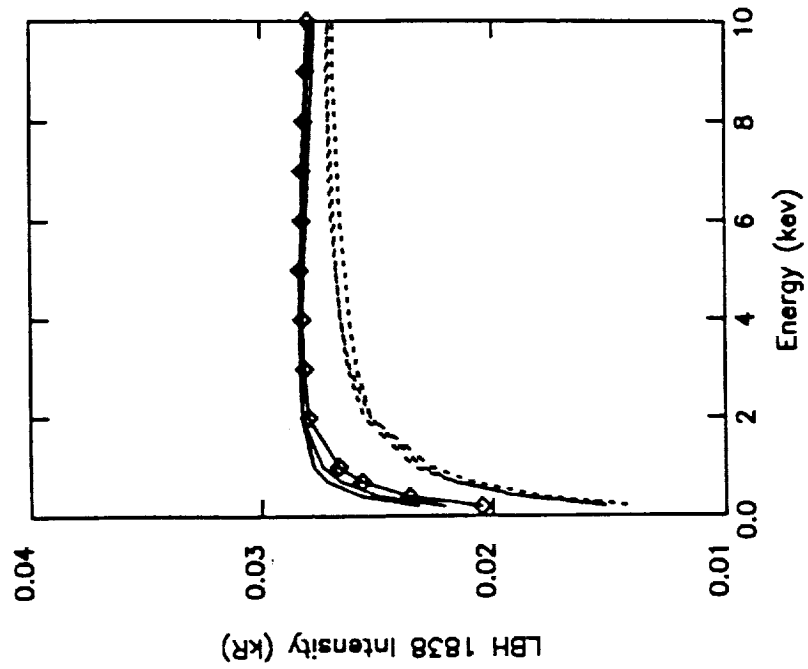
OI 1356, LBH<sub>short</sub>, LBH<sub>long</sub>

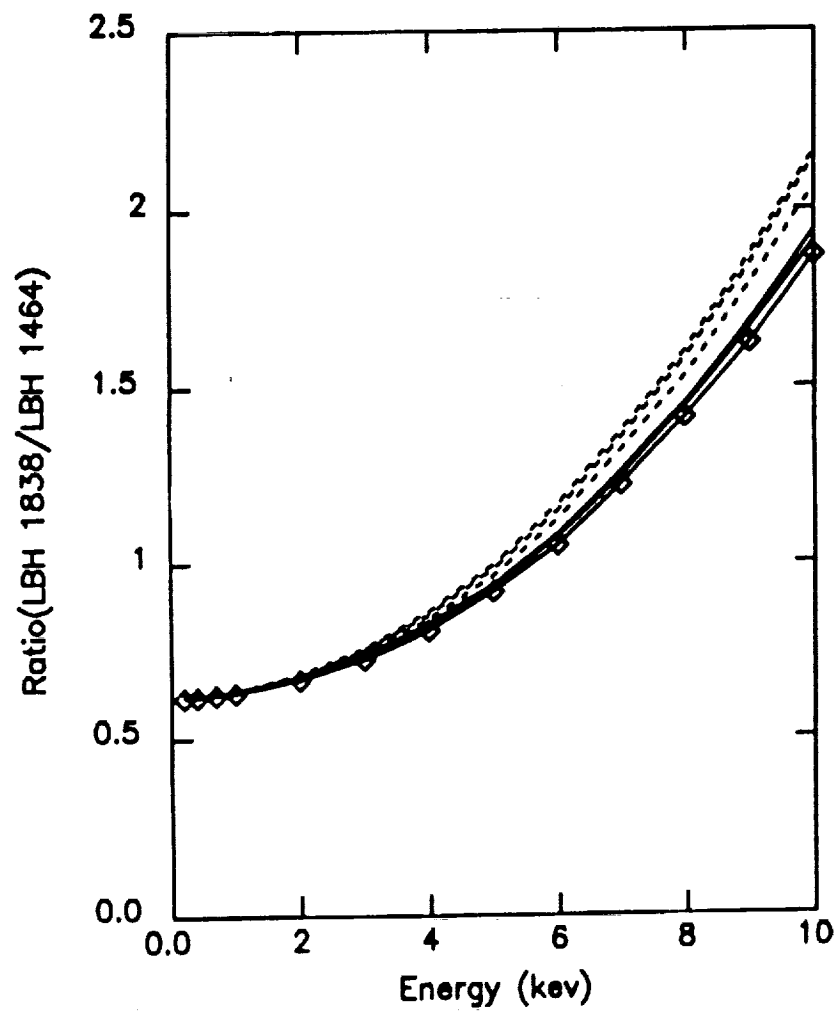
Perturbed single atmospheric constituents.

Looked at seasonal and solar variations.

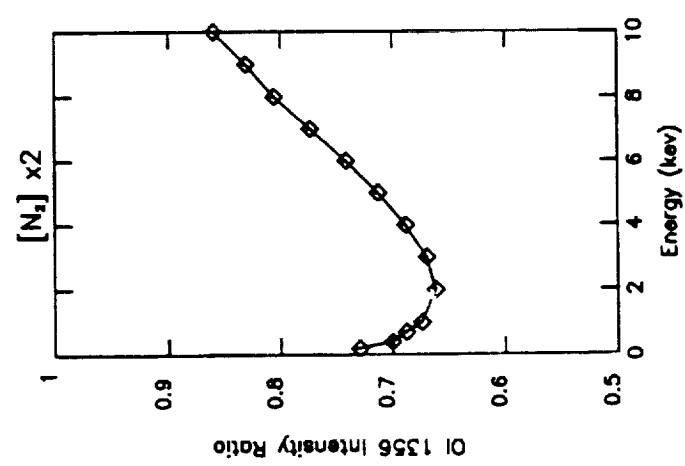
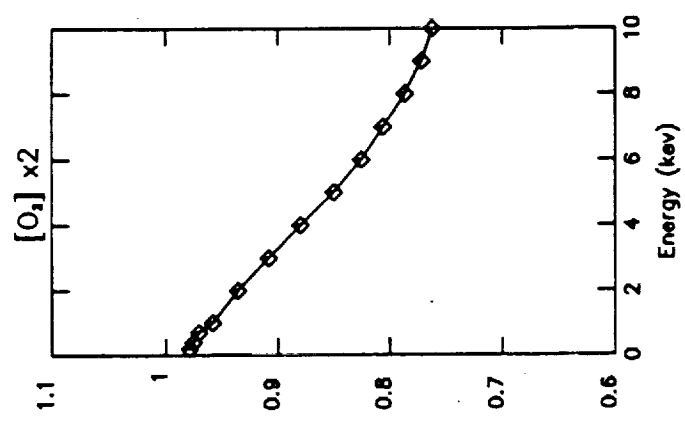
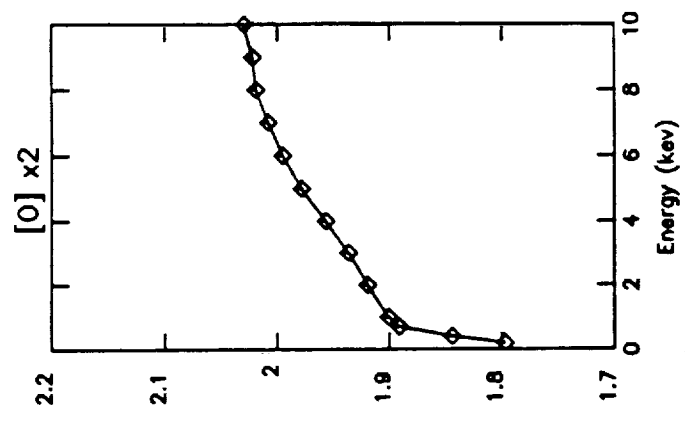




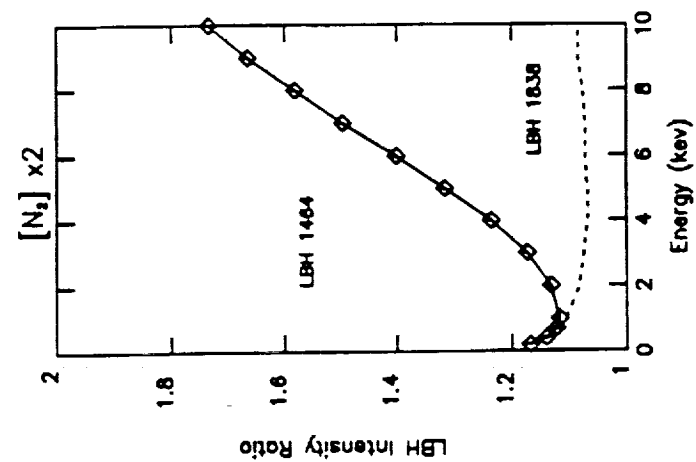
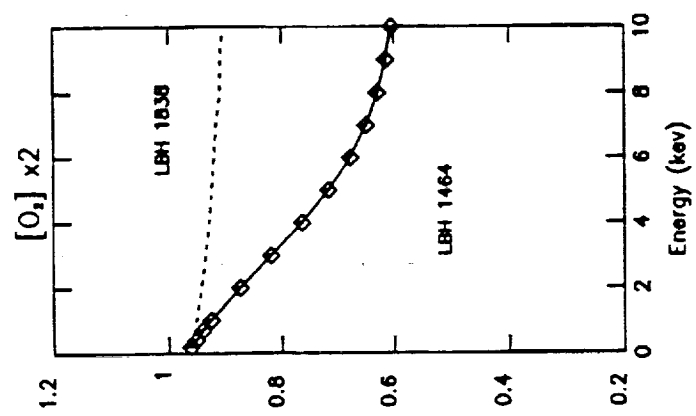
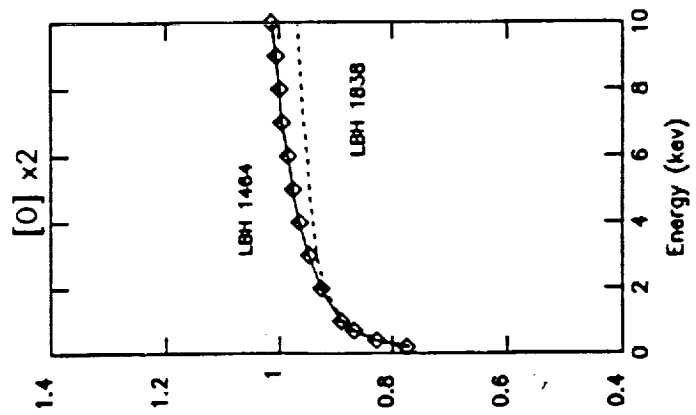








OI 1356 Intensity Ratio



## CONCLUSIONS

---

Intensity Ratios Available:

$$\frac{OI\ 1356}{LBH_{SHORT}} / \frac{LBH_{LONG}}{LBH_{LONG}}$$

Sensitivity & Variability Being Studied

Nature of Corrections Being Defined



# The Dependence of Modeled OI 1356 and N<sub>2</sub> Lyman Birge Hopfield Auroral Emissions on the Neutral Atmosphere

G. A. GERMANY AND M. R. TORR

*Space Science Laboratory, NASA Marshall Space Flight Center, Huntsville, Alabama*

P. G. RICHARDS AND D. G. TORR

*University of Alabama in Huntsville, Huntsville, Alabama*

Images of the entire auroral oval at carefully selected wavelengths contain information on the global energy influx due to energetic particles and some information on the characteristic energy of the precipitating particles. In this paper we investigate the sensitivity of selected auroral emissions to changes in the neutral atmosphere. In particular, we examine the behavior of OI 1356 Å and two Lyman Birge Hopfield (LBH) bands and their ratios to each other with changing atmospheric composition. The two LBH bands are selected so that one lies in the region of strong O<sub>2</sub> absorption (1464 Å) and one lies at a wavelength where O<sub>2</sub> absorption is effectively negligible (1838 Å). We find that for anticipated average uncertainties in the neutral atmosphere (factor of 2 at auroral altitudes), the resultant change in the modeled intensities is comparable to or less than the uncertainty in the neutral atmosphere. The smallest variations, for example, are for I 1838 (approximately 10 to 20%) while the largest variation is seen in the OI 1356 Å emission which is linear with [O] to within 20%. We have also investigated the dependence of these intensities, and their ratios, to much larger changes in the composition (i.e., [O]/[N<sub>2</sub>]) such as might be encountered in large magnetic storms, or over seasonal or solar cycle extremes. We find that the variation in the I 1356/I 1838 ratio over the equivalent of a solar cycle is less than 50%. The summer-to-winter changes are approximately a factor of 2. The I 1356/I 1838 ratio is a very sensitive indicator of the characteristic energy, showing a change of 13 over the energy range 200 eV to 10 keV. The corresponding change in the LBH long-to-short wavelength ratio is much less (about a factor of 3). However, the latter is insensitive to changes in the neutral atmosphere (<20% changes in LBH emission ratio for large changes in N<sub>2</sub>). The three emissions therefore potentially provide a most valuable diagnostic of particle characteristic energy and energy flux.

## 1. INTRODUCTION

While in situ observations of energetic particles provide accurate information on the particle characteristics at the point of measurement, imaging from space of the entire auroral oval holds the potential for providing details on total auroral energy influx, estimates of the characteristic energy of the auroral particles, and the capability to map and relate the footprint of this derived information back along the magnetic field lines to various regions of the magnetosphere. Auroral imaging in the vacuum ultraviolet permits observations of the regions of interest under both day and night conditions. Work by *Rees and Luckey* [1974] on the ratios of visible emissions, UV emission intensity calculations by *Strickland et al.* [1983], and analysis of UV auroral spectra by *Ishimoto et al.* [1988] all indicate the potential value of using ratios of emission intensities to study auroral processes. A major focus of work in this area at the present time is to establish the quantitative footing on which such determinations can be placed.

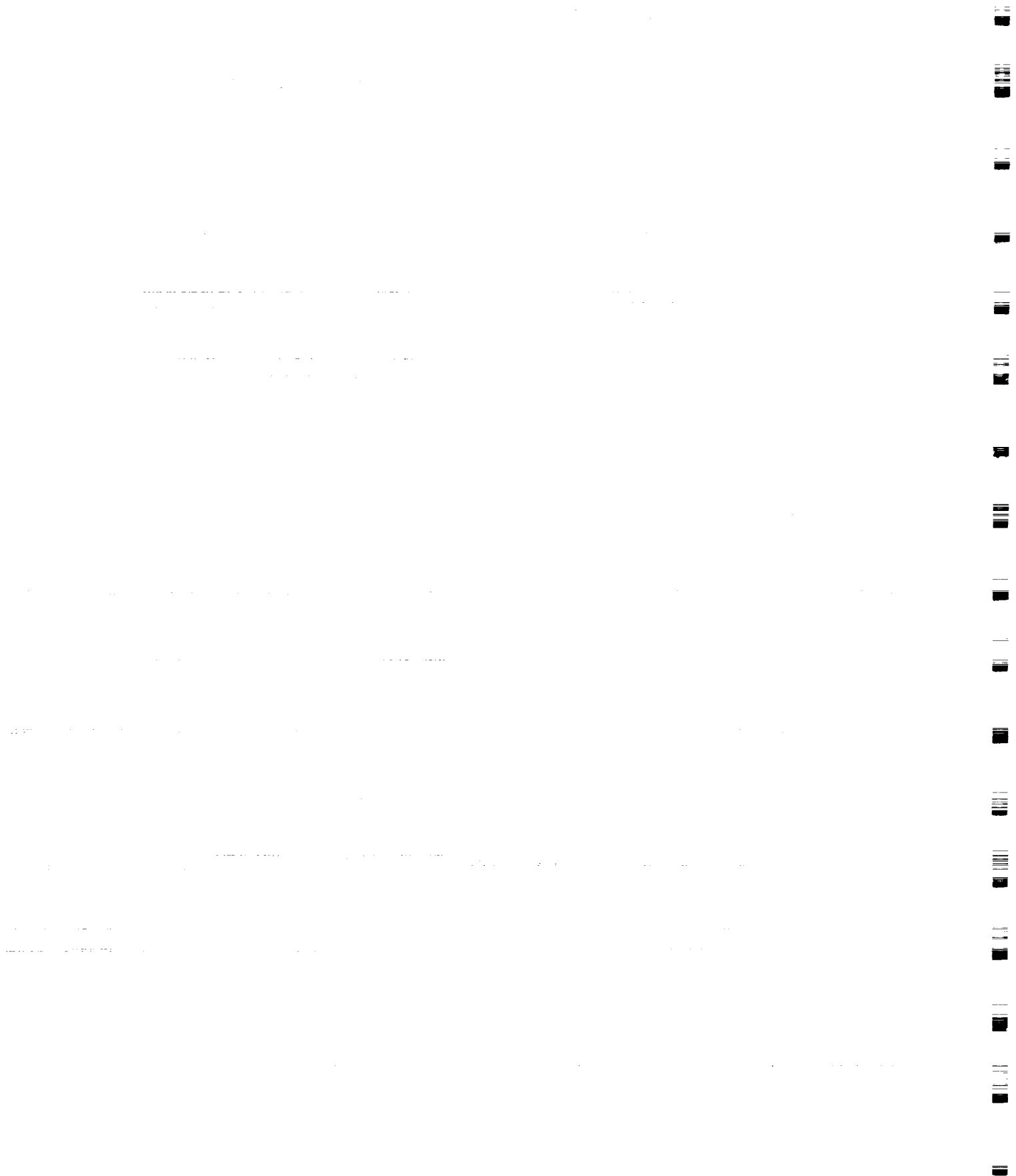
With the exception of H I Ly $\alpha$ , the OI multiplets at 1304 Å and 1356 Å and the N<sub>2</sub> Lyman Birge Hopfield (LBH) bands are the most prominent vacuum ultraviolet auroral emissions. The OI 1304 Å emission has a high efficiency for multiple scattering. As a result, it has limited use for actual auroral imaging, although it does have potential value as an indicator of the O concentration. While the 1356 Å emission does undergo multiple scattering, the efficiency is relatively small [*Strickland and Anderson*, 1983] and we ignore multiple scattering for I 1356 for this study. Similar

considerations allow us to also ignore multiple scattering for the N<sub>2</sub> LBH emissions that are also considered in this study. The OI 1356 Å emission is absorbed increasingly by O<sub>2</sub> with decreasing altitude. Thus its intensity varies strongly (inversely) with increasing depth of penetration of the incident auroral electrons and hence with increasing energy. The N<sub>2</sub> LBH transitions are electric dipole forbidden and the only prominent excitation mechanism is electron impact. The LBH emission may therefore serve as a direct measure of the total energy flux of charged particles into the atmosphere. The longer wavelength LBH bands, which lie outside the region of substantial O<sub>2</sub> absorption, are useful indicators of the total energy influx, while the long-to-short wavelength LBH intensity ratio provides information on the O<sub>2</sub>, and thus also some information on energy. These are the emissions (OI 1356, long and short wavelength LBH) on which we shall concentrate in this study.

The purpose of this paper is to examine the sensitivity of these emissions to both likely uncertainties and anticipated changes in the neutral atmosphere. This is just one step in the process of making quantitative interpretations of auroral images, but an important one. We will consider other aspects (energy spectral characteristics and wavelength spectral extraction) elsewhere. In this paper we conduct a series of sensitivity studies using an auroral emission code that has been developed by our group [*Richards and Torr*, 1990]. The results are discussed below.

## 2. DESCRIPTION OF AURORAL CODE

The behavior of auroral OI 1356 and N<sub>2</sub> LBH emissions has been studied with the use of an auroral computer model. The model is a two-stream auroral electron energy loss code that determines the energy degradation of the primary spectrum as a func-



USE OF SNAKES  
TO EXTRACT AURORAL OVAL

Bob Clauer

11:00 16 August

# **Computer Automated Analysis of Auroral Images Obtained from High Altitude Polar Satellites**

C. Robert Clauer  
Ramin Samadani  
Domingo Mihovilovic  
John Vesecky  
Peter Banks  
Gio Wiederhold

STAR Laboratory, Stanford University, Stanford, CA.

John Craven  
Lou Frank

Dept. of Physics and Astronomy, University of Iowa, Iowa City, IA

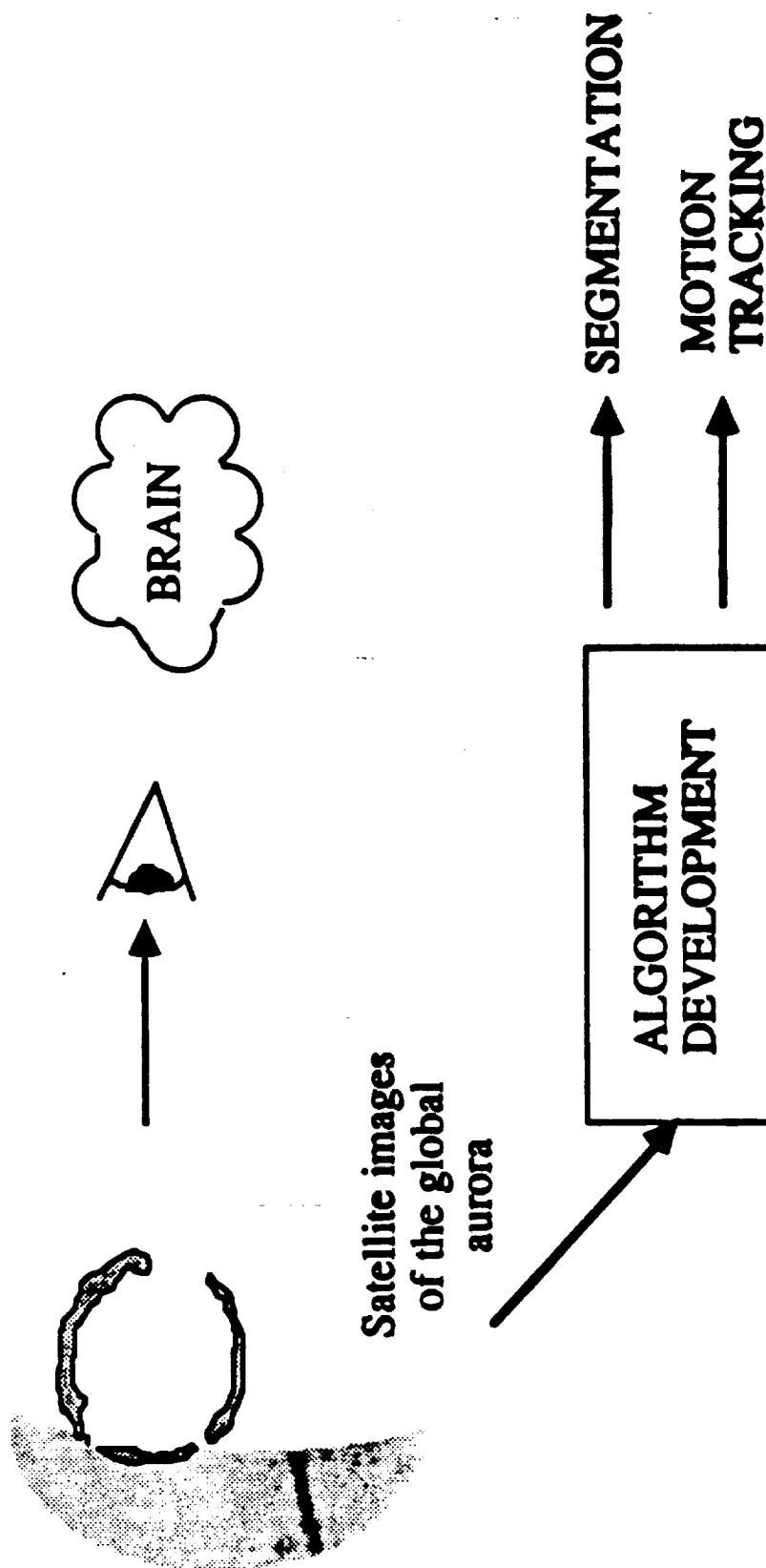
Over half a million auroral images presently exist in the DE-1 image database. The extraction of quantitative parameters from the images is extremely labor intensive. Thus, detailed analysis of the presently existing images greatly exceeds the manpower available. In addition, future satellite missions will provide more images at a greater rate and spatial resolution. One must conclude then, that automation is necessary to extract the information held within the existing data bases and it is imperative to process the anticipated large volume of expected images.



## COMPUTER IMAGE ANALYSIS RESEARCH GOALS

---

OF INTEREST TO: R. Samadani, D. Mihovilovic, G. Wiederhold,...



ORIGINAL PAGE IS  
OF POOR QUALITY

# **GEOPHYSICAL RESEARCH GOALS**

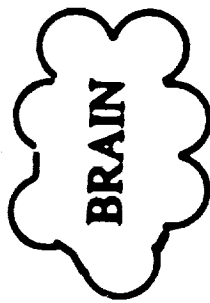
---

**OF INTEREST TO: C.R. Clauer, P.M. Banks, J.F. Vesecky,....**

**UNDERSTANDING  
OF MAGNETOSPHERE,  
IONOSPHERE, SUN,...**



**Satellite images  
of the global  
aurora**



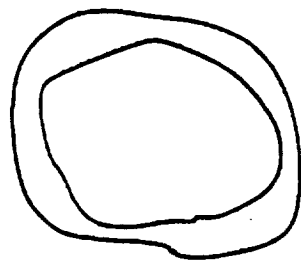
**GEOMETRY**

**MENSURATION**

**STATISTICS**

## BOUNDARIES PROVIDE MUCH USEFUL INFORMATION

---



+

SATELLITE  
EPHEMERIS  
DATA

=

- 1) Area of the polar cap.
- 2) Intensity as a function of local time.
- 3) Total integrated auroral intensity.
- 4) Width as a function of local time.

## METHODS EXPLORED FOR FINDING THE BOUNDARIES

---

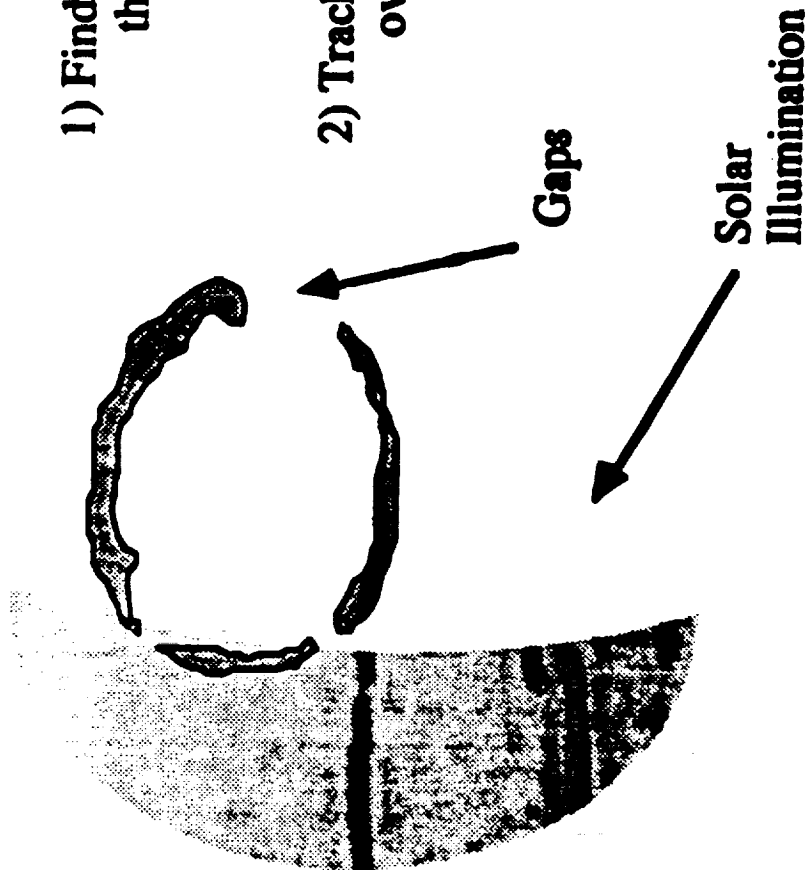
- 1) Edge detection.
- 2) Global and local thresholds.
- 3) Region growing.
- 4) Morphological methods.
- 5) Fitting of parametric models.
- 6) Regularized segmentation.
- 7) Elastic model dynamic simulations or snakes.  
Kass, Terzopoulos, Witkin, 1987.  
Samadani, 1989.  
Wiederhold, Brinkley, Samadani and Clauer, 1989.

## FINDING THE AURORA OVAL

---

1) Find the geometric information describing the aurora oval.

2) Track the geometric changes in the aurora oval over time.



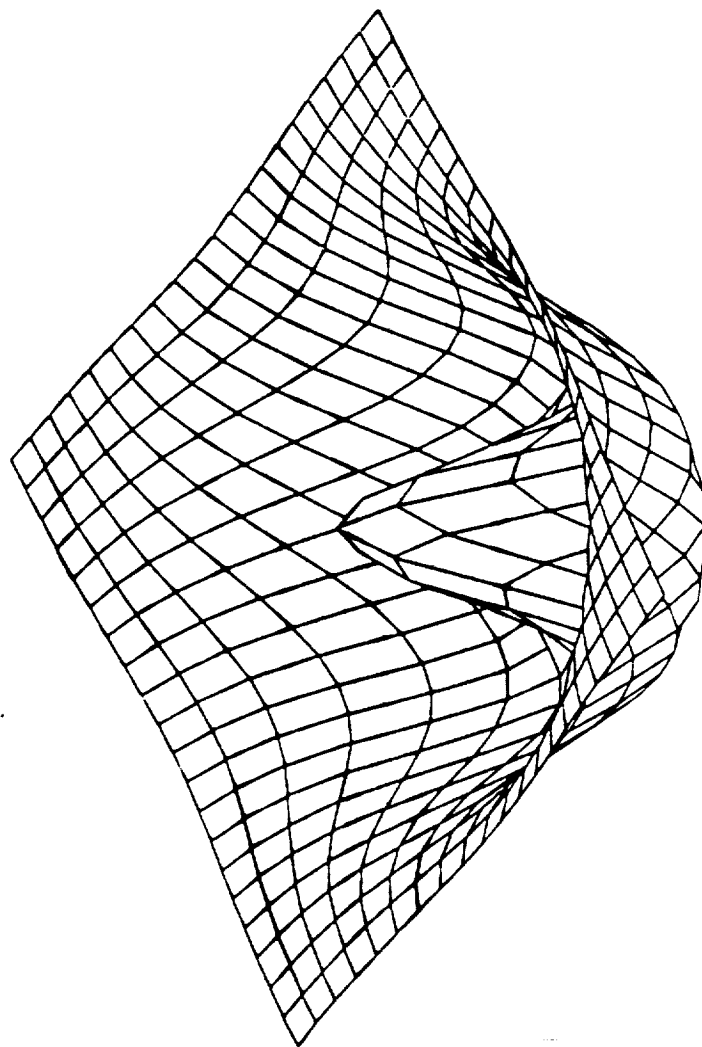
## METHODS EXPLORED FOR FINDING THE BOUNDARIES

---

- 1) Edge detection.
- 2) Global and local thresholds.
- 3) Region growing.
- 4) Morphological methods.
- 5) Fitting of parametric models.
- 6) Regularized segmentation.
- 7) Elastic model dynamic simulations or snakes.  
Kass, Terzopoulos, Witkin, 1987.  
Samadani, 1989.  
Wiederhold, Brinkley, Samadani and Clauer, 1989.

TWO DIMENSIONAL IMAGE INTERPRETED AS A POTENTIAL FIELD

---

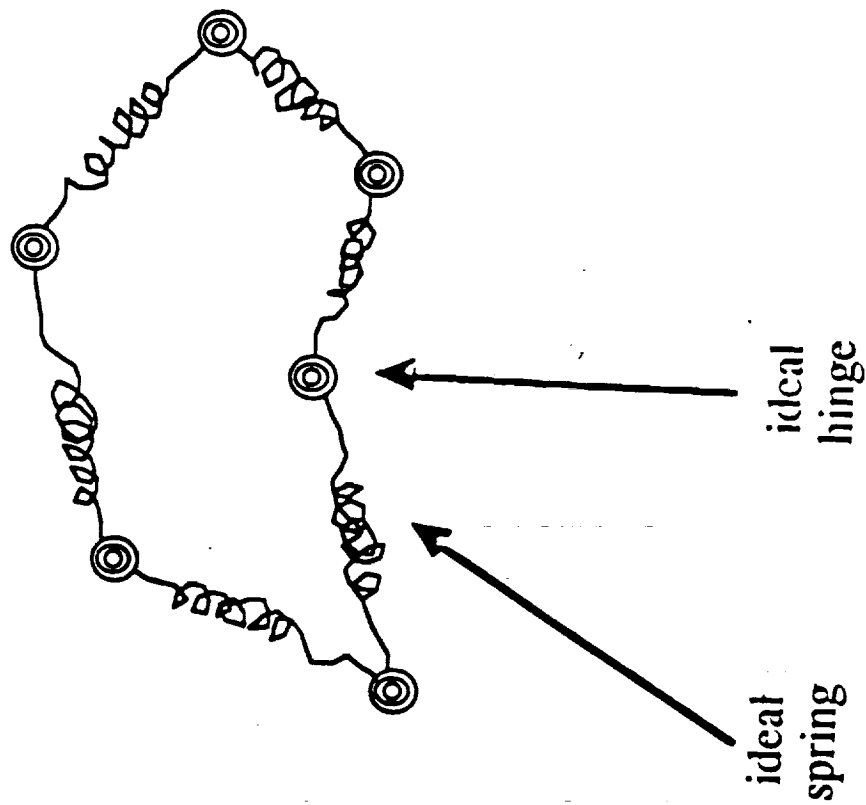


## PHYSICAL INTERPRETATION FOR DISCRETIZED SNAKES

---

1) Two dimensional damped spring-hinge model.

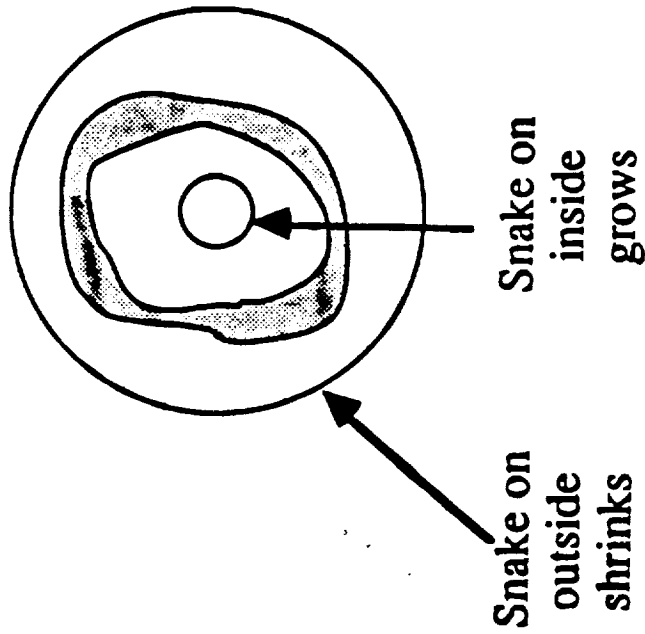
2) Image provides potential which exerts forces on the system of particles.





## WHY USE SNAKES?

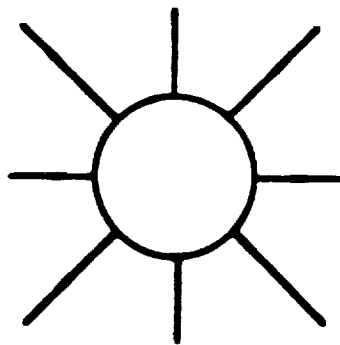
---



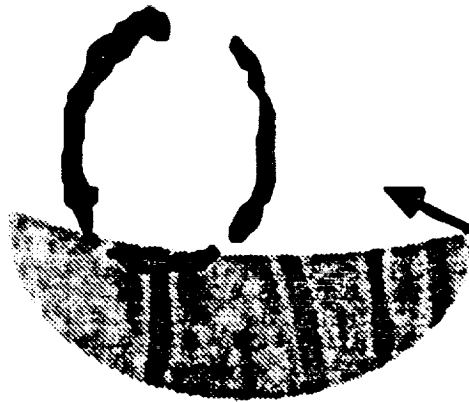
- 1) They provide a natural way to incorporate rough initial knowledge of auroral position.
- 2) They provide smooth, closed curves to fit the data even when there are gaps.
- 3) A sign change allows the tracking of inner and outer boundaries or of the maximum intensity boundary.
- 4) They provide a natural method for analyzing a time sequence of images.
- 5) They are conceptually simple. Physicists like to see a "physics" analogy used for image processing.

# ORBIT DATA

---



Sun location



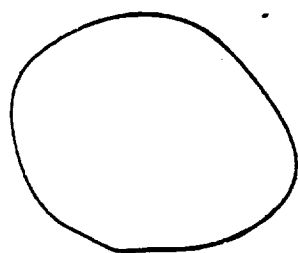
Latitude and longitude of a pixel  
(Thanks to Rick Rairden)



Satellite  
location

## USING A SNAKE ON ONE IMAGE IN A SEQUENCE

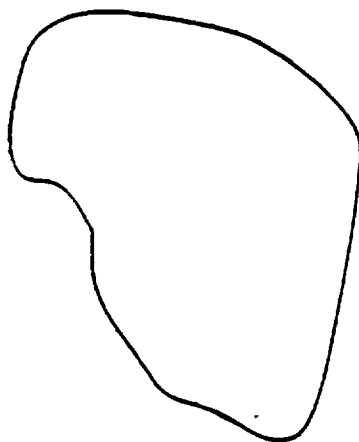
---



initial condition is  
given by  $u(s,0)$



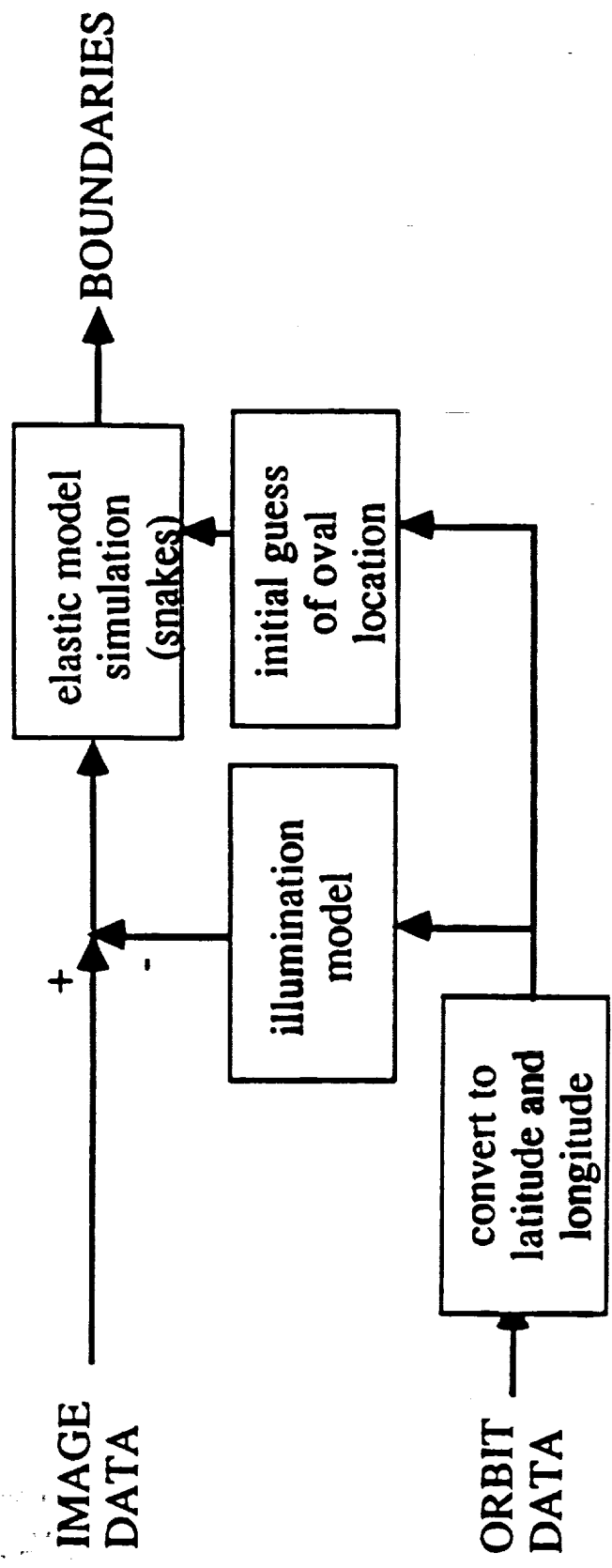
solve for  
 $u(s,t)$



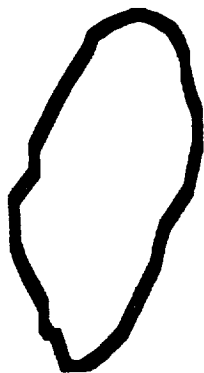
solution is given by  
 $u(s,\text{infinity})$

ORIGINAL PAGE IS  
OF POOR QUALITY

# BLOCK DIAGRAM FOR AUTOMATED BOUNDARY EXTRACTION



AUTOMATED CHECK: IS THE CURVE SIMPLE?

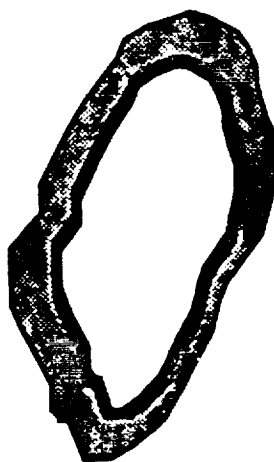


OKAY

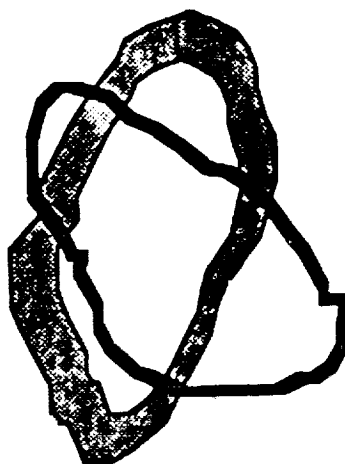


NOT OKAY

AUTOMATED CHECK: IS THE CURVE ALONG A BOUNDARY?



OKAY



NOT OKAY

ORIGINAL PAGE IS  
OF POOR QUALITY

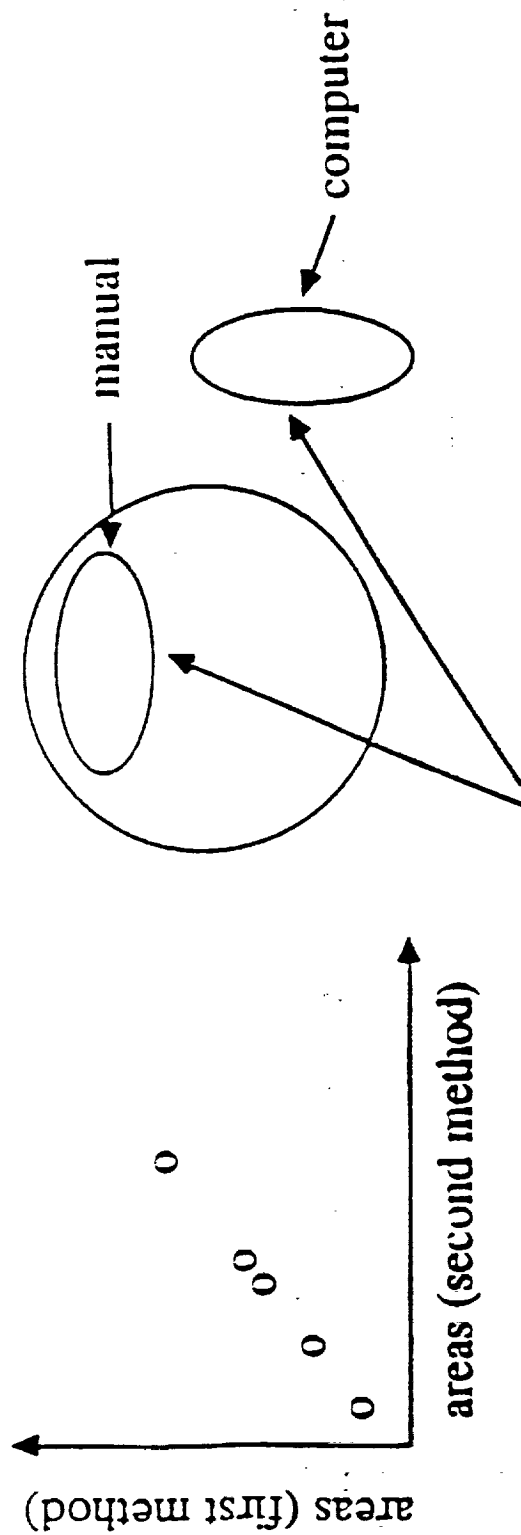
Handwritten signature or mark.

## EVALUATION

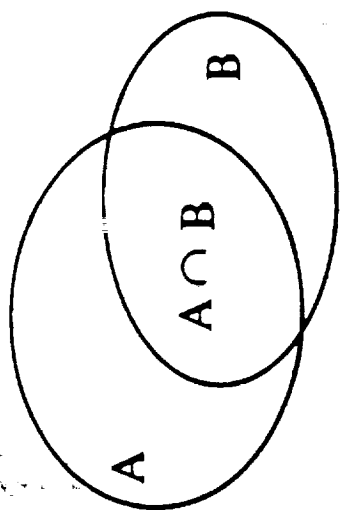
---

- 1) No "right" answer, so compare the system to manual measurements.
- 2) But first check the variation in the manual measurements.
- 3) The general issue is, how do you compare two curves?

## COMPARISON OF AREAS INSIDE THE CURVES



# COMPARISON OF OVERLAP OF THE CURVES



$$B \supseteq A$$



(1,1)

$$A = B$$

$$A \supseteq B$$

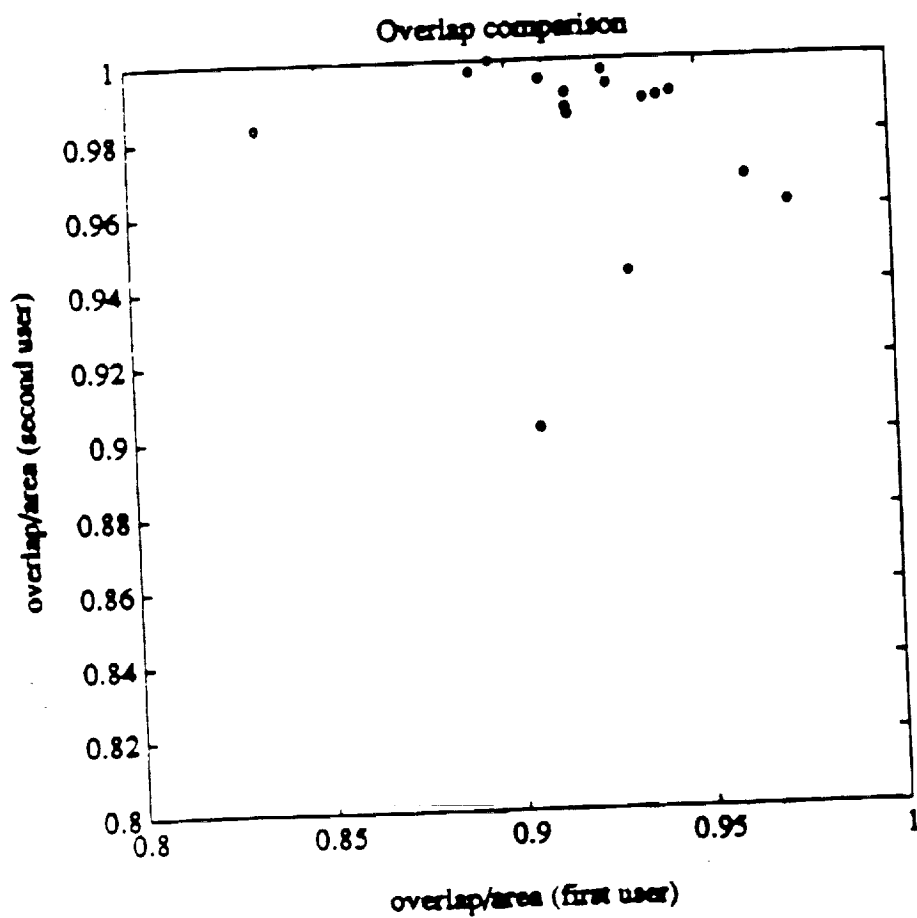
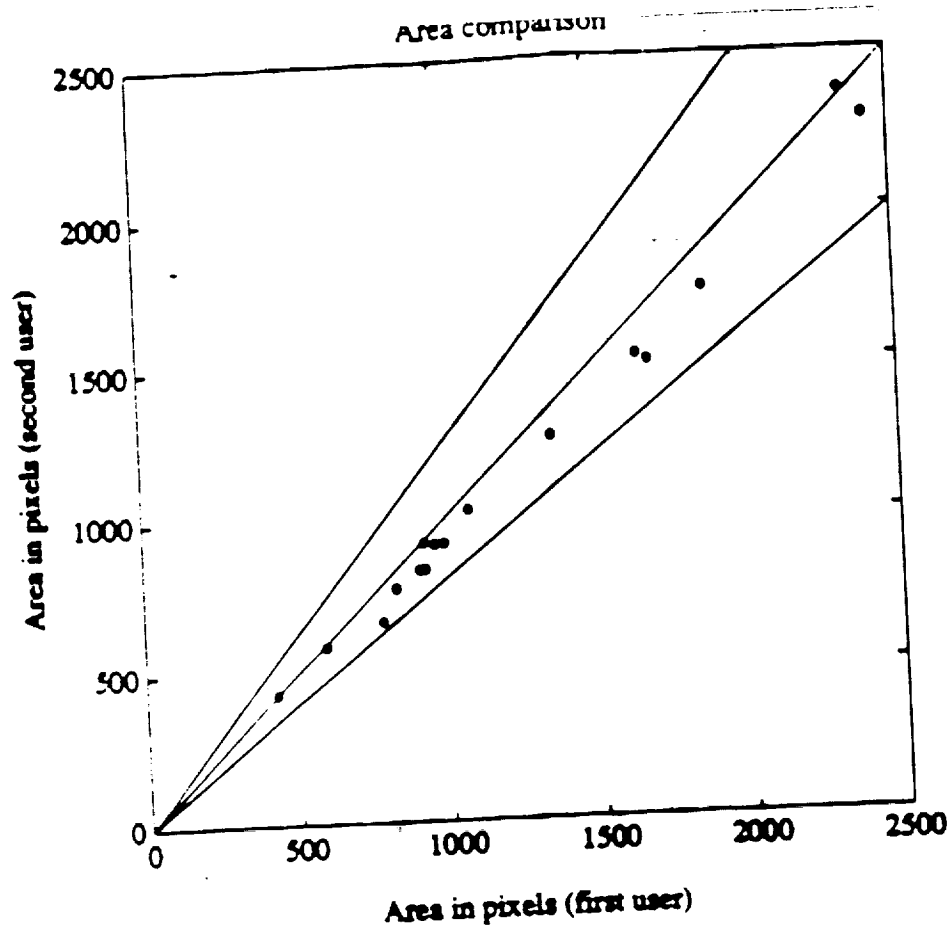
$$\frac{\#A \cap B}{\#A}$$

(0,0)

$$\frac{\#A \cap B}{\#B}$$

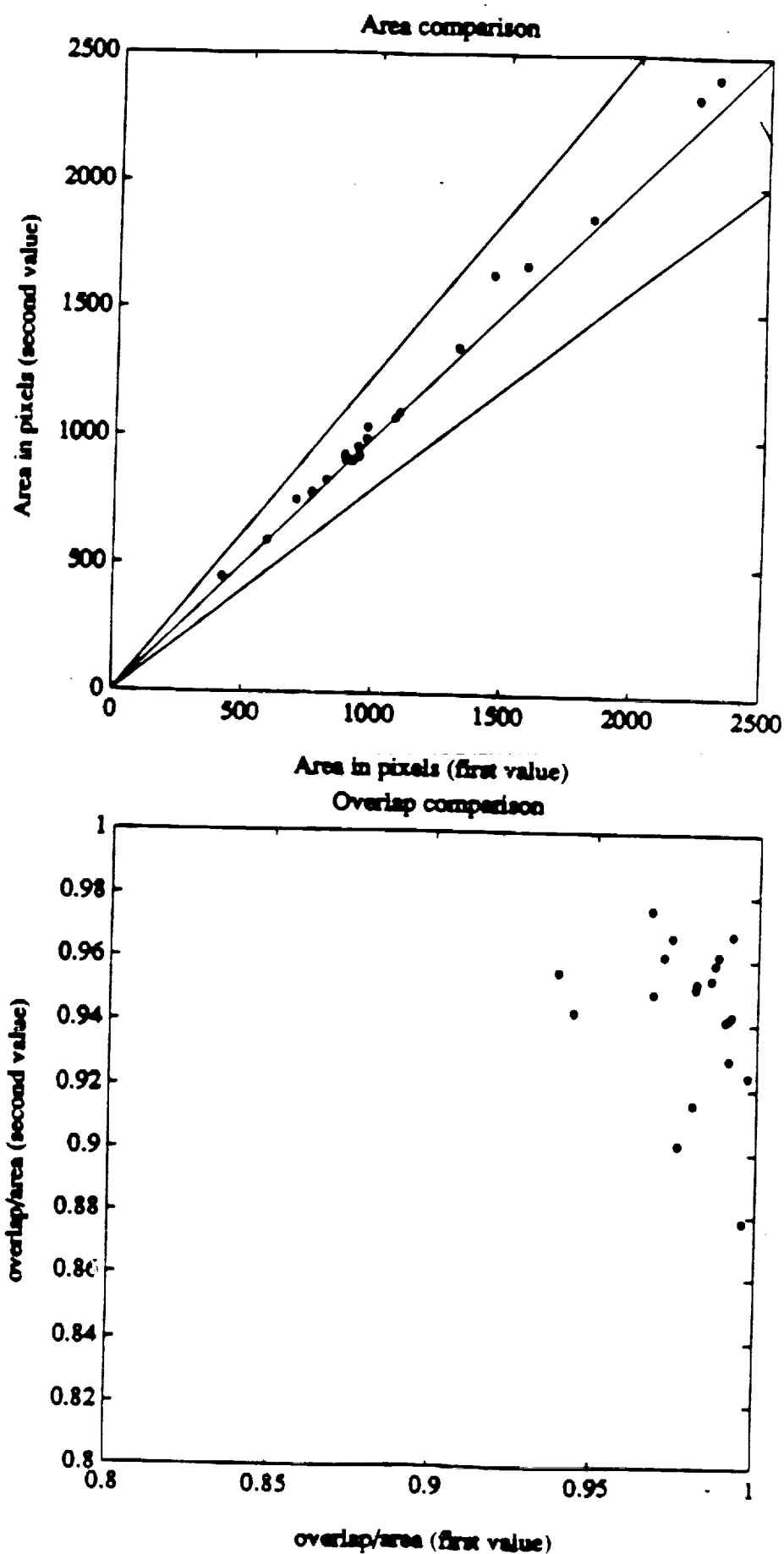
$$A \cap B = \phi$$





ORIGINAL PAGE IS  
OF POOR QUALITY

Figure 1. Comparison of manually generated curves by two people on the



ORIGINAL PAGE IS  
OF POOR QUALITY

Figure 10: Comparison of manually generated curves by the same person

in one system, but at two different times. a. Area comparison. b. Overlap

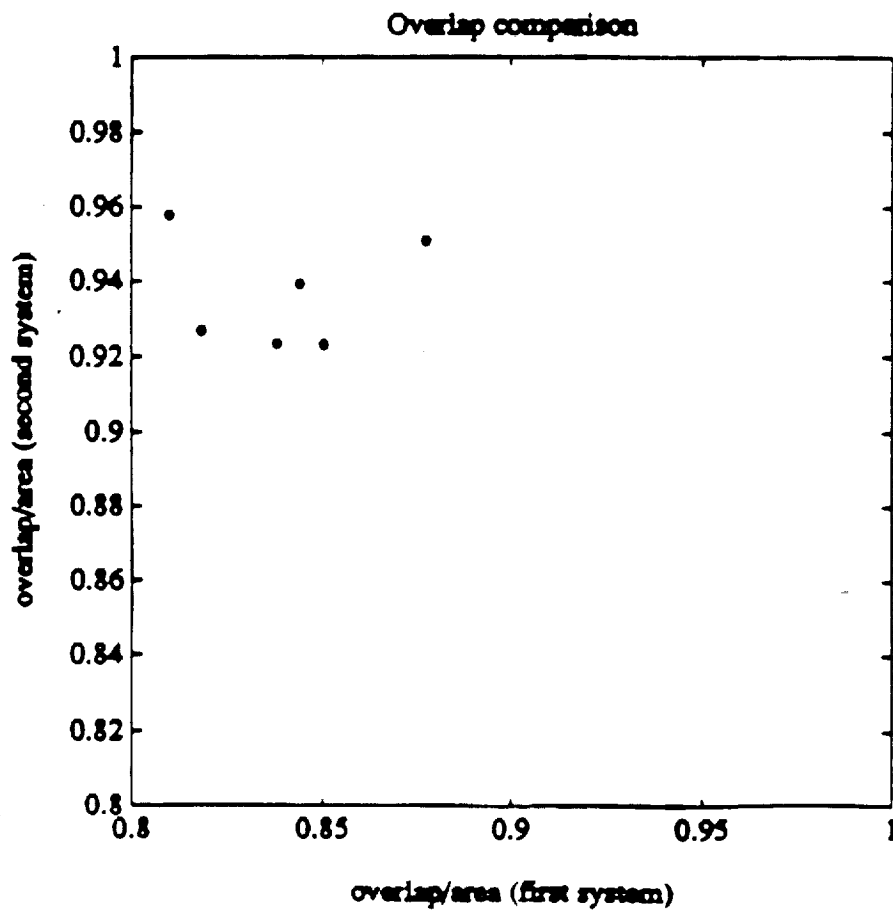
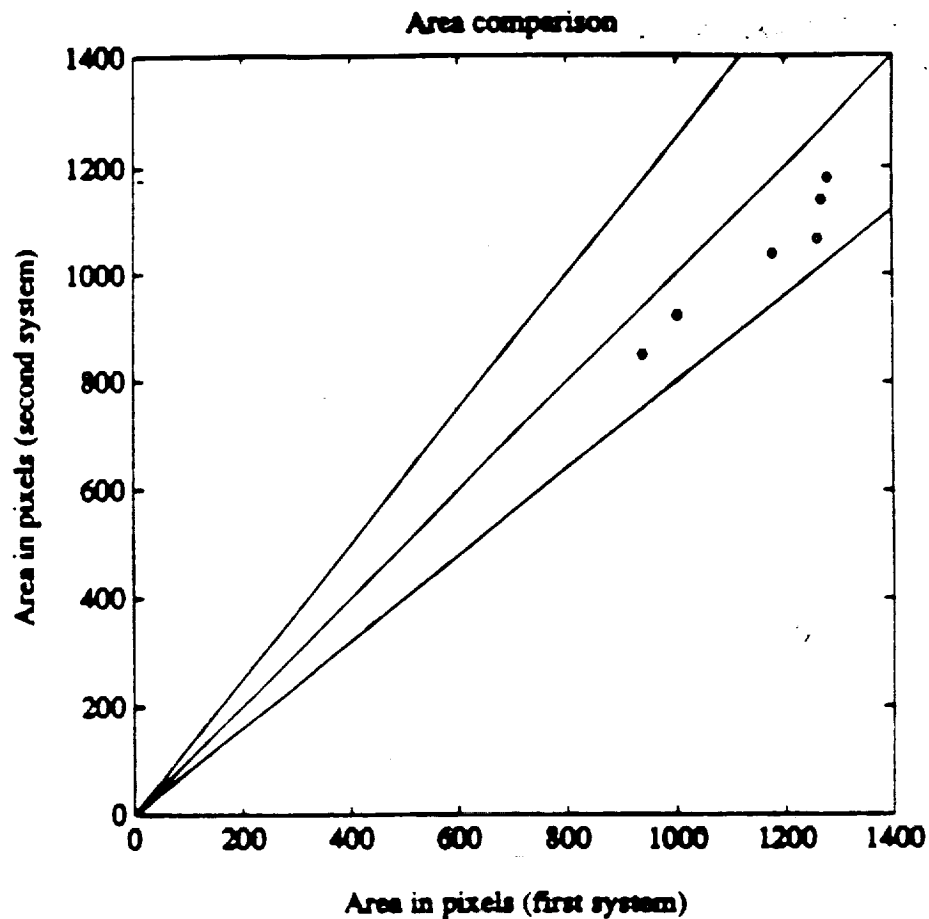
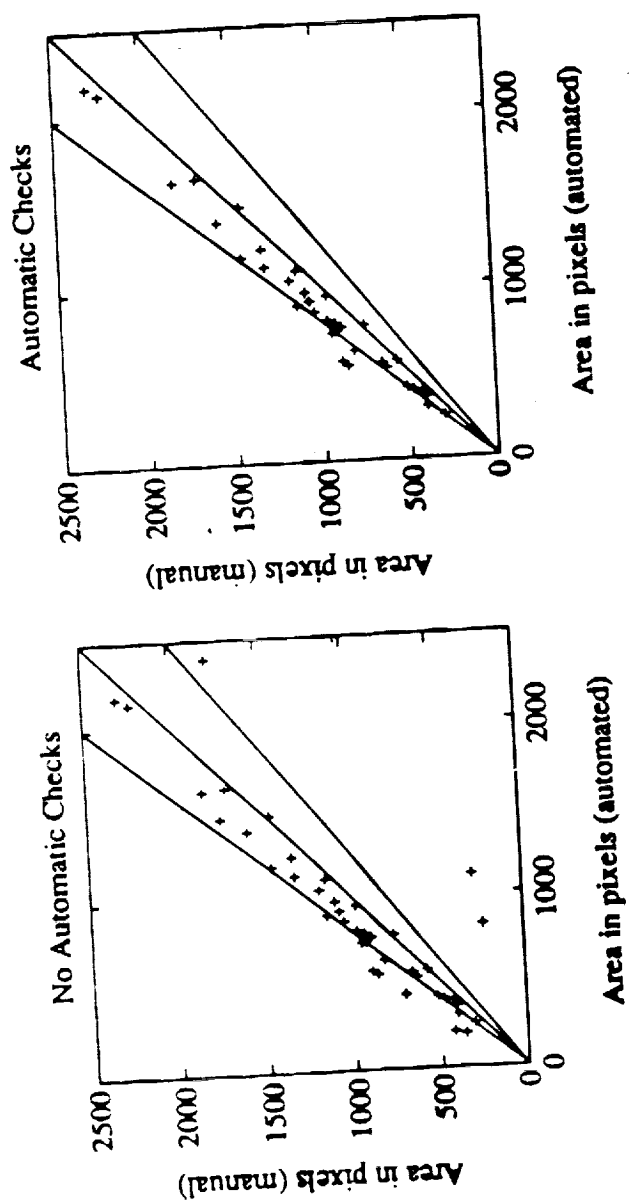


Figure 9: Comparison of manually generated curves by two people on different computer systems. a) Area comparison b) Overlap comparison.

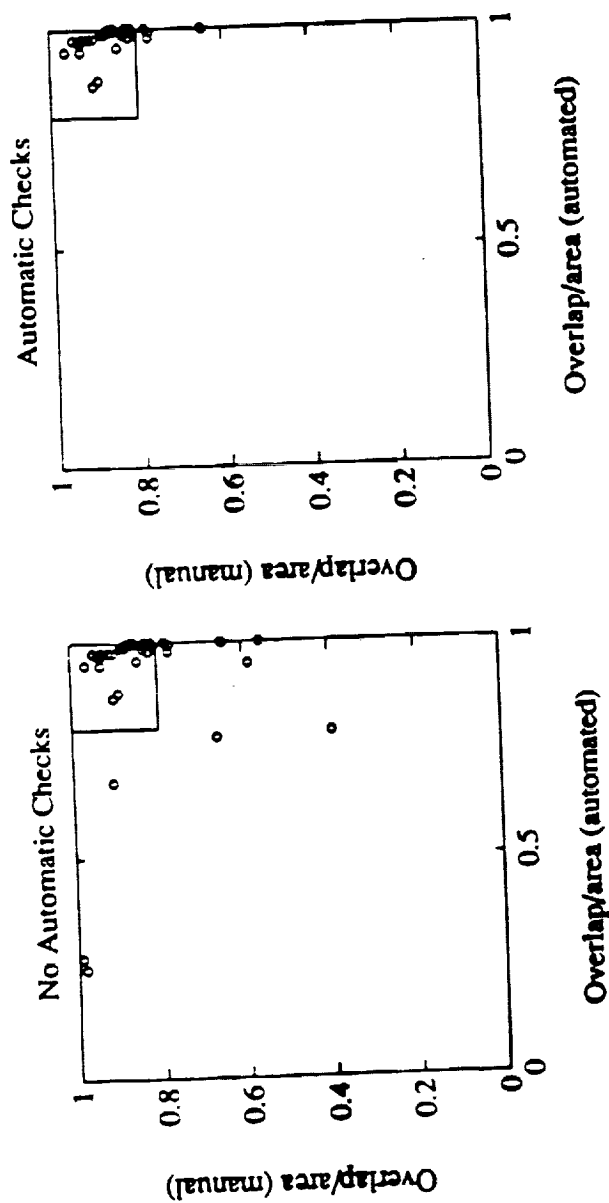
ORIGINAL PAGE IS  
OF POOR QUALITY

# AREA COMPARISONS (WITH AND WITHOUT CHECKS)



ORIGINAL PAGE IS  
OF POOR QUALITY

# OVERLAP COMPARISONS (WITH AND WITHOUT CHECKS)



ORIGINAL PAGE IS  
OF POOR QUALITY



# Evaluation of an Elastic Curve Technique For Finding the Auroral Oval From Satellite Images Automatically

RAMIN SAMADANI, MEMBER, IEEE, DOMINGO MIHOVILOVIC, C. ROBERT CLAUER, GIO WIEDERHOLD, MEMBER, IEEE, JOHN D. CRAVEN, AND LOUIS A. FRANK

**Abstract**—The DE-1 satellite has gathered over 500 000 images of the Earth's aurora using ultraviolet and visible light photometers. A feature having geophysical significance is the inner boundary of the auroral oval. Manual methods are currently used for feature extraction. An automated algorithm is described for finding the inner boundary based on a recently proposed computer vision technique. The algorithm is analogous to solving the equations of motion for an elastic curve, where the forces are provided by the image. The resulting equilibrium position of the elastic curve provides an automated method for finding the shape and location of the inner boundary of the auroral oval. Two methods, both based on comparisons with manual measurements, are developed for the evaluation of the automated algorithm. The first method compares the areas within the automated and the manual boundaries. The second method measures the overlap between the interiors of the two boundaries. The expected variation between two sets of manual measurements is used to set an upper bound to the allowed discrepancy between the automated results and a single set of manual measurements. The algorithm, when tested with 71 satellite images, is found to perform best for those images without overlap between the aurora and the dayside hemisphere.

## I. INTRODUCTION

THE AURORA polaris is the result of processes that exchange energy between the solar wind (the expanding outer atmosphere of the sun) and the Earth's magnetic field. Images now available from high-altitude polar satellites provide the first global characterization of auroral activity from a single measurement within a single data set [1]. Of particular interest for the understanding of the physical processes of the aurora is the identification of the inner boundary of the auroral oval. From this boundary, useful quantitative parameters can be extracted [2]. For example, the area within the inner boundary varies, and this is thought to be related to the amount of magnetic

Manuscript received October 9, 1989; revised February 26, 1990. This work was partially supported by the Center for Excellence in Space Data Information Systems, and by NASA through Grants NAGW419, NAGW1634, and NAGS-483.

R. Samadani, D. Mihovilovic, and C. R. Clauer are with the Department of Electrical Engineering, 202 Durand Building, Stanford University, Stanford, CA 94305.

G. Wiederhold is with the Departments of Computer Science and Medicine, Stanford University, Stanford, CA 94305.

J. D. Craven and L. A. Frank are with the Department of Physics and Astronomy, University of Iowa, Iowa City, IA 52242.

IEEE Log Number 9036051

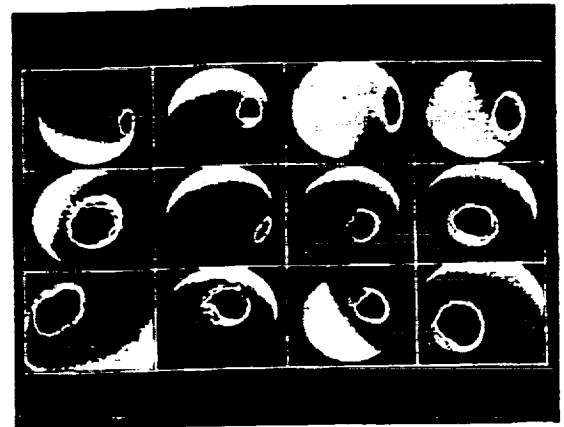


Fig. 1. Manually generated inner boundaries for 12 DE images.

energy stored in the magnetic field lines that map into this area.

Presently, the boundaries are extracted manually. Fig. 1 shows the results of manual extraction of inner boundaries of the auroral oval for several images. The boundaries are superimposed on the original DE-1 images, which were gathered using a photometer sensitive to ultraviolet radiation. The crescent shapes in the images are due to solar illumination of the dayside hemisphere. The illuminated rings are the aurora, resulting from the excitation and ionization of the upper atmospheric gasses by the precipitation of energetic electrons.

Detailed analysis of the existing and expected images greatly exceeds the manpower available. Hence automation is necessary to aid in extracting the information from the images. In this paper, we discuss the application of computer vision techniques to semiautomate the quantitative analysis of the auroral images with particular attention to the evaluation of the efficacy of the techniques.

From the point of view of a computer vision researcher, the satellite images of the aurora present interesting new challenges in object recognition and object tracking that are different from the most frequently reported applications. With notable exceptions [3]–[5], the two most common assumptions made for current applications are that the objects of interest are rigid and that parametric descriptions of the expected shapes of the objects are pos-

-----

-----

-----

-----

-----

-----

-----

-----

-----

-----

-----

-----

-----

-----

-----

-----

-----

-----

-----

-----

-----

-----

-----



LBH & NI CROSS SECTIONS

Joe Ajello

11:45 16 August



A Reexamination of Important N<sub>2</sub> Cross Sections by Electron Impact  
With Application to the Dayglow: The Lyman-Birge-Hopfield Band  
System and N I (119.99 nm)

J. M. AJELLO ✓

Jet Propulsion Laboratory, California Institute of Technology, Pasadena

D. E. SHEMANSKY

Lunar and Planetary Laboratory, University of Arizona, Tucson

GLYNN A. GERMANY

The far ultraviolet emission spectrum (120 to 210 nm) of electron-excited N<sub>2</sub> has been obtained in a crossed-beam laboratory experiment. The cross section of the Lyman-Birge-Hopfield (LBH) band system ( $a^1\Pi_u \rightarrow X^1\Sigma_g^+$ ) has been remeasured using experimental techniques we have previously developed for this metastable transition. The improved laboratory data set for the  $a^1\Pi_u$  state allows a determination of the excitation, emission, and predissociation cross section from threshold to 200 eV for use in planetary atmosphere models of the dayglow and aurora. An analytic fit to the experimental cross section allows accurate estimates to arbitrarily high excitation energy. The close agreement in both energy dependence and absolute cross section values between the emission measurements, presented here, and published electron scattering results shows cascade is small ( $<5\%$ ). The total excitation cross section for the N<sub>2</sub>  $a^1\Pi_u$  state is estimated to be  $6.22 \pm 1.37 \times 10^{-18} \text{ cm}^2$  at 100 eV. The absence of emission bands for  $v' \geq 7$  suggests the predissociation yield is unity. The excitation function of each vibrational level is found to have the same shape to within 5%. In the low-energy region,  $\epsilon < 20 \text{ eV}$ , differences in excitation threshold lead to a significant departure of the relative vibrational cross sections from the Franck-Condon distribution. Thus the relative LBH vibrational population distribution in a planetary dayglow or aurora is affected by the energy distribution of the electron flux; and we show that atmospheric models need to include this threshold effect. The N I (119.99 nm) cross section has also been remeasured and found to be  $3.48 \pm 0.77 \times 10^{-18} \text{ cm}^2$  at 200 eV on the basis of a comparison with Lyman  $\alpha$  emission from dissociative excitation of H<sub>2</sub>.

## INTRODUCTION

We present the N<sub>2</sub> electron impact excitation cross sections in the vacuum ultraviolet (VUV) from 40 to 210 nm in a two-part series. From an instrumental point of view the VUV spectrum of N<sub>2</sub> can be conveniently separated into two spectral regions: the extreme ultraviolet (EUV) from 40 to 120 nm and the far ultraviolet (FUV) from 120 to 210 nm. In the EUV region, channeltron detectors (or windowless photomultipliers) are used, and in the FUV, photomultiplier detectors with vacuum-sealed photocathodes. In this paper we concentrate on the FUV region. We show in Figure 1 a calibrated, optically thin electron impact-induced fluorescence spectrum (relative accuracy  $\sim 20\%$ ) from 50 to 190 nm at 100 eV electron impact energy. Approximately 100 features can be identified at the instrumental resolution of 0.4 nm. Clearly, the EUV is more intense than the FUV. Both regions are rich in atomic lines and molecular features.

In order to model atmospheric UV emissions by N<sub>2</sub> it is necessary to begin the calculation by having at hand a reliable set of laboratory cross section data. To date there has not been a complete study of the entire VUV spectral range with the goal of providing all of the significant cross sections. We provide such a data set at an accuracy of  $\sim 20\%$  and identification of all features in Figure 1, beginning with the FUV spectral region.

The Lyman-Birge-Hopfield (LBH) band system is a prom-

inent and important UV emission source in the terrestrial dayglow and aurora. The sole excitation source of the LBH band system is direct electron impact [Meier *et al.*, 1980], and because of this fact it should in principle be a direct monitor of total energy deposition. Rocket and satellite spectra of the FUV region of the dayglow and aurora [Gentieu *et al.*, 1979; Park *et al.*, 1977; Huffman *et al.*, 1980; Takacs and Feldman, 1977; Rottman *et al.*, 1973; Paresce *et al.*, 1972] have measured emissions from both atomic nitrogen multiplets and the LBH band system. Additionally, in the outer solar system the LBH band system, many N I and N II atomic multiplets, and several molecular Rydberg systems were detected in the Titan atmosphere by the Voyager ultraviolet spectrometer [Strobel and Shemansky, 1982]. Detailed studies show that the radiation from the atomic nitrogen multiplets arises principally from dissociative excitation (earth aurora, Titan dayside emissions) and direct electron excitation of atomic nitrogen (earth dayglow) [Meier *et al.*, 1980; Park *et al.*, 1977].

We have established a laboratory program at the Jet Propulsion Laboratory (JPL) to measure a primary data set consisting of calibrated optically thin VUV fluorescence spectra (40–200 nm) and absolute excitation cross sections (0–0.5 keV) for stable gases which are candidate species for electron impact in the upper atmosphere of the planets and in the atmospheres of cool stars and interstellar molecular clouds. We have made the first steps in this program by completing studies of the singlet states of H<sub>2</sub> [Ajello *et al.*, 1982, 1984; Shemansky and Ajello, 1983], the benchmark dissociative cross section of H<sub>2</sub> to produce Lyman  $\alpha$  [Shemansky *et al.*, 1985a], the atomic emissions of He [She-



UVI FILTERS

Doug Torr

1:30 16 August

# VUV Thin Films

## Part I:

Optical constants of  $\text{BaF}_2$ ,  $\text{CaF}_2$ ,  $\text{LaF}_3$ ,  $\text{MgF}_2$ ,  
 $\text{Al}_2\text{O}_3$ ,  $\text{HfO}_2$ , and  $\text{SiO}_2$  thin films in the VUV

Muamer Zukic, Douglas G. Torr  
University of Alabama in Huntsville  
Department of Physics  
Huntsville, Alabama 35899  
and

James F. Spann, and Marsha R. Torr  
George C. Marshall Space Flight Center  
Huntsville, Alabama 35812

### Abstract

The optical constants of  $\text{MgF}_2$  (bulk) and  $\text{BaF}_2$ ,  $\text{CaF}_2$ ,  $\text{LaF}_3$ ,  $\text{MgF}_2$ ,  $\text{Al}_2\text{O}_3$ ,  $\text{HfO}_2$ , and  $\text{SiO}_2$  films deposited on  $\text{MgF}_2$  substrates are determined from photometric measurements through an iteration process of matching calculated and measured values of the reflectance and transmittance in the vacuum ultraviolet wavelength region from 120 nm - 230 nm. The potential use of the listed fluorides and oxides as vacuum ultraviolet coating materials is discussed in Part II of the paper.

ORIGINAL PAGE IS  
OF POOR QUALITY

# VUV Thin Films

## Part II:

### Vacuum ultraviolet all-dielectric narrowband filters

Muamer Zukic, Douglas G. Torr

University of Alabama in Huntsville

Department of Physics

Huntsville, Alabama 35899

and

James F. Spann, and Marsha R. Torr

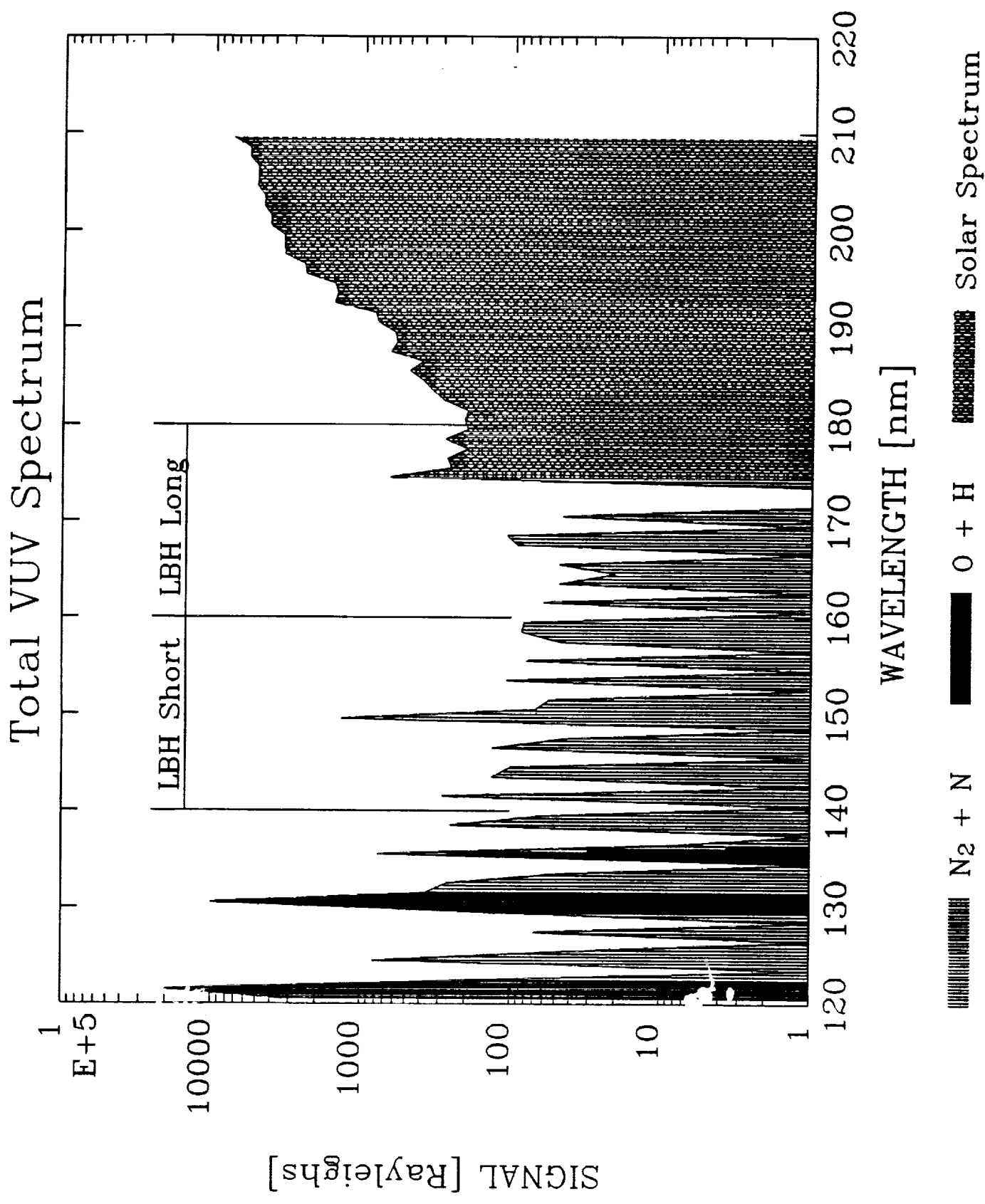
George C. Marshall Space Flight Center

Huntsville, Alabama 35812

#### Abstract

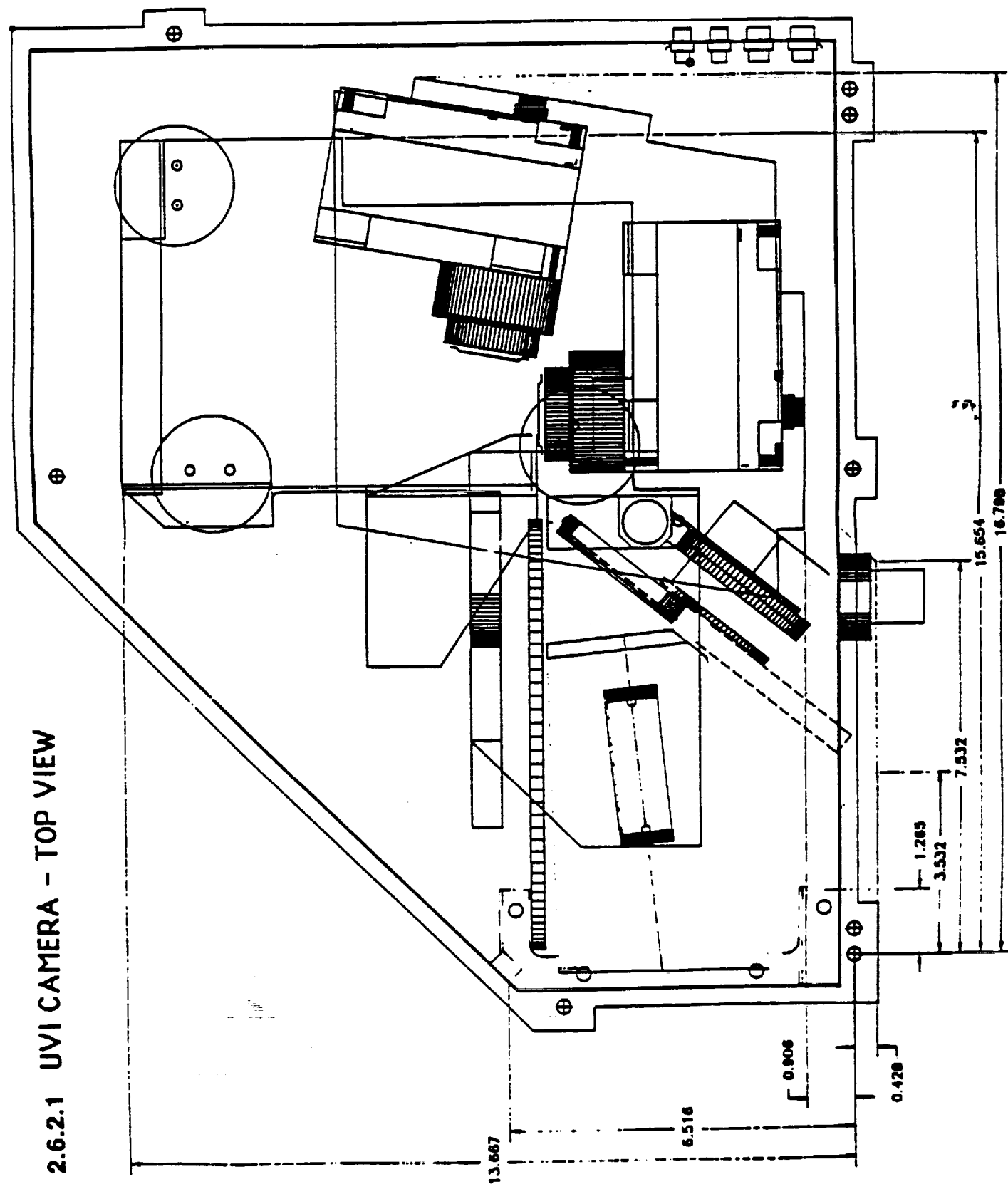
We report the design and performance of the narrowband transmission filters employing the rapidly changing extinction coefficient that is characteristic of  $\text{BaF}_2$  and  $\text{SiO}_2$  films within certain wavelength intervals in the vacuum ultraviolet. We demonstrate the design concept for two filters centered at 135 nm for  $\text{BaF}_2$  and at 141 nm for  $\text{SiO}_2$ . It is found that these filters provide excellent narrowband spectral performance when combined with narrowband reflection filters. The filter centered at 135 nm has a peak transmittance of 24% and a bandwidth of 4 nm at full width half maximum for collimated incident light. The transmittance for  $\lambda_0 \leq 130$  nm is less than 0.1% and for  $138 \leq \lambda_0 \leq 230$  nm the average transmittance is less than 3%. Another filter centered at 141 nm, has a peak transmittance of 25% and a bandwidth of 3.5 nm.

ORIGINAL PAGE IS  
OF POOR QUALITY





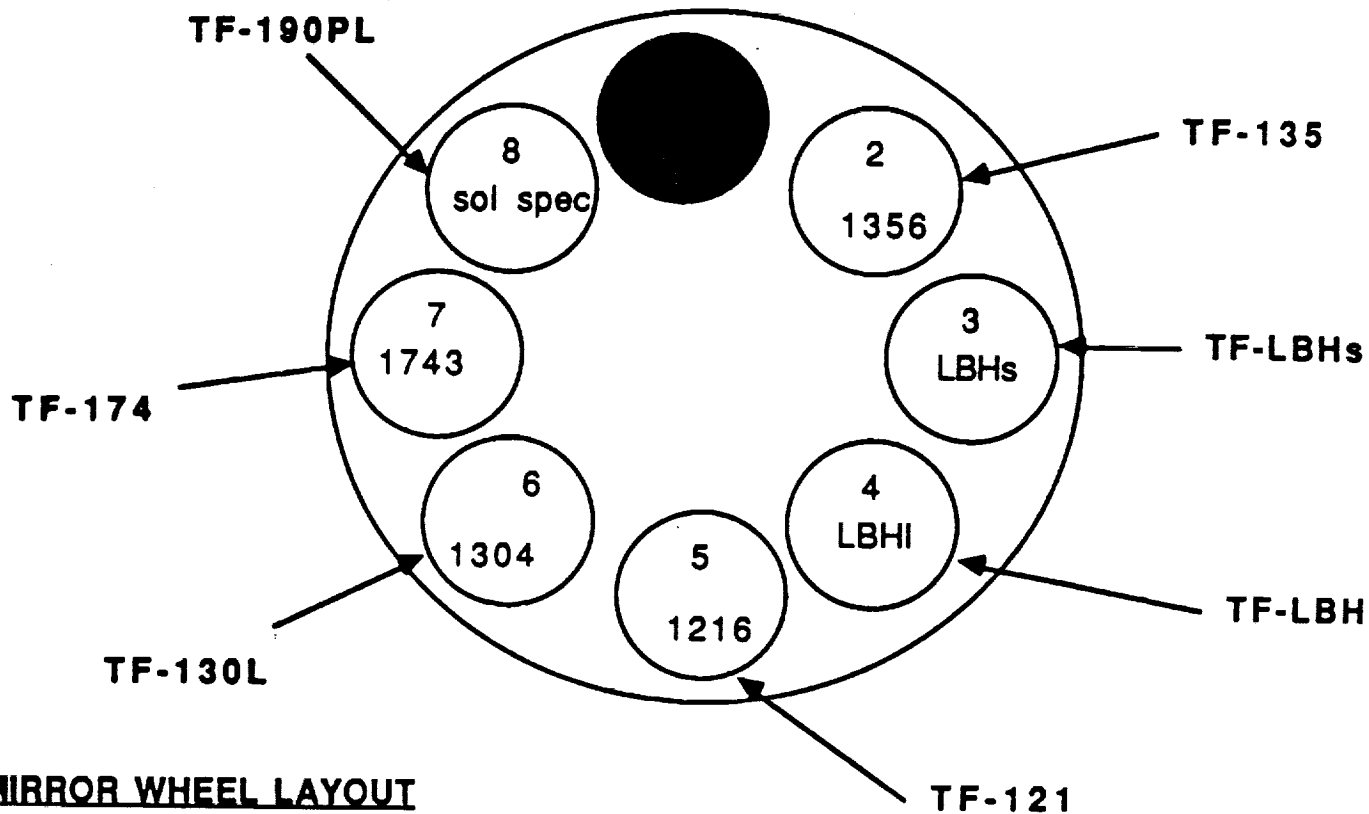
# 2.6.2.1 UVI CAMERA - TOP VIEW



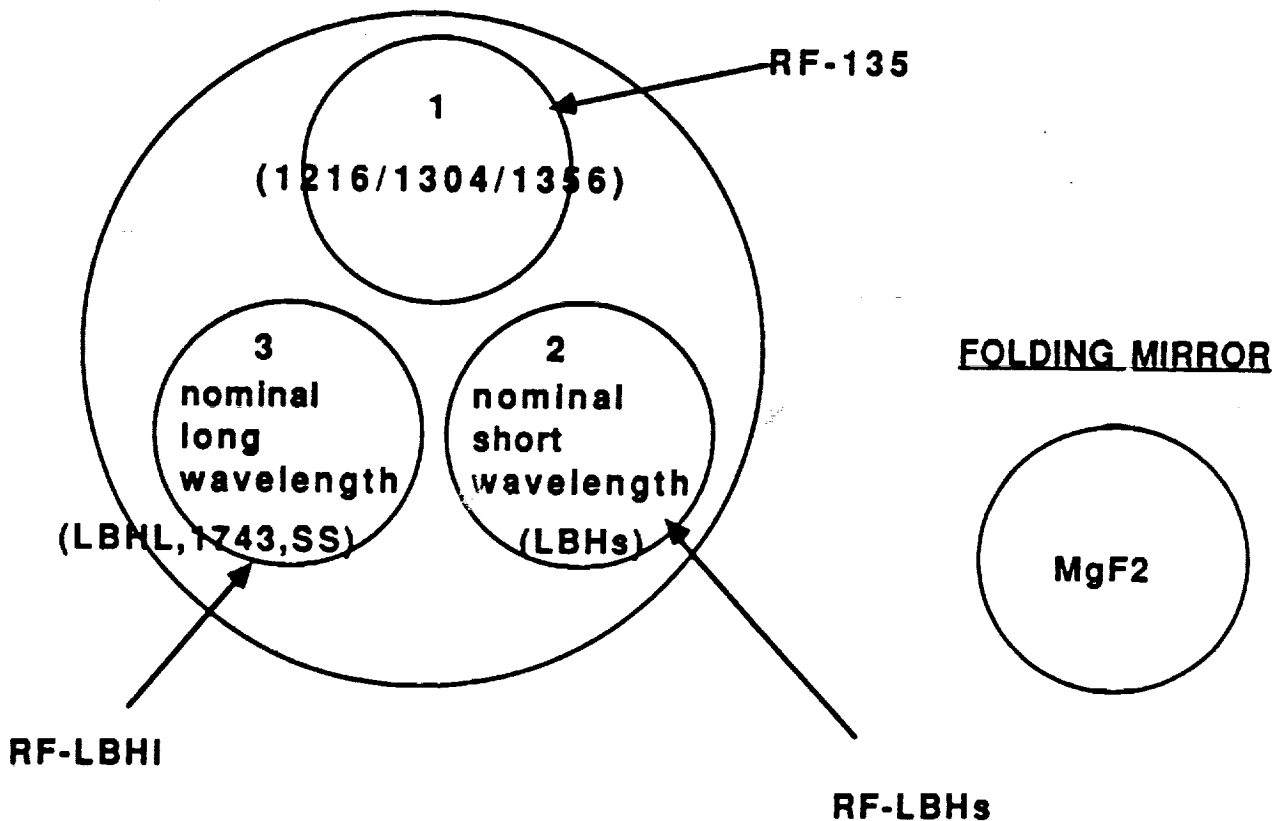
ORIGINAL PAGE IS  
OF POOR QUALITY

# UVI FILTER WHEEL LAYOUT

Date: 6/18/90

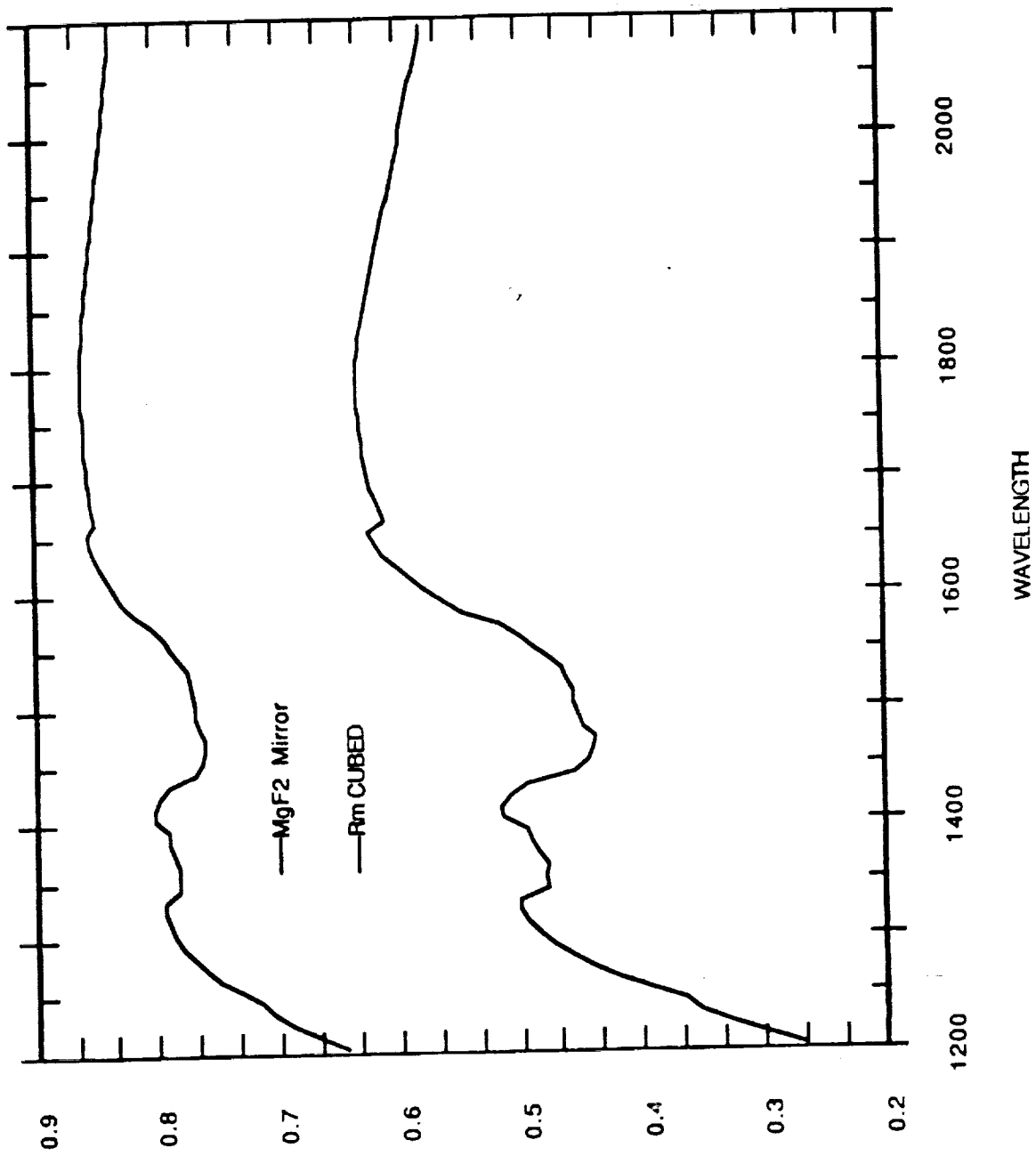


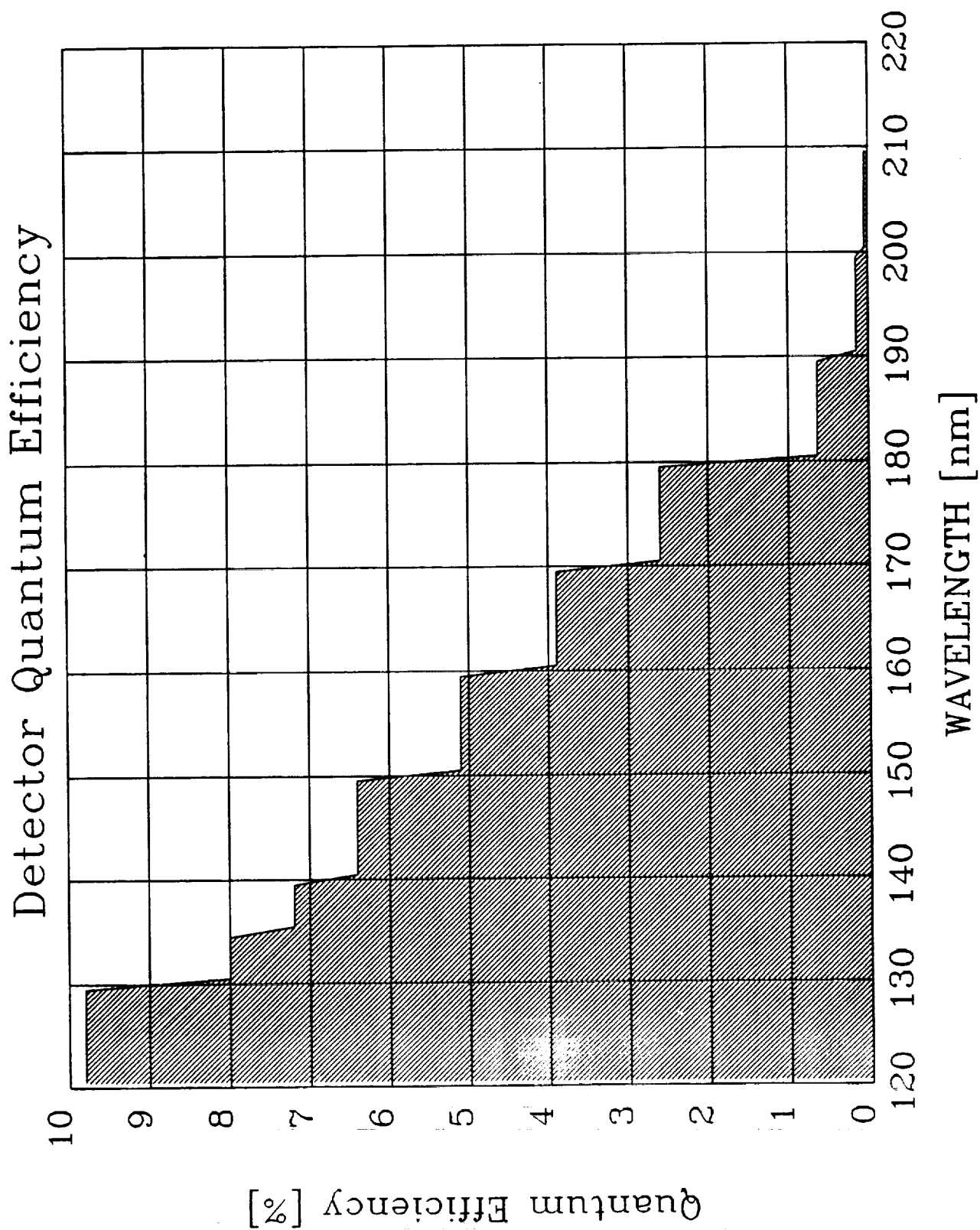
## MIRROR WHEEL LAYOUT

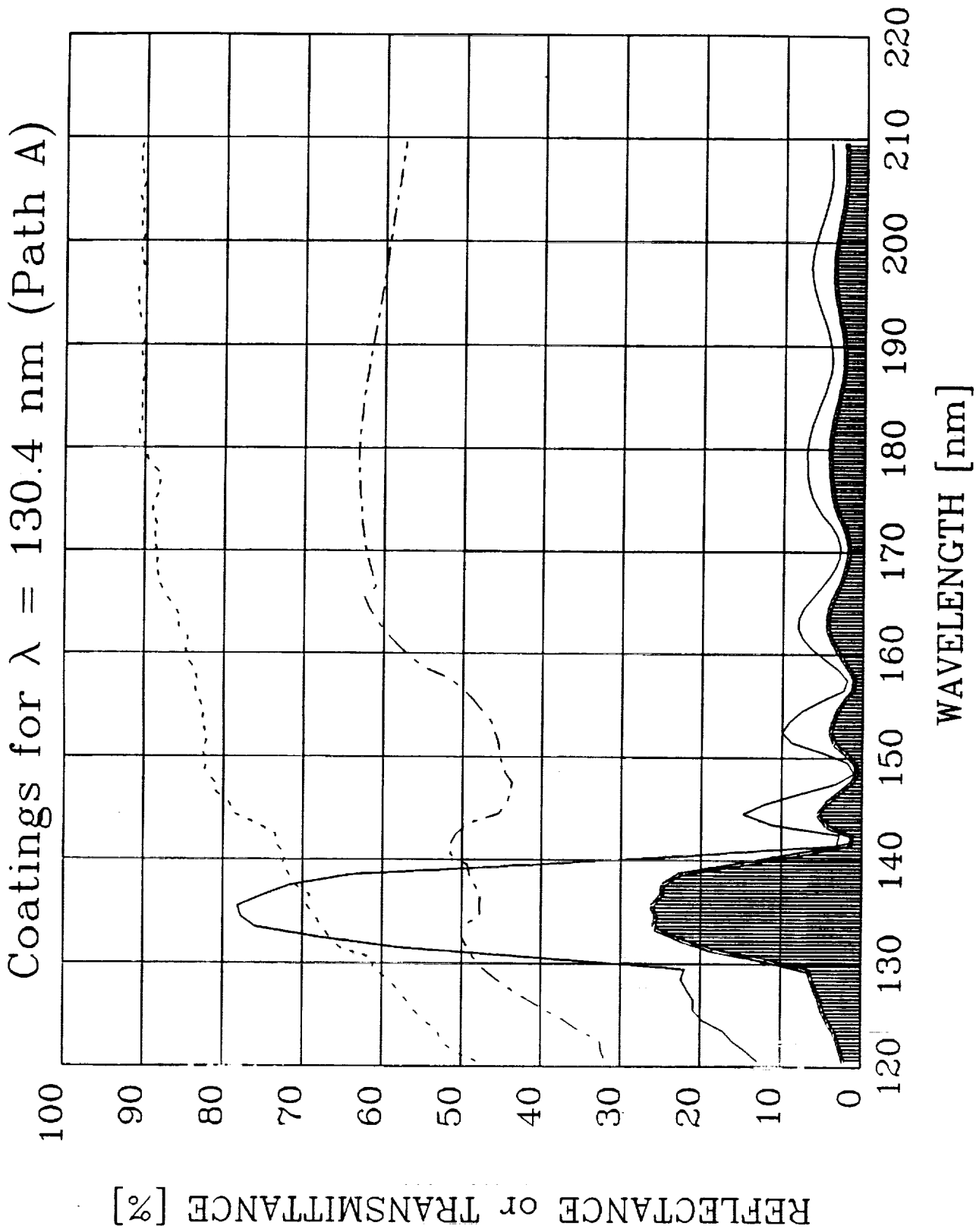


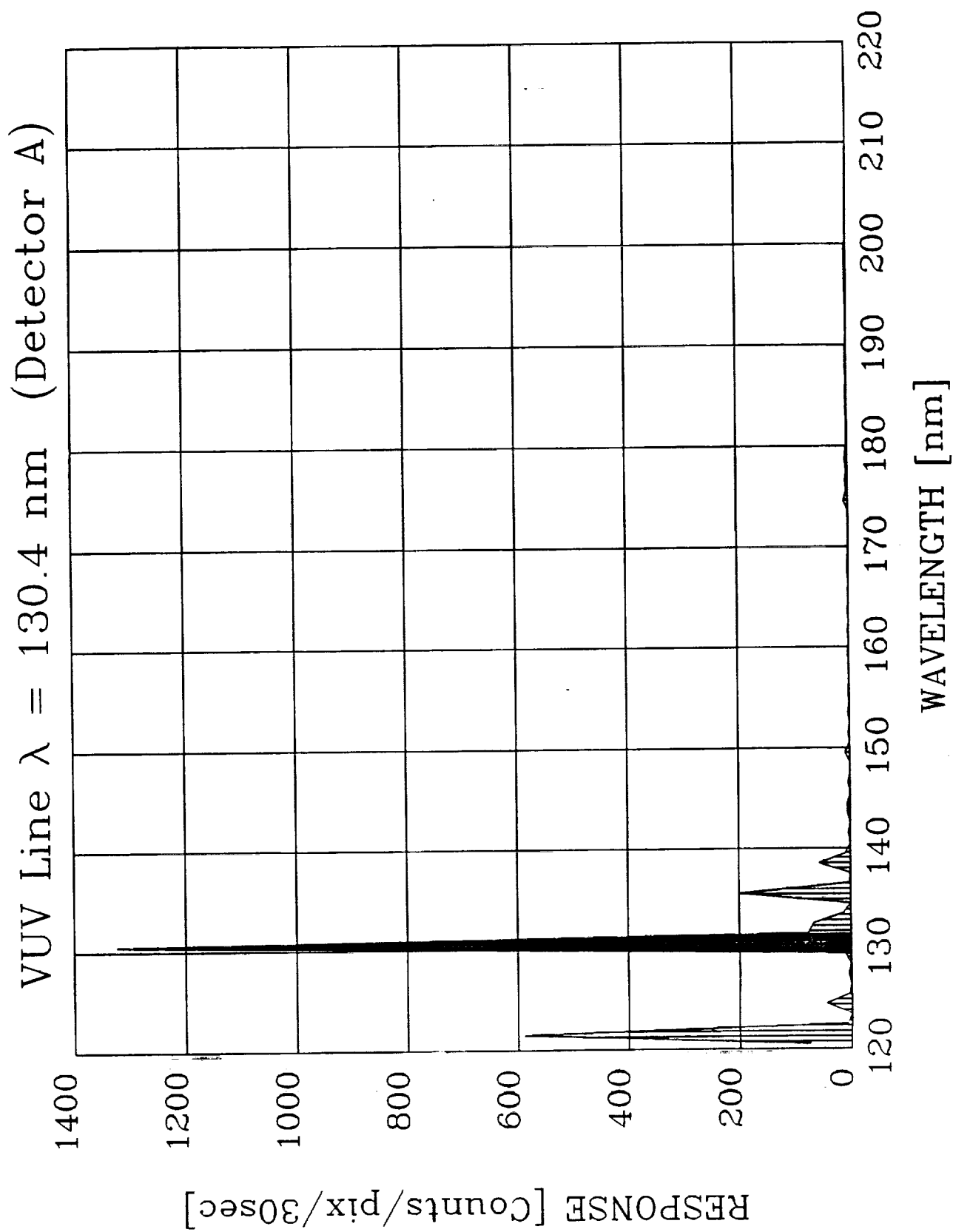
# ULTRAVIOLET IMAGER FILTER SUMMARY:

PARAMETERS	1216A	1304A	1356A	LBHS	LBHL	1743	SOLSPEC
TRANSMISSION FILTER:	Action 1216	TF-130L	TF-135	TF-LBHs	TF-LBHI	TF-174	TF-190PL
SUBSTRATE NUMBER OF LAYERS	MgF2	MgF2 26	MgF2 29	BaF2 35	Fused Silica 35	Fused Silica 29	Fused Silica 19
FILM MATERIALS	MgF2/Al	MgF2/BaF2	MgF2/BaF2	MgF2/LaF3	MgF2/LaF2	MgF2/LaF3	Al2O3/MgF2
1st REFLECTION FILTER:	RF-135	RF-135	RF-135	RF-LBHs	RF-LBHI	RF-LBHI	RF-LBHI
SUBSTRATE NUMBER OF LAYERS	Pyrex 29	Pyrex 29	Pyrex 29	Pyrex 35	Pyrex 25	Pyrex 25	Pyrex 25
FILM MATERIALS	MgF2/BaF2	MgF2/BaF2	MgF2/BaF2	MgF2/LaF3	MgF2/LaF3	MgF2/LaF3	MgF2/LaF3



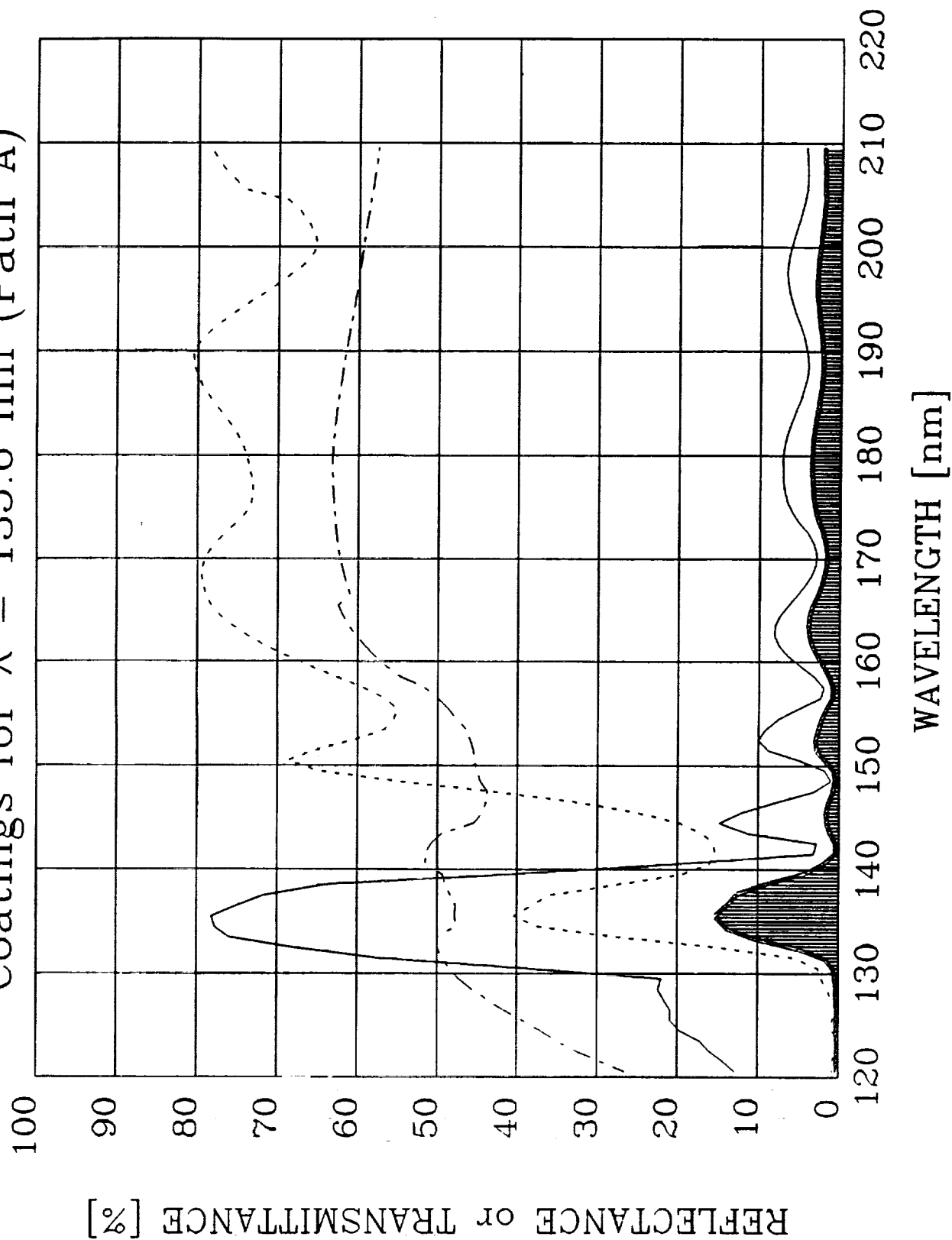




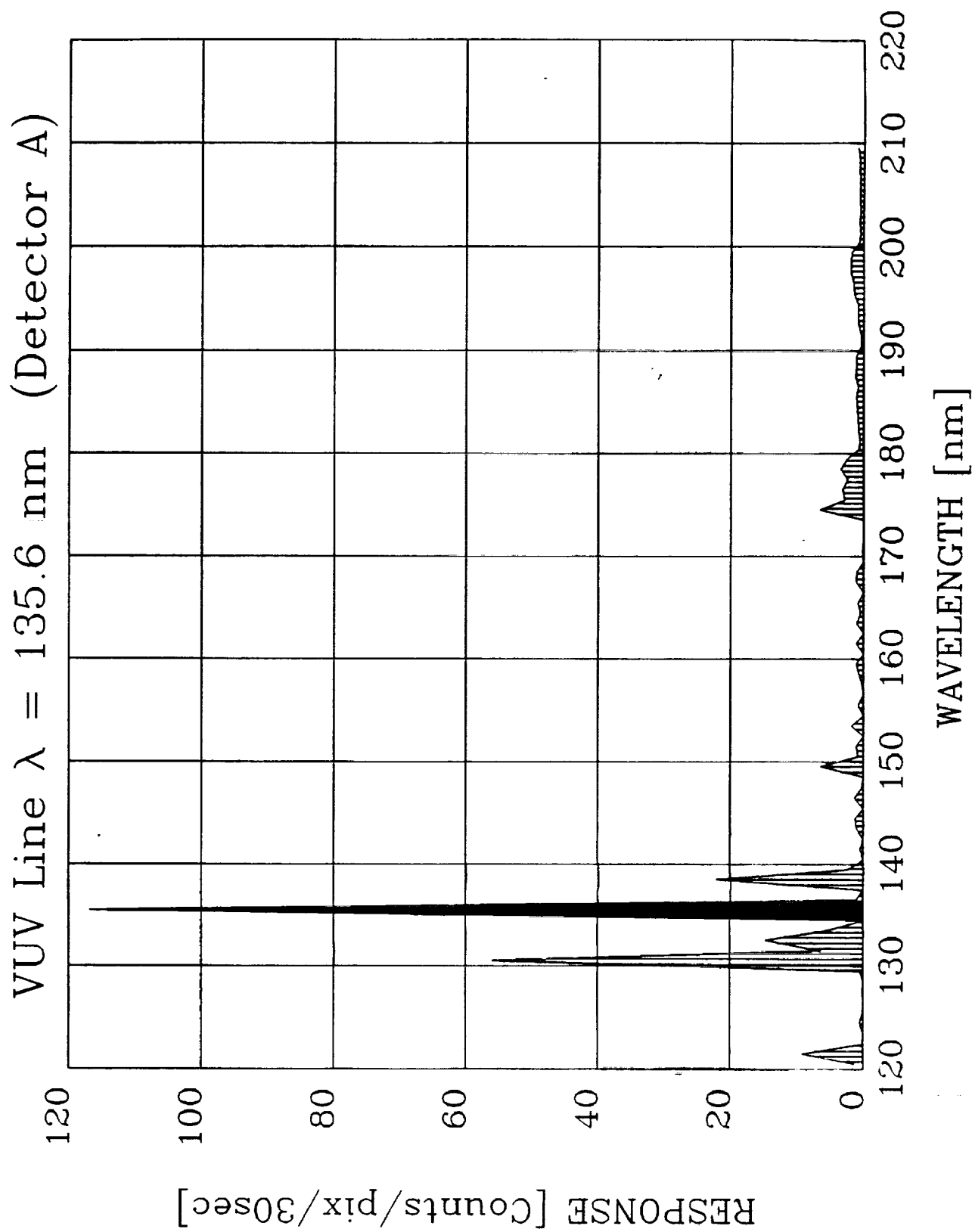


Signal to Noise Ratio = 83.848042

# Coatings for $\lambda = 135.6$ nm (Path A)

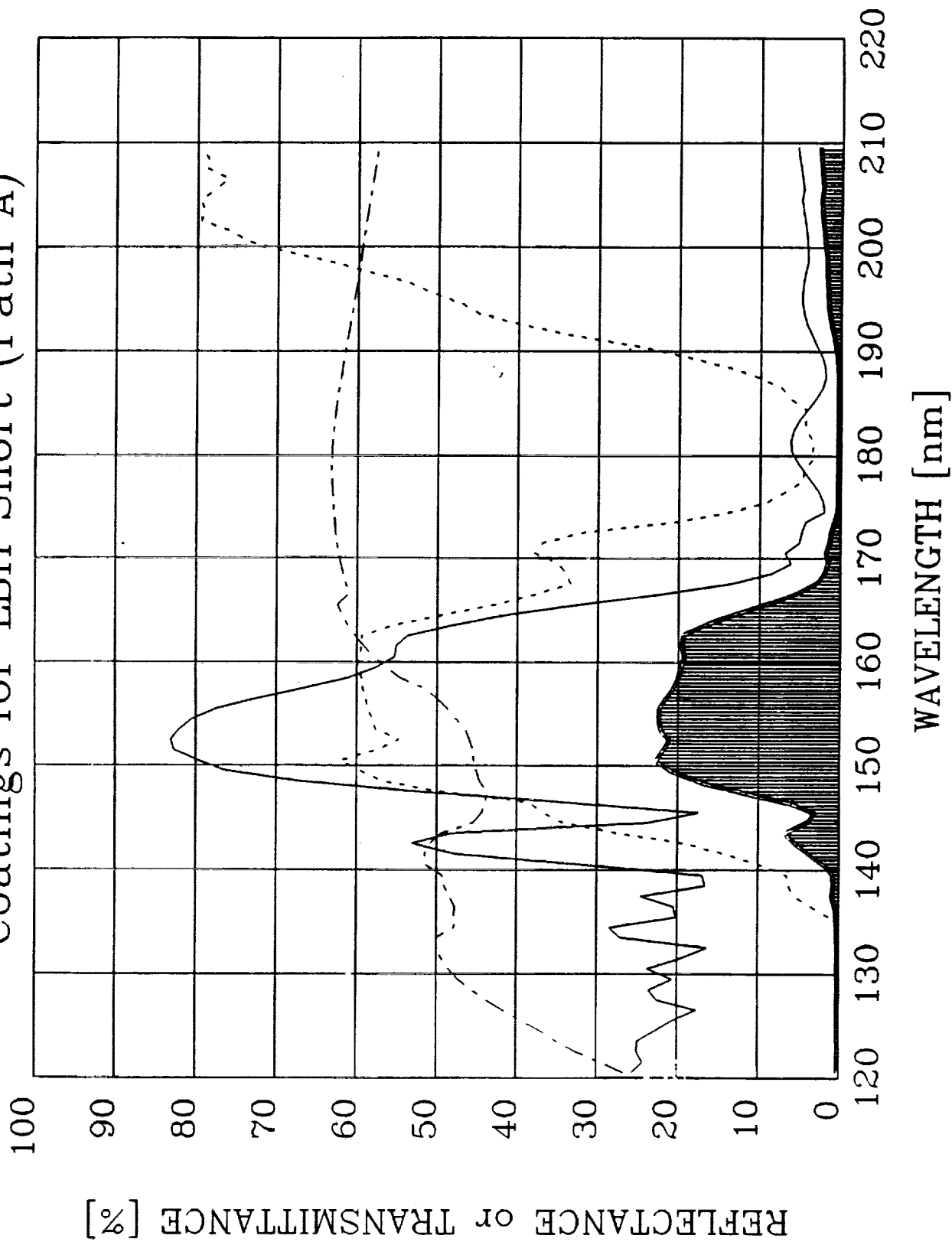


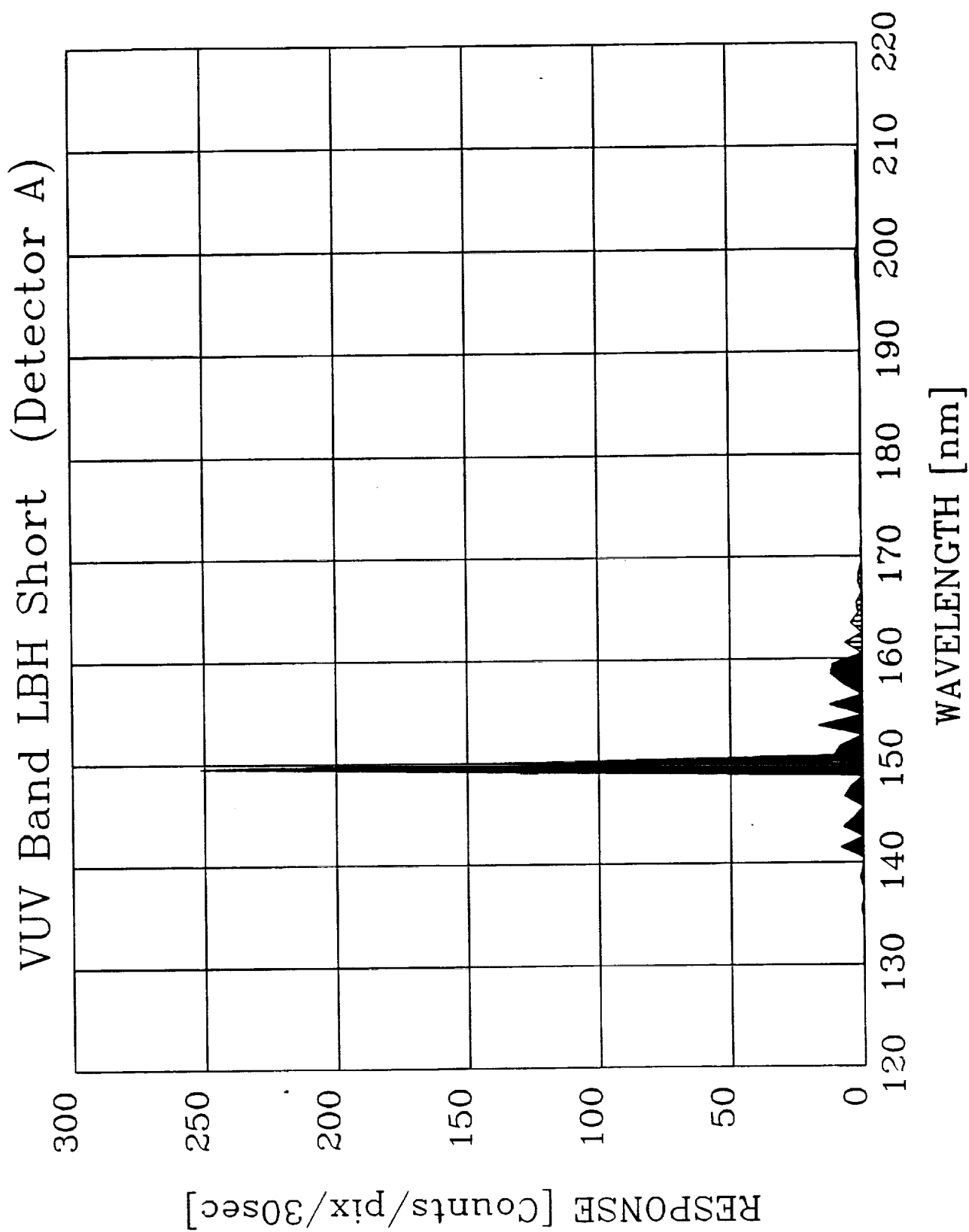




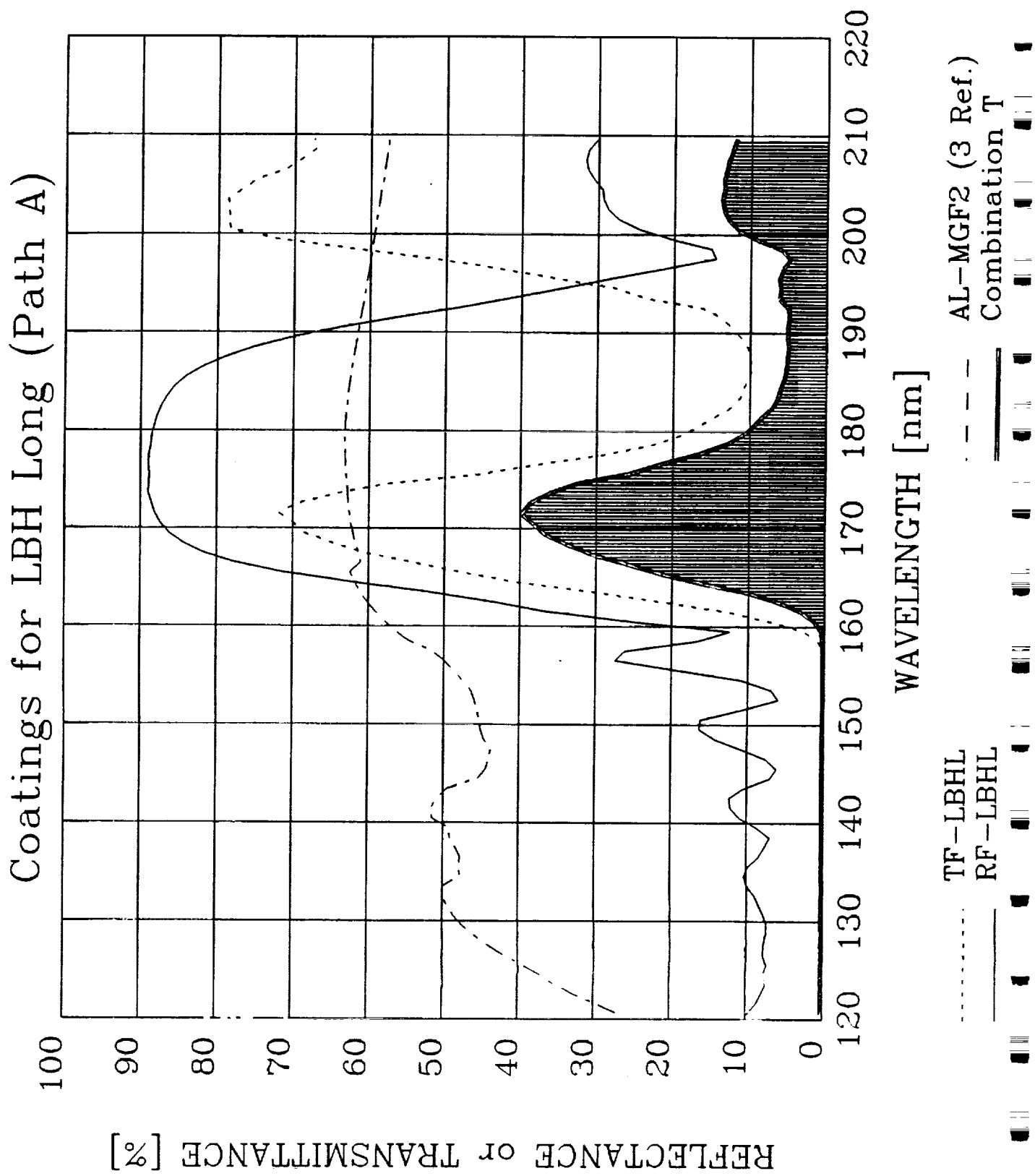
Signal to Noise Ratio = 20.606875

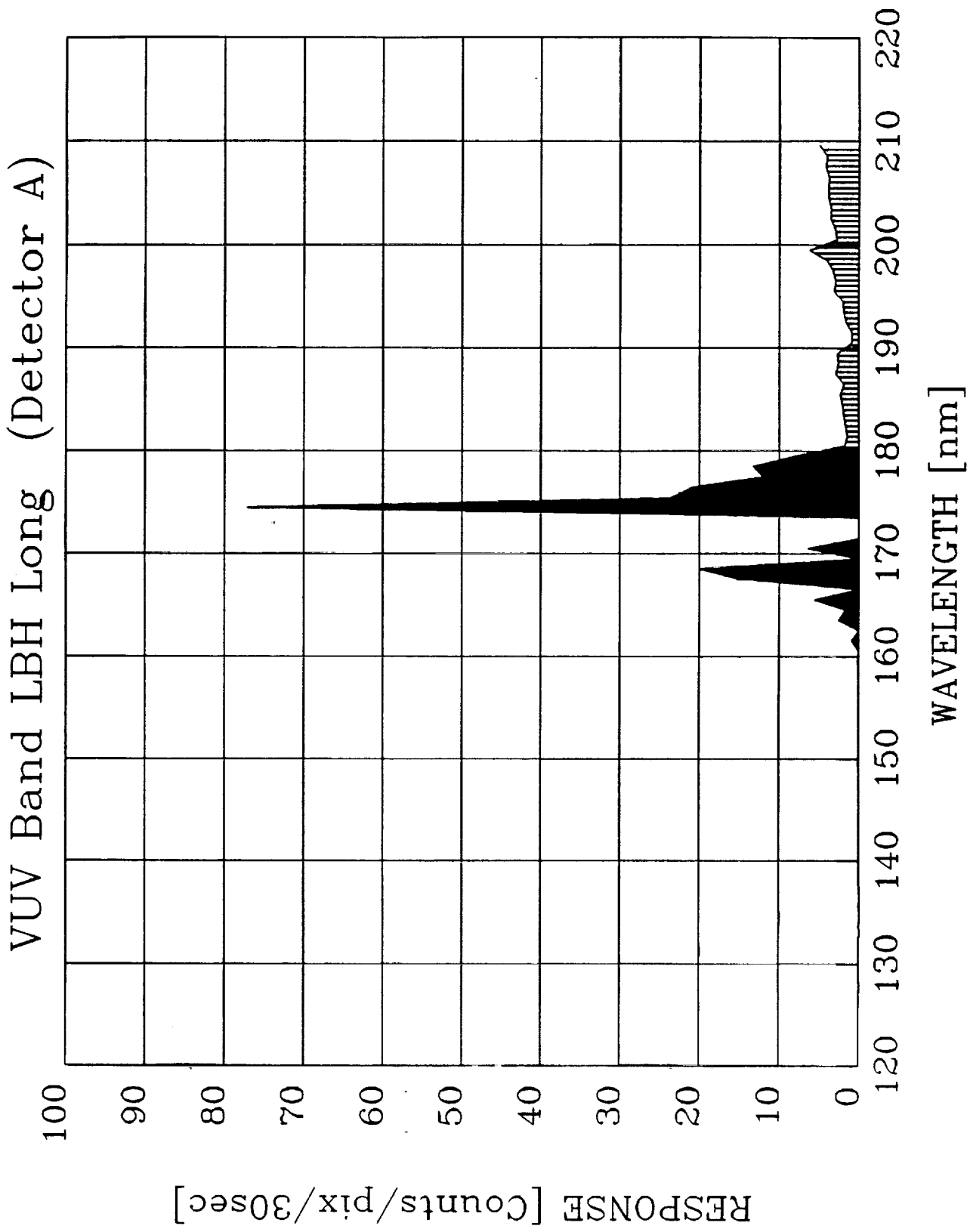
# Coatings for LBH Short (Path A)



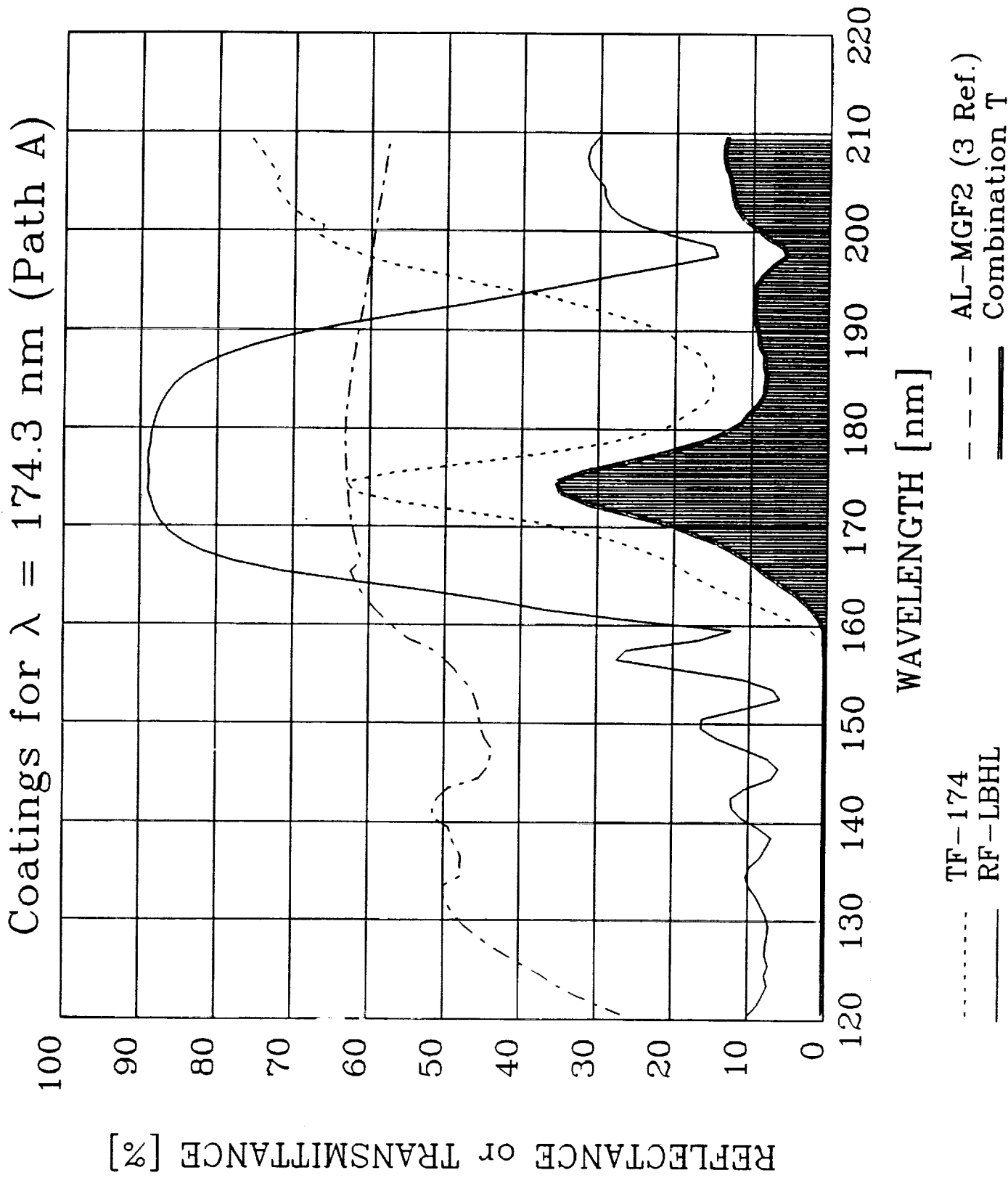


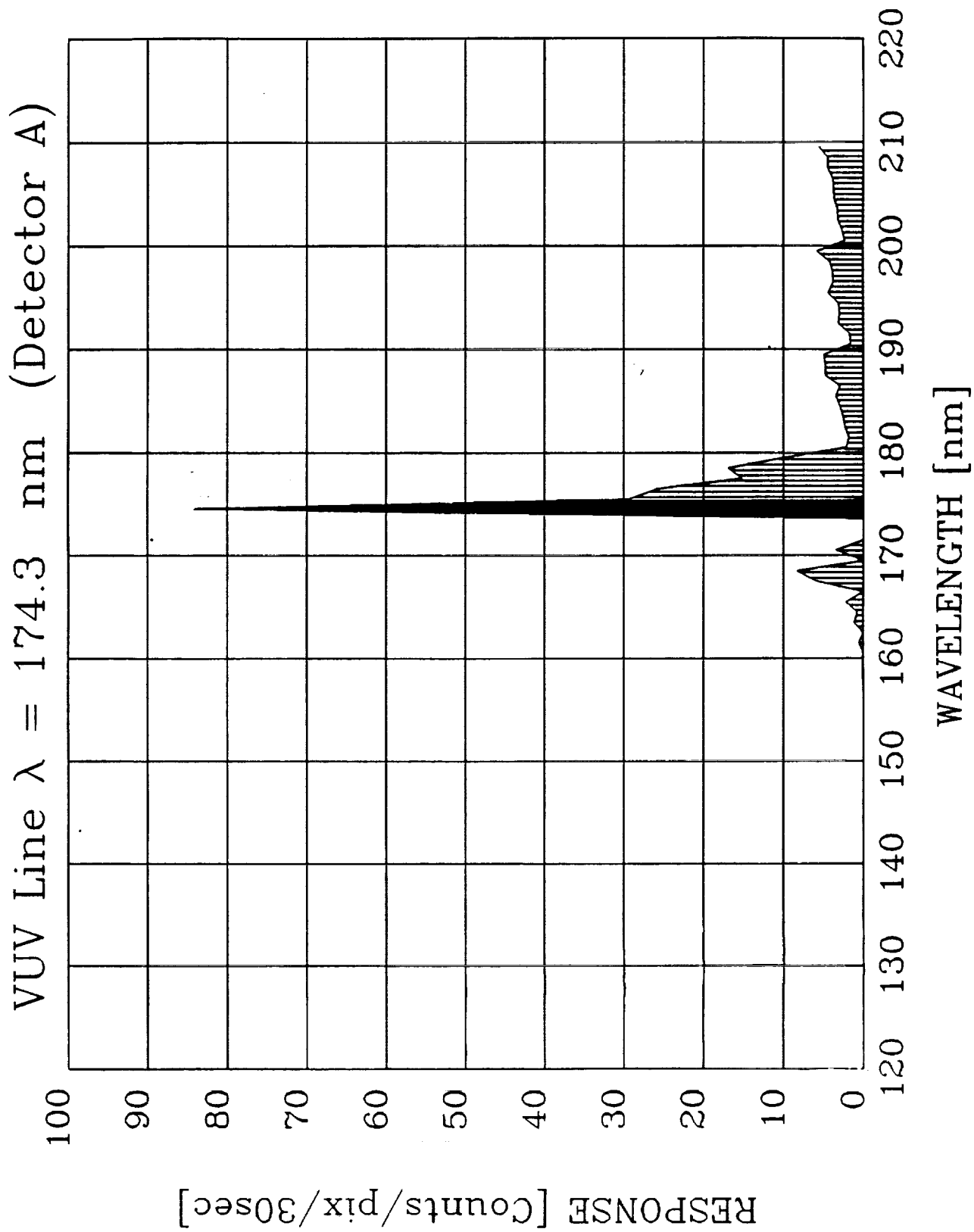
Signal to Noise Ratio = 57.567165





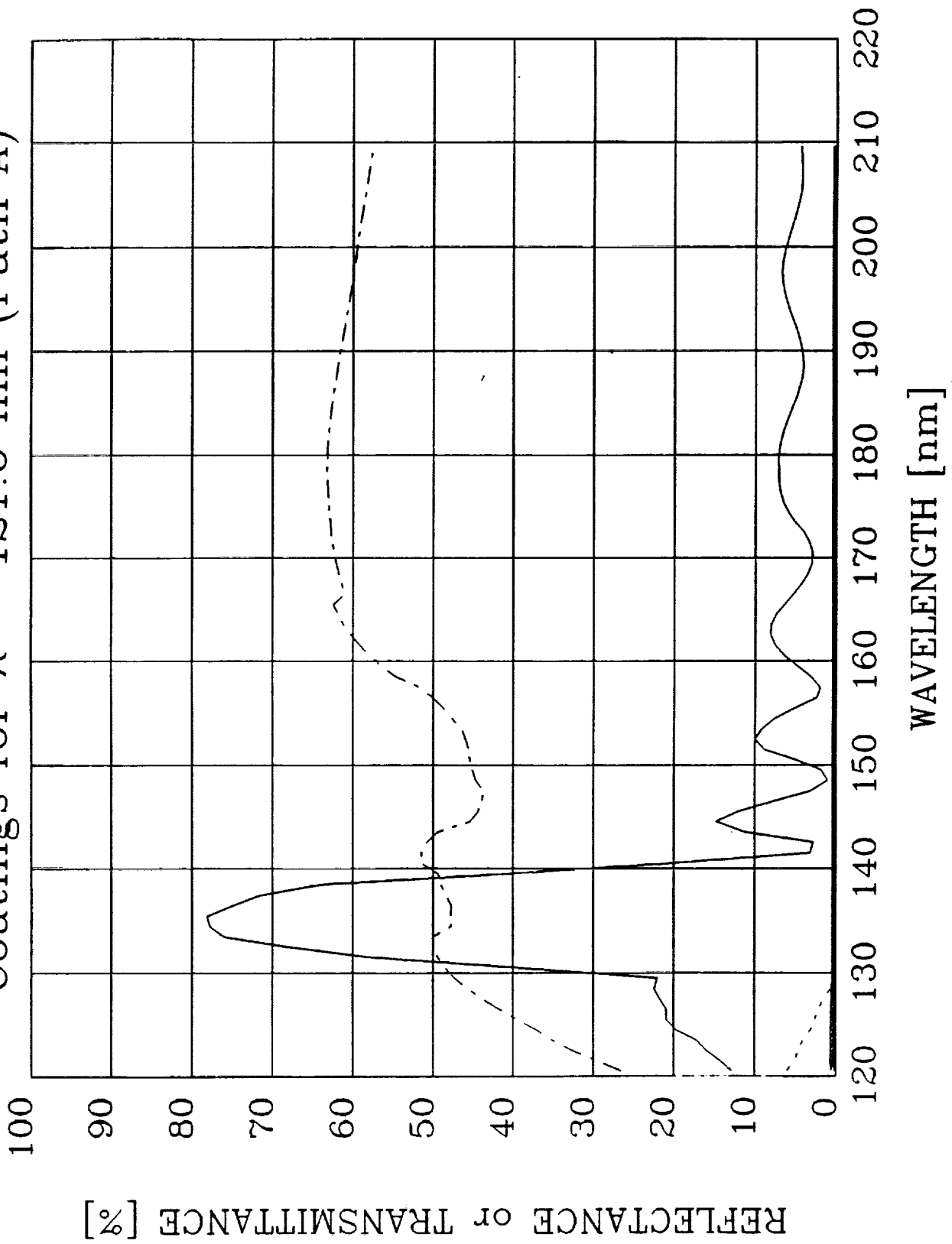
Signal to Noise Ratio = 38.685591



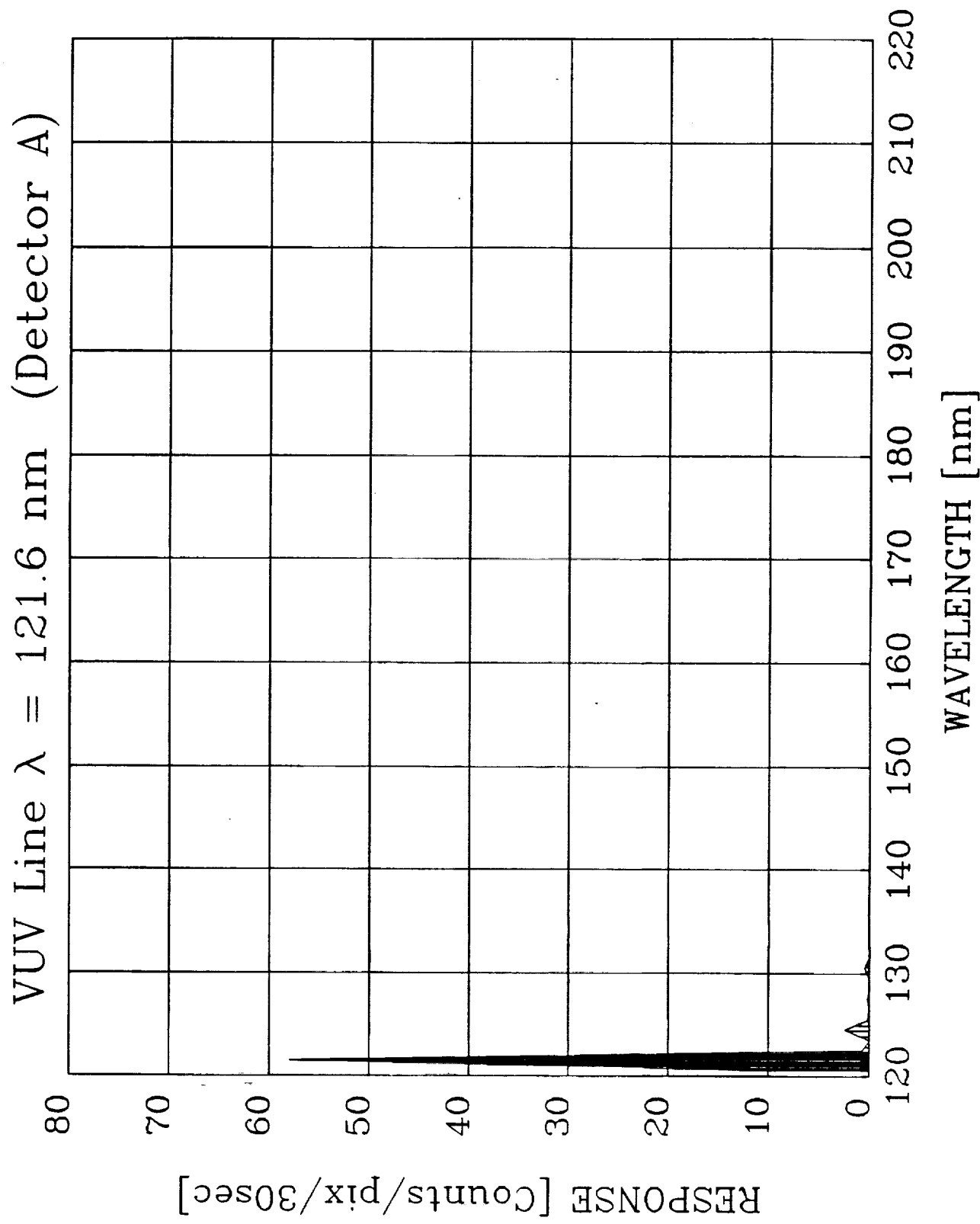


Signal to Noise Ratio = 18.116952

Coatings for  $\lambda = 121.6$  nm (Path A)

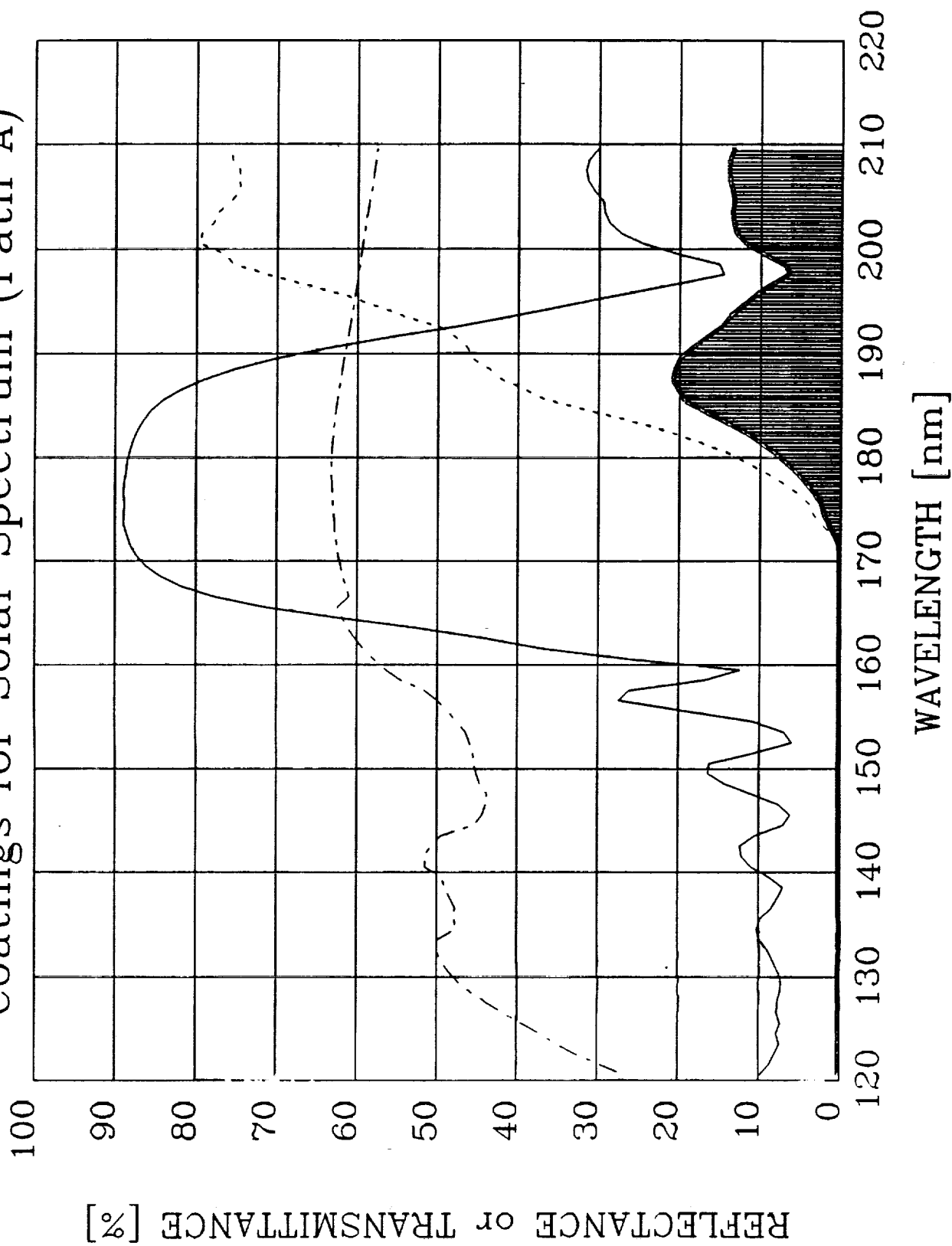


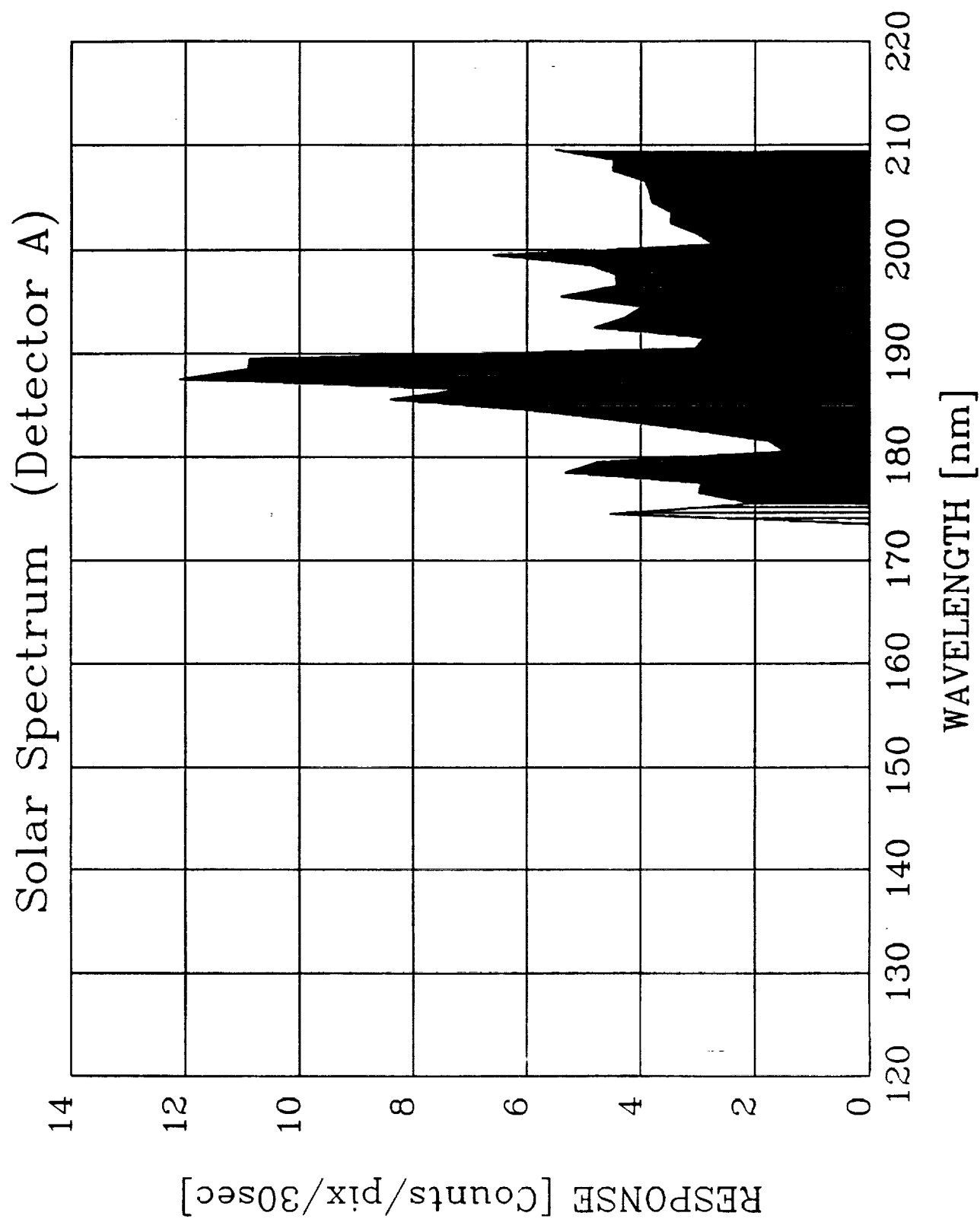




Signal to Noise Ratio = 23.430963

# Coatings for Solar Spectrum (Path A)





# FIELD LINE MAPPING

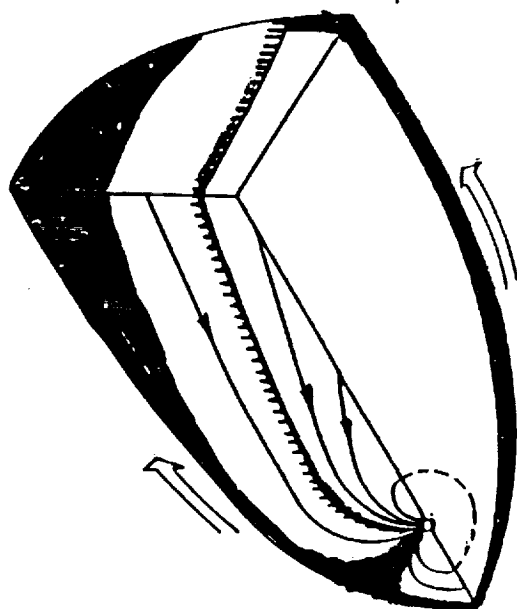
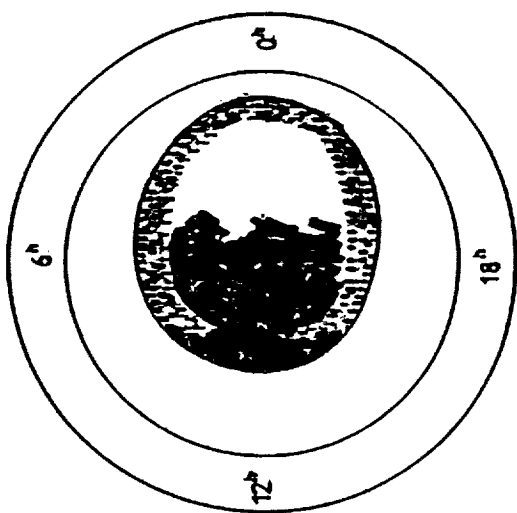
Bob Clauer



2:00 16 August




## **FIELD LINE MAPPING**

**(Ionospheric Signatures of Magnetospheric Processes)**

1. Mapping Particle Trajectories, Magnetic Fields, Currents  
Requires knowledge of:
  - A. Magnetic Field Structure
  - B. Field-aligned potential drop
  - C. Transmission Properties of magnetospheric and ionospheric Plasma
  - D. Feedback
2. Magnetopause Boundary Layers
  - A. Plasma Mantle
  - B. Interior Cusp
  - C. Low-Latitude Boundary Layer
3. Plasma Sheet Boundary Layer
4. Ring Current and Plasma Sheet





 RING CURRENT  
 PLASMA SHEET

 PLASMA  
 BOUNDARY  
 LAYER

 LOW-LATITUDE  
 BOUNDARY  
 LAYER

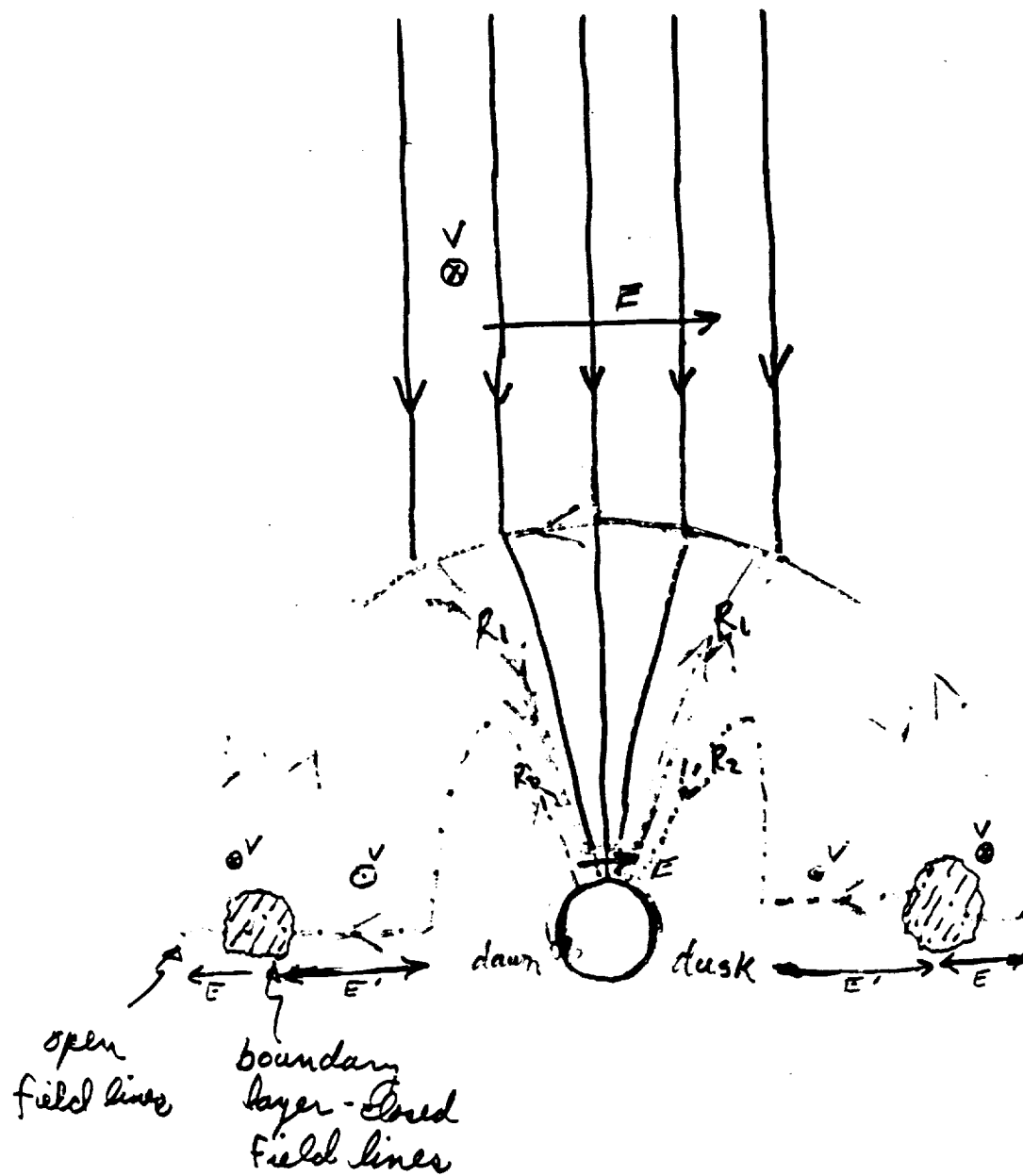
 INTERIOR  
 CUSP (EL)

 PLASMA  
 MANTLE

MAGNETOPAUSE BOUNDARY LAYERS

*Vasyliunas, 1979*

ORIGINAL PAGE IS  
OF POOR QUALITY



View from Sun

ORIGINAL PAGE IS  
OF POOR QUALITY

